CLASSIFICATION OF HARDWOOD SPECIES USING MULTIRESOLUTION FEATURE EXTRACTION TECHNIQUES

Ph.D. THESIS

by

YADAV ARVINDKUMAR RAMREKHA

DEPARTMENT OF ELECTRICAL ENGINEERING
INDIAN INSTITUTE OF TECHNOLOGY ROORKEE
ROORKEE – 247667 (INDIA)

AUGUST, 2015

CLASSIFICATION OF HARDWOOD SPECIES USING MULTIRESOLUTION FEATURE EXTRACTION TECHNIQUES

A THESIS

Submitted in partial fulfilment of the requirements for the award of the degree

of

DOCTOR OF PHILOSOPHY

in

ELECTRICAL ENGINEERING

by

YADAV ARVINDKUMAR RAMREKHA

DEPARTMENT OF ELECTRICAL ENGINEERING
INDIAN INSTITUTE OF TECHNOLOGY ROORKEE
ROORKEE – 247667 (INDIA)

AUGUST, 2015

INDIAN INSTITUTE OF TECHNOLOGY ROORKEE
ROORKEE

CANDIDATE'S DECLARATION

I hereby certify that the work which is being presented in the thesis entitled **"CLASSIFICATION OF HARDWOOD SPECIES USING MULTIRESOLUTION FEATURE EXTRACTION TECHNIQUES"** in partial fulfilment of the requirements for the award of the Degree of Doctor of Philosophy and submitted in the Department of Electrical Engineering of the Indian Institute of Technology Roorkee is an authentic record of my own work carried out during a period from July, 2012 to August, 2015 under the supervision of Dr. R. S. Anand, Professor, and Dr. M. L. Dewal, Ex-Professor, Department of Electrical Engineering, Indian Institute of Technology Roorkee, Roorkee, & Dr. Sangeeta Gupta, Head-Wood Anatomy Discipline, Botany Division, Forest Research Institute, Dehradun.

The matter presented in the thesis has not been submitted by me for the award of any other degree of this or any other Institute.

(**YADAV ARVINDKUMAR RAMREKHA**)

This is to certify that the above statement made by the candidate is correct to the best of our knowledge.

(R. S. Anand)	(M. L. Dewal)	(Sangeeta Gupta)
Supervisor	Supervisor	Supervisor

Dated: _____

ABSTRACT

Identification of wood is an important and difficult issue to deal with because of its complex biological structure. Correct identification of wood species is necessary for price fixation, fraudulent checking, protection of threatened plant and tree species at risk, and helping custom officials in proper assessment of wood species and implementation of tariffs accordingly. Wood is by and large classified into hardwood (HW) and softwood (SW) species. Softwood trees have limited number of cell types, which makes discrimination of softwood species a difficult task. On the other hand, hardwood species have a complex cellular structure and are easy to distinguish amongst the similar species.

The wood identification task is accomplished by using 1) traditional, and 2) machine vision based methods. In, traditional approaches, wood experts usually identify the wood species by examining surface of the wood specimen at two different stages, first with the naked eye, then with a magnifier. Recognition of large volumes of wood species, employing traditional approach is prolonged, erroneous and unfeasible sometimes. To overcome the problems associated with the traditional methods of wood identification, machine vision technology was employed for wood identification. It works on the principle of obtaining certain statistical parameter of the wood species; thus, helpful in minimizing the error in wood identification. The machine vision based systems outperform experienced officers when large volumes of wood species are to be identified repeatedly with utmost accuracy, without getting fatigued.

The macroscopic, microscopic and stereogram images of wood species have been used by the researchers for forest/wood species classification. A comprehensive analysis of the state-of-the-art work published in the area of forest/wood species classification shows that different texture features and classification algorithms are used for wood species identification. Further, microscopic images of wood carries significant information useful in its precise identification as compared to limited information possessed by macroscopic images. Hence, current work utilizes microscopic images for hardwood species identification.

The classification accuracy of hardwood species can be improved either by getting appropriate discernible texture features from the image using suitable feature extraction technique and/or by using suitable classifier. However, performance of the classifiers highly depends on the quality of its input features. This has been the motivation behind the proposal of using multiresolution texture feature extraction techniques to extract the significant features of the hardwood specie images for their efficient classification.

In the light of the above background, the objectives of the present research work have been broadly categorized as design and development of suitable feature extraction techniques, and determination of vessel elements of hardwood species. Thus, the key objectives of this research work are formulated as: (1) Design and development of multiresolution texture feature

extraction techniques to acquire substantial information of the microscopic images of hardwood species, useful in their classification; (2) Employing feature dimensionality and feature selection techniques to investigate their effect in improving the classification of hardwood species; (3) Selection of appropriate multiclass classification algorithms to evaluate the effectiveness of multiresolution feature extraction techniques for classification of hardwood species, and determining the best combination of feature extraction and classification algorithms for better discrimination of hardwood species; and (4) Segmentation and determination of vessel elements to compute their hydraulic conductivity and lumen resistivity.

To accomplish the above objectives, initially the state-of-the-art texture feature extraction techniques have been investigated for the classification of hardwood species. The texture descriptors produced by the state-of-the-art texture feature extraction techniques are based on spatial interactions over a fixed neighbourhood size on single scale image, which is appropriate for micro-texture analysis only. But, the microscopic images of hardwood species have four key elements namely vessels, rays, parenchyma and fibres, that too of varied shapes and sizes. In order to identify these images efficiently, it must be analysed at several scales of resolution as referred above. The smaller objects are the candidates to be examined at higher resolutions; whereas large size objects need to be examined at coarse view (lower) resolutions. To achieve multiresolution features, the images are decomposed at several levels of resolution; wherein each of the subimages coefficients contain varied and valuable information. Thereafter, the texture feature extraction techniques namely variants of local binary pattern (LBP), local configuration pattern (LCP), local ternary pattern (LTP), completed local binary pattern (CLBP) and local phase quantization (LPQ) are chosen to extract significant information from multiresolution images. The feature vector data obtained from each of the subimages are concatenated to increase the significant information of the images.

The multiresolution based texture feature extraction techniques have tendency to produce large number of complex features and many of the features may not be significant. Keeping this aspect in mind, feature selection and feature dimensionality reduction techniques have been employed not only to improve the classification accuracy but at the same time to minimize the computation time needed by classification algorithms. The principal component analysis (PCA) has been incorporated to reduce feature vector data dimensions by computing a few orthogonal linear combinations of the original dataset features with maximal variance. In addition, the minimal redundancy maximal relevance (mRMR) feature selection technique based on mutual information quotient has been chosen to eliminate the irrelevant features, and retain a subset of features that efficiently describes the observed input data.

The classification algorithms do play important role in improving the overall classification accuracy. Thus, four widely used classification algorithms, namely, linear discriminant analysis (LDA), random forest (RF), linear SVM and radial basis function (RBF) kernel SVM have been

employed to see the effect of features produced by proposed texture feature extraction techniques on the classification accuracy. Further, the performance of proposed feature extraction techniques, have been assessed with two different approaches; namely, 1) The 10-fold cross validation, and 2) Randomly divided database (RDD). Furthermore, under the individual approaches the results have further been categorized under full feature vector data (FFVD), PCA reduced feature vector data and mRMR feature selection based reduced feature vector data.

The present research work initially, examines the efficiency of several state-of-the-art texture feature extraction techniques for the classification of hardwood species. The selection of the feature extraction techniques have been based on their performance achieved in the various areas of image processing applications.

In the objectives mentioned in the beginning, the transform domain techniques have been opted here due to their multiresolution capability for analysing images at different frequencies for several levels of resolutions. The different frequency sub-band images provide substantial information about the various objects of the images compared to the information obtained from spatial domain grayscale images.

In, multiresolution feature extraction technique category, first approach has been design of the binary wavelet transform (BWT) based texture feature extraction techniques. By and large, the grayscale images have been utilized for extraction of texture features. It has been observed that the most significant bit (MSB), bit-plane (b7) of grayscale image contributes ample amount of information to the overall image. Thus, the BWT based LBP variants texture feature extraction techniques have been proposed to classify the hardwood species. The performance of BWT based LBP variants texture feature extraction technique has been found comparatively superior or at par with most of the state-of-the-art texture feature extraction techniques for hardwood species' classification.

The BWT based LBP variants have used only the MSB bit to extract the texture features of images; thus, the classification accuracy cannot be improved beyond a specific limit as the MSB bit does not correspond to 100% information about the image. To further enrich the quality of texture features, texture feature extraction techniques based on the Gaussian image pyramid (GP) model has been proposed. The selection of GP has been based on less computational efforts required in its implementation. Amongst, the GP based texture feature extraction techniques, the Gaussian image pyramid based local phase quantization (GPLQP) technique has produced the best classification accuracy, better than the techniques discussed in the preceding paragraphs.

In addition, the discrete wavelet transform (DWT) based LBP (DWTLBP) variants texture feature extraction techniques have been chosen for hardwood species classification as DWT has the property to emphasize the directional information of the images. The texture features

obtained from these directional subimages further help to the enrichment of feature vector data; which in turn help in better discrimination of the hardwood species. Amongst the proposed DWT based LBP variants texture feature extraction techniques, the DWT based uniform completed local binary pattern ($DWTCLBP^{u2}$) texture features processed by mRMR feature selection technique has yielded the best classification accuracy.

Further, to improve the classification accuracy of hardwood species, DWT based hybrid texture feature extraction techniques have been proposed; where, DWT decomposed subimages have been profound to be used with LBP and first-order statistics (FOS) techniques to get the tentative features. Moreover, it is proposed to fuse the features obtained from LBP and FOS methods. This technique thereafter is investigated to extract the texture features of both, the grayscale and color (RGB) images. It is observed that the mRMR feature selection based texture features of discrete wavelet transform based first-order statistics and local binary pattern histogram Fourier features (DWTFOSLBP-HF) technique produces the best classification accuracy for both types of images. Also, the texture features acquired by DWTFOSLBP-HF texture feature extraction technique for hardwood species are of excellent quality and no significant information loss is observed when grayscale image is employed for the classification in place of RGB image.

For the purpose of evaluating the performance of the proposed features extraction techniques with the help of classifiers, an open access database of hardwood species consisting of 75 different categories has been selected. These microscopic images of hardwood species are correctly labelled by the experts in the laboratory of wood anatomy at Federal University of Parana, Curitiba, Brazil.

In addition to the above classification work, a platform independent tool based on simple digital image processing technique has been developed to quantify the vessel elements of hardwood species. A prototype model has been developed and has been tested on several microscopic images prepared at the Xylarium (DDw) of the Wood Anatomy Discipline of the Forest Research Institute, Dehradun. The analysis of the experimental work suggests that with the help of appropriate parameter selection, the vessel elements are being extracted for most of the images. Further, along with the extraction of vessel elements, the proposed model is capable of computing the hydraulic conductivity and lumen resistivity of the vessel elements, which in turn provides helping hand to the wood anatomist in characterizing the woods.

In nutshell, the significant contribution of this thesis work can be summed up as the proposed multiresolution feature extraction techniques, which help in to extract the discernible features of the microscopic images of hardwood species and the improvement in the classification accuracy because of them. The determination of vessel elements while using segmentation approach can be considered as the further contribution.

ACKNOWLEDGEMENTS

I owe my gratitude to all those people who have made this dissertation possible and because of whom my research experience has been one that I will cherish forever.

I wish to express deep sense of gratitude and sincere thanks to my thesis supervisors, Dr. R. S. Anand, Professor and Dr. M. L. Dewal, Ex-Professor, Department of Electrical Engineering, Indian Institute of Technology Roorkee, Roorkee, & Dr. Sangeeta Gupta, Head-Wood Anatomy Discipline, Botany Division, Forest Research Institute, Dehradun, for their invaluable inspiration, competent guidance, wholehearted cooperation, motivation and help in carrying out this research work.

I would like to thank members of my examining committee, Dr. Vinod Kumar, Professor & Chairman DRC and Dr. Indra Gupta, Associate Professor, Department of Electrical Engineering & Dr. M. J. Nigam, Professor, Department of Electronics and Communication Engineering, Indian Institute of Technology Roorkee, Roorkee, for their vigilant examination of the work and instrumental suggestions. I also take this opportunity to thank Dr. Vinay Pant, Assistant Professor, Dr. P. Sumathi, Assistant Professor, Dr. G. N. Pillai, Professor, Dr. Pramod Agarwal, Professor & Dean Academics, and Dr. S. P. Srivastava, Head, Department of Electrical Engineering, IITR, Roorkee, for their continuous support.

I would like to express earnest gratitude to Prof. Luiz Eduardo S. Oliveira, Federal University of Parana (UFPR), Department of Informatics, for providing microscopic images of hardwood species for academic research purpose. Further, I am grateful to the anonymous reviewers for providing valuable suggestions for improving the work.

I am really thankful to Mr. Arun Balodi, Mr. Bhavik Patel, Mr. Yogesh Saria, Mr. Jayendra Kumar, Mr. Sachin Singh, Mr. Roshan Kumar, Mr. Milan Singh, Mr. Nagshettappa Biradar, Mr. Uday Joshi, Mr. Marmik Bhavsar, Ms. Nisha Shah, Mr. Ankit Srivastava, Ms. Nidhi Chauhan, Mr. Chandrasekhar shitole, Dr. Yantindra kumar and Dr. Divyang Pandya for their constant care and support during my entire research work. It is a pleasure to acknowledge the support extended by all the laboratory and administrative staff.

I also take this opportunity to express my heartfelt gratitude to Dr. Jayesh Patel, President, Dr. Devanshu Patel, Vice Presiden, Parul University, and the Principal, Dr. Vilin Parekh, Parul Institute of Engineering and Technology, Waghodia, Vadodara, for sponsoring me for the doctoral research work at IIT Roorkee. I also thank and sincerely acknowledge the financial support and assistantship provided by the QIP Centre, Indian Institute of Technology, Roorkee, during the research work.

I would like to thank to all my family members, especially my parents, who constantly encouraged and provided moral and social support during my research. Their sacrifice in difficult times not only boosted my morale but also provided motivation and enthusiasm in my research

work. Very special thanks to my wife, Neelam for being a constant companion in my ups and downs at Roorkee. Piyush and Vaani owe a special mention as they sacrificed the time that rightfully belonged to them. Their smiling faces always kept me lively. Special thanks to Mr. Ashok Yadav and Mr. Rajan Yadav who have been continuous source of moral support to me during my research work.

At the outset, I also thank almighty god for giving me strength, courage, health and wisdom helpful in completion of my research work. Last but not the least, I am thankful to all those who have helped me directly or indirectly in the successful completion of this thesis.

(YADAV ARVINDKUMAR RAMREKHA)

CONTENTS

LIST OF FIGURES

LIST OF TABLES

LIST OF ABBREVIATIONS

1D	One dimensional
2D	Two dimensional
ACA	Ant clustering algorithm
ALBP	Adaptive local binary patterns
ANN	Artificial neural network
ASM	Active shape model
BGLAM	Basic gray level aura matrix
BGP	Binary gabor pattern
BP	Back-propagation
BWT	Binary wavelet transform
$BWTCLBP^{ri}$	Binary wavelet transform based rotation invariant completed local binary pattern
$BWTCLBP^{riu2}$	Binary wavelet transform based rotation invariant uniform completed local binary pattern
$BWTCLBP^{u2}$	Binary wavelet transform based uniform completed local binary pattern
CA	Classification accuracy
CIELUV	International Commission on Illumination
CLBP	Completed local binary pattern
$CLBP^{u2}$	Completed uniform local binary pattern
CoALBP	Co-occurrence among Adjacent LBP
DenseCLBP	Dense completed local binary pattern
CSLBP	Centre symmetric local binary pattern
DLEP	Directional local extrema patterns
DWT	Discrete wavelet Transform
DWTCLBP	Discrete wavelet transform based completed local binary patterns
$DWTCLBP^{u2}$	Discrete wavelet transform based completed uniform local binary pattern
DWTFOSLBP-HF	Discrete wavelet transform based first-order statistics local binary pattern histogram Fourier features
$DWTFOSLBP^{ri}$	Discrete wavelet transform based first-order statistics rotation invariant local binary patterns
$DWTFOSLBP^{riu2}$	Discrete wavelet transform based first-order statistics- rotation invariant uniform local binary patterns
$DWTFOSLBP^{u2}$	Discrete wavelet transform based first-order statistics uniform local binary patterns
DWTLBP	Discrete wavelet transform based local binary patterns
DWTLBP-HF	Discrete wavelet transform based local binary patterns histogram Fourier features
$DWTLBP^{ri}$	Discrete wavelet transform based rotation invariant local binary pattern
$DWTLBP^{riu2}$	Discrete wavelet transform based rotation invariant uniform local binary patterns
$DWTLBP^{u2}$	Discrete wavelet transform based uniform local binary patterns
FOS	First-order statistics
FFDV	Full feature vector data
FS	Feature selection
FVDN	Feature vector data normalization
GP	Gaussian image pyramid

GLAC	Gradient local auto-correlation
GLCM	Gray level co-occurrence matrix
GLRLM	Gray level run length matrix
$GPLBP^{ri}$	Gaussian image pyramid based rotation invariant local binary pattern
$GPLBP^{riu2}$	Gaussian image pyramid based rotation invariant uniform local binary patterns
$GPLBP^{u2}$	Gaussian image pyramid based uniform local binary patterns
$GPLCP^{ri}$	Gaussian image pyramid based rotation invariant local configuration patterns
$GPLCP^{riu2}$	Gaussian image pyramid based rotation invariant uniform local configuration patterns
$GPLCP^{u2}$	Gaussian image pyramid based uniform local configuration patterns
GPLPQ	Gaussian image pyramid based local phase quantization
GSVD	Generalized singular value decomposition
HSV	Hue, saturation, and value
IDL	Image decomposition level
KDA	Kernel discriminant analysis
KNN	K nearest neighborhood
LBP	Local binary pattern
LBP-HF	Local binary pattern histogram Fourier features
LBP^{ri}	Rotation invariant local binary pattern
LBP^{riu2}	Rotation invariant uniform local binary pattern
LBP^{u2}	Uniform local binary pattern
LCP	Local configuration pattern
LCP^{ri}	Rotation invariant local configuration pattern
LCP^{riu2}	Rotation invariant uniform local configuration pattern
LCP^{u2}	Uniform local configuration pattern
LDA	Linear discriminant analysis
LDP	Local derivative patterns
LPQ	Local phase quantization
LSB	Least significant bit
LTCoP	Local ternary co-occurrence pattern
LTP	Local ternary pattern
MLP	Multilayer perceptron
MLP-BP-ANN	Multilayer perceptron back- propagation artificial neural network
MMI	Mask matching image
MRLBP	Multiresolution local binary pattern
mRMR	Minimal redundancy-maximal relevance
MSB	Most significant bit
NN	Nearest neighbourhood
NoF	Number of features
PC	Principal component
PCA	Principal component analysis
RBF	Radial basis function
RDD	Random divided database
RF	Random forest
ROI	Region of interest
SD	Standard deviation
SPPD	Statistical properties of pore distribution

SVM	Support vector machine
WT	Wavelet transform
%CA±SD	Percentage classification accuracy plus/minus standard deviation

CHAPTER 1. INTRODUCTION

This chapter presents an overview of the research work carried out in this work. At the outset, the need of wood identification, challenges & motivation, wood anatomy and methods of wood identification are presented. Further, a comprehensive review of the work carried out for the classification of forest/wood species by employing feature extraction and machine learning techniques have been discussed. Based on the literature review the objectives of the present study have been formulated. The organisation of the thesis is given at the end of the chapter.

Trees are considered to be friend of all living beings on this earth as they provide them life (oxygen), shelter (House), food, and fuel for good living. Wood is considered to be one of the nature's supreme souvenirs for mankind. In India some trees are deified (sacred), as "Vriksha Devta" which are considered to be holy and the people ought to worship them. The Tulsi, Pipal, Banyan, Goolar, and Neem are the trees that are worshipped in India. India has rich forest resources, and not less than 1400 species of trees are commercially exploited for wood (timber) in different parts of India.

1.1 NEED OF WOOD IDENTIFICATION

Recognition (identification) of wood is an important and difficult issue to deal with because of its complex biological structure. Wood must satisfy certain prerequisites in order to be the most suitable and appropriate for the manufacturing of different products. For certain applications, physical properties of wood (i.e., density, hardness, durability, bending strength, and stability) are of utmost importance. Other applications may have specific requirement of texture pattern, grain and color (i.e., decorative objects). Hence, from industry perspective, identification of wood is essential as its characteristics vary widely [82]. Correct identification of wood species is crucial for many reasons as given below:

1. Accurate recognition of wood species is essential for price fixation based on color, texture, scent, hardness, durability, availability and rational use of available resources.
2. To check on fraud as some timber traders have tendency to amalgamate different types of wood so as to increase their profit margin.
3. To strengthen the endeavour of wood trading countries to fight against the illegal logging and smuggling of precious woods (i.e., sandalwood), and protection of threatened plant and tree species at risk.
4. Provide helping hand to custom officials in proper assessment of wood species and implementation of tariffs accordingly [217].

1.2 WOOD IDENTIFICATION CHALLENGES

The major challenge in wood identification is the non-availability of infrastructure (Xylarium, micro slides and literature for comparing the microstructure of unknown wood sample with the known) and the scarcity of highly skilled manpower with proven experience in the said field. Further, imparting training to human officers to attain an expertise in identification of wood is a time-consuming process. Nowadays, occupation as a wood certification officer is neither easy nor lucrative and likelihood of unfairness and oversight cannot be denied. Moreover, identification of large quantity of wood samples is not only time consuming, but erroneous and impractical to implement in real world applications. There is no systematic classification procedure for wood identification and, thus, a specie has to be identified based on the combination of its microstructure features. In tropical countries there is huge hardwood diversity. India alone has over 1200 hardwood species and, therefore, memorizing the microstructure of all the species is next to impossible. Thus, to effectively address the above said issues researchers are looking into the possibility of coming up with computer assisted forest species/hardwood species identification system.

Most of the problems related to the identification of wood material are similar to those for any of the biological material [54, 127, 161, 162] such as insufficient foundation for comparison and reference base. Further, there is also incorrect interpretation of keys by the users due to lack of knowledge for wood identification. The limitations of the traditional techniques have opened the new way for wood identification which is machine vision based. This has been the first motivation for this task. The core goal of machine vision based identification system in the context of wood identification is to achieve quantifiable, repeatable and reliable pattern recognition results [217].

In order to understand the object of interest (wood), in the present work an effort has been made to introduce the basic wood anatomy which is discussed in brief in the following subsection.

1.3 WOOD ANATOMY

The surfaces of wood can be categorized into three classes as illustrated in Fig. 1.1; each of which speaks about the surface uncovered during the process of marking.

1. Cross-section surface or Transverse plane: Parallel to the long axis of the stem,
2. Radial surface: Perpendicular to growth rings and the long axis of the stem,
3. Tangential surface: Tangent to the growth rings.

The cross-sectional surface of wood images contain ample information necessary to discriminate the wood species. The microscopic structure of maple (angiosperm wood) in three different views are illustrated in Fig. 1.2.

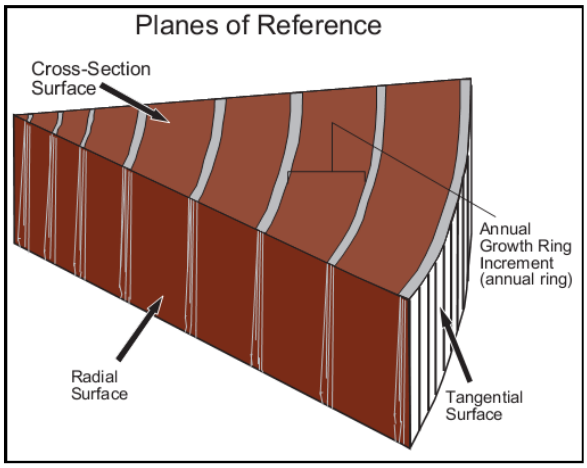

Fig. 1.1 The three reference planes of wood [19].

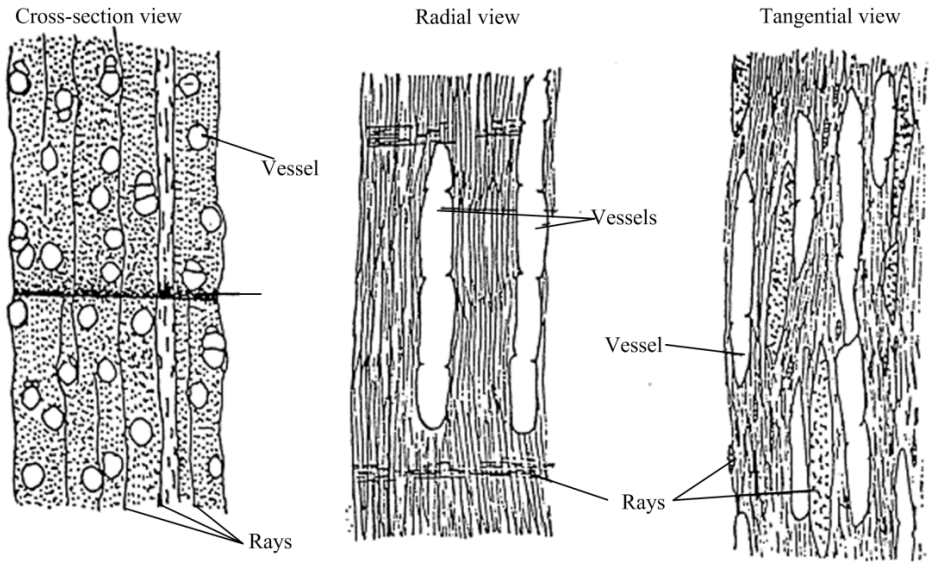

Fig. 1.2 Microscopic structure of angiosperm wood (maple) [252].

1.4 MACRO CROSS-SECTION CHARACTERISTICS OF TREE-STEM

The tree stem cross-section view is depicted in Fig. 1.3. Primary layers of wood tissue consist of bark, vascular cambium, sapwood, heartwood, growth ring, earlywood and latewood which are described as follows:

- Bark: An outer, protective covering layer of tree, made up of non-functional pholem and corky tissues, contains oil and wax. Bark helps to moderate interior temperature, reduces water loss, and gives protection against external injury. Small openings that permit gas exchange is known as lenticels. It is further categorised into outer bark and inner bark. Outer bark *is a* non-functioning pholem, acts as insulation for tree, protects tree from insects, disease attacks, other injuries, fire, extreme heat and cold conditions. The inner bark is a soft, spongy, and functioning pholem that transports sugar from the foliage in the tree crown to other branches, stems and the roots.

- Vascular cambium: It is a layer of cells, found between the sapwood and the inner bark. The xylem and pholem cells are produced by vascular cambium, both contribute in the growth of the tree. The vascular cambium also helps in formation of annual ring inside the tree and new bark outside the tree.
- Sapwood: It is a new and functioning xylem and has lighter color than heartwood as shown in Fig. 1.3. Main function of sapwood is transportation of water from roots to crown of the tree for photosynthesis. It also moves resin (pitch) through the tree for preventing any of the infections that take place due to the damage incurred by insects or animals. The inner portion of sapwood has dead cells, and the active cells are normally found in the outer portion.

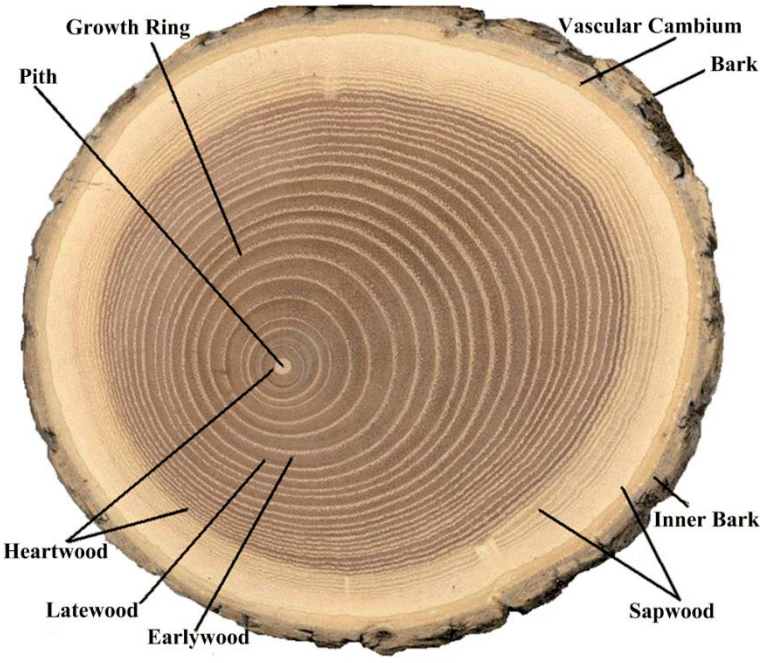

Fig. 1.3 Tree stem cross-section view.

- Growth rings: Wood formation during a period of one year is known as growth ring of the tree. The wood material developed inside a growth ring is attributable to the changes that occur during the growing season, known as earlywood and latewood. Growth rings may vary in width as a result of different climatic conditions. The earlywood (springwood) formation in wood takes place during spring and early summer season at the beginning of the growing season when warm and wet conditions promote rapid growth. In hardwood, earlywood cells (vessels) have large diameters and thin cell walls. The formation of latewood (summerwood) takes place in the late summer and fall towards the end of the growing season, when dryer conditions slow down the development of new wood growth. Latewood occurs at the outer region of a growth ring and the vessels are either absent or have small size diameter with greatly thickened cell walls.

- Pith: Pith is made up of sapling cells and is found in the centre of the trunk.
- Heartwood: Heartwood is an old and inactive xylem infiltrated by resins and gums; it has been once a sapwood and has darker shade due to a variety of chemicals. Its function is to provide support to the tree.

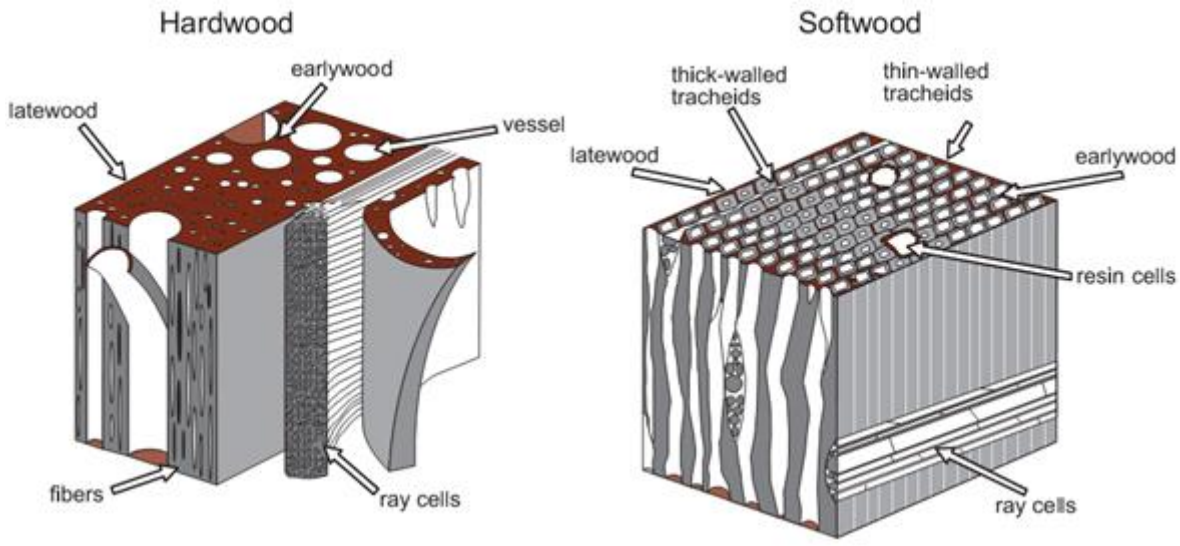

Fig. 1.4 Three-dimensional view of hardwood and Softwood species samples [19].

In general, the wood species are classified as hardwood and softwood. The phrase hardwood and softwood are used only to reference the taxonomical distribution that separates a specie from the other specie and has little to do with the actual hardness or softness of the wood. A number of softwood species may not be soft and hardwood species may not be hard. The 3-dimensional view of hardwood and softwood species is shown in Fig. 1.4.

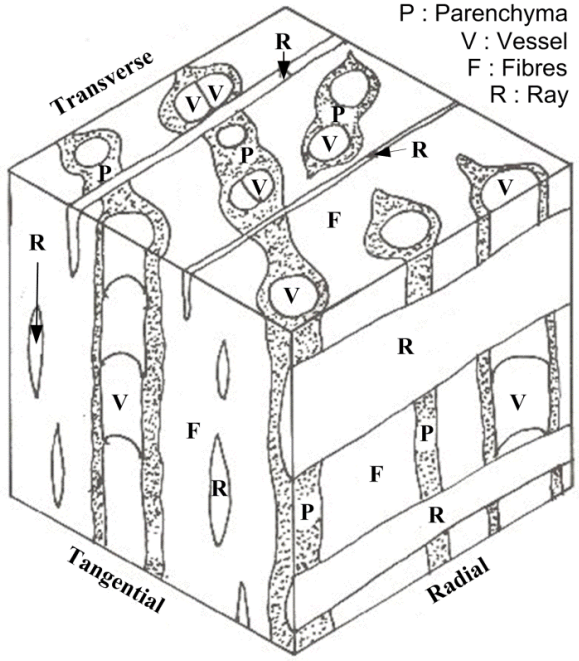

Fig. 1.5 Cube of hardwood species showing three planes of section and arrangement of principle tissues of the xylem [246].

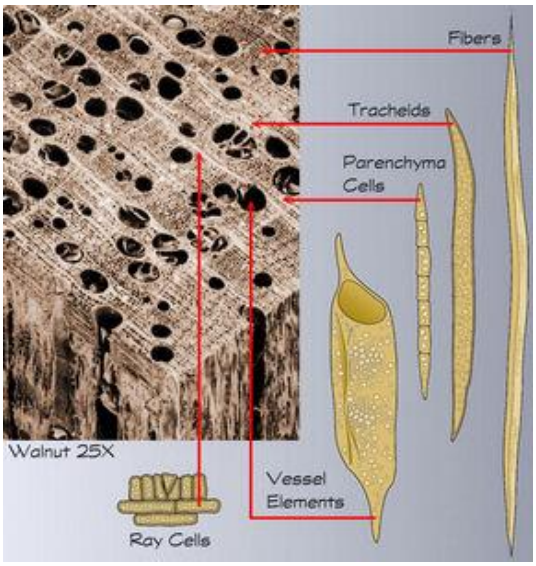

Fig. 1.6 Microscopic structure of cells of hardwood specie [248].

Softwood (gymnosperm) trees are conifers and use cones for seed reproduction; consist of 90% - 95% of cells called longitudinal tracheid's and have simple cellular structure. Softwoods don't contain vessels elements, contain long fiber, are lighter in weight, straight grained, and relatively homogenous. The hardwood species (angiosperm) are leaf bearing trees, possess complex cellular structures. Hardwood species have four significant elements namely, vessels, fibres, parenchymas and rays that are useful in their identification. The arrangement of these elements in all the three views (transverse, tangential and radial) are depicted in Fig. 1.5; whereas Fig. 1.6 shows these elements in the cross-section view only. Concise description of these elements are as follows:

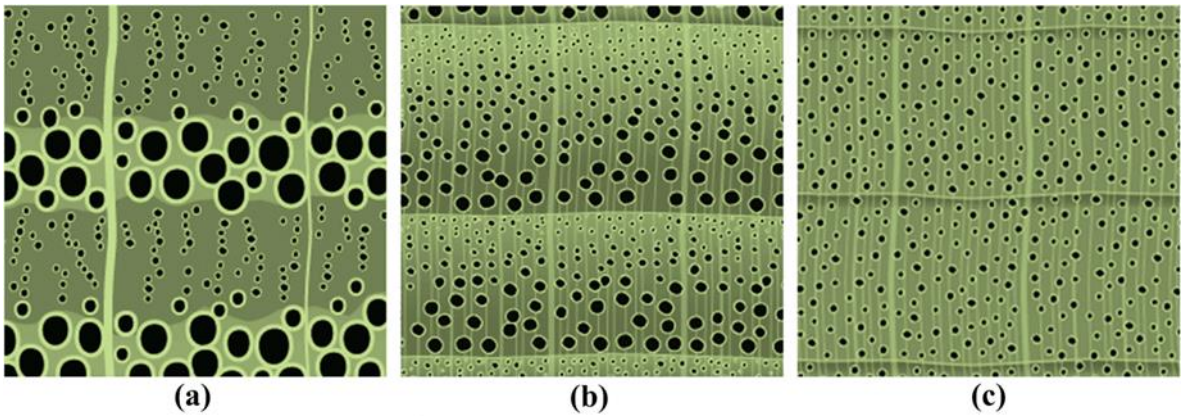

Fig. 1.7 Hardwood species a) Ring porous b) Semi-ring porous, and c) Diffuse porous [254].

1.4.1 Vessel

Vessel elements known as pores in the cross-sectional view of the image vary greatly in size, shape, number and spacing from one specie to another in earlywood to latewood zone. Vessels have large diameter compared to any other cells in the hardwood structure. Using hand lens of 10x power one can determine whether vessels elements are present or not. The hardwood

species are further categorised into ring, semi-ring and diffuse porous based on the arrangement of pores in a growth ring. The schematic representation of the same is given in Fig. 1.7.

- Ring porous: Each growth ring of the hardwood species has a band of earlywood vessels (pores) of considerably large size; easily visible in the macroscopic image, and a band of latewood vessels of minor size that sometimes need use of magnifying lens for viewing (Fig. 1.7 (a)).
- Semi ring porous: In each growth ring, the pores in the earlywood zone have larger diameter that progressively decreases in size as pores enter the latewood zone (Fig. 1.7 (b)).
- Diffuse porous: Pores are of uniform size across the entire growth ring. All the pores are of considerably tiny size, which requires use of 10x lens to see them in the macroscopic images of hardwood species (Fig. 1.7 (c)).

1.4.2 Vessel (Pore) Arrangements

In cross-section view the relative position of pore with respect to each other is useful for describing vessel elements. Different species of hardwood have unique vessel arrangements, as depicted in Fig. 1.8.

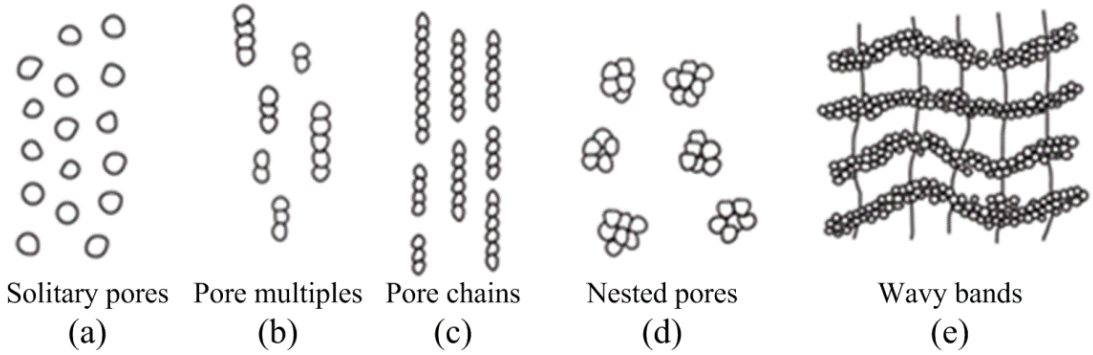

Fig. 1.8 Pore arrangements [251].

- Solitary pores: Solitary pores are single pores, which do not touch other pores and are evenly spaced across the cross-section (Fig. 1.8 (a)).
- Pore multiples: In pore multiples, two to five pores appear grouped together. It usually occur in radial rows, but can take place in both radial and tangential directions (Fig. 1.8 (b)).
- Pore chains: In Fig. 1.8 (c) an arrangement is shown where pore multiples appear in radial direction only.
- Nested pores (clusters): More number of pores come in contact with each other in both radial and tangential directions as shown in Fig. 1.8 (d).
- Wavy bands (ulmiform): As shown in Fig. 1.8 (e), the pores are arranged in irregular concentric bands.

1.4.3 Fiber

Fibres (technically called fibre tracheids) are abundant, long, round in cross section, needle-like cells having thickened walls as shown in Fig. 1.6. They provide mechanical support to the tree, and are heavily lignified xylem cells [19]. They are usually 0.5 to 1.5 mm long, 20-30 μm diameter, 20%-75% by volume and 40%-90% by weight of wood.

1.4.4 Ray

Rays are not easily visible with naked eye; these are characterized by the narrow stripe or lines, series of cells radiating from the centre towards the bark across the tree cookie as shown in Fig. 1.6. Rays have perpendicular orientation to the main axis of the stem of the wood. The size and distribution of rays on the cross-section are quite unique for many species and used to separate groups of species. The functions of rays are to allow horizontal movement of sap and minerals in stem and storage of carbohydrate [19]. Rays can be used as key characteristic to identify the wood species in the radial or tangential surface. Rays vary not only in width, but also in height. The height of ray varies between species from barely small to several inches high and is best observed from the tangential surface.

1.4.5 Parenchyma

The small, thin-walled, longitudinal cells that provide food storage, sparse in softwoods but are often quite significantly dense in hardwoods [19]. There are many species with visible and unique arrangements of parenchyma cells that offer a clear structural feature for decisive identification. They are categorised into 1) paratracheal, and 2) apotracheal parenchyma's.

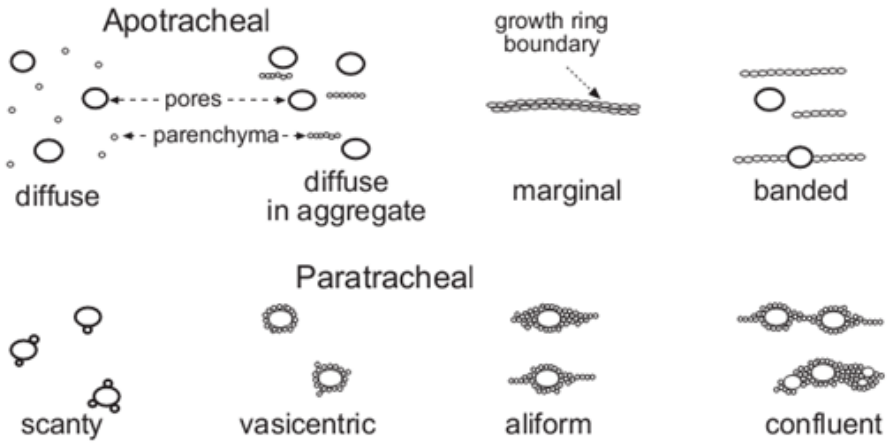

Fig. 1.9 Parenchyma arrangements around hardwood pores [19].

As shown in Fig. 1.9, the paratracheal parenchyma make contact with the vessels (pores) in cross-section view, whereas apotracheal parenchymas are separated from pores by fibres or rays. Paratracheal parenchyma appears in many forms, namely, scanty, vasicentric, aliform and confluent. Similarly, apotracheal parenchyma are categorised into diffuse, diffuse in aggregates, marginal and banded forms.

Identification of timber and tree becomes difficult when their fruit-lets and leaves are axed from its trunk. Therefore, in such cases, one has to rely on physical, macroscopic and microscopic features of wood for their identification. Sometimes, identification of wood is not easy as the biological deterioration, stains, and aging that can alter wood by transforming its look. Further, the wood elements/samples kept in outdoor conditions, are exposed to direct sunlight and rain may lead to changes in the characteristics of wood such as color and weight. Further, the wood elements can become darker due to application of oil, wax and polish treatment [71; 83]. In wood industry, one of the many ways to improve the quality is to identify and verify the wood before the process starts. Like humans, unique cellular structure of the wood species (which vary among the intra-species) acts as a blueprint for its identification [19].

1.5 WOOD IDENTIFICATION METHODS

There are two methods normally used for wood identification:

1. Traditional methods, and
2. Machine vision based methods

1.5.1 Traditional Methods

For many decades, traditional approaches have been instrumental in wood identification. Wood experts usually identify the wood species by examining surface of the wood specimen at two different stages, first with the naked eye, then with a magnifier. With the naked eyes, the wood expert can observe the weight, color, scent, feel, odour, hardness, and texture of the wood surface. This stage basically examines the physical characteristic that the wood species possess. A sharp pocket knife is used to unwrap (peel) the wood surface to acquire a clear and smooth cross-section. Using a magnifier (i.e., 10x hand lens), the wood expert will be able to observe the anatomical characteristics of the cross-sectional surface of the wood. The distinctive features of wood cross-section such as vessels and parenchymas are examined for hardwood species, whereas, in case of softwood species that do not possess vessels and has trivial (insignificant) parenchyma and rays. Therefore, for softwood species characteristics like, growth rings and resin canals, etc., are examined for the identification purpose [14]. However, for more reliable results, cross-sectional micro-structures of the wood samples are analysed in the laboratory and their features are compared with available samples of hardwood species for identification [12].

The process of analysis of anatomical features is the most important aspect of wood species identification. The methods such as visual comparison, dichotomous key and multiple entry keys are employed for wood identification based on their characteristics observed under macroscopic view.

1.5.1.1 Visual comparison

Recognizing wood species by comparing them, are popularly used for many types of living things. The majority of field guides will demonstrate similar species in the same section so that the user can use it to determine the species [111]. The wood anatomical characteristics are required to be compared with the information provided in the field guides. The disadvantage associated with visual comparison method is that the comparison between similar species might be tedious, when the differences are very small and difficult to be observed. Further, the other difficulty associated with looks-like (comparison) method is when looking at a wood specie one has never seen before and categorizing them to a particular category. One of the probable reason is that most of the wood species apt to give the impression of another wood specie [84].

1.5.1.2 Dichotomous key

The dichotomous key is another popular method used in the identification of plants, wood, animals, etc. The dichotomous key presents a series of paired, contrasting options at any stage in the selection process [250, 253]. One option has to be selected at each branching point [40] that leads to another two options. Different keys lead to another pair of keys until the correct answer (one or more taxa is suggested) is found. Further, it is necessary to check the obtained results (taxa) against reliable reference materials. Dichotomous key is simple and comprehensible but at the same time tends to cause errors in case the keys have longer sequences. The Fig. 1.10 shows the part of dichotomous key to select conifer or broadleaf tree [250, 253]. The disadvantage of this method is, if incorrect decision is taken at an intermediate stage (branching point), then the end result will be affected and the correct identification will not be achieved. Also, if a particular genus or specie is not included/incorporated in the dichotomous keys, no match will be found [130].

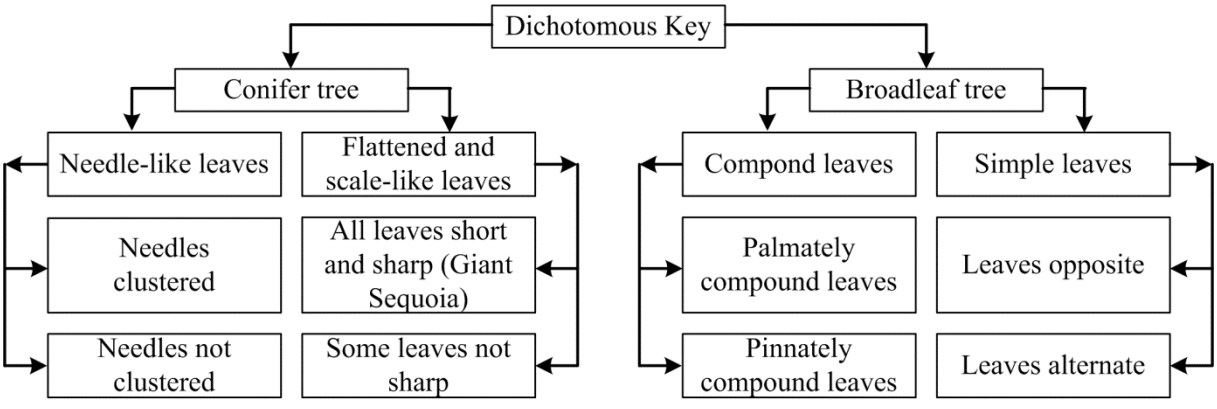

Fig. 1.10 The dichotomous key [250, 253].

1.5.1.3 Multiple entry key

The synoptical key is one of the most simple multiple entry key that lists for each diagnostic feature the taxa that have particular features, and the examples of such keys are given in [51, 129, 130, 205]. The advantages of these keys are the sequence of characters employed in an

identification process that is motivated by the unidentified wood sample, as opposed to the author of the key. In fact, the primary application of multiple entry card was for wood identification [37, 163]. The multiple entry keys have one card per taxon. These cards have perforated edges, and the perforations are numbered sequentially. Each numbered perforation correspond to one feature. In case, if a wood has particular feature, the edge of the card will be notched to point out the existence of that particular feature. In order to identify an unknown wood sample, a pointer is passed through a stack of cards at a perforation corresponding to a feature perceived in the wood. The card of species that possess feature for a given wood sample is dropped, or else the card of species stay on the needle. The sorting process is repeated until a single or only a few cards remain.

In these keys, only one feature is used at a time, and the observer has the flexibility to select the number of features and the sequence in which these features are used, which makes it useful for unknowns in which some features cannot be observed. Further, addition of new species to key is done by inserting a new entry to the computer database. Multiple entry keys are easily computerized, so this is no longer a limitation. The Princes Rodborough microscopic key to hardwoods is one of the most valuable multiple entry keys [20].

1.5.2 Drawbacks of Traditional Methods of Wood Identification

Recognition of large volumes of wood species, employing traditional approach is prolonged, erroneous and unfeasible sometimes. Further, imparting training to wood identification officers to get an expertise in identification of wood is a time-consuming process. Only few certified and trained officers are available for identification of wood, because occupation as a wood certification officer is neither easy nor lucrative and the possibility of unfairness and oversight cannot be denied. Sometimes, the experienced officer gets promoted and may not be able to pass his experience to his juniors. Examining several trucks of wood log is tedious task for an individual and, manual assessment of the wood sample can be very subjective. At present, timber is examined by naked eye or sometimes with the aid of a magnifier, by comparing and analysing the main features of wood i.e. texture. It is not easy even for seasoned expert to identify woods by using microscopic images as it requires plenty of study and rich knowledge of wood microstructure, using traditional method of identification. Further, there might be chances of intentional or unintentional human error/biasness in the identification of wood by the expert.

1.5.3 Machine Vision Based Wood Identification

To overcome the problems associated with the traditional methods of wood identification, machine vision technology was employed for wood identification. Machine vision technology of wood identification is analogous to human visual system. The most basic methodology is to use sensors to acquire wood image, pre-process, extract texture feature or segment the image, and

then compare the features or segmented image with the available database. If the same specie features/segmented image is available in the database, match will be found and the wood specie gets identified. The wood identification using machine vision technique works on the principle of obtaining certain statistical parameter of the wood species. Therefore, it is able to reduce the wood identification error, contrast to traditional method of wood identification, where identification is subjective to individual.

Machine vision based technology has existed in the forest product industry since the early 1980's. Several computer packages have been developed for wood identification and are being widely used [30, 70, 86, 216, 218, 247,255]. Most research has been made in the development of automatic visual inspection systems in the wood industry for the purpose of grading of hardwood lumber [39], trimming and edging based on the quality of the wood and the presence of defects. These machines used technologies and devices such as ultrasound, microwave, nuclear magnetic resonance, X-ray, laser ranging, cameras and spectrometers which are rather expensive [40, 44, 98, 195]**.** The machine vision techniques have given two-fold milling and sorting speeds and an increase of 10-20% in the productivity in wood industry has been reported.

Researchers are showing interest in machine vision based automatic identification of wood because of the accuracy of identification. Further, for a given sample of wood, the recognition accuracy will be same if the identification process is repeated 1000 times, whereas, if the same sample of wood is shown to hundreds of people having expertise in wood identification, it is not guaranteed that the sample will be identified as same wood specie because of human constraints.

The enormous computing power capacity of machines and several fold increase in the storage capacity has given rise to use of machine vision technology in the field of wood identification. The machine vision based systems outperform experienced officers when large volumes of wood species are to be identified repeatedly with utmost accuracy, without getting fatigued. Thus, machine vision based wood identification techniques have emerged as an alternative in overcoming deficiencies associated with traditional approaches.

1.6 APPLICATIONS OF WOOD

Some of the application of wood are as follows:

1. Wood has drawn attention of forensic experts, archaeologists, art historians and palaeontologists, and all living things on this earth for centuries. Art historians use evidence from wooden frames and panels to establish the authenticity and provenance of an art work [79, 217].
2. Forensic value, e.g. determining whether wooden fragments at the scene of a crime match those taken from the clothing or a vehicle belonging to a suspect.

3. Different tree species and wood anatomies characterize different climates [19]. Therefore, identification of ancient woods helps to reconstruct ancient ecosystems and documentation of climate change.
4. Palaeontologists are interested in knowing what trees were present when dinosaurs lived, and in what type of vegetation early primates and hominids evolved.
5. Geologically ancient woods provide information helpful for explaining present-day distributions of plants, the history of particular families and genera, and the past distribution and diversity of woody plants.
6. Woody remains provide significant information to the archaeologists useful for reconstructing trade routes.
7. The unique characteristics and comparatively huge quantity of wood have made it a natural material of choice in construction industry.
8. The wood is a useful raw material for furniture, railway sleepers, tools, shipping and process industry, saw mill, paper & pulp industry, etc.

1.7 LITERATURE REVIEW

The machine vision based forest/hardwood species identification techniques were introduced by several researchers. These techniques have shown ability in performing the task with reasonable accuracy based on the statistical information (texture features) extracted from the images of various wood species. The different techniques proposed for wood identification till present have considered the macroscopic, microscopic and stereogram images. From the literature review, it is observed that texture features obtained in combination with classifiers have produced reasonably better classification accuracy for forest/hardwood species. A brief review of these developed are presented below:

To begin with, Travis *et al.,* [203], in year 1996 have introduced use of image processing techniques for the quantitative measurements of anatomical features of individual cells, their number and size with the help of image skeltonization and distance transform. These measurements were then used to classify cells into 7 categories with discriminant analysis using cross-validation approach. Modasia *et al.,* [132] in year 2005 have made use of digital image processing (DIP) and artificial neural network (ANN) techniques, and they reported a classification accuracy of 75%, for microscopic images of wood. In the followed year 2006, Mu *et al.,* [134] have proposed a non-destructive method of detection and classification of rotten knot and hollow heartwood defects. The position and size of wood defects were considered as the extracted features, and ANN as a classifier. The proposed technique in this case had requirement of extensive computation time.

In the year 2008, Zhang *et al.,* [237] proposed a technique for recognition of wood defects. They have used discrete wavelet transform (DWT), non-negative matrix factorization (NMF) and

dual tree complex wavelet transform (DTCWT) to extract features of wood images. A verification rate above 90% was reported with support vector machine (SVM) classifier.

During the year 2007-2010, few researchers have used gray level co-occurrence matrix (GLCM) to extract number of texture features from wood images [200, 98, 22, 201, 208]. Subsequently, they have used different classifiers like multilayer perceptron back propagation artificial neural network (MLP-BP-ANN) [200], Pearson correlation [98], energy value [22], & SVM [201, 208] and achieved classification accuracy of 75% [200], 95% [98], high accuracy [22], 80% [201], & 91.70% [208], respectively. Tou *et al.*, in the year 2009 [202] have done comparison of GLCM, Gabor filters and fusion of Gabor filters & GLCM feature extraction techniques for classification of six wood species of CAIRO wood database. They have reported the best classification accuracy of 85% for covariance matrix of Gabor filtered images of wood species. In the year 2009, You and Cai [228] have employed the principal component analysis (PCA), 2DPCA, $(2D)^2$PCA and linear discriminant analysis (LDA) to extract texture features for the classification of wood species. The performance reported for LDA was a bit superior to PCA for cross-section images of wood, but inferior to 2DPCA and $(2D)^2$PCA.

Paula Filho *et al.*, in year 2009 [166] have presented a database of 11 different species of the Brazilian flora. The feature vector data comprises 18 features extracted from CIELUV, HSV and RGB color models, and 24 features produced by GLCM matrix. A recognition accuracy of 82% was reported using MLP classifier. Nasirzadeh *et al.*, in year 2010 [145] used local binary pattern (LBP) variants for texture feature extraction and nearest neighbourhood (NN) as a classifier. The local binary patterns histogram Fourier features (LBP-HF) have reported 96.60% accuracy compared to 91% recognition accuracy obtained by the traditional rotation invariant local binary pattern (LBP^{ri}) method. In the same year, Yusof *et al.*,[234] have used collective features obtained by Gabor filter and GLCM techniques from macroscopic images of wood and attained a recognition rate of 90.33% for test data using MLP-ANN classifier. In the same year, Harjoko and Gasim [75] have used four feature extraction methods (binary image without threshold, binary image with threshold, edge detection, and RGB image) for wood identification, and reported a classification accuracy of 88% using ANN-BP classifier. In the year 2010, Piuri and Scotti [171] also have proposed a system to use fluorescence spectra for wood type classification. The input spectra was partitioned into different uniformly spaced bands. The energy of each band was used as input, and a classification error of 1.1±0.2 % was reported by SVM classifier for A-type dataset.

In the year 2011, Khairuddin *et al.*, [97] have introduced basic gray level aura matrix (BGLAM) and statistical properties of pore distribution (SPPD) methods to extract texture features of wood images. Successively, before applying these features to the final classification stage, pre-classification task was carried out by K-means clustering followed by dimensionality reduction using LDA and kernel discriminant analysis (KDA)/generalized singular value

decomposition (GSVD). This scheme has resulted into a classification accuracy of 96.15% using K-NN as classifier. This work has been followed by Khalid *et al.*, [99, 100], who have employed BGLAM and SPPD to extract texture features, followed by a pre classification stage consisting of K-means clustering and KDA. Further, two classifiers, LDA and K nearest neighbourhood (KNN) have been used and an increase in the classification accuracy from 84% to 96.92% for LDA has been reported. Sun *et al.,* [196] in the same year, have presented a clustering and sifting operations to emphasize the key points of Gabor features. To measure the distance between two signatures earth movers distance (EMD) method was used, and best classification accuracy of 97.50% was reported with NN classifier.

Followed by the above work, Harjoko *et al.*, [76] have extracted R, G, B, entropy, contrast, energy, correlation, homogeneity, gray level and standard deviation (SD) features of 15 commercial woods. A recognition accuracy of 95% was recorded for testing dataset using ANN classifier. Also, Mallik *et al.*, [122] have presented a scheme to classify wood species (scanning electron microscopy micrographs). The images are first enhanced and then segmented. Subsequently, five features namely rectangularity, circularity, average area, number of tracheid's and distance between tracheid's are extracted from segmented images. Amongst seven different classifiers used for classification KNN, SVM and neural networks have reported better classification accuracy.

Wang *et al.*, [211] in year 2012 have extracted statistical features namely, mean, standard deviation (SD), entropy and contrast from stereogram images of wood using a Gabor filter bank. Among different combinations, fusion of entropy, mean and SD features classified with NN classifier achieved a classification accuracy of 94.58%. In the same year, Martins *et al.*, [126] have used local phase quantization (LPQ) and variants of LBP as textural descriptors and SVM as classifier. The classification accuracy reported by LPQ and LBP descriptors individually was 79.82% and 76.16%, respectively. Further, the combination of LPQ and $LBP^{ri}_{8,2}$ descriptors feature vector data has produced the best result of 86.47%. Later, Pan and Kudo [160, 158] proposed two direction insensitive feature sets (nearest-pore pair and diameter-changes of pore elements) for feature extraction and C4.5, SVM and Naive Bayes as classifier. Naive Bayes classifier has given the best classification accuracy of 83.70% using diameter-changes feature. The only difficulty encountered was into discrimination between semi-ring porosity and other two kinds of porosity. Following above work, Ma and Wang [118] have employed higher-order local autocorrelation (HLAC) method to extract texture features from several blocks of wood images. A classification accuracy of 79% has been reported with SVM classifier. The classification accuracy obtained for blocked HLAC texture features was improved by about 21% compared to the original HLAC features.

In the year 2103, Yusof *et al.*, [233] proposed a kernel genetic algorithm for selection of nonlinear features of macroscopic images of tropical wood species obtained by GLCM, BGLAM and SPPD techniques. This approach has not only brought in dimensionality reduction, also achieved better classification accuracy of 98.69% with LDA classifier. Subsequently, a pre-classifier approach that uses fuzzy-logic concept was used by Yusof *et al.*, [232] to cluster the database. The experimental outcome has reported classification accuracy of 93% compared to 88.90% accuracy achieved without employing fuzzy-logic pre-classifier. In the same year, Ahmad and Yusof [2], employed ant clustering algorithm (ACA) to train and test the feature dataset obtained by BGLAM and SPPD techniques. They have reported a classification accuracy of 96.75% for the experimental work performed using 24 clusters. Wang *et al.,* [213] in the same year, employed a mask matching image (MMI) feature extraction technique to obtain features of wood stereogram images. Further, KNN and SVM classifiers were examined and a classification accuracy of 86.53% was achieved for statistical features of MMI with SVM classifier. Similar type of work followed later.

Martins *et al.*, [125] have presented a database of microscopic images of 112 forest species (37 softwood and 75 hardwood). In addition, they obtained structural, GLCM and LBP features of these species, and a classification accuracy of 98.60% and 86% was reported for two-class and multi-class (112) classification using SVM classifier. Afterwards, Cavalin *et al*., [31] extracted GLCM, LBP, and LPQ features from the images obtained by quad-tree decomposition method. The combination of GLCM and LPQ features have achieved a recognition accuracy of 93.20% with SVM classifier. A binary particle swarm optimization technique was proposed by Hasan *et al*., [78] to optimize the parameters and feature selection process of GLCM and KNN method to enhance the classification accuracy. Zhao [240], proposed a system to acquire RGB image of wood species. The image is then converted to grayscale image and the histogram of the grayscale image was used as feature for wood species recognition. A snake model is first applied to the histogram of the standard specimen of the image, which is then applied to the test specimen. The initial and final snakes are then compared with the histogram of the test image. This scheme certainly discriminates the interspecific and intraspecific color variations.

In the year 2013 itself, Wang *et al*., [212] presented an automatic recognition method for stereogram images of 24 wood species based on Gabor method. The grayscale images are convolved with 40 Gabor patterns and from these images mean and SD features were extracted using sub block partitioning approach. The use of sub block features extraction has given better results than several contemporary methods. Later, Gasim *et al*., [57] have proposed a wood identification system that extracts features of wood image by subdividing them into sub blocks. The entropy, SD and correlation (GLCM) features were then extracted from grayscale and edge detected images. A classification accuracy of 95% was achieved with ANN classifier. Later,

Gasim *et al*., [56, 77] have combined six and seven features extracted from edge detection and RGB images, respectively. They have achieved 100% accuracy for training data (2000 images) and 95% accuracy for testing data (500 images).

Similarly, in same year Ahmad and Yusof [3] have obtained 157 features from the wood images using BGLAM (136 features) and SPPD (21 features) methods. Further, to improve the classification accuracy they employed Kohonen self organizing map (KSOM) to cluster and classify the tropical wood species data. In addition, Yusof *et al*., [231] have proposed another tropical wood species recognition system using pore count based fuzzy data management. The test data is first categorized into four groups based on their pore size. Later, each group data was separately classified using multilayer feed forward neural network (MLP-FF-NN).

Followed after the above work, Kapp *et al*., [94] in the year 2014, have investigated the effectiveness of multiple feature sets (LBP and LPQ) for forest species (macroscopic and microscopic) recognition. The analysis of the results revealed that for microscopic images the classification accuracy of 74.58% was obtained using single feature vector. Further, an improved classification accuracy of about 95.68% has been achieved by multiple feature set approach with Gaussian kernel SVM classifier.

Later, Paula Filho *et al*., [167] proposed a two level divide-and-conquer classification strategy to categorize the macroscopic images of 41 species with the help of SVM classifier. Feature set obtained by a combination of several feature extraction techniques were classified with 6 number of classifiers and reported best recognition accuracy of 97.77%. Taman *et al*., [197] have extracted features of wood knot images (CAIRO UTM database) using GLCM, and used binary gravitational search algorithm (BGSA) for feature selection. The proposed approach has reported good accuracy with KNN classifier. Since for automated wood classification, the classifier requires most of the resources and is computationally expensive. Thus, to accelerate the classifiers performance the hardware implementation of classifier is needed. Therefore, Kusuma *et al*., [107] in 2014 itself have proposed a floating-point to fixed-point conversion for hardware implementation of LDA classifier. This approach has witnessed lowest hardware cost compared to sequential search and Matlab fixed-point toolbox. Subsequently, the 32 bit fixed-point implementation of LDA has achieved a classification accuracy of 94.82% compared to 95% accomplished with original implementation for recognition of tropical wood species [106]. Later, Hafemann *et al*., [72] have introduced a deep learning approach known as convolutional neural networks (CNN), for classification of macroscopic and microscopic image of wood species. A classification accuracy of 95.77±0.27% and 97.32±0.21% were attained for macroscopic and microscopic images, respectively. For microscopic images the proposed method has attained higher classification accuracy, whereas in case of macroscopic images comparatively lower classification accuracy has been reported compared to the cotemporary techniques.

Followed by the above work of 2014, Zhao *et al*., [241] in same year have proposed a feature level fusion approach for wood species identification. They have designed a system to acquire the wood images. Subsequently, color, GLCM and spectral features were extracted. The fusion of these features classified with fuzzy BP neural network has resulted into a classification accuracy 95% for 5 wood species better than the accuracy obtained for combination of color and GLCM texture features. Further, Zhao *et al*., [242] have converted color wood surface image a V1V2I color-base image and obtained corresponding grey histograms for V1 and V2. The ASM was then employed to accomplish the curve deformation of standard specimen's histogram curve, and then the same ASM was applied on the histogram curve of the test specimen. Comparison of the initial and final ASM with the histogram curve of the test specimen was performed to recognize the wood. The proposed approach has reported a mean recognition accuracy of 90% for 5 different wood species.

In the year 2015, Martins *et al*., [124] have used 10 descriptors to extract features of forest species images. Further, they have used dynamic classifier selection and dissimilarity feature vector representation for wood species recognition. By incorporating probabilistic information in dynamic selection of classifier (DSC) technique based on multiple classifier behaviour, a recognition accuracy of 93.03% was reported.

Further, for wood anatomist the anatomical parameters of wood species are of special interest as they are helpful in characterisation of wood. Therefore, the machine vision based methods have been developed for segmentation and extraction of wood elements. In the work reported by QI *et al*., [178] in year 2008, they proposed a method to identify hardwood species using only pore features obtained from cross-sectional images. The mathematical morphology was employed for automatic classification of the hardwood species into ring, semi-ring and diffuse porous wood based on the pore features (distribution of pores is described by calculation of their mean square error (MSE) extracted from hardwood species. Later, in the year 2009, Wang *et al*., [209, 210], have proposed an adaptive method (genetic algorithm) to obtain optimal threshold of closed region area for pore segmentation. Experimental outcome on images of hardwood species reveals that the threshold obtained by the genetic algorithm is much more efficient than the ordinary enumeration algorithm. Besides, majority of the pores were extracted barring some very small ones with the help of threshold obtained from proposed technique.

In addition, Yu *et al*., [229] in the year 2009, have used computers to measure cellular tissue proportions of broad leaved (vessel, fibre and xylem ray) and coniferous (resin canal tracheid and ray) tree. The results obtained were compared with conventional methods (weighing and grid counting) and found to be accurate, efficient and time saving. Kennel *et al*., [95] in year 2010, proposed an automatic method of cell files recognition in light microscopic images of conifer wood. The method comprises watershed segmentation to extract anatomical structures of the image, followed by identification of cells using classification and regression tree

(CART) method, and then recognition of cell files. The results obtained on 10 different tree species were encouraging, and are yet to be adapted for hardwood species. Lei and Yan [109], in the same year observed that the physical properties of wood mainly depends on the characteristics of basic units of wood called cells. In the following year, Pan and Kudo [159], have used the radius of structuring element decided by the mathematical morphology with a variable structuring element, which has resulted into decent quality segmentation for 25 out of 30 wood samples, whereas 5 samples were found to have conflicting radii. The only drawback noticeable was time required to execute the segmentation was considerably on the higher side.

Scholz *et al*., [182], in the year 2013 have carried out an investigation on various methods useful for wood conduits quantification. Several hardware and image analysis tools useful in the quantification of wood have been reported for better understanding of wood anatomy. Later, Guang-Sheng and Peng, [63] have proposed a robust method of wood cell identification. The images were segmented by dual threshold method, of which the edge contours of the multiple cells are obtained by geodesic active contour (GAC). Subsequently, PCA was employed to get improved accuracy for wood cell recognition.

1.8 RESEARCH OBJECTIVES OF THE PRESENT STUDY

The microscopic images of wood provide sufficient information for accurate classification of variety of woods in contrast to macroscopic images that reveal only limited amount of information [160]. Taking into account the work reported by various researchers in the available literature on classification of wood images, it is understood that the recognition accuracy, can be improved by employing a suitable texture feature descriptor for acquiring significant texture information of an image. Softwood trees (Gymnosperms) have a simple cellular structure, and because of a limited number of cell types, it turns out to be difficult task to discriminate softwood species from one another [19]. Unlike their counterparts, hardwood species have a complex cellular structure and are easy to distinguish amongst the similar species. Vessels, fibers, parenchymas and rays are the four major elements useful in the identification of hardwood species. Vessels, also known as pores (in cross-section view) are the missing elements in softwood species. In the above perspective, in the present work, several multiresolution based texture feature extraction techniques for microscopic images of hardwood species have been proposed. The research objectives for hardwood species classification using their microscopic images are as follows

1. The key objective of this proposal is to develop an "Automatic wood identification system using digital image processing tools" based on the microscopic images of wood. The hardwood species classification task has been divided into three key stages namely feature extraction, feature selection/dimensionality reduction and classification.
2. Feature extraction: The effectiveness and efficiency of wood species identification primarily depend on the quality of the texture features extracted from the microscopic images of

hardwood species. Therefore, the emphasis in this work has been to propose efficient feature extraction techniques for classification of hardwood species which are listed below.

- A survey on the performance of the state-of-the-art texture feature extraction techniques for grayscale images,
- Binary wavelet transform (BWT) based texture feature extraction techniques for grayscale images,
- Gaussian image pyramid (GP) based texture feature extraction techniques for grayscale images,
- Discrete wavelet transform (DWT) based texture feature extraction techniques for grayscale images, and
- Discrete wavelet transform (DWT) based hybrid texture feature extraction techniques for grayscale and color images.

3. Feature selection: The proposed texture feature extraction techniques produce large complex features, and among them several features may not be significant for discrimination of the hardwood species. Thus, in order to reduce the feature vector data and improve the hardwood species classification accuracy a feature selection technique, minimal redundancy maximal relevance (mRMR) and feature dimensionality reduction technique, principal component analysis (PCA) have been investigated.
4. Classification: The selection of classifier further enhances the efficiency of the classification system. Therefore, linear SVM, radial basis function (RBF) kernel SVM, random forest (RF) and LDA classifier have been investigated to get the optimum classification accuracy from the wood identification system.
5. Segmentation and determination of vessel elements: The vessel elements are one of the most important features that is used for identification of hardwood species. Further, the number and size of vessels provide information about the hydraulic conductivity of the wood. Thus, this part of the proposed work deals with the measurement of the vessel elements and their hydraulic conductivity.

1.9 ORGANIZATION OF THE THESIS

The thesis contains eight chapters, out of that, the first chapter deals with the introduction, literature review and research objectives of the present study. The remaining part of the thesis is structured as follows:

Chapter 2 presents brief theoretical background of the state-of-the-art texture feature extraction techniques, feature vector data normalisation, feature selection, feature dimensionality reduction and the four classifiers used in the wood identification task. Further, the effectiveness of the state-of-the-art texture feature extraction techniques for the classification of hardwood species is also evaluated.

Chapter 3, detailed description of one dimensional (1D) and two dimensional (2D) binary wavelet transform (BWT) is presented. The BWT based texture feature extraction technique for extraction of significant feature vector data from grayscale images of hardwood species is discussed which is followed by the investigation of the effectiveness of the said technique for the classification of hardwood species.

A concise description of the Gaussian image pyramid (GP) approach for image decomposition is presented in *Chapter 4*. The GP based texture feature extraction techniques are presented to get the significant features of grayscale images of hardwood species. Finally, the efficiency of these techniques for the classification of hardwood species is presented.

Chapter 5 presents detailed description of the DWT based texture feature extraction techniques to extract the feature vector data of grayscale images of hardwood species. The effectiveness of these techniques are also examined for the classification of hardwood species images.

Chapter 6 presents description of the DWT based hybrid texture feature extraction techniques for grayscale and color images of hardwood species. The effectiveness of these techniques are then investigated for the classification of hardwood species.

Chapter 7 presents an approach for segmentation and determination of vessel elements followed by computation of their hydraulic conductivity and lumen resistivity.

The conclusions drawn from the exhaustive experimentation work carried out in the present research work are presented in *Chapter 8*. The chapter also presents the limitations of the present work emphasizing the scope for future research in this field.

CHAPTER 2. STATE-OF-THE-ART TEXTURE FEATURE EXTRACTION TECHNIQUES

This chapter investigates the state-of-the-art texture features in the classification of hardwood species. The chapter starts with concise description of the feature extraction techniques followed by the performance evaluation of these techniques by different classifiers.

2.1 STATE-OF-THE-ART TEXTURE FEATURE EXTRACTION TECHNIQUES

Texture features [18, 81, 85, 90, 101, 114, 164, 181, 227, 235] play very important role in the classification of image database. Here in this work some widely used texture feature descriptors [17, 18] are employed and their effectiveness for the classification of hardwood species database into 75 classes has been studied. The techniques are listed below.

1 First-order statistics
2 Gray level co-occurrence matrices
3 Gray level run length matrices
4 Gabor filter
5 Local binary pattern
6 Uniform local binary pattern
7 Rotation invariant local binary pattern
8 Rotation invariant uniform local binary pattern
9 Local binary pattern histogram Fourier features
10 Adaptive local binary pattern
11 Co-occurrence among adjacent local binary pattern
12 Center-symmetric local binary pattern
13 Completed local binary pattern
14 Dense completed local binary pattern
15 Local directional pattern
16 Local ternary pattern
17 Local ternary co-occurrence pattern
18 Local configuration pattern
19 Local phase quantization
20 Gradient local auto-correlation
21 Binary Gabor pattern

The brief description of each of the techniques is presented in the following sub-sections:

2.1.1 First-order Statistics (FOS)

The FOS is one of the simplest and computationally efficient technique for describing texture by using the intensity histogram of an image [103]. In FOS, the main features that are taken into consideration are mean(m), SD(σ), skewness (μ_3) and kurtosis (μ_4). For a grayscale image, mean is a measure of the average intensity of pixels, while SD is a measure of contrast. Skewness is a measure of symmetry (it deals with the degree of histogram asymmetry around the mean) and kurtosis is the descriptor of the shape of probability distribution. The formula for each of the FOS feature descriptor is given by Eqs. (2.1 - 2.5) [60]:

$$m = \sum_{i=0}^{L-1} z_i p(z_i) \tag{2.1}$$

$$\sigma^2 = \sum_{i=0}^{L-1} (z_i - m)^2 \, p(z_i) \tag{2.2}$$

$$\sigma = \sqrt{\sigma^2} \tag{2.3}$$

$$\mu_3 = \sum_{i=0}^{L-1} (z_i - m)^3 \, p(z_i) \tag{2.4}$$

$$\mu_4 = \sum_{i=0}^{L-1} (z_i - m)^4 \, p(z_i) \tag{2.5}$$

where, z stands for image intensity and $p(z_i)$ signifies corresponding histogram.

2.1.2 Gray Level Co-occurrence Matrix (GLCM)

Haralick *et al.*, [74] have introduced GLCM (also known as gray tone spatial dependence matrix: GTSDM) which has been extensively used to extract texture features of grayscale images. In this method, a statistical descriptor, co-occurrence matrix is generated, that is measure of how often different combination of pixel gray values with specified distance and orientations occur in an image. The GLCM [46] based features have advantage over the texture information computed using only histogram, as they don't carry any information about the relative position of the pixels with respect to each other.

Consider, $f\{f(x,y), 0 \le x \le M-1, 0 \le y \le N-1\}$, a $M \times N$ size image with L gray (intensity) levels. The GLCM matrix G is a square matrix of order L. Each $(i, j)^{th}$ entry in G represents the number of times a pixel with gray level i is adjacent to a pixel with gray level j. Different spatial distance and 4 directions (i.e., 0°, 45°, 90° and 135°) are used to generate GLCM matrices. Thereafter, second order statistical texture features are computed from the GLCM matrices. The 18 features of GLCM investigated here consist of 13 features proposed by Haralick *et al.* [74] and 5 features proposed by Soh and Tsatsoulis [191], which are listed in Table 2.1. The detailed mathematical description of these features is available in [74,136, 191].

Table 2.1 Second-order statistical texture features calculated from GLCM matrix.

Sr. No.	Features	Sr. No.	Features
1	Angular second moment (f1)	10	Difference variance (f10)
2	Contrast (f2)	11	Difference entropy (f11)
3	Correlation (f3)	12	Information measure of correlation1 (f12)
4	Sum of squares (variance) (f4)	13	Information measure of correlation2 (f13)
5	Inverse difference moment (f5)	14	Autocorrelation
6	Sum average (f6)	15	Dissimilarity
7	Sum variance (f7)	16	Cluster shade
8	Sum entropy (f8)	17	Cluster prominence
9	Entropy (f9)	18	Maximum probability

2.1.3 Gray Level Run Length Matrix (GLRLM)

Galloway [55] proposed a higher-order statistical texture feature measure technique known as Gray level run length matrices. The GLRLM generates a 2D matrices having elements L×R, where L stands for number of gray level; R is the longest run. Each element of GLRLM matrices has information about number of times the original image has run of length *j* of gray level intensity *i*, in the given direction. The higher-order statistical texture features computed from GLRLM matrices are listed in Table 2.2.

Table 2.2 GLRLM statistical texture features

Authors	Sr. No.	Features
Galloway [55]	1	Short runs emphasis (SRE)
	2	Long runs emphasis (LRE)
	3	Gray level non-uniformity (GLN)
	4	Run length non-uniformity (RLN)
	5	Run percentage (RP)
Chu *et al.*, [35]	6	Low gray level runs emphasis (LGRE)
	7	High gray level runs emphasis(HGRE)
Albregtsen [6]	8	Short run low gray-level emphasis (SRLGE)
	9	Short run high gray-level emphasis (SRHGE)
	10	Long run low gray-level emphasis (LRLGE)
	11	Long run high gray-level emphasis (LRLGE)

2.1.4 Gabor Filter

The Gabor wavelets (Gabor filters) with various orientations and frequencies, effectively mimic the human visual system [46]. It has been widely used for pattern analysis, texture feature extraction and classification due to their illumination, rotation, scale, and translation invariance properties [46, 62, 73, 104, 105, 179]. The Gabor filter expression in the spatial domain is given by [46]:

$$G(x,y;\lambda,\theta,\psi,\sigma,\gamma) = \exp\left(\frac{x'^2+\gamma^2 y'^2}{2\sigma^2}\right)\cos\left(2\pi\frac{x'}{\lambda}+\psi\right) \tag{2.6}$$

$$x' = x\cos(\theta)+y\sin(\theta) \tag{2.7}$$

$$y' = y\cos(\theta)-x\sin(\theta) \tag{2.8}$$

where, λ: Wavelength of the cosine factor, ψ : Phase offset,

γ: Spatial aspect ratio, σ : Sigma of the Gaussian envelope, and

θ: Orientation of the normal to parallel stripes of Gabor function.

Each of the texture image is convolved with 40 Gabor filters (5 scales and and 8 orientations; 45°, 90°, 135°, 180°, 225°, 270°, 315° and 360°) as shown in Fig. 2.1. Subsequently mean, standard deviation and entropy features are calculated from these images.

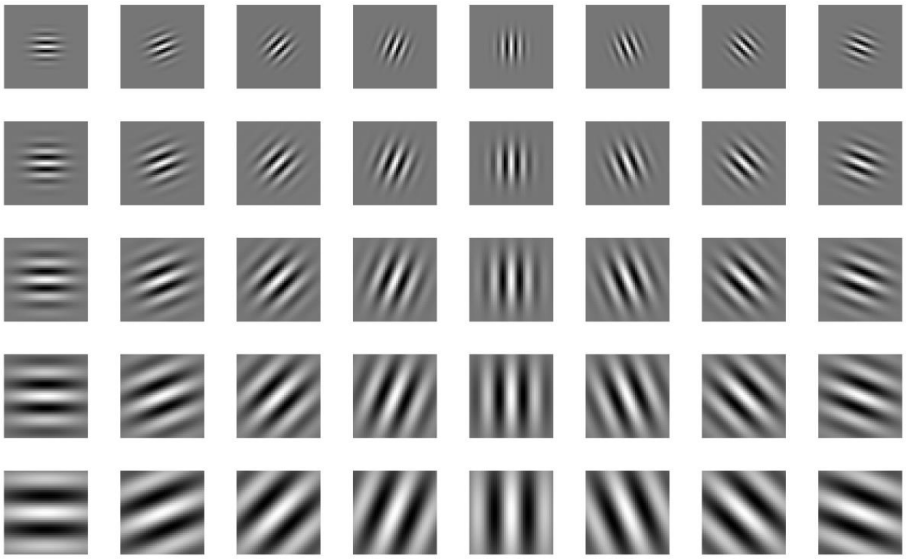

Fig. 2.1 Gabor filters (5 scales and and 8 orientations).

2.1.5 Local Binary Pattern (LBP)

Ever since LBP's introduction by Ojala *et al.*, 1994 [150, 151], it has been used as a dominant texture descriptor technique for image analysis due to its discriminative information representation capacity. Some of the areas where LBP has shown its potentials are face recognition, object identification, demographic classification, etc. This technique is considered to be an easy, yet computationally efficient [141, 142, 143, 151]. A circular neighbourhood of variable size was proposed in [152] to overcome the inadequacy of original LBP operator of 3×3 neighbourhood size that cannot capture the dominant texture features in large-scale structures.

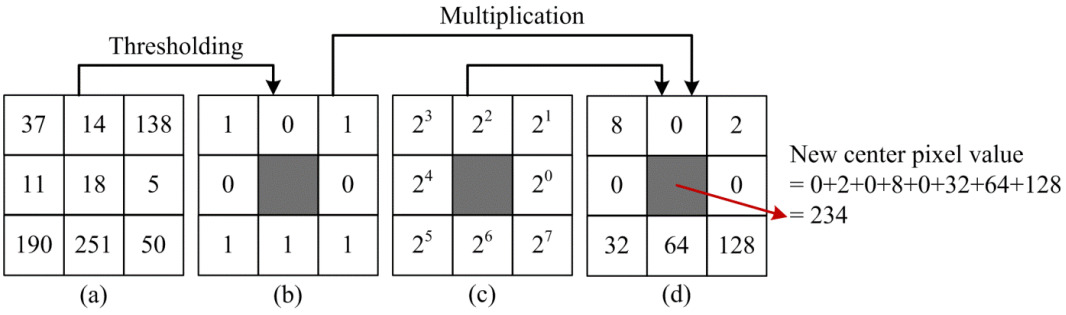

Fig. 2.2 The LBP computation process a) 3×3 local window image, (b) thresholding, (c) weight and d) new center pixel value (decimal).

The LBP label for a centre pixel coordinate (x,y) of an image is given by [152]:

$$LBP_{P,R}(x,y)=\sum_{p=0}^{P-1}s(g_p-g_c))2^p \tag{2.9}$$

where, the gray value of the pixel of interest (central pixel) and p neighbours of the centre pixel is represented by g_c and g_p, respectively. Also, $s(z)=\begin{Bmatrix}0, & z<0\\ 1, & z\geq0\end{Bmatrix}$ symbolizes thresholding function. In $LBP_{P,R}$ operator, *P* stands for number of sampling points on circular

neighbourhood, whereas *R* is the spatial resolution of the neighbourhood. Bilinear interpolation is applied to pixel values if the sampling points are not part of integer coordinates. The LBP operator produces 256-dimensional texture descriptor for a given image. The pictorial representation of calculation of new centre pixel value for LBP is shown in Fig. 2.2.

2.1.6 Uniform Local Binary Pattern (LBP^{u2})

The LBP patterns are said to be uniform patterns, if at most 2 bit wise transition (1 to 0 or 0 to 1) is reported in the circular binary pattern of LBP [152]. The LBP^{u2} histogram comprises separate bin for uniform patterns and only single bin is assigned to all the non-uniform patterns. For a given pattern of P bits, $P(P-1)+3$ output bins are produced. The reduction in non-uniform patterns is due to the fact that in natural images the LBP patterns are mostly uniform. Further, uniform patterns of texture images account for about 90% of the entire pattern with (8, 1) neighbourhood and close to 70% for (16, 2) neighbourhood [169]. The LBP^{u2} produces 59-dimensional texture descriptors.

2.1.7 Rotation Invariant Local Binary Pattern (LBP^{ri})

The rotation of an image results into diverse LBP codes. To address the issue of the image rotation effect, LBP^{ri} has been proposed in [152, 119, 170]. Thus, to make all the versions of binary codes the same, the LBP codes are rotated back to reference pixel position to nullify the consequence of translation of a pixel location. The $\text{LBP}^{ri}_{P,\,R}$ is generated by circularly rotating the basic LBP code and considering the pattern which has a minimum value as given by [152, 119, 170]:

$$\text{LBP}^{ri}_{P,R} = \min_i \left\{ ROR\left(LBP_{P,R}, i\right) \right\} \tag{2.10}$$

where, $i = 0, 1, 2, \ldots, P-1$. The circular bit-by-bit right shift operation is performed on x (a P-bit number) for i times by the function $ROR(x, i)$. The $\text{LBP}^{ri}_{P,\,R}$ descriptor produces overall 36-bin histograms for each image due to 36 diverse, 8 bit rotation invariant codes [119, 170].

2.1.8 Rotation Invariant Uniform Local Binary Pattern (LBP^{riu2})

To overcome the disadvantages associated with $\text{LBP}^{ri}_{P,\,R}$ (poor performance because of crude quantization of angular space at 45°) $\text{LBP}^{riu2}_{P,R}$ was proposed [119]. If a pattern has uniformity value $U \leq 2$, it is known as "uniform" pattern defined as follows [119]:

$$U(x) = \sum_{p=0}^{P-1} F_b\left(x \oplus ROR(x,1), p\right) \tag{2.11}$$

where, *b* stands for binary numbers. Given a binary number *x*, the circularly consecutive binary bits *b* are obtained by [119]:

$$F_b(x,i) = ROR(x,i) \cdot \left(2^b - 1\right) \tag{2.12}$$

The bitwise logical operators "XOR" and "AND" are denoted by '$\oplus$' and '$\cdot$' (dot) operator, respectively and for a given bit sequence, *i* signifies the index of least significant bit (LSB). The rotation of uniform codes towards their minimum value generates $(P+1)$ patterns. Merely counting the number of one's in the "uniform" patterns, binary number generates $\text{LBP}_{P,R}^{riu2}$ pattern code. The other patterns are marked "miscellaneous" and grouped into a single value as given by [111]:

$$\text{LBP}_{P,R}^{riu2} = \begin{cases} \sum_{p=0}^{P-1} s\left(g_p - g_c\right), U\left(G_P\right) \le 2 \\ P+1 \qquad\qquad ,otherwise \end{cases} \tag{2.13}$$

The $\text{LBP}_{P,R}^{riu2}$ produces 10-bin histograms.

2.1.9 Local Binary Pattern Histogram Fourier Features (LBP-HF)

A rotation invariant LBP-HF that retains the most discriminative characteristics, is obtained by taking the discrete Fourier transform (DFT) of $\text{LBP}_{P,R}^{u2}$ [4, 238]. The LBP-HF is constructed globally for the entire image compared to other histogram based invariant texture descriptor methods which have normalization of rotation in the local region. The LBP-HF's are invariant to cyclic shifts along the rows of input histogram, and are said to be invariant to the rotary motion of an input image $f(x, y)$ [4]. The DFT is used to construct the features as given by [4, 238]:

$$H(n,u) = \sum_{r=0}^{P-1} h_l\left(U_P(n,r)\right) e^{-i2\pi ur/P} \tag{2.14}$$

where, $H(n,u)$ corresponds to the DFT of the nth row of LBP^{u2} histogram $h_l\left(U_P(n,r)\right)$. It produces 38-bin histograms for a given texture image.

2.1.10 Adaptive Local Binary Pattern (ALBP)

The LBP descriptor doesn't provide information about orientation. To compensate the local spatial structure changes, Guo *et al*., 2010 [68] have proposed an adaptive local binary pattern that enhances images classification efficiency by minimizing the variations of the oriented mean and standard deviation of absolute local difference $|g_c - g_p|$. A weight parameter (w_p) given in Eq. (2.15) is introduced to minimize the overall directional differences $|g_c - w_p * g_p|$ along diverse orientations. The objective function for ALBP is expressed by [68]:

$$w_p = \arg\min_{w} \left\{ \sum_{i=1}^{N} \sum_{j=1}^{M} \left| g_c(i,j) - w.g_p(i,j) \right|^2 \right\} \tag{2.15}$$

where, *N* and *M* are the number of rows and columns of the image, respectively. For each of the orientations $2\pi p / P$ of entire image, a weight factor w_p is approximated. The expression for ALBP is then given by Eq. (2.16)

$$ALBP_{P,R} = \sum_{p=0}^{P-1} s\left(g_p * w_p - g_c\right) 2^p,\ s(x) = \begin{cases} 1, x \geq 0 \\ 0, x < 0 \end{cases} \tag{2.16}$$

2.1.11 Co-occurrence of Adjacent Local Binary Pattern (CoALBP)

Nosaka *et al.* [149] have proposed co-occurrence of adjacent local binary patterns to improve the performance of conventional LBP. The LBP does not consider the spatial relations among multiple LBPs, while in CoALBP the co-occurrence is measured among multiple LBPs and yet it retains the characteristics and robustness against deviation in illumination of LBP. The co-occurrence of the entire permutation (combination) of LBPs is obtained with the help of autocorrelation matrices (computed from two measured LBPs). In this method to reduce the computational cost of calculating the centre pixel value two sparser configurations are taken into consideration. The LBP (+) configuration takes into account two horizontal and two vertical pixels; whereas LBP (×) configuration considers the four diagonal pixels as given by [149]:

$$LBP(+):\ Nn = 4,\ s_i \in \left\{ (\pm \Delta s, 0)^T, (0, \pm \Delta s)^T \right\} \tag{2.17}$$

$$LBP(\times):\ Nn = 4,\ s_i \in \left\{ (\pm \Delta s, \pm \Delta s)^T, (\pm \Delta s, \mp \Delta s)^T \right\} \tag{2.18}$$

Subsequently, the co-occurrence of LBPs is effectively computed by converting each LBP to vector $(f \in R^{Np})$ given by [149]:

$$f_i(r) = \delta_{i,I(b(r))} \tag{2.19}$$

where, N_P stands for number of possible LBPs, $\delta_{i,j}$ is Kronecher's delta and $i, I\left(b(r)\right)$ is the label of $b(r)$. The co-occurrence of LBP is computed by talking into account $N_P \times N_P$ auto-correlation matrix given by [140]:

$$H(a) = \sum_{r \in I} f(r) f(r + a)^T \tag{2.20}$$

where, *a* is the displacement vector from the reference LBP to its neighbour LBP. Finally, these matrices are vectorised and combined to form a $4N_P^2$ dimensional feature vector data.

2.1.12 Center-Symmetric Local Binary Pattern (CSLBP)

Heikkila *et al.*, [80] proposed CSLBP descriptor to reduce long histogram produced by LBP descriptor. The new center pixel value in CSLBP (encompassing the advantageous characteristics of texture and gradient based features [243]) is produced by comparing center

symmetric pixels, contrary to comparing each of the neighborhood pixels with center pixels in LBP. The schematic representation for CSLBP descriptor is given in Fig. 2.3.

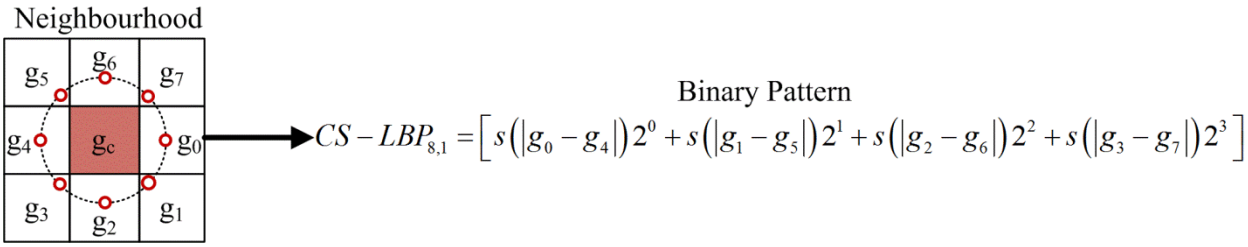

Fig. 2.3 CS-LBP features (considering neighbourhood size of 8 pixels).

For 8 neighbors total 2^4 (16) binary patterns are produced by CSLBP whereas LBP produces 2^8 (256) binary patterns. Mathematically, CSLBP is expressed as [80]:

$$\text{CS-LBP}_{P,R,Th}(x,y)=\sum_{p=0}^{\frac{P}{2}-1}s\left(g_p-g_{p+\frac{N}{2}}\right)2^p,\ s(m)=\begin{cases}1, & m>Th\\ 0, & otherwise\end{cases} \tag{2.21}$$

In the above Eq. (2.21), g_p and $g_{p+\frac{N}{2}}$ denote the gray values of center-symmetric pairs of P evenly spaced pixels on a circle of radius R. For flat image regions, the robustness of CS-LBP descriptor is enhanced by selecting small value of threshold (Th).

2.1.13 Completed Local Binary Pattern (CLBP)

Guo *et al.* [67] have proposed completed local binary pattern (CLBP) to enhance the significant texture feature extraction capability of LBP. Fig. 2.4 (a) shows 3×3 block of an image having center pixel value 34. The local difference, sign component and magnitude components are illustrated in Fig. 2.4 (b), (c) and (d) respectively.

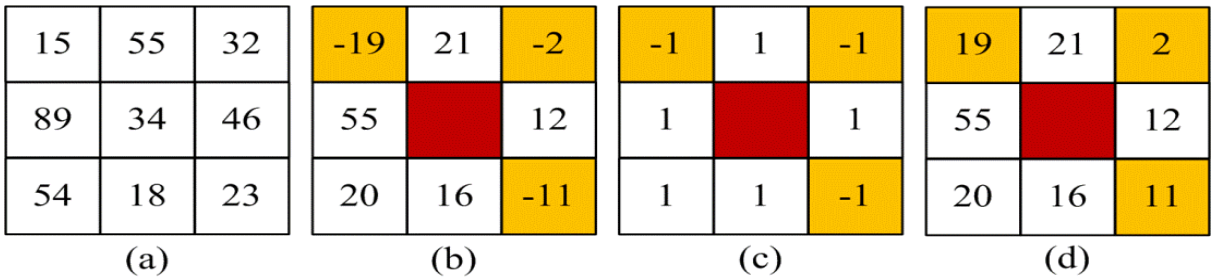

Fig. 2.4 (a) 3×3 block of image, (b) local difference (g_p-g_c) (c) sign component, and (d) magnitude component.

The structure of CLBP is depicted in Fig. 2.5. In CLBP, two components namely local difference and centre gray level are obtained from the grayscale image. The sign (S) and magnitude (M) components of local difference is produced by employing local difference sign-magnitude transform (LDSMT) as given by [67]:

$$d_p = g_p - g_c = s_p * m_p,\ and \begin{cases} s_p = sign\left(d_p\right) \\ m_p = \left|d_p\right| \end{cases} \tag{2.22}$$

where, m_p and $s_p = \begin{cases} 1, d_p \geq 0 \\ -1, d_p < 0 \end{cases}$ are magnitude and sign of d_p, respectively. The CLBP_Sign (*CLBP_S*) and CLBP_Magnitude (*CLBP_M*) operator characterizes the complementary components of image's local structure. Also, the CLBP_Center (*CLBP_C*) operator is produced by converting centre pixel into binary code employing global thresholding [238]. The CLBP is better texture feature descriptor than LBP [66]. Here, *CLBP_S*, and *CLBP_M* operator are concatenated to shape the CLBP histogram.

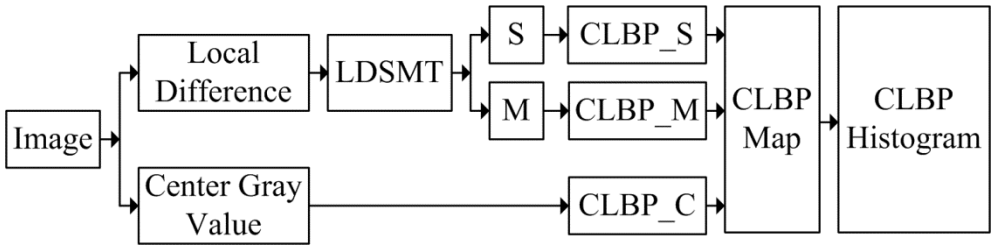

Fig. 2.5 Structure of CLBP

2.1.14 Dense Completed Local Binary Pattern (DenseCLBP)

Ylioinas *et al.*, [225] have introduced dense sampling based LBP in order to improve the performance of conventional LBP technique (making it robust against the noise). The drawbacks associated with LBPs are overcome by incorporating the dense sampling encoding approach for calculating additional discriminative and stable LBP texture descriptors. In this method, small steps are taken into consideration for shifting the operator over the image, as opposed to shifting the operator along each center pixel position. Further, bilinear interpolation is used to calculate the samples that do not fall at the center pixel location. Each new pixel turn out to be permutation of its weighted neighbourhood compared to a single pixel as in the original image. Therefore, the new pixel has additional low frequency information (by and large gives basic structure of the original image). Further, the noise present in the high frequency content of the image gets covered up due to averaging of neighbourhood. The dense sampling concept is further applied to the CLBP technique for producing dense completed local binary pattern (DenseCLBP) descriptors.

2.1.15 Local Directional Pattern (LDP)

Jabid *et al*., [87] have proposed LDP for face recognition application. In LDP, for each pixel position the edge response value is calculated in 8 directions using Kirsch mask in a local 3×3 neighborhood region. The LDP descriptor works effectively in the presence of noise compared to LBP, because the edge gradients are relatively more stable than the pixel intensity value [244]. The Kirsch mask in all the eight directions are shown in Fig. 2.6.

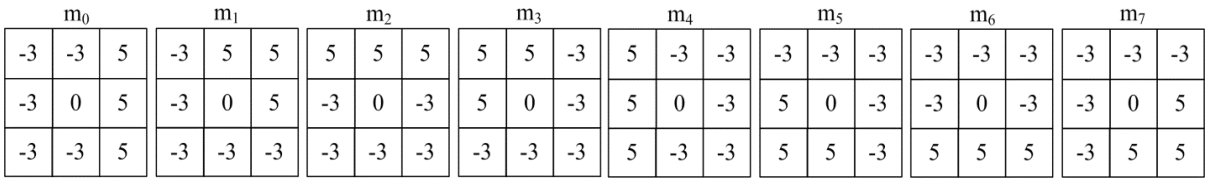

Fig. 2.6 Kirsch masks in eight directions.

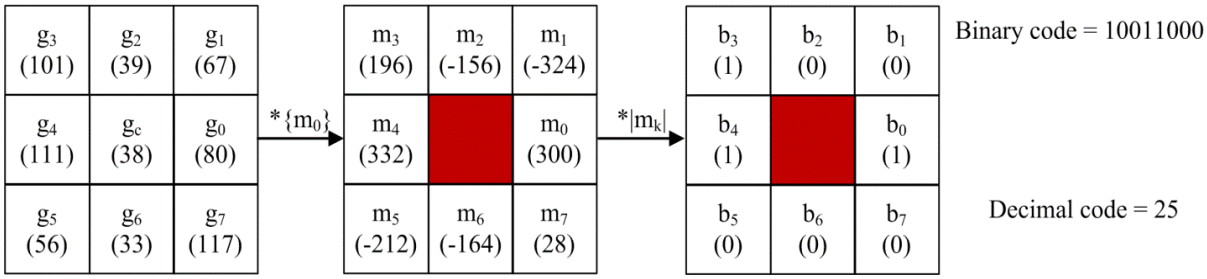

Fig. 2.7 Procedure to calculate LDP code for k=3.

Subsequently, the relative edge response for each pixel location produces the 8-bit LDP code. The top k response values are set to 1 whereas remaining values are set to 0. The complete procedure for calculating the LDP code for top 3 values for 3×3 neighbourhood image is presented in Fig. 2.7. In this example, the central pixel value at location g_c (38) is now replaced by LDP decimal code 25.

2.1.16 Local Ternary Pattern (LTP)

Tan and Triggs [198] have proposed LTP (generalization of LBP), a discriminative texture descriptor which is robust against noise specially in near-uniform regions of image. Contrary to LBP which thresholds the neighbouring pixels to binary values (0, 1), the LTP uses three values (i.e., 1, 0 and -1). The schematic for LTP descriptor is illustrated in Fig. 2.8.

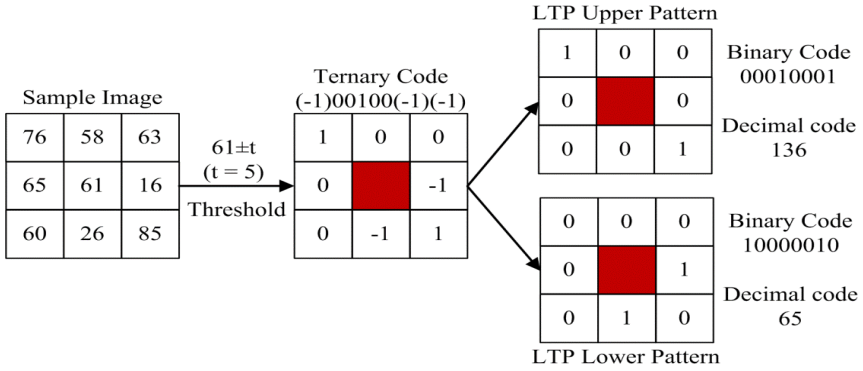

Fig. 2.8 LTP calculation process

The thresholding expression for LTP is given by:

$$s'\left(x,g_c,th\right)=\begin{cases}+1, & x\geq g_c+th\\ 0, & \left|x-g_c\right|<th\\ -1, & x\leq g_c-th\end{cases} \tag{2.23}$$

where, $x = g_p - g_c, g_c$ is gray value of centre pixel, g_p gray value of neighbourhood pixel and th is user specified threshold value. All the gray levels in the range of $\pm th$ is quantized to zero. Further, gray levels above $(g_c + th)$ and below $(g_c - th)$ is quantized to +1 and -1, respectively.

2.1.17 Local Ternary Co-occurrence Pattern (LTCoP)

The LTCoP feature descriptor was introduced by Murala and Jonathan [139] for image retrieval application.

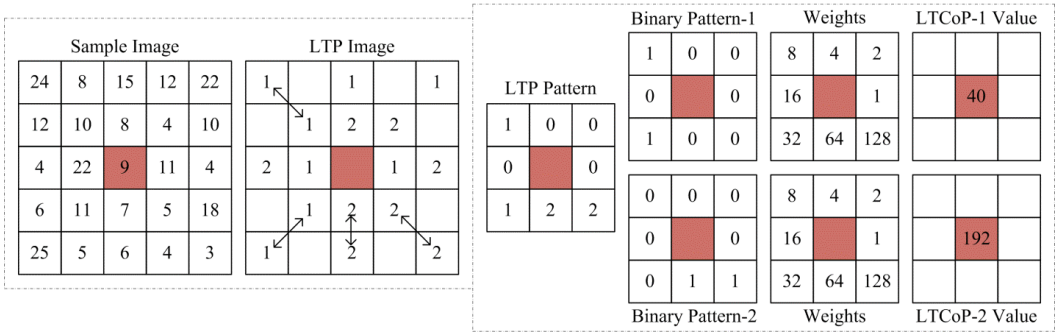

Fig. 2.9 Illustration of LTCoP computation.

The gray level values of center pixels and its surrounding neighbors are used to compute the LTP edges. Thereafter, the LTCoP encodes the co-occurrence of similar LTP edges. The LTCoP has established its superiority for MRI and CT image retrieval, as it integrates the concept of LDP, LTP, and co-occurrence matrices. The LTCoP computation is depicted in Fig. 2.9. The LTCoP is expressed by:

$$\text{LTCoP} = \begin{bmatrix} s\left(I^1_{P,R}(g_1), I^1_{P,R+1}(g_1)\right), \\ s\left(I^1_{P,R}(g_2), I^1_{P,R+1}(g_2)\right), \ldots \\ \ldots, s\left(I^1_{P,R}(g_p), I^1_{P,R+1}(g_p)\right) \end{bmatrix} \tag{2.24}$$

$$s(x,y) = \begin{cases} 1 \; if \; x = y = 1 \\ 2 \; if \; x = y = 2 \\ 0 \; else \end{cases} \tag{2.25}$$

where, $I^1_{P,R}(g_i)$ and $I^1_{P,R+1}(g_i)$ represents ternary values [139]. The LTCoP generates ternary pattern that is subsequently converted into two binary patterns by using the concept of LTP. A feature vector of length 2^P is generated for a local pattern having *P* neighbourhoods. Although LTP gives comparatively better results but it is achieved at higher computational cost.

2.1.18 Local Configuration Pattern (LCP)

Guo *et al*., [65] have proposed local configuration pattern descriptor appropriate for modeling the microscopic configuration of an image. The LCP descriptor is produced by means of local

structural and microscopic configuration information of the image. The local structural information is obtained by combining local variance information together with rotation invariant LBP descriptor. On the other hand, the microscopic configuration information employs image configuration and pixel-wise interaction. Modeling of microscopic configuration is given by:

$$E\left(a_{0,\ldots}a_{p-1}\right)=\left|g_c-\sum_{i=0}^{p-1}a_i g_i\right| \tag{2.26}$$

where, g_i and g_c are neighboring and central pixel intensity values, respectively. The $a_i\left(i=0\,to\,P-1\right)$ is weighting factor associated with g_i and E is reconstruction error in relation to a_i. Reconstruction error for each pattern is minimized by the least squares estimation. The features generated so has both the magnitude and pixel-wise interaction information.

$$H_L\left(k\right)=\sum_{i=0}^{P-1}A_L\left(i\right).e^{-j2\pi ki/P} \tag{2.27}$$

where, $H_L\left(k\right)$ and $A_L\left(i\right)$ are k^{th} element of H_L and i^{th} element of A_L, respectively. The magnitude part of H_L is expressed as,

$$\left|H_L\right|=\left[\left|H_L\left(0\right)\right|;\left|H_L\left(1\right)\right|;\ldots;\left|H_L\left(P-1\right)\right|\right] \tag{2.28}$$

The LCP feature is thus given by

$$\text{LCP}=\left[\left[\left|H_0\right|;O_0\right];\left[\left|H_1\right|;O_1\right];\ldots;\left[\left|H_{q-1}\right|;O_{q-1}\right]\right] \tag{2.29}$$

where, $\left|H_i\right|$ is calculated by Eq. (2.28) with respect to i^{th} pattern of interest. Further, O_i is occurrence of the i^{th} pattern of interest and q is total number of patterns of interest. The detailed mathematical information of LCP is given in [65].

2.1.19 Local Phase Quantization (LPQ)

The LPQ texture descriptor, which is insensitive to image blurring has been introduced by Ojansivu and Heikkil [153] originally for face recognition. In this approach, for a given image, at each pixel location over a local region (rectangular neighborhood) two dimensional short term Fourier transform (2D-STFT) is calculated to obtain the local phase information. This transformation is known as local phase quantization (LPQ) owing to phase quantization of 2D-STFT information. The local frequency is calculated by using a STFT on a local region (rectangular $M\times M$ neighborhoods N_x) at each pixel location of the image $f\left(x\right)$ is expressed by:

$$\text{F(u,x)}=\sum_{y\in N_x}f(x-y)e^{(-j2\pi u^T y)}=w_{\text{u}}^T f_x \tag{2.30}$$

where, w_u is window function defining the neighborhood N_x at frequency u, while f_x is a vector that has all N^2 image samples from N_x. In this method, local Fourier complex coefficients are calculated at four frequency points, $u_1 = [a,0]^T$, $u_2 = [0,a]^T$, $u_3 = [a,a]^T$ and $u_4 = [a,-a]^T$ corresponding to 2D- frequencies, where a is scalar such that $H(u_i) > 0$.

$$F(x) = \left[F(u_1,x), F(u_2,x), F(u_3,x), F(u_4,x)\right] \tag{2.31}$$

$$G(x) = \left[Re\{F(x)\}, Im\{F(x)\}\right] \tag{2.32}$$

$$q_j = \begin{cases} 1, & g_j \geq 0 \\ 0, & \text{otherwise} \end{cases} \tag{2.33}$$

where q_j is j^{th} component of the vector $G(x)$. The LPQ is expressed by:

$$f_{LPQ}(x) = \sum_{j=1}^{8} q_j . 2^{(j-1)} \tag{2.34}$$

The eight binary coefficients q_j are represented as integer values between 0-255 using Eq. (2.33). Finally the histogram of these values from all locations is composed and used as 256-dimensional feature vector. The detailed mathematical description for LPQ is available in [145, 153, 154].

2.1.20 Gradient Local Auto-correlation (GLAC)

Kobayashi and Otsu [102] proposed GLAC, a shift-invariant image feature extraction technique. In contrast to the texture feature extraction techniques which are based on histogram, GLAC is a 2nd order statistics of gradient and hence extracts more discriminative and richer information of an image. As stated in [102] the GLAC makes use of "spatial and oriental auto-correlations of local image gradients". The GLAC inherit the advantageous properties of higher-order local autocorrelation (HLAC) and the image gradients are sparsely expressed with reference to their orientations and magnitudes.

2.1.21 Binary Gabor Pattern (BGP)

Zhang *et al.*, [236] have proposed a robust and efficient descriptors known as binary Gabor pattern (BGP) for texture classification. The BGP employs *J* Gabor filters (g_0 to g_{j-1}) with *J* different orientations. The texture image is convolved with these *J* Gabor filters. The radius of the filter mask is represented by *R*. For a circular image patch *p* having radius *R* is centered at location x on the image. Multiplying image patch *p* pixel-wise with *J* filters and later summing up all the elements produces a response vector $r = \{r_j : | j = 0,1,\ldots,J-1\}$. A binary vector $b = \{b_j : | j = 0,1,\ldots,J-1\}$ is produced by binarizing *r*. The BGP is then expressed by:

$$BGP = \sum_{j=0}^{j} b_j \cdot 2^j \tag{2.35}$$

For a given 2^J binary patterns (*b* has *J* elements), the BGP operator generates 2^J output values. The rotation invariant binary Gabor pattern (BGP_{ri}) is defined by:

$$BGP_{ri} = \max\left\{ROR\left(BGP, j\right) | j = 0,1,\ldots,J\right\} \tag{2.36}$$

where, $ROR\left(x, j\right)$ performs circular bitwise right shift operation on *x* (*J*-bit number) for *j* number of times.

2.2 FEATURE DIMENSIONALITY REDUCTION

With the high-dimensional features, computational requirement of classifier increases and the classification accuracy may not be improved due to high-dimensional features. Therefore, a feature dimension reduction technique [27, 223] is required to transform the data from high-dimensional space to low-dimensional space. The endeavour of feature dimensionality reduction is to retain the best subset of features of the full feature dataset [221, 222]. The dimension of feature vector data can be reduced by following two methods such as PCA (feature dimensionality reduction) and mRMR (feature selection).

2.2.1 Principal Component Analysis (PCA)

The PCA is one of the widely used linear transformation technique [26]. The PCA reduces data dimensions by computing a few orthogonal linear combinations of the original dataset features with maximal variance. The PCA involves calculating the Eigen values and Eigen vectors of the covariance matrix of the original feature matrix. The eigenvectors characterized by largest Eigen value is known as first principal component (PC). The second PC is orthogonal to first PC with second largest variance, and so on. The first several PC's have most of the variance, which is sufficient to represent the original data without losing much of the information.

2.2.2 Minimal Redundancy Maximal Relevance (mRMR)

The key objective of feature selection (FS) technique is to eliminate the irrelevant features, and retain a subset of features that efficiently describes the observed input data. The FS facilitates in reducing the effect of curse of dimensionality, gives better insight of data, and improves the performance of classifier by using a subset of features as input [32, 140]. The FS techniques are categorized into filter, wrapper and embedded methods in the context of classification [180]. The filter techniques are fast, computationally efficient and independent of classification algorithms. The mRMR feature selection technique based on mutual information quotient proposed by Peng *et al*. [168] is a multivariate filter technique that has been chosen in this work.

2.3 CLASSIFIERS

Four classifiers, namely, linear discriminant analysis (LDA), random forest (RF) and two variants of SVM, viz., linear and radial basis function (RBF) kernel have been used here for hardwood species classification. These classifiers are briefly explained in the following subsections:

2.3.1 Linear Discriminant Analysis

The LDA is a simple, powerful and mathematically robust classifier, which often constructs models with accuracy equivalent to other methods [113]. The need of low computational complexity and immunity to over fit, facilitated LDA classifier to be widely used in applications such as brain computer interface (BCI), face and object recognition [59, 113, 135, 199], image retrieval [224], bioinformatics and tropical wood species identification [233], etc. The LDA was originally proposed as Fisher's discriminant analysis [53] for binary class problem. It works on the concept of projecting data in high-dimensional feature space to low-dimensional features space. The LDA searches for a linear combination of variables (features) that is best to discriminate among the given classes. The LDA has been extended for multiclass problem using (p -1) discriminant function for p classes and is known as multiple discriminant analysis [113, 199]. The LDA classifier has been investigated only for PCA reduced feature dataset. The LDA cannot be employed directly to high dimensional features and small sample size set [224], because of the fact that within class scatter matrix is always singular [15, 38].

2.3.2 Random Forest

The RF classifier is an ensemble machine learning technique, which builds several classification and regression trees by incorporating additional layer of randomness to bagging [21]. It has been widely used as a classifier in bioinformatics, geology and pattern recognition [42]. It is robust against over fitting, handles large dataset, computationally efficient, and easy to implement.

2.3.3 Support Vector Machine

The SVM, an efficient and robust supervised classifier, gives excellent generalization performance and has been fruitfully applied to several pattern recognition problems in signal and image processing [34, 42, 96, 117, 120, 219, 220]. It was initially proposed as binary classifier [41, 88]. Let (x_i, y_i) for $i = 1, 2, 3,...,I,$ represents a particular set of instance-label pairs, $x_i \in R^n$, $y_i \in \{+1,-1\}$, then the SVM binary classifier predicts a label y, in y_i for a given testing instance x. The optimization problem for binary classification is defined as follows [52]:

$$\min_{w} \frac{1}{2} w^T w + C \sum_{i=1}^{I} \xi\left(w; x_i, y_i\right)$$

Subject to constraint,

$$y_i\left(w^T x_i + b\right) - 1 \geq 0, \forall i \tag{2.37}$$

where, $\xi\left(w; x_i, y_i\right)$ is a loss function and *C* (nonnegative) is a penalty parameter (cost factor). The binary class SVM is extended for multiclass classification using approaches such as, "one against one", "one against all", and "directed acyclic graph" [172]. Further, a multiclass SVM classifier proposed by Crammer and Singer [43] involves solving single optimization problem only. The linear SVM and RBF kernel SVM (nonlinear) are briefly described here:

2.3.4 Linear SVM

These days, linear classifier is method of choice as it works directly on the given input data space. The linear SVM classifier is ideal for a dataset having massive features, and is sparse in nature. It is considered to be efficient and enjoys faster training and testing procedure [16, 230]. The multi class SVM proposed by Crammer and Singer [43] has been used in linear SVM classifier, here. The decision function for p class is expressed by [52]:

$$f\left(x\right) = argmax_{p=1,2,\ldots,P}\left(w_p^T x_i\right) \tag{2.38}$$

2.3.5 Radial Basis Function Kernel SVM

When the training set is inseparable in the original space, the original input data $\mathbf{x}_i$ are mapped into a high dimensional space $\Phi\left(\mathbf{x}_i\right)$, in which mapped data are linearly separable. The expression for decision rule is given as [33, 185]:

$$f\left(x\right) = sgn\left(\sum_{i=1}^{l} \alpha_i y_i k\left(x_i, x_j\right) + b\right) \tag{2.39}$$

where, $k\left(x_i, x_j\right)$ is a kernel function and α_i signify the Lagrange multipliers (for dual optimization problems) which describes the optimal separating hyperplane. The radial basis function is one of the most popular kernel function and is given by [33]:

$$K\left(x_i, x_j\right) = e^{\left(-\gamma x_i - x_j^2\right)},\ \gamma > 0 \tag{2.40}$$

where, γ is the kernel parameter.

2.4 MICROSCOPIC IMAGE DATABASE OF HARDWOOD SPECIES

In the present work, an open access database of hardwood species consisting of 75 different categories has been selected for investigation. Each of the seventy five hardwood species contain twenty samples (20). Thus, in all they form set of 1500 samples. These microscopic images of hardwood species are correctly labelled by the experts in the laboratory of wood anatomy at Federal University of Parana, Curitiba, Brazil [125]. The family, gender, and specie of each of the hardwood species are listed in Table 2.3. The image acquisition and sample preparation process is briefly described here for the sake of completeness. Initially, the wood

cube is boiled in order to soften it to get the samples. Then, a sliding microtome is incorporated to obtain wood samples of about 25 µm thickness. Thereafter, triple staining technique is used to color the veneer that is followed by dehydration process which makes use of rinsing the sample with an ascending alcohol series. Finally, Olympus Cx40 microscope with 100x zoom is employed to obtain the images from the sheet of wood which generates images of 1024 × 768 pixel resolution.

Table 2.3 List of hardwood species.

Sr. No.	Family	Gender	Species	Sr. No.	Family	Gender	Species
1	Ephedraceae	Ephedra	*Californica*	39	Lauraceae	Nectandra	*Sp*
2	Lecythidaceae	Cariniana	*Estrellensis*	40	Lauraceae	Ocotea	*Porosa*
3	Lecythidaceae	Couratari	*Sp*	41	Lauraceae	Persea	*Racemosa*
4	Lecythidaceae	Eschweiler	*Matamata*	42	Annonaceae	Porcelia	*Macrocarp*
5	Lecythidaceae	Eschweleir	*Chartaceae*	43	Magnoliaceae	Magnolia	*Grandiflora*
6	Sapotaceae	Chrysophy	*Sp*	44	Magnoliaceae	Talauma	*Ovata*
7	Sapotaceae	Micropholi	*Guianensis*	45	Melastomatace	Tibouchiana	*Sellowiana*
8	Sapotaceae	Pouteria	*Pachycarpa*	46	Myristicaceae	Virola	*Oleifera*
9	Fabaceae-Cae.	Copaifera	*Trapezifolia*	47	Myrtaceae	Campomanesia	*Xanthocar*
10	Fabaceae-Cae.	Eperua	*Falcata*	48	Myrtaceae	Eucalyptus	*Globulus*
11	Fabaceae-Cae.	Hymenae	*Courbaril*	49	Myrtaceae	Eucalyptus	*Grandis*
12	Fabaceae-Cae.	Hymenae	*Sp*	50	Myrtaceae	Eucalyptus	*Saligna*
13	Fabaceae-Cae.	Schizolobi	*Parahyba*	51	Myrtaceae	Myrcia	*Racemulos*
14	Fabaceae-Fab.	Pterocarp	*Violaceus*	52	Vochysiaceae	Erisma	*Uncinatum*
15	Fabaceae-Mim.	Acacia	*Tucunamensi*	53	Vochysiaceae	Qualea	*Sp*
16	Fabaceae-Mim.	Anadenan	*Colubrina*	54	Vochysiaceae	Vochysia	*Laurifolia*
17	Fabaceae-Mim.	Anadenan	*Peregrina*	55	Proteaceae	Grevillea	*Robusta*
18	Fabaceae-Fab.	Dalbergia	*Jacaranda*	56	Proteaceae	Grevillea	*Sp*
19	Fabaceae-Fab.	Dalbergia	*Spruceana*	57	Proteaceae	Roupala	*Sp*
20	Fabaceae-Fab.	Dalbergia	*Variabilis*	58	Moraceae	Bagassa	*Guianensis*
21	Fabaceae-Mim.	Dinizia	*Excelsa*	59	Moraceae	Brosimum	*Alicastrum*
22	Fabaceae-Mim.	Enterolobi	*Schomburgkii*	60	Moraceae	Ficus	*Gomelleira*
23	Fabaceae-Mim.	Inga	*Sessilis*	61	Rhamnaceae	Hovenia	*Dulcis*
24	Fabaceae-Mim.	Leucaena	*Leucocephala*	62	Rhamnaceae	Rhamnus	*Frangula*
25	Fabaceae-Fab.	Lonchocar	*Subglaucesce*	63	Rosaceae	Prunus	*Sellowii*
26	Fabaceae-Mim.	Mimosa	*Bimucronata*	64	Rosaceae	Prunus	*Serotina*
27	Fabaceae-Mim.	Mimosa	*Scabrella*	65	Rubiaceae	Faramea	*Occidentali*
28	Fabaceae-Fab.	Ormosia	*Excelsa*	66	Meliaceae	Cabralea	*Canjerana*
29	Fabaceae-Mim.	Parapipta	*Rigida*	67	Meliaceae	Carapa	*Guianensis*
30	Fabaceae-Mim.	Parkia	*Multijuga*	68	Meliaceae	Cedrela	*Fissilis*
31	Fabaceae-Mim.	Piptadenia	*Excelsa*	69	Meliaceae	Khaya	*Ivorensis*
32	Fabaceae-Mim.	Pithecello	*Jupunba*	70	Meliaceae	Melia	*Azedarach*
33	Rubiaceae	Psychotria	*Carthagenens*	71	Meliaceae	Swietenia	*Macrophyll*
34	Rubiaceae	Psychotria	*Longipes*	72	Rutaceae	Balfourodendro	*Riedelianu*
35	Bignoniaceae	Tabebuia	*Alba*	73	Rutaceae	Citrus	*Aurantium*
36	Bignoniaceae	Tabebuia	*Sp*	74	Rutaceae	Fagara	*Rhoifolia*
37	Oleaceae	Ligustrum	*Lucidum*	75	Simaroubaceae	Simarouba	*Amara*
38	Lauraceae	Nectandra	*Rigida*				

2.5 METHODOLOGY

2.5.1 Procedural Steps

The complete procedural steps for the classification of microscopic images of hardwood species using state-of-the-art texture feature extraction techniques with the help of classifiers is shown in Fig. 2.10.

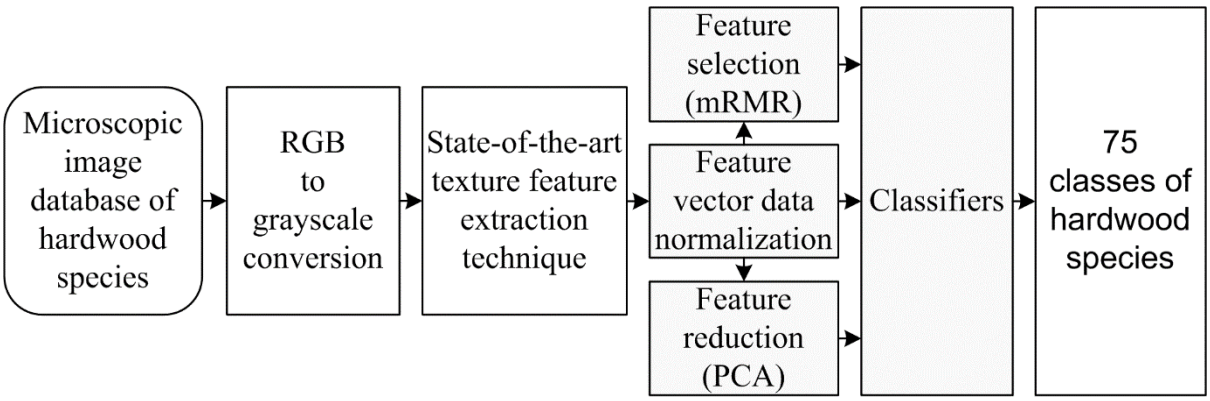

Fig. 2.10 Hardwood species classification using state-of-the-art texture feature extraction technique.

A brief description of these procedures are as described below:

1. The microscopic images of hardwood species are added with color information to enhance certain anatomical features of hardwood species. Thus, the pre-processing step is involved to obtain grayscale image from color (RGB) image, resulting into significant reduction of computational time during texture feature extraction. The expression for RGB to grayscale conversion is given by [92]:

$$G_{luminance} = 0.2989 \times R + 0.5878 \times G + 0.1140 \times B \quad (2.41)$$

where, $G_{luminance}$ represents grayscale image achieved by considering luminance information only and eliminating the hue and saturation information of color image. The R, G and B signify red, green and blue components of color image, respectively.

2. Texture features of grayscale images are then extracted from state-of-the-art texture feature extraction techniques.
3. The feature vector data produced so has been normalised in the range 0 to 1, thus rendering it in the form useful as an input to the classifier. The feature vector data is normalized using Eq. (2.42):

$$F_{Norm} = \left(\frac{F - \min(F)}{\max(F) - \min(F)} \right) \quad (2.42)$$

where, F_{Norm} : normalized feature vector data, and F: original feature vector data.

4. The feature vector data is then given as input to different classifiers into three different manners (full feature vector data (FFVD), the PCA reduced feature vector data and the

mRMR feature selection based reduced feature vector data) for classifying the microscopic images of hardwood species database into 75 categories.

5. The best combination of texture feature extraction technique and classifier is then identified on the basis of the superlative classification accuracy.

2.5.2 Approaches used for Performance Evaluation of Feature Extraction Techniques

The performance of the feature extraction techniques for classification of hardwood species have been investigated employing two strategies: (1) 10-fold cross validation and (2) randomly dividing the database. These approaches are discussed in following subsections:

2.5.2.1 10-fold cross validation

In this approach, the classification task employs 10-fold cross validation [58] to produce the end result by dividing the whole feature dataset into 10 uniform folds. The primary reason for using 10-fold cross validation is to ensure that the results remain unbiased to given partitioned data. Out of 10- folds, nine are considered as training data and remaining one is used as test data. Hence, 90% data is used for training and 10% data is used for test purpose. The process is then repeated 10 times so that each sample is used as test data. The final outcome is the average of all the 10 results.

2.5.2.2 Randomly divided database (RDD)

In this section total available dataset of microscopic image of hardwood specie is randomly divided [34] into fixed training and testing subsets for each individual species. The investigations have been carried out with four different proportions of training and testing datasets as given below:

1. 80% data for training and 20% data for testing (80/20)
2. 70% data for training and 30% data for testing (70/30)
3. 60% data for training and 40% data for testing (60/40)
4. 50% data for training and 50% data for testing (50/50)

2.6 EXPERIMENTAL RESULTS AND DISCUSSION

The experimental work presented in this section investigates the efficacy of the state-of-the-art texture feature extraction techniques for the classification of microscopic images of hardwood species database into 75 classes with the help of classifiers. The four classifiers used in this work are linear SVM, RBF kernel SVM, LDA and RF classifiers. The linear and RBF kernel SVM classifiers have been examined by means of MATLAB implementations of LibLINEAR [52] and LIBSVM [33] tools, respectively. The LDA classifier has been implemented with the help of built-in function available in MATLAB R2013a. Further, the RF classifier is performed using Matlab implementation of RF_MexStandalone-v0.02 tool [249].

2.6.1 Parameter Selection

The GLCM technique generates 18 features in each direction for a given neighbourhood distance. The neighbourhood distance (d) in the range 1-10 has been investigated and d=9 has been selected as it yields best result. Further, these features are calculated in four directions (0°, 45°, 90° and 135°).

In order to get Gabor texture features, the grayscale image is convolved with Gabor filters and produces 40 Gabor patterns for each grayscale image [73]. Subsequently, FOS texture features namely, mean, standard deviation (SD) and entropy are calculated from each of the Gabor pattern images.

The *P* and *R* parameter values are considered as 8 and 1, respectively, for all the variants of LBP (LBP, LBP^{u2}, LBP^{ri}, LBP^{riu2}, LBP-HF, $CLBP^{u2}$, $ALBP^{u2}$, $ALBP^{ri}$ and $ALBP^{riu2}$) because these values have yielded fast and accurate feature extraction as represented by [7]. Further, for texture images, uniform patterns account for approximately 90% of all patterns when using the (8, 1) neighbourhood and these patterns account for around 70% in the (16, 2) neighbourhood. The use of LBP^{riu2} having $P = 8$ and $R = 1$ has also reported the best result compared to (P, R) pair values of (16, 2) and (24, 3) [152]. Furthermore, the *R* parameter is usually chosen small because the correlation between pixels decreases with distance, and a lot of the texture information can be obtained from local neighbourhoods [80].

For the variants of LTP (viz., LTP^{u2}, LTP^{ri}, LTP^{riu2}) the threshold value, $th = 5$ has been chosen as it produces the best result [198]. For LCP variant the number of neighbouring sample have been fixed to 8 [65].To extract LPQ texture features the local window size has been chosen as 3×3 (default value). The STFT with Gaussian window (Gaussian quadrature filter pair) has been used for local frequency estimation and the coefficients are decorrelated [153], as the information is maximally conserved in scalar quantization when the samples to be quantized are statistically independent.

For linear SVM classifier, the optimum value of C has been selected by searching in the range (10^{-4}, 10^{-3},…, 10^{+5}), whereas the optimum value of *C* and gamma (γ) has been selected by using grid search method in the range (10^{-4},10^{-3},…,10^{+5}) for RBF kernel SVM classifier [36]. The tolerance of termination criteria (ξ) value has been tested in the range (0.1, 0.01, 0.001, and 0.0001) and found that ξ = 0.01 gives the best trade-off between classification accuracy and computational time. Also, the bias (b) parameter value has been selected as 1 for SVM implementation.

The LDA classifier has been investigated only for PCA reduced feature dataset. The LDA cannot be employed directly to high dimensional features and small sample size set [224], because of the fact that the within class scatter matrix is always singular [15, 38].

The RF classifier needs to optimize number of trees $(nTree)$ and number of randomly chosen features $(mTry)$ for generating a prediction model. Typically, 500 to 2000 trees are grown and the results aggregated by averaging [173]. Here, *nTree* values have been varied in the range of 100 to 1000 and it has been found that addition of number of trees beyond 450 to 500 were not having significant improvement in the classification accuracy for our dataset. Thus, as a trade-off between classification accuracy and computational time, $nTree$ = 500 [5, 115] and $\text{mTry} = \text{floor}\left(\sqrt{\text{number of features}}\right)$ [5, 49] has been selected in this experimentation.

2.6.2 Experimental Results

The classification accuracy of the state-of-the-art texture feature extraction techniques has been computed using the earlier discussed classifiers, who have been selected on the basis of their general performance for pattern recognition and classification task. The classification accuracy has been computed under three different categories viz., full feature vector data (FFVD), PCA reduced feature vector data and mRMR feature selection based reduced feature vector data. To compute the performance of feature extraction techniques two approaches viz., 10- fold cross validation and randomly divided database (RDD) selection has been adapted. Then, the comprehensive results are presented under two subsections of 10-fold cross validation and RDD selection. Further, under the individual approaches the results have further been categorised under FFVD, PCA reduced feature vector data and minimal redundancy maximal relevance (mRMR) feature selection based reduced feature vector data.

2.6.3 Performance Evaluation of State-of-the-art Texture Feature Extraction Techniques using 10-fold Cross Validation Approach

The classification accuracy obtained for full feature vector data, PCA reduced dimension feature vector data and mRMR feature selection based reduced feature vector data is discussed in the following subsections.

2.6.3.1 Full feature vector data (FFVD)

The classification accuracy achieved using FFVD of several state-of-the-art texture feature extraction techniques for grayscale image of hardwood species is presented in Table 2.4. The classification accuracy obtained with the texture features using three different classifiers is discussed below:

Linear SVM classifier: The feature vector data of BGP texture feature extraction technique has achieved highest classification accuracy of 95.93±1.52% with 216-dimension features. The second best classification accuracy of 95.20±1.20% has been attained by COALBP48 texture features (1024). The feature vector data of FOS techniques has presented worst classification accuracy of 15.80 ± 2.59%, amongst the state-of-the-art texture feature extraction techniques.

RBF kernel SVM classifier: The best classification accuracy of 94.13±2.24% has been obtained using FFVD of BGP texture feature extraction technique. The FFVD of COALBP48 texture feature extraction technique has achieved the second best classification accuracy of 91.67±1.14%. Further, the least classification accuracy of 38.67±2.08% has been obtained with FFVD of FOS technique.

RF classifier: The FFVD of BGP texture feature extraction technique has attained the best classification accuracy of 86.27±1.37%. The second best classification accuracy of 85.00±1.89% has been obtained by FFVD of COALBP48 texture feature extraction technique. Similar to all other classifiers, in this case too, the lowest classification accuracy of 33.13±2.72% has been accomplished by FFVD of FOS technique.

Table 2.4 Classification accuracy achieved using full feature vector data

Technique	Feature extraction time in seconds	% CA±SD achieved by classifiers			
		NoF	Linear SVM	RBF kernel SVM	RF
GLCM	0.3468	72	80.47±3.32	73.67±3.25	53.93±2.74
GLRLM	4.0733	44	75.20±3.13	68.67±4.30	47.20±4.12
FOS	0.1694	4	15.80±2.59	38.67±2.08	33.13±2.72
Gabor	9.3753	120	93.47±1.43	90.20±3.25	77.80±3.14
LBP	0.1351	256	89.73±2.90	87.93±2.16	69.33±1.83
LBP^{u2}	0.2592	59	79.73±2.88	81.47±2.64	69.27±2.52
LBP^{ri}	0.2621	36	77.33±2.86	79.07±3.31	53.47±2.98
LBP^{riu2}	0.2497	10	63.53±3.16	67.07±2.71	41.60±4.23
LBP-HF	0.2594	38	71.60±1.51	71.40±1.49	65.47±3.20
LPQ	0.2795	256	90.80±2.13	87.00±2.18	70.53±1.96
GLAC	0.1407	105	83.53±2.98	74.80±4.28	51.00±3.60
CSLBP	4.4766	16	43.33±3.84	50.13±4.20	38.53±4.60
$CLBP^{u2}$	0.3124	118	87.40±2.14	86.13±2.59	73.53±3.16
LDP	0.4137	256	76.80±2.10	78.93±3.41	58.33±4.41
LTP^{u2}	0.3853	118	88.40±2.11	87.13±2.88	74.73±3.69
LTP^{ri}	0.3865	72	86.46±1.77	85.86±2.32	61.40±4.61
LTP^{riu2}	0.4069	20	79.86±2.10	79.93±1.76	55.86±4.21
$ALBP^{u2}$	0.6445	59	80.33±3.02	81.40±2.58	69.06±4.01
$ALBP^{ri}$	0.5911	36	75.53±1.72	78.13±3.15	56.07±4.18
$ALBP^{riu2}$	0.5823	10	62.00±3.29	67.87±4.42	43.80±2.51
LCP^{u2}	0.5200	81	81.53±3.01	84.33±2.93	75.27±2.57
LCP^{ri}	0.6589	81	77.27±3.44	77.60±2.27	70.93±2.93
LCP^{riu2}	0.7185	81	82.80±3.24	82.13±2.52	73.20±3.79
BGP	2.6857	216	**95.93±1.52**	**94.13±2.24**	**86.27±1.37**
LTCoP	4.5533	256	90.93±1.81	86.33±1.57	68.27±3.17
CoALBP12	0.2926	1024	94.06±1.55	90.93±2.13	79.87±2.17
CoALBP24	0.3048	1024	94.53±1.28	91.60±0.78	83.20±1.62
CoALBP48	0.3323	1024	95.20±1.20	91.67±1.14	85.00±1.89
DenseCLBP	1.8823	118	89.67±1.37	86.60±2.16	75.93±3.02

Amongst other LBP variants (i.e., LBP, LBP^{u2}, LBP^{ri}, LBP^{riu2}, LBP-HF, $CLBP^{u2}$, $ALBP^{u2}$, $ALBP^{ri}$, $ALBP^{riu2}$), the LBP texture features have given the best classification accuracy results though it is poorer than the rest of the above discussed techniques. The classification accuracy results produced by rest of the state-of-the-art texture features extraction techniques by three classifiers are also listed in Table 2.4. The percentage classification accuracy results obtained by state-of-the-art texture feature extraction techniques are graphically illustrated as shown in

Fig. 2.11. The superiority of BGP and COALBP48 texture feature extraction techniques are clearly visible in Fig. 2.11.

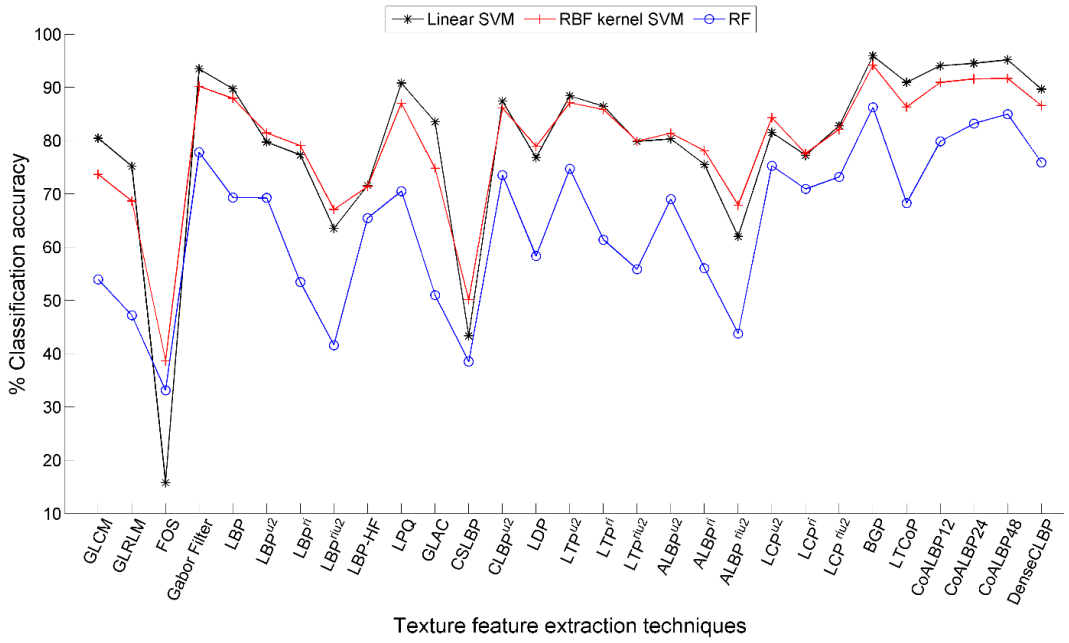

Fig. 2.11 Classification accuracy achieved using FFVD.

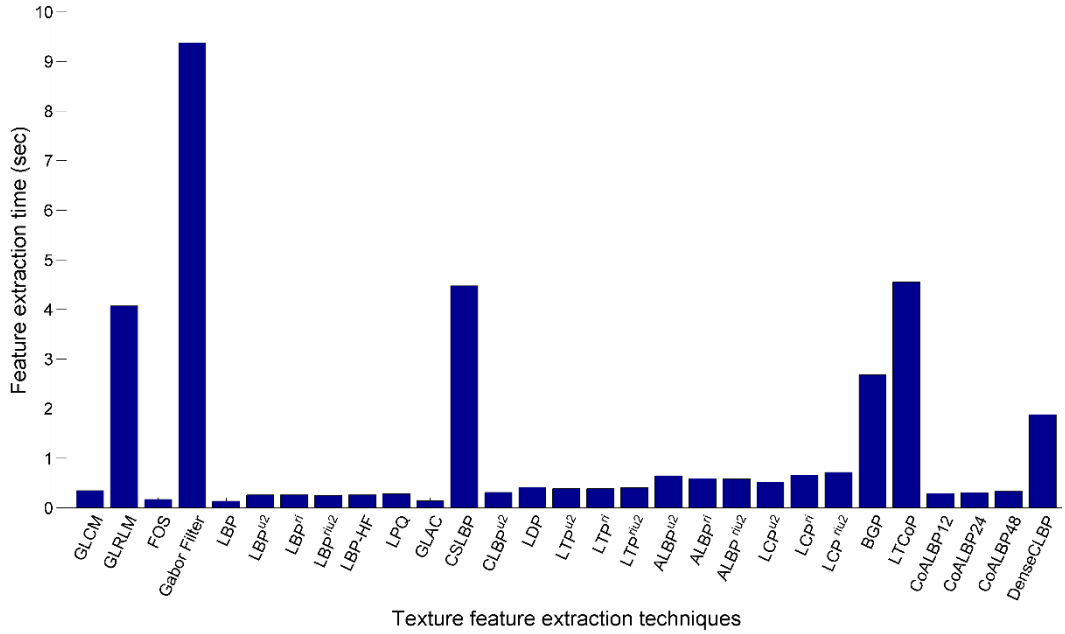

Fig. 2.12 Feature extraction time for single grayscale image.

In Fig. 2.12, time taken by each of the state-of-the art texture feature extraction techniques for single image is presented. It is evident that Gabor texture extraction technique takes maximum time (9.3753 second) to produce features of a single grayscale image. Similarly, CSLBP, BGP, LTCOP and DenseCLBP do need more time for texture feature extraction. In contrast to rest of the techniques, the LBP variants have taken minimum time for feature extraction as is evident from Fig. 2.12.

The error bar plot with standard deviation (SD) for classification accuracy achieved by texture feature extraction techniques is shown in Fig. 2.13. It is again observed that BGP texture feature extraction technique has produced best classification accuracy with minimum value of SD for all the three classifiers compared to rest of the texture feature extraction techniques. Another observation which needs to be emphasized is that the linear SVM classifier has achieved comparatively better classification accuracy compared to the RBF kernel SVM and RF classifier for most of the state-of-the-art texture feature extraction techniques.

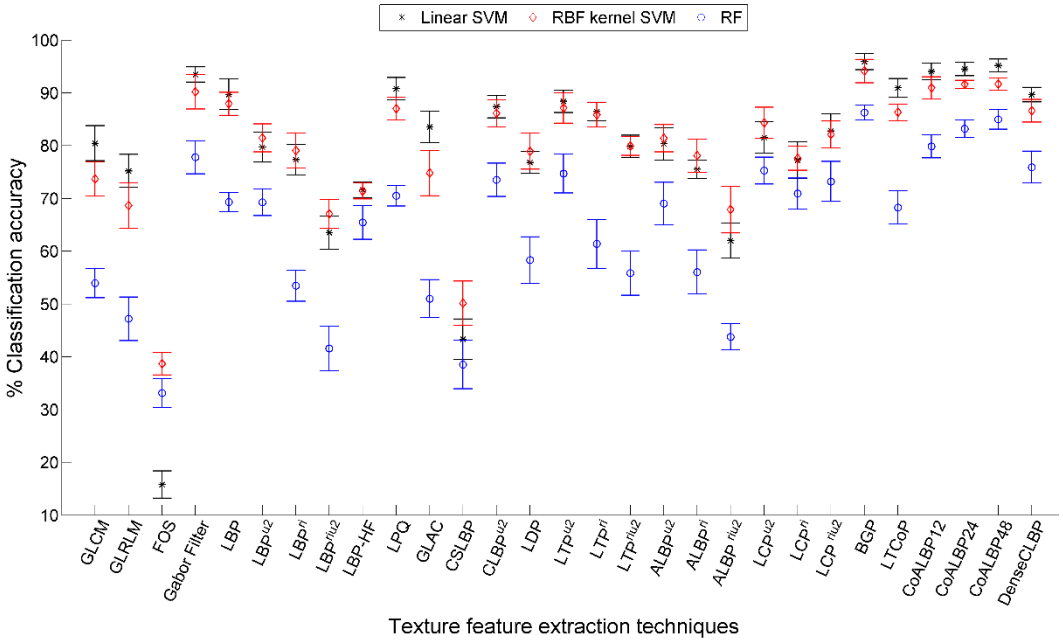

Fig. 2.13 Error bar plot with SD using FFVD.

2.6.3.2 The PCA dimensionality reduced feature vector data

In this section, the PCA is used to reduce the dimensionality of feature vector data. The classification accuracy results obtained by the PCA based reduced feature vector data of state-of-the-art texture feature extraction techniques with different classifiers are presented in Table 2.5, and has been concisely discussed henceforth:

Linear SVM classifier: The PCA reduced feature vector data of BGP feature extraction technique yields 95.20±1.50% classification accuracy, compared to 95.93±1.55% classification accuracy achieved by FFVD of BGP. Though, the achieved accuracy is relatively lower but it has been achieved with 175 features only in comparison to 216 features considered for FFVD.

RBF kernel SVM classifier: Amongst the proposed feature extraction techniques, the PCA reduced feature vector data of BGP texture feature extraction technique has achieved a classification accuracy of 94.47±1.33% using 150 features only, which is better than the classification accuracy (94.13±2.24%) achieved for FFVD of BGP.

RF classifier: For PCA reduced feature vector data of BGP feature extraction techniques, the RF classifier has also obtained much better classification accuracy (91.47±2.22%) with 75 features only compared to 86.27±1.37% classification accuracy produced by FFVD of BGP.

LDA classifier: Further, the LDA classifier has also been investigated with PCA reduced feature vector data and it has achieved a classification accuracy of 96.33±1.14% with 225 features of CoALBP24 feature extraction techniques. Further, the PCA reduced feature vector data of BGP feature extraction techniques has also achieved a classification accuracy of 95.87±1.25% using 210 features.

Table 2.5 Classification accuracy achieved using PCA based reduced feature vector data.

Technique	%CA±SD achieved by classifiers							
	NoF	Linear SVM	NoF	RBF kernel SVM	NoF	LDA	NoF	RF
GLCM	50	79.40±2.91	40	70.93±3.77	65	82.80±2.53	60	82.87±2.04
GLRLM	40	73.13±3.58	25	65.13±4.17	40	72.40±4.20	40	78.13±2.39
FOS	4	18.53±2.07	4	36.33±4.21	4	29.00±2.52	4	34.73±4.57
Gabor	115	93.33±1.63	115	90.22±3.11	110	94.20±1.14	115	93.93±1.73
LBP	200	89.87±2.53	175	87.93±1.73	250	87.80±1.63	100	84.60±2.94
LBP^{u2}	55	79.27±1.95	55	81.40±2.64	50	81.00±1.81	50	83.33±1.72
LBP^{ri}	35	77.07±3.45	30	78.93±3.33	35	76.00±3.47	30	77.40±1.49
LBP^{riu2}	8	58.80±3.51	8	66.00±2.81	8	56.47±4.55	9	68.60±3.78
LBP-HF	35	70.13±1.96	35	71.53±1.51	35	78.87±2.04	35	76.47±3.28
LPQ	125	90.27±2.31	200	87.13±2.33	105	89.93±3.29	75	88.33±3.67
GLAC	75	81.40±2.62	25	70.93±2.88	100	83.60±2.07	75	86.60±2.89
CSLBP	15	41.60±4.81	16	47.27±3.18	15	43.93±4.61	15	58.20±3.71
$CLBP^{u2}$	115	87.53±1.66	100	86.07±2.60	95	87.47±1.91	50	85.93±2.40
LDP	100	76.53±3.40	75	77.93±4.59	35	72.60±2.46	75	76.93±3.52
LTP^{u2}	115	87.67±2.90	100	87.47±2.20	115	88.73±1.35	75	89.27±0.97
LTP^{ri}	70	85.87±2.26	60	85.33±3.10	70	86.20±2.72	60	83.73±3.22
LTP^{riu2}	18	77.07±3.22	15	79.06±4.49	18	75.40±3.39	18	83.13±2.55
$ALBP^{u2}$	55	80.00±3.49	40	81.20±3.16	50	79.80±3.28	50	81.80±2.53
$ALBP^{ri}$	35	74.00±2.75	30	78.80±2.55	35	74.33±2.48	35	76.27±3.11
$ALBP^{riu2}$	9	55.20±3.39	9	67.27±2.78	9	57.27±2.52	9	68.00±3.69
LCP^{u2}	50	81.33±3.06	75	85.93±2.07	50	82.27±3.08	50	80.40±3.57
LCP^{ri}	60	78.46±3.57	50	77.33±2.47	50	83.67±2.10	60	80.06±1.95
LCP^{riu2}	60	82.80±2.81	75	82.13±2.45	50	86.27±2.07	60	85.33±2.79
BGP	**175**	**95.20±1.50**	**150**	**94.47±1.33**	**210**	**95.87±1.25**	**75**	**91.47±2.22**
LTCoP	200	90.53±2.22	175	86.47±2.09	125	89.73±1.10	50	87.00±1.81
CoALBP12	250	93.53±1.78	250	91.47±3.26	175	95.73±1.78	150	91.73±1.38
CoALBP24	300	94.67±1.75	225	91.53±3.00	**225**	**96.33±1.14**	125	93.60±2.36
CoALBP48	250	95.13±1.18	250	91.80±3.14	225	95.53±0.83	125	92.60±2.48
DenseCLBP	115	89.80±2.16	50	86.67±2.95	110	90.86±1.75	75	89.80±2.95

The feature vector data of BGP texture feature extraction techniques has achieved best classification accuracy with all the classifiers, whereas the FOS techniques has presented lowest classification accuracies. The classification accuracy obtained by the other feature extraction techniques have also been listed in Table 2.5. The results obtained by PCA based reduced feature dataset is compared with the FFVD. It is also evident from Table 2.5 that the PCA based reduced feature vector data has obtained classification accuracy which is

comparable to the classification accuracy achieved with FFVD. The RF classifier has demonstrated maximum rise in the classification accuracy for PCA based reduced feature vector data for all the state-of-the-art texture feature extraction techniques in comparison to their FFVD.

The comparison of classification accuracy achieved by four classifiers for state-of-the-art texture feature extraction techniques using PCA reduced feature vector data is presented in Fig. 2.14. Further, error bar plot with SD for the classification accuracy achieved by all the texture feature extraction techniques discussed in this chapter are shown in Fig. 2.15. In this case, the CoALBP24 has produced best classification accuracy (96.33±1.14%) with smaller value of SD, whereas, the BGP has also achieved a classification accuracy of 95.87±1.25% with smaller value of SD by using LDA classifier.

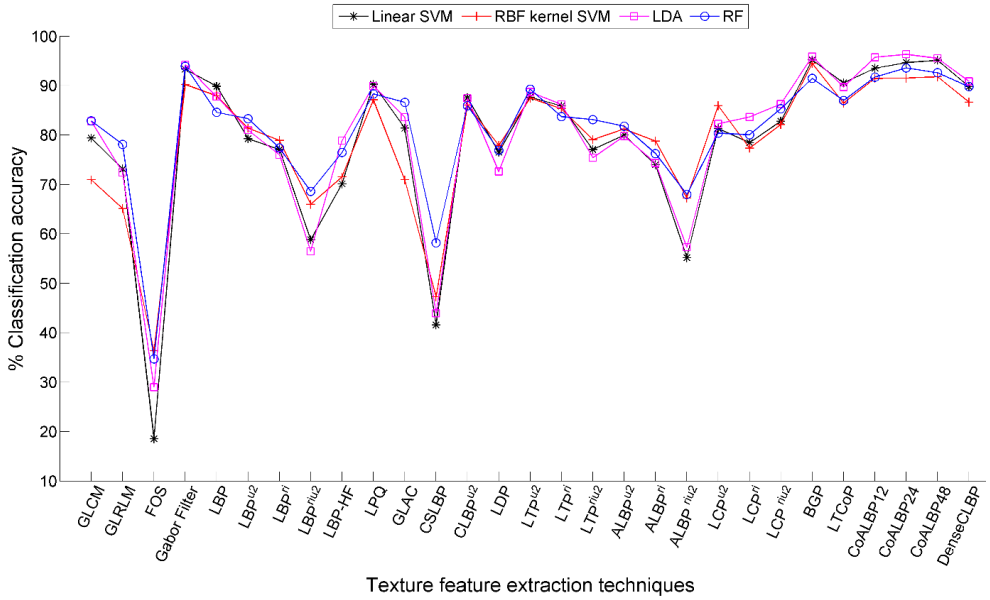

Fig. 2.14 Classification accuracy achieved using PCA reduced feature vector data.

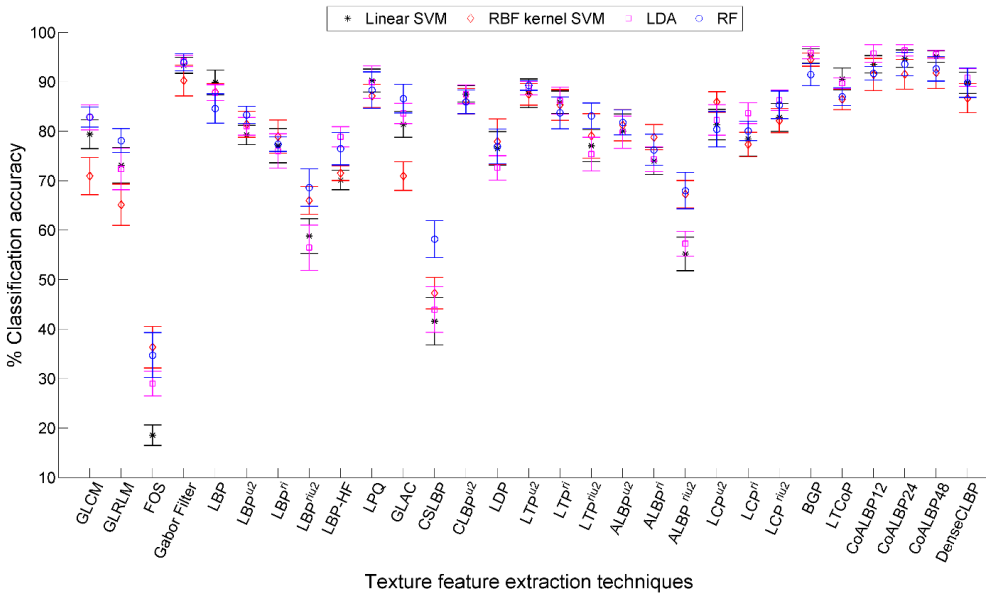

Fig. 2.15 Error bar plot with SD using PCA reduced feature vector data.

2.6.3.3 The mRMR feature selection based reduced feature vector data

The Table 2.6 enlists the classification accuracy results obtained by the state-of-the-art texture feature extraction techniques using mRMR feature selection based feature vector data.

Linear SVM classifier: Amongst the state-of-the-art texture feature extraction techniques, the best classification accuracy of 95.60±1.78% has been achieved with mRMR processed subset (200 features) of FFVD of BGP technique. This classification accuracy is slightly lesser than 95.93±1.52% accuracy obtained by FFVD (216 features) of BGP technique.

Table 2.6 Classification accuracy achieved using mRMR feature selection based reduced feature vector data.

Technique	% CA±SD achieved by classifiers					
	NoF	Linear SVM	NoF	RBF kernel SVM	NoF	RF
GLCM	60	80.80±3.45	60	73.47±3.05	70	55.27±4.30
GLRLM	40	74.33±3.57	40	61.60±4.12	40	47.53±2.18
FOS	4	16.73±1.79	4	36.20±2.93	4	34.47±3.81
Gabor	100	93.67±1.64	100	91.07±2.39	75	79.93±2.36
LBP	250	89.53±3.06	225	87.40±1.92	150	71.27±3.51
LBP^{u2}	55	76.93±3.31	55	79.73±2.54	55	69.07±3.59
LBP^{ri}	35	76.33±2.51	35	78.53±3.01	30	54.26±4.36
LBP^{riu2}	9	59.80±3.76	9	64.67±2.96	9	42.67±4.23
LBP-HF	37	71.80±2.37	37	71.13±1.89	37	64.40±5.28
LPQ	255	90.67±1.94	175	86.87±2.11	175	72.53±2.72
GLAC	100	83.27±3.09	100	66.27±3.80	100	52.47±5.81
CSLBP	15	42.00±2.88	15	46.87±4.10	15	38.07±3.89
$CLBP^{u2}$	115	87.20±2.53	115	85.40±2.54	115	73.87±2.39
LDP	75	76.80±2.10	125	78.33±3.52	175	59.80±4.09
LTP^{u2}	115	87.40±3.12	115	87.00±2.52	75	75.13±2.67
LTP^{ri}	72	86.87±2.18	70	85.73±2.52	30	63.13±3.63
LTP^{riu2}	18	79.93±2.46	18	78.20±2.01	18	56.00±3.91
$ALBP^{u2}$	55	78.00±3.53	55	80.33±3.05	50	68.73±4.54
$ALBP^{ri}$	35	75.00±2.02	35	77.07±2.27	35	55.87±4.56
$ALBP^{riu2}$	10	62.00±3.30	9	63.60±4.03	9	43.20±1.96
LCP^{u2}	75	79.93±3.33	70	83.47±3.17	60	75.60±2.07
LCP^{ri}	50	79.47±2.84	50	80.87±3.39	50	71.27±3.49
LCP^{riu2}	70	82.27±2.60	25	83.60±2.65	60	74.80±2.88
BGP	**200**	**95.60±1.78**	**175**	**94.47±2.16**	**75**	**88.80±1.85**
LTCoP	225	90.40±2.11	200	86.33±2.16	125	69.27±3.56
CoALBP12	400	92.93±2.18	300	90.47±2.09	225	82.73±3.36
CoALBP24	450	94.80±1.43	300	91.33±1.51	175	85.13±3.03
CoALBP48	400	94.47±1.00	300	92.20±0.83	150	87.07±1.84
DenseCLBP	115	89.33±1.47	115	86.67±2.37	75	76.40±2.46

RBF kernel SVM classifier: The mRMR selected feature subset (175 features) of BGP texture feature extraction technique has achieved the best classification accuracy of 94.47±2.16%, which is relatively better than 94.13±2.24% classification accuracy obtained by FFVD (216 features) of BGP technique.

RF classifier: The RF classifier has achieved the best classification accuracy of 88.80±1.85% for mRMR selected feature subset (75 features) of BGP texture feature extraction technique.

This accuracy is reasonably better than the highest classification accuracy (86.27±1.37%) obtained by the FFVD (216 features) of BGP technique.

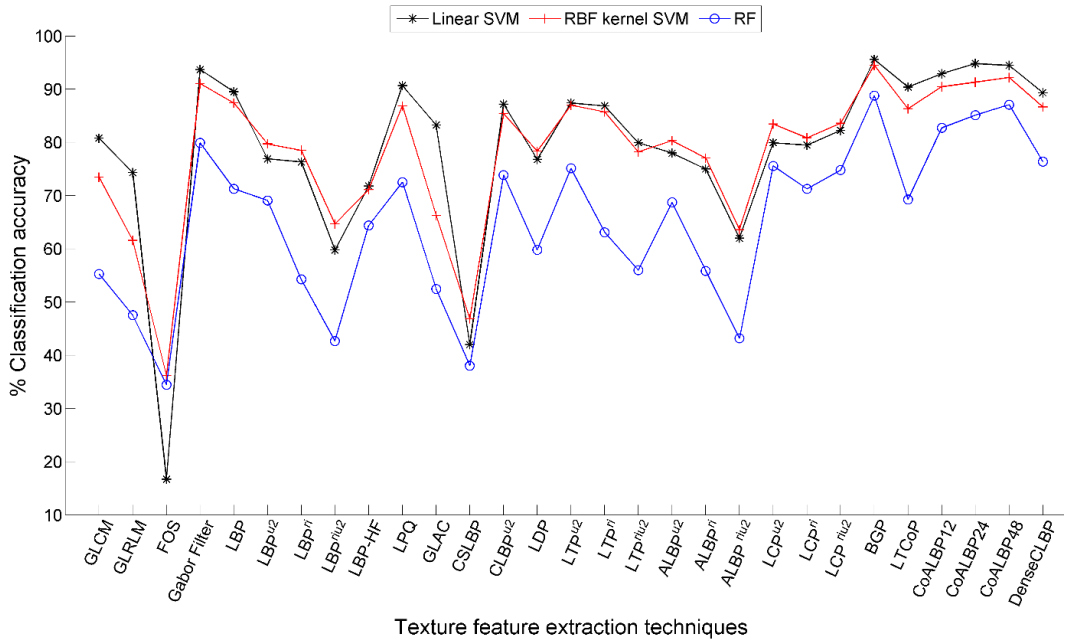

Fig. 2.16 Classification accuracy achieved using mRMR feature selection based reduced feature data.

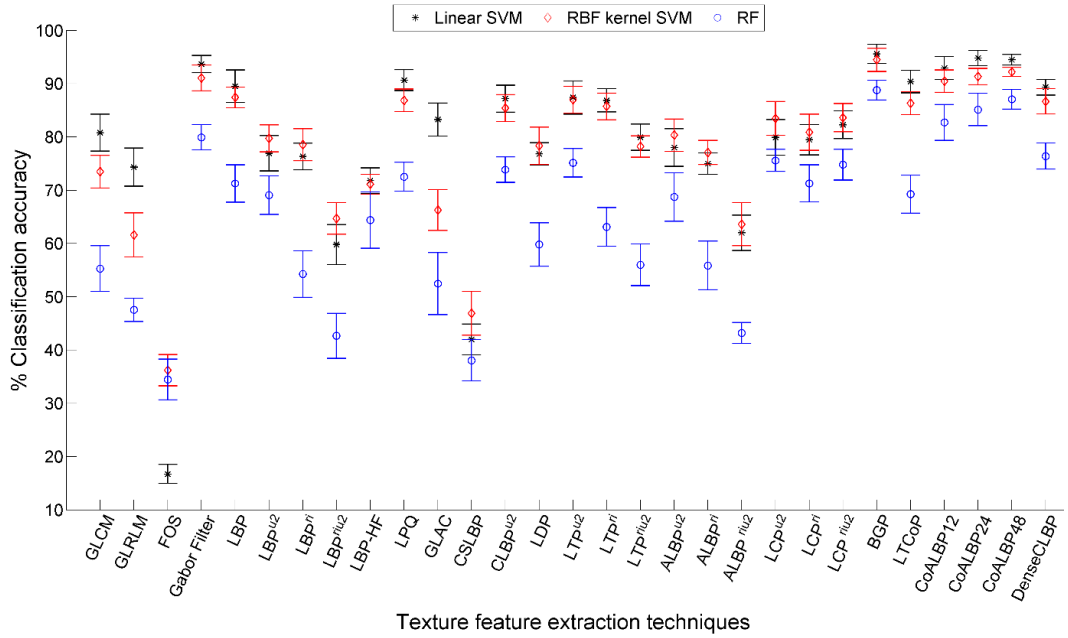

Fig. 2.17 Error bar plot with SD using mRMR feature selection based reduced feature vector data.

The classification accuracy results achieved by other texture feature extraction techniques are listed in Table 2.6. The classification accuracy results achieved by mRMR feature selection based BGP texture features are much closer to the results obtained by FFVD and PCA based reduced feature vector data of BGP techniques using linear SVM and RBF kernel SVM classifiers. The RF classifier, on the other hand has produced relatively better

classification accuracy as compared to FFVD, and relatively lower classification accuracy compared to PCA based reduced feature vector data for BGP feature extraction technique.

The graphical representation of state-of-the-art texture feature extraction techniques for mRMR feature selection based reduced feature vector data of state-of-the-art texture feature extraction techniques are illustrated in Fig. 2.16. The linear SVM classifier seems to be outperforming rest of the classifiers for all the feature extraction techniques. In Fig. 2.17, the error bar plot with SD using mRMR feature selection based reduced feature vector data has been presented. It is evident from Fig. 2.17 that for mRMR feature selection based reduced feature vector data, BGP has achieved lowest SD value. Further, BGP has marginally outperformed COALBP12, COALBP24, COALBP48, Gabor filter and LPQ techniques.

2.6.4 Performance Evaluation of State-of-the-art Texture Feature Extraction Techniques using Randomly Divided Database (RDD)

2.6.4.1 Full feature vector data (FFVD)

The classification accuracy achieved by state-of-the-art texture feature extraction techniques for different ratios of training and testing data is listed in Table 2.7.

Linear SVM classifier: Amongst the studied texture feature extraction techniques, FFVD of BGP technique yields best classification accuracy of 94.33%, 88%, 85.33% and 82.40% for 80/20, 70/30, 60/40 and 50/50 proportions of training and testing data of RDD, respectively. The 2nd best classification accuracy has been attained by FFVD of COALBP48 technique, whereas FFVD of Gabor filter technique attains the 3rd best classification accuracy. Similar to above, the FFVD of FOS texture feature extraction technique has resulted into lowest classification accuracy. The classification accuracy achieved by other texture feature extraction techniques are also listed in Table 2.7 for comparison purpose.

RBF kernel SVM classifier: The feature vector data produced by BGP texture feature extraction technique has obtained best classification accuracy of 88%, 87.33% and 83% for 80/20, 70/30 and 60/40 proportions of training and testing data of RDD, respectively. Further, the feature vector data obtained by COALBP48 texture feature extraction technique has given the best classification accuracy of 79.33% for 50/50 proportions of training and testing data of RDD. The classification accuracy achieved by other texture feature extraction techniques are also listed in Table 2.7.

RF classifier: In case of RF classifier, again the BGP texture features have achieved best classification accuracy of 82.33% and 79.33% for 80/20 and 70/30 training and testing ratios of RDD. The FFVD of COALBP48 technique, however has achieved maximum classification accuracy of 76.33% and 73.87% for 60/40 and 50/50 training and testing ratios of RDD, respectively, which is also listed in Table 2.7.

Table 2.7 Classification accuracy achieved by full feature vector data for different proportions of training and testing data of RDD using three classifiers.

Technique	% CA achieved by classifiers for different proportions of training and testing data											
	LSVM				RBF kernel SVM				RF			
	80/20	70/30	60/40	50/50	80/20	70/30	60/40	50/50	80/20	70/30	60/40	50/50
GLCM	76.33	75.33	69.00	67.47	67.00	65.11	62.00	61.07	50.00	47.56	47.33	46.67
GLRLM	70.67	64.44	60.17	59.47	61.67	54.89	52.17	50.80	42.67	39.56	38.67	37.07
FOS	10.66	10.88	12.66	10.53	28.67	24.44	23.67	24.00	27.67	22.67	21.33	22.33
Gabor	87.00	84.44	82.50	80.80	84.00	81.33	76.00	73.47	72.00	68.44	64.67	64.40
LBP	83.67	80.22	75.83	70.67	78.33	72.67	68.33	65.60	60.33	54.44	53.67	52.13
LBP^{u2}	74.67	68.00	66.50	62.13	71.67	66.00	61.67	57.87	60.00	51.78	50.00	46.53
LBP^{ri}	68.00	69.55	66.33	63.60	69.00	66.89	64.00	60.27	45.67	41.78	41.50	34.93
LBP^{riu2}	61.00	57.11	55.00	54.13	63.67	58.67	57.83	53.33	36.00	33.78	35.00	32.00
LBP-HF	65.67	58.00	55.00	50.93	65.67	58.44	52.50	49.33	57.00	51.56	51.67	48.00
LPQ	83.67	77.78	74.50	72.40	78.67	71.78	67.50	63.60	62.33	54.44	51.67	49.87
GLAC	77.33	73.11	68.00	66.40	64.00	59.56	56.00	49.60	40.67	34.22	37.17	35.20
CSLBP	33.00	32.22	31.33	29.33	35.67	34.44	34.16	31.60	27.67	24.89	25.33	22.53
$CLBP^{u2}$	79.00	74.89	72.50	68.53	76.00	70.67	67.17	63.60	61.67	57.33	57.50	55.60
LDP	71.33	68.67	62.83	61.33	70.00	63.33	58.17	56.67	49.67	42.44	42.33	40.93
LTP^{u2}	83.00	79.56	75.17	74.40	79.33	72.67	68.00	67.60	66.67	62.00	60.17	57.60
LTP^{ri}	83.67	80.89	79.00	76.13	80.00	75.77	73.67	70.40	59.67	54.22	50.83	46.53
LTP^{riu2}	74.67	71.78	70.00	67.33	72.67	72.00	69.17	65.60	49.00	47.33	46.50	42.93
$ALBP^{u2}$	74.00	68.44	66.00	61.33	74.67	65.56	60.50	58.00	60.33	51.78	50.67	47.87
$ALBP^{ri}$	70.00	68.00	64.00	61.60	70.67	66.89	64.50	61.73	50.33	47.33	43.33	39.07
$ALBP^{riu2}$	53.33	50.67	50.83	50.13	59.67	52.22	52.33	50.13	49.67	47.11	42.33	40.27
LCP^{u2}	76.00	69.33	65.00	62.40	76.00	70.67	70.33	64.67	68.67	61.78	57.67	55.60
LCP^{ri}	70.67	64.89	64.00	61.33	66.67	64.89	64.83	57.07	63.00	56.44	56.67	52.13
LCP^{riu2}	74.33	71.56	68.83	66.67	70.00	69.33	65.50	61.60	63.33	61.11	59.17	55.87
BGP	**94.33**	**88.00**	**85.33**	**82.40**	**88.00**	**87.33**	**83.00**	78.80	**82.33**	**79.33**	75.50	71.73
LTCoP	85.00	79.33	76.83	73.33	75.00	70.89	67.83	64.93	60.33	53.33	51.33	52.00
CoALBP12	88.67	84.44	81.33	77.47	85.33	80.00	74.50	71.87	71.33	64.89	63.50	60.93
CoALBP24	89.67	86.89	82.33	80.80	85.33	82.00	76.67	72.93	77.67	73.56	68.67	65.47
CoALBP48	90.33	86.44	85.50	84.53	85.33	83.33	80.83	**79.33**	80.33	76.44	**76.33**	**73.87**
DenseCLBP	84.33	79.78	75.50	72.40	82.00	74.89	69.50	68.27	68.67	64.67	60.17	59.87

The graphical illustration for 80/20, 70/30, 60/40 and 50/50 training and testing data ratios of RDD is given in Fig. 2.18, Fig. 2.19, Fig. 2.20, and Fig. 2.21, respectively. It is clearly visible from these figures that the FFVD of BGP texture feature extraction techniques has established its superiority amongst other feature extraction techniques for RDD.

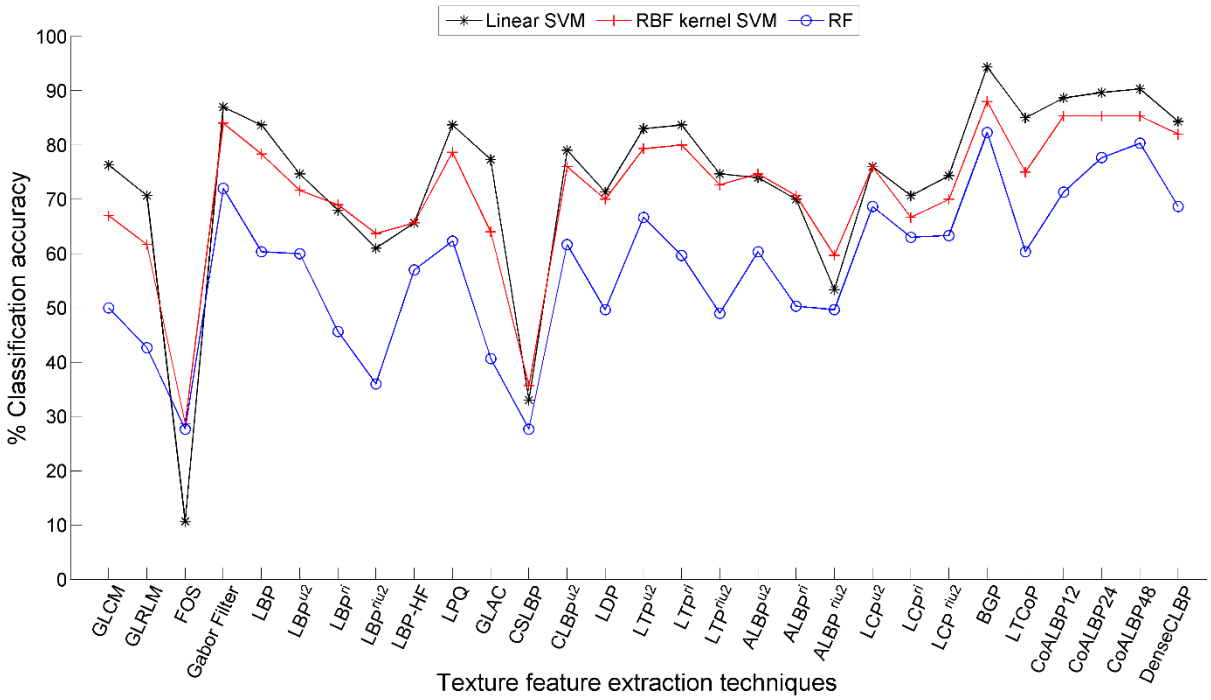

Fig. 2.18 Classification accuracy achieved for 80/20 proportion of training and testing data of RDD.

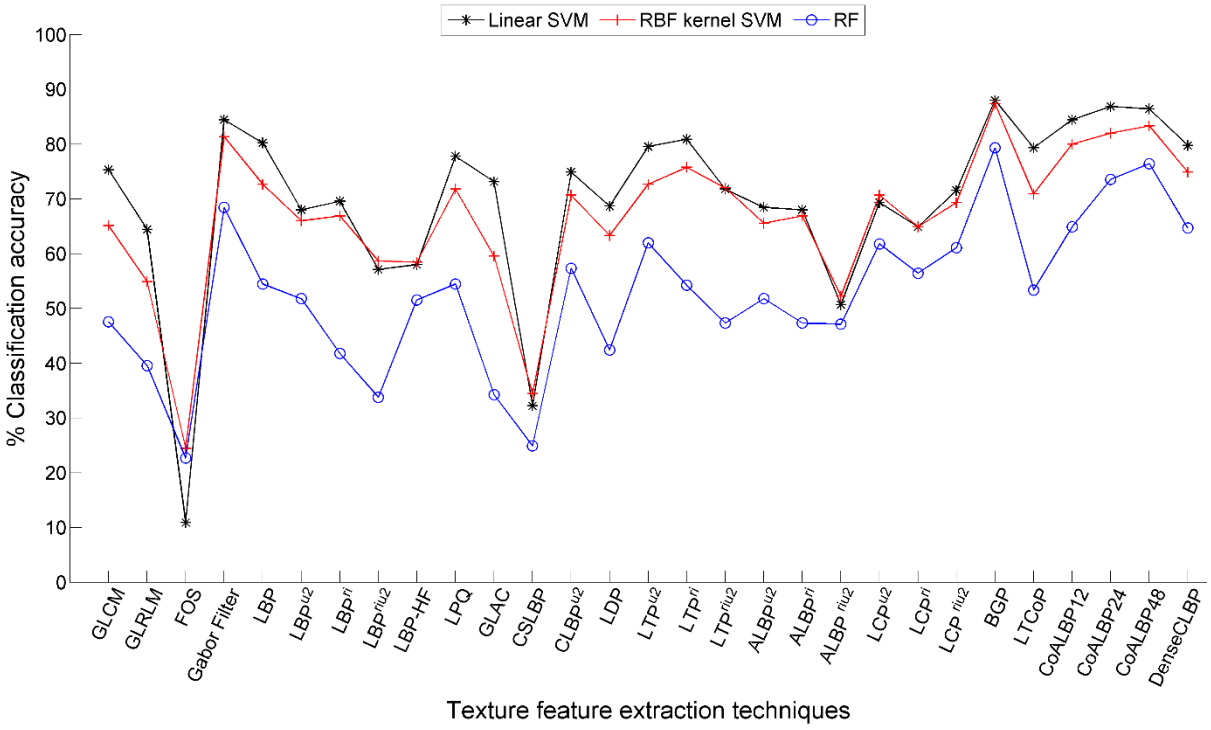

Fig. 2.19 Classification accuracy achieved for 70/30 proportion of training and testing data of RDD.

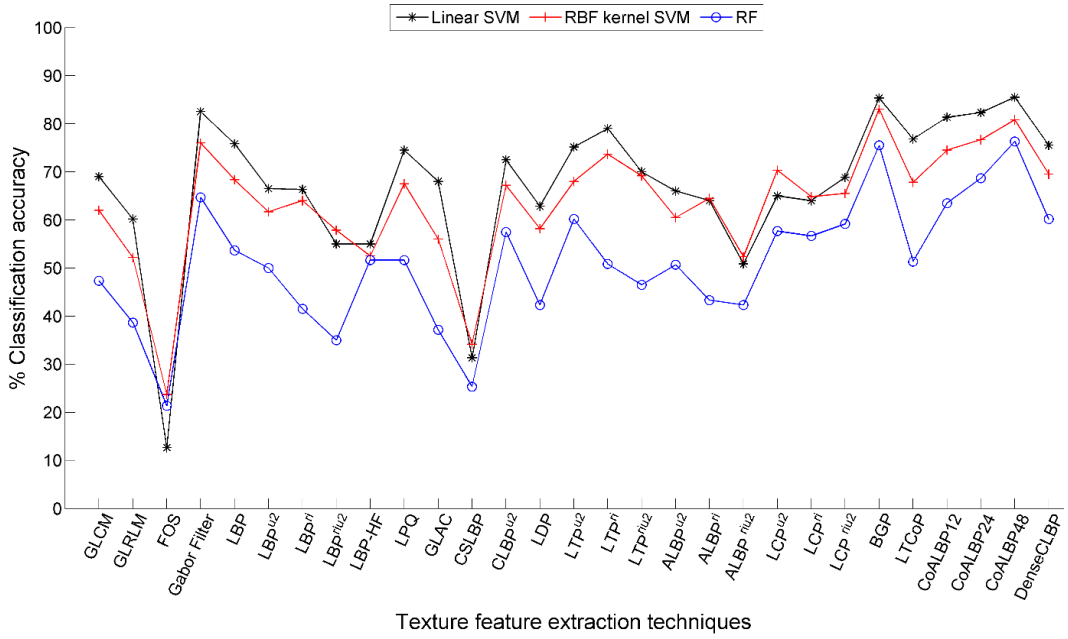

Fig. 2.20 Classification accuracy achieved for 60/40 proportion of training and testing data of RDD.

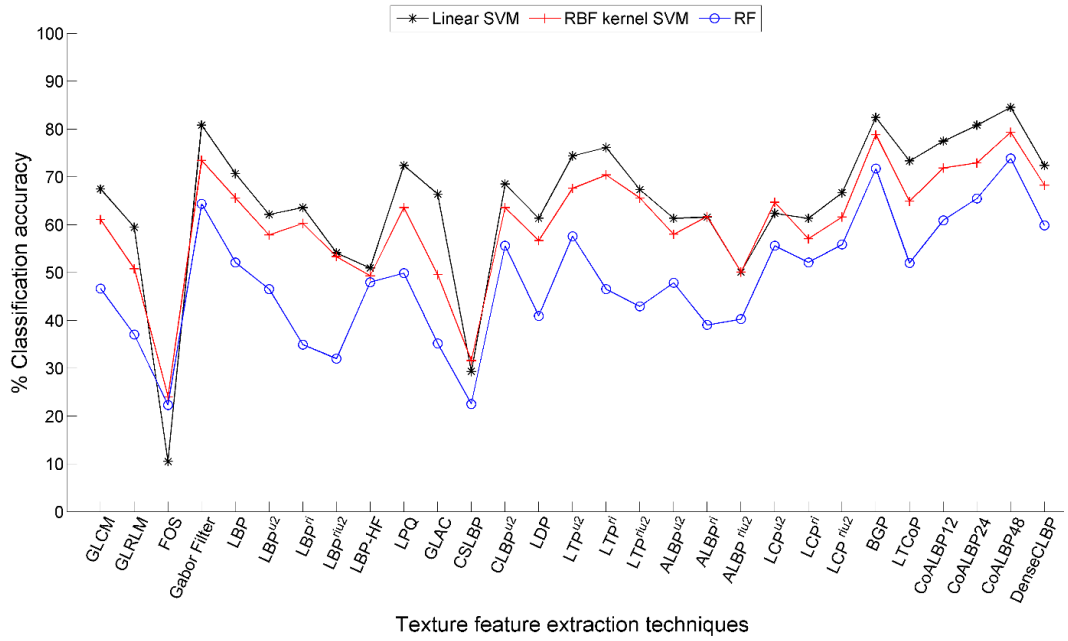

Fig. 2.21 Classification accuracy achieved for 50/50 proportion of training and testing data of RDD.

2.6.4.2 The PCA dimensionality reduced feature vector data

The classification accuracy results obtained by the PCA based reduced feature vector data by linear SVM, RBF kernel SVM, RF and LDA classifier has been listed in Table 2.8, Table 2.9, Table 2.10 and Table 2.11 respectively.

Linear SVM classifier: The PCA reduced feature vector data of BGP technique has produced the best classification accuracy of 92.33% (125 features), 87.56% (175 features) and 85.50% (175 features) for 80/20, 70/30 and 60/40 training and testing ratios of RDD, respectively. In addition, the PCA reduced feature vector data of COALBP48 technique has achieved the best

classification accuracy of 84.40% (225 features) for 50/50 training and testing ratio of RDD (Table 2.8).

Table 2.8 Classification accuracy achieved by PCA reduced feature vector data for different proportions of training and testing data of RDD using linear SVM classifier.

Technique	NoF	80/20	NoF	70/30	NoF	60/40	NoF	50/50
GLCM	50	76.67	50	75.77	50	69.83	50	68.40
GLRLM	35	70.33	30	65.78	35	61.17	40	59.47
FOS	4	18.33	4	18.22	4	18.50	4	19.20
Gabor	100	87.33	100	85.33	100	83.67	100	80.67
LBP	150	84.00	175	79.33	150	75.67	200	70.93
LBP^{u2}	58	76.00	58	67.78	58	65.12	50	62.27
LBP^{ri}	30	72.67	35	71.33	35	68.50	30	65.20
LBP^{riu2}	9	52.00	9	51.56	9	47.66	9	45.20
LBP-HF	37	64.00	37	58.00	37	56.33	37	52.00
LPQ	175	82.67	175	76.40	200	74.50	75	71.47
GLAC	75	76.33	100	72.67	100	68.33	100	65.47
CSLBP	16	31.33	12	30.22	12	30.50	12	28.93
$CLBP^{u2}$	110	82.00	110	76.00	115	73.67	115	69.87
LDP	75	69.00	75	67.78	75	63.67	75	61.33
LTP^{u2}	75	83.67	50	77.78	115	74.83	115	73.20
LTP^{ri}	65	80.00	70	78.89	65	79.33	65	75.60
LTP^{riu2}	18	74.33	18	72.00	18	69.83	18	66.13
$ALBP^{u2}$	50	74.33	40	68.44	55	67.17	55	62.53
$ALBP^{ri}$	30	69.33	35	68.22	35	65.00	35	62.67
$ALBP^{riu2}$	9	54.67	9	53.78	9	52.33	9	49.47
LCP^{u2}	60	77.67	70	70.89	70	66.67	50	62.93
LCP^{ri}	60	70.33	60	66.89	60	64.67	60	62.13
LCP^{riu2}	50	75.67	70	71.33	70	70.00	50	67.73
BGP	**125**	**92.33**	**175**	**87.56**	**175**	**85.50**	100	82.80
LTCoP	175	83.00	150	80.22	175	77.50	225	72.53
CoALBP12	200	88.67	250	84.22	250	81.00	450	77.87
CoALBP24	250	89.67	225	87.33	300	82.33	150	80.80
CoALBP48	225	90.33	175	86.89	225	84.50	**225**	**84.40**
DenseCLBP	100	84.67	110	79.33	110	75.33	100	72.27

RBF kernel SVM classifier: The PCA reduced feature vector data of BGP technique has produced the best classification accuracy of 88.33% (100 features), 87.33% (200 features), and 82.83% (125 features) for 80/20, 70/30 and 60/40 training and testing ratios of RDD, respectively. Further, PCA reduced feature vector data of COALBP48 technique has achieved the best classification accuracy of 79.60% (400 features), for 50/50 training and testing ratios of RDD (Table 2.9).

Table 2.9 Classification accuracy achieved by PCA reduced feature vector data for different proportions of training and testing data of RDD using RBF kernel SVM classifier.

Technique	NoF	80/20	NoF	70/30	NoF	60/40	NoF	50/50
GLCM	70	67.67	50	66.44	50	62.17	60	60.93
GLRLM	30	63.00	40	56.44	30	52.50	40	51.73
FOS	3	29.67	3	27.77	3	27.83	3	26.00
Gabor	100	84.33	118	81.78	110	75.67	100	73.47
LBP	150	79.00	175	73.33	150	68.50	225	65.60
LBP^{u2}	50	72.00	58	66.44	58	61.33	58	58.13
LBP^{ri}	20	71.00	35	68.22	30	65.33	35	61.46
LBP^{riu2}	9	65.33	9	56.89	9	55.67	9	51.60
LBP-HF	37	66.33	30	58.67	37	52.17	37	49.33
LPQ	125	79.00	100	71.78	150	67.17	100	63.47
GLAC	75	63.67	100	60.44	50	55.67	100	49.87
CSLBP	15	37.67	15	34.22	15	33.17	15	32.53
$CLBP^{u2}$	100	76.33	100	70.89	115	67.17	115	64.00
LDP	125	70.67	200	63.33	250	58.00	225	56.80
LTP^{u2}	75	80.67	75	72.89	100	68.17	100	68.13
LTP^{ri}	70	80.00	60	75.56	70	73.33	70	70.80
LTP^{riu2}	18	73.00	15	70.67	15	68.33	18	66.40
$ALBP^{u2}$	45	74.00	50	66.00	50	60.50	45	57.87
$ALBP^{ri}$	35	72.00	35	68.44	25	65.00	35	62.53
$ALBP^{riu2}$	9	62.67	9	55.56	9	55.50	9	51.20
LCP^{u2}	60	76.33	70	70.44	50	70.33	50	65.20
LCP^{ri}	70	68.33	50	65.56	50	64.67	70	58.27
LCP^{riu2}	60	71.00	50	70.00	50	66.50	50	61.87
BGP	**100**	**88.33**	**200**	**87.33**	**125**	**82.83**	125	78.93
LTCoP	75	77.67	100	71.78	150	67.83	200	64.93
CoALBP12	250	85.67	250	80.00	200	74.67	400	72.40
CoALBP24	75	86.00	150	82.22	400	74.67	300	73.20
CoALBP48	125	86.33	100	83.55	250	80.67	**400**	**79.60**
DenseCLBP	50	82.00	75	75.11	50	70.17	100	68.53

RF classifier: The PCA reduced feature vector data of COALBP48 technique has produced the best classification accuracy of 88.33% (200 features), 84.44% (75 features), 83.17% (125 features) and 82.27% (100 features) for 80/20, 70/30, 60/40 and 50/50 training and testing ratios of RDD, respectively (Table 2.10).

LDA classifier: The PCA reduced feature vector data of BGP technique has produced the best classification accuracy of 92.00% (210 features), 90.20% (125 features), 89% (75 features) and 85.73% (100 features) for 80/20, 70/30, 60/40 and 50/50 training and testing ratios of randomly divided database, respectively (Table 2.11).

Table 2.10 Classification accuracy achieved by PCA reduced feature vector data for different proportions of training and testing data of RDD using RF classifier.

Technique	NoF	80/20	NoF	70/30	NoF	60/40	NoF	50/50
GLCM	60	78.67	60	76.00	60	72.83	60	70.67
GLRLM	35	75.00	30	67.33	40	66.00	40	64.80
FOS	4	29.67	4	30.44	4	29.83	4	29.46
Gabor	110	89.67	50	86.22	50	84.17	110	81.60
LBP	50	79.00	100	71.11	50	68.33	75	66.27
LBP^{u2}	55	76.33	35	68.22	55	65.17	45	61.87
LBP^{ri}	30	68.00	35	64.44	25	63.83	25	61.20
LBP^{riu2}	9	63.33	9	56.67	9	55.50	9	54.40
LBP-HF	35	68.67	35	63.33	35	60.50	35	57.60
LPQ	125	82.00	75	73.56	75	73.00	50	68.80
GLAC	100	81.33	75	73.78	75	69.83	50	66.93
CSLBP	15	43.00	15	44.44	15	42.83	15	39.47
$CLBP^{u2}$	50	79.33	50	73.11	75	69.83	75	65.47
LDP	75	68.00	50	64.00	50	61.50	75	58.00
LTP^{u2}	75	81.67	110	75.78	110	71.00	50	68.93
LTP^{ri}	50	76.00	50	74.89	25	72.50	25	68.67
LTP^{riu2}	18	76.33	15	72.44	18	70.67	18	67.60
$ALBP^{u2}$	55	74.00	50	68.89	45	62.33	35	61.47
$ALBP^{ri}$	35	68.33	35	65.78	35	62.50	35	60.13
$ALBP^{riu2}$	9	61.67	9	55.11	9	55.00	9	52.93
LCP^{u2}	60	72.33	50	65.33	60	63.50	60	60.67
LCP^{ri}	70	71.67	60	69.56	60	68.50	60	63.07
LCP^{riu2}	75	80.33	60	75.11	60	73.33	60	72.00
BGP	50	86.00	100	82.89	50	81.17	100	80.40
LTCoP	100	79.67	75	74.00	50	73.50	75	71.20
CoALBP12	125	83.67	150	80.22	150	78.33	100	74.27
CoALBP24	125	86.67	100	82.44	150	80.50	150	77.20
CoALBP48	**200**	**88.33**	**75**	**84.44**	**125**	**83.17**	**100**	**82.27**
DenseCLBP	115	82.67	75	78.44	100	74.33	75	72.53

It is observed that in most of the cases, the PCA reduced feature vector data of BGP technique yields best classification accuracy amongst the state-of-the-art texture feature extraction techniques. The PCA reduced feature vector data of COALBP48 technique closely follows the results produced by BGP technique. The least classification accuracy has been reported for PCA reduced feature vector data of FOS technique amongst all the texture feature extraction techniques examined here, for hardwood species database classification.

The graphical illustration for 80/20, 70/30, 60/40 and 50/50 training and testing data ratios of RDD is given in Fig. 2.22, Fig. 2.23, Fig. 2.24 and Fig. 2.25, respectively. It is clearly visible from these figures that the PCA reduced feature vector data of BGP texture feature extraction technique has established its superiority over other feature extraction techniques for RDD. It is worth noting that amongst all the four classifiers, the PCA reduced feature vector data has given better performance with linear SVM classifier for most of the texture feature extraction

techniques considered in this discussion. However, RF classifier yields relatively lower classification accuracy in comparison to other three classifiers. Though, PCA reduced feature vector data has achieved relatively lower classification accuracy compared to FFVD, but these accuracies were obtained using smaller number of feature vector data compared to full feature vector data, requiring less computation time in classification.

Table 2.11 Classification accuracy achieved by PCA reduced feature vector data for different proportions of training and testing data of RDD using LDA classifier.

Technique	NoF	80/20	NoF	70/30	NoF	60/40	NoF	50/50
GLCM	50	77.67	60	75.33	40	74.00	60	73.20
GLRLM	35	69.67	35	65.33	44	65.67	40	64.80
FOS	4	27.33	4	26.22	4	28.00	4	27.20
Gabor	75	91.33	118	89.33	75	86.17	75	85.60
LBP	125	81.33	200	76.89	100	75.00	100	74.40
LBP^{u2}	40	78.33	40	70.44	50	68.00	20	61.86
LBP^{ri}	35	71.33	35	68.89	35	66.33	35	65.07
LBP^{riu2}	9	54.67	9	50.67	9	53.00	9	52.40
LBP-HF	37	76.00	37	72.00	37	71.17	37	69.60
LPQ	125	84.00	200	78.22	125	77.16	125	74.00
GLAC	75	78.67	75	72.67	75	70.00	100	68.00
CSLBP	15	35.67	15	33.33	15	30.00	10	28.67
$CLBP^{u2}$	75	83.33	75	79.11	75	75.50	75	71.33
LDP	30	63.33	30	61.78	30	60.50	30	59.33
LTP^{u2}	75	84.33	115	80.00	50	77.17	50	74.00
LTP^{ri}	40	80.00	50	78.00	60	77.67	60	76.40
LTP^{riu2}	15	72.00	15	67.56	15	66.50	15	64.67
$ALBP^{u2}$	50	75.33	55	69.56	55	68.00	40	64.67
$ALBP^{ri}$	25	69.00	25	67.78	35	66.00	35	64.67
$ALBP^{riu2}$	9	55.33	9	51.78	9	52.00	9	51.33
LCP^{u2}	54	79.67	50	73.56	54	71.67	54	69.20
LCP^{ri}	54	80.33	54	77.33	54	77.00	54	75.87
LCP^{riu2}	54	85.67	54	80.44	54	79.83	54	77.20
BGP	**210**	**92.00**	**125**	**90.22**	**75**	**89.00**	**100**	**85.73**
LTCoP	200	84.33	100	81.56	100	80.50	100	78.67
CoALBP12	225	90.00	200	88.44	200	86.67	150	83.87
CoALBP24	250	92.00	225	90.22	250	87.50	225	84.13
CoALBP48	175	90.00	125	88.67	150	87.33	150	85.33
DenseCLBP	75	85.33	50	80.89	50	78.17	50	76.27

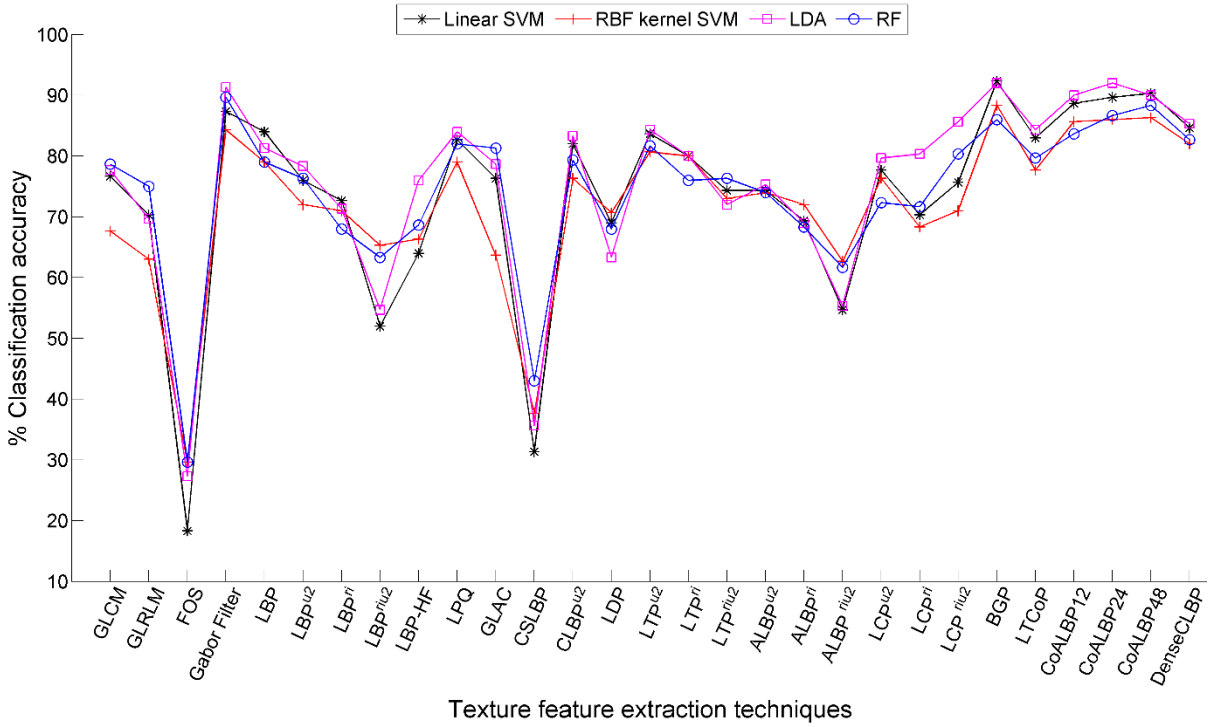

Fig. 2.22 Classification accuracy achieved for 80/20 proportion of training and testing data of RDD.

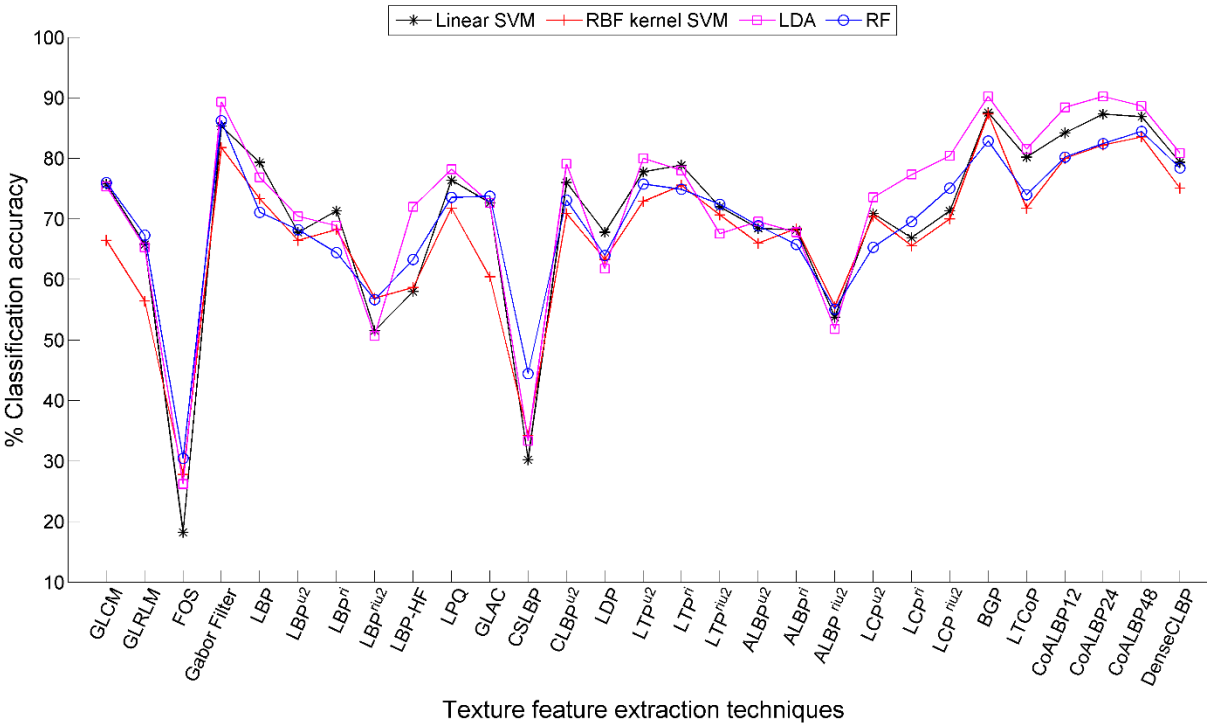

Fig. 2.23 Classification accuracy achieved for 70/30 proportion of training and testing data of RDD.

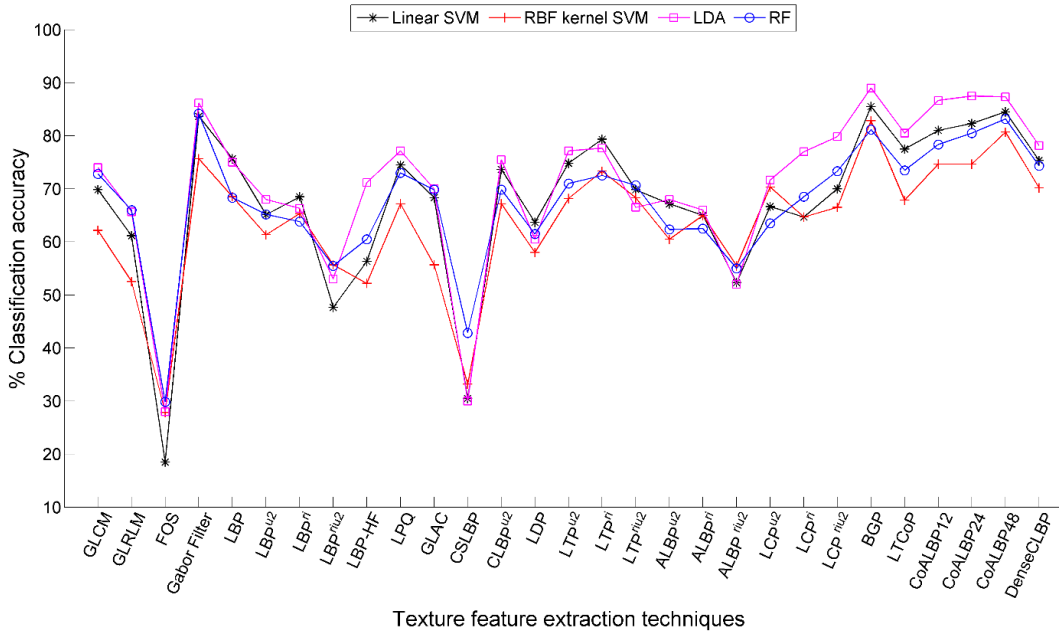

Fig. 2.24 Classification accuracy achieved for 60/40 proportion of training and testing data of RDD.

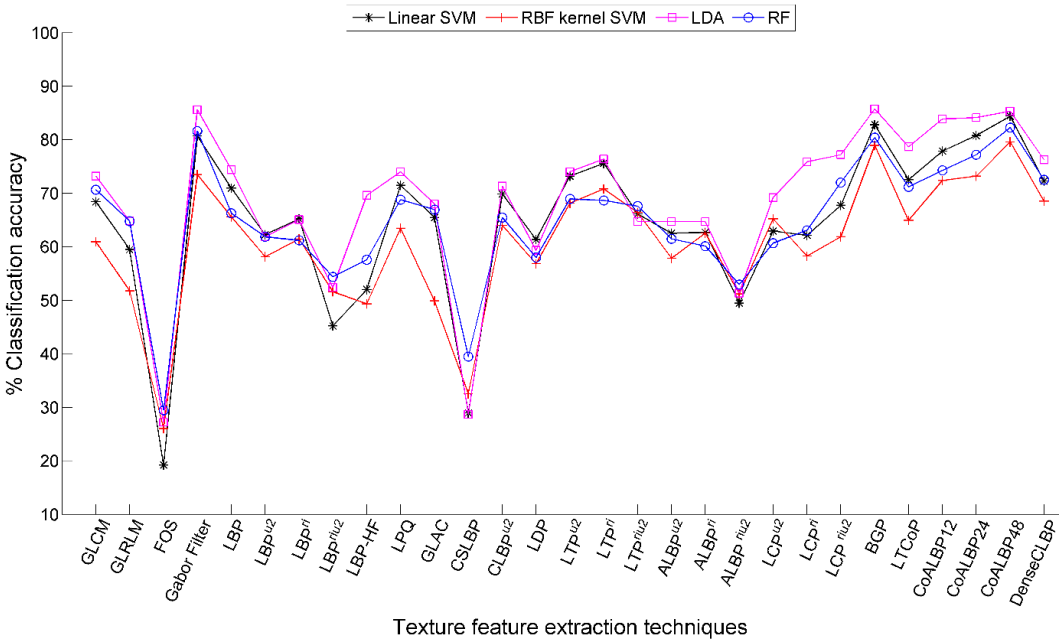

Fig. 2.25 Classification accuracy achieved for 50/50 proportion of training and testing data of RDD.

2.6.4.3 The mRMR feature selection based reduced feature vector data

The classification accuracy results obtained by the mRMR feature selection based reduced feature vector data of RDD through linear SVM, RBF kernel SVM and RF classifiers has been presented in Table 2.12, Table 2.13 and Table 2.14, respectively.

Linear SVM classifier: The mRMR feature selection based reduced feature vector data of BGP technique yields the best classification accuracy of 92.67% (200 features), 88.67% (150 features), 86.67% (150 features) and 84% (150 features) for 80/20, 70/30, 60/40 and 50/50 training and testing ratios of RDD, respectively (Table 2.12). The 2nd best classification accuracy

has been presented by mRMR feature selection based reduced feature vector data of CoALBP48 technique as listed in Table 2.12.

RBF kernel SVM classifier: The mRMR feature selection based reduced feature vector data of BGP technique has yet again produced the best classification accuracy of 89% (150 features), 87.11% (150 features) and 84.50% (150 features) for 80/20, 70/30 and 60/40 training and testing ratios of RDD, respectively. Further, the mRMR feature selection based reduced feature vector data of COALBP48 technique has achieved best classification accuracy of 81.47% (200 features) for 50/50 training and testing ratios of randomly divided database (Table 2.13).

Table 2.12 Classification accuracy achieved by mRMR feature selection based reduced feature vector data for different proportions of training and testing data of RDD using linear SVM classifier.

Technique	NoF	80/20	NoF	70/30	NoF	60/40	NoF	50/50
GLCM	70	76.00	70	75.33	70	69.50	70	67.60
GLRLM	30	57.00	40	52.89	35	51.83	35	49.47
FOS	4	16.67	4	16.00	4	16.00	4	14.80
Gabor	115	86.67	115	85.11	110	82.50	110	80.80
LBP	250	83.33	250	80.44	250	76.17	250	71.33
LBP^{u2}	55	72.33	55	66.00	55	64.67	50	60.40
LBP^{ri}	35	71.33	35	65.56	35	63.33	35	59.60
LBP^{riu2}	9	61.00	9	57.11	9	53.67	9	54.13
LBP-HF	37	66.67	37	57.55	37	52.33	37	50.80
LPQ	175	84.33	175	79.33	175	74.67	175	72.93
GLAC	100	75.67	100	73.11	100	68.50	100	66.67
CSLBP	15	33.00	15	32.89	15	31.50	15	30.93
$CLBP^{u2}$	75	79.67	115	75.78	100	73.13	100	69.07
LDP	125	71.33	125	68.67	125	62.83	125	61.33
LTP^{u2}	100	83.67	100	79.33	100	76.17	115	73.33
LTP^{ri}	70	82.33	70	79.78	70	78.33	70	76.00
LTP^{riu2}	18	75.00	18	71.33	18	69.33	18	66.00
$ALBP^{u2}$	55	72.00	55	67.33	55	65.67	55	60.93
$ALBP^{ri}$	35	70.33	35	67.33	35	65.00	35	63.87
$ALBP^{riu2}$	9	50.00	9	50.22	9	48.50	9	48.27
LCP^{u2}	70	74.47	75	71.56	75	64.67	70	62.67
LCP^{ri}	60	76.00	60	70.44	60	68.67	60	65.73
LCP^{riu2}	25	79.67	50	72.89	25	72.33	70	67.33
BGP	**200**	**92.67**	**150**	**88.67**	**150**	**86.67**	**150**	**84.00**
LTCoP	225	85.00	250	79.56	225	76.50	250	73.60
CoALBP12	300	88.33	400	84.67	350	80.17	350	76.93
CoALBP24	300	88.67	400	86.44	350	83.50	350	81.60
CoALBP48	**400**	**89.67**	**450**	**85.11**	**400**	**83.67**	**350**	**83.07**
DenseCLBP	110	84.33	110	79.56	110	75.83	110	72.13

Table 2.13 Classification accuracy achieved by mRMR feature selection based reduced feature vector data for different proportions of training and testing data of RDD using RBF kernel SVM classifier.

Technique	NoF	80/20	NoF	70/30	NoF	60/40	NoF	50/50
GLCM	70	68.00	70	64.67	70	61.67	70	60.40
GLRLM	30	57.00	40	52.89	35	51.83	35	49.47
FOS	4	37.00	4	35.11	4	33.83	4	33.07
Gabor	115	84.00	115	81.55	115	76.00	110	74.93
LBP	150	78.33	250	72.89	250	68.50	175	65.47
LBP^{u2}	55	69.33	55	66.00	55	60.33	55	56.93
LBP^{ri}	35	71.33	35	66.89	35	64.50	30	61.07
LBP^{riu2}	9	63.67	9	58.67	9	57.83	9	53.33
LBP-HF	37	65.67	37	58.00	37	53.00	37	49.73
LPQ	175	79.67	225	71.56	225	67.33	200	64.00
GLAC	100	61.33	100	54.00	100	49.33	100	46.40
CSLBP	15	36.33	16	34.44	15	33.83	15	33.00
$CLBP^{u2}$	100	76.33	100	71.11	100	67.00	115	63.87
LDP	125	69.33	75	63.11	50	57.33	50	56.67
LTP^{u2}	100	80.67	110	73.11	75	69.33	100	68.13
LTP^{ri}	50	79.33	70	76.00	70	73.33	70	70.40
LTP^{riu2}	18	73.00	18	70.44	18	66.83	18	65.20
$ALBP^{u2}$	40	69.67	55	64.00	50	59.50	55	57.60
$ALBP^{ri}$	35	71.33	35	68.88	30	64.33	35	62.13
$ALBP^{riu2}$	9	58.67	9	52.89	9	51.67	9	48.53
LCP^{u2}	60	76.33	50	71.78	75	70.17	70	65.47
LCP^{ri}	60	72.67	60	69.56	70	65.83	60	61.33
LCP^{riu2}	25	77.33	25	71.78	25	71.17	25	68.53
BGP	**150**	**89.00**	**150**	**87.11**	**150**	**84.50**	150	80.53
LTCoP	175	75.00	175	71.11	225	67.83	225	65.73
CoALBP12	350	86.00	350	79.78	450	75.33	400	71.87
CoALBP24	300	85.33	350	83.17	350	77.83	350	74.80
CoALBP48	350	88.00	150	83.56	200	82.83	**200**	**81.47**
DenseCLBP	75	83.33	115	75.11	100	70.00	115	68.53

RF classifier: The mRMR feature selection based reduced feature vector data of BGP technique yields the best classification accuracy of 85.33% (150 features), 82.67% (75 features), 80% (100 features) and 76.40% (50 features) for 80/20, 70/30, 60/40 and 50/50 training and testing ratios of RDD, respectively (Table 2.14). For RF classifier, the feature vector data of BGP technique has outperformed all other feature extraction techniques examined for the classification of hardwood species.

The graphical illustration for 80/20, 70/30, 60/40 and 50/50 training and testing data ratios of RDD is given in Fig. 2.26, Fig. 2.27, Fig. 2.28 and Fig. 2.29, respectively. It is clearly visible from these figures that the mRMR feature selection based reduced feature vector data of BGP texture feature extraction techniques has established its superiority over other feature extraction techniques for RDD. It is worth noting that amongst all the classifiers, the mRMR feature selection based reduced feature vector data has given better performance with linear

SVM classifier for most of the texture feature extraction techniques considered in this discussion. The RF classifier yields relatively lower classification accuracy in comparison to other classifiers. Though, the mRMR feature selection based reduced feature vector has achieved relatively lower classification accuracy compared to FFVD, but these accuracies were obtained using smaller number of feature vector data compared to the full feature vector data.

Table 2.14 Classification accuracy achieved by mRMR feature selection based reduced feature vector data for different proportions of training and testing data of RDD using RF classifier.

Technique	NoF	80/20	NoF	70/30	NoF	60/40	NoF	50/50
GLCM	60	51.33	50	49.11	50	48.83	70	46.67
GLRLM	30	41.00	30	38.00	35	37.83	35	46.53
FOS	4	33.67	4	29.33	4	28.17	4	27.60
Gabor	50	76.67	50	73.11	50	68.31	75	67.20
LBP	100	64.67	175	56.44	175	55.00	125	53.47
LBP^{u2}	50	58.00	55	52.22	55	50.67	50	48.40
LBP^{ri}	35	48.33	35	44.89	35	41.50	35	36.80
LBP^{riu2}	9	34.88	9	34.50	9	34.33	9	31.73
LBP-HF	37	58.33	37	50.89	37	52.00	37	48.13
LPQ	150	65.67	75	57.11	225	54.50	75	51.07
GLAC	50	42.33	50	38.89	25	40.50	25	37.87
CSLBP	15	29.67	15	25.78	15	28.83	15	25.07
$CLBP^{u2}$	75	64.00	75	59.78	100	57.83	100	56.33
LDP	175	52.67	175	46.22	125	44.17	75	42.53
LTP^{u2}	75	67.33	110	63.33	100	61.00	110	58.13
LTP^{ri}	50	58.33	50	56.22	50	52.33	50	47.87
LTP^{riu2}	15	50.33	18	49.11	15	46.83	15	44.40
$ALBP^{u2}$	50	59.00	50	51.78	50	50.50	55	49.33
$ALBP^{ri}$	25	50.00	25	47.56	25	42.83	35	40.93
$ALBP^{riu2}$	9	35.00	9	33.11	9	31.33	9	29.07
LCP^{u2}	70	68.67	60	62.67	70	60.00	25	58.13
LCP^{ri}	50	63.00	50	58.00	25	57.17	75	53.87
LCP^{riu2}	25	68.00	25	62.22	70	60.33	25	57.60
BGP	**150**	**85.33**	**75**	**82.67**	**100**	**80.00**	**50**	**76.40**
LTCoP	150	63.33	200	55.78	175	54.33	175	53.60
CoALBP12	200	75.33	200	69.56	150	66.83	350	63.73
CoALBP24	275	79.00	250	75.33	275	73.00	150	69.07
CoALBP48	275	80.67	175	76.89	350	77.67	200	74.40
DenseCLBP	100	71.33	100	66.22	110	62.67	50	61.47

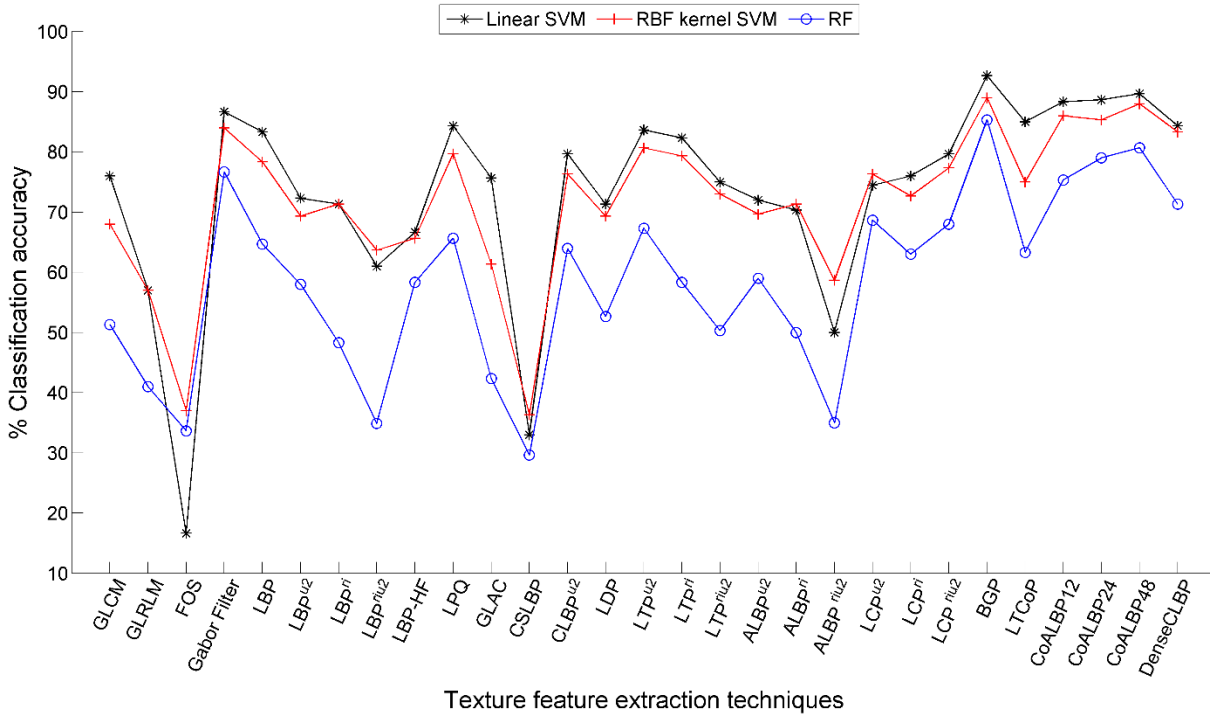

Fig. 2.26 Classification accuracy achieved for 80/20 proportion of training and testing data of RDD.

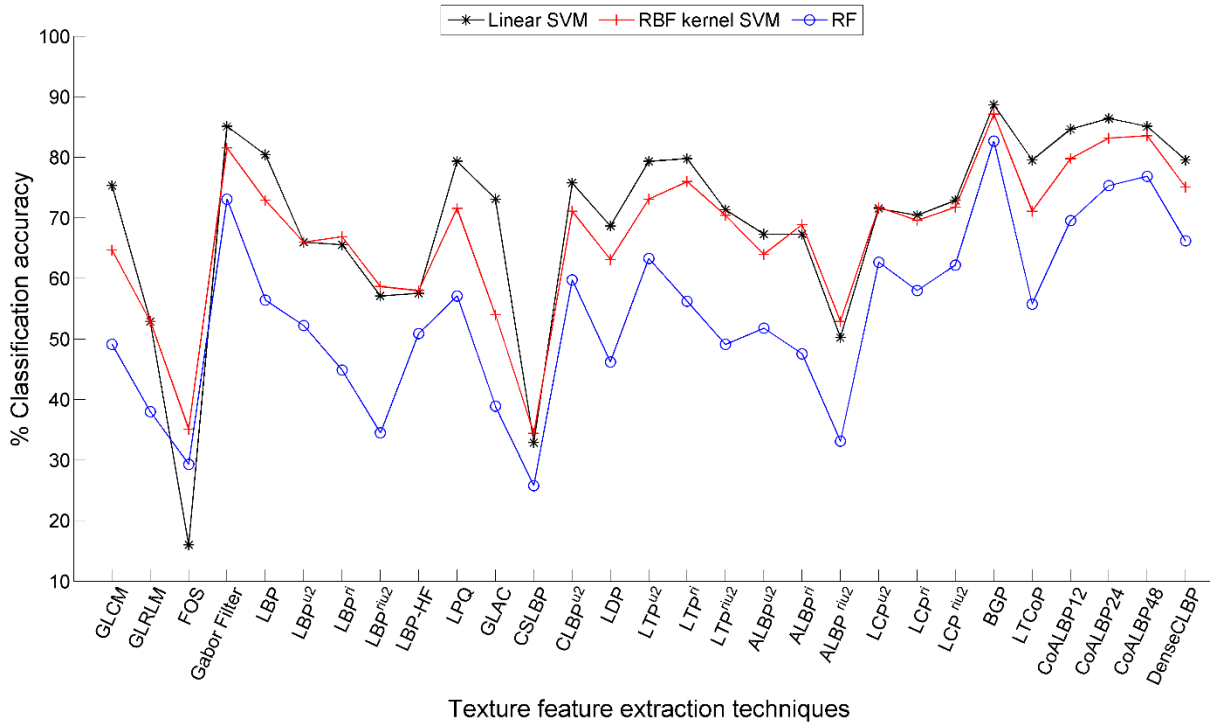

Fig. 2.27 Classification accuracy achieved for 70/30 proportion of training and testing data of RDD.

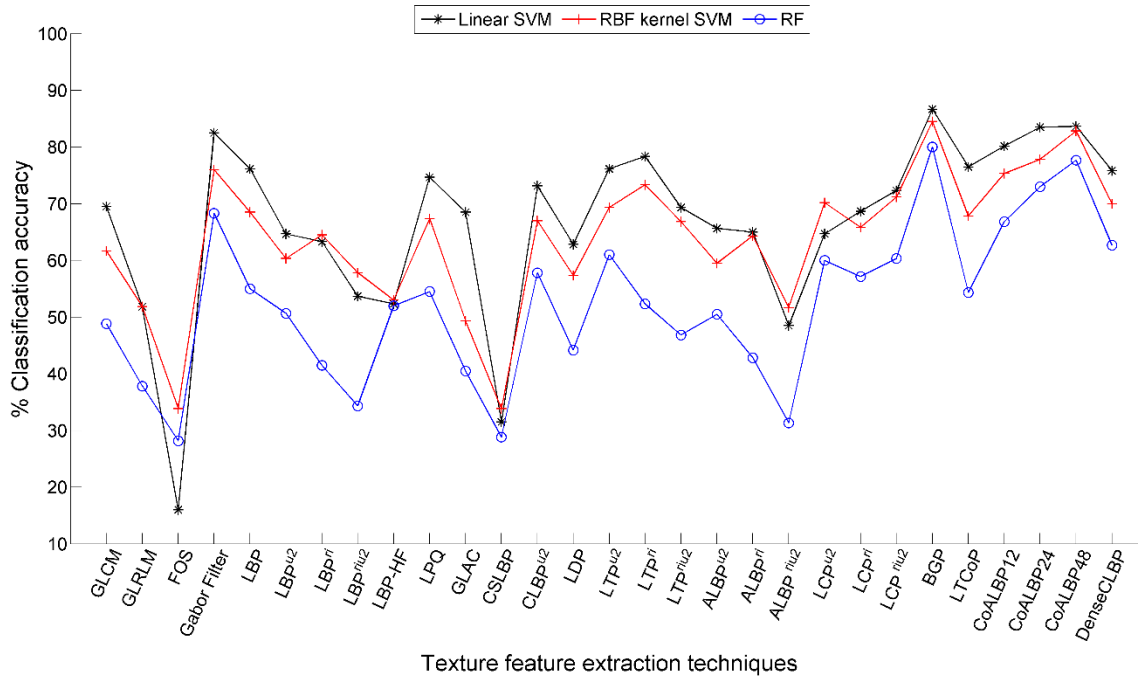

Fig. 2.28 Classification accuracy achieved for 60/40 proportion of training and testing data of RDD.

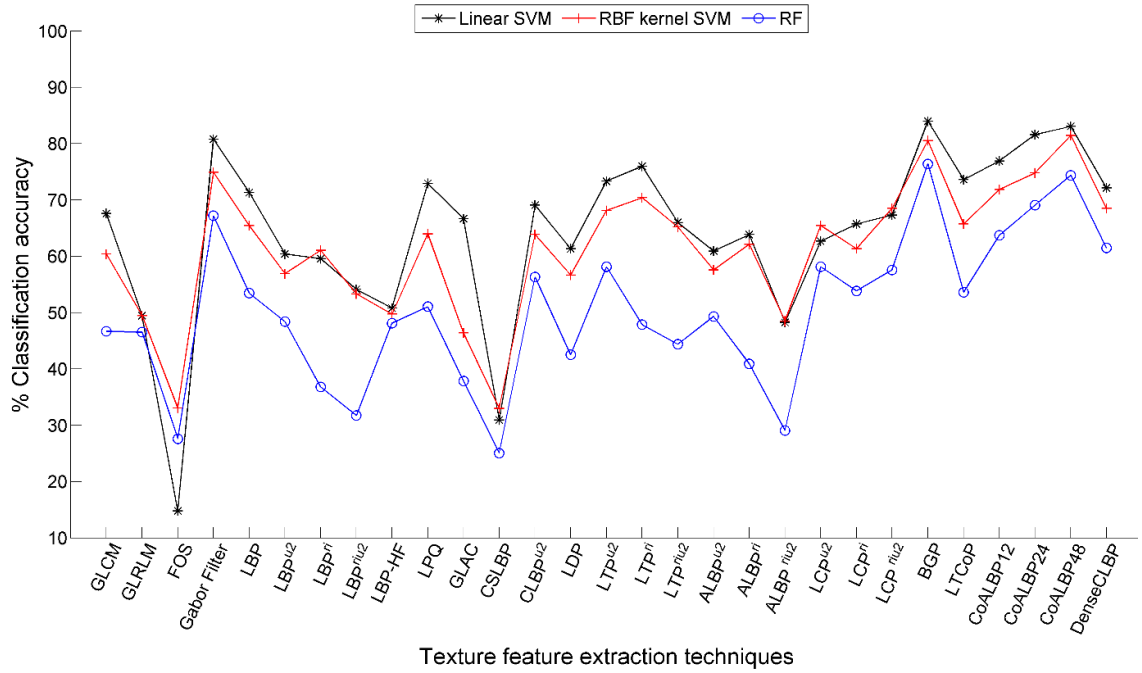

Fig. 2.29 Classification accuracy achieved for 50/50 proportion of training and testing data of RDD.

2.7 SUMMARY

In this chapter, the efficacy of the state-of-the-art texture feature extraction techniques have been investigated for the classification of microscopic images of hardwood species into 75 categories with the help of classifiers. The efficiency of the state-of-the-art texture feature extraction techniques have been tested using two different approaches, namely 1) 10-fold cross validation and 2) randomly divided database. Further, in both the approaches 3 cases are

discussed (viz., FFVD, PCA reduced feature vector data and mRMR feature selection based feature vector data).

The best classification accuracy of 95.93±1.52% has been achieved by FFVD data of BGP texture feature extraction techniques using linear SVM classifier. The PCA reduced feature vector data of CoALBP24 texture feature extraction technique has attained maximum classification accuracy of 96.33±1.14% with the help of LDA classifier. Further, the mRMR feature selection based feature vector data of BGP texture feature extraction techniques has again produced the best classification accuracy of 95.60±1.78% when classified with linear SVM classifier. The CoALBP12, CoALBP24, CoALBP48, Gabor filter, LBP and LTCoP feature extraction techniques have also produced better results compared to rest of the state-of-the-art texture feature extraction techniques. It is to be emphasized that Gabor filter, LTCoP and BGP techniques took 9.3753, 4.5533 and 2.6857 seconds, respectively, to extract the texture features of individual image. The feature vector data of CoALBP48 and CoALBP24 texture feature extraction techniques have attained classification accuracies of 95.20±1.20% and 94.47±1.00% through FFVD and mRMR feature selection based feature vector data respectively with linear SVM classifier. In addition, a classification accuracy of 95.53±0.83% has been obtained for PCA reduced feature vector data of BGP texture feature extraction technique using LDA classifier. The feature vector data of FOS technique has obtained lowest classification accuracy amongst the techniques tested here.

For RDD, four different proportions of training and testing ratios of the feature vector dataset has been investigated. In this case also, BGP texture feature extraction technique has achieved the best classification accuracy over other texture feature extraction techniques. The FFVD of BGP texture feature extraction technique with linear SVM classifier has produced the best classification accuracies of 94.33%, 88%, 85.33% and 82.40% for 80/20, 70/30, 60/40 and 50/50 training and testing ratios of RDD, respectively. Further, the PCA reduced feature vector data of BGP technique has produced classification accuracy of 92.67% (RBF kernel SVM classifier) 90.22% (LDA classifier), 89 %(LDA classifier) and 85.73% (LDA classifier) for 80/20, 70/30, 60/40 and 50/50 training and testing ratios of RDD, respectively.

The mRMR feature selection based reduced feature vector data of BGP technique yields the best classification accuracy of 92.67%, 88.67%, 86.67% and 84.00% for 80/20, 70/30, 60/40 and 50/50 training and testing ratios of RDD, respectively, with linear SVM classifier.

Thus, it is observed that the BGP technique outperforms the other state-of-the-art texture feature extraction techniques except one case where CoALBP48 produce better classification accuracy. The linear SVM, RBF kernel SVM and LDA classifier give better performance, whereas RF classifier gives poor performance, comparatively.

CHAPTER 3. BWT BASED TEXTURE FEATURE EXTRACTION TECHNIQUES

This chapter investigates the binary wavelet transform (BWT) based LBP variants texture features for classification of hardwood species. The chapter starts with concise description of the BWT, proposed hardwood species classification methodology, followed by assessment of effectiveness of proposed techniques with the help of different classifiers.

3.1 INTRODUCTION

Local texture pattern approaches have achieved best results for specific datasets. In reality, individual local descriptor technique have failed to produce better results for all the datasets. Thus, an opportunity of enhancing the texture descriptors do exist by bringing in together more descriptors or extracting texture features from transform domain images [61].

The wavelet transforms (WT) are found in wide range of image processing applications for analysing images at several resolutions [165,186]. This analysis is analogous to the human visual perception system which evaluates the images simultaneously at several scales/levels of resolution [103, 239]. Further, WT has ability to efficiently represent most of the signal energy by small number of transformation coefficients.

In order to effectively address the issue of texture classification [10,184], the problem is generally sub-divided into texture feature extraction and classification. Since, the primary goal is to enhance the classification accuracy, hence employing appropriate classification algorithm may accomplish the task of texture classification efficiently. Similarly, making use of a feature extractor that is capable of acquiring essential features too play a crucial role. If the significant features are utilized as input to the classifier then reasonably better classification accuracy can be achieved.

By and large, the grayscale images have been utilized for extraction of texture features. In image compression applications, the bit-plane slicing approach has been used. The most significant bit (MSB), bit-plane (b7) of grayscale image contributes ample amount of information to the overall image. Thus, the aim of the present work is to investigate the impact of the MSB bit-plane for feature extraction and classification. Further, to get the time-frequency localization, 2D-BWT is performed. The BWT has been used for biomedical image indexing and retrieval [138] and progressive medical image coding [93].

Thus, in view of the above discussion, this work presents an efficient texture feature extraction method that integrates BWT and LBP variants to obtain significant texture features of an image. Further to assess the effectiveness of the proposed texture feature approach four classifiers (Section 2.3) have been chosen.

3.2 BINARY WAVELET TRANSFORM (BWT) FOR GRAYSCALE IMAGE: A REVIEW

A brief description of one-dimensional (1D) and two-dimensional (2D) BWT is presented in the following subsection.

3.2.1 One-dimensional BWT (1D-BWT)

The realization of BWT on binary images is identical to implementation of real wavelet transform (RWT) on grayscale images [156]. For a given 1D signal x of length 1×N, W_T (BWT coefficient matrix) is given by Eq. (3.1)

$$\boldsymbol{W_T} = \left[C\ D\right]^T \tag{3.1}$$

where, $C = \left(\bar{c}\,|_{s=0},\ \bar{c}\,|_{s=2}, \bar{c}\,|_{s=4}, \ldots, \bar{c}\,|_{s=N-2}\right)^T$, $D = \left(\bar{d}\,|_{s=0},\ \bar{d}\,|_{s=2}, \bar{d}\,|_{s=4}, \ldots, \bar{d}\,|_{s=N-2}\right)^T$ and $\bar{c}\,|_{s=k}$ describe a vector whose elements are circularly shifted sequence of $\bar{c}$ by k. The C^T is the transpose of C, and

$$\bar{c} = \left\{c_0, c_1, \ldots, c_{S-1}\right\}^T \tag{3.2}$$

$$\bar{d} = \left\{d_0, d_1, \ldots, d_{S-1}\right\}^T \tag{3.3}$$

where, c_i and d_i are the scaling (approximate) and wavelet (detail) filter coefficients, respectively, whereas S correspond to number of scales. The expression for BWT is then given by:

$$y = \boldsymbol{W_T} x \tag{3.4}$$

An in-place implementation for realization of BWT has been proposed by Pan et al. [157]. The 32 different pairs of binary filters for filter lengths equal to 8 are categorized in four groups based on total number of "1" in the binary filters as listed in Table 3.1.

Table 3.1 Filter groups of length-8 binary filters for BWT

Group	Low pass filter (LPF)	High pass filter (HPF)
1	{0,1,0,0,0,0,0,0}	{1,1,0,0,0,0,0,0}
2	{1,1,1,0,0,0,0,0}	{1,1,0,0,0,0,0,0}
3	{1,1,1,1,0,0,0,1}	{1,1,0,0,0,0,0,0}
4	{1,1,1,1,1,1,1,0}	{1,1,0,0,0,0,0,0}

The odd and even number samples of the signal x are divided into two sequences to have an in-place implementation structure. Further, these sequences are updated in accordance with the filter coefficients produced by low pass filter (LPF) and the high pass filter (HPF). In order to produce the transformed output the LPF and HPF outputs are interleaved together. In this work, group 1 filter is used to implement BWT as illustrated in Fig. 3.1.

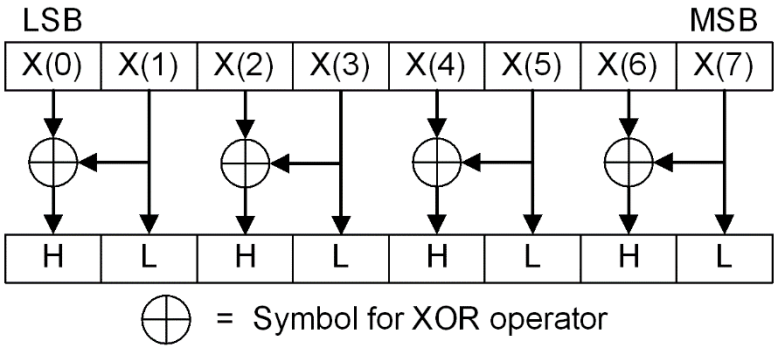

Fig. 3.1 In-place implementation of group 1 filter of 1D-BWT filter.

The X(0) and X(7) are the LSB and MSB bit of sequence, respectively. In the given sequence X(0), X(2), X(4), and X(6) are odd-indexed numbers, whereas X(1), X(3), X(5) and X(7) are even-indexed numbers. The even-indexed numbers represent LPF output, while exclusive-OR (XOR) operation of odd-indexed number with subsequent even-indexed numbers produce HPF output.

3.2.2 Two-dimensional BWT (2D-BWT)

Murala *et al*., [138] proposed a separable 2D-BWT by applying associated 1D filter bank on each row of the binary image followed by applying 1D filter bank on each of the column of the resultant coefficients (H and L) as pictorially represented in Fig. 3.2.

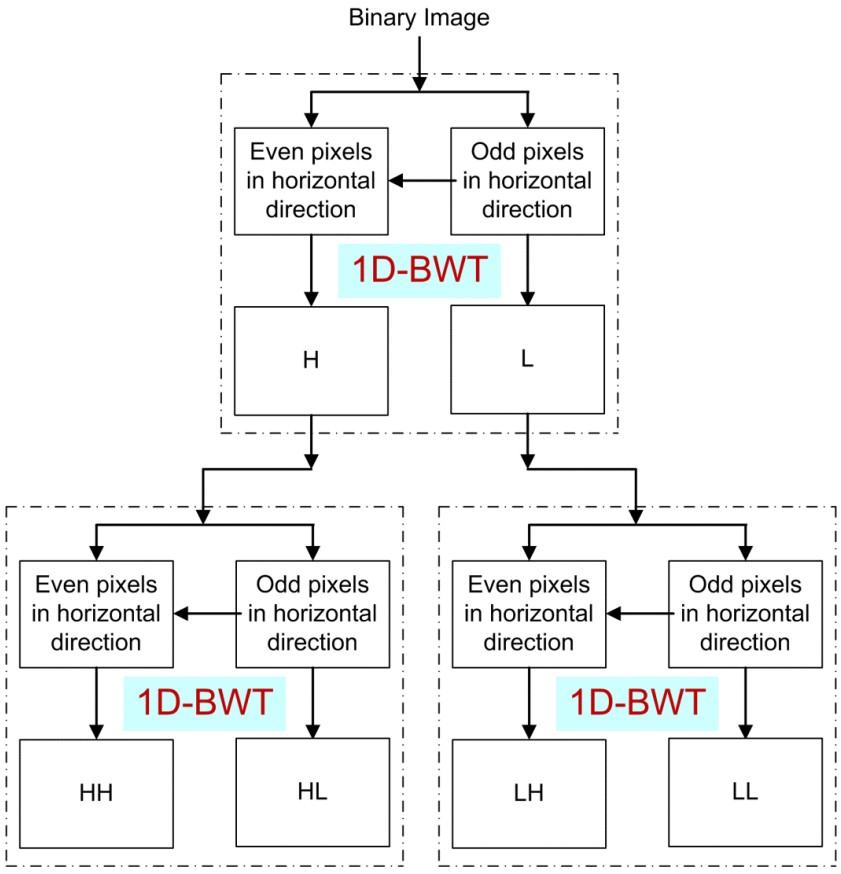

Fig. 3.2 Separable 2D-BWT implementation at the 1st scale/level for binary image.

The binary image decomposition at 1st level/scale employing 2D-BWT generates one approximate (LL) subimage and three detail (LH, HL and HH) subimages. In order to generate higher level of decomposition, approximate subimage is further processed to produce four subimages. Further, the idea is applied on grayscale image by converting it to 8 binary bit-planes; later each bit-plane is processed through 2D-BWT. An illustration of 2D-BWT grayscale image decomposition is shown in Fig. 3.3. The image is first divided into 8-binary images; each of the image is then processed by BWT that produces four (LL, LH, HL and HH) images. These images are later subjected to $CLBP^{u2}$ texture descriptor method. The CLBP_Sign (*CLBP_S*) and CLBP_Magnitude (*CLBP_M*) image for 8th bit-plane is shown in Fig. 3.3. The original *CLBP_S* image is not visible clearly for LL_CLBP_S, therefore the improved *CLBP_S* images are also set aside next to the original *CLBP_S* images for illustration purpose only.

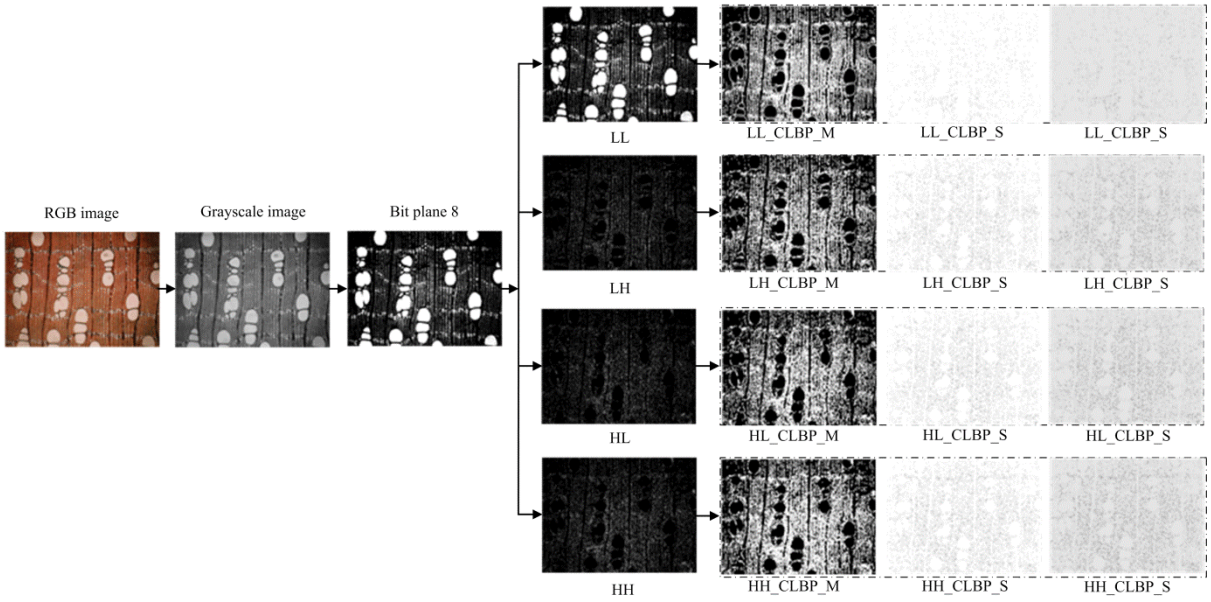

Fig. 3.3 The $CLBP^{u2}$ texture descriptor images of b_7 bit-plane of grayscale image generated by 2D-BWT image decomposition.

3.3 PROPOSED METHODOLOGY

3.3.1 Procedural Steps

In the proposed framework, the task of image classification is divided into four different phases, namely, preprocessing, texture feature extraction, feature selection and classification. The block diagram of BWT based LBP variants texture feature extraction techniques for classification of hardwood species is illustrated in Fig. 3.4.

A brief description of these procedures are as described below:

1. The color (RGB) image is converted to grayscale image using Eq. (2.4.1).
2. The significant texture features of the grayscale image are achieved by a 2D-DWT based texture feature extraction techniques, illustrated as dotted segment in Fig. 3.4. Initially, the

bit-plane slicing approach is used to transform grayscale image to binary image (b_0 to b_7). The b_0 correspond to least significant bit (LSB) and b_7 is most significant bit (MSB) plane. The higher-order bit-plane possess vital amount of visually significant information. Therefore, b_7 bit-plane of each image is decomposed up to 5 different levels/scales (S1 to S5) with the help of 2D-BWT. The 2D-BWT decomposes the MSB bit plane (b_7) into four (LL, LH, HL, and HH) equal-size subimages at the 1st level of image decomposition. The approximation (LL) coefficient of preceding level is further decomposed into four equal-size subimages at the subsequent level of image decomposition. Subsequently, LBP variants are employed to get texture features of each of the subimages up to 5 scales (S1 to S5). Further, at each scale of image decomposition, the histograms obtained by LBP variants from the four subimages are concatenated to form a feature vector data. For instance, the $CLBP^{u2}$ texture descriptor produces 118-dimensional features for each image, therefore, 472-dimensional feature vector data is produced at 1st level of image decomposition.

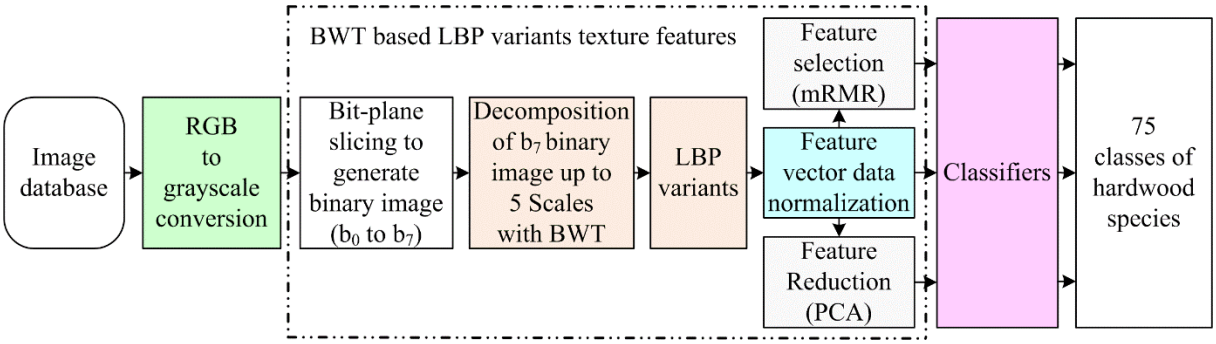

Fig. 3.4 Block diagram of 2D-BWT based LBP variants texture features for image classification

3. The feature vector data produced so has been normalized to accommodate the various values into a range 0 to 1 using Eq. (2.42), to give equal weightage to all the features.
4. The feature vector data is then given as input to different classifiers into three different manners (FFVD, the PCA reduced feature vector data and the mRMR feature selection based reduced feature vector data) for classifying the microscopic images of hardwood species database into 75 categories.
5. The best combination of BWT based LBP variants texture feature extraction technique and classifier is then identified on the basis of the superlative classification accuracy. Thus, on the basis of combination of BWT with different variants LBP texture feature descriptors, following texture feature extraction techniques are proposed here, and they are listed as below with their notations and variations.

BWTLBP Binary wavelet transform based local binary pattern
$BWTLBP^{u2}$ Binary wavelet transform based uniform local binary pattern
$BWTLBP^{ri}$ Binary wavelet transform based uniform rotation invariant local binary pattern
$BWTLBP^{riu2}$ Binary wavelet transform based rotation invariant uniform local binary pattern
BWTLBP-HF Binary wavelet transform based local binary pattern histogram Fourier features

$BWTCLBP^{u2}$	Binary wavelet transform based uniform completed local binary pattern
$BWTCLBP^{ri}$	Binary wavelet transform based rotation invariant completed local binary pattern
$BWTCLBP^{riu2}$	Binary wavelet transform based rotation invariant uniform completed local binary pattern

3.3.2 Approaches used for Performance Evaluation of Feature Extraction Techniques

The performance of the BWT based LBP variants feature extraction techniques for classification of hardwood species have been investigated by employing two strategies: (1) 10-fold cross validation and (2) randomly dividing the database (Section 2.5.2)

3.4 EXPERIMENTAL RESULTS AND DISCUSSION

The experimental work presented in this section investigates the effectiveness of the BWT based LBP variants texture feature extraction techniques for the classification of microscopic images of hardwood species database into 75 classes with the help of classifiers. The classifiers used for the investigation are linear SVM, RBF kernel SVM, LDA and RF classifiers (Section 2.3).

3.4.1 Parameter Selection

The selection of parameters for efficient implementation of LBP feature extraction techniques and classifiers have been discussed in detail in Section 2.6.1.

3.4.2 Experimental Results

The classification accuracy of the BWT based LBP variants texture feature extraction techniques for microscopic images of hardwood species have been computed using four classifiers. As discussed in Section 2.6.2, analysis of the results here is also presented in the similar manner.

3.4.3 Performance Evaluation of BWT based LBP Variants Texture Feature Extraction Techniques using 10-fold Cross Validation Approach

3.4.3.1 Full feature vector data (FFVD)

The classification accuracy achieved by BWT based LBP variants texture features for grayscale image of hardwood species database is presented in Table 3.2. The classification accuracy obtained by the texture features using three different classifiers is discussed below:

Linear SVM classifier: The FFVD of $BWTCLBP^{ri}$ feature extraction technique has given the best classification accuracy of 95.47±1.75% using 864-dimensional feature vector data. Further, second best classification accuracy of 95.07±0.72% (1416 features) has been obtained by FFVD of $BWTCLBP^{u2}$ texture feature extraction technique. Among the proposed feature extraction techniques, the least classification accuracy of 83.20±3.32% (456 features) has been attained for FFVD produced by BWTLBP-HF feature extraction technique.

Table 3.2 Classification accuracy achieved using full feature vector data.

Proposed techniques	IDL	Feature extraction time in seconds	NoF	% CA±SD achieved by classifiers		
				Linear SVM	RBF kernel SVM	RF
BWTLBP	1	0.4160	1024	84.27±3.10	84.80±3.81	78.53±2.53
	2	0.4888	2048	89.47±2.63	87.87±2.81	83.47±2.47
	3	0.5105	3072	91.67±2.58	89.13±2.13	85.40±2.48
	4	0.5403	4096	90.33±2.21	86.93±2.60	84.67±2.41
	5	0.5618	5120	89.20±2.17	85.07±2.44	84.67±2.43
$BWTLBP^{u2}$	1	0.5159	236	85.60±1.99	86.67±3.69	75.93±3.49
	2	0.5967	472	89.93±2.34	91.20±1.85	84.27±2.61
	3	0.6211	708	91.40±2.36	92.53±1.96	87.53±2.18
	4	0.6321	944	90.40±2.18	90.73±2.23	87.93±2.32
	5	0.6400	1180	87.67±2.48	89.73±2.63	87.40±2.07
$BWTLBP^{ri}$	1	0.5172	144	77.00±3.15	81.00±2.16	70.60±2.14
	2	0.5925	288	87.67±3.00	86.80±2.33	80.60±2.02
	3	0.6129	432	89.40±2.25	89.13±3.12	84.60±2.46
	4	0.6230	576	86.73±2.05	86.67±3.43	84.20±2.79
	5	0.6361	720	84.93±1.97	84.47±1.69	83.67±2.50
$BWTLBP^{riu2}$	1	0.5097	40	77.60±3.64	82.00±2.47	63.13±4.03
	2	0.5898	80	86.60±1.79	88.47±1.78	76.87±2.11
	3	0.6181	120	89.47±2.15	90.07±1.80	82.13±2.31
	4	0.6223	**160**	88.00±1.94	87.80±1.18	**83.07±2.27**
	5	0.6833	200	84.60±2.76	84.53±2.31	82.73±1.52
BWTLBP-HF	1	0.5225	152	69.87±3.29	70.60±3.08	72.27±4.10
	2	0.6110	304	76.93±2.95	80.87±2.90	84.47±2.39
	3	0.6414	**456**	**83.20±3.32**	**84.73±2.23**	88.00±2.01
	4	0.6689	608	82.53±2.22	85.33±2.59	87.60±1.84
	5	0.6909	760	81.60±2.52	83.87±2.91	86.40±1.73
$BWTCLBP^{u2}$	1	0.5810	472	90.27±1.58	90.40±2.30	81.60±3.50
	2	0.6708	944	94.53±1.33	93.07±1.73	88.80±1.63
	3	0.7245	**1416**	**95.07±0.72**	**93.87±1.53**	**91.27±0.97**
	4	0.7498	1888	94.20±0.71	93.00±1.34	90.13±1.36
	5	1.2905	2360	92.53±1.43	91.40±1.46	90.27±1.45
$BWTCLBP^{ri}$	1	0.5698	288	88.60±3.10	88.67±3.00	77.27±2.62
	2	0.6899	576	92.47±2.39	91.33±2.27	85.87±1.83
	3	0.6929	**864**	**95.47±1.75**	93.20±1.60	88.40±1.92
	4	0.6970	1152	93.47±1.75	90.67±1.99	88.07±2.62
	5	0.7049	1440	91.67±1.92	87.93±1.62	87.53±1.60
$BWTCLBP^{riu2}$	1	0.5435	80	87.00±2.74	89.20±1.66	75.53±2.79
	2	0.6446	160	91.53±1.78	92.20±1.04	83.80±2.31
	3	0.6578	240	94.13±2.28	**93.73±2.58**	**89.27±2.28**
	4	0.6631	320	93.67±1.41	93.27±1.79	88.67±2.55
	5	0.6764	400	91.13±2.06	90.73±1.87	88.80±2.08

RBF kernel SVM classifier: Amongst the proposed feature extraction techniques, the best classification accuracy of 93.87±1.53% has been obtained for FFVD produced by $BWTCLBP^{u2}$ feature extraction technique. Further, the FFVD of $BWTCLBP^{riu2}$ texture feature extraction technique has achieved slightly lower classification accuracy (93.73±2.58%) in comparison of $BWTCLBP^{u2}$ technique. However, least classification accuracy of 84.73±2.23% has been achieved for FFVD of BWTLBP-HF texture feature extraction technique.

RF classifier: This classifier has achieved the best classification accuracy of 91.27±0.97% for FFVD produced by BWTCLBP^{u2} texture feature extraction technique; whereas the FFVD of BWTCLBP^{riu2} technique has obtained the 2nd best classification accuracy of 89.27±2.28%. Further, the lowest classification accuracy of 83.07±2.27% has been attained for FFVD produced by BWTLBP^{riu2} feature extraction technique.

It has been observed that the best classification accuracy has been achieved at the 3rd scale of image decomposition by most of the proposed feature extraction techniques using all the three classifiers. In addition, among all the three classifiers the best classification accuracy is achieved by linear SVM classifier; whereas, RF classifier has given comparatively lower classification accuracy. The classification accuracy achieved by the three classifiers have been compared and the same is illustrated in Fig. 3.5. The graphical representation reveals that BWTCLBP^{ri} feature extraction technique has given the best classification accuracy with linear SVM classifier.

The time taken by the proposed texture feature extraction techniques for feature vector data generation of single image is also listed in Table 3.2. The BWTCLBP^{ri} feature extraction technique requires 0.6929 sec/image for extracting the texture features of given individual images as shown in Fig. 3.6

The error bar plot with SD for BWT based LBP variants feature extraction techniques has been shown in Fig. 3.7. The observation on Fig. 3.7 suggests that the FFVD of BWTCLBP^{ri} feature extraction technique at the 3rd level of image decomposition yields best classification accuracy with lower value of standard deviation (95.47±1.75%).

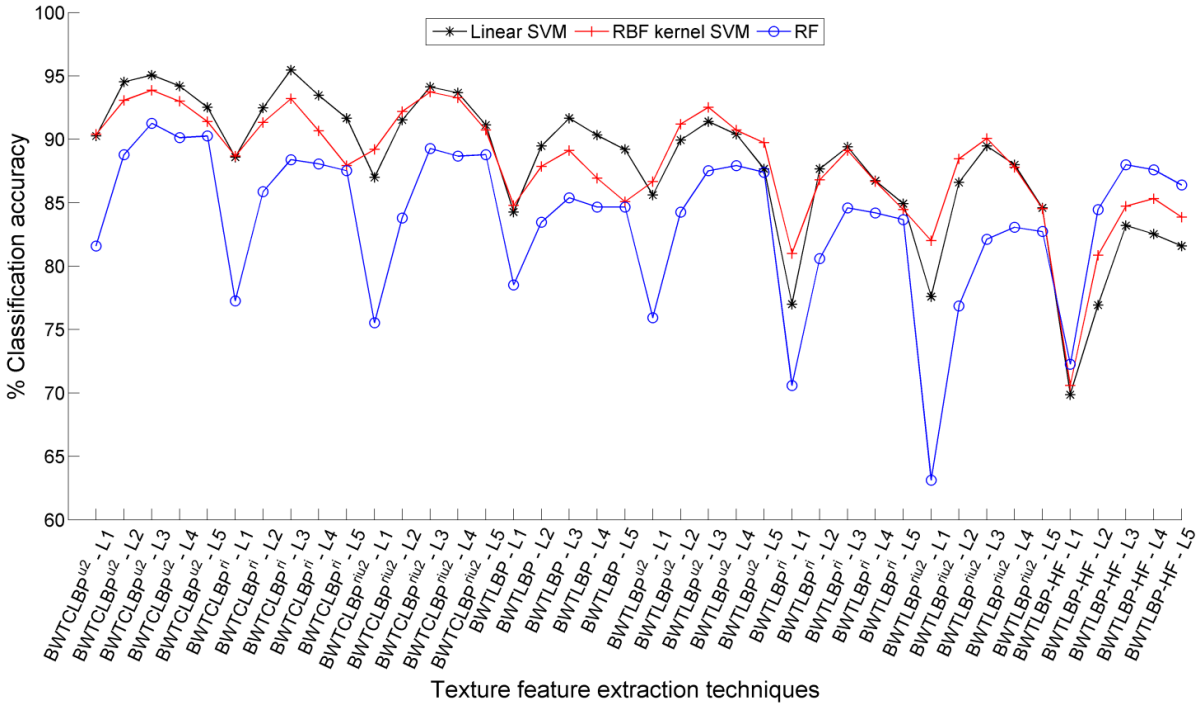

Fig. 3.5 Classification accuracy achieved using FFVD.

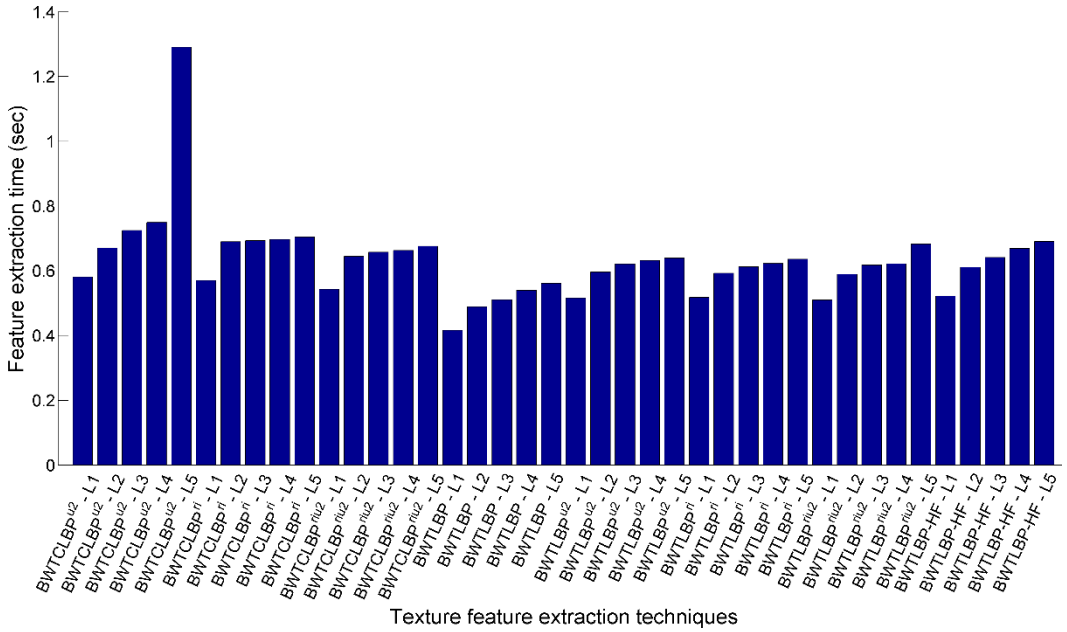

Fig. 3.6 Feature extraction time for single grayscale image.

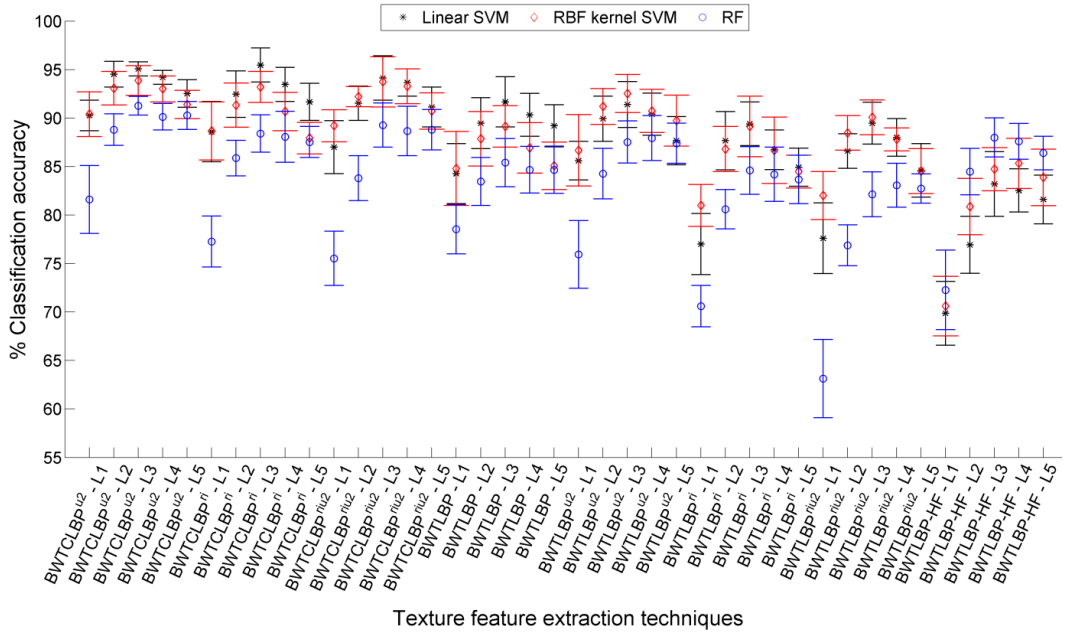

Fig. 3.7 Error bar plot with SD using FFVD.

3.4.3.2 The PCA dimensionality reduced feature vector data

Further to improve the classification accuracy of hardwood species classification the PCA has been employed to reduce the dimensionality of feature vector data. The performance of feature extraction techniques for different classifiers are listed in Table 3.3 and has been concisely discussed hereafter:

Linear SVM classifier: The best classification accuracy of 94.93±1.18% has been achieved by the PCA reduced feature vector data of BWTCLBP^{u2} feature extraction technique (100 features). Compared to the classification accuracy obtained by FFVD (95.07±0.72%), the PCA reduced

feature vector data has given slightly lower classification accuracy but using much lower feature dimension (100 features) compared to FFVD (1416 features).

Table 3.3 Classification accuracy achieved using PCA based reduced feature vector data.

Proposed techniques	IDL	%CA±SD achieved by classifiers							
		NoF	Linear SVM	NoF	RBF kernel SVM	NoF	LDA	NoF	RF
	1	250	81.33±3.68	50	87.47±2.03	50	82.53±3.95	50	83.13±3.22
	2	50	87.60±2.36	50	92.87±1.91	100	89.67±1.81	50	89.80±2.72
BWTLBP	3	50	91.40±2.60	50	94.13±2.49	100	92.00±1.99	**50**	**91.87±1.96**
	4	100	90.07±3.02	50	94.53±1.96	50	92.07±1.95	50	89.80±2.95
	5	50	89.20±2.45	50	93.53±2.42	100	90.87±2.61	50	89.80±2.95
	1	225	85.20±2.37	100	87.47±3.26	100	83.60±1.81	50	82.47±3.61
	2	300	89.87±1.77	300	91.27±2.64	450	89.27±1.87	50	86.27±2.29
$BWTLBP^{u2}$	3	50	90.80±2.41	50	93.13±0.95	50	90.07±1.67	50	89.60±1.84
	4	200	89.13±1.60	50	92.33±2.36	50	89.93±1.79	50	88.07±2.04
	5	50	86.93±2.71	50	91.33±1.81	50	89.20±1.43	50	86.67±2.35
	1	135	76.20±3.16	100	81.27±3.55	140	84.73±2.28	144	71.53±3.14
	2	250	87.93±3.27	200	86.80±1.83	280	90.53±1.47	50	81.07±2.42
$BWTLBP^{ri}$	3	300	87.93±2.30	50	90.60±2.58	400	90.93±1.73	50	85.47±2.43
	4	300	85.60±1.64	150	88.33±3.21	400	87.93±2.60	50	84.33±2.88
	5	300	81.20±2.17	50	85.93±2.12	400	84.20±3.03	50	81.33±1.51
	1	35	76.60±2.28	30	80.86±2.86	36	80.20±2.88	35	77.13±1.22
	2	75	86.27±1.64	70	88.53±1.80	72	88.87±1.51	70	83.80±1.91
$BWTLBP^{riu2}$	3	110	88.40±1.97	100	89.80±3.57	108	92.33±1.19	110	84.00±1.86
	4	150	87.07±2.33	100	88.27±2.60	144	92.60±1.27	150	80.20±2.69
	5	175	83.33±3.03	175	84.40±1.94	180	93.00±1.81	180	74.73±3.26
	1	140	69.27±3.29	125	70.60±3.51	148	87.27±1.73	148	68.40±1.55
	2	300	75.67±3.19	250	81.00±3.46	296	92.27±1.41	280	75.27±3.59
BWTLBP-HF	3	300	80.33±2.87	300	84.40±2.80	444	93.40±1.42	50	78.80±2.15
	4	300	78.27±2.95	300	85.40±2.50	500	88.27±1.70	50	81.33±1.89
	5	300	76.27±2.83	250	84.53±2.77	50	83.13±1.48	50	80.13±2.17
	1	250	90.67±1.57	150	90.07±1.62	400	90.33±2.60	50	87.53±2.90
	2	300	94.27±1.34	200	93.33±2.22	300	94.00±2.53	50	90.27±1.87
$BWTCLBP^{u2}$	3	**100**	**94.93±1.18**	**250**	**94.80±2.15**	200	94.33±1.14	**50**	**91.80±1.67**
	4	250	93.53±0.89	50	94.73±1.42	200	93.80±1.00	50	89.80±1.57
	5	50	91.87±1.83	50	93.60±1.51	200	92.67±1.51	50	89.20±1.21
	1	250	88.00±2.88	200	88.40±2.27	200	90.47±1.72	100	82.33±2.21
	2	250	92.40±1.76	250	91.73±1.18	300	93.13±1.48	50	86.67±1.47
$BWTCLBP^{ri}$	3	250	93.40±2.07	100	93.93±1.92	300	93.67±1.38	50	89.53±2.22
	4	250	92.47±1.91	50	92.80±2.17	400	92.47±1.41	50	88.80±2.22
	5	250	90.00±1.37	150	92.33±2.54	250	90.67±1.22	50	86.20±1.81
	1	70	87.80±1.99	150	89.60±2.74	72	88.07±1.87	60	85.00±1.67
	2	125	91.47±2.03	150	92.13±2.17	144	93.33±1.30	50	88.40±1.94
$BWTCLBP^{riu2}$	3	225	94.67±2.15	150	93.67±1.92	216	95.60±1.18	75	88.40±1.78
	4	300	93.60±0.84	200	93.00±2.09	**288**	**95.73±0.84**	50	86.07±1.59
	5	300	90.67±2.04	250	90.87±1.91	350	95.06±1.45	50	83.93±2.80

RBF kernel SVM classifier: Amongst the proposed feature extraction techniques, the PCA reduced feature vector data of BWTCLBP^{u2} texture feature extraction technique has attained slightly better classification accuracy of 94.80±2.15% (250 features) compared to 93.87±1.53% accuracy presented by FFVD.

RF classifier: The PCA reduced feature vector data of BWTCLBP^{u2} texture feature extraction technique has obtained the best classification accuracy of 91.80±1.67% using 50-dimensional feature vector data which is slightly better than the FFVD (91.27±0.97%) with 1416-dimenisonal feature vector data. The BWTLBP has obtained a classification accuracy of 91.87±1.96% using 50-dimensional feature vector data better than the 86.40±3.03% accuracy presented by FFVD of BWTLBP feature extraction techniques.

LDA classifier: This classifier has achieved the best classification accuracy of 95.73±0.84% for PCA reduced feature vector data of BWTCLBP^{riu2} texture feature extraction technique using 288-dimemnsional feature vector data. The classification accuracy obtained by the other feature extraction techniques have also been better than the rest of the three classifiers in this segment of PCA reduced dimensionality feature vector data.

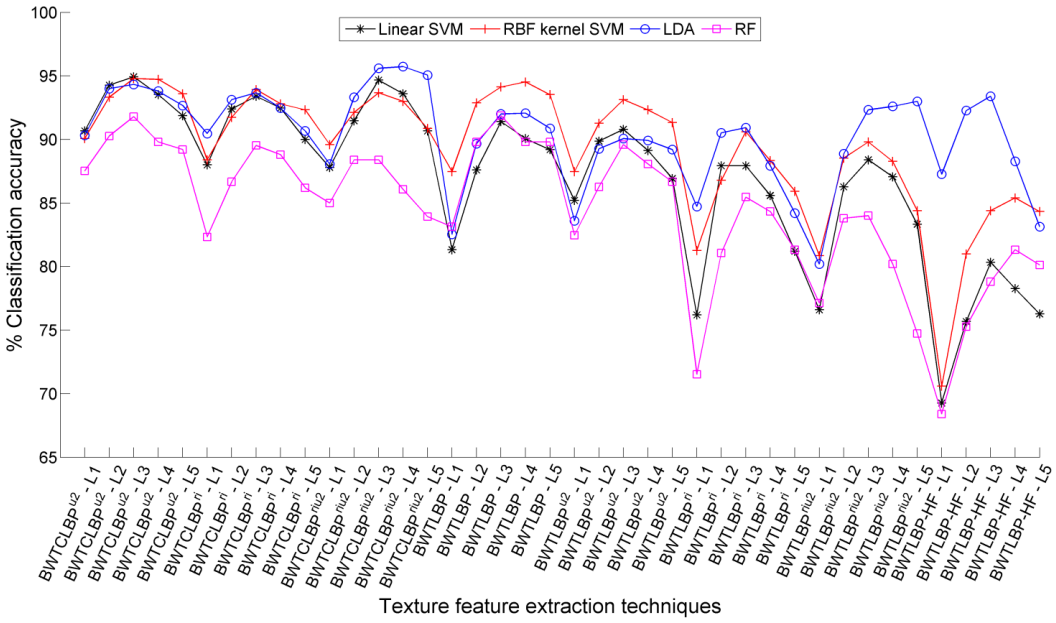

Fig. 3.8 Classification accuracy achieved using PCA reduced feature vector data.

The classification accuracy has not been improved by large margin with PCA reduced feature vector data but comparable classification accuracy has been obtained with lower dimensional feature vector data. In this segment, the LDA classifier has produced maximum classification accuracy for the feature vector data produced by BWTCLBP^{riu2} texture feature extraction techniques at the 3rd level of image decomposition. The graph depicting the comparison of the classification accuracy obtained by four different classifiers is shown in Fig. 3.8. Further, the error bar plot representation of the same is given in Fig. 3.9, which suggests that PCA reduced feature vector data of BWTCLBP^{riu2} texture feature extraction technique has

achieved the best classification accuracy with lower SD value using LDA classifier.

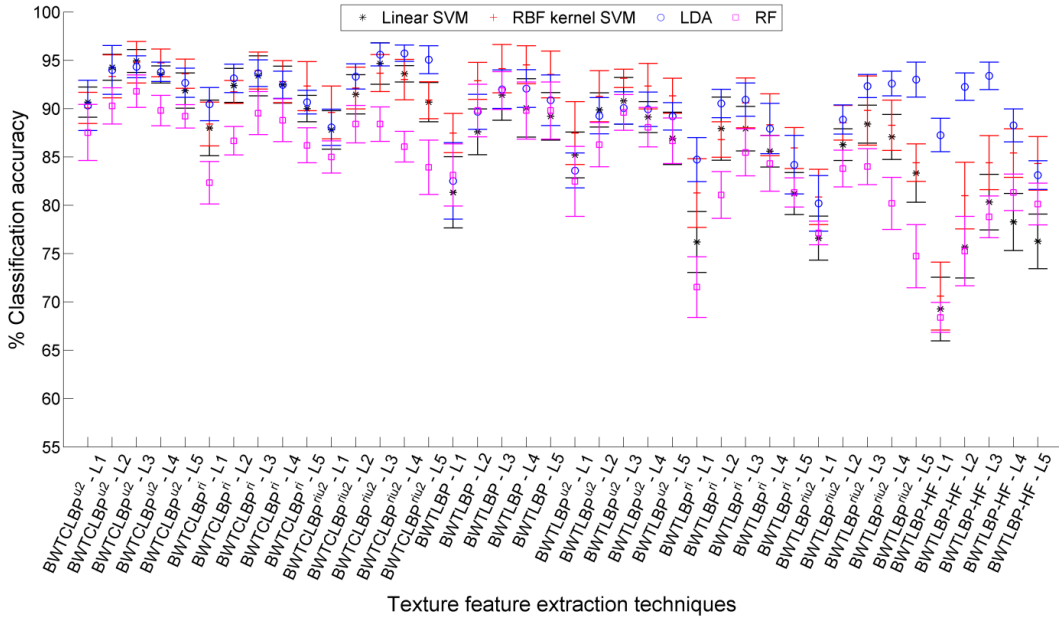

Fig. 3.9 Error bar plot with SD using PCA reduced feature vector data.

3.4.3.3 The mRMR feature selection based reduced feature vector data

The subset of feature vector data obtained by mRMR feature selection method has been investigated here to see their effect on the classification accuracy produced for hardwood species classification. The classification accuracy results achieved by three different classifiers are listed in Table 3.4. The performance of texture feature extraction techniques by different classifiers are as follows:

Linear SVM classifier: Amongst the proposed feature extraction techniques, the highest classification accuracy of 96.20±1.41% has been achieved by mRMR processed subset (300 features) of FFVD of BWTCLBP^{ri} technique at the 4th level of image decomposition. This classification accuracy is comparatively better than 95.47±1.75% accuracy obtained by FFVD of BWTCLBP^{ri} technique (864-dimensional feature) at the 3rd level of image decomposition.

RBF kernel SVM classifier: The mRMR selected feature subset (200 features) of FFVD produced by BWTCLBP^{ri} texture feature extraction technique at the 4th level of image decomposition has achieved the best classification accuracy of 96.87±1.18%. This classification accuracy is far better than 93.20±1.60% accuracy obtained by FFVD of BWTCLBP^{ri} technique (864 features).

RF classifier: The RF classifier has achieved the best classification accuracy of 92.80±1.88% for mRMR selected feature subset (150 features) of FFVD produced by BWTCLBP^{u2} texture feature extraction technique at the 4th level of image decomposition. This classification accuracy has been relatively better than the highest classification accuracy (91.27±0.97%) produced by FFVD of BWTCLBP^{u2} texture feature extraction technique.

Table 3.4 Classification accuracy achieved using mRMR feature selection based reduced feature vector data.

Proposed techniques	IDL	% CA±SD achieved by classifiers					
		NoF	Linear SVM	NoF	RBF kernel SVM	NoF	RF
BWTLBP	1	300	85.07±1.92	300	87.60±1.58	300	81.33±2.89
	2	300	92.60±1.95	300	93.13±1.18	300	85.27±2.99
	3	300	92.60±1.52	300	93.33±1.04	300	86.40±3.03
	4	300	92.60±1.71	300	93.67±1.23	200	86.53±2.33
	5	300	92.67±1.60	300	93.60±1.23	200	86.73±1.82
$BWTLBP^{u2}$	1	225	85.07±2.33	200	87.00±3.57	150	77.00±3.70
	2	200	90.53±1.77	200	92.07±2.44	250	85.67±1.87
	3	250	92.53±2.01	300	94.13±1.88	250	89.53±1.72
	4	250	92.80±1.93	300	94.00±2.15	300	89.67±2.11
	5	300	93.00±1.81	300	94.07±2.12	300	89.60±2.31
$BWTLBP^{ri}$	1	125	74.80±3.06	125	78.87±3.27	75	69.27±3.21
	2	250	87.33±2.20	100	88.13±2.68	150	81.73±1.92
	3	150	90.33±1.97	200	91.13±1.91	100	86.67±1.22
	4	200	91.33±1.91	100	92.60±2.30	200	86.93±1.26
	5	200	91.33±1.78	150	91.93±2.34	300	86.80±2.46
$BWTLBP^{riu2}$	1	40	77.60±3.64	35	79.60±3.02	30	62.40±2.31
	2	80	86.67±1.72	70	87.47±2.74	60	77.07±2.45
	3	120	89.47±2.14	100	89.27±2.19	110	83.13±2.93
	4	150	85.93±2.42	150	88.33±2.04	150	82.73±1.62
	5	150	84.07±1.92	50	85.47±0.98	50	82.60±2.28
BWTLBP-HF	1	50	79.00±2.88	50	82.13±2.89	50	78.13±4.26
	2	150	87.80±2.35	100	90.47±1.14	150	85.87±1.85
	3	150	93.60±0.95	150	94.13±2.13	200	89.27±1.62
	4	200	93.20±1.66	100	93.87±1.13	200	89.27±2.54
	5	200	93.07±2.69	100	93.67±2.36	200	89.00±1.34
$BWTCLBP^{u2}$	1	300	91.00±1.64	200	90.80±2.17	300	82.67±2.91
	2	300	94.87±1.41	150	95.40±0.73	150	89.53±1.89
	3	300	95.73±1.55	150	96.27±0.95	300	91.93±1.82
	4	300	95.80±1.22	250	96.47±1.34	**150**	**92.80±1.88**
	5	300	95.87±1.12	150	96.40±1.48	150	92.40±1.70
$BWTCLBP^{ri}$	1	250	88.07±3.05	250	88.67±2.74	100	80.13±2.75
	2	150	93.27±1.84	150	94.13±1.72	100	87.87±2.22
	3	150	95.93±1.62	150	96.00±1.41	150	91.07±1.14
	4	**300**	**96.20±1.41**	**200**	**96.87±1.18**	150	91.80±1.57
	5	300	95.87±1.03	300	96.47±0.89	200	91.27±2.28
$BWTCLBP^{riu2}$	1	70	88.73±1.52	70	88.33±1.73	50	76.13±2.81
	2	125	92.53±1.83	100	92.40±2.07	50	85.93±1.73
	3	200	93.80±1.91	200	93.80±2.59	100	89.40±1.73
	4	100	93.20±1.17	100	94.47±1.00	150	89.87±0.61
	5	100	93.47±1.25	100	94.80±0.76	200	89.53±1.60

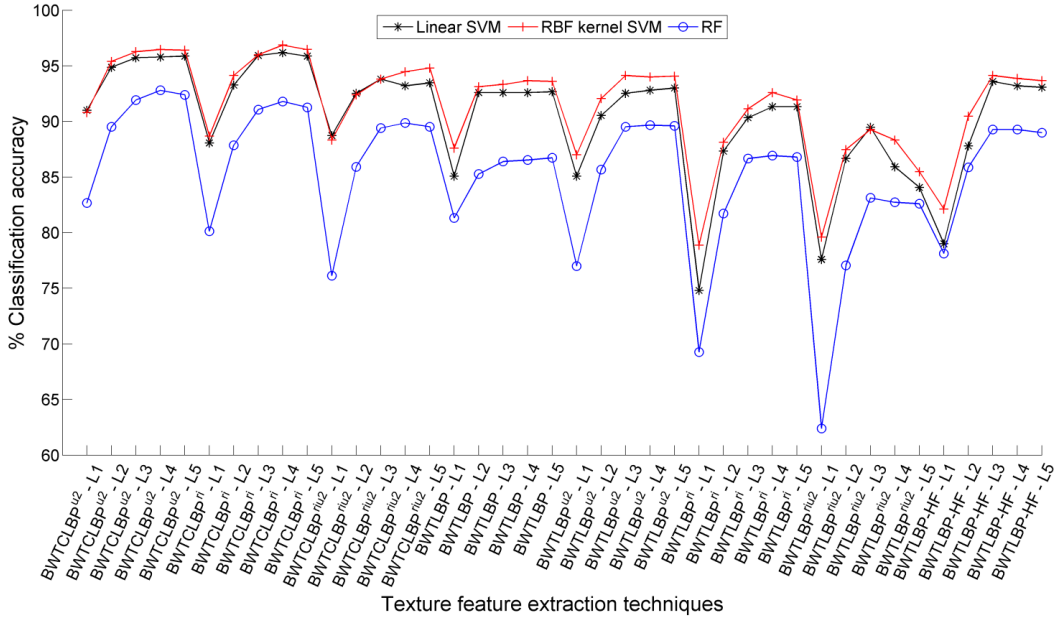

Fig. 3.10 Classification accuracy achieved using mRMR feature selection based reduced feature vector data.

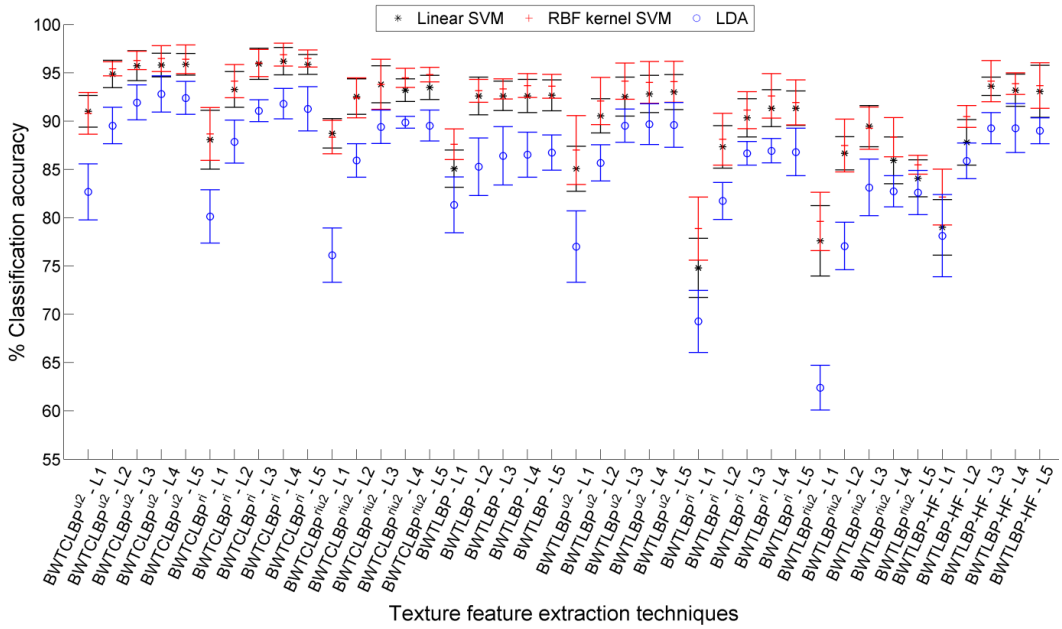

Fig. 3.11 Error bar plot with SD using mRMR feature selection based reduced feature vector data.

The classification accuracy results are plotted in Fig. 3.10. Further, the error bar plot with SD for the same has been illustrated in Fig. 3.11**.** These figures depict that BWTCLBP^{ri} technique has produced best classification accuracy at the 4th level of image decomposition that too with lower value of SD.

The analysis of Table 3.2 suggests that as the level of image decomposition increases, the length of the feature vector data also increases. The classification accuracy results for FFVD of BWT based LBP variants texture feature extraction techniques using different classifiers increased up to 3rd level of image decomposition and thereafter either it remains same or

decreases a little bit. It is noticeable that the increase in the classification accuracy has been attained at the cost of additional computation time. Therefore, the texture descriptors beyond 5th level of image decomposition have not been investigated.

Further, employing PCA (dimensionality reduction) and mRMR (feature selection) techniques have not only reduced the computational time for classification algorithms but also shown considerable improvement in the classification accuracy for hardwood species classification into seventy five categories. It is also observed from Table 3.2, Table 3.3 and Table 3.4 that the proposed feature extraction techniques have produced better classification accuracy compared to the original LBP variants as discussed in Chapter 2.

3.4.4 Performance Evaluation of BWT based LBP Variants Texture Feature Extraction Techniques using Randomly Divided Database (RDD)

3.4.4.1 Full feature vector data (FFVD)

The classification accuracy achieved by BWT based LBP variants texture feature extraction techniques for different ratios of training and testing data has been listed in Table 3.5.

Linear SVM classifier: Amongst the proposed texture feature extraction techniques, the BWTCLBP^{riu2} technique has produced significant feature vector data which yields best classification accuracy of 92.33%, 90.89%, 89.50% and 87.07% for 80/20, 70/30, 60/40 and 50/50 training and testing ratios of RDD, respectively. Further, the BWTCLBP^{u2} technique has achieved the 2nd best classification accuracy of 91.67%, 90.22%, 88.50% and 86.80% for 80/20, 70/30, 60/40 and 50/50 training and testing ratios of RDD, respectively. Both of these classification accuracies are achieved by the texture feature vector data obtained at the 3rd level of image decomposition.

RBF kernel SVM classifier: The classification accuracy results using RBF kernel SVM classifier for proposed texture extraction techniques is also presented in Table 3.5. Here, the best classification accuracy of 91%, 88.67%, 85.33% and 84.13% has been achieved for 80/20, 70/30, 60/40 and 50/50 training and testing ratios of RDD, respectively, for BWTLBP^{ri} techniques' feature vector data. The BWTLBP technique has achieved the 2nd best classification accuracy as listed in Table 3.5.

RF classifier: As given in Table 3.5, the feature vector data produced by BWTCLBP^{u2} feature extraction technique has given the best classification accuracy for different proportions of training and testing data of RDD, respectively amongst the proposed techniques using RF classifier. The BWTCLBP^{u2} features have achieved classification accuracy of 89.33%, 85.56%, 84% and 81.33% for 80/20, 70/30, 60/40 and 50/50 training and testing ratios, respectively, at the 4th level of image decomposition.

Table 3.5 Classification accuracy achieved by full feature vector data for different proportions of training and testing data of RDD using three classifiers.

Proposed technique	IDL	% CA achieved by classifiers for different proportions of training and testing data											
		LSVM				RBF kernel SVM				RF			
		80/20	70/30	60/40	50/50	80/20	70/30	60/40	50/50	80/20	70/30	60/40	50/50
BWTLBP	1	77.67	75.11	72.17	70.53	84.67	82.44	77.83	74.53	72.67	68.67	65.17	62.27
	2	84.33	82.44	80.00	77.87	89.00	86.89	83.83	81.60	78.67	76.67	74.83	70.13
	3	85.67	83.78	82.67	80.40	90.67	89.11	86.33	83.33	81.00	78.89	76.17	72.67
	4	83.00	81.11	81.83	80.00	90.33	87.11	84.33	82.80	81.00	78.89	74.67	71.73
	5	81.67	80.89	80.83	78.93	89.33	84.89	83.17	80.93	81.00	77.78	76.67	72.27
$BWTLBP^{u2}$	1	81.67	78.22	75.50	72.67	84.67	79.33	77.17	75.20	70.00	64.00	60.17	60.40
	2	85.00	85.33	83.17	78.80	87.33	84.67	82.67	78.40	82.67	75.33	74.33	70.67
	3	86.33	86.44	84.50	81.60	87.33	86.44	84.50	81.87	86.00	80.67	79.67	75.47
	4	86.67	85.78	85.33	82.27	86.00	83.33	81.83	79.33	88.33	84.44	79.50	75.20
	5	83.00	81.56	81.00	79.20	84.67	81.56	80.17	78.00	86.33	82.44	79.33	76.67
$BWTLBP^{ri}$	1	74.33	70.44	67.50	65.33	85.00	81.33	80.00	76.53	62.33	63.33	58.83	56.27
	2	81.67	80.67	77.67	76.40	88.00	86.89	83.83	82.93	81.00	75.11	71.33	66.93
	3	87.67	84.22	81.67	81.33	**91.00**	**88.67**	**85.33**	**84.13**	84.00	80.00	77.33	73.20
	4	83.67	80.44	78.67	76.00	89.67	87.78	85.83	83.73	84.67	80.00	77.00	75.07
	5	82.33	77.56	74.83	72.13	88.67	84.67	83.83	81.87	82.67	80.22	77.00	73.33
$BWTLBP^{riu2}$	1	76.00	70.40	68.33	65.47	80.00	74.89	70.33	67.20	58.67	54.67	53.83	49.73
	2	83.00	81.11	79.50	78.27	83.33	80.67	78.17	72.80	76.33	71.77	67.17	64.27
	3	84.00	82.44	82.17	79.20	83.67	81.33	79.83	76.27	80.00	76.67	72.00	70.53
	4	85.33	82.89	80.17	78.40	82.67	78.89	77.33	75.07	79.67	75.33	73.33	72.13
	5	82.33	78.67	76.50	73.60	79.67	77.33	75.83	72.27	79.67	76.00	74.50	71.33
BWTLBP-HF	1	59.00	54.44	53.50	50.53	81.67	78.89	73.83	70.93	72.00	67.11	64.83	62.80
	2	74.33	68.22	67.00	63.20	89.00	83.78	80.33	76.40	84.67	77.33	75.83	73.73
	3	78.67	74.67	73.67	69.47	89.33	87.11	83.17	79.87	85.67	81.11	80.33	77.87
	4	80.33	75.11	73.67	71.60	88.67	85.56	82.50	80.13	87.33	81.11	81.00	77.60
	5	79.67	74.00	71.33	68.53	87.67	82.44	80.00	78.13	85.33	82.22	81.17	78.27
$BWTCLBP^{u2}$	1	88.00	85.56	83.67	79.73	77.00	71.11	68.00	64.53	77.33	71.56	69.17	65.60
	2	90.67	88.67	88.50	84.67	84.00	82.00	77.50	73.20	85.67	81.78	82.00	77.07
	3	91.33	90.22	89.00	85.73	87.33	82.89	81.17	77.20	88.33	86.22	83.17	80.67
	4	91.93	90.00	88.67	86.13	83.67	78.89	77.17	72.93	**89.33**	**85.56**	**84.00**	**81.33**
	5	91.93	88.00	87.67	85.73	82.00	78.22	74.83	71.73	89.00	85.56	83.17	80.80
$BWTCLBP^{ri}$	1	84.00	82.44	80.00	76.13	78.00	74.89	73.17	69.87	72.33	67.33	66.00	64.27
	2	89.33	88.44	86.83	83.33	83.67	83.56	79.83	77.33	83.67	78.67	77.00	73.47
	3	**91.67**	**90.22**	**88.50**	**86.80**	88.33	84.22	80.50	78.80	88.00	82.22	81.17	78.53
	4	90.67	88.00	86.17	84.67	86.00	82.67	80.00	78.27	88.33	84.22	82.17	78.27
	5	89.67	85.33	83.67	82.40	82.33	78.22	77.00	73.73	86.33	82.89	81.00	78.40
$BWTCLBP^{riu2}$	1	84.33	82.22	79.17	77.47	63.67	61.33	59.17	55.73	70.33	64.00	65.00	61.60
	2	90.00	88.44	86.17	84.27	80.00	73.33	71.67	67.20	85.33	78.89	76.50	72.80
	3	**92.33**	**90.89**	**89.50**	**87.07**	82.00	79.78	76.67	73.07	86.67	83.33	81.67	79.07
	4	91.33	90.00	88.57	86.67	82.33	78.22	76.67	74.00	87.67	84.44	81.83	79.73
	5	89.00	87.33	85.67	82.93	81.00	77.11	74.17	72.00	87.67	83.33	81.83	79.73

The classification accuracies obtained by the three different classifiers are compared for each of the four (80/20, 70/30, 60/40 and 50/50) training and testing ratios, and are graphically

illustrated in Fig. 3.12, Fig. 3.13, Fig. 3.14 and Fig. 3.15, respectively. It is evident from these figures that texture feature vector data produced by most of the proposed feature extraction techniques yield best classification accuracy with linear SVM classifier; whereas, the least classification accuracy has been achieved using RF classifier.

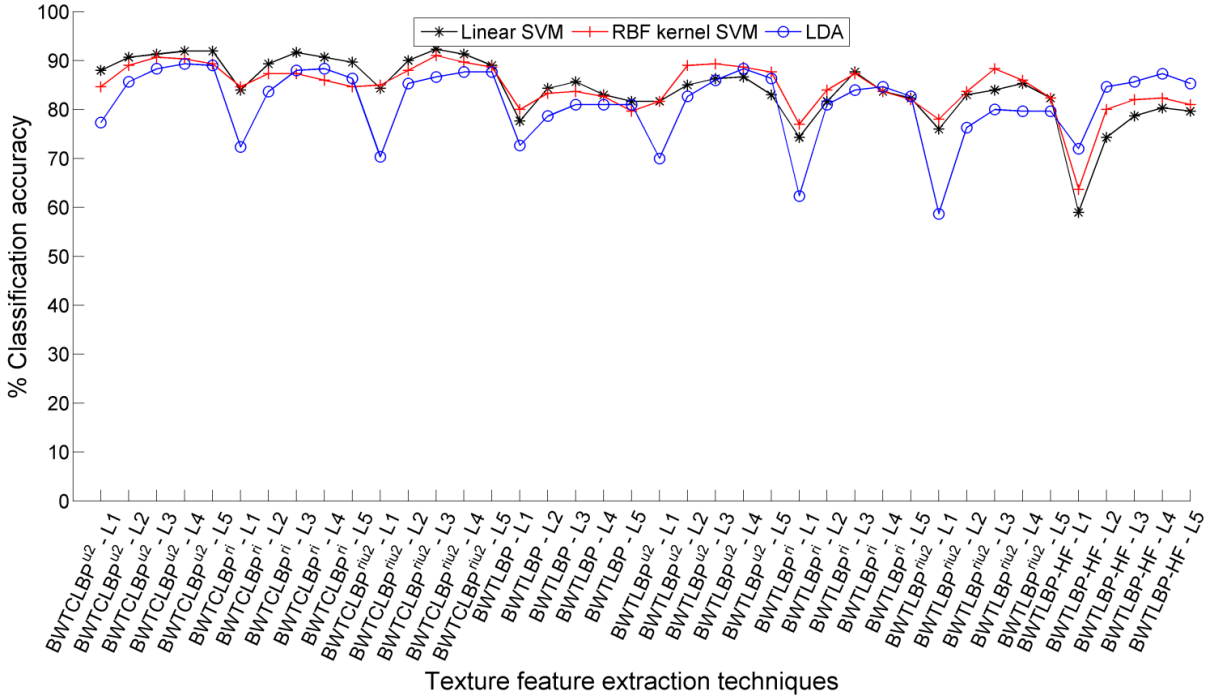

Fig. 3.12 Classification accuracy achieved for 80/20 proportion of training and testing data of RDD.

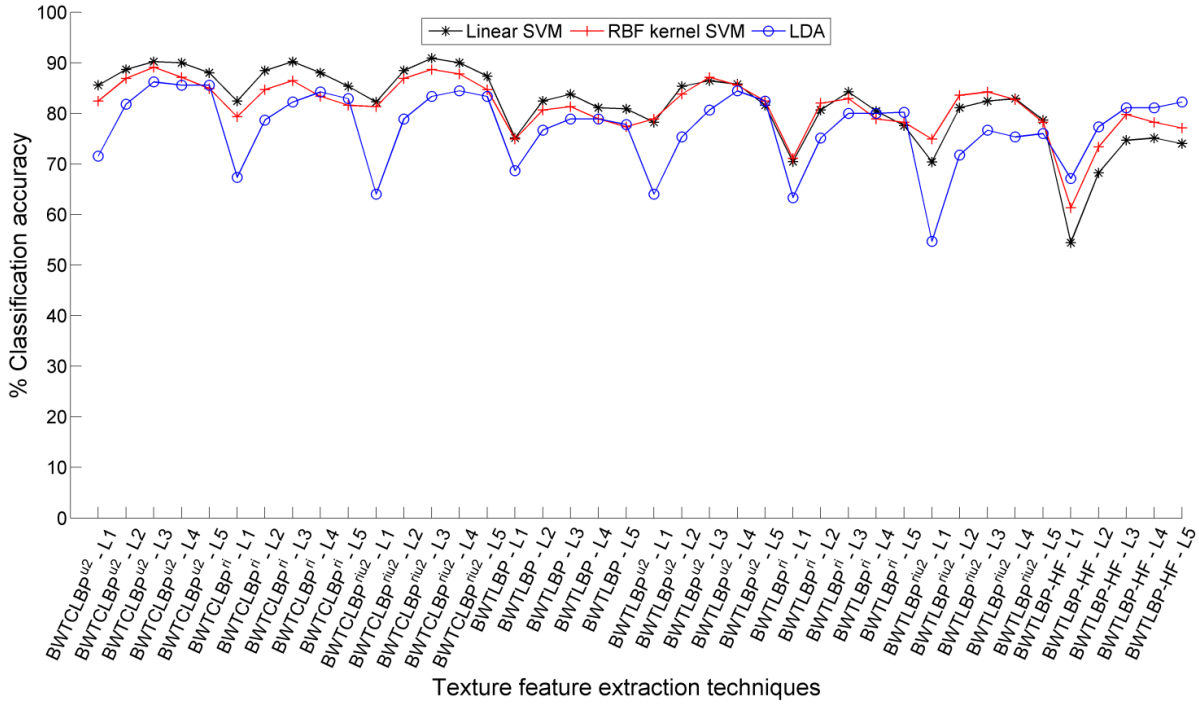

Fig. 3.13 Classification accuracy achieved for 70/30 proportion of training and testing data of RDD.

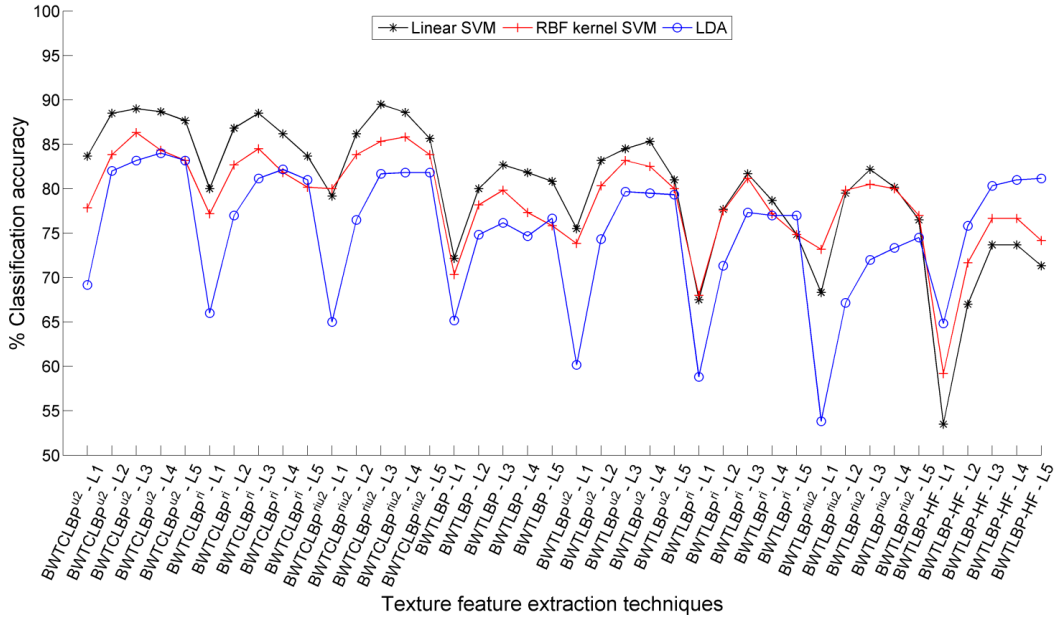

Fig. 3.14 Classification accuracy achieved for 60/40 proportion of training and testing data of RDD.

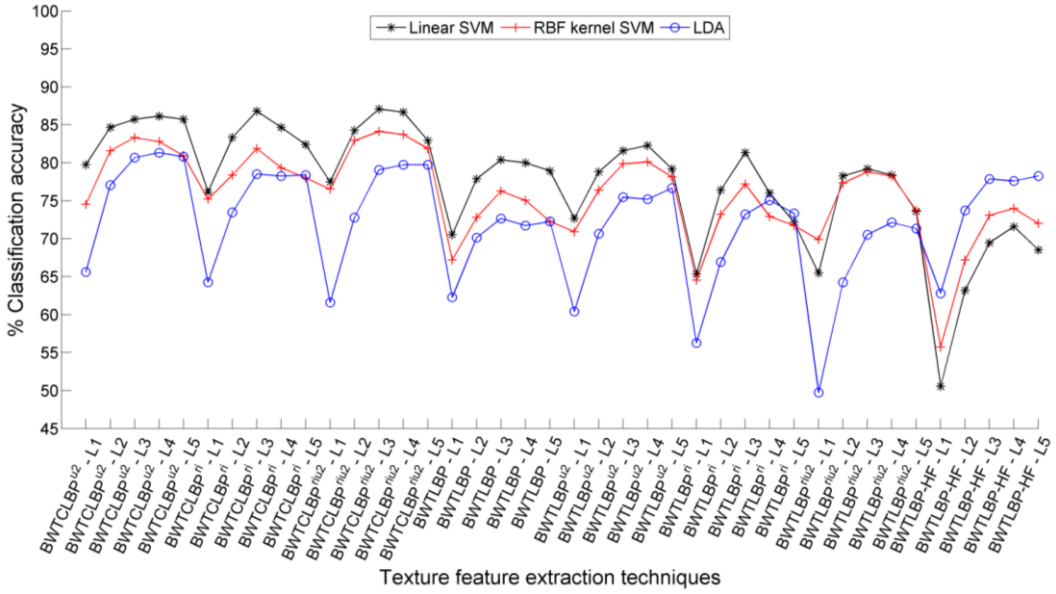

Fig. 3.15 Classification accuracy achieved for 50/50 proportion of training and testing data of RDD.

3.4.4.2 The PCA dimensionality reduced feature vector data

The classification accuracy results obtained by the PCA based reduced feature vector data using linear SVM, RBF kernel SVM, LDA and RF classifier has been listed in Table 3.6, Table 3.7, Table 3.8, and Table 3.9, respectively.

Linear SVM classifier: The PCA dimensionality reduced feature vector data of the $BWTCLBP^{riu2}$ technique has yielded the best classification accuracy of 92.67% (200 features), 91.33% (250 features), 89.33% (250 features) and 86.80% (300 feature) for 80/20, 70/30, 60/40 and 50/50 training and testing ratios of RDD, respectively. The aforesaid classification accuracy is obtained for feature vector data produced at the 4^{th} level of image decomposition. This

classification accuracy is better than the FFVD produced by the BWTCLBP^{riu2} technique with high-dimensional features (Table 3.6).

Table 3.6 Classification accuracy achieved by PCA reduced feature vector data for different proportions of training and testing data of RDD using linear SVM classifier.

Technique	IDL	NOF	80/20	NOF	70/30	NOF	60/40	NOF	50/50
	1	250	77.33	300	74.44	150	70.83	250	68.00
	2	50	86.67	50	81.78	50	81.00	100	78.27
BWTLBP	3	50	88.00	50	86.00	50	84.00	100	81.60
	4	50	88.67	50	86.44	100	82.33	50	80.40
	5	100	84.00	50	82.44	100	79.83	50	78.53
	1	200	81.33	225	76.89	225	73.83	225	72.00
	2	50	85.33	200	85.33	250	82.33	250	79.07
BWTLBP^{u2}	3	50	89.33	50	86.00	250	83.50	300	81.33
	4	50	86.33	50	84.67	250	83.50	150	81.33
	5	50	82.67	50	82.22	50	80.00	200	78.13
	1	125	72.00	125	69.56	125	64.83	125	62.53
	2	250	83.67	275	82.22	275	78.50	275	76.27
BWTLBP^{ri}	3	250	87.67	300	84.67	300	81.00	300	80.00
	4	300	81.33	50	78.89	300	75.67	50	74.53
	5	300	77.33	300	75.78	50	71.83	50	70.40
	1	35	76.33	30	69.78	35	68.50	30	64.13
	2	70	83.67	70	81.33	70	79.00	60	76.67
BWTLBP^{riu2}	3	100	85.67	100	83.56	100	82.17	110	80.27
	4	125	85.67	125	82.44	150	80.33	125	77.33
	5	150	80.67	175	78.44	175	75.50	150	71.60
	1	125	60.00	125	55.78	100	54.83	125	51.60
	2	250	75.00	250	68.67	250	67.17	250	63.33
BWTLBP-HF	3	300	78.00	300	74.89	300	72.67	300	66.80
	4	250	75.67	50	72.67	200	70.33	50	67.60
	5	250	76.00	50	70.22	250	69.00	300	65.87
	1	100	87.33	100	84.44	250	82.83	300	79.07
	2	100	90.00	250	90.00	250	87.50	250	84.13
BWTCLBP^{u2}	3	150	92.33	300	90.67	300	88.50	150	86.27
	4	200	92.67	100	89.56	250	89.00	300	85.73
	5	100	90.33	300	88.89	100	86.67	50	85.60
	1	200	83.33	250	82.22	275	79.50	275	75.47
	2	200	89.33	200	88.67	250	87.00	250	83.73
BWTCLBP^{ri}	3	200	91.00	300	90.20	200	88.83	300	86.13
	4	300	90.33	100	88.89	100	85.50	300	84.67
	5	100	86.00	250	84.89	200	82.67	50	82.13
	1	60	83.67	60	82.20	70	79.33	70	77.20
	2	150	89.00	100	88.22	125	86.33	125	84.67
BWTCLBP^{riu2}	3	225	92.00	200	90.67	200	89.33	200	87.33
	4	**200**	**92.67**	**250**	**91.33**	**250**	**89.33**	**300**	**86.80**
	5	250	89.67	300	86.89	250	85.00	250	82.67

RBF kernel SVM classifier: A classification accuracy of 91.67% (250 features, 4th IDL), 89.33% (200 features, 4th IDL), 86.83% (200 features, 3rd IDL) and 84% (200 features, 5th IDL) has been obtained for 80/20, 70/30, 60/40 and 50/50 training and testing ratios of RDD, respectively. These results have been achieved by PCA based dimensionality reduced feature vector data of

the BWTCLBP^{u2} technique. These classification accuracy results are slightly lower than the accuracy presented by the FFVD of BWTCLBP^{u2} technique (Table 3.7).

Table 3.7 Classification accuracy achieved by PCA reduced feature vector data for different proportions of training and testing data of RDD using RBF kernel SVM classifier.

Technique	IDL	NOF	80/20	NOF	70/30	NOF	60/40	NOF	50/50
	1	150	84.00	50	79.78	100	73.17	50	71.20
	2	100	88.33	50	87.56	100	83.17	50	78.67
BWTLBP	3	50	90.67	50	89.11	50	86.00	50	83.60
	4	50	90.00	50	89.56	50	85.50	50	84.00
	5	50	88.67	50	86.44	100	84.67	50	82.00
	1	100	81.67	100	79.11	225	78.83	150	71.20
	2	50	89.00	50	86.00	50	80.50	200	76.93
BWTLBP^{u2}	3	50	92.00	50	89.11	50	84.17	100	81.87
	4	50	91.33	100	87.11	50	84.17	50	83.20
	5	50	91.00	50	86.67	50	83.67	50	81.73
	1	125	77.00	100	71.78	100	68.33	50	64.93
	2	200	83.67	250	82.00	250	77.50	275	73.87
BWTLBP^{ri}	3	250	87.33	50	86.67	50	82.17	50	78.40
	4	100	84.67	100	81.33	50	78.67	50	76.13
	5	50	85.00	50	81.11	50	77.83	50	75.33
	1	35	78.00	35	74.89	35	73.00	35	69.20
	2	70	84.67	75	84.22	50	79.83	60	77.33
BWTLBP^{riu2}	3	100	88.33	100	84.67	100	81.00	100	79.87
	4	100	85.67	150	82.67	150	80.50	100	78.27
	5	150	82.67	175	78.44	150	77.17	150	73.73
	1	125	63.67	125	61.11	125	59.33	125	55.47
	2	250	80.00	250	73.78	250	72.00	300	67.33
BWTLBP-HF	3	50	82.67	300	79.33	300	76.00	250	73.73
	4	100	81.67	100	78.89	50	76.67	300	74.00
	5	200	83.33	300	76.89	200	75.33	200	72.53
	1	50	85.67	50	83.57	200	77.67	100	75.60
	2	100	90.00	150	88.67	300	84.17	150	82.27
BWTCLBP^{u2}	3	300	90.67	200	89.33	**200**	**86.83**	200	83.73
	4	**250**	**91.67**	**100**	**89.11**	50	85.33	60	83.60
	5	100	91.67	300	87.78	50	86.00	**50**	**84.00**
	1	275	84.00	150	80.22	150	78.17	200	75.60
	2	150	87.33	50	84.89	150	82.17	150	79.07
BWTCLBP^{ri}	3	50	89.00	150	87.56	200	84.50	150	82.40
	4	100	88.67	100	87.11	100	84.00	100	81.47
	5	150	87.00	50	84.67	50	82.83	150	80.40
	1	50	85.33	60	81.56	70	80.33	60	76.80
	2	50	89.00	50	86.44	50	83.67	150	82.93
BWTCLBP^{riu2}	3	150	91.00	225	88.89	200	85.33	200	84.13
	4	150	90.33	150	87.56	200	86.00	200	83.60
	5	300	88.67	200	84.89	200	83.67	250	82.13

LDA classifier: Amongst the proposed feature extraction techniques, the PCA based dimensionality reduced feature vector data of the BWTCLBP^{riu2} technique has attained the highest classification accuracy at the 4th level of image decomposition. The obtained classification accuracy results are 93% (200 features), 92% (250 features), 90% (250 features) and 87.87% (250 features) for 80/20, 70/30, 60/40 and 50/50 training and testing ratios of RDD,

respectively (Table 3.8). The classification accuracy results produced by LDA classifier has been much better than the classification accuracy obtained by other classifiers.

Table 3.8 Classification accuracy achieved by PCA reduced feature vector data for different proportions of training and testing data of RDD using LDA classifier.

Technique	IDL	NOF	80/20	NOF	70/30	NOF	60/40	NOF	50/50
	1	150	76.00	50	75.57	50	75.17	50	71.20
	2	50	87.67	50	85.77	50	83.00	50	80.67
BWTLBP	3	50	89.00	50	87.78	50	87.33	50	84.53
	4	50	91.33	50	88.44	50	88.00	50	84.13
	5	50	89.33	100	86.00	50	84.50	50	82.27
	1	200	81.33	100	74.67	50	73.17	100	70.00
	2	300	85.33	100	84.44	100	83.00	50	79.60
$BWTLBP^{u2}$	3	50	90.00	50	86.67	50	87.00	50	82.67
	4	50	88.33	100	87.33	50	86.00	50	84.13
	5	50	88.33	50	87.11	50	85.67	50	83.60
	1	135	81.00	135	76.00	135	74.17	135	69.20
	2	250	87.67	250	85.33	275	80.83	275	76.67
$BWTLBP^{ri}$	3	150	87.00	300	86.00	50	82.17	50	80.27
	4	50	83.67	50	80.67	50	78.67	50	78.93
	5	50	82.33	50	80.67	50	79.83	50	77.33
	1	35	76.67	35	72.89	35	72.33	35	70.13
	2	72	85.67	72	83.56	72	82.67	72	81.33
$BWTLBP^{riu2}$	3	100	87.00	104	86.22	104	85.67	104	83.73
	4	144	89.67	125	86.22	144	86.33	144	84.67
	5	172	87.33	150	85.56	172	84.33	172	82.80
	1	125	83.67	144	79.11	144	77.50	144	74.13
	2	250	88.33	275	84.89	275	81.83	275	78.40
BWTLBP-HF	3	300	84.67	300	81.78	300	77.33	50	73.47
	4	50	85.00	50	81.11	50	80.50	50	75.47
	5	100	83.67	50	80.22	50	79.16	50	75.73
	1	250	86.67	50	82.00	100	82.67	50	78.40
	2	300	90.33	300	90.22	200	87.67	150	84.67
$BWTCLBP^{u2}$	3	250	91.33	200	90.44	50	89.00	50	86.80
	4	150	92.67	100	90.44	50	89.50	50	87.60
	5	250	92.00	100	90.00	200	88.50	50	85.47
	1	200	89.00	272	85.56	150	83.00	150	78.53
	2	250	92.00	250	90.22	300	88.50	250	84.40
$BWTCLBP^{ri}$	3	200	91.67	200	89.33	50	88.17	50	86.27
	4	100	90.00	100	88.67	100	88.00	100	86.27
	5	150	89.00	150	86.44	150	86.33	50	83.60
	1	72	84.67	72	81.78	72	82.00	72	79.87
	2	125	90.67	144	88.89	125	89.00	125	86.27
$BWTCLBP^{riu2}$	3	216	91.67	216	90.89	200	90.00	216	87.73
	4	**200**	**93.00**	**250**	**92.00**	**250**	**90.00**	**250**	**87.87**
	5	250	90.33	250	88.44	300	87.67	200	84.67

Table 3.9 Classification accuracy achieved by PCA reduced feature vector data for different proportions of training and testing data of RDD using RF classifier.

Technique	IDL	NOF	80/20	NOF	70/30	NOF	60/40	NOF	50/50
	1	50	81.67	50	73.78	50	71.17	50	68.53
	2	50	85.67	100	83.11	50	78.50	50	75.33
BWTLBP	3	50	88.67	**50**	**86.00**	50	83.17	**50**	**80.67**
	4	**50**	**89.33**	50	84.89	50	82.33	50	78.80
	5	50	87.00	50	84.22	**50**	**83.17**	50	79.87
	1	50	78.00	50	73.33	50	69.50	100	66.13
	2	50	79.73	100	77.11	50	73.67	50	70.13
$BWTLBP^{u2}$	3	50	85.67	100	79.56	50	78.33	50	76.00
	4	50	86.67	50	82.00	50	78.17	50	76.27
	5	50	87.00	50	80.00	50	77.50	50	76.40
	1	50	66.67	50	62.89	50	59.33	50	56.53
	2	100	75.00	100	74.89	50	71.67	50	67.60
$BWTLBP^{ri}$	3	50	80.67	50	78.44	50	76.17	50	73.47
	4	50	80.67	50	77.33	50	77.00	50	74.40
	5	100	79.33	50	76.22	50	74.00	50	71.87
	1	35	72.33	35	65.33	35	64.83	35	62.00
	2	70	81.67	75	75.33	75	73.33	75	69.60
$BWTLBP^{riu2}$	3	115	83.33	115	77.56	100	76.50	115	72.67
	4	150	80.00	150	74.22	100	72.00	150	67.73
	5	50	71.33	150	67.56	50	63.83	175	61.47
	1	125	58.00	125	55.56	125	55.67	125	48.93
	2	250	67.33	50	64.67	50	60.17	250	60.00
BWTLBP-HF	3	50	76.33	100	71.78	50	73.67	50	69.60
	4	50	79.67	50	75.33	50	73.67	50	69.60
	5	100	78.00	50	74.22	50	73.50	50	70.00
	1	50	85.67	150	76.22	50	74.83	50	71.20
	2	50	86.33	50	82.22	50	80.67	100	76.67
$BWTCLBP^{u2}$	3	50	88.67	50	84.89	50	84.50	100	80.67
	4	50	88.00	50	83.56	50	82.50	50	80.27
	5	50	85.67	50	82.44	50	83.00	50	80.93
	1	50	79.67	100	75.78	100	73.00	50	69.87
	2	50	84.00	50	81.11	50	77.67	50	76.53
$BWTCLBP^{ri}$	3	50	86.33	50	84.22	50	80.33	50	79.73
	4	50	86.33	50	82.00	50	81.67	50	78.93
	5	100	83.00	50	80.22	50	77.83	50	77.60
	1	60	82.33	60	78.22	70	76.00	50	71.60
	2	50	86.00	50	80.22	150	79.33	50	77.20
$BWTCLBP^{riu2}$	3	100	85.67	50	82.22	100	81.17	50	78.13
	4	50	83.67	50	81.33	50	80.83	50	78.27
	5	50	82.33	50	78.22	50	75.67	50	74.00

RF classifier: In this case the classification accuracy results of 89.33% (50 features, 4^{th} IDL), 86% (50 features, 3^{rd} IDL), 83.17% (50 features, 5^{th} IDL) and 80.67% (50 features, 3^{rd} IDL) for 80/20, 70/30, 60/40 and 50/50 training and testing ratios of RDD, respectively, has been obtained by PCA dimensionality reduced feature vector data of BWTLBP technique (Table 3.9).

The said classification accuracy results are poor than results obtained with the help of other classifiers.

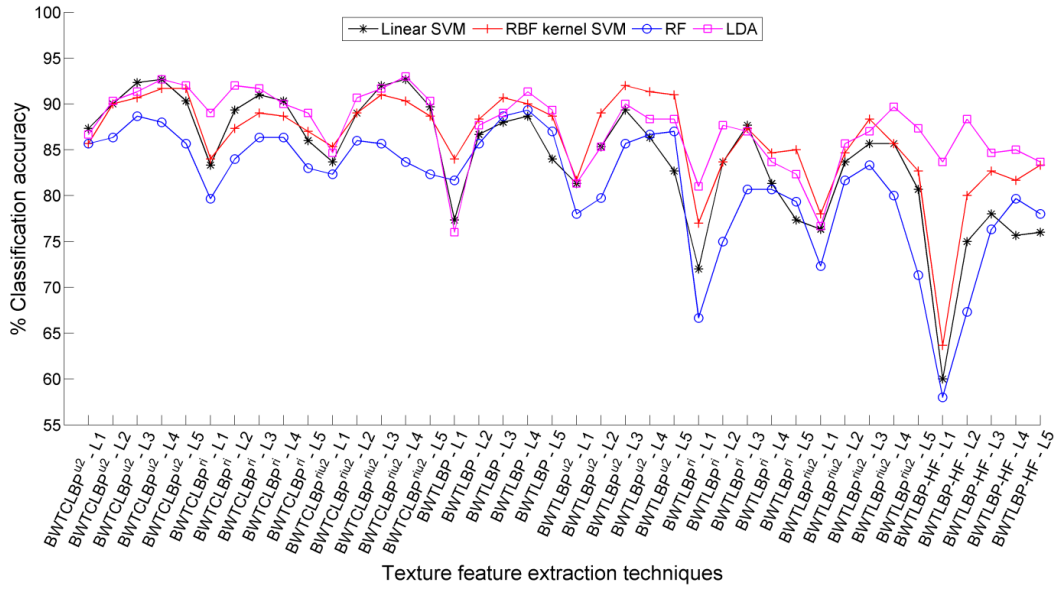

Fig. 3.16 Classification accuracy achieved for 80/20 proportion of training and testing data of RDD.

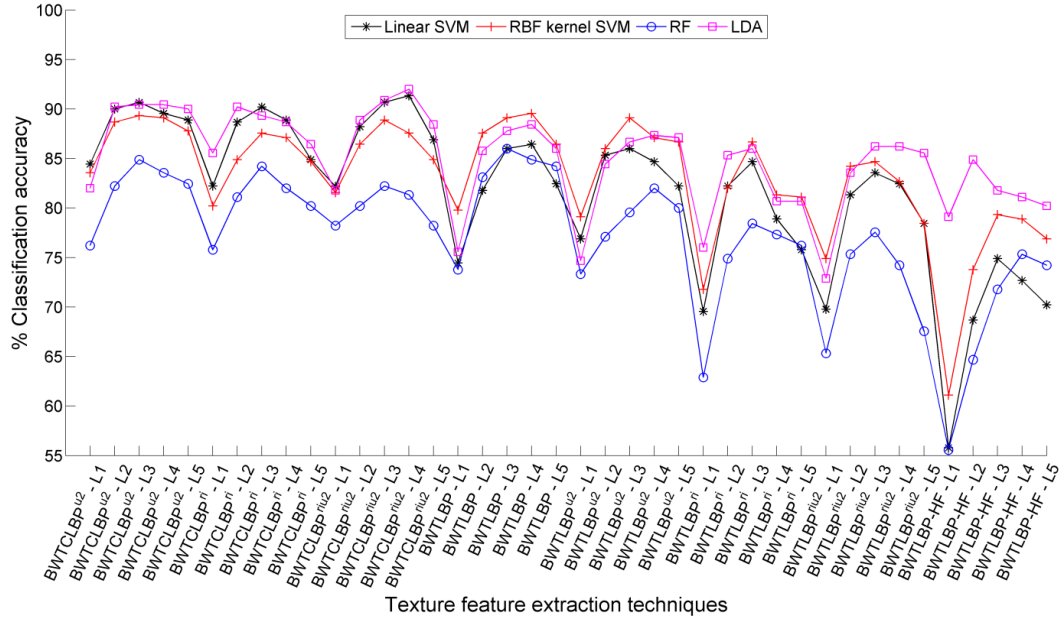

Fig. 3.17 Classification accuracy achieved for 70/30 proportion of training and testing data of RDD.

The classification accuracies obtained by four different classifiers are compared for each of the four (80/20, 70/30, 60/40 and 50/50) training and testing data ratios of RDD, and are illustrated in Fig. 3.16, Fig. 3.17, Fig. 3.18 and Fig. 3.19, respectively. It has been observed from the analysis of the PCA based dimensionality reduced feature vector data that amongst the 4 classifiers, the LDA classifier yields the best classification accuracy for $BWTCLBP^{riu2}$ feature extraction technique. The LDA classifier has not only given the best classification accuracy results, but also requires minimum time to complete the classification task, compared to other

three classifiers. The linear SVM classifier has given the 2nd best classification accuracy; whereas the RF classifier has presented lowest classification accuracy results. Thus, it can be said that incorporating PCA for feature dimensionality reduction has improved the performance of proposed feature extraction techniques for hardwood species classification with low-dimensionality features.

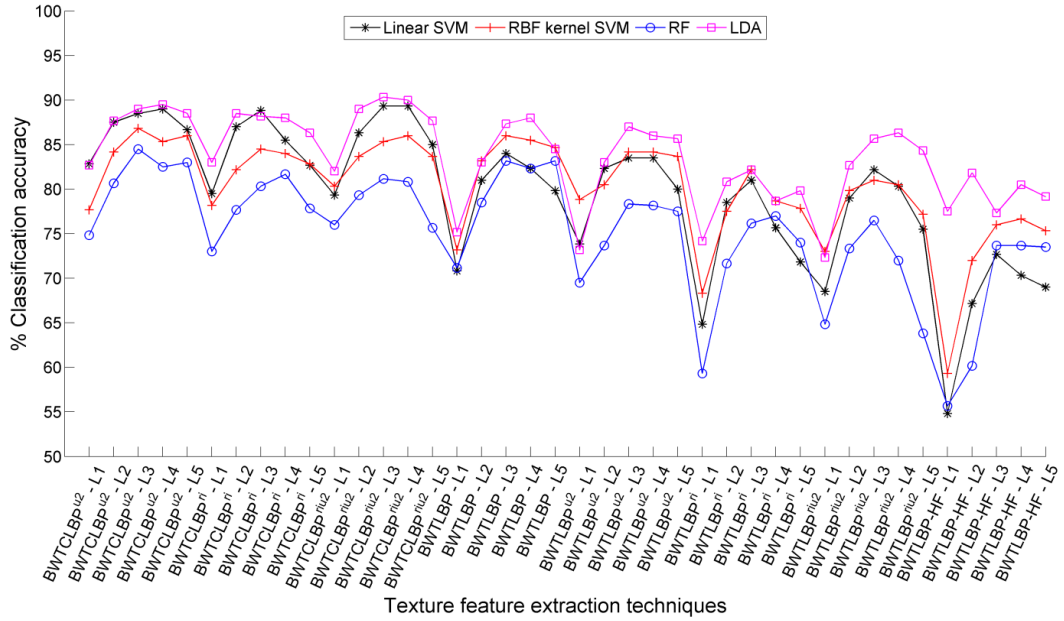

Fig. 3.18 Classification accuracy achieved for 60/40 proportion of training and testing data of RDD.

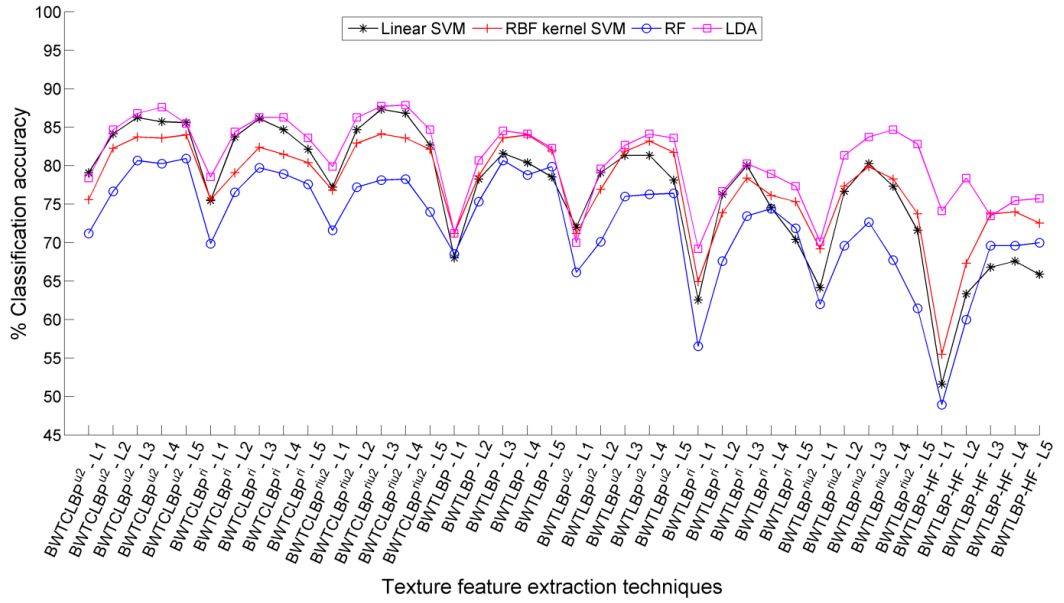

Fig. 3.19 Classification accuracy achieved for 50/50 proportion of training and testing data of RDD.

3.4.4.3 The mRMR feature selection based reduced feature vector data

The classification accuracy results achieved by the mRMR feature selection based reduced feature vector data of propose feature extraction techniques with three different classifiers have

been presented in Table 3.10, Table 3.11 and Table 3.12, respectively. The classification accuracy results obtained by each of the classifiers are as follows:

Table 3.10 Classification accuracy achieved by mRMR feature selection based reduced feature vector data for different proportions of training and testing data of RDD using linear SVM classifier.

Technique	IDL	NOF	80/20	NOF	70/30	NOF	60/40	NOF	50/50
	1	150	79.67	150	76.89	150	74.67	250	70.13
	2	250	88.00	250	85.78	250	84.67	300	82.80
BWTLBP	3	250	87.67	300	86.67	300	85.00	300	83.87
	4	250	88.33	250	87.11	300	86.00	300	84.67
	5	300	88.33	300	87.56	300	85.83	300	84.40
	1	150	82.33	150	78.00	200	75.17	225	72.93
	2	250	87.33	250	86.44	250	84.33	250	80.13
$BWTLBP^{u2}$	3	200	87.33	200	88.89	200	86.33	250	83.73
	4	150	89.33	200	88.67	200	87.00	250	85.60
	5	300	89.67	250	88.67	250	87.67	250	85.87
	1	125	71.67	125	67.11	125	62.67	125	61.07
	2	100	86.00	100	82.22	100	78.83	275	76.13
$BWTLBP^{ri}$	3	300	87.67	300	86.00	300	84.00	300	82.27
	4	300	89.33	250	86.67	200	85.33	150	83.33
	5	300	90.33	300	88.44	300	85.00	150	83.47
	1	35	76.00	35	69.11	35	67.00	35	62.80
	2	75	83.67	70	80.89	70	79.00	70	77.87
$BWTLBP^{riu2}$	3	110	85.33	110	82.89	110	82.50	110	79.60
	4	125	83.67	125	80.67	150	80.17	150	78.67
	5	150	82.33	175	77.78	150	77.17	150	74.67
	1	50	77.00	50	73.33	50	73.50	50	68.13
	2	100	85.67	100	82.67	100	80.50	100	78.27
BWTLBP-HF	3	100	89.33	50	88.22	50	87.67	50	85.20
	4	150	91.33	150	89.78	150	88.50	150	86.27
	5	100	90.67	250	88.67	200	87.50	200	85.60
	1	300	88.67	200	86.67	250	83.83	250	85.60
	2	200	92.00	200	90.22	200	88.33	200	85.73
$BWTCLBP^{u2}$	3	250	93.00	250	92.67	250	91.50	300	89.20
	4	250	93.33	250	93.11	150	90.83	150	89.33
	5	150	93.00	250	92.89	300	90.67	300	90.13
	1	275	85.67	250	82.44	250	79.50	250	76.00
	2	100	92.33	100	90.00	100	88.50	250	85.07
$BWTCLBP^{ri}$	3	250	93.33	250	92.67	250	90.83	200	89.07
	4	200	94.33	150	93.78	150	90.83	150	89.87
	5	**250**	**95.67**	**150**	**93.78**	**250**	**91.50**	**250**	**90.53**
	1	70	83.67	75	81.56	70	78.67	70	77.87
	2	125	90.00	50	88.67	100	86.33	150	83.73
$BWTCLBP^{riu2}$	3	225	92.00	225	91.11	200	89.00	225	87.07
	4	300	92.00	300	90.89	300	88.33	300	86.44
	5	50	91.67	150	89.33	100	88.67	100	86.80

Linear SVM classifier: The subset of feature vector data of $BWTCLBP^{ri}$ technique produced by mRMR feature selection technique yields the best classification accuracy of 95.67% (250 features), 93.78% (150 features), 91.50% (250 features) and 90.53% (250 features) for 80/20, 70/30, 60/40 and 50/50 training and testing ratios of RDD, respectively (Table 3.10).

Table 3.11 Classification accuracy achieved by mRMR feature selection based reduced feature vector data for different proportions of training and testing data of RDD using RBF kernel SVM classifier.

Technique	IDL	NOF	80/20	NOF	70/30	NOF	60/40	NOF	50/50
	1	150	84.33	150	80.22	250	76.00	150	71.47
	2	200	87.67	300	86.67	300	85.83	300	80.80
BWTLBP	3	300	89.67	300	88.67	300	86.17	250	83.47
	4	300	89.67	300	88.00	300	86.67	300	84.13
	5	300	89.33	300	88.00	300	86.17	250	83.33
	1	150	83.00	150	80.44	100	47.33	200	71.07
	2	250	90.67	250	86.89	200	83.50	150	80.13
$BWTLBP^{u2}$	3	150	90.33	200	90.44	200	87.83	200	85.60
	4	250	91.33	250	91.56	250	88.67	300	86.00
	5	150	91.00	300	90.67	300	88.67	200	85.87
	1	125	77.67	125	71.56	125	66.67	125	63.73
	2	150	85.00	150	82.22	275	77.67	200	74.00
$BWTLBP^{ri}$	3	100	88.33	150	86.22	100	84.50	150	82.53
	4	100	89.33	100	87.33	150	85.50	150	84.53
	5	200	89.00	200	87.78	200	85.67	150	84.67
	1	35	78.67	35	73.11	35	70.00	35	66.80
	2	60	85.00	70	82.67	75	79.50	75	76.93
$BWTLBP^{riu2}$	3	115	87.67	115	84.00	115	80.50	115	79.33
	4	150	85.67	150	81.78	150	79.33	150	77.33
	5	50	84.33	50	80.44	50	77.83	50	78.27
	1	50	78.33	50	74.89	50	72.17	50	70.27
	2	100	88.33	50	84.89	50	81.50	50	78.53
BWTLBP-HF	3	50	89.33	100	89.11	100	85.67	100	83.87
	4	100	90.67	100	88.44	150	86.17	200	84.40
	5	50	91.33	50	89.33	150	86.33	150	84.53
	1	150	87.33	200	83.56	200	79.67	150	76.53
	2	150	92.00	150	90.00	150	87.17	200	85.20
$BWTCLBP^{u2}$	3	100	92.33	250	92.44	250	90.17	250	87.87
	4	200	93.67	150	91.78	100	90.00	200	88.93
	5	250	94.00	300	92.00	300	90.33	200	88.93
	1	275	84.33	150	80.89	250	78.50	275	76.13
	2	150	91.67	100	88.44	100	86.00	100	83.47
$BWTCLBP^{ri}$	3	150	92.33	150	90.89	150	89.17	100	88.00
	4	150	93.33	150	92.00	150	90.33	100	89.07
	5	**200**	**94.33**	**200**	**92.22**	**200**	**90.50**	**100**	**89.47**
	1	75	85.00	60	81.56	75	79.67	70	76.93
	2	125	89.67	125	87.11	100	85.67	50	83.60
$BWTCLBP^{riu2}$	3	50	90.67	150	89.78	100	87.33	50	85.87
	4	100	90.67	100	90.22	100	88.67	100	86.93
	5	100	90.33	150	89.33	100	88.50	100	87.07

RBF kernel SVM classifier: In this case, also the subset of feature vector data of $BWTCLBP^{ri}$ technique processed through mRMR feature selection technique yields the best classification accuracy of 94.33% (200 features), 92.22% (200 features), 90.50% (200 features) and 89.07% (100 features) for 80/20, 70/30, 60/40 and 50/50 training and testing ratios of RDD, respectively (Table 3.11).

Table 3.12 Classification accuracy achieved by mRMR feature selection based reduced feature vector data for different proportions of training and testing data of RDD using RF classifier.

Technique	IDL	NOF	80/20	NOF	70/30	NOF	60/40	NOF	50/50
	1	100	72.67	300	71.33	300	68.50	300	66.13
	2	300	79.67	250	77.78	300	76.17	300	72.80
BWTLBP	3	100	82.67	150	80.00	150	78.17	250	76.40
	4	100	83.67	200	80.44	200	80.33	200	76.13
	5	150	82.00	150	79.56	200	78.67	250	75.60
	1	100	71.33	150	66.67	150	63.83	100	61.87
	2	150	83.67	100	79.11	200	77.67	150	73.87
$BWTLBP^{u2}$	3	100	88.67	150	87.56	250	85.33	150	81.20
	4	200	89.67	150	86.44	150	84.83	200	81.60
	5	250	89.33	150	86.22	250	85.50	150	82.27
	1	50	69.33	100	63.78	100	60.33	125	57.60
	2	100	83.67	50	79.56	50	77.17	50	72.80
$BWTLBP^{ri}$	3	150	87.33	100	84.44	50	83.17	50	80.40
	4	150	89.00	100	85.11	200	83.67	50	80.00
	5	250	87.33	150	85.33	100	82.33	100	80.80
	1	30	59.00	30	55.11	30	52.00	30	49.73
	2	50	77.00	70	72.67	50	69.83	50	65.20
$BWTLBP^{riu2}$	3	110	83.00	110	78.00	100	76.00	100	72.13
	4	50	81.33	50	78.89	50	76.83	50	73.20
	5	50	84.00	50	79.11	50	77.83	50	74.80
	1	50	73.67	50	69.56	50	69.67	50	64.40
	2	200	85.67	100	81.33	200	78.83	50	76.53
BWTLBP-HF	3	300	88.33	50	86.00	150	84.16	50	81.87
	4	300	89.33	150	85.11	150	85.67	100	81.73
	5	250	87.33	100	85.78	150	84.16	100	81.87
	1	250	78.33	150	74.89	50	71.50	250	69.07
	2	200	88.33	200	84.89	200	83.17	300	79.60
$BWTCLBP^{u2}$	3	200	90.00	300	88.44	250	86.50	250	84.00
	4	100	90.33	200	88.89	200	87.00	250	84.93
	5	**250**	**90.67**	**300**	**89.33**	**300**	**87.17**	**250**	**85.33**
	1	100	77.33	50	72.00	50	69.50	50	67.20
	2	300	87.00	150	83.78	100	82.50	100	80.13
$BWTCLBP^{ri}$	3	300	90.00	100	89.11	100	87.67	150	85.20
	4	100	90.33	150	87.55	100	87.33	150	86.40
	5	100	89.67	100	88.67	100	87.83	150	85.87
	1	50	73.00	40	69.11	50	67.67	40	64.27
	2	50	86.00	50	83.11	50	80.17	50	77.20
$BWTCLBP^{riu2}$	3	150	88.67	200	86.00	150	85.00	50	81.33
	4	150	88.67	150	87.33	100	86.50	100	83.47
	5	200	88.33	100	86.89	100	86.33	100	83.73

RF classifier: The mRMR feature selection based feature vector data of $BWTCLBP^{u2}$ technique yields the best classification accuracy result of 90.67% (250 features), 89.33% (300 features), 87.17% (300 features) and 84.93% (250 features) for 80/20, 70/30, 60/40 and 50/50 training and testing ratios of RDD, respectively (Table 3.12).

Interestingly, all the three classifiers have achieved the best classification accuracies by the feature vector data produced by the BWT based LBP variants at the 5th level of image decomposition (IDL). Further, employing mRMR feature selection technique for reducing the

number of features has paid off with better classification accuracy compared to FFVD along with requirement of lower classification time due to low-dimensional features.

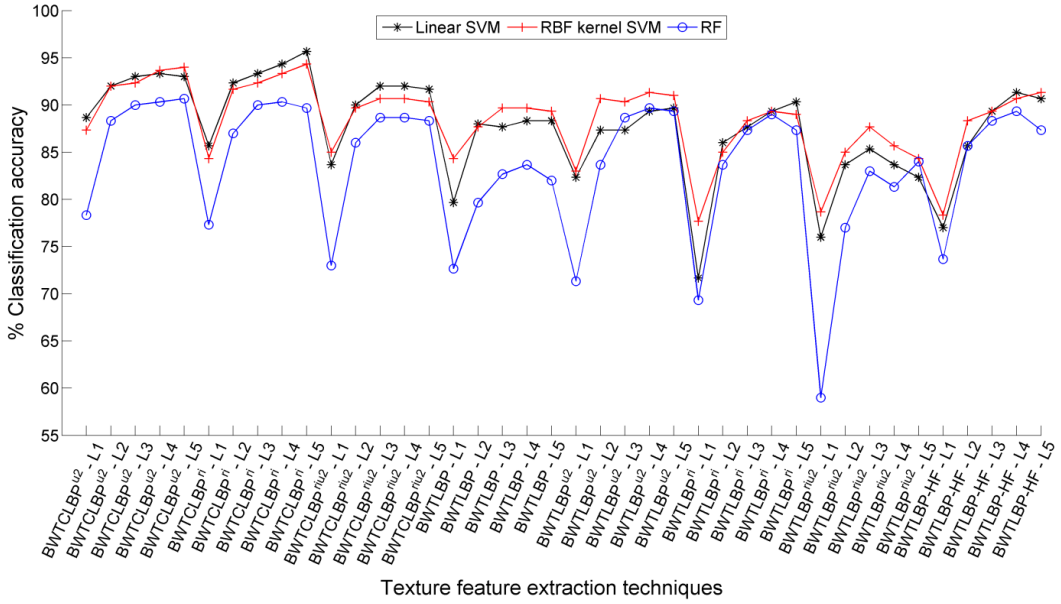

Fig. 3.20 Classification accuracy achieved for 80/20 proportion of training and testing data of RDD.

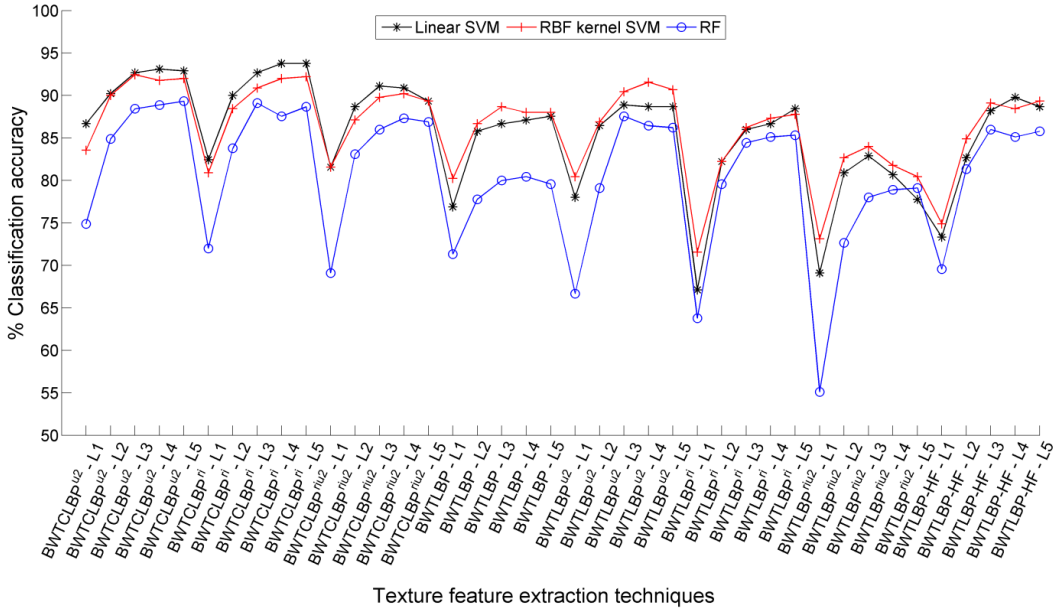

Fig. 3.21 Classification accuracy achieved for 70/30 proportion of training and testing data of RDD.

The classification accuracies obtained by three different classifiers are compared for each of the four (80/20, 70/30, 60/40 and 50/50) training and testing ratios of RDD, and are illustrated in Fig. 3.20, Fig. 3.21, Fig. 3.22 and Fig. 3.23, respectively. The analysis of these graphs advocates that BWT based LBP variants ($BWTCLBP^{ri}$) texture features have given the best classification accuracy with linear SVM classifier; whereas comparatively lower classification accuracy has been produced by RF classifier.

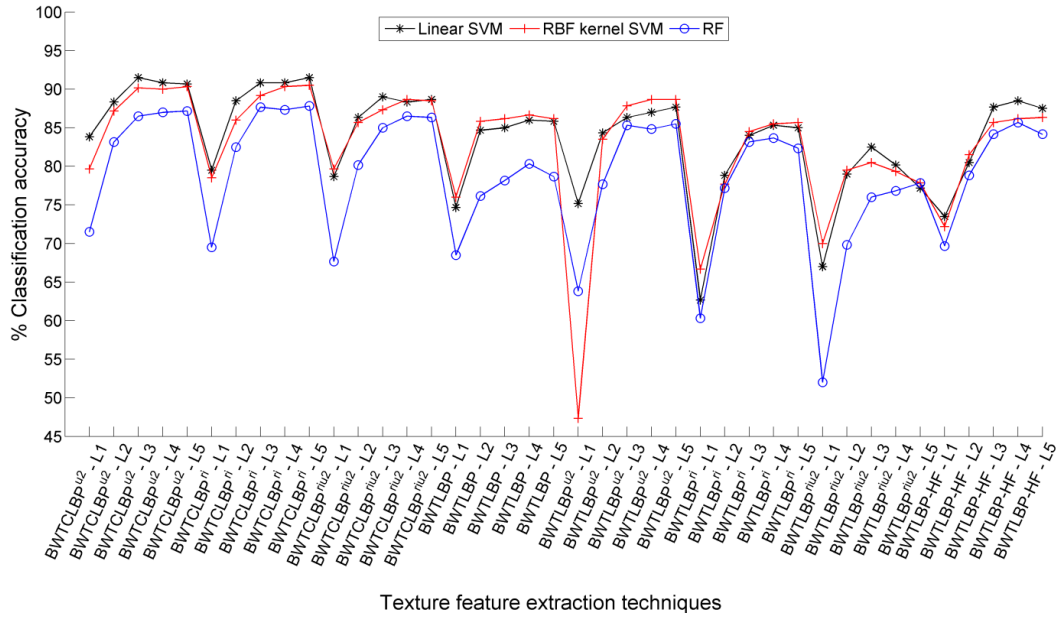

Fig. 3.22 Classification accuracy achieved for 60/40 proportion of training and testing data of RDD.

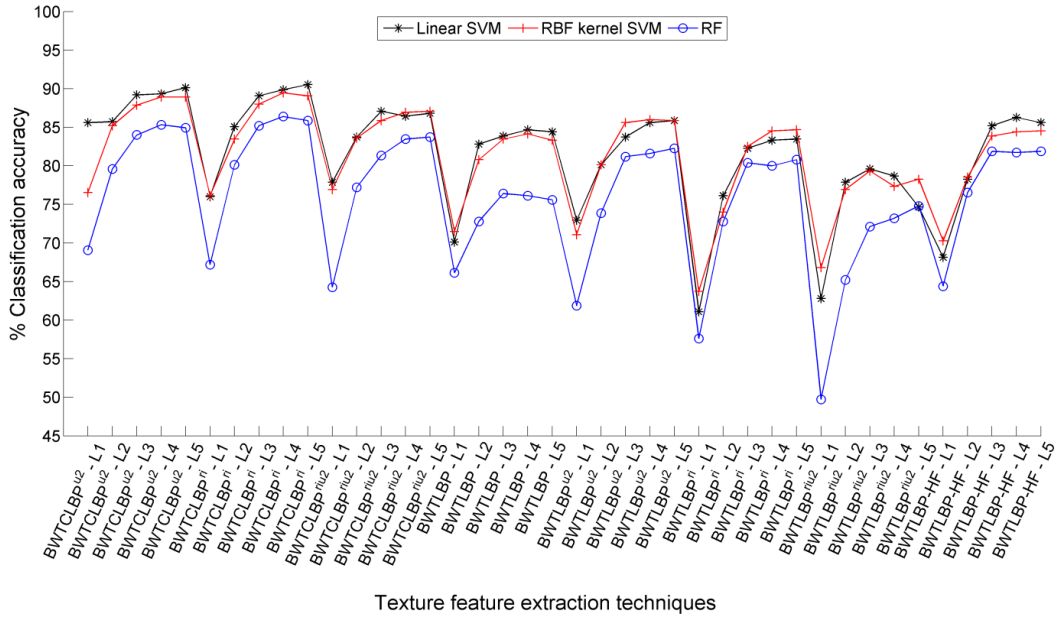

Fig. 3.23 Classification accuracy achieved for 50/50 proportion of training and testing data of RDD.

Thus, employing feature dimensionality reduction/feature selection technique has not only reduced the computational time of classifiers but also shown considerable improvement in the classification accuracy for hardwood species classification into seventy five categories. It is also observed that the performance of variants of LBP texture feature extraction techniques have been improved by including grayscale image transformation with gray-level slicing, and BWT transform followed by extraction of texture features from these transformed images.

The performance of BWT based texture feature extraction techniques has been comparatively superior/at par with most of the state-of-the-art texture feature extraction techniques possibly because of the following reasons: the texture descriptors produced by the

state-of-the-art texture feature extraction techniques are based on spatial interactions over a fixed neighborhood size on single scale image, which is appropriate for micro-texture analysis only. The microscopic images of hardwood species have four key elements namely vessels, rays, parenchyma and fibers, that too of varied shapes and sizes. In order to identify these images efficiently, it must be analyzed at several scales of resolution. The smaller objects are to be examined at higher resolutions; whereas large size objects need to be examined at coarse view (lower) resolutions. For this reason, the images are decomposed by BWT wherein each of the subimages' coefficients contain varied and valuable information. In addition, to extract features from several level/scale images, LBP variants are preferred due to the most prominent and simple computational requirement. Though, distinguishing features are obtained from low resolution subimages but alone they are not capable enough to discriminate amongst the hardwood species. Therefore, the texture descriptors of several scale resolution images are combined to get more significant feature vector data to discriminate the hardwood species database.

3.5 SUMMARY

The effectiveness of the BWT based LBP variants texture feature extraction techniques have been investigated for the classification of microscopic images of hardwood species into 75 categories with the help of classifiers. Two different approaches, namely 1) 10-fold cross validation and 2) randomly divided database (RDD) have been chosen to test the efficiency of the proposed techniques. Further, three case studies are discussed (viz., FFVD, PCA dimensionality reduced feature vector data and mRMR feature selection based reduced feature vector data) in both the approaches.

In case of 10-fold cross validation approach, the FFVD (864 features) produced by $BWTCLBP^{ri}$ feature extraction technique at the 3^{rd} level of image decomposition yields best classification accuracy with lower value of SD (95.47±1.75%) using linear SVM classifier. Further, the LDA classifier yields the best classification accuracy result of 95.73±0.84% for PCA reduced feature vector data of $BWTCLBP^{riu2}$ texture feature extraction technique (288 features). The mRMR selected feature subset (200 features) of $BWTCLBP^{ri}$ texture feature extraction technique (at the 4^{th} level of image decomposition) has achieved the best classification accuracy of 96.87±1.18% using RBF kernel SVM classifier**.**

The aforesaid classification accuracy (96.87±1.18%) produced by $BWTCLBP^{ri}$ texture feature extraction technique is comparatively better than the classification accuracy (96.33±1.14%) achieved by the PCA reduced feature vector data of CoALBP24 texture feature extraction technique (Chapter 2). Further, it is worthwhile to point out that only MSB bit-plane of gray scale image used by BWT based LBP variants texture feature extraction technique has

achieved slightly better classification accuracy compared to 8-bit plane image (grayscale image) used by CoALBP24 texture feature extraction technique.

Further, in 2nd approach, four different proportions of training and testing ratios of randomly divided database have been studied. Amongst the proposed texture feature extraction techniques, FFVD of $BWTCLBP^{riu2}$ technique has achieved the best classification accuracy of 92.33%, 90.89%, 89.50% and 87.07% for 80/20, 70/30, 60/40 and 50/50 training and testing ratios of RDD, respectively, using linear SVM classifier.

The PCA dimensionality reduced feature vector data of $BWTCLBP^{riu2}$ technique has obtained the best classification accuracy results of 93% (200 features), 92% (250 features), 90% (250 features) and 87.87% (250 features) for 80/20, 70/30, 60/40 and 50/50 training and testing ratios of RDD, respectively, with LDA classifier.

The subset of feature vector data of $BWTCLBP^{ri}$ technique selected by mRMR feature selection technique yields the best classification accuracy of 95.67% (250 features), 93.78% (150 features), 91.50% (250 features) and 90.53% (250 features) for 80/20, 70/30, 60/40 and 50/50 training and testing ratios of RDD, respectively, with linear SVM classifier. The aforementioned classification accuracies are much better than the classification accuracy produced by BGP (state-of-the-art) feature extraction technique (94.33%, 88%, 85.33% and 82.40% for 80/20, 70/30, 60/40 and 50/50 training and testing ratios of RDD, respectively), using linear SVM classifier.

Thus, it is summarised that the performance of LBP variants texture feature extraction techniques have been significantly improved by incorporating grayscale image transformation with gray-level slicing and BWT transform followed by extraction of texture features from these transformed images. The MSB bit of grayscale image has significant information which can be used to deliver comparatively good classification accuracy using BWT transform. Further, the performance of BWT based LBP variants technique have been found comparatively superior or at par with most of the state-of-the-art texture feature extraction techniques for hardwood species classification.

CHAPTER 4. GAUSSIAN IMAGE PYRAMID BASED TEXTURE FEATURE EXTRACTION TECHNIQUES

This chapter explores the effectiveness of Gaussian image pyramid (GP) based texture feature extraction techniques for classification of hardwood species. The chapter starts with concise description of the GP, proposed (GP based texture features) methodology for hardwood species classification and subsequently assessment of effectiveness of the proposed feature extraction techniques using different classifiers.

4.1 INTRODUCTION

Multi-resolution texture feature extraction techniques have been widely used to extract the significant features of the image that is difficult to obtain from the original image (single resolution image). Although a number of multi-resolution approaches are available, Gaussian image pyramid (GP) has been preferred here because it requires less computational efforts. Image pyramid is useful for illustrating images at several resolutions [1, 25] and has been used for texture analysis [108] due to local averages at various scales [24]. In GP, moving from bottom to top of the pyramid, produces images of reduced size and resolution. The base image of the pyramid has high resolution, while the top (apex) of the pyramid has low resolution. The original image G_0 is convolved with Gaussian kernel function (low pass filter) and sub-sampled to generate next level of pyramid image G_1. In order to generate the next higher level of image G_2, the G_1 image is convolved with Gaussian kernel and sub-sampled. This process of image convolution and sub-sampling is repeated for the *N* (desired) level of image pyramid. The formula for the GP [24] for original (base) image $f(x,y)$ is given by Eq. (4.1),

$$G_0(x,y) = f(x,y) \tag{4.1}$$

$$G_l(x,y) = \sum_{m=-2}^{2}\sum_{n=-2}^{2} w(m,n)G_{(l-1)}(2x+m,2y+n), 0 \le l \le N \tag{4.2}$$

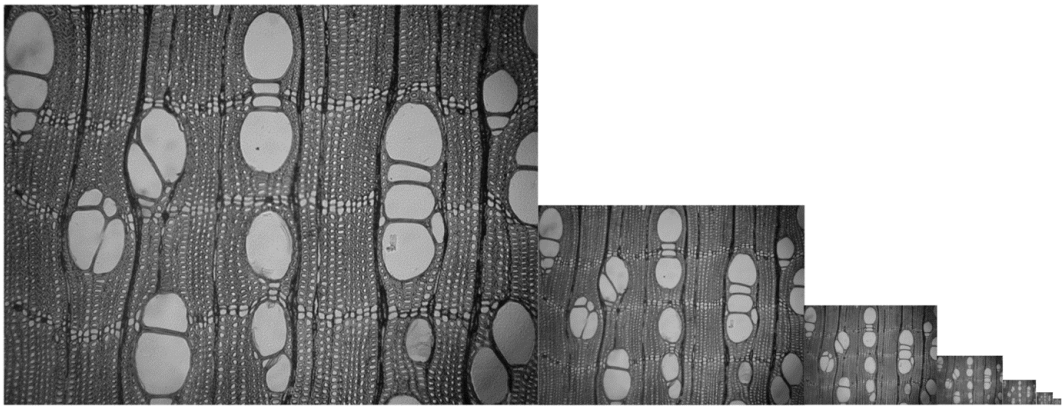

Fig. 4.1 Gaussian image pyramid of *Guianensis* species at G_0 to G_6 levels.

In Eq. (4.1), $G_0(x,y)$ is first level image (viz., base image) produced by GP. In Eq. (4.2), $G_l(x,y)$ is the l^{th} level image produced by GP, and $w(m,n)$ is a weighting function (generating kernels). The generating kernel $w(m,n)$ approximates a Gaussian function (Gaussian pyramid). These kernels are identical at all levels, symmetric and separable. As a special case, the GIP for *Guianensis* species [125] of Sapotaceae family is shown at G_0 to G_6 levels in Fig. 4.1.

4.2 PROPOSED METHODOLOGY

4.2.1 Procedural Steps

The procedural steps involved in present work used for classification of microscopic images of hardwood species is represented in the form of block schematic and is shown in Fig. 4.2.

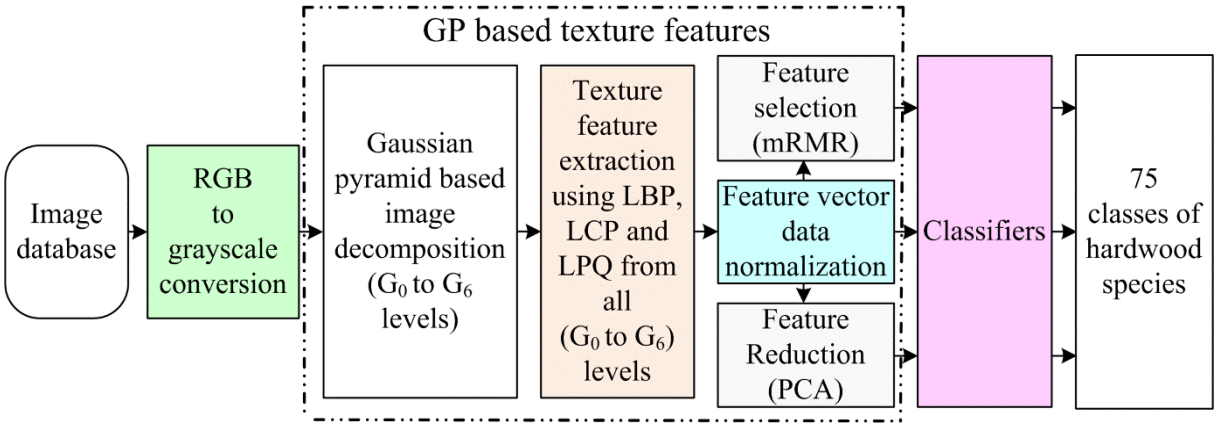

Fig. 4.2 Schematic for classification of hardwood species using Gaussian image pyramid based texture feature extraction techniques.

The complete classification process consists of three stages: pre-processing, feature extraction and classification.

1. In pre-processing, microscopic images are converted to grayscale model from RGB model using Eq. (2.41).
2. In the second stage, these images are transformed to multiresolution images by means of GP. The GP model at G_0 to G_6 levels has been achieved by convolving grayscale images with the Gaussian kernel (low pass filter). From each GP decomposed images, texture features are extracted using different texture descriptors like LBP, LCP and LPQ. The texture features produced by these feature extraction techniques produces a wide range of numerical values.
3. A normalization process is thus considered necessary to make the feature vector data suitable for directly applying it to the classifier. The feature vector data has been normalised in the range 0 to 1 using Eq. (2.42).
4. Each and every level of multiresolution image has significantly distinctive information about the original image. Therefore, combining them together produces efficient feature

vector data useful in the categorization of hardwood species. The normalized texture feature vectors are combined cumulatively to form level 1 to level 7 feature vectors as given by Eq. (4.3).

$$F_L = \sum_{I=1}^{I=L} G_I \tag{4.3}$$

where, F_L stands for feature vector data obtained at level L and, G_I signifies the texture features obtained by LBP or LCP or LPQ feature extraction technique from the I^{th} level of Gaussian processed grayscale image.

5. The PCA and mRMR techniques are employed in the third stage to reduce the dimensions of feature vector data.
6. In the final stage, four classifiers have been employed to classify the hardwood species into 75 categories using GP based texture feature vector data. Consequently, the best combination of texture feature technique with classifier is obtained to classify the hardwood species decided on the basis of the best classification accuracy. Thus, on the basis of combination of GP with different variants of texture feature descriptors, following texture feature extraction techniques are proposed here, and they are listed as below with their notations and variations.

$GPLBP^{u2}$ Gaussian image pyramid based uniform local binary pattern

$GPLBP^{ri}$ Gaussian image pyramid based rotation invariant local binary pattern

$GPLBP^{riu2}$ Gaussian image pyramid based rotation invariant uniform local binary pattern

$GPLCP^{u2}$ Gaussian image pyramid based uniform local configuration pattern

$GPLCP^{ri}$ Gaussian image pyramid based rotation invariant local configuration pattern

$GPLCP^{riu2}$ Gaussian image pyramid based rotation invariant uniform local configuration pattern

GPLPQ Gaussian image pyramid based local phase quantization

4.2.2 Approaches used for Performance Evaluation of Feature Extraction Techniques

The performance of the GP based feature extraction techniques for classification of hardwood species have been investigated employing two strategies: (1) 10-fold cross validation and (2) randomly dividing the database (Section 2.5.2).

4.3 EXPERIMENTAL RESULTS AND DISCUSSION

The experimental work presented in this section investigates the effectiveness of the GP based texture feature extraction techniques for the classification of microscopic images of hardwood species database into 75 classes with the help of classifiers. The four classifiers used for the investigation are linear SVM, RBF kernel SVM, LDA and RF classifiers (Section 2.3).

4.3.1 Parameter Selection

The selection of parameters for efficient implementation of various feature extraction techniques (LBP, LCP and LPQ) and classifiers have been discussed in detail in Section 2.6.1.

4.3.2 Experimental Results

The classification accuracy obtained by the GP based texture feature extraction techniques for microscopic images of hardwood species have been computed using four classifiers. Similar to presentation of results in Chapter 3, here also results have been presented for different categories, and different sets of feature vector data (Section 2.6.2).

4.3.3 Performance Evaluation of GP based Texture Feature Extraction Techniques using 10-fold Cross Validation Approach

4.3.3.1 Full feature vector data (FFVD)

The percentage classification accuracy attained by the GP based texture features for grayscale image of hardwood species database is presented in Table 4.1. The classification accuracy obtained by the proposed texture features using three different classifiers is discussed below:

Linear SVM classifier: The FFVD of GPLPQ feature extraction technique has given the best classification accuracy of 98.20±1.04% with feature vector dimension of 1024. Further, the 2nd best classification accuracy of 95.73±2.39% (236 features) has been achieved by FFVD produced by GPLBP^{u2} texture feature extraction technique. The FFVD produced by GPLBP^{riu2} feature extraction technique has given a classification accuracy of 91.20±1.53% (50 features), which is lowest among the proposed feature extraction techniques.

RBF kernel SVM classifier: Using this classifier the best classification accuracy of 97.67±1.05% has been attained with FFVD (1024 features) produced by GPLPQ feature extraction technique, which is the best among the proposed feature extraction techniques. The FFVD of GPLBP^{u2} texture feature extraction technique has obtained the 2nd best classification accuracy of 95.40±1.23% with 295-dimensional feature vector data. On the other hand, least classification accuracy of 91.00±2.13% (40 features) has been achieved by feature vector data of GPLBP^{riu2} texture feature extraction technique.

RF classifier: This classifier has given the best classification accuracy of 94.27±1.76% for FFVD **(**1280 features**)** produced by GPLPQ texture feature extraction technique. Further, the FFVD produced by GPLCP^{riu2} technique has obtained the 2nd best classification accuracy of 93.13±2.06% for 486-dimensional feature vector data**.** In addition, among the proposed feature extraction techniques, the least classification accuracy of 85.33±2.47% has been achieved by FFVD of GPLBP^{riu2} feature extraction technique.

Table 4.1 Classification accuracy achieved using full feature vector data.

Proposed techniques	IDL	Feature extraction time in seconds	NoF	% CA±SD achieved by classifiers		
				Linear SVM	RBF kernel SVM	RF
GPLBP^{u2}	1	0.2920	59	79.20±2.96	81.40±2.64	69.27±2.52
	2	0.3164	118	91.53±1.43	90.47±1.69	81.60±2.73
	3	0.3320	177	93.60±1.83	94.00±1.63	85.60±3.07
	4	0.3410	**236**	**95.73±2.39**	95.07±1.48	89.27±1.35
	5	0.3462	**295**	95.07±1.18	**95.40±1.23**	90.33±2.07
	6	0.3536	354	94.07±2.21	95.13±1.25	90.67±2.80
	7	0.3648	413	93.40±2.64	94.00±1.29	90.87±2.37
GPLBP^{ri}	1	0.3039	36	77.33±2.86	78.80±2.57	53.93±2.78
	2	0.3139	72	88.53±1.43	87.07±1.96	73.33±1.99
	3	0.3290	108	91.86±3.23	91.00±1.86	82.60±2.89
	4	0.3335	144	91.53±2.51	91.87±2.17	84.93±2.58
	5	0.3364	180	91.93±1.84	92.67±1.96	86.93±2.14
	6	0.3427	216	91.07±2.04	92.67±1.67	87.80±1.51
	7	0.3475	252	89.80±2.47	90.47±2.47	86.73±2.05
GPLBP^{riu2}	1	0.2868	10	63.53±3.15	66.00±2.96	41.87±3.69
	2	0.3139	20	81.60±2.45	83.20±2.03	64.93±2.07
	3	0.3208	30	88.40±1.69	89.06±1.69	74.93±2.97
	4	0.3217	**40**	90.00±1.44	**91.00±2.13**	80.07±3.21
	5	0.3301	**50**	**91.20±1.53**	89.40±1.48	84.00±3.93
	6	0.3341	**60**	88.60±1.67	90.00±1.50	**85.33±2.47**
	7	0.3355	70	87.80±1.66	88.30±0.84	84.73±1.92
GPLCP^{u2}	1	0.5367	81	65.33±5.03	71.73±3.43	65.40±2.75
	2	0.6647	162	83.33±2.33	84.33±3.33	77.80±2.11
	3	0.6673	243	89.00±1.81	90.53±1.36	84.07±1.97
	4	0.6907	324	91.73±1.41	92.80±1.74	88.40±2.42
	5	0.7033	405	92.13±1.71	92.86±1.63	88.80±1.03
	6	0.7333	486	92.60±2.21	93.40±1.55	89.27±1.19
	7	0.7473	567	92.47±1.96	93.80±1.60	90.07±1.52
GPLCP^{ri}	1	0.6363	81	67.13±2.36	63.07±4.55	63.47±4.03
	2	0.6849	162	79.93±2.74	80.33±3.44	76.13±2.17
	3	0.7771	243	87.47±2.60	88.20±2.33	87.07±1.81
	4	0.8190	324	89.20±1.90	91.20±1.71	90.27±1.67
	5	0.8257	405	90.67±1.80	92.27±1.57	92.13±1.21
	6	0.8341	486	91.87±1.90	92.67±1.40	92.53±1.40
	7	0.8392	567	90.93±1.75	92.07±1.34	92.67±1.83
GPLCP^{riu2}	1	0.7553	81	73.67±2.93	71.13±5.31	69.00±4.51
	2	0.9360	162	85.40±2.72	84.93±2.72	81.53±1.69
	3	0.9760	243	89.60±1.89	91.07±2.18	88.73±2.00
	4	0.9633	324	92.33±2.11	92.67±1.50	92.40±1.76
	5	0.9733	405	94.07±1.73	93.67±1.44	92.80±1.88
	6	0.9640	**486**	93.80±1.13	94.13±1.85	**93.13±2.06**
	7	1.0247	567	93.13±1.57	93.67±1.37	92.93±2.07
GPLPQ	1	0.2979	256	93.20±1.83	89.06±1.69	78.07±2.25
	2	0.3120	512	96.67±0.94	94.33±1.01	87.33±2.33
	3	0.3275	768	97.33±1.30	97.13±1.13	93.00±1.58
	4	0.3498	**1024**	**98.20±1.04**	**97.67±1.05**	93.80±2.11
	5	0.3679	1280	97.80±1.37	97.47±1.17	**94.27±1.76**
	6	0.3919	1536	97.33±1.47	97.07±1.26	94.20±2.14
	7	0.3960	1792	96.87±1.78	96.73±1.39	93.87±1.96

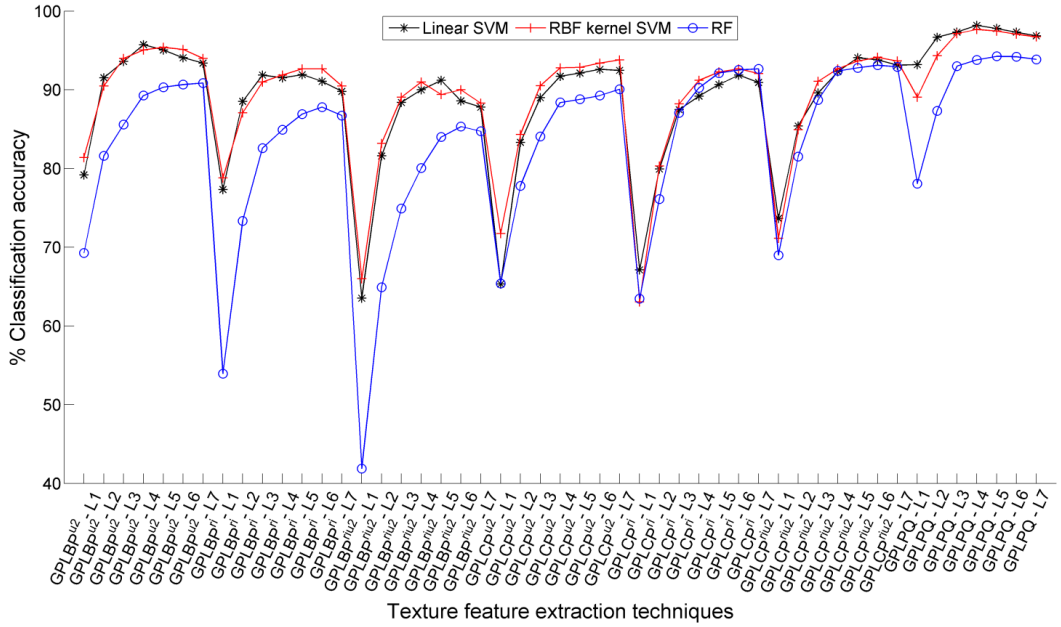

Fig. 4.3 Classification accuracy achieved using FFVD.

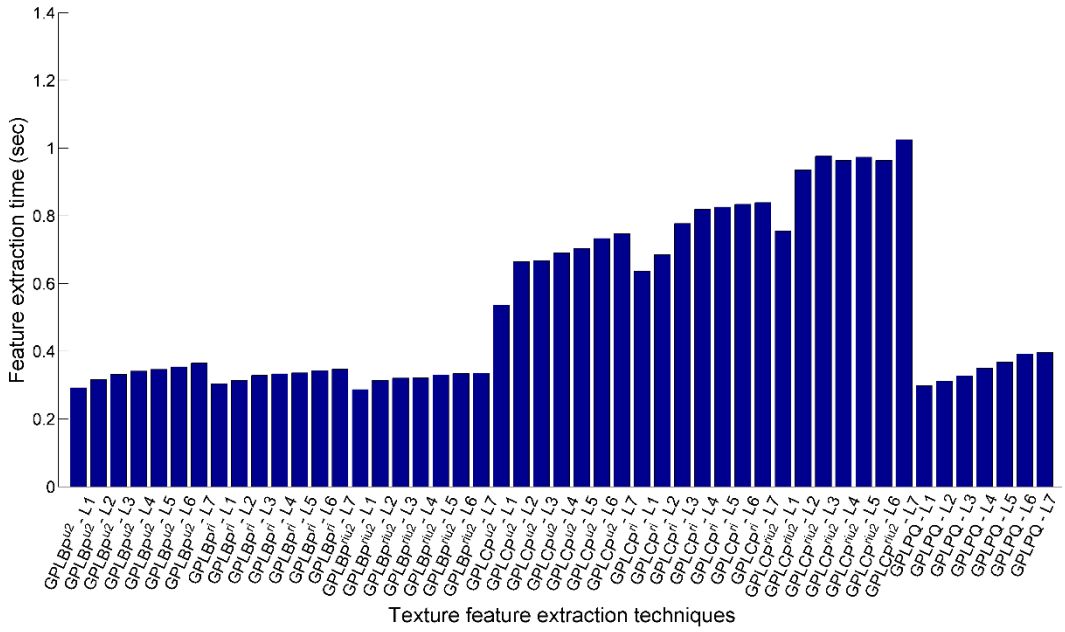

Fig. 4.4 Feature extraction time for single grayscale image.

Here, it has been observed that the best classification accuracy has been achieved at the 4th level of image decomposition by most of the GP based texture feature extraction techniques using all the three classifiers. In addition, among all the three classifiers the best classification accuracy is achieved by linear SVM classifier; whereas, RF classifier yields comparatively lower classification accuracy. The classification accuracy obtained by all the three classifiers have been compared and the same is illustrated in Fig. 4.3. The graphical illustration reveals that GPLPQ texture feature extraction technique has given the best classification accuracy with linear SVM classifier.

Further, the time required by the proposed texture feature extraction techniques for single image is also listed in Table 4.1. The GPLPQ feature extraction technique requires 0.3498 seconds/image for extracting the texture features of given individual images as shown in Fig. 4.4. This feature extraction time is much less than the BWTCLBP^{ri} feature extraction technique which takes 0.6929 seconds/image. The error bar plot for FFVD is shown in Fig. 4.5. The assessment of Fig. 4.5 suggests that the FFVD produced by GPLPQ feature extraction technique at the 4th level of image decomposition yields best classification accuracy of 98.20±1.04% with lower SD value. The GPLPQ feature extraction technique have achieved slightly lower classification accuracy (97.67±1.05%) with RBF kernel SVM classifier, while the RF classifier has given lowest classification accuracy (94.27±1.76%).

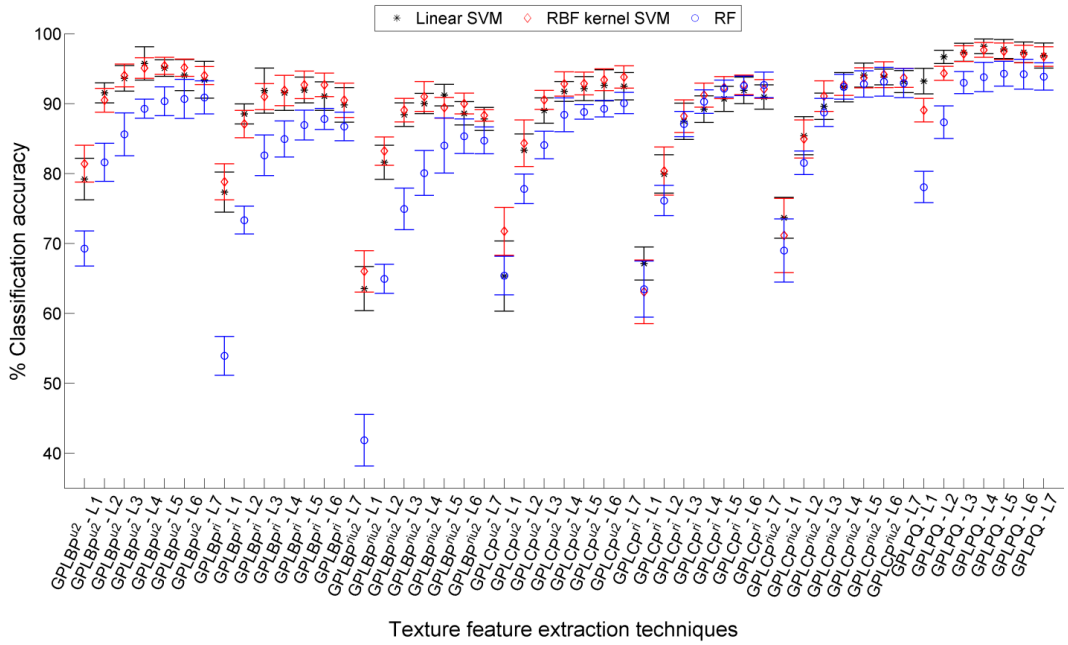

Fig. 4.5 Error bar plot with SD using FFVD.

4.3.3.2 The PCA dimensionality reduced feature vector data

In order to improve the classification accuracy of hardwood species classification, the PCA has been employed to reduce the dimensionality of full feature vector data. The performance of feature extraction techniques with PCA using different classifiers has been listed in Table 4.2 and are succinctly discussed henceforth:

Linear SVM classifier: Here, the PCA reduced feature vector data of GPLPQ feature extraction technique yields the best classification accuracy of 98.20±1.04%, which is similar to the classification accuracy achieved by FFVD; but has been achieved using only 350-dimensional feature vector data compared to 1024-dimensional feature vector data at the 4th level of image decomposition.

Table 4.2 Classification accuracy achieved using PCA based reduced feature vector data.

Proposed techniques	IDL	%CA±SD achieved by classifiers							
		NoF	Linear SVM	NoF	RBF kernel SVM	NoF	RF	NoF	LDA
$GPLBP^{u2}$	1	50	78.93±2.02	55	81.40±2.64	40	83.20±2.43	50	81.00±1.81
	2	110	90.73±2.38	100	90.53±1.65	110	90.07±1.90	100	91.33±1.18
	3	170	93.53±1.66	150	94.07±1.15	50	90.00±1.78	170	95.67±1.14
	4	200	95.27±1.20	225	95.13±1.41	100	90.73±1.90	232	97.33±1.41
	5	275	95.13±1.81	275	95.40±1.24	50	90.53±1.63	290	97.67±1.34
	6	325	93.87±2.33	250	95.20±1.25	100	88.93±2.67	348	97.80±1.57
	7	350	92.33±2.62	250	94.00±1.30	200	84.20±3.08	348	97.80±1.57
$GPLBP^{ri}$	1	35	77.07±3.45	30	78.93±3.33	35	76.87±1.69	35	76.00±3.47
	2	65	88.13±1.96	65	87.07±1.86	50	84.73±2.44	70	89.80±1.48
	3	100	91.33±2.69	75	91.33±1.83	75	87.87±3.14	105	94.47±1.51
	4	125	91.20±2.59	100	92.00±2.55	125	87.60±1.26	140	96.00±1.13
	5	170	91.53±1.51	170	92.67±2.01	170	84.93±2.07	175	96.80±1.50
	6	200	90.87±2.01	200	92.67±1.66	200	84.13±2.96	208	96.67±1.04
	7	200	89.40±2.42	225	90.47±2.48	225	81.53±1.89	208	96.67±1.04
$GPLBP^{riu2}$	1	8	58.53±3.40	8	66.00±2.81	8	67.40±3.70	9	58.40±3.95
	2	15	79.47±2.41	15	83.00±2.33	15	84.20±2.67	18	81.00±2.04
	3	25	87.60±1.78	25	88.60±1.31	25	89.67±2.58	27	89.67±1.92
	4	35	89.93±1.62	35	91.33±2.04	35	90.73±0.97	36	92.60±1.87
	5	45	90.80±1.29	40	89.47±1.43	45	91.00±1.84	45	93.60±1.45
	6	50	88.93±1.78	40	89.93±1.39	55	91.00±1.55	54	94.40±1.51
	7	50	88.20±1.91	50	88.40±0.95	60	89.67±3.03	54	94.40±1.51
$GPLCP^{u2}$	1	50	69.20±3.61	50	72.00±3.20	60	66.73±3.58	54	75.53±3.81
	2	100	83.40±2.78	125	84.67±3.22	100	76.33±2.76	108	88.20±2.29
	3	150	89.60±2.11	200	90.60±1.35	200	81.07±3.69	162	93.86±1.17
	4	200	91.27±1.52	300	92.80±1.74	200	82.87±3.81	216	95.67±0.96
	5	250	91.53±2.06	200	92.80±1.72	50	82.47±2.79	250	95.47±0.88
	6	300	92.20±2.27	250	93.40±1.55	50	83.20±3.20	300	95.60±1.18
	7	300	92.27±2.25	500	93.93±1.68	50	84.00±3.05	314	95.53±1.09
$GPLCP^{ri}$	1	50	68.13±3.28	50	63.87±4.75	60	75.47±3.92	54	82.80±2.61
	2	125	79.60±3.18	125	80.53±3.38	150	81.73±4.28	108	93.67±1.92
	3	200	86.93±2.76	150	88.33±2.31	150	84.33±2.16	162	96.33±1.01
	4	250	89.80±1.94	200	91.20±1.72	200	85.27±1.79	216	97.20±0.93
	5	300	90.47±1.78	200	92.33±1.67	200	85.20±2.22	270	97.07±0.84
	6	250	91.73±2.00	250	92.80±1.36	300	85.40±3.36	305	96.60±0.86
	7	300	90.87±1.94	200	92.33±1.05	200	83.87±2.82	305	96.60±0.86
$GPLCP^{riu2}$	1	60	73.93±2.84	50	71.33±4.88	70	83.07±3.13	54	85.67±2.15
	2	100	85.07±2.90	125	85.07±2.63	100	86.80±2.82	100	94.00±1.30
	3	150	90.07±1.92	150	91.13±2.25	200	88.40±1.41	162	97.20±1.21
	4	250	92.53±1.50	200	92.80±1.60	150	86.67±1.89	200	98.13±0.82
	5	250	93.60±1.78	200	93.67±1.45	250	86.93±1.78	270	98.13±0.69
	6	300	94.20±0.94	350	94.20±1.69	250	86.60±1.59	324	97.87±0.76
	7	300	92.80±1.63	300	93.80±1.34	350	85.93±2.40	324	97.87±0.76
GPLPQ	1	150	93.27±1.62	150	89.40±1.39	150	88.20±1.57	150	91.93±2.56
	2	300	96.40±1.23	250	94.53±1.17	150	93.73±1.86	300	96.53±0.69
	3	200	97.53±1.14	200	97.47±0.93	100	94.27±1.84	450	98.33±1.10
	4	**350**	**98.20±1.04**	**250**	**97.87±1.08**	**100**	**94.33±1.76**	**500**	**98.73±1.15**
	5	350	98.00±1.22	150	97.67±1.01	150	94.20±2.04	450	98.53±0.82
	6	500	97.07±1.38	150	97.73±1.10	50	93.47±2.13	500	98.13±1.08
	7	550	96.93±1.00	100	97.73±1.23	50	92.87±2.65	550	97.47±0.82

RBF kernel SVM classifier: Amongst the proposed feature extraction techniques, the PCA reduced feature vector data of GPLPQ texture feature extraction technique has attained slightly better classification accuracy of 97.87±1.08% (250 features) compared to 97.67±1.05% (1024 features) classification accuracy presented by FFVD of GPLPQ technique.

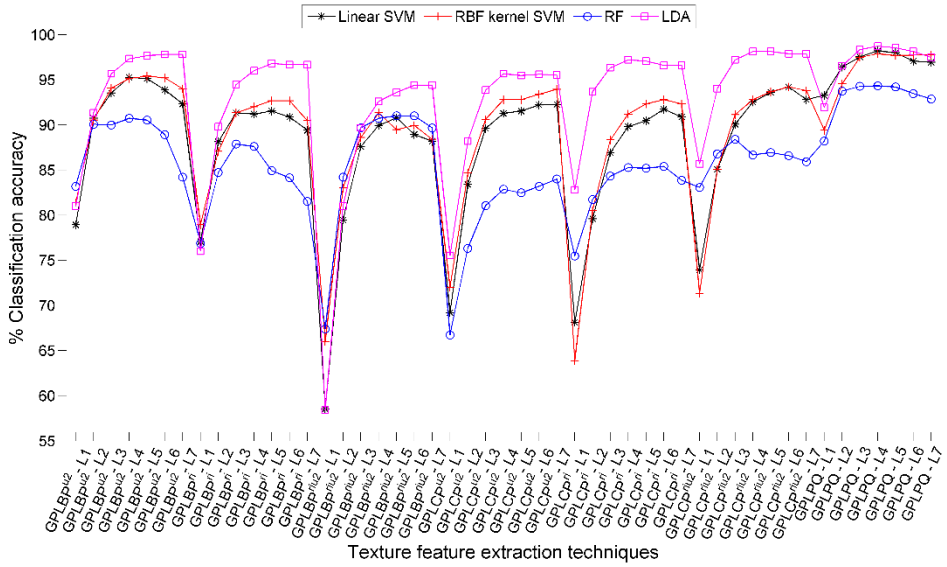

Fig. 4.6 Classification accuracy achieved using PCA reduced feature dataset.

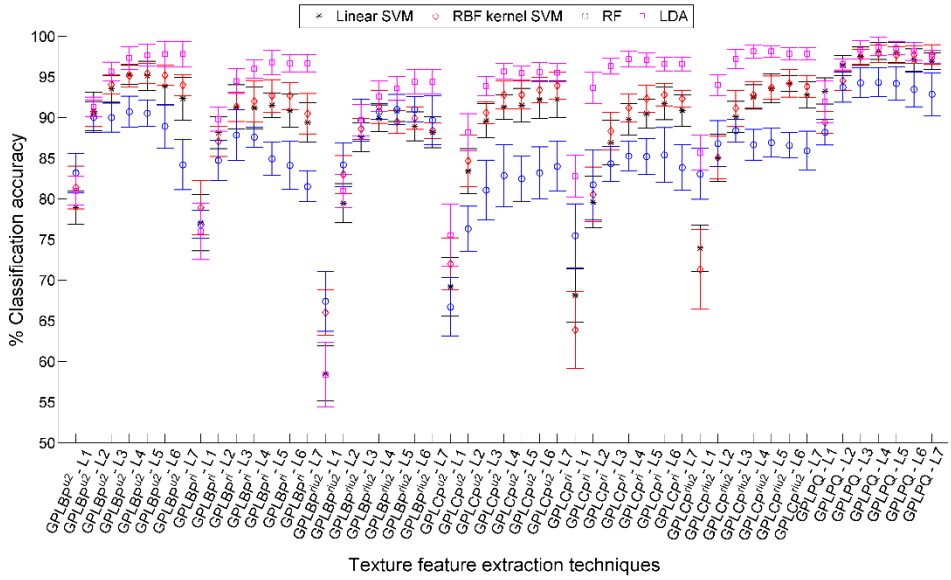

Fig. 4.7 Error bar plot with SD using PCA reduced feature vector data.

RF classifier: The PCA reduced feature vector data of GPLPQ texture feature extraction technique has obtained the best classification accuracy of 94.33±1.76% using 100-dimensional feature vector data only, which is slightly better than the accuracy yielded by the FFVD (94.27±1.76%) of GPLPQ with 1280-dimenisonal feature vector data.

LDA classifier: This classifier has given the best classification accuracy of 98.73±1.15% for PCA reduced feature vector data of GPLPQ texture feature extraction techniques with 500-dimemnsional feature vector data. The classification accuracy obtained by the other feature

extraction techniques have also been better than the rest of the three classifiers used in this experimental work with PCA reduced dimensionality feature vector data.

The classification accuracy achieved with PCA reduced dimensional feature vector data are at par with the FFVD, but has been obtained using low-dimensional feature vector data. The LDA classifier has obtained maximum classification accuracy for the feature vector data produced by GPLPQ texture feature extraction techniques at the 4th level of image decomposition. The graph depicting the comparison of the classification accuracy obtained by four different classifiers is shown in Fig. 4.6. Further, the error bar plot representation of the same is given in Fig. 4.7. The graphical illustration also supports the statement that GPLPQ texture features classified with LDA classifier present the best classification accuracy results.

4.3.3.3 The mRMR feature selection based reduced feature vector data

The subset of feature vector data obtained by mRMR feature selection method has been investigated to see their effect on the classification accuracy produced for hardwood species classification. The classification accuracy results achieved by three different classifiers are listed in Table 4.3. The performance of texture feature extraction techniques with different classifiers are as follows:

Linear SVM classifier: Amongst the proposed feature extraction techniques, the highest classification accuracy of 98.13±0.93% has been achieved by mRMR processed subset (550 features) of FFVD produced by GPLPQ technique at the 6th and 7th level of image decomposition. This classification accuracy is slightly lesser than 98.20±1.04% accuracy obtained by FFVD of GPLPQ technique (1024 features) at the 4th level of image decomposition.

RBF kernel SVM classifier: The mRMR selected feature subset (200 features) of GPLPQ texture feature extraction technique (FFVD produced at the 6th and 7th level of image decomposition) has achieved the best classification accuracy of 98.13±1.08%. This classification accuracy is relatively better than 97.67±1.05% accuracy obtained by FFVD of GPLPQ technique (1024 features) at the 4th level of image decomposition.

RF classifier: The RF classifier has achieved a classification accuracy of 94.53±1.69% for mRMR selected feature subset (300 features) of FFVD produced by GPLPQ texture feature extraction technique at the 5th level of image decomposition. This classification accuracy has been relatively better than the highest classification accuracy (94.27±1.76%) produced by GPLPQ texture feature extraction technique for FFVD (1280-dimensional feature) at the 5th level of image decomposition.

The classification accuracy results are plotted in Fig. 4.8, and the error bar plot for the same has been illustrated in Fig. 4.9. These figures depict that GPLPQ texture feature extraction techniques have produced best classification accuracy at the 6th and 7th level of image decomposition that too with lower value of SD using linear SVM classifier.

Table 4.3 Classification accuracy achieved using mRMR feature selection based reduced feature vector data.

Proposed techniques	IDL	% CA±SD achieved by classifiers					
		NoF	Linear SVM	NoF	RBF kernel SVM	NoF	RF
$GPLBP^{u2}$	1	55	76.93±3.31	55	79.73±2.54	55	69.93±4.60
	2	110	91.07±1.78	115	90.33±1.78	115	81.73±2.14
	3	170	93.47±1.83	170	93.87±1.36	100	86.13±3.37
	4	225	95.47±2.15	225	95.07±1.38	225	89.47±1.29
	5	250	95.33±1.86	275	95.47±1.60	150	90.53±2.68
	6	200	94.80±1.57	300	95.47±1.17	250	91.40±1.46
	7	250	95.13±1.81	250	94.80±1.12	350	91.00±1.67
$GPLBP^{ri}$	1	35	76.33±2.52	35	78.53±3.01	35	54.87±2.95
	2	65	87.53±1.54	65	87.27±1.73	65	75.60±3.71
	3	100	91.53±2.98	100	91.13±2.01	50	84.20±2.37
	4	75	91.00±1.45	75	91.80±2.52	75	87.13±2.69
	5	170	91.67±2.02	100	93.27±1.49	50	88.80±2.89
	6	100	92.60±1.35	100	92.73±1.15	100	89.07±2.29
	7	150	91.73±2.37	150	92.87±2.33	225	88.60±2.21
$GPLBP^{riu2}$	1	8	54.13±3.57	8	61.40±3.80	8	67.40±3.70
	2	15	79.00±2.78	15	81.20±2.08	15	84.20±2.67
	3	25	87.00±2.29	25	88.33±1.34	25	89.67±2.58
	4	35	88.93±2.02	35	90.80±1.74	35	90.73±0.97
	5	45	89.20±1.60	45	88.93±1.38	45	91.00±1.84
	6	55	88.00±1.63	55	88.87±1.54	55	91.00±1.55
	7	65	87.47±1.80	50	88.47±0.83	60	89.67±3.03
$GPLCP^{u2}$	1	75	69.87±3.16	50	71.80±3.27	60	66.33±2.02
	2	150	82.40±2.42	150	84.00±3.43	150	78.33±3.02
	3	100	89.13±2.42	200	91.13±1.60	150	85.47±1.72
	4	200	92.93±1.51	200	94.13±1.57	100	90.00±1.63
	5	150	93.47±1.69	150	94.87±1.22	150	91.40±1.46
	6	150	93.60±1.48	150	94.87±1.41	150	92.13±1.69
	7	150	93.73±1.70	250	94.80±2.06	100	91.73±1.34
$GPLCP^{ri}$	1	60	67.87±3.04	70	64.80±4.81	70	64.33±4.15
	2	100	82.13±1.93	50	82.20±2.70	50	77.80±2.83
	3	100	90.07±2.50	100	90.80±2.51	200	88.20±2.65
	4	100	93.40±1.68	50	95.00±1.27	100	92.07±1.87
	5	100	94.33±1.34	100	95.13±1.72	50	93.27±1.68
	6	150	94.47±1.34	100	95.40±1.59	100	93.40±1.62
	7	100	94.20±1.63	150	95.00±1.58	150	94.00±1.18
$GPLCP^{riu2}$	1	60	76.53±2.63	50	72.40±4.59	75	68.87±4.00
	2	50	87.00±2.38	50	86.20±2.20	50	81.53±3.30
	3	100	92.87±1.63	100	94.47±1.37	50	89.33±1.37
	4	100	95.07±1.38	100	95.87±1.63	250	93.33±1.18
	5	100	96.40±1.10	100	97.67±1.26	100	94.33±1.67
	6	200	96.07±1.31	100	96.73±1.02	50	94.47±1.04
	7	100	96.67±1.54	100	96.67±1.44	250	94.33±0.79
GPLPQ	1	200	93.27±1.55	200	88.87±1.54	150	78.33±1.55
	2	450	96.60±1.06	250	94.80±1.25	300	88.67±2.90
	3	500	97.80±1.30	300	97.00±1.19	250	93.47±1.43
	4	550	97.93±1.15	400	98.07±1.52	250	94.47±1.60
	5	400	98.07±1.11	350	98.07±1.27	**300**	**94.53±1.69**
	6	**550**	**98.13±0.93**	**200**	**98.13±1.08**	200	94.33±1.45
	7	**550**	**98.13±0.93**	**200**	**98.13±1.08**	200	94.47±1.14

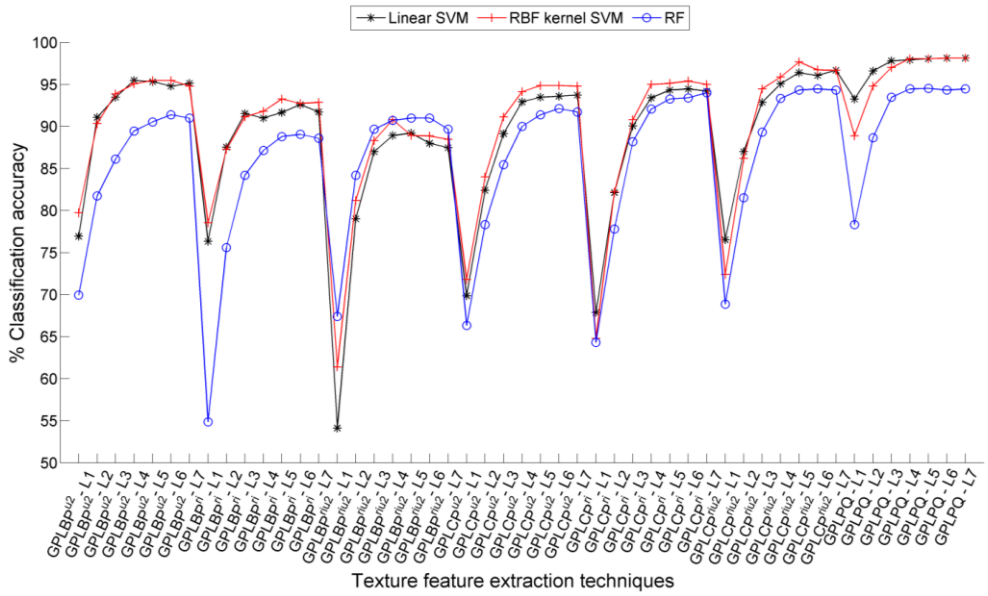

Fig. 4.8 Classification accuracy achieved using mRMR feature selection based reduced feature vector data.

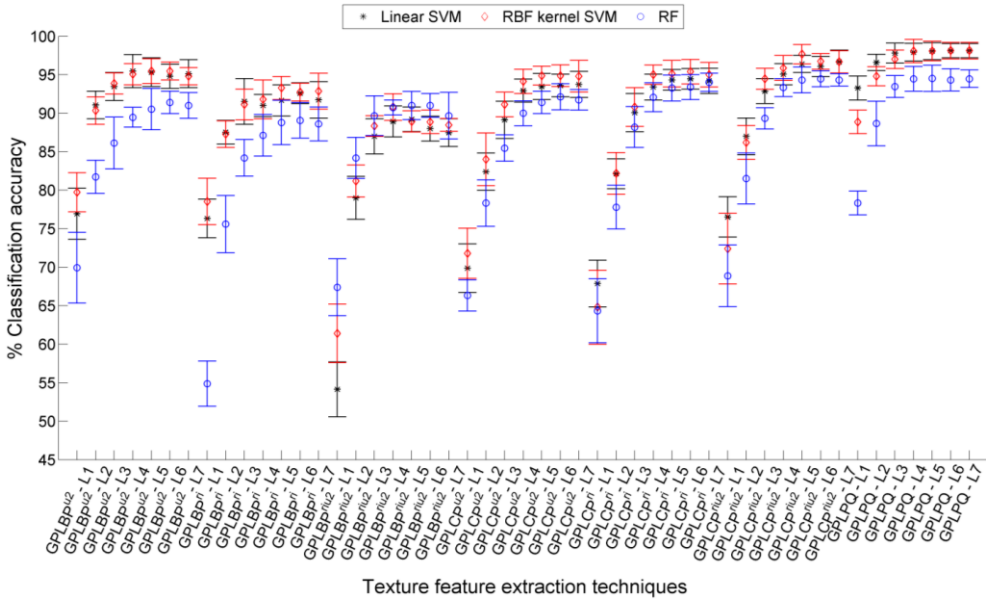

Fig. 4.9 Error bar plot with SD using mRMR feature selection based reduced feature vector data.

It is observed from Table 4.1 that the length of the feature vector data increases as the level of image decomposition increases. The classification accuracy results for full feature vector data of GP based texture feature extraction techniques using three different classifiers have gone up in the range of 4th to 6th level of image decomposition and thereafter either it remains same or decreases a little bit. Further, in case of feature vector data of GPLCP^{u2} feature extraction technique, the increase in the classification accuracy has been observed for both, RBF kernel SVM and RF classifiers. It is noticeable that the increase in the classification accuracy has been attained at the cost of additional computation time. Therefore, the texture descriptors beyond 7th level of image decomposition has not been investigated.

Further, employing PCA (dimensionality reduction) and mRMR (feature selection) technique has not only reduced the computational time but also shown considerable improvement in the classification accuracy for hardwood species' classification. It is also observed from Table 4.1, Table 4.2 and Table 4.3 that the GP based feature extraction techniques have achieved better classification accuracy compared to the original LBP variants and BWT based LBP variants feature extraction techniques as discussed in Chapter 2 and Chapter 3.

4.3.4 Performance Evaluation of GP based Texture Feature Extraction Techniques using Randomly Divided Database (RDD)

4.3.4.1 Full feature vector data (FFVD)

The classification accuracy achieved by GP based texture feature extraction techniques for different ratios of training and testing data has been listed in Table 4.4.

Linear SVM classifier: Amongst the proposed texture feature extraction techniques, the FFVD produced by GPLPQ technique has produced significant feature vector data which yields best classification accuracy of 95.33% (at 4^{th} IDL), 93.78% (at 4^{th} IDL), 91% (at 4^{th} IDL) and 89.07% (at 5^{th} IDL) for 80/20, 70/30, 60/40 and 50/50 training and testing ratios of RDD, respectively.

RBF kernel SVM classifier: Using RBF kernel SVM classifier, the best classification accuracy of 93.33% (at 5^{th} IDL), 91.78% (at 5^{th} IDL), 88.17% (at 5^{th} IDL) and 84.53% (at 4^{th} IDL) has been achieved for 80/20, 70/30, 60/40 and 50/50 training and testing ratios of RDD, respectively. These classification accuracies have been achieved for FFVD produced by GPLPQ texture feature extraction technique (Table 4.4).

RF classifier: As listed in Table 4.4 the FFVD produced by GPLPQ feature extraction technique has given the best classification accuracy for different proportions of training and testing data of RDD, amongst the proposed techniques using RF classifier. The GPLPQ features have achieved classification accuracy of 89.33% (at 5^{th} IDL), 87.56% (at 6^{th} IDL), 86.17% (at 7^{th} IDL) and 81.60% (at 5^{th} IDL) for 80/20, 70/30, 60/40 and 50/50 proportions of training and testing data, respectively.

The classification accuracies obtained by the three different classifiers are compared for each of the four (80/20, 70/30, 60/40 and 50/50) training and testing ratios, and are graphically illustrated in Fig. 4.10, Fig. 4.11, Fig. 4.12 and Fig. 4.13, respectively. It is clear from these figures that texture feature vector data produced by most of the GP based texture feature extraction techniques yielded the best classification accuracy with linear SVM classifier. Whereas, the least classification accuracy for the GP based texture feature extraction techniques has been achieved with RF classifier.

Table 4.4 Classification accuracy achieved by full feature vector data for different proportions of training and testing data of RDD using three classifiers.

Proposed techniques	IDL	% CA achieved by classifiers for different proportions of training and testing data											
		Linear SVM				RBF kernel SVM				RF			
		80/20	70/30	60/40	50/50	80/20	70/30	60/40	50/50	80/20	70/30	60/40	50/50
$GPLBP^{u2}$	1	74.67	68.00	66.33	62.13	70.33	66.00	61.67	57.87	59.33	53.11	51.00	47.60
	2	85.00	81.33	78.33	76.67	84.67	81.11	75.33	73.33	76.33	69.78	67.00	64.80
	3	87.33	85.56	83.17	80.40	89.00	84.89	81.50	78.40	80.33	78.00	73.17	70.80
	4	92.00	87.87	85.83	84.13	90.00	87.56	85.83	82.67	87.33	81.56	78.67	75.87
	5	90.67	88.00	87.67	83.33	90.67	87.78	85.83	82.67	86.00	83.56	81.83	78.40
	6	91.00	88.22	86.00	83.73	90.33	89.11	86.00	82.93	87.00	83.56	81.83	79.07
	7	89.67	86.67	83.67	82.80	89.00	87.11	84.50	81.87	87.33	83.56	81.50	79.33
$GPLBP^{ri}$	1	68.00	69.56	66.33	63.60	69.00	66.89	64.00	60.27	47.00	42.22	40.17	37.20
	2	85.67	82.44	81.50	77.07	82.67	78.89	74.33	71.47	71.67	67.33	63.17	62.13
	3	87.67	87.11	84.00	80.53	86.00	85.56	81.67	77.60	80.33	76.67	74.67	70.53
	4	89.67	86.89	85.83	82.40	88.67	88.22	84.33	80.13	83.33	81.78	78.83	75.33
	5	86.33	84.89	84.67	83.20	88.00	86.44	84.50	81.07	85.00	82.44	82.67	78.80
	6	86.67	85.11	86.00	82.00	88.33	86.44	84.83	81.07	85.00	82.89	82.83	79.33
	7	86.00	84.22	83.50	78.80	86.67	82.89	81.33	78.93	85.67	83.56	81.17	79.73
$GPLBP^{riu2}$	1	61.00	57.11	57.67	54.13	63.67	58.67	57.83	53.33	34.67	34.44	35.00	30.93
	2	79.00	75.33	75.33	71.47	80.00	76.67	70.50	67.60	61.00	59.33	54.83	52.93
	3	86.67	83.56	81.17	78.53	86.00	82.89	80.00	77.47	76.33	69.33	67.67	64.40
	4	88.67	84.22	83.67	82.93	87.67	84.44	81.83	78.27	77.67	75.78	73.33	71.60
	5	87.00	85.56	85.50	83.73	86.33	84.44	84.33	79.87	81.33	79.33	80.00	75.87
	6	86.00	84.22	82.50	82.53	85.67	84.00	82.67	81.20	82.33	80.89	79.83	76.67
	7	85.67	81.33	81.50	81.07	84.00	81.78	79.33	79.07	82.67	78.44	78.50	76.27
$GPLCP^{u2}$	1	61.33	57.78	50.67	52.40	64.00	58.44	53.50	52.67	56.33	51.11	48.83	47.87
	2	78.33	71.78	69.17	64.40	80.00	74.22	69.00	65.73	71.00	66.22	61.33	59.33
	3	83.67	80.67	76.17	73.07	83.67	80.89	76.17	74.67	78.33	74.00	72.83	70.40
	4	86.33	83.11	81.50	79.07	85.33	83.11	80.67	79.47	83.00	80.44	78.50	76.27
	5	86.33	83.33	82.00	80.27	87.00	85.11	82.83	80.40	84.67	82.67	82.17	79.07
	6	86.33	85.11	83.33	80.40	87.00	84.67	83.33	82.00	83.67	81.33	80.83	78.67
	7	87.00	85.56	83.83	79.73	86.33	84.67	83.33	82.00	84.00	81.33	81.33	77.20
$GPLCP^{ri}$	1	57.33	50.89	49.17	46.00	53.00	45.56	46.67	43.87	51.67	46.89	45.67	45.87
	2	72.33	67.56	64.83	62.00	71.67	66.67	63.67	60.40	68.00	61.11	59.83	58.40
	3	80.33	77.33	75.83	74.40	82.67	78.22	75.17	73.07	82.00	80.44	78.00	76.40
	4	84.00	79.56	79.50	78.27	87.00	84.67	79.83	78.40	85.67	86.22	84.50	80.80
	5	86.33	84.22	81.00	79.07	87.33	83.11	84.00	80.40	87.67	87.56	85.67	83.20
	6	87.00	83.56	83.00	79.47	85.67	84.44	83.33	80.80	88.00	87.56	86.00	84.00
	7	87.33	83.33	81.67	79.47	87.33	83.56	83.00	81.47	87.67	87.33	87.00	84.27
$GPLCP^{riu2}$	1	66.67	60.22	57.67	51.73	62.33	56.22	52.83	50.53	58.00	51.11	53.00	48.80
	2	78.67	75.11	71.50	68.93	76.67	73.56	71.17	66.93	73.67	72.44	67.50	65.73
	3	85.33	82.22	79.00	78.00	85.33	81.56	78.83	76.27	84.67	82.22	80.17	78.27
	4	86.67	85.33	83.00	80.67	87.67	85.78	81.67	80.27	88.33	86.89	87.83	82.13
	5	89.00	86.44	84.50	81.60	90.00	87.33	83.83	81.73	90.00	88.22	88.50	84.40
	6	90.67	87.56	84.83	83.33	89.67	88.89	85.67	83.20	89.67	89.11	89.17	86.13
	7	90.00	86.00	85.00	82.67	89.33	88.67	85.00	83.07	88.67	88.89	89.67	84.00
GPLPQ	1	87.33	81.11	77.67	75.20	82.67	75.33	69.17	68.00	72.67	64.44	60.50	57.47
	2	92.67	88.67	85.83	83.07	89.67	84.67	79.83	76.93	84.67	77.56	76.17	71.60
	3	95.00	92.22	90.33	86.80	92.67	90.44	84.67	82.13	88.67	84.44	82.00	79.07
	4	**95.33**	**93.78**	**91.00**	88.93	92.33	91.33	87.50	**85.33**	89.00	86.67	84.67	80.93
	5	93.33	92.67	90.00	**89.07**	**93.33**	**91.78**	**88.17**	84.53	**89.33**	85.78	84.83	**81.73**
	6	91.67	90.89	89.33	87.73	92.67	91.33	87.67	84.17	88.00	**87.56**	85.83	81.60
	7	94.33	90.44	89.00	87.73	92.33	90.00	86.83	84.40	89.33	87.11	**86.17**	81.47

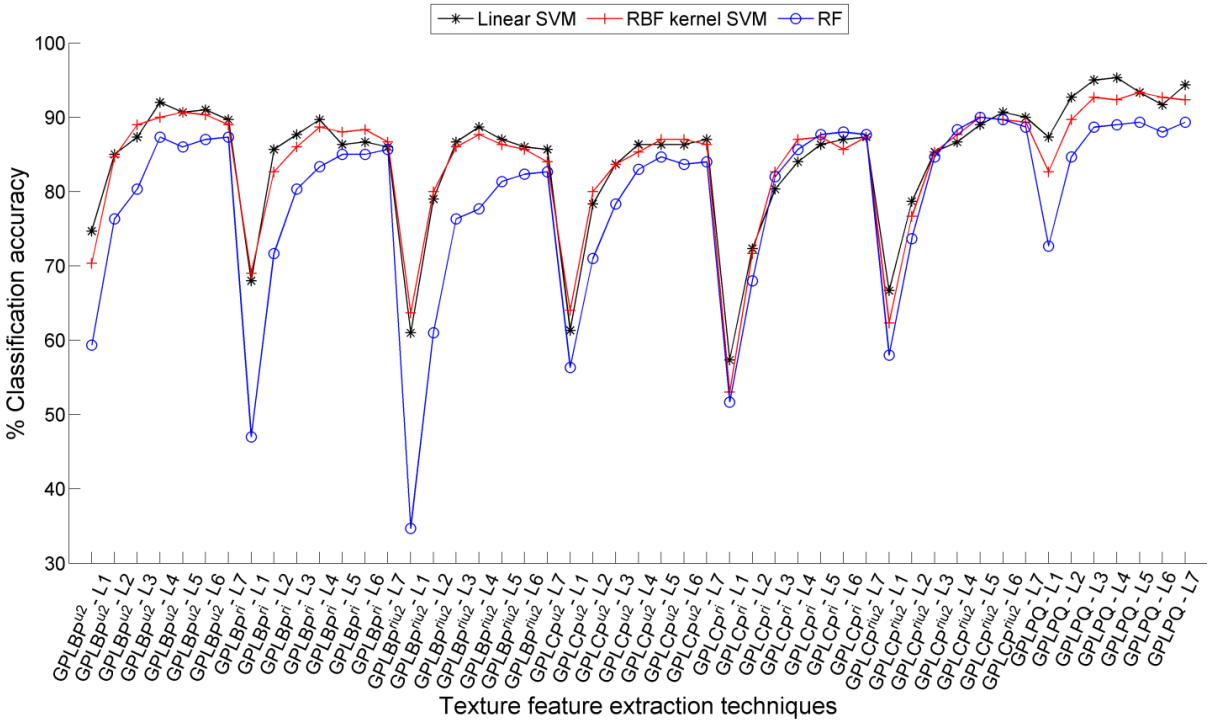

Fig. 4.10 Classification accuracy achieved for 80/20 proportion of training and testing data of RDD.

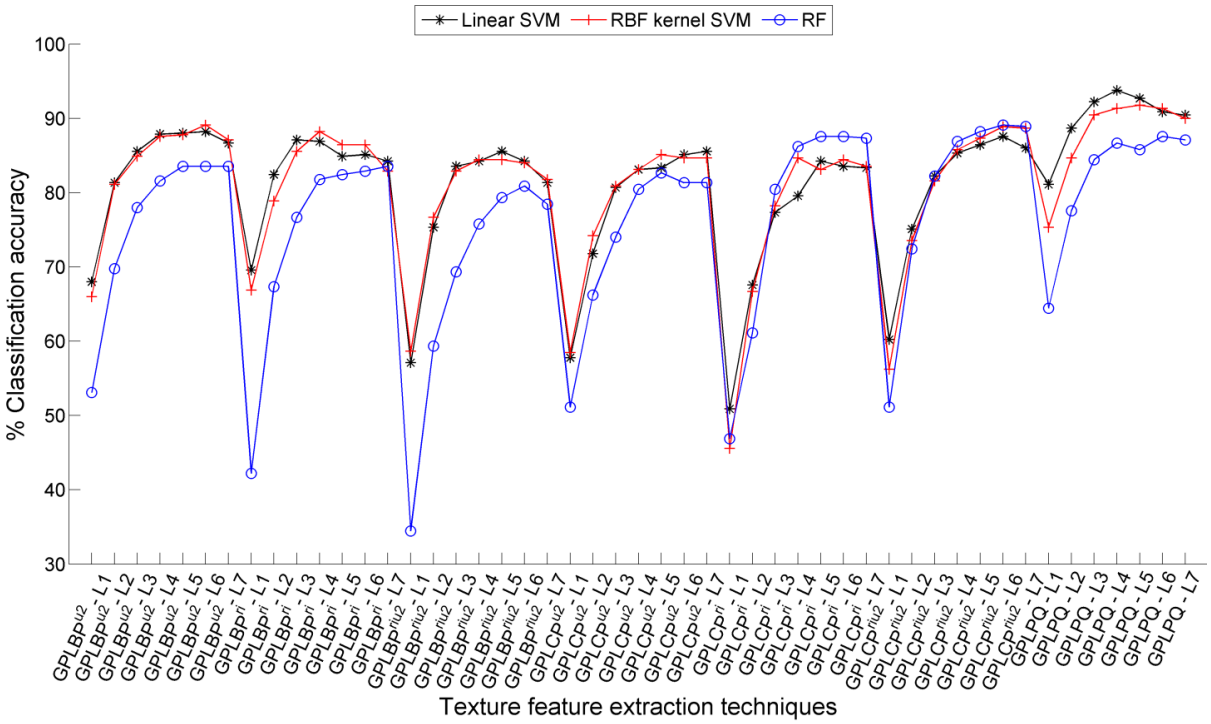

Fig. 4.11 Classification accuracy achieved for 70/30 proportion of training and testing data of RDD.

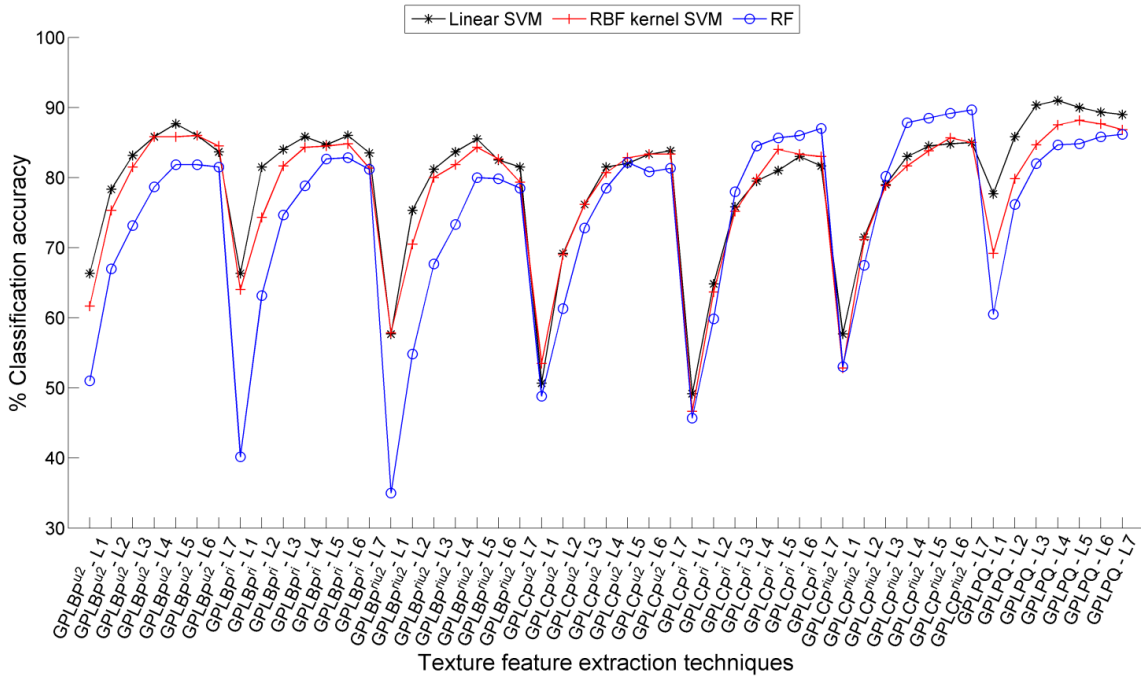

Fig. 4.12 Classification accuracy achieved for 60/40 proportion of training and testing data of RDD.

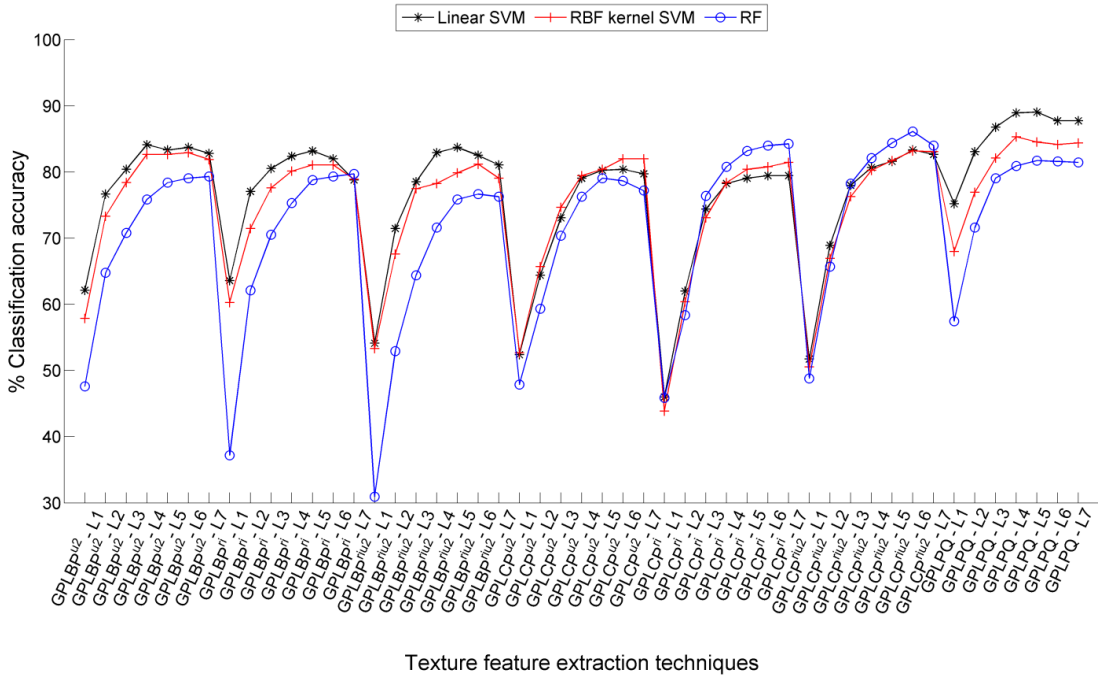

Fig. 4.13 Classification accuracy achieved for 50/50 proportion of training and testing data of RDD.

4.3.4.2 The PCA dimensionality reduced feature vector data

The classification accuracy results obtained by the PCA based reduced feature vector data using linear SVM, RBF kernel SVM, LDA and RF classifier has been listed in Table 4.5, Table 4.6, Table 4.7 and Table 4.8, respectively.

Linear SVM classifier: The PCA dimensionality reduced feature vector data of the GPLPQ technique yields the best classification accuracy of 95% (150 features, at 4th IDL), 93.56% (200

features, at 3rd IDL), 91.33% (450 features, at 4th IDL) and 88.67% (500 features, at 4th IDL) for 80/20, 70/30, 60/40 and 50/50 training and testing ratios of RDD, respectively. This classification accuracy is marginally lower than the accuracy achieved for FFVD of GPLPQ technique with high-dimensional features (Table 4.5).

Table 4.5 Classification accuracy achieved by PCA reduced feature vector data for different proportions of training and testing data of RDD using linear SVM classifier.

Techniques	IDL	NOF	80/20	NOF	70/30	NOF	60/40	NOF	50/50
GPLBP^{u2}	1	50	76.33	55	68.00	55	65.17	50	62.27
	2	110	84.67	100	80.67	110	77.83	110	76.13
	3	100	86.00	170	85.33	170	82.33	150	79.47
	4	200	90.67	150	88.00	225	86.67	150	84.27
	5	150	90.00	100	87.11	150	86.83	275	83.47
	6	200	89.33	200	88.22	250	85.67	250	82.93
	7	200	88.67	350	86.67	250	83.33	250	81.73
GPLBP^{ri}	1	30	72.67	35	71.33	35	68.50	30	65.20
	2	65	85.67	60	81.56	60	81.50	60	77.07
	3	100	86.67	100	85.56	75	83.67	75	80.27
	4	125	87.67	125	84.89	125	85.17	125	81.87
	5	170	87.67	170	84.89	170	84.50	170	82.40
	6	200	85.67	200	84.67	200	83.67	200	79.87
	7	225	82.00	150	82.22	200	82.33	200	77.87
GPLBP^{riu2}	1	8	55.33	8	53.33	8	51.50	8	49.73
	2	15	75.33	15	72.89	15	71.67	15	70.67
	3	25	83.33	25	80.67	25	80.00	25	77.33
	4	30	87.00	35	84.00	35	83.17	65	81.07
	5	45	86.33	45	85.78	45	83.83	45	83.60
	6	55	85.00	55	83.33	50	82.00	55	81.47
	7	60	84.33	60	82.67	60	80.17	60	79.73
GPLCP^{u2}	1	60	64.00	60	57.33	60	51.83	60	51.20
	2	100	79.00	100	73.11	125	67.50	100	66.13
	3	150	84.00	150	79.78	200	76.33	200	74.53
	4	250	87.00	200	83.33	200	81.17	250	78.80
	5	250	85.67	250	82.67	250	82.00	250	79.33
	6	250	87.00	300	84.89	250	82.50	300	80.40
	7	300	86.33	300	84.44	300	82.83	300	79.20
GPLCP^{ri}	1	60	58.67	60	53.33	60	49.50	60	46.40
	2	100	73.00	100	68.89	100	66.00	125	62.67
	3	150	80.67	200	77.78	150	75.83	150	75.33
	4	200	83.00	150	79.78	150	80.00	200	78.27
	5	250	86.67	250	84.00	300	81.50	200	79.33
	6	250	87.33	250	85.11	300	82.17	250	80.27
	7	250	87.67	250	85.11	250	81.83	250	80.40
GPLCP^{riu2}	1	50	68.00	50	60.22	50	58.33	50	50.44
	2	100	78.00	100	74.00	100	71.67	100	67.87
	3	150	85.00	150	80.22	150	78.33	150	77.47
	4	150	86.00	200	84.22	200	83.67	150	79.73
	5	200	88.33	250	84.44	200	84.33	200	82.53
	6	300	90.33	250	86.67	250	85.83	300	83.20
	7	200	88.67	250	85.33	300	84.50	200	82.67
GPLPQ	1	100	86.00	100	82.00	200	77.50	200	74.40
	2	200	92.00	150	89.33	350	85.83	300	81.73
	3	250	95.00	**200**	**93.56**	250	90.17	350	86.40
	4	**150**	**95.00**	100	93.33	**450**	**91.33**	**500**	**88.67**
	5	250	94.00	450	92.67	400	89.83	450	88.67
	6	150	91.67	200	91.56	200	90.00	200	88.40
	7	350	94.33	150	91.78	300	90.00	150	87.60

Table 4.6 Classification accuracy achieved by PCA reduced feature vector data for different proportions of training and testing data of RDD using RBF kernel SVM classifier.

Techniques	IDL	NOF	80/20	NOF	70/30	NOF	60/40	NOF	50/50
	1	50	72.00	50	66.22	55	61.33	40	58.00
	2	100	85.33	100	80.89	50	76.33	100	73.60
	3	170	89.33	150	84.67	100	81.67	150	78.67
$GPLBP^{u2}$	4	150	90.00	200	88.22	225	85.83	225	82.53
	5	50	92.00	150	88.00	100	86.00	100	82.93
	6	150	90.33	100	89.33	300	86.17	150	83.33
	7	250	89.67	150	87.33	300	84.83	350	82.00
	1	20	71.00	35	68.22	30	65.33	35	61.87
	2	50	82.67	65	78.89	65	74.50	60	71.47
	3	50	86.33	50	85.33	75	82.00	75	77.33
$GPLBP^{ri}$	4	100	89.00	100	88.00	75	84.17	125	79.60
	5	150	88.33	150	86.44	150	84.67	170	81.67
	6	200	88.67	150	86.44	200	84.83	200	81.20
	7	200	87.00	150	83.11	150	81.17	150	78.93
	1	8	64.00	8	57.11	8	56.67	8	53.20
	2	15	79.33	15	75.11	15	70.17	15	66.27
	3	25	86.33	25	82.89	25	80.00	20	77.07
$GPLBP^{riu2}$	4	35	87.67	30	84.44	35	82.67	35	78.40
	5	40	86.00	45	84.44	45	84.33	45	80.00
	6	55	85.33	55	83.56	55	82.67	50	81.33
	7	50	83.33	60	81.56	65	79.83	65	79.07
	1	70	63.00	75	57.78	70	54.17	70	52.13
	2	100	79.67	150	74.00	150	69.17	150	66.80
	3	100	86.00	100	83.33	100	77.50	100	72.67
$GPLCP^{u2}$	4	150	88.00	100	85.56	100	82.67	150	82.00
	5	50	90.00	50	86.89	200	84.17	150	83.60
	6	50	89.33	100	86.22	150	84.17	150	84.00
	7	50	90.00	50	86.67	150	84.83	150	84.00
	1	50	53.33	50	46.89	50	47.67	60	44.80
	2	100	71.67	100	67.78	100	65.00	100	61.07
	3	150	82.67	150	78.00	150	75.67	150	72.93
$GPLCP^{ri}$	4	100	87.00	150	84.67	150	79.83	200	78.13
	5	200	88.00	200	83.56	250	83.83	300	80.53
	6	200	86.33	200	84.44	250	83.33	200	80.93
	7	200	87.33	200	84.00	200	83.17	250	81.73
	1	50	64.00	50	55.78	100	54.67	150	50.13
	2	100	76.67	100	74.67	100	72.00	100	67.20
	3	100	85.67	100	81.78	200	78.67	200	76.53
$GPLCP^{riu2}$	4	150	88.00	200	86.00	200	82.00	150	80.67
	5	300	90.33	150	87.11	200	84.00	250	81.47
	6	250	89.67	200	88.89	200	85.83	250	83.20
	7	200	89.33	250	88.67	200	84.83	250	83.07
	1	200	82.33	200	74.89	150	69.33	150	67.87
	2	150	89.67	200	85.56	150	80.50	200	77.33
	3	50	92.67	200	90.67	300	85.67	300	82.40
GPLPQ	4	50	92.33	100	92.00	200	88.00	100	86.00
	5	**150**	**94.33**	150	92.67	**150**	**89.00**	**200**	**86.40**
	6	50	94.00	**50**	**92.89**	200	88.67	50	86.00
	7	50	94.67	50	92.67	50	88.17	50	86.00

Table 4.7 Classification accuracy achieved by PCA reduced feature vector data for different proportions of training and testing data of RDD using LDA classifier.

Techniques	IDL	NOF	80/20	NOF	70/30	NOF	60/40	NOF	50/50
	1	40	78.33	40	70.44	40	68.00	30	65.87
	2	100	86.33	100	81.78	100	81.83	50	77.20
	3	170	90.67	150	89.33	150	86.83	170	83.07
$GPLBP^{u2}$	4	225	94.00	225	92.67	225	89.67	100	86.93
	5	150	93.33	250	92.89	275	91.00	150	88.13
	6	300	93.00	325	93.56	150	90.33	200	88.00
	7	300	93.00	325	93.56	150	90.33	250	88.00
	1	35	71.33	35	68.89	35	66.33	35	65.07
	2	70	87.33	70	84.22	70	83.33	70	82.53
	3	105	93.00	105	90.44	105	88.67	105	87.20
$GPLBP^{ri}$	4	140	94.67	140	92.67	140	90.33	140	89.33
	5	175	95.00	175	93.11	175	91.50	175	89.73
	6	208	95.00	208	93.78	208	92.00	208	89.47
	7	208	95.00	208	93.78	208	92.00	208	89.47
	1	9	54.67	9	50.67	9	53.00	9	52.40
	2	18	79.67	18	74.44	18	74.83	18	73.33
	3	27	86.67	27	84.00	27	85.33	27	83.33
$GPLBP^{riu2}$	4	36	89.73	35	87.56	35	88.33	35	86.53
	5	45	90.33	45	89.11	45	90.33	45	88.13
	6	54	90.33	54	90.00	54	91.00	54	89.33
	7	54	90.33	54	90.00	54	91.00	54	89.33
	1	50	71.33	50	64.22	54	62.17	54	60.40
	2	100	84.00	100	80.44	108	78.33	108	75.87
	3	162	89.67	162	88.22	162	87.50	162	83.87
$GPLCP^{u2}$	4	216	92.67	216	90.67	216	88.33	216	85.20
	5	270	92.67	270	91.11	270	88.83	270	85.47
	6	314	93.00	314	89.56	314	88.00	300	83.33
	7	314	93.00	314	89.56	314	88.00	300	83.60
	1	54	75.67	50	72.67	54	71.67	54	68.00
	2	108	91.00	100	85.78	108	86.33	108	83.20
	3	162	94.00	162	91.33	150	90.17	162	89.07
$GPLCP^{ri}$	4	216	94.67	216	94.22	216	92.33	200	90.13
	5	250	94.67	270	93.78	200	92.00	200	91.20
	6	300	94.33	300	93.78	305	91.67	300	89.07
	7	300	94.33	300	93.78	305	91.67	300	89.20
	1	54	80.00	54	76.44	54	76.83	54	74.53
	2	108	92.33	100	89.56	100	89.67	100	85.87
	3	150	94.33	150	94.00	150	92.83	150	90.80
$GPLCP^{riu2}$	**4**	200	95.67	250	95.33	**300**	**94.67**	250	92.80
	5	**250**	**96.33**	**250**	**96.22**	250	94.33	**250**	**93.73**
	6	300	95.33	300	94.44	324	93.83	300	92.67
	7	300	95.33	300	94.22	324	93.83	300	92.53
	1	255	87.33	200	82.89	200	81.17	200	78.93
	2	150	91.67	300	90.22	100	89.17	100	85.47
	3	350	94.67	250	93.78	450	91.50	200	88.80
GPLPQ	**4**	**250**	**95.00**	**100**	**94.44**	**250**	**91.83**	100	90.00
	5	200	95.00	150	93.56	350	91.83	**100**	**90.93**
	6	100	94.67	200	93.78	200	91.67	200	89.33
	7	300	94.33	200	92.44	150	91.33	50	88.67

Table 4.8 Classification accuracy achieved by PCA reduced feature vector data for different proportions of training and testing data of RDD using RF classifier.

Techniques	IDL	NOF	80/20	NOF	70/30	NOF	60/40	NOF	50/50
	1	40	75.67	30	67.56	50	64.33	50	62.67
	2	100	84.00	50	78.22	50	74.67	50	72.00
	3	170	85.67	100	82.22	50	79.17	50	76.93
$GPLBP^{u2}$	4	50	85.33	150	83.33	50	81.00	50	78.53
	5	50	85.33	100	82.67	50	83.00	50	78.93
	6	150	82.33	150	81.11	50	78.83	50	75.33
	7	50	80.00	50	77.33	50	77.00	100	72.13
	1	35	68.33	35	64.00	20	63.33	35	62.53
	2	50	79.67	65	74.89	65	74.50	65	70.00
	3	75	82.67	100	78.89	75	77.50	75	76.00
$GPLBP^{ri}$	4	100	81.67	100	80.44	100	79.33	100	76.27
	5	150	81.67	100	78.67	150	75.83	150	74.13
	6	150	79.00	100	78.89	50	76.67	50	73.20
	7	200	76.00	150	76.00	150	76.67	150	70.80
	1	8	60.00	8	54.22	8	54.33	8	54.67
	2	15	81.33	15	72.67	15	71.50	15	68.80
	3	25	85.33	25	80.89	25	79.83	25	78.93
$GPLBP^{riu2}$	4	35	86.33	30	82.67	35	83.00	35	79.47
	5	45	88.00	45	85.56	45	83.83	45	81.60
	6	55	85.33	55	86.67	50	85.00	50	82.13
	7	65	84.33	65	83.78	60	82.83	60	80.80
	1	60	56.33	70	51.33	60	49.50	60	47.73
	2	100	68.33	125	62.89	100	61.50	125	56.80
	3	243	76.00	100	68.89	100	67.83	100	63.73
$GPLCP^{u2}$	4	50	78.67	100	73.56	150	71.00	150	67.87
	5	50	79.00	50	74.00	100	72.33	100	68.53
	6	250	78.00	50	75.56	50	74.67	50	72.80
	7	150	78.33	50	75.78	50	74.00	50	71.33
	1	60	66.67	70	60.67	50	59.00	50	56.13
	2	150	75.33	100	70.44	100	66.83	100	63.07
	3	150	77.00	150	71.11	150	71.00	150	66.67
$GPLCP^{ri}$	4	200	79.67	200	76.00	150	74.67	200	68.27
	5	150	81.33	150	76.44	150	74.67	150	70.40
	6	250	81.33	50	76.22	300	74.33	20	72.27
	7	300	78.33	300	75.33	50	73.17	250	70.80
	1	60	75.67	50	69.56	60	68.00	60	64.80
	2	125	79.67	150	76.44	100	74.67	100	70.53
	3	200	79.67	200	75.56	150	74.83	200	69.33
$GPLCP^{riu2}$	4	150	83.00	200	78.22	150	76.00	150	72.80
	5	150	78.00	200	75.56	150	73.17	250	71.33
	6	300	83.33	300	78.44	300	75.50	300	72.13
	7	50	81.33	350	79.33	350	75.50	300	71.60
	1	50	82.33	100	79.11	50	76.00	50	70.67
	2	250	87.67	150	84.89	100	82.00	150	77.47
	3	100	89.67	150	86.44	50	84.00	100	80.80
GPLPQ	**4**	100	90.00	50	87.33	**50**	**85.83**	150	83.33
	5	**150**	**90.67**	**100**	**88.89**	50	85.67	**150**	**84.00**
	6	300	89.00	50	86.89	250	85.33	100	83.33
	7	50	89.67	50	87.56	50	85.67	50	82.40

RBF kernel SVM classifier: A classification accuracy of 94.33% (150 features, at 5th IDL), 92.89% (50 features, at 6th IDL), 89% (150 features, at 5th IDL) and 86.40% (200 features, at 5th IDL) has been obtained for 80/20, 70/30, 60/40 and 50/50 training and testing ratios of RDD, respectively. The classification accuracy has been achieved by PCA dimensionality reduced feature vector data of GPLPQ technique; found to be reasonably better than the accuracy presented by FFVD of GPLPQ technique (Table 4.6).

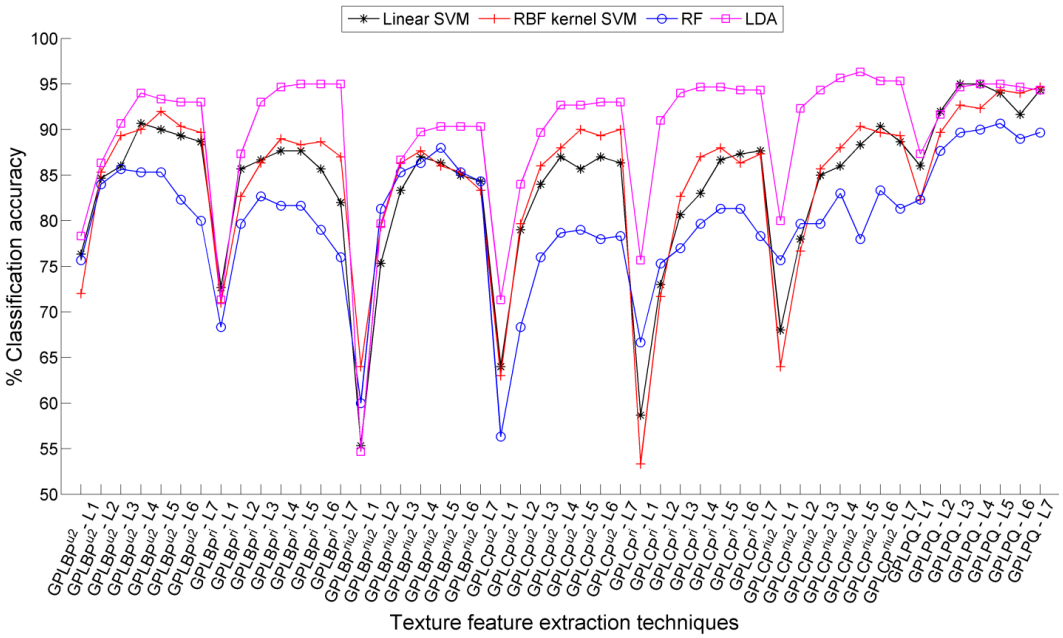

Fig. 4.14 Classification accuracy achieved for 80/20 proportion of training and testing data of RDD.

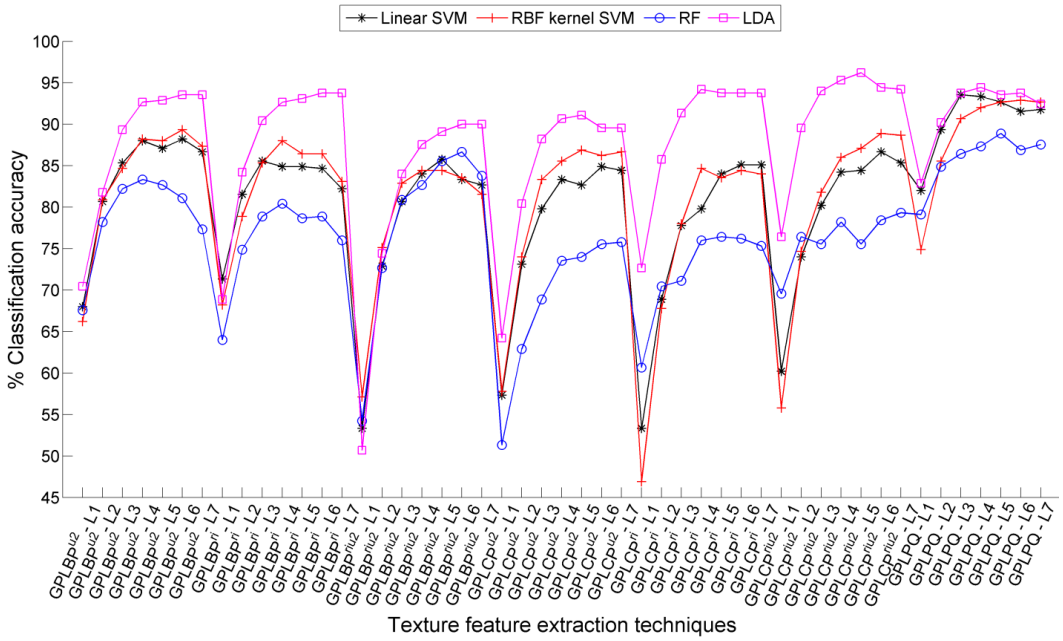

Fig. 4.15 Classification accuracy achieved for 70/30 proportion of training and testing data of RDD.

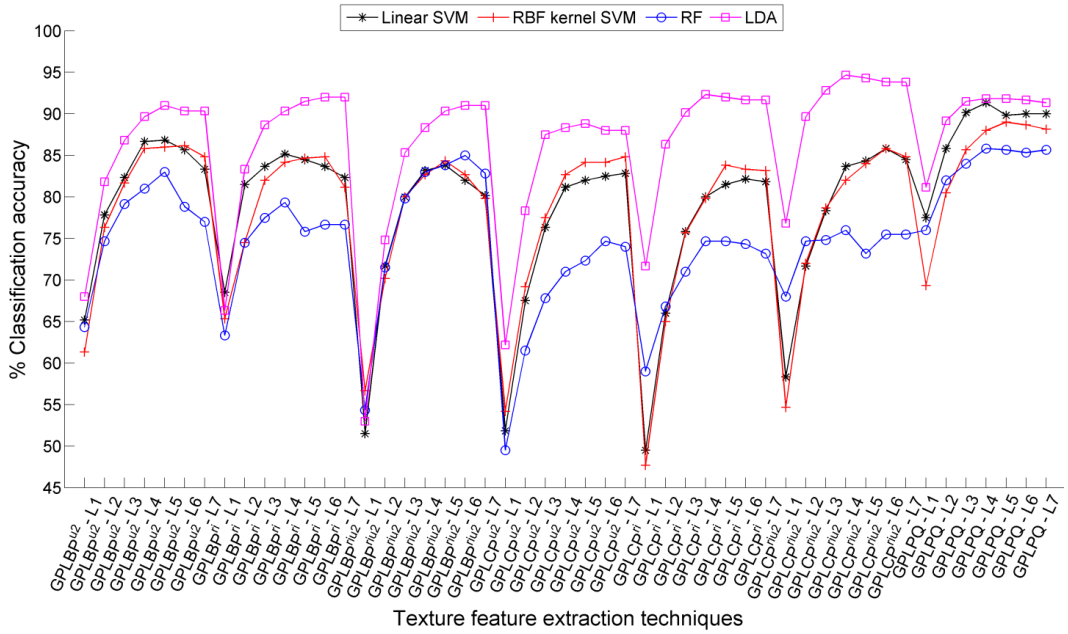

Fig. 4.16 Classification accuracy achieved for 60/40 proportion of training and testing data of RDD.

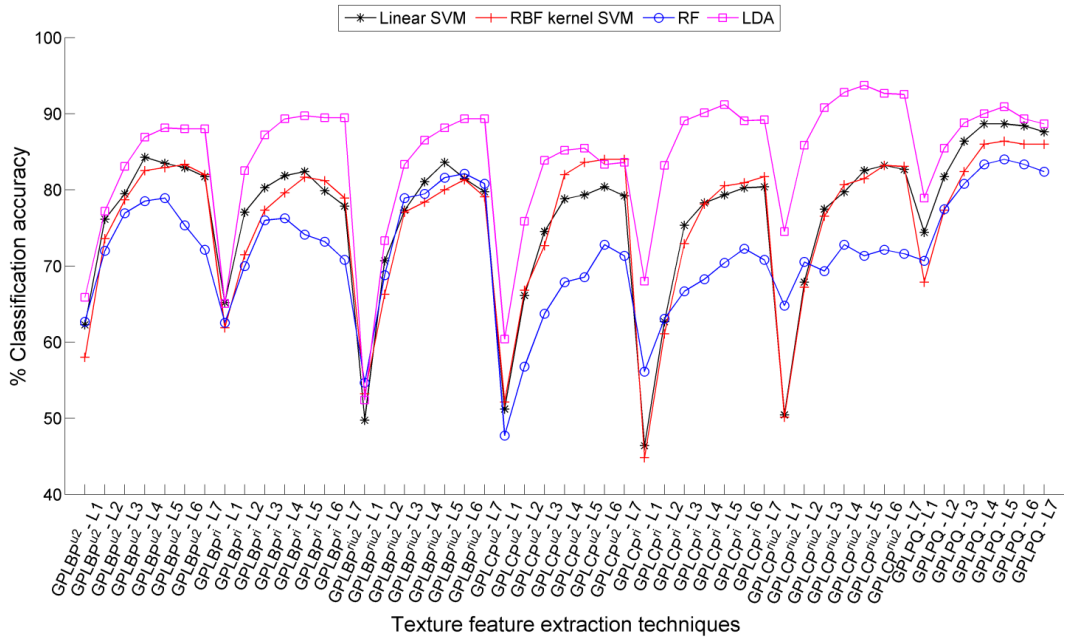

Fig. 4.17 Classification accuracy achieved for 50/50 proportion of training and testing data of RDD.

LDA classifier: Amongst the proposed feature extraction techniques, the PCA dimensionality reduced feature vector data of the GPLCP^{riu2} technique has attained the highest classification accuracy. The obtained classification accuracy results are 96.33% (250 features, at 5th IDL), 96.22% (250 features, at 5th IDL), 94.67% (300 features, at 4th IDL) and 93.73% (250 features, at 5th IDL) for 80/20, 70/30, 60/40 and 50/50 training and testing ratios of RDD, respectively (Table 4.7). Further, the PCA dimensionality reduced feature vector data of the GPLPQ technique has attained the 2nd best classification accuracy. The obtained classification accuracy results are 95% (250 features, at 4th IDL), 94.44% (100 features, at 4th IDL), 91.83% (250

features, at 4th IDL) and 90.93% (100 features, at 5th IDL) for 80/20, 70/30, 60/40 and 50/50 training and testing ratios of RDD, respectively (Table 4.7).

RF classifier: In this case the classification accuracy results of 90.67% (150 features, at 5th IDL), 88.89% (100 features, at 5th IDL), 85.83% (50 features, at 4th IDL) and 84% (150 features, at 5th IDL) for 80/20, 70/30, 60/40 and 50/50 training and testing ratios of RDD, respectively, has been obtained by GPLPQ technique with PCA dimensionality reduced feature vector data (Table 4.8).

The graphical illustration of PCA reduced feature vector data of GP based texture feature extraction techniques are shown in Fig. 4.14, Fig. 4.15, Fig. 4.16 and Fig. 4.17 for 80/20, 70/30, 60/40 and 50/50 training and testing ratios of RDD, respectively. It is clearly visible that the PCA reduced feature vector data has achieved the best classification accuracy with LDA classifier, whereas RF classifier has given the lowest classification accuracy among the four different classifiers. Thus, it can be said that incorporating PCA for feature dimensionality reduction has improved the performance of GP based texture feature extraction techniques for hardwood species classification with low-dimensional feature vector data.

4.3.4.3 The mRMR feature selection based reduced feature vector data

The classification accuracy results achieved by the mRMR feature selection based reduced feature vector data of GP based texture feature extraction techniques with three different classifiers have been presented in Table 4.9, Table 4.10 and Table 4.11, respectively. The classification accuracy results obtained by each of the classifiers are as follows:

Linear SVM classifier: The subset of feature vector data of GPLPQ technique produced by mRMR feature selection technique yields the best classification accuracy of 95.67% (450 features, at 5th IDL), 93.56% (550 features, at 4th IDL), 90.67% (550 features, at 5th IDL) and 89.60% (450 features, at 6th IDL) for 80/20, 70/30, 60/40 and 50/50 training and testing ratios of RDD, respectively (Table 4.9).

RBF kernel SVM classifier: In this case, also, the subset of feature vector data of GPLPQ technique processed through mRMR feature selection technique yields the best classification accuracy of 94.67% (250 features, at 5th IDL), 92.89% (200 features, at 5th IDL), 91% (200 features, at 6th IDL) and 88.40% (200 features, at 6th IDL) for 80/20, 70/30, 60/40 and 50/50 training and testing ratios of randomly divided database, respectively (Table 4.10).

RF classifier: The mRMR feature selection based feature vector data of GPLPQ technique yield the best classification accuracy result of 90.33% (200 features, at 5th IDL), 89.56% (150 features, at 5th IDL), 87.83% (300 features, at 6th IDL) and 85.23% (100 features, at 6th IDL) for 80/20, 70/30, 60/40 and 50/50 training and testing ratios of RDD, respectively (Table 4.11).

Interestingly, all the three classifiers have achieved the best classification accuracies for feature vector data produced by the GP based texture features at the 5th and 6th level of image

decomposition. Also, employing mRMR feature selection technique for reducing the number of features, has given marginally lower classification accuracy compared to FFVD, but with lesser number of features.

Table 4.9 Classification accuracy achieved by mRMR feature selection based reduced feature vector data for different proportions of training and testing data of RDD using linear SVM classifier.

Technique	IDL	NOF	80/20	NOF	70/30	NOF	60/40	NOF	50/50
	1	55	72.33	55	66.00	55	64.67	55	65.13
	2	110	84.33	110	81.33	100	78.00	115	76.00
	3	170	87.67	150	85.33	170	82.50	170	79.73
$GPLBP^{u2}$	4	225	92.00	200	87.53	200	86.33	200	83.73
	5	100	92.33	200	88.22	200	87.17	250	83.33
	6	250	92.00	200	88.44	300	87.50	250	84.13
	7	250	92.00	200	88.67	300	86.50	300	84.27
	1	30	68.33	30	68.22	30	67.67	30	64.80
	2	60	84.67	60	81.78	65	81.33	65	77.47
	3	100	88.33	100	86.67	100	84.67	75	81.20
$GPLBP^{ri}$	4	75	89.00	75	86.67	100	85.67	75	82.27
	5	100	89.33	100	87.56	150	84.83	170	83.20
	6	100	88.00	100	86.22	150	85.67	100	83.47
	7	100	88.00	100	85.78	100	85.17	150	82.40
	1	8	55.33	80	79.33	8	48.33	8	47.87
	2	15	75.67	15	72.22	15	69.33	15	68.40
	3	25	85.00	25	83.33	25	80.33	25	76.80
$GPLBP^{riu2}$	4	35	87.67	35	84.22	35	82.17	35	82.27
	5	45	86.67	45	84.00	45	83.50	45	83.47
	6	55	84.67	55	82.00	55	80.67	55	79.87
	7	50	84.67	50	81.11	65	80.50	65	79.20
	1	50	64.33	70	57.78	50	53.83	50	52.40
	2	150	78.67	150	72.44	150	67.50	150	64.93
	3	100	85.00	100	82.22	225	76.83	100	73.87
$GPLCP^{u2}$	4	150	89.67	200	87.33	150	83.00	200	82.00
	5	200	89.00	150	87.33	200	84.17	200	82.40
	6	150	88.67	150	86.22	200	84.00	200	82.53
	7	200	88.33	200	85.78	250	84.50	200	82.13
	1	75	63.33	60	54.67	60	51.67	60	48.93
	2	50	75.33	100	71.33	100	67.00	100	65.47
	3	50	86.00	100	82.00	50	79.83	100	78.13
$GPLCP^{ri}$	4	100	89.33	100	87.56	50	84.17	100	83.87
	5	50	92.00	50	81.11	100	89.17	100	87.47
	6	100	91.67	100	90.89	100	88.67	100	87.20
	7	100	91.33	100	89.33	100	87.83	100	87.20
	1	50	67.67	60	63.33	60	58.67	50	54.53
	2	100	81.33	100	76.22	100	74.17	50	72.93
	3	150	88.67	150	87.11	150	84.17	150	81.20
$GPLCP^{riu2}$	4	100	92.00	100	91.78	100	89.17	100	87.73
	5	150	93.33	150	92.44	150	91.33	100	88.00
	6	150	93.00	150	92.89	150	90.17	150	88.27
	7	150	94.00	150	92.00	150	90.50	150	89.07
	1	100	86.00	200	80.89	200	78.17	200	75.47
	2	250	93.00	400	90.00	350	86.33	450	84.00
	3	400	95.33	450	92.22	450	89.50	400	86.67
GPLPQ	**4**	250	95.00	**350**	**93.56**	350	90.50	200	89.47
	5	**450**	**95.67**	550	92.89	**550**	**90.67**	400	89.20
	6	550	95.67	300	92.44	450	90.00	**450**	**89.60**
	7	550	95.67	300	92.44	450	90.00	450	89.60

Table 4.10 Classification accuracy achieved by mRMR feature selection based reduced feature vector data for different proportions of training and testing data of RDD using RBF kernel SVM classifier.

Technique	IDL	NOF	80/20	NOF	70/30	NOF	60/40	NOF	50/50
$GPLBP^{u2}$	1	55	69.33	55	66.00	55	60.33	55	56.93
	2	115	85.00	115	80.67	100	75.67	115	73.07
	3	170	89.33	170	85.33	170	82.17	170	78.40
	4	225	90.00	225	87.33	225	85.50	150	82.40
	5	275	91.67	275	88.00	275	86.67	250	83.33
	6	200	91.00	300	88.44	150	86.67	150	84.27
	7	150	91.00	350	87.78	200	86.17	150	84.00
$GPLBP^{ri}$	1	35	70.00	35	66.89	35	65.00	30	61.07
	2	60	82.33	60	78.44	60	75.00	60	71.33
	3	50	88.33	75	86.00	50	83.00	75	79.20
	4	75	88.67	75	87.56	75	85.50	75	83.07
	5	100	88.00	100	87.56	100	86.00	100	83.73
	6	100	88.67	100	87.78	200	85.67	100	84.40
	7	100	87.67	100	86.67	100	85.00	100	83.20
$GPLBP^{riu2}$	1	8	57.00	8	49.33	8	51.50	8	48.53
	2	15	76.00	15	72.44	15	68.83	15	66.40
	3	25	84.67	25	82.00	25	78.33	25	76.27
	4	35	88.00	35	84.44	35	82.17	35	78.80
	5	45	86.67	40	85.11	45	83.67	45	80.00
	6	50	84.33	50	83.11	50	82.33	55	81.73
	7	60	84.00	65	83.11	50	82.33	50	80.40
$GPLCP^{u2}$	1	70	63.00	75	57.78	70	54.17	50	52.53
	2	100	79.67	150	74.00	150	69.17	150	66.80
	3	150	86.33	100	83.33	100	77.50	150	76.40
	4	200	88.00	150	85.11	100	82.67	100	81.47
	5	50	90.00	50	86.89	250	85.00	150	83.60
	6	50	89.33	100	86.22	250	84.67	150	84.00
	7	50	90.00	50	86.67	150	84.83	150	84.00
$GPLCP^{ri}$	1	50	58.67	50	51.11	50	46.83	60	45.87
	2	50	76.67	50	72.44	50	68.33	50	65.47
	3	100	88.00	50	83.33	50	81.00	50	77.60
	4	100	91.33	100	88.44	100	87.17	100	83.20
	5	50	91.33	50	90.44	50	89.00	50	86.40
	6	200	91.67	100	90.00	100	88.67	100	86.27
	7	200	91.67	100	89.33	100	88.00	100	86.40
$GPLCP^{riu2}$	1	70	65.00	50	58.89	50	56.17	50	52.00
	2	50	79.67	50	76.89	50	73.83	50	71.87
	3	50	90.00	50	87.33	50	84.00	100	82.53
	4	100	92.33	50	91.78	100	88.67	100	86.40
	5	150	94.33	150	92.00	50	89.17	100	89.20
	6	100	93.33	150	92.22	200	89.50	150	89.07
	7	200	92.67	100	91.56	150	90.00	150	88.40
GPLPQ	1	100	82.33	200	74.67	150	71.00	150	69.20
	2	250	90.67	200	85.78	200	82.33	150	79.47
	3	300	92.33	150	90.67	200	87.50	200	84.27
	4	200	93.67	150	92.44	150	90.33	150	87.73
	5	**250**	**94.67**	**200**	**92.89**	200	90.83	200	88.00
	6	200	94.00	200	92.89	**200**	**91.00**	**200**	**88.40**
	7	200	94.00	200	92.89	200	91.00	200	88.40

Table 4.11 Classification accuracy achieved by mRMR feature selection based reduced feature vector data for different proportions of training and testing data of RDD using RF classifier.

Technique	IDL	NOF	80/20	NOF	70/30	NOF	60/40	NOF	50/50
$GPLBP^{u2}$	1	55	59.07	55	52.00	55	51.17	50	48.53
	2	100	74.67	110	71.11	50	67.67	100	66.00
	3	100	80.33	150	77.78	150	74.50	150	72.53
	4	225	85.33	225	81.78	200	80.00	200	77.33
	5	275	87.33	200	84.67	275	82.00	250	79.60
	6	200	88.33	150	84.22	150	83.63	100	80.80
	7	150	87.00	250	84.67	150	82.67	150	80.27
$GPLBP^{ri}$	1	35	49.00	30	44.44	35	42.00	30	36.80
	2	50	72.67	60	67.78	50	64.33	65	62.67
	3	50	82.00	50	77.78	50	77.33	50	73.60
	4	50	85.67	50	81.33	75	81.00	75	78.40
	5	100	88.00	100	84.00	100	85.33	100	81.20
	6	100	87.33	100	84.44	100	84.83	100	82.00
	7	150	88.00	150	84.44	100	83.67	100	80.80
$GPLBP^{riu2}$	1	8	35.00	8	33.78	8	33.50	8	31.60
	2	15	62.67	15	58.22	15	55.00	15	51.87
	3	20	76.67	25	70.67	20	67.67	20	64.13
	4	25	80.00	35	76.89	30	74.67	30	72.53
	5	40	82.67	30	80.22	40	79.83	40	77.20
	6	50	83.33	50	81.33	50	80.33	50	78.27
	7	60	82.33	60	79.78	50	80.33	65	77.47
$GPLCP^{u2}$	1	75	57.67	60	52.67	70	49.50	70	48.27
	2	125	72.67	150	66.22	150	63.33	125	60.67
	3	50	79.67	50	75.56	100	73.33	150	72.27
	4	100	85.33	100	82.44	100	82.83	100	78.93
	5	50	86.00	150	85.33	50	83.17	150	80.53
	6	200	86.33	100	86.44	50	83.83	150	80.93
	7	100	87.33	50	85.33	150	83.83	100	80.67
$GPLCP^{ri}$	1	70	52.67	75	49.56	50	48.83	50	45.73
	2	100	72.00	50	65.33	50	64.33	50	62.40
	3	100	84.00	150	80.89	50	79.33	100	76.27
	4	50	89.00	100	87.33	100	87.00	100	83.73
	5	50	90.00	100	89.11	100	88.83	100	86.13
	6	150	90.33	250	89.56	100	89.00	200	85.47
	7	150	89.33	50	88.67	150	88.00	150	86.27
$GPLCP^{riu2}$	1	50	58.67	50	53.11	50	52.67	50	49.73
	2	50	78.67	50	74.00	50	70.17	50	67.87
	3	100	87.67	50	84.44	50	81.67	50	79.47
	4	50	90.00	100	89.56	50	87.33	100	84.80
	5	100	91.33	100	89.56	200	89.33	100	86.80
	6	150	91.67	150	90.22	300	89.33	150	87.20
	7	150	91.67	150	91.56	300	89.50	150	86.80
GPLPQ	1	50	72.00	50	63.78	100	63.33	100	58.53
	2	150	85.00	450	80.22	350	76.83	100	72.53
	3	100	88.33	150	86.67	150	85.00	100	80.80
	4	200	90.00	250	88.89	200	86.67	350	84.93
	5	**200**	**90.33**	**150**	**89.56**	200	87.67	200	84.93
	6	250	90.00	200	88.89	**300**	**87.83**	**100**	**85.20**
	7	200	90.00	200	89.78	300	87.33	100	85.20

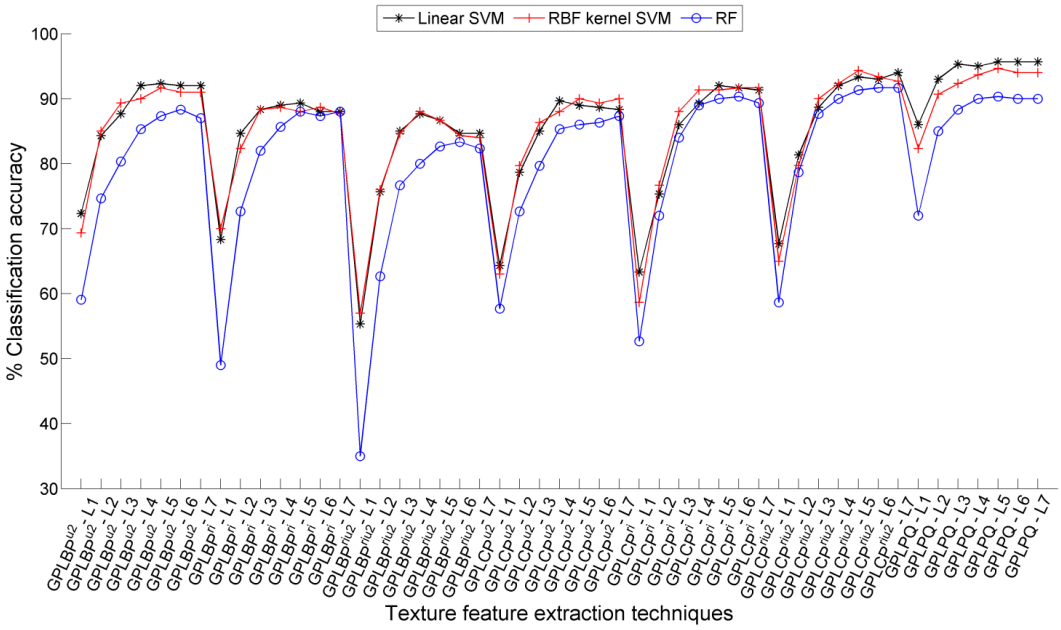

Fig. 4.18 Classification accuracy achieved for 80/20 proportion of training and testing data of RDD.

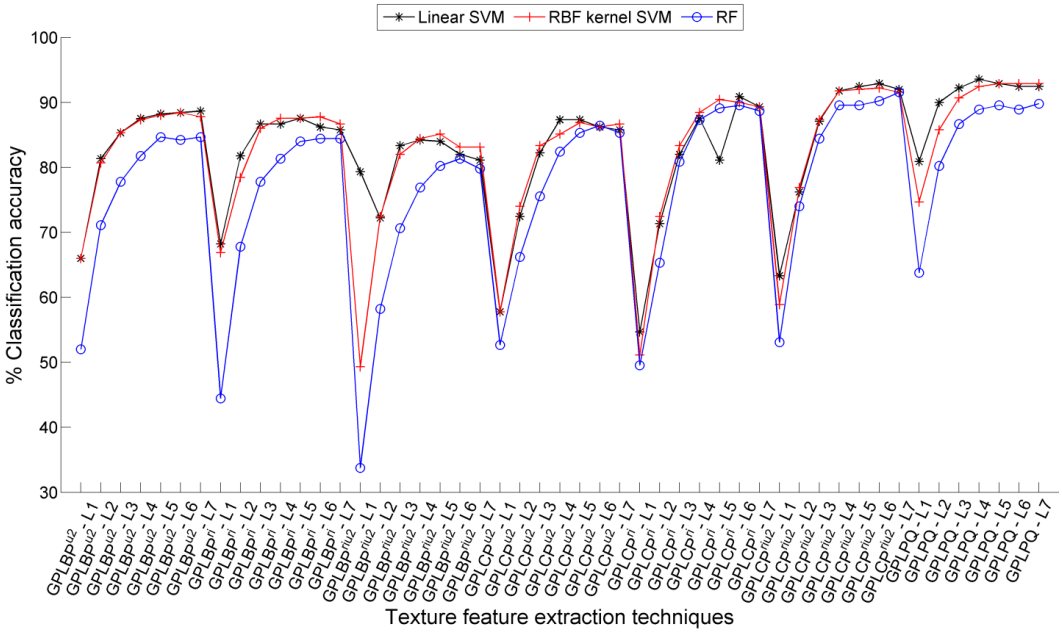

Fig. 4.19 Classification accuracy achieved for 70/30 proportion of training and testing data of RDD.

The classification accuracies obtained by three different classifiers are compared for each of the four (80/20, 70/30, 60/40 and 50/50) training and testing ratios, and are illustrated in Fig. 4.18, Fig. 4.19, Fig. 4.20 and Fig. 4.21, respectively. The analysis of these graphs advocates that GP based texture feature extraction technique (GPLPQ) has given the best classification accuracy with linear SVM classifier; whereas comparatively lower classification accuracy has been reported by RF classifier.

Thus, employing feature dimensionality reduction/feature selection technique has not only reduced the computational time but also shown considerable improvement in the classification accuracy for hardwood species classification. It is also observed that the performance of variants

of LBP, LCP and LPQ texture feature extraction techniques have been improved by involving Gaussian image pyramid approach followed by extraction of texture features from these transformed images.

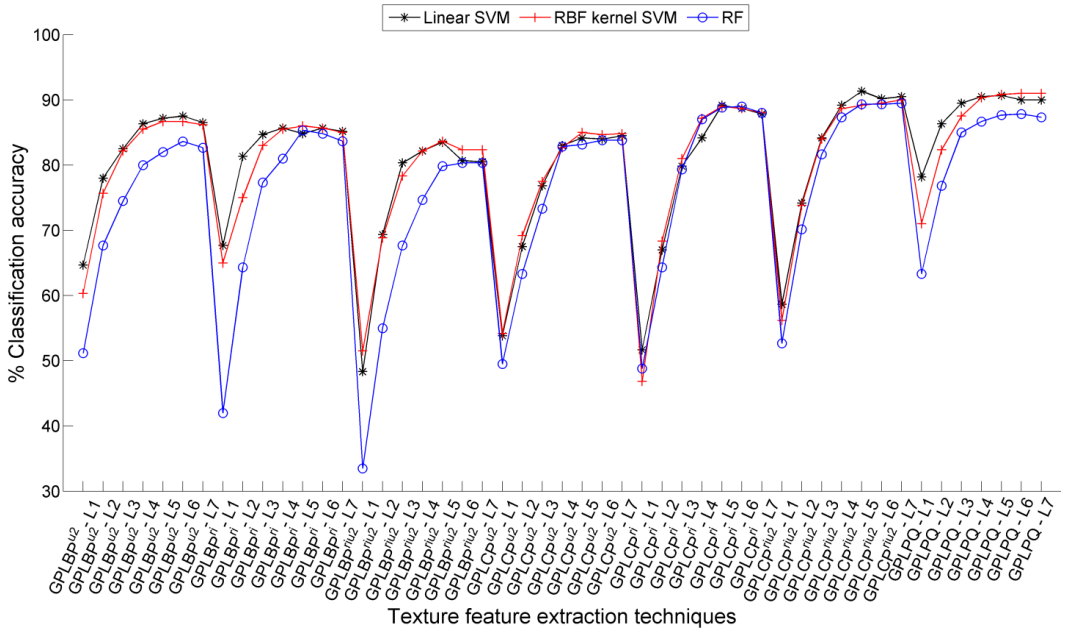

Fig. 4.20 Classification accuracy achieved for 60/40 proportion of training and testing data of RDD.

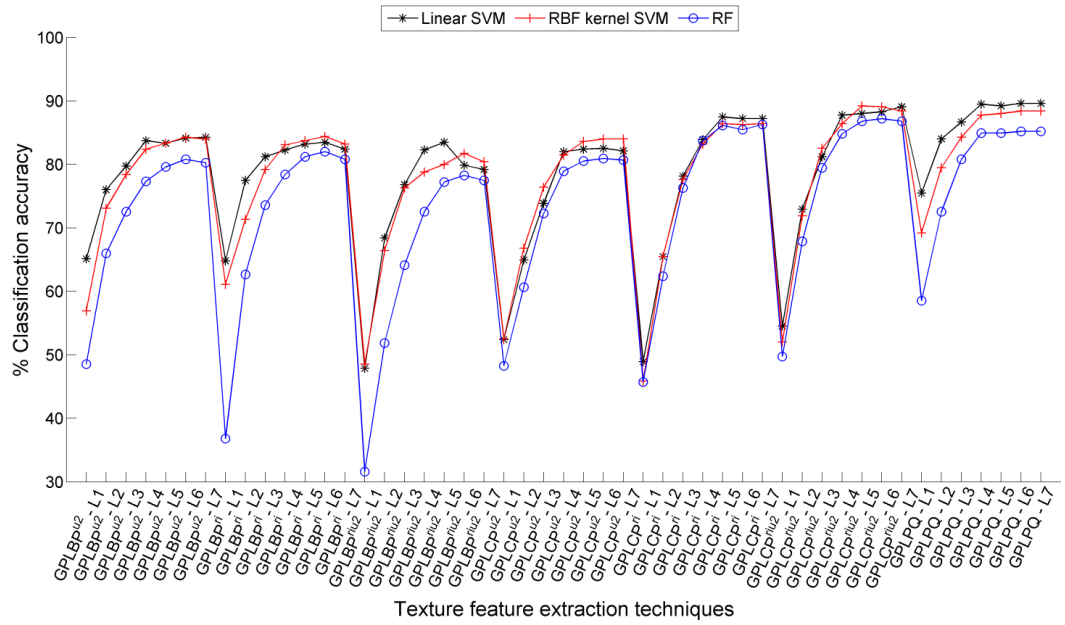

Fig. 4.21 Classification accuracy achieved for 50/50 proportion of training and testing data of RDD.

The performance of GP based texture feature extraction technique has been comparatively superior/at par with most of the state-of-the-art texture feature extraction techniques possibly because of the following reasons:

As discussed in Chapter 3, the microscopic images of hardwood species are required to be analyzed at several scale of resolutions for better discrimination among the wood species. For this reason, the images are decomposed by GP wherein each of the subimages coefficients contain varied and valuable information. In addition, to extract features from several level images, LBP, LCP and LPQ are preferred due to their simple computational requirement. Though, distinguishing features are obtained from low resolution subimages but alone they are not sufficient to discriminate amongst the hardwood species. Therefore, the texture descriptors of several scale resolution images are combined to get more significant feature vector data to discriminate among the hardwood species.

4.4 SUMMARY

The efficiency of the GP based texture feature extraction techniques for the classification of microscopic images of hardwood species into 75 categories have been examined with the help of classifiers. Two different approaches, 10-fold cross validation and randomly divided database (RDD) has been chosen to test the efficiency of proposed techniques. Further, for both the approaches, three different case studies are discussed (viz., FFVD, PCA reduced feature vector data and mRMR feature selection based feature vector data).

In case of 10-fold cross validation approach, the FFVD (1024 features) of GPLPQ feature extraction technique at the 4^{th} level of image decomposition yields best classification accuracy with lower value of standard deviation (98.20±1.04%), using linear SVM classifier. The LDA classifier yields the best classification accuracy of 98.73±1.15% for PCA reduced feature vector data of GPLPQ texture feature extraction technique (500 features). The mRMR selected feature subset (550 features) of GPLPQ technique has achieved the best classification accuracy of 98.13±0.93% using linear SVM classifier**.**

In case of RDD, amongst the proposed texture feature extraction techniques, the FFVD of GPLPQ technique has achieved the best classification accuracies of 95.33%, 93.78%, 91% and 88.93% for 80/20, 70/30, 60/40 and 50/50 training and testing ratios of RDD, respectively, with linear SVM classifier. The PCA dimensionality reduced feature vector data of $GPLCP^{riu2}$ technique has obtained the best classification accuracy results of 96.33% (250 features), 96.22% (250 features), 94.67% (300 features) and 93.73% (250 features) for 80/20, 70/30, 60/40 and 50/50 training and testing ratios of RDD, respectively, using LDA classifier. The subset of feature vector data of GPLPQ technique selected by mRMR feature selection technique yields the best classification accuracies of 95.67% (450 features), 92.89% (550 features), 90.67% (550 features) and 89.20% (400 features) for 80/20, 70/30, 60/40 and 50/50 training and testing ratios of RDD, respectively, using linear SVM classifier.

Thus, it is concluded that the performance of variants of LBP, LCP and LPQ texture feature extraction techniques have been significantly improved by incorporating Gaussian image

processing based image decomposition, followed by extraction of texture features from these transformed images. Further, the performance of GP based texture feature extraction techniques have been comparatively superior compared to the state-of-the-art and BWT based texture feature extraction techniques for hardwood species classification. The time taken by the proposed techniques for feature extraction is much lower than the BWT based texture feature extraction techniques (Chapter 3).

CHAPTER 5. DWT BASED TEXTURE FEATURE EXTRACTION TECHNIQUES

This chapter explores the effectiveness of discrete wavelet transform (DWT) based local binary pattern (LBP) variants texture feature extraction techniques for classification of hardwood species. The chapter starts with concise description of the DWT, proposed DWT based texture feature extraction techniques for hardwood species classification and subsequently evaluation of the effectiveness of these techniques using different classifiers.

5.1 INTRODUCTION

A mathematical tool employed in the hierarchical decomposition of a signal/image is known as discrete wavelet transform (DWT). Ever since its introduction, due to its multi-resolution capability, DWT [8, 91, 23, 103, 121, 176, 177, 183, 188, 189, 226] has been efficiently explored in a wide range of applications like image analysis, object recognition [9], denoising, segmentation, compression, biomedical imaging, fingerprint anti-spoofing [146] and texture feature extraction, etc. The DWT has gained popularity in image processing applications for efficiently providing spatial-frequency information [48, 69, 116, 137, 147, 148, 187]. The significant elements of 2D-DWT includes four critical elements, one scaling function $\varphi(x,y)$, and three wavelet functions ($\psi^H(x,y)$, $\psi^V(x,y)$ and $\psi^D(x,y)$), which are product of two one dimensional (1D) functions. The ψ^{H}, ψ^{V} and ψ^{D} wavelets are useful in the measurement of gray level variations in the horizontal, vertical and diagonal directions, respectively. The scaled φ and translated ψ basis functions are defined as follows [60]:

$$\varphi_{j,r,c}(x,y) = 2^{j/2}\varphi\left(2^j x - r, 2^j y - c\right) \tag{5.1}$$

$$\psi^i_{j,r,c}(x,y) = 2^{j/2}\psi^i\varphi\left(2^j x - r, 2^j y - c\right),\ i = \{H,V,D\} \tag{5.2}$$

The DWT expression to an image $f(x,y)$ of size $M \times N$ is given by:

$$W_\varphi(j_0,r,c) = \frac{1}{\sqrt{MN}}\sum_{x=0}^{M-1}\sum_{y=0}^{N-1} f(x,y)\varphi_{j_0,r,c}(x,y) \tag{5.3}$$

$$W^i_\psi(j,r,c) = \frac{1}{\sqrt{MN}}\sum_{x=0}^{M-1}\sum_{y=0}^{N-1} f(x,y)\phi_{j0,r,c}(x,y),\ i = \{H,V,D\} \tag{5.4}$$

In above equation j_0 is an arbitrary starting scale. The $W_\varphi(j_0,r,c)$ coefficients produce approximation of image $f(x,y)$ at j_0 scale and $W^i_\psi(j,r,c)$ coefficients provide diagonal, vertical and horizontal details at scale $j \geq j_0$.

A compactly supported orthogonal wavelet having pre-assigned degree of smoothness was designed by Ingrid Daubechies [194]. It has been used in several image processing applications [214]. Daubechies wavelet family is characterized by time invariance, produces real

number coefficients, asymmetrical and has a sharp filter transition band that is useful in minimizing the edge effects between the frequency bands. The fractal like self-symmetry property facilitates fast wavelet transform in computation, also for a given support it offers the highest number of vanishing moments [194].

The requirement for the significant texture features is based on the following facts. It is known that the microscopic images of hardwood species contain four key elements namely, vessels, rays, parenchyma and fibres. These elements are of numerous sizes and shapes. As the visual perception evaluates images on various levels of resolution at the same time, the multiresolution analysis capability of DWT is helpful in detecting features at a unique resolution which is undetectable at any other resolution. Further, the LBP variants are well-known for their ability of extracting significant features of images. Thus, the features obtained by combining DWT and LBP variants at several level of image decomposition extracts distinctive features. Furthermore, combining these features together at several level of image decomposition improves discrimination capability of classifier for hardwood species.

As an visual illustration, the DWTCLBP^{u2} (*CLBP_Sign* + *CLBP_Magnitude*) texture images obtained up to the 3rd level of image decomposition for grayscale image of *Aurantium* species is shown in Fig. 5.1. It is noticed that each level of subimages of *CLBP_Sign* and *CLBP_Magnitude* have significant information which is combined together to get the discriminative texture features.

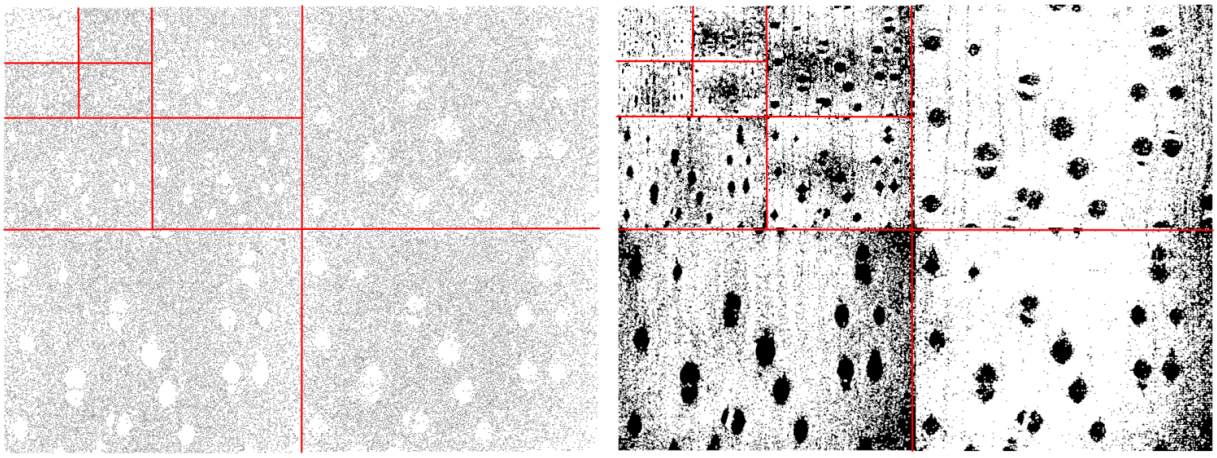

Fig. 5.1 The *Aurantium* species image at 3rd level of image decomposition by DWT, (a) *CLBP_S* texture image, and (b) *CLBP_M* texture image.

5.2 PROPOSED METHODOLOGY

5.2.1 Procedural Steps

The algorithmic steps for the classification of microscopic images of hardwood species is shown in Fig. 5.2. The four key steps involved to accomplish hardwood species classification task are pre-processing, texture feature extraction, feature dimension reduction and classification.

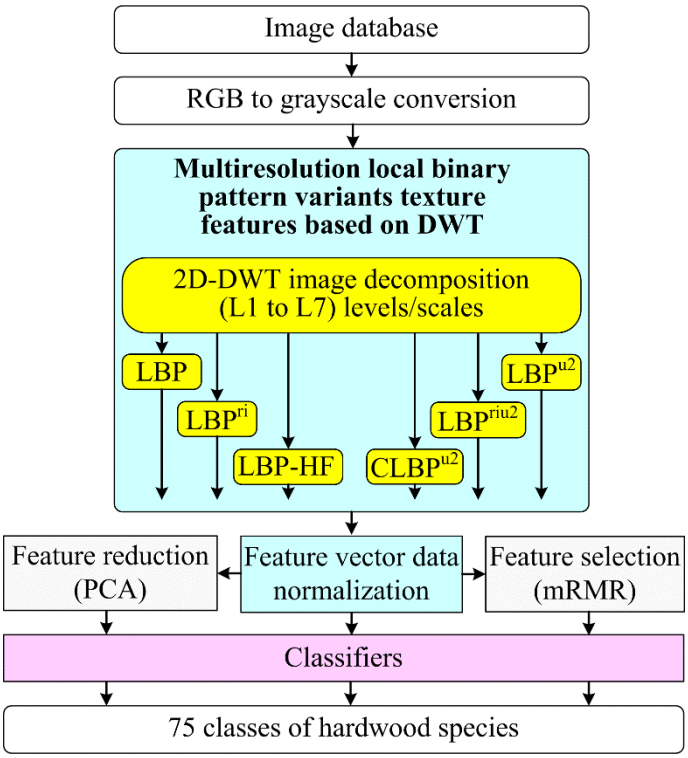

Fig. 5.2 Block diagram of proposed multiresolution local binary pattern (MRLBP) variants based texture features for hardwood species classification.

1. The pre-processing step is involved to obtain grayscale image from color (RGB) image using Eq. (2.41).
2. In the second step (texture feature extraction), these grayscale images are first decomposed by DWT to seven different levels/scales (L1 to L7) incorporating Daubechies wavelet (db2) as decomposition filter. The transformation is carried out to obtain significant features of the image at unique resolution that are unnoticeable at any other resolution. The decomposition process divides grayscale image into four identical quarter-size subimages, viz., approximation (LL1), horizontal (LH1), vertical (HL1) and diagonal (HH1) components at the 1st level of image decomposition. Subsequently, the LL1 component is decomposed into four equal quarter-size subimages (LL2, LH2, HL2 and HH2) at the 2nd level of image decomposition. This procedure of subdividing the approximation component is repeated till defined level of image decomposition is reached. Thereafter, texture features are extracted from each of the subimages at different levels (L1 to L7) of image decomposition. To extract significant features of the image, six texture descriptors namely LBP, LBP^{u2}, LBP^{ri}, LBP^{riu2}, LBP-HF and CLBP^{u2} are used. Thus, on the basis of combination of DWT with different variants of LBP following multiresolution local binary pattern variants **(**MRLBP) variants based texture feature extraction techniques are proposed here and they are listed below.

DWTLBP Discrete wavelet transform based local binary pattern

DWTLBP^{u2} Discrete wavelet transform based uniform local binary pattern

$DWTLBP^{ri}$	Discrete wavelet transform based rotation invariant local binary pattern
$DWTLBP^{riu2}$	Discrete wavelet transform based rotation invariant uniform local binary pattern
DWTLBP-HF	Discrete wavelet transform based local binary pattern histogram Fourier features
$DWTCLBP^{u2}$	Discrete wavelet transform based uniform completed local binary pattern

3. Further, these texture feature vectors containing various range of values are normalized in the range of 0 to 1, thus rendering it in the form useful as an input to the classifier. The feature vector data is normalized using Eq. (2.42).
4. The proposed texture descriptors produce large complex features, and among them several features may not be significant for discrimination of the hardwood species. Thus, in order to reduce the feature dimensions, PCA (feature dimension reduction technique) and mRMR (feature selection technique) is employed in the third step.
5. In the final step, four different machine learning algorithms have been employed to classify the given hardwood species into 75 different classes using these texture features. Further, the effectiveness of the MRLBP variants based texture feature extraction techniques has been observed on the basis of the classification accuracy obtained through the classifiers. Consequently, the best combination of texture descriptor and classifier is identified on the basis of the best classification accuracy.

5.2.2 Approaches used for Performance Evaluation of Feature Extraction Techniques

The performance of the DWT based texture feature extraction techniques for classification of hardwood species have been investigated employing two strategies: (1) 10-fold cross validation and (2) randomly dividing the database (Section 2.5.2).

5.3 EXPERIMENTAL RESULTS AND DISCUSSION

The experimental work presented in this section investigates the efficiency of the MRLBP variants based texture feature extraction techniques for the classification of microscopic images of hardwood species database into 75 classes with the help of classifiers. The classifiers used for the investigation are linear SVM, RBF kernel SVM, LDA and RF classifiers (Section 2.3).

5.3.1 Parameter Selection

The selection of parameters for efficient implementation of various feature extraction techniques and classifiers have been discussed in detail in Section 2.6.1.

5.3.2 Experimental Results

The classification accuracy obtained by the DWT (MRLBP variants) based texture feature extraction techniques for microscopic images of hardwood species have been computed using

four classifiers. As discussed in Section 2.6.2 analysis of the results here is also presented in the similar manner.

5.3.3 Performance Evaluation of DWT based Texture Feature Extraction Techniques using 10-fold Cross Validation Approach

5.3.3.1 Full feature vector data (FFVD)

The percentage classification accuracy attained by the DWT based texture feature extraction techniques for grayscale image of hardwood species database is presented in Table 5.1. The classification accuracy obtained by the proposed texture features using three different classifiers are discussed below:

Linear SVM classifier: The texture feature vector data of DWTCLBP^{u2} feature extraction technique has given the best classification accuracy of 97.40±1.06% with texture feature vector dimension of 1416. In addition, the second best classification accuracy of 96.27±1.73% (3072 features) has been achieved by texture feature vector data produced by DWTLBP texture feature extraction technique. The least classification accuracy of 93.60±1.81% (120 features) has been achieved by using texture feature vector data produced by DWTLBP^{riu2}, among the proposed feature extraction techniques. All these classification accuracies are reported for texture feature vector data generated at the 3rd level of image decomposition.

RBF kernel SVM classifier: With this classifier, the best classification accuracy of 97.00±1.10% has been attained using feature vector data (2360 features) produced by DWTCLBP^{u2} feature extraction technique, which is the best among the proposed feature extraction techniques. The feature vector data of DWTLBP^{u2} texture feature extraction technique has obtained the second best classification accuracy of 96.07±1.24% with 1180-dimensional feature vector data. These classification accuracies are achieved for texture feature vector data produced at the 5th level of image decomposition. On the other hand, the least classification accuracy of 93.80±2.18% (160 features) has been achieved by feature vector data of DWTLBP^{riu2} texture feature extraction technique at the 4th level of image decomposition.

RF classifier: This classifier has given the best classification accuracy of 93.67±1.38% for texture feature vector data (2360 features) produced by DWTCLBP^{u2} texture feature extraction technique. The texture feature vector data produced by of DWTLBP-HF technique has obtained the second best classification accuracy of 92.07±1.24% for 760-dimensional feature vector data**.** In addition, among the proposed feature extraction techniques, the least classification accuracy of 88.60±1.15% (200 features) has been attained by using FFVD produced by DWTLBP^{riu2} feature extraction technique. These classification accuracies are obtained for FFVD produced at the 5th level of image decomposition.

Table 5.1 Classification accuracy achieved using full feature vector data.

Proposed techniques	IDL	Feature extraction time in seconds	NoF	% CA±SD achieved by classifiers		
				Linear SVM	RBF kernel SVM	RF
DWTLBP	1	0.1753	1024	92.40±2.11	90.47±1.37	79.73±2.63
	2	0.2133	2048	95.53±1.34	93.73±1.84	87.13±2.92
	3	0.2291	**3072**	**96.27±1.73**	94.87±1.86	89.53±1.78
	4	0.2431	4096	96.00±1.83	95.13±2.06	89.60±1.58
	5	0.2556	5120	95.73±1.38	94.07±2.00	89.47±1.69
	6	0.2681	6144	94.73±1.49	93.67±1.94	90.00±2.06
	7	0.2802	7168	94.60±1.90	93.40±1.76	89.93±2.00
$DWTLBP^{u2}$	1	0.2692	236	90.00±1.86	89.60±2.16	78.53±2.22
	2	0.3161	472	94.87±1.69	94.00±1.81	85.93±2.00
	3	0.3398	708	95.67±1.45	96.00±1.91	90.00±1.69
	4	0.3525	944	95.80±1.34	95.87±1.72	91.60±1.30
	5	0.3617	**1180**	95.80±2.09	**96.07±1.24**	91.93±1.46
	6	0.3681	1416	94.60±2.10	94.73±0.86	91.60±1.45
	7	0.3752	1652	94.47±1.44	94.53±1.33	91.07±1.86
$DWTLBP^{ri}$	1	0.2738	144	83.13±3.11	85.87±2.51	74.53±2.86
	2	0.3272	288	91.87±2.13	91.87±2.13	83.27±1.68
	3	0.3523	432	94.33±1.55	94.13±1.25	87.67±1.34
	4	0.3718	576	94.73±1.35	94.67±1.94	88.93±1.34
	5	0.3881	720	93.80±2.13	94.13±1.66	88.27±1.51
	6	0.4026	864	92.40±2.31	93.87±1.50	88.73±1.55
	7	0.4182	1008	91.53±1.69	92.53±1.72	89.13±1.04
$DWTLBP^{riu2}$	1	0.2631	40	81.07±2.31	82.87±2.55	67.33±2.93
	2	0.3073	80	90.73±1.71	91.73±1.70	79.80±1.72
	3	0.3321	**120**	**93.60±1.81**	92.40±2.04	84.93±1.92
	4	0.3406	**160**	92.87±1.30	**93.80±2.18**	88.33±1.45
	5	0.3455	**200**	92.20±1.83	93.07±1.67	**88.60±1.15**
	6	0.3494	240	90.87±1.22	92.87±1.83	88.27±1.48
	7	0.3538	280	88.53±1.96	91.20±1.80	88.27±1.47
DWTLBP-HF	1	0.2785	152	79.40±2.71	80.67±2.93	78.13±1.72
	2	0.3339	304	89.00±2.44	90.13±2.72	86.00±1.94
	3	0.3611	456	91.40±2.14	93.27±2.10	90.40±1.23
	4	0.3817	608	92.80±1.63	94.07±1.82	91.00±1.14
	5	0.3985	**760**	93.80±1.54	94.40±0.95	**92.07±1.24**
	6	0.4299	912	93.40±1.06	93.93±1.06	91.67±1.41
	7	0.4486	1064	92.00±1.47	93.47±1.88	92.00±1.63
$DWTCLBP^{u2}$	1	0.3160	472	93.33±1.94	91.73±2.85	84.00±2.04
	2	0.3847	944	96.40±1.30	95.13±1.86	89.80±1.94
	3	0.4070	**1416**	**97.40±1.06**	96.80±1.74	92.87±1.34
	4	0.4162	1888	97.00±1.41	96.93±1.05	93.20±1.66
	5	0.4380	**2360**	96.80±1.03	**97.00±1.10**	**93.67±1.38**
	6	0.4435	2832	96.40±0.84	95.93±0.97	93.13±1.51
	7	0.4480	3304	96.13±1.29	95.47±0.98	93.13±1.41

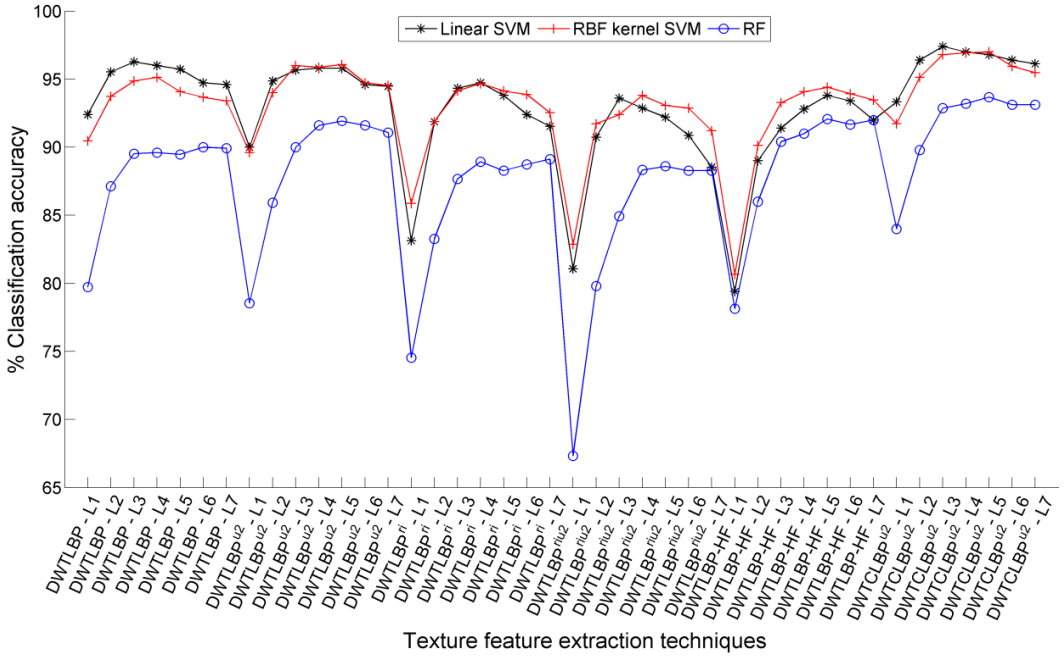

Fig. 5.3 Classification accuracy achieved using FFVD.

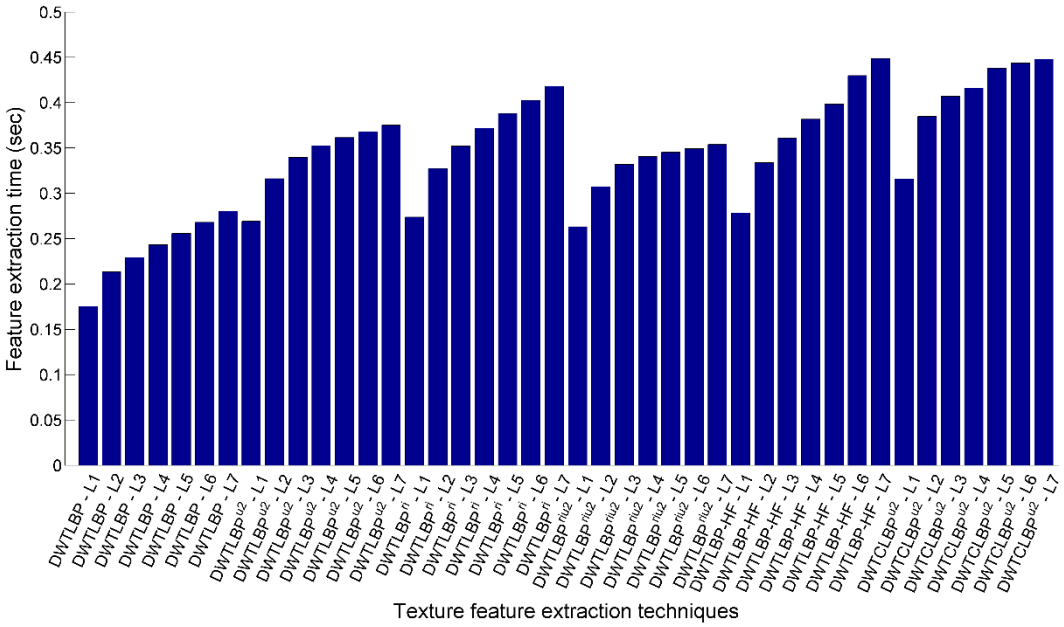

Fig. 5.4 Feature extraction time for single grayscale image.

Here, it has been observed that the best classification accuracy has been achieved by most of the MRLBP variants based texture features obtained between the 3rd to 5th levels of image decomposition with all the classifiers. In addition, among the three classifiers the superlative classification accuracy is achieved with linear SVM classifier; whereas, RF classifier yields comparatively lower classification accuracy. The classification accuracy obtained by the three classifiers have been compared and the same is illustrated in Fig. 5.3. The graphical illustration also reveals that DWTCLBP^{u2} texture feature extraction technique has given the best classification accuracy with linear SVM classifier.

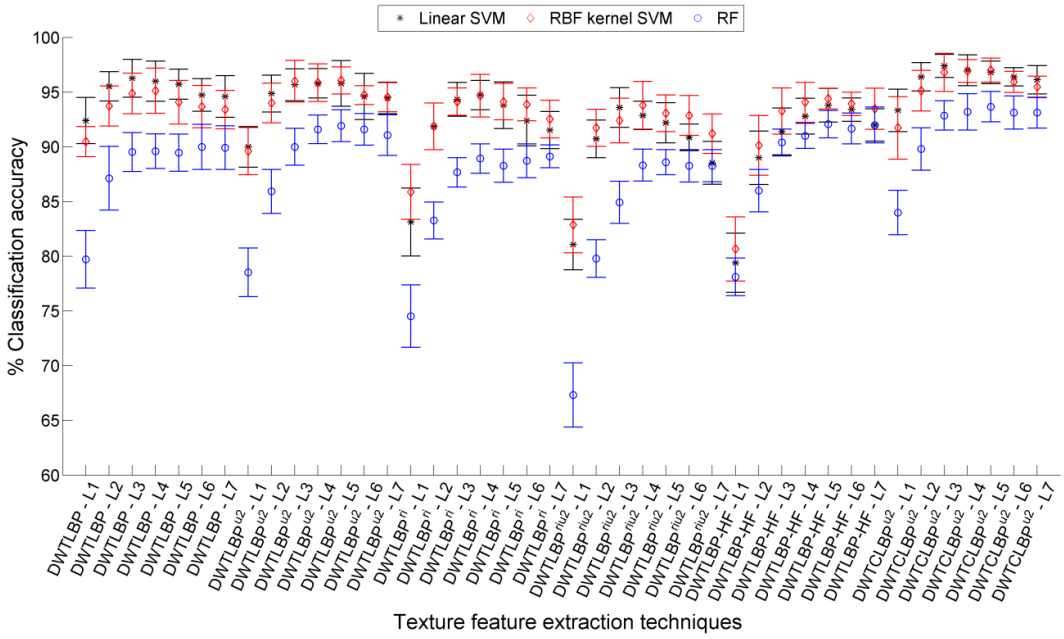

Fig. 5.5 Error bar plot with SD using FFVD.

Further, the time required by the proposed texture feature extraction techniques for feature vector data generation for single image is also listed in Table 5.1. The DWTCLBP^{u2} feature extraction technique has achieved best classification accuracy of 97.40±1.06% at the 3rd level of image decomposition, which requires 0.4070 seconds for extracting the texture features of given individual images as shown in Fig. 5.4; which is much better than the time taken by the BWTCLBP^{ri} feature extraction technique (0.6929 seconds/image). The assessment of the error bar plot with SD for FFVD is shown in Fig. 5.5, reveals that the feature vector data achieved by DWTCLBP^{u2} feature extraction technique at the 3rd level of image decomposition yields the best classification accuracy of 97.40±1.06% with lesser value of SD. The DWTCLBP^{u2} feature extraction technique has achieved slightly lower classification accuracy (97.00±1.10%) with RBF kernel SVM classifier, while the RF classifier has given lowest classification accuracy (93.67±1.38%).

5.3.3.2 The PCA dimensionality reduced feature vector data

In order to improve the classification accuracy of hardwood species classification the PCA has been employed to reduce the dimensionality of full feature vector data. The performance of feature extraction techniques with PCA using different classifiers are listed in Table 5.2 and has been succinctly discussed henceforth:

Linear SVM classifier: Here, the PCA reduced feature vector data of DWTCLBP^{u2} feature extraction technique yields the best classification accuracy of 97.60±1.05%, which is slightly better than the FFVD of DWTCLBP^{u2} feature extraction technique (97.40±1.04%). Further, the classification accuracy has been achieved using only 75-dimensional feature vector data generated at the 5th level of image decomposition compared to 1416-dimensional features of

FFVD produced at the 3rd level of image decomposition.

Table 5.2 Classification accuracy achieved using PCA based reduced feature vector data.

Proposed techniques	IDL	%CA±SD achieved by classifiers							
		NoF	Linear SVM	NoF	RBF kernel SVM	NoF	LDA	NoF	RF
	1	150	92.67±1.57	250	91.13±1.44	100	91.67±1.81	50	88.67±2.31
	2	375	96.00±1.54	300	94.80±1.93	300	95.67±1.92	50	92.87±2.01
	3	325	96.73±1.35	200	96.73±1.73	125	96.80±1.43	50	94.07±1.31
DWTLBP	4	**100**	97.13±1.18	175	**97.07±1.51**	125	96.67±1.47	150	94.13±1.88
	5	**100**	**97.40±1.35**	150	97.00±1.01	150	95.67±1.45	50	94.60±1.65
	6	100	96.93±0.90	125	96.60±1.06	75	95.80±1.48	50	93.80±1.81
	7	75	96.60±0.97	175	96.47±1.22	150	96.00±1.22	50	94.07±1.90
	1	200	88.93±1.76	100	90.00±2.13	225	89.27±1.73	50	86.47±1.99
	2	425	94.40±2.18	150	93.80±2.31	200	94.27±1.30	50	89.73±1.67
	3	275	95.60±1.48	200	96.13±1.74	500	95.87±1.17	50	92.73±1.76
$DWTLBP^{u2}$	4	600	95.80±1.41	550	96.20±1.54	150	95.73±1.58	50	92.27±1.30
	5	525	95.80±1.69	350	96.40±1.10	350	95.27±2.21	50	92.80±1.50
	6	550	94.27±1.94	50	96.20±0.95	125	94.33±1.31	50	93.00±1.45
	7	350	94.07±1.46	100	95.67±1.45	125	94.93±1.45	50	92.40±1.14
	1	125	81.87±2.75	125	85.80±2.52	125	86.13±2.89	100	74.07±4.29
	2	275	91.67±2.07	150	92.20±1.99	275	94.13±1.36	100	84.93±2.60
	3	375	94.27±1.67	300	94.20±1.34	400	95.33±1.22	50	89.40±1.46
$DWTLBP^{ri}$	4	475	94.40±1.05	50	94.80±1.03	525	94.60±1.95	50	89.67±2.25
	5	425	93.60±1.94	300	94.40±1.51	450	93.47±1.29	50	88.67±1.37
	6	350	92.20±2.11	500	93.93±1.49	225	93.07±1.48	50	89.13±1.48
	7	525	91.53±1.83	175	93.47±1.69	50	91.53±0.63	50	87.00±1.84
	1	35	80.47±2.76	25	82.67±2.74	35	82.27±2.11	35	81.53±2.35
	2	65	90.93±1.76	75	91.73±1.70	72	91.80±0.95	50	86.20±1.22
	3	105	93.33±2.22	85	92.87±2.01	105	94.60±1.15	100	89.33±2.18
$DWTLBP^{riu2}$	4	135	93.00±1.34	155	94.33±1.64	125	95.73±1.26	155	88.40±2.18
	5	125	92.47±1.78	95	93.13±2.09	180	95.67±0.96	175	86.20±2.44
	6	225	90.80±1.60	175	92.93±1.89	195	96.00±1.09	225	83.80±2.31
	7	245	88.53±2.22	225	91.13±1.69	235	95.60±1.23	250	82.27±2.61
	1	150	76.93±2.65	125	80.73±2.77	125	88.13±2.74	125	73.30±2.63
	2	300	88.47±2.48	250	90.13±2.79	275	94.47±1.37	250	79.53±3.76
	3	350	91.47±1.83	350	93.27±2.10	425	95.87±1.43	50	85.60±3.19
DWTLBP-HF	4	500	92.53±1.74	450	94.00±1.13	550	96.40±1.26	50	87.93±1.76
	5	475	93.47±1.43	450	94.60±0.91	575	94.80±2.01	50	85.93±1.79
	6	550	93.33±1.04	250	94.33±1.45	525	92.93±1.64	50	87.73±1.84
	7	575	92.00±1.72	550	93.67±2.04	500	92.33±2.04	50	84.73±2.05
	1	200	93.33±1.54	250	91.73±2.78	125	94.00±1.75	150	90.07±2.82
	2	375	96.40±1.64	250	95.27±1.73	200	96.60±0.91	150	91.87±1.50
	3	575	97.40±1.31	350	97.00±1.38	**325**	**97.87±0.82**	100	94.80±1.91
$DWTCLBP^{u2}$	4	275	97.40±1.19	75	97.40±1.35	250	97.53±0.95	100	94.33±1.97
	5	**75**	**97.60±1.05**	**100**	**97.60±1.23**	350	97.13±1.22	50	95.20±1.29
	6	100	97.00±1.34	250	97.07±1.00	325	96.87±1.22	**50**	**95.40±1.31**
	7	100	96.60±1.46	175	97.07±1.23	175	96.67±1.22	50	94.53±2.24

RBF kernel SVM classifier: Amongst the proposed feature extraction techniques, the PCA reduced feature vector data of DWTCLBP^{u2} techniques has attained slightly better classification accuracy of 97.60±1.23% (100 features) compared to 97.00±1.10% (2360 features) presented by full feature vector data. In addition, the aforesaid feature vector data are obtained at the 5th level of image decomposition.

RF classifier: The PCA reduced feature vector data of DWTCLBP^{u2} texture feature extraction technique has achieved the best classification accuracy of 95.40±1.31% using 325-dimensional feature vector data only. This is slightly better than the classification accuracy (93.67±1.38%) yielded by the FFVD of DWTCLBP^{u2} texture feature extraction technique (2360 features).

LDA classifier: This classifier has given the best classification accuracy of 97.87±0.82% for PCA reduced feature vector data of DWTCLBP^{u2} texture feature extraction technique (325 features). The said classification accuracy has been achieved for the feature vector data produced at the 3rd level of image decomposition.

The classification accuracy achieved with PCA reduced dimensional feature vector data is at par/superior than their FFVD, but has been obtained using lower-dimensional features. Among the classifiers, the LDA classifier has obtained maximum classification accuracy for the feature vector data produced at the 3rd level of image decomposition by DWTCLBP^{u2} texture feature extraction technique. The graph depicting the comparison of the classification accuracy obtained by four different classifiers is shown in Fig. 5.6. Further, the error bar plot representation of the same is given in Fig. 5.7. The graphical illustration also supports the statement that DWTCLBP^{u2} texture features classified with LDA classifier presents the superior classification accuracy amongst the proposed techniques with different classifiers.

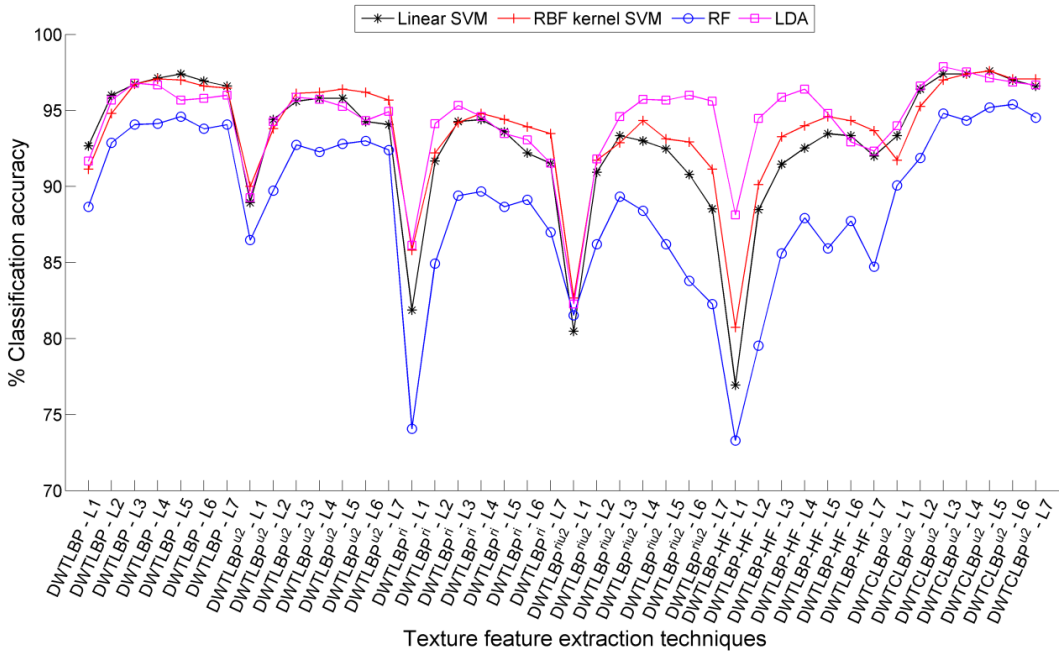

Fig. 5.6 Classification accuracy achieved using PCA reduced feature vector data.

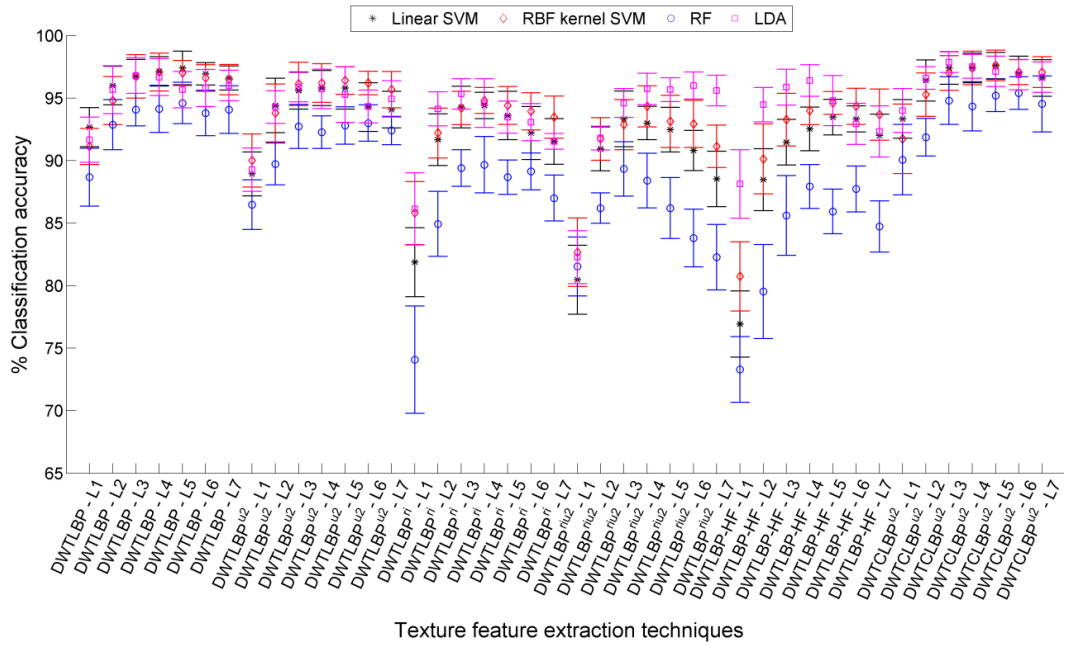

Fig. 5.7 Error bar plot with SD using PCA reduced feature vector data.

5.3.3.3 The mRMR feature selection based reduced feature vector data

The subset of feature vector data obtained by mRMR feature selection method has been investigated to see their effect on the classification accuracy produced for hardwood species classification. The classification accuracy results achieved by three different classifiers are listed in Table 5.3. The classification accuracy results are plotted in Fig. 5.8. Further, the error bar plot for the same has been illustrated in Fig. 5.9. The performance of texture feature extraction techniques with different classifiers are as follows:

Linear SVM classifier: Amongst the proposed feature extraction techniques, the highest classification accuracy of 98.33±0.72% has been achieved by mRMR processed subset (550 features) of FFVD of DWTCLBP^{u2} technique, at the 6th and 7th level of image decomposition. This classification accuracy is comparably better than 97.40±1.06% accuracy obtained by FFVD of DWTCLBP^{u2} technique (1416 features) at the 3rd level of image decomposition.

RBF kernel SVM classifier: The mRMR selected feature subset (550 features) of DWTCLBP^{u2} texture feature extraction technique (feature vector data produced at the 4th level of image decomposition) has achieved the best classification accuracy of 98.40±1.00%. This classification accuracy is relatively better than 97.00±1.10% accuracy obtained by FFVD of DWTCLBP^{u2} technique (2360 features) at the 5th level of image decomposition.

RF classifier: The RF classifier has achieved a classification accuracy of 95.40±1.31% for mRMR selected feature subset (50 features) of DWTCLBP^{u2} texture feature extraction technique (at the 6th level of image decomposition). This accuracy is reasonably better than the highest classification accuracy (93.67±1.38%) obtained by the FFVD (2360 features) of DWTCLBP^{u2} texture feature extraction technique, at the 5th level of image decomposition.

Table 5.3 Classification accuracy achieved using mRMR feature selection based reduced feature vector data.

Technique	IDL	% CA±SD achieved by classifiers					
		NoF	Linear SVM	NoF	RBF kernel SVM	NoF	RF
DWTLBP	1	550	93.33±1.91	350	92.13±1.98	200	83.20±3.45
	2	550	96.27±1.64	500	95.67±1.23	300	89.93±1.52
	3	600	97.47±1.21	450	97.27±0.97	300	92.00±2.81
	4	550	97.67±1.41	450	97.80±1.00	300	93.27±2.66
	5	**550**	**97.87±1.57**	**450**	**97.87±1.17**	150	93.47±2.33
	6	500	97.73±1.55	500	97.67±0.90	500	93.53±1.83
	7	500	97.73±1.55	500	97.67±0.90	350	93.20±0.93
$DWTLBP^{u2}$	1	200	89.33±1.18	150	90.60±2.91	150	79.67±3.85
	2	300	95.13±1.22	250	94.40±1.78	300	87.53±2.22
	3	400	96.20±1.14	350	96.67±1.54	300	91.93±2.56
	4	300	96.87±1.44	200	97.20±0.82	300	92.93±1.84
	5	400	97.33±1.33	200	97.47±0.97	300	93.53±1.51
	6	300	97.47±1.03	200	97.60±0.90	250	93.47±2.49
	7	400	97.60±1.38	200	97.60±0.95	300	93.40±2.12
$DWTLBP^{ri}$	1	140	83.00±3.10	125	85.93±2.07	125	74.20±4.09
	2	200	92.93±0.95	200	91.93±1.35	100	85.07±2.42
	3	400	94.87±1.18	300	95.13±1.22	100	88.67±2.55
	4	250	96.13±0.88	150	95.80±1.60	150	90.73±2.44
	5	300	96.13±0.82	100	96.13±0.88	100	90.67±1.54
	6	300	96.67±0.94	150	96.60±1.35	150	90.73±2.68
	7	300	96.80±0.98	150	96.67±1.35	150	91.53±2.85
$DWTLBP^{riu2}$	1	35	79.87±2.45	35	82.60±1.84	30	66.80±4.28
	2	50	91.00±1.27	50	91.67±1.94	50	80.40±2.11
	3	100	93.33±1.81	100	92.93±1.76	150	86.47±2.29
	4	125	93.20±1.43	150	93.93±1.39	150	88.33±2.40
	5	150	93.60±2.04	100	93.00±1.55	150	89.13±2.72
	6	150	94.13±1.83	150	93.87±1.17	150	89.47±2.84
	7	150	93.67±1.76	150	93.60±1.51	250	88.93±1.14
DWTLBP-HF	1	200	89.33±1.18	50	83.53±2.88	125	73.30±2.63
	2	300	95.13±1.22	50	92.20±2.16	250	79.53±3.76
	3	400	96.20±1.14	100	95.73±1.51	50	85.60±3.19
	4	300	96.87±1.44	50	97.27±1.45	50	85.93±1.79
	5	400	97.33±1.33	150	97.67±1.01	50	87.93±1.76
	6	300	97.47±1.03	150	97.47±1.29	50	87.73±1.84
	7	400	97.60±1.38	150	97.53±1.37	50	84.73±2.05
$DWTCLBP^{u2}$	1	250	93.87±1.29	300	92.93±2.56	150	90.07±2.82
	2	450	96.73±1.11	250	96.40±1.73	150	91.87±1.50
	3	500	98.07±0.97	400	98.07±0.91	100	94.80±1.91
	4	**500**	98.27±0.90	**550**	**98.40±1.00**	100	94.33±1.97
	5	**350**	**98.33±1.14**	300	98.33±0.65	50	95.20±1.29
	6	**550**	98.33±0.72	450	98.60±0.91	**50**	**95.40±1.31**
	7	550	98.33±0.72	450	98.60±0.80	50	94.53±2.24

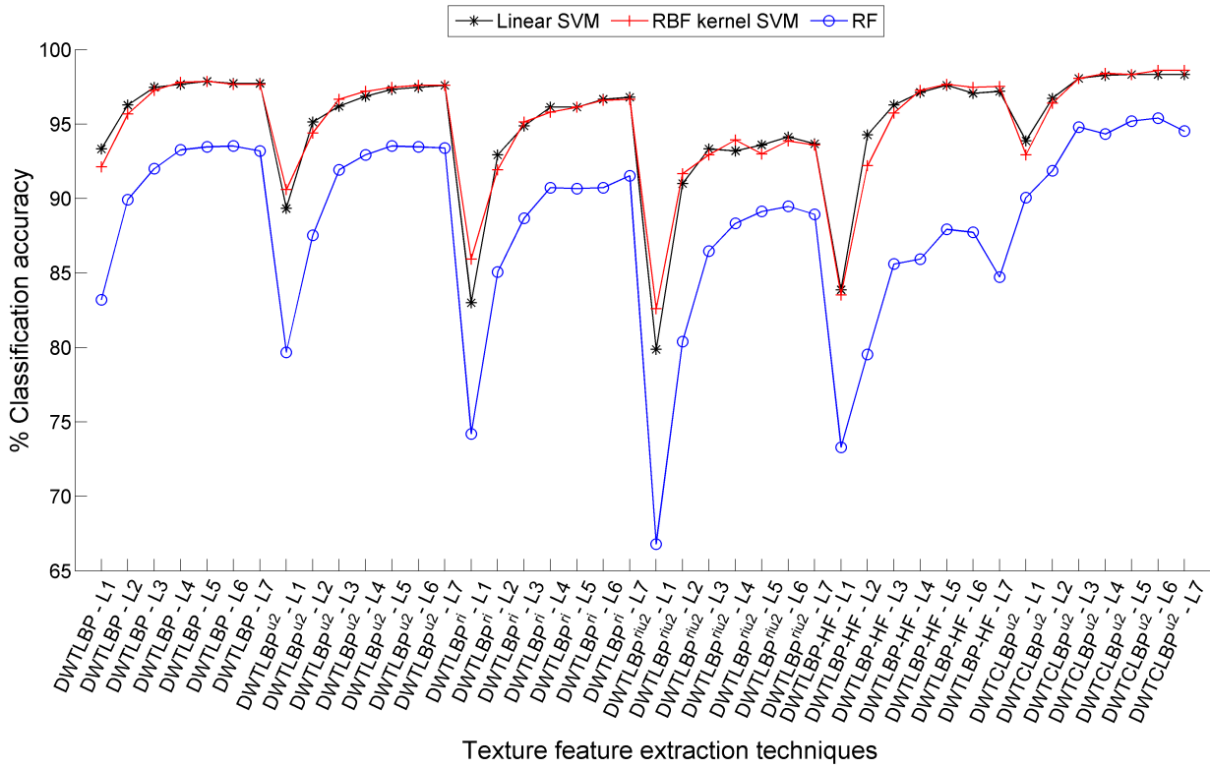

Fig. 5.8 Classification accuracy achieved using mRMR feature selection based reduced feature vector data.

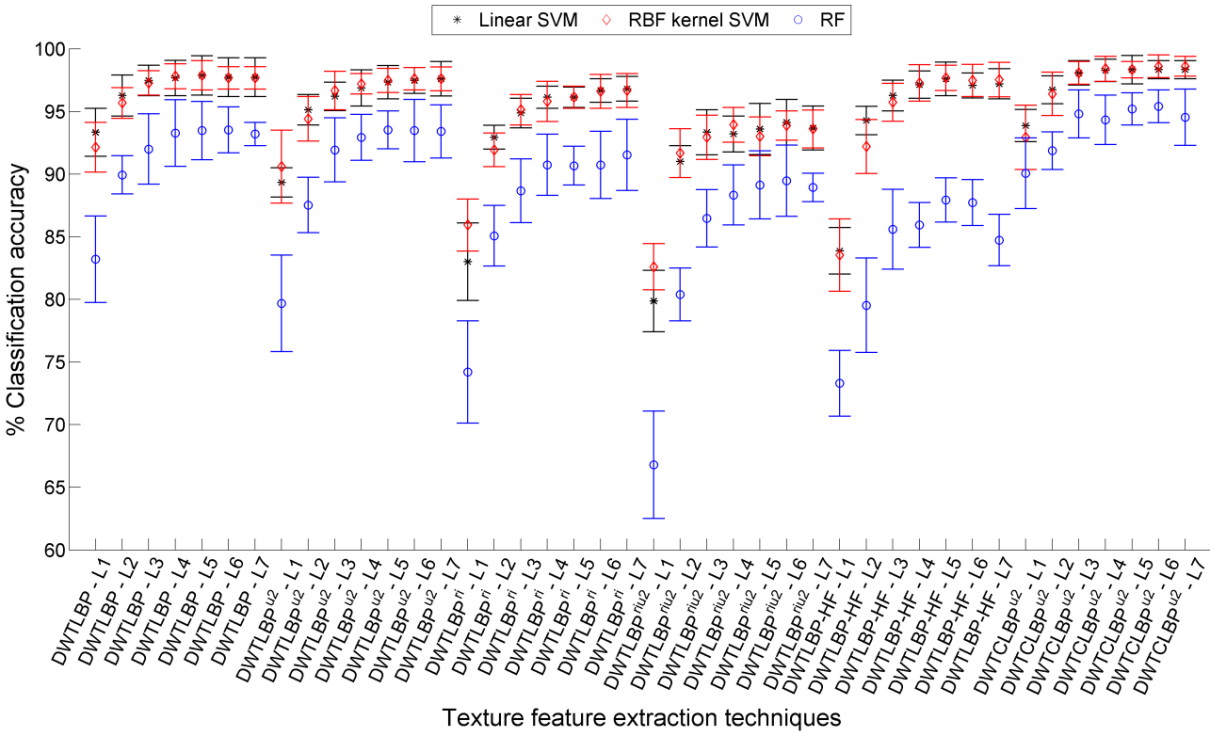

Fig. 5.9 Error bar plot with SD using mRMR feature selection based reduced feature vector data.

The analysis of Table 5.3 suggests that among the proposed texture feature extraction techniques, the mRMR selected feature subset of DWTCLBP^{u2} technique has achieved the best classification accuracy of 98.40±1.00% with RBF kernel SVM classifier**.**

It is observed from Table 5.1 that as the level of image decomposition increases, the length of the feature vector data also increases. The classification accuracy results for the FFVD of DWT based texture feature extraction techniques using different classifiers have grown up in the range of 3rd to 5th level of image decomposition and thereafter either it remains same or decreases a little bit. It is noticeable that the increase in the classification accuracy has been attained at the cost of additional computation time. Therefore, the DWT based texture descriptors beyond 7th level of image decomposition has not been investigated.

Further, employing PCA (dimensionality reduction) and mRMR (feature selection) technique has not only reduced the computational time but at the same time has shown considerable improvement in the classification accuracy of hardwood species. It is also observed from Table 5.1, Table 5.2 and Table 5.3 that the DWT based LBP variants texture feature extraction techniques have achieved better classification accuracy compared to the original LBP variants feature extraction techniques as given in Chapter 2.

5.3.4 Performance Evaluation of GP based Texture Feature Extraction Techniques using Randomly Divided Database (RDD)

5.3.4.1 Full feature vector data (FFVD)

The classification accuracy achieved by DWT (MRLBP variants) based texture feature extraction techniques for different ratios of training and testing data is listed in Table 5.4.

Linear SVM classifier: Amongst the proposed texture feature extraction techniques, DWTCLBP^{u2} has produced significant feature vector data that yields best classification accuracy of 94.33% (at 4th IDL), 93%(at 3rd IDL), 92.17% (at 4th IDL) and 90.93% (at 4th IDL) for 80/20, 70/30, 60/40 and 50/50 training and testing ratios of RDD, respectively (Table 5.4).

RBF kernel SVM classifier: Using RBF kernel SVM classifier, the best classification accuracy of 92% (at 4th IDL), 92% (at 5th IDL), 90.33% (at 5th IDL) and 88.67% (at 5th IDL) has been achieved for 80/20, 70/30, 60/40 and 50/50 training and testing ratios of RDD, respectively as listed in Table 5.4 .

RF classifier: As given in Table 5.4, the feature vector data produced by DWTCLBP^{u2} feature extraction technique has given the best classification accuracy for different proportions of training and testing data of RDD, amongst the proposed techniques using RF classifier. The DWTCLBP^{u2} features (at the 5th level of image decomposition) have achieved classification accuracy of 88.67% (at 6th IDL), 87.56% (at 5th IDL), 87.83% (at 5th IDL) and 85.33% (at 5th IDL) for 80/20, 70/30, 60/40 and 50/50 training and testing ratios of RDD, respectively.

The classification accuracies obtained by the three different classifiers are compared for each of the four (80/20, 70/30, 60/40 and 50/50) training and testing ratios, and are graphically illustrated in Fig. 5.10, Fig. 5.11,Fig. 5.12 and Fig. 5.13, respectively.

Table 5.4 Classification accuracy achieved by full feature vector data for different proportions of training and testing data of RDD using three classifiers.

Technique	IDL	% CA achieved by classifiers for different proportions of training and testing data											
		LSVM				RBF kernel SVM				RF			
		80/20	70/30	60/40	50/50	80/20	70/30	60/40	50/50	80/20	70/30	60/40	50/50
DWTLBP	1	88.00	84.22	81.00	75.73	83.67	82.44	76.33	72.13	73.67	68.67	69.67	63.73
	2	91.33	89.56	87.33	83.47	87.00	85.78	82.50	77.73	81.67	79.78	77.50	75.33
	3	93.67	91.78	90.00	87.60	89.00	87.56	85.33	81.07	82.67	82.22	80.83	78.93
	4	92.67	91.33	91.17	87.87	87.00	88.22	87.00	82.93	85.33	83.33	83.00	80.80
	5	92.33	90.67	90.33	88.27	86.67	86.44	87.17	83.47	84.67	83.11	82.67	80.13
	6	91.33	90.00	90.33	88.00	86.00	86.00	85.83	82.83	84.67	83.11	81.83	81.47
	7	92.00	89.11	89.83	87.33	85.00	84.67	85.00	81.73	83.67	82.89	82.67	81.73
$DWTLBP^{u2}$	1	81.33	78.67	76.83	73.87	81.67	78.67	73.50	71.20	68.67	65.78	64.83	63.33
	2	87.33	86.00	82.83	81.47	87.00	84.89	82.67	79.07	80.00	77.11	77.16	72.93
	3	90.00	89.56	89.00	86.53	88.67	88.00	84.83	82.13	84.67	83.56	81.83	78.93
	4	90.67	89.56	88.83	88.53	90.33	89.11	87.67	84.93	85.67	84.22	84.67	83.07
	5	91.33	90.44	90.17	87.60	88.67	89.33	88.00	85.47	87.00	84.44	84.00	82.40
	6	90.33	89.78	89.33	87.47	88.67	89.11	87.33	84.40	87.00	83.11	84.67	81.73
	7	89.00	89.56	88.33	86.27	87.33	89.11	87.67	83.73	86.33	84.89	84.33	81.47
$DWTLBP^{ri}$	1	77.67	71.33	70.50	67.47	79.00	73.78	70.83	68.53	68.00	61.56	60.17	59.47
	2	89.00	85.33	83.83	79.60	87.00	83.78	82.33	77.33	82.33	76.89	75.67	70.00
	3	89.00	86.89	86.00	84.67	89.00	87.78	85.83	82.27	83.33	81.33	81.00	76.40
	4	89.67	89.78	87.83	85.73	87.33	88.00	85.83	82.53	85.67	83.56	82.33	78.93
	5	89.00	87.56	87.50	85.60	88.33	86.00	85.67	82.53	85.33	82.44	82.67	79.60
	6	88.33	88.00	86.83	84.13	89.00	86.22	86.33	82.27	84.00	84.44	84.83	80.27
	7	86.33	84.67	85.00	82.93	86.33	86.00	85.67	81.87	84.00	82.67	83.00	80.53
$DWTLBP^{riu2}$	1	77.00	72.89	71.67	69.47	74.33	71.33	69.17	65.20	55.67	52.22	52.50	50.40
	2	88.33	86.22	84.17	81.60	87.67	83.11	82.00	77.73	80.00	74.44	71.00	68.13
	3	90.33	90.44	87.83	84.93	88.67	87.78	85.17	82.40	79.33	77.78	77.33	75.33
	4	89.33	90.00	87.33	86.80	89.00	89.11	87.17	86.00	83.33	82.44	81.67	78.40
	5	88.33	88.22	86.50	85.07	88.33	88.22	85.83	84.80	85.33	82.89	81.17	79.33
	6	87.67	86.67	84.83	82.40	88.67	88.00	84.67	82.93	85.00	83.77	82.83	79.87
	7	85.00	84.00	81.50	80.40	86.67	86.22	84.33	81.33	84.33	82.67	81.83	79.73
DWTLBP-HF	1	72.00	68.44	65.50	62.00	70.67	67.33	66.17	62.53	70.33	68.00	64.17	63.47
	2	86.00	82.00	79.33	75.87	85.00	81.11	80.83	75.47	82.67	78.89	76.83	75.47
	3	89.67	86.00	84.17	82.13	89.67	87.33	83.83	81.33	87.00	82.89	83.00	81.33
	4	89.67	88.00	86.83	84.00	89.00	87.78	87.17	83.33	89.00	85.56	85.17	82.93
	5	89.67	88.89	88.17	84.17	88.67	89.11	88.50	84.93	87.33	87.56	85.83	84.00
	6	90.67	90.22	87.50	83.87	89.00	88.44	86.83	84.53	88.33	85.77	86.00	83.20
	7	87.67	88.22	86.00	83.87	87.67	88.00	86.83	83.73	87.67	87.33	86.33	84.00
$DWTCLBP^{u2}$	1	88.67	84.22	83.17	80.00	85.33	82.67	79.33	76.00	76.33	71.56	69.83	68.13
	2	91..67	90.00	88.00	84.53	90.00	87.78	84.50	81.47	85.67	82.00	79.50	79.47
	3	92.33	**93.00**	89.83	88.27	90.00	89.56	86.33	83.87	86.67	85.11	85.83	83.33
	4	**94.33**	92.67	**92.17**	**90.93**	**92.00**	90.67	89.33	87.73	88.00	86.67	86.33	84.80
	5	94.00	92.44	91.83	90.80	91.33	**92.00**	**90.33**	**88.67**	88.00	**87.56**	**87.83**	**85.33**
	6	93.33	92.44	92.00	90.93	91.00	91.33	89.67	87.60	**88.67**	86.67	87.67	85.20
	7	92.33	91.56	91.33	90.13	90.67	90.89	89.50	87.47	87.67	86.89	88.00	84.13

It is apparent from these figures that texture feature vector data produced by most of the DWT (MRLBP variants) based texture feature extraction techniques yield best classification accuracy with linear SVM classifier; whereas, the least classification accuracy has been achieved with RF classifier. Further, the classification accuracy obtained by other MRLBP variants texture feature extraction techniques have obtained better classification accuracy results compared to the classification accuracy achieved by state-of-the-art LBP variants texture feature extraction techniques.

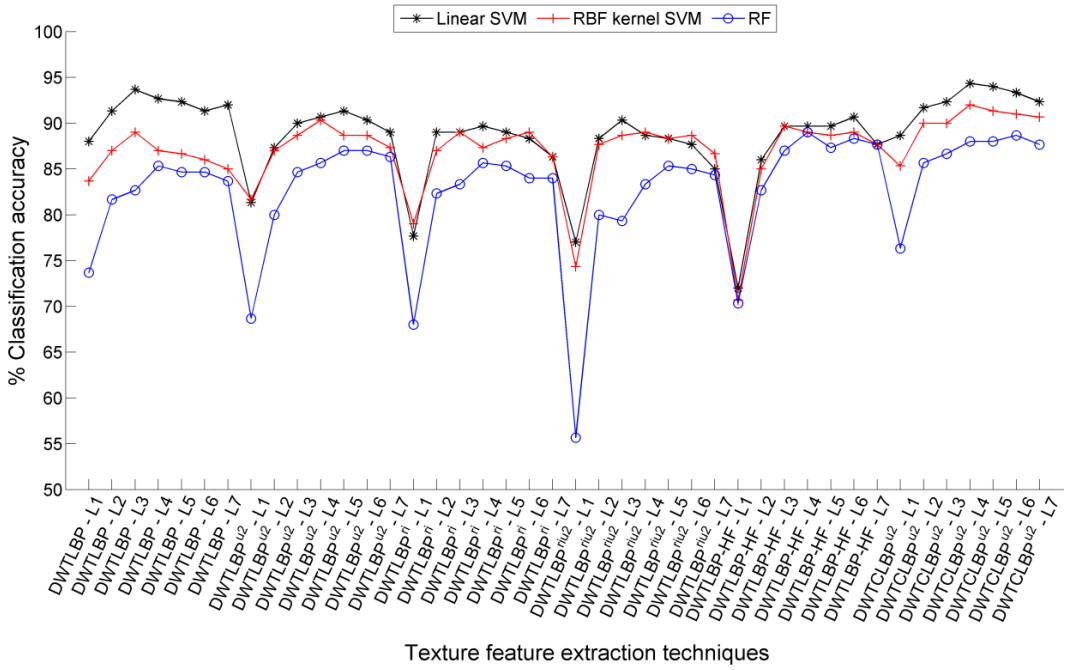

Fig. 5.10 Classification accuracy achieved for 80/20 proportion of training and testing data of RDD.

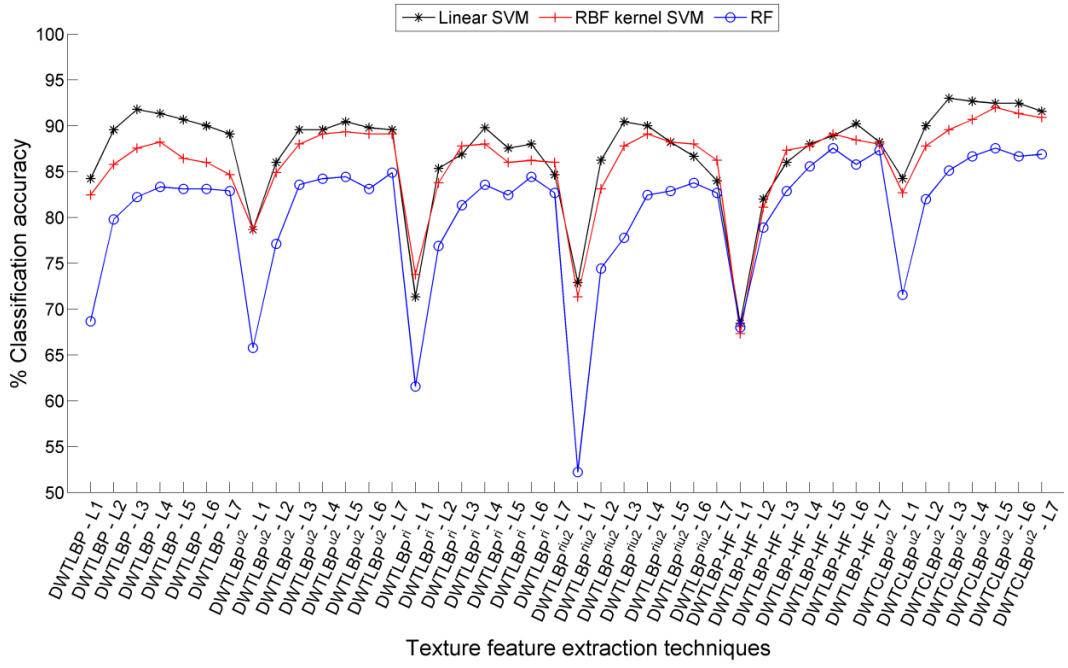

Fig. 5.11 Classification accuracy achieved for 70/30 proportion of training and testing data of RDD.

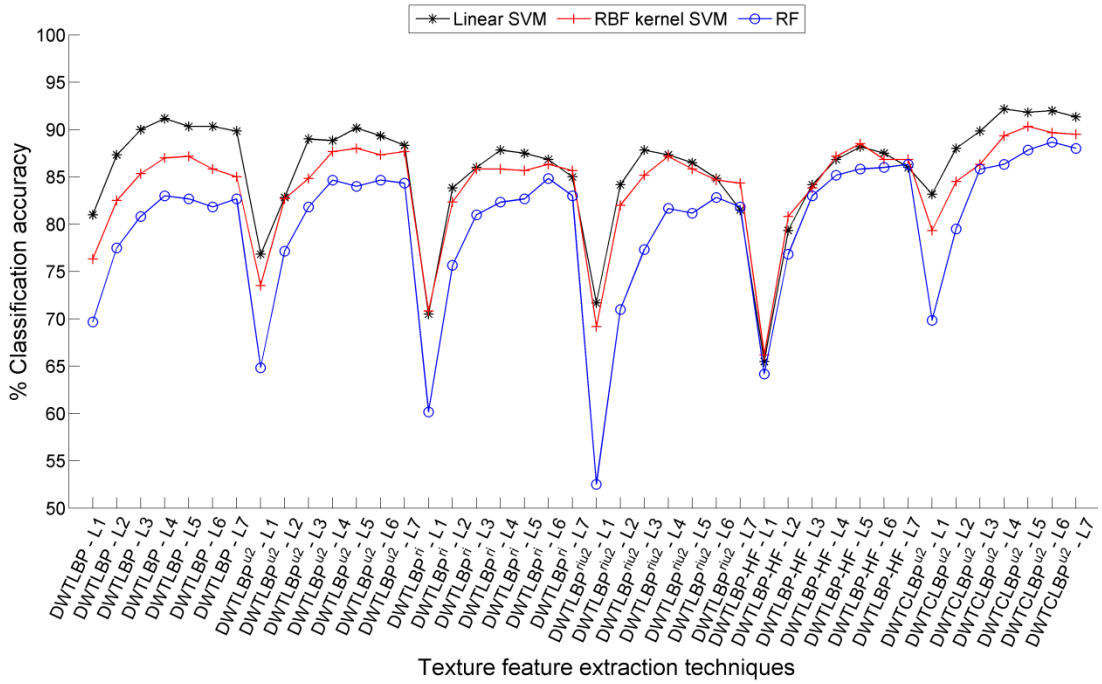

Fig. 5.12 Classification accuracy achieved for 60/40 proportion of training and testing data of RDD.

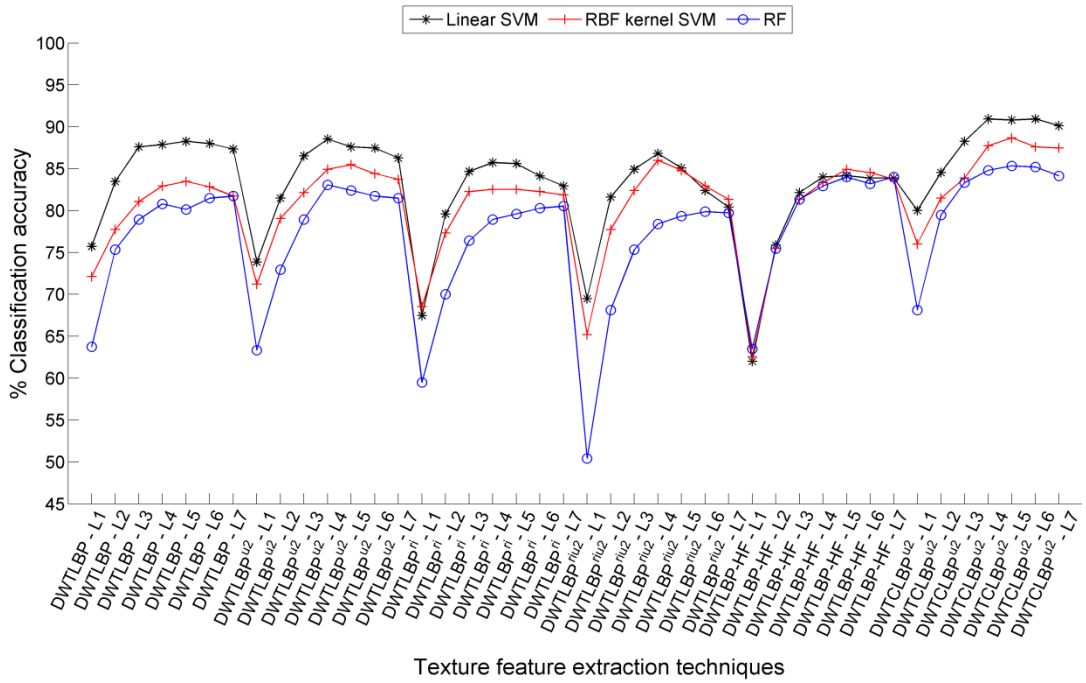

Fig. 5.13 Classification accuracy achieved for 50/50 proportion of training and testing data of RDD.

5.3.4.2 The PCA dimensionality reduced feature vector data

The classification accuracy results obtained by the PCA reduced feature vector data using four different classifiers are concisely discussed here forth:

Linear SVM classifier: The PCA dimensionality reduced feature vector data of the DWTCLBP^{u2} technique yields the best classification accuracy of 94.67% (450 features, at 4th IDL), 93.56% (450 features, at 5th IDL), 92.50% (450 features, at 6th IDL) and 90.67% (350 features, at 6th IDL)

for 80/20, 70/30, 60/40 and 50/50 training and testing ratios of RDD, respectively. This classification accuracy is comparable to the accuracy achieved with FFVD of DWTCLBP^{u2} technique with high-dimensional features (Table 5.5).

Table 5.5 Classification accuracy achieved by PCA reduced feature vector data for different proportions of training and testing data of RDD using linear SVM classifier.

Technique	IDL	NoF	80/20	NoF	70/30	NoF	60/40	NoF	50/50
	1	150	87.33	600	84.00	100	81.00	550	77.07
	2	150	92.33	350	91.78	300	88.17	500	83.73
	3	300	94.33	100	93.11	550	91.17	450	88.67
DWTLBP	4	100	93.67	150	92.67	100	91.67	150	89.87
	5	100	94.00	100	93.33	100	91.33	100	88.93
	6	150	93.67	100	92.67	400	91.00	100	88.53
	7	100	94.33	150	92.67	150	91.00	150	88.67
	1	225	82.67	100	78.67	200	76.67	200	73.20
	2	250	87.33	150	86.00	300	83.67	250	80.67
	3	50	90.33	50	90.22	300	88.50	400	86.40
DWTLBP^{u2}	4	50	90.67	50	91.56	300	89.50	400	87.87
	5	50	91.33	100	91.78	350	89.83	350	87.33
	6	100	91.00	200	90.44	300	89.00	50	86.13
	7	100	89.00	50	88.67	300	88.00	400	85.73
	1	125	76.67	125	72.00	125	70.67	125	68.13
	2	250	88.33	250	84.89	200	83.33	250	79.87
	3	350	89.00	300	87.33	150	86.00	250	84.53
DWTLBP^{ri}	4	150	89.67	450	89.11	300	87.00	400	85.73
	5	300	88.67	500	88.00	450	86.83	250	85.07
	6	450	88.67	150	86.67	350	86.00	500	84.53
	7	500	85.33	450	84.00	500	84.00	450	82.53
	1	35	74.33	30	72.22	30	72.33	30	67.87
	2	70	88.33	70	85.11	75	83.83	70	81.33
	3	100	91.33	100	90.22	100	88.17	100	85.33
DWTLBP^{riu2}	4	100	89.67	125	90.00	125	87.83	125	86.67
	5	200	88.33	150	88.22	150	87.33	175	85.20
	6	200	87.67	150	86.44	200	84.17	225	81.73
	7	200	83.00	250	84.00	250	81.33	250	80.53
	1	150	72.33	150	67.78	150	65.50	125	62.00
	2	200	88.33	250	82.22	250	79.00	300	76.13
	3	300	89.00	350	86.44	350	83.33	300	81.20
DWTLBP-HF	4	400	90.33	350	88.00	450	86.00	450	84.00
	5	400	90.67	550	89.78	550	88.50	550	84.67
	6	350	91.00	350	90.44	500	87.00	550	83.20
	7	450	87.33	500	88.00	400	86.00	550	82.27
	1	200	88.67	200	84.00	200	83.50	350	80.27
	2	250	91.00	150	90.44	450	87.17	300	84.67
	3	400	92.67	150	92.00	250	90.33	300	88.80
DWTCLBP^{u2}	**4**	**450**	**94.67**	200	93.33	150	91.33	550	90.67
	5	350	94.00	**450**	**93.56**	250	92.00	100	90.53
	6	450	94.00	600	93.11	**450**	**92.50**	**350**	**90.67**
	7	600	93.33	50	92.89	150	91.50	150	90.53

RBF kernel SVM classifier: A classification accuracy of 93.33% (50 features, at 6th IDL), 93.33% (150 features, at 7th IDL), 91.50% (150 features, at 6th IDL) and 89.87% (50 features, at 5th IDL) has been obtained for 80/20, 70/30, 60/40 and 50/50 training and testing ratios of RDD,

respectively. These results have been achieved by PCA dimensionality reduced feature vector data of the DWTCLBP^{u2} technique, and are reasonably better than the accuracy presented by the FFVD of DWTCLBP^{u2} technique (Table 5.6).

Table 5.6 Classification accuracy achieved by PCA reduced feature vector data for different proportions of training and testing data of RDD using RBF kernel SVM classifier.

Technique	IDL	NoF	80/20	NoF	70/30	NoF	60/40	NoF	50/50
	1	100	84.33	450	82.44	250	77.50	250	74.13
	2	200	88.67	200	87.33	300	83.50	100	79.60
	3	150	91.00	200	90.67	200	87.17	150	83.87
DWTLBP	4	300	91.33	250	91.33	200	89.83	150	86.80
	5	200	92.67	100	92.00	150	89.67	100	87.07
	6	150	92.33	100	92.00	150	90.33	150	87.47
	7	150	91.33	150	92.89	300	90.00	100	87.07
	1	150	82.67	150	79.33	100	74.67	100	71.73
	2	100	87.00	150	85.56	150	82.67	300	79.07
	3	50	90.00	50	89.56	100	86.83	100	83.60
DWTLBP^{u2}	4	100	90.33	100	90.22	100	88.17	150	86.00
	5	150	90.00	50	90.22	150	89.67	50	86.53
	6	50	89.67	50	91.11	100	90.00	100	87.33
	7	100	89.67	100	90.22	150	89.00	150	86.67
	1	125	79.67	100	74.00	125	71.33	100	69.07
	2	150	86.67	100	83.56	250	82.17	250	77.47
	3	300	89.33	20	88.89	200	85.67	200	82.80
DWTLBP^{ri}	4	50	89.67	50	88.67	200	86.33	50	84.67
	5	50	89.00	50	86.89	50	86.17	50	83.73
	6	50	87.67	150	87.56	150	86.67	50	84.53
	7	150	88.00	100	86.44	50	85.50	50	83.87
	1	30	75.33	35	70.89	35	69.83	35	65.73
	2	50	87.67	50	83.33	50	82.00	60	77.33
	3	50	89.67	100	88.00	50	85.83	100	82.53
DWTLBP^{riu2}	4	100	89.67	100	89.56	100	87.50	150	85.87
	5	175	89.00	150	88.22	100	86.00	150	84.93
	6	200	88.67	200	87.78	200	84.50	225	83.07
	7	200	86.67	250	86.44	200	84.17	250	81.47
	1	100	70.67	100	67.56	125	66.33	150	62.80
	2	150	85.00	200	81.33	200	80.50	300	75.60
	3	150	89.67	150	87.33	300	83.67	400	81.47
DWTLBP-HF	4	100	89.67	150	88.44	400	87.67	450	83.60
	5	100	90.33	150	89.33	500	88.33	50	86.67
	6	250	91.33	100	90.00	250	87.67	50	87.07
	7	50	88.00	150	88.00	350	87.67	50	84.27
	1	200	85.67	150	82.89	100	80.17	400	76.13
	2	300	90.00	400	88.22	250	85.17	300	82.13
	3	150	91.33	150	90.00	300	86.67	300	85.20
DWTCLBP^{u2}	4	500	92.67	200	92.67	150	90.83	100	88.80
	5	250	93.00	250	92.89	250	91.50	**50**	**89.87**
	6	**50**	**93.33**	200	92.89	**150**	**91.50**	100	89.73
	7	100	93.33	**150**	**93.33**	100	90.83	150	89.47

RF classifier: In this case, the classification accuracy results of 91.33% (150 features, at 6th IDL), 89.78% (100 features, at 5th IDL), 89.33% (100 features, at 6th IDL) and 87.60% (50 features, at 6th IDL) for 80/20, 70/30, 60/40 and 50/50 training and testing ratios of RDD,

respectively, has been obtained by DWTCLBP^{u2} technique with PCA dimensionality reduced feature vector data (Table 5.7).

Table 5.7 Classification accuracy achieved by PCA reduced feature vector data for different proportions of training and testing data of RDD using RF classifier.

Technique	IDL	NoF	80/20	NoF	70/30	NoF	60/40	NoF	50/50
	1	50	83.33	100	78.44	100	76.50	50	73.87
	2	50	87.67	150	84.89	50	84.50	100	79.20
	3	100	89.33	100	88.00	100	88.33	100	85.73
DWTLBP	4	50	90.67	50	90.44	150	90.00	50	86.67
	5	100	89.67	100	88.67	50	88.17	100	85.33
	6	100	90.33	50	87.56	50	87.50	150	85.87
	7	100	89.00	50	87.78	100	87.67	50	85.87
	1	50	79.67	50	72.00	50	71.83	50	66.80
	2	50	83.67	50	79.78	50	77.83	100	73.87
	3	100	86.67	50	85.33	50	84.50	50	80.80
DWTLBP^{u2}	4	150	87.00	100	86.67	100	86.33	50	84.27
	5	150	86.67	50	86.44	50	86.33	50	85.33
	6	100	86.67	50	87.56	50	86.50	50	85.20
	7	250	85.33	50	86.00	50	84.83	50	83.67
	1	50	72.67	50	64.89	50	61.50	100	61.60
	2	50	80.67	50	76.89	50	76.17	50	72.00
	3	50	85.67	50	84.00	200	81.67	50	79.20
DWTLBP^{ri}	4	50	84.00	50	83.33	50	83.33	50	82.13
	5	50	85.33	50	84.22	50	83.83	50	81.73
	6	50	85.67	50	84.67	50	82.67	50	82.13
	7	150	83.67	50	82.22	50	82.67	50	80.40
	1	30	78.00	35	73.78	35	69.33	35	69.73
	2	50	80.00	60	79.33	60	78.83	60	76.00
	3	110	85.67	100	85.56	100	82.50	110	80.93
DWTLBP^{riu2}	4	150	85.33	100	86.00	100	83.67	100	82.27
	5	175	83.33	100	80.00	175	79.83	100	76.80
	6	225	81.00	225	79.56	200	78.17	150	75.87
	7	250	78.33	150	76.89	50	75.33	50	74.00
	1	150	69.00	150	62.89	150	58.67	150	58.53
	2	250	76.00	150	68.22	200	66.33	100	66.00
	3	200	81.67	50	78.00	50	75.67	50	73.07
DWTLBP-HF	4	100	82.67	100	80.22	50	79.67	50	77.07
	5	50	85.67	50	82.22	150	80.67	50	78.67
	6	50	85.33	50	83.33	50	81.83	50	78.67
	7	50	82.67	50	81.56	50	78.33	50	76.13
	1	100	84.00	100	80.67	50	77.00	50	74.13
	2	100	87.00	50	84.44	150	81.33	250	76.40
	3	50	89.00	350	88.00	100	87.33	100	85.20
DWTCLBP^{u2}	4	150	90.00	50	89.33	50	88.67	50	87.20
	5	100	91.00	**50**	**89.78**	150	88.50	50	87.33
	6	**150**	**91.33**	100	89.33	**100**	**89.33**	**50**	**87.60**
	7	50	89.33	50	89.78	50	88.33	50	87.60

Table 5.8 Classification accuracy achieved by PCA reduced feature vector data for different proportions of training and testing data of RDD using LDA classifier.

Technique	IDL	NoF	80/20	NoF	70/30	NoF	60/40	NoF	50/50
	1	150	87.33	150	82.89	100	83.50	50	81.87
	2	300	92.00	200	91.11	50	89.00	50	86.53
	3	300	93.33	100	93.33	100	92.67	100	90.00
DWTLBP	4	200	92.67	150	93.11	150	92.33	100	90.53
	5	200	93.33	150	93.33	50	92.67	50	90.40
	6	200	94.67	200	92.89	50	92.67	50	90.53
	7	150	94.67	100	93.33	100	93.17	50	90.93
	1	100	84.33	100	80.00	100	78.67	50	76.80
	2	250	89.33	200	88.00	200	86.67	150	82.67
	3	100	91.00	300	91.11	150	89.83	100	88.00
$DWTLBP^{u2}$	4	100	92.33	150	91.11	100	91.17	50	88.80
	5	50	91.33	50	91.11	50	90.33	50	88.80
	6	150	91.67	50	91.56	50	90.50	50	87.87
	7	50	90.33	50	90.67	50	89.50	50	87.60
	1	140	83.67	140	79.56	140	78.50	140	75.73
	2	280	90.67	280	88.67	250	88.17	280	83.07
	3	400	92.33	420	90.22	350	89.00	300	86.13
$DWTLBP^{ri}$	4	350	91.33	250	89.56	250	88.17	150	85.47
	5	450	91.00	200	88.89	100	88.00	100	86.13
	6	400	89.67	150	88.67	50	88.17	50	87.60
	7	150	88.67	50	87.11	50	88.17	50	87.33
	1	35	78.67	35	74.22	36	75.50	36	75.87
	2	50	88.00	50	86.67	50	87.83	60	86.00
	3	100	91.67	108	92.22	100	91.67	108	89.47
$DWTLBP^{riu2}$	4	125	93.67	144	92.67	144	92.33	125	90.13
	5	150	93.33	175	92.67	180	91.83	175	89.33
	6	200	93.00	200	92.44	200	91.67	200	89.73
	7	225	93.33	225	91.33	225	91.17	225	89.87
	1	148	85.67	148	80.44	148	79.67	148	77.07
	2	250	90.67	275	88.67	296	88.33	296	83.87
	3	444	92.00	444	90.22	444	90.00	400	84.67
DWTLBP-HF	4	350	90.67	150	88.89	200	89.00	200	85.60
	5	300	91.00	150	89.11	100	88.00	100	84.80
	6	200	90.33	200	89.33	50	88.33	50	86.00
	7	50	89.33	50	88.67	50	87.50	50	85.73
	1	100	91.00	100	86.89	100	87.50	100	84.13
	2	450	93.00	100	90.89	250	89.67	150	86.27
	3	100	93.33	100	93.33	100	91.83	100	91.47
$DWTCLBP^{u2}$	4	200	94.33	**200**	**94.22**	**200**	**93.00**	**200**	91.47
	5	450	95.33	200	94.22	250	92.67	**100**	**92.00**
	6	**350**	**95.67**	350	94.00	50	91.83	150	91.20
	7	100	94.67	200	94.00	50	92.33	100	90.67

LDA classifier: Amongst the proposed feature extraction techniques, the PCA dimensionality reduced feature vector data of the $DWTCLBP^{u2}$ technique has achieved classification accuracy

of 95.67% (350 features, at 6th IDL), 94.22% (200 features, at 4th IDL), 93% (200 features, at 4th IDL) and 92% (100 features, at 5th IDL) for 80/20, 70/30, 60/40 and 50/50 training and testing ratios of randomly divided database, respectively (Table 5.8).

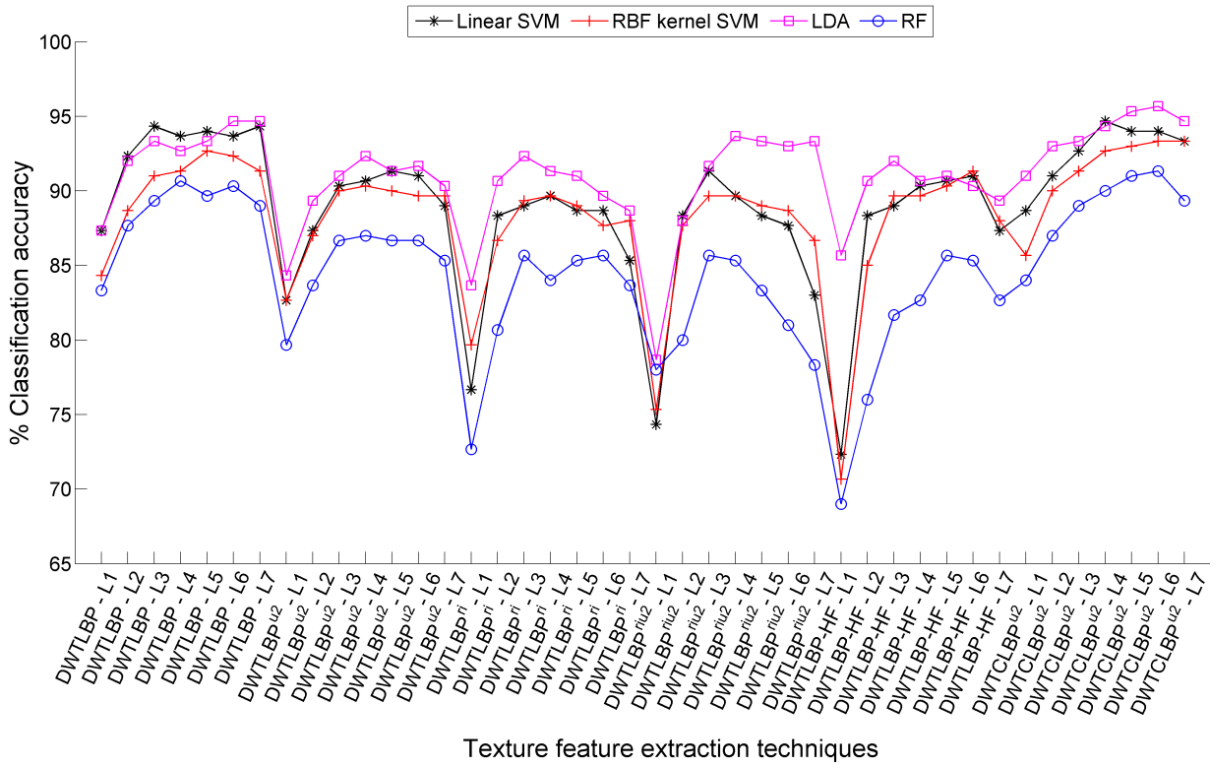

Fig. 5.14 Classification accuracy achieved for 80/20 proportion of training and testing data of RDD.

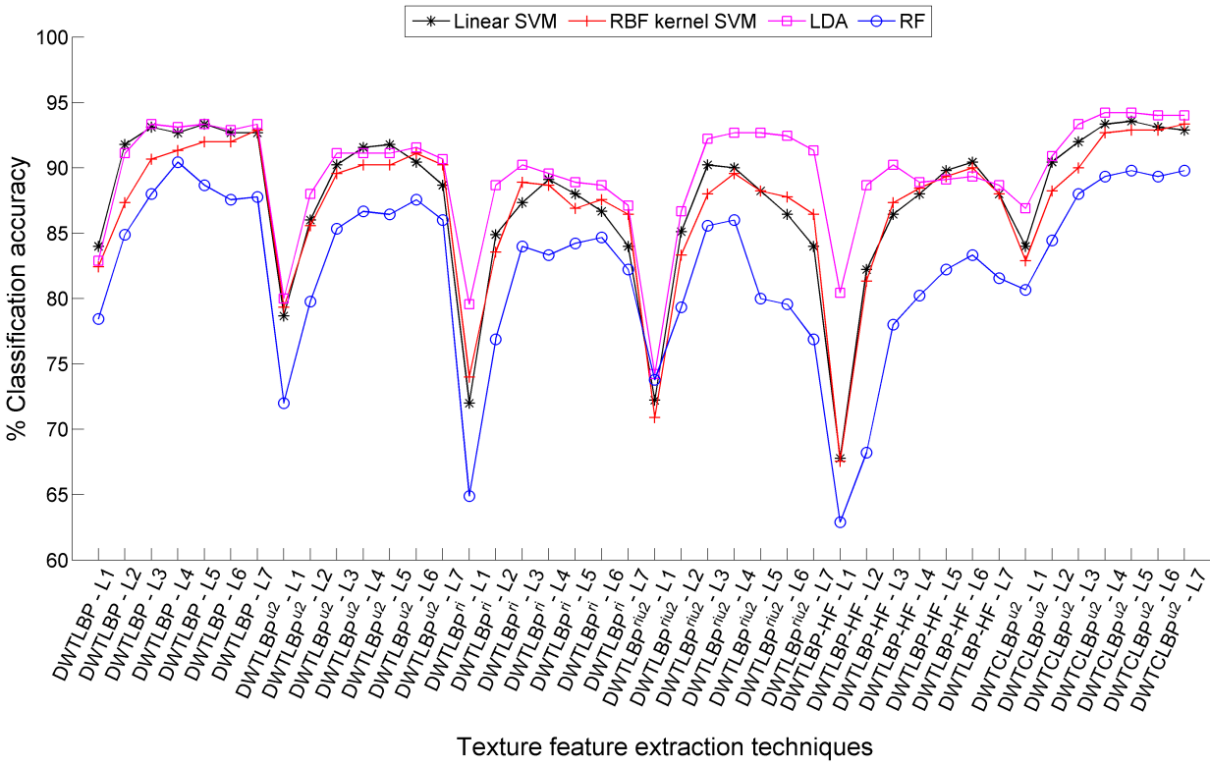

Fig. 5.15 Classification accuracy achieved for 70/30 proportion of training and testing data of RDD.

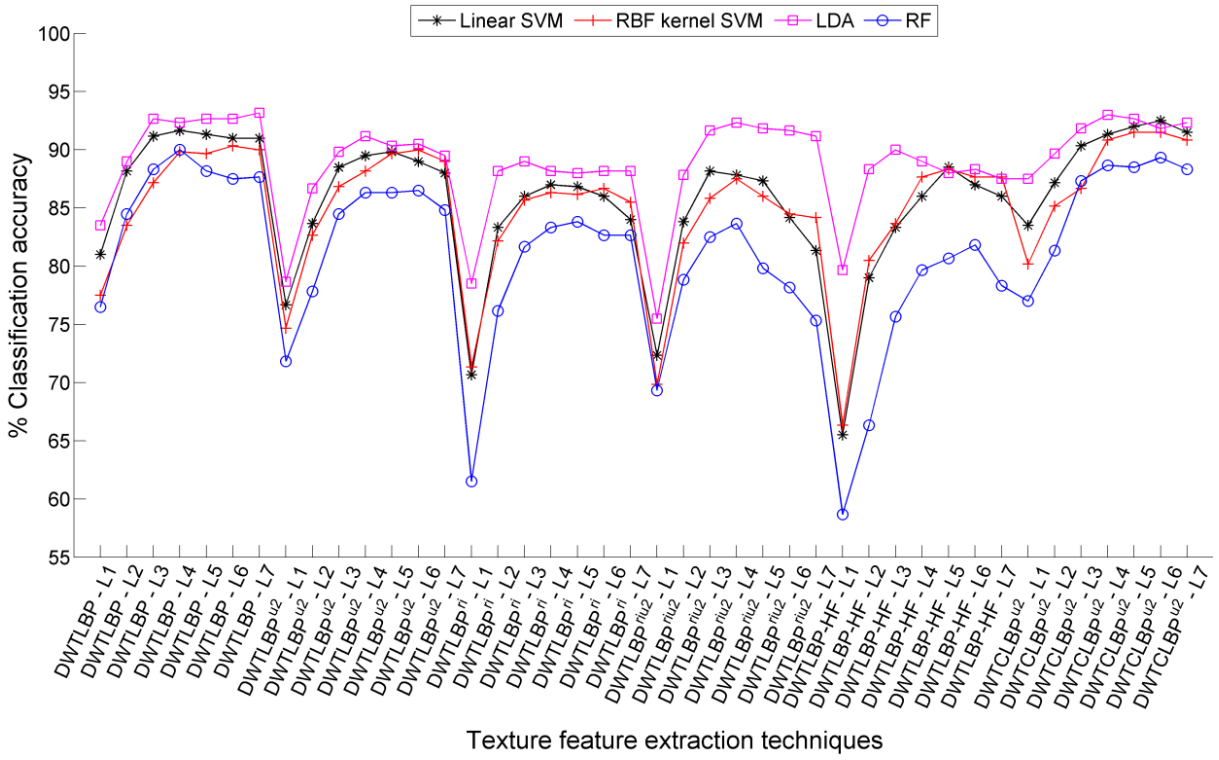

Fig. 5.16 Classification accuracy achieved for 60/40 proportion of training and testing data of RDD.

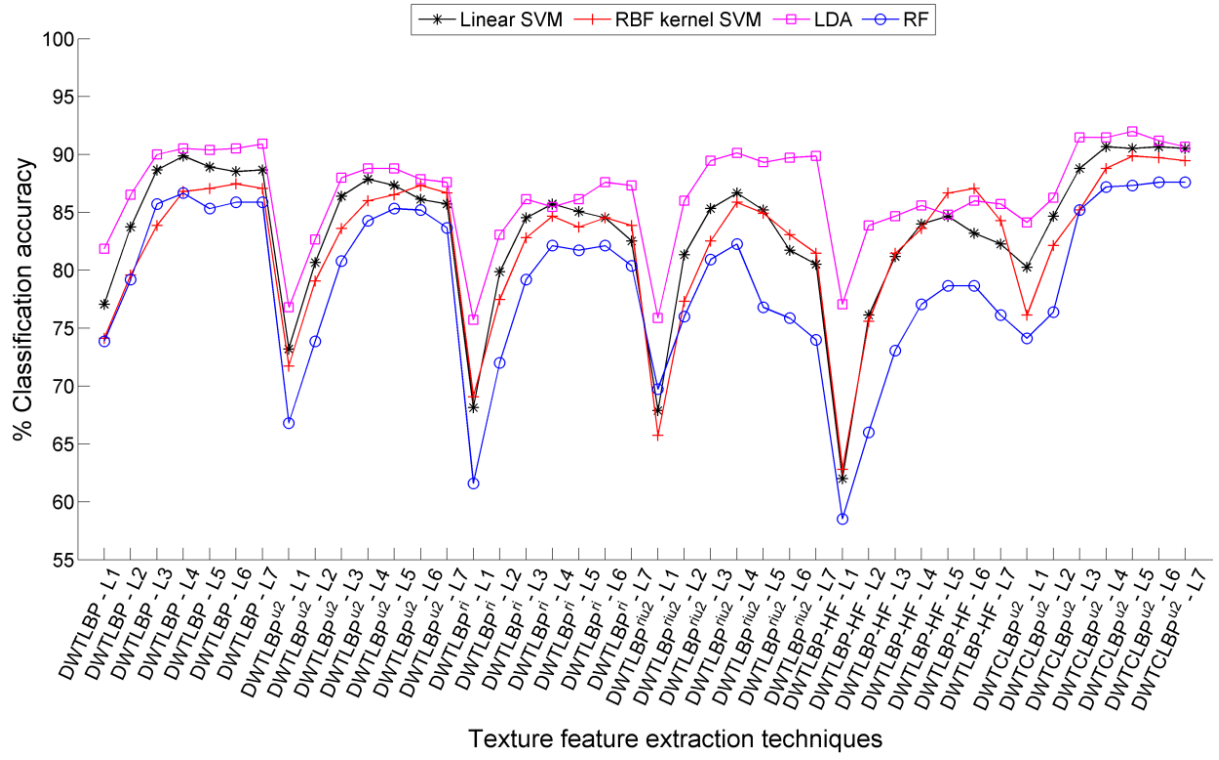

Fig. 5.17 Classification accuracy achieved for 50/50 proportion of training and testing data of RDD.

The graphical illustration of PCA reduced feature vector data of MRLBP variants based texture feature extraction techniques are shown in Fig. 5.14, Fig. 5.15, Fig. 5.16 and Fig. 5.17 for 80/20, 70/30, 60/40 and 50/50 training and testing ratios of randomly divided database,

respectively. It is clearly visible that the PCA reduced feature vector data has given the best classification accuracy with LDA classifier, whereas RF classifier has achieved the lowest classification accuracy among the classifiers. Thus, it is understood that incorporating PCA for feature dimensionality reduction has improved the performance of MRLBP variants based texture feature extraction techniques for hardwood species classification with low-dimensional feature vector data.

5.3.4.3 The mRMR feature selection based reduced feature vector data

The classification accuracy results achieved by the mRMR feature selection based reduced feature vector data of proposed texture feature extraction techniques with three different classifiers have been presented in Table 5.9, Table 5.10 and Table 5.11, respectively. The classification accuracy results obtained by each of the classifiers for MRLBP variants based texture feature extraction techniques are discussed below:

Linear SVM classifier: The subset of feature vector data of DWTCLBP^{u2} texture feature extraction technique, produced by mRMR feature selection technique, yields the best classification accuracy of 97.33% (300 features), 96.67% (350 features), 94.33% (400 features) and 93.60% (350 features) for 80/20, 70/30, 60/40 and 50/50 training and testing ratios of RDD, respectively (Table 5.9).

RBF kernel SVM classifier: Here, also the subset of feature vector data of DWTCLBP^{u2} technique processed through mRMR feature selection technique yields the best classification accuracy of 96% (200 features), 95.56% (250 features), 93.83% (300 features) and 92.80% (300 features) for 80/20, 70/30, 60/40 and 50/50 training and testing ratios of RDD, respectively (Table 5.10).

RF classifier: The mRMR feature selection based feature vector data of DWTCLBP^{u2} technique yields the best classification accuracy of 92.67% (200 features, at 4th IDL), 91.56% (200 features, at 7th IDL), 90.33% (100 features, at 6th IDL) and 88.27% (450 features, at 6th IDL) for 80/20, 70/30, 60/40 and 50/50 training and testing ratios of RDD, respectively (Table 5.11).

Interestingly, the linear SVM and RBF kernel SVM classifiers have achieved the best classification accuracies for feature vector data produced by the DWTCLBP^{u2} texture features at the 7th level of image decomposition. Further, other MRLBP variants based texture feature extraction techniques have improved the classification accuracy in comparison to the state-of-the-art LBP variants texture feature extraction techniques. Also, employing mRMR feature selection technique for reducing the number of features has given much better classification accuracy compared to the full feature vector data, that too with lower-dimensional feature vector data.

Table 5.9 Classification accuracy achieved by mRMR feature selection based reduced feature vector data for different proportions of training and testing data of RDD using linear SVM classifier.

Technique	IDL	NoF	80/20	NoF	70/30	NoF	60/40	NoF	50/50
	1	400	89.67	350	85.56	500	82.00	350	77.60
	2	550	93.33	550	92.22	550	88.33	500	84.53
	3	350	95.00	400	93.78	500	91.50	400	89.07
DWTLBP	4	400	95.33	400	94.22	500	92.00	400	90.67
	5	700	95.33	300	93.78	300	92.50	400	90.80
	6	500	95.00	300	94.00	300	92.17	350	90.93
	7	500	95.00	300	94.00	350	92.17	400	90.80
	1	100	83.00	200	80.22	200	76.67	225	74.00
	2	300	89.33	250	87.33	300	85.33	250	82.67
	3	200	92.00	350	90.89	500	89.33	400	87.60
$DWTLBP^{u2}$	4	250	94.33	300	93.11	500	92.17	450	90.67
	5	200	94.00	200	94.00	500	92.33	450	90.67
	6	150	94.33	200	94.00	250	91.67	250	90.53
	7	200	94.67	150	94.00	500	92.17	450	90.40
	1	125	77.00	125	71.56	125	71.17	125	66.93
	2	250	89.00	250	86.22	250	84.50	250	80.13
	3	200	91.00	250	88.22	250	87.33	200	85.87
$DWTLBP^{ri}$	4	100	92.67	250	91.33	350	86.67	200	87.47
	5	500	94.33	100	92.44	250	90.50	450	87.87
	6	250	92.67	200	92.67	200	90.17	500	88.67
	7	200	93.33	200	93.11	200	90.67	500	89.47
	1	35	77.33	35	74.67	35	73.17	35	69.87
	2	75	86.67	70	84.67	70	83.83	60	80.67
	3	100	91.33	115	90.22	115	88.00	110	85.47
$DWTLBP^{riu2}$	4	150	89.67	150	89.33	125	87.50	150	87.20
	5	175	88.67	175	88.67	175	87.33	100	87.33
	6	100	90.33	100	89.33	150	87.33	100	86.67
	7	150	89.33	100	88.89	100	88.33	100	87.47
	1	50	72.33	50	70.44	50	69.17	50	65.73
	2	150	88.67	50	86.22	100	84.67	100	81.60
	3	100	93.00	100	91.56	100	90.33	150	88.67
DWTLBP-HF	4	100	93.67	100	92.89	300	91.00	200	90.40
	5	50	93.33	200	93.33	350	92.33	200	91.47
	6	50	94.00	200	93.33	250	91.83	200	91.20
	7	150	94.00	200	93.57	350	92.50	100	92.40
	1	250	89.00	200	85.56	450	83.50	200	79.87
	2	200	92.00	500	91.56	250	88.83	150	86.80
	3	250	95.33	200	94.89	300	92.00	200	90.80
$DWTCLBP^{u2}$	4	200	97.00	350	95.11	300	93.33	400	92.40
	5	300	96.33	300	95.33	400	94.00	450	93.20
	6	300	97.33	400	96.22	350	94.17	350	93.60
	7	**350**	**97.33**	**350**	**96.67**	**400**	**94.33**	**350**	**93.60**

Table 5.10 Classification accuracy achieved by mRMR feature selection based reduced feature vector data for different proportions of training and testing data of RDD using RBF kernel SVM classifier.

Technique	IDL	NoF	80/20	NoF	70/30	NoF	60/40	NoF	50/50
	1	150	87.33	250	83.78	200	78.67	250	76.00
	2	400	90.00	250	90.00	450	87.17	450	84.13
	3	300	93.33	300	92.89	350	90.67	150	87.47
DWTLBP	4	150	94.00	150	93.33	150	91.67	200	89.73
	5	200	94.00	300	93.56	400	91.83	450	90.00
	6	200	94.00	200	93.56	500	92.00	450	90.13
	7	200	94.00	200	93.56	500	92.00	400	92.00
	1	150	84.00	150	80.44	150	74.67	150	72.53
	2	150	87.67	250	86.22	100	85.33	100	81.07
	3	150	90.67	150	89.78	250	88.50	150	86.67
$DWTLBP^{u2}$	4	350	92.00	100	91.56	200	91.17	350	89.60
	5	100	92.67	150	92.44	450	92.00	300	90.53
	6	100	92.67	100	93.11	200	92.00	300	90.80
	7	100	93.67	100	93.33	250	92.00	250	90.80
	1	100	80.33	125	74.89	125	71.67	125	68.93
	2	200	88.33	100	84.89	150	82.83	100	79.60
	3	150	90.67	200	89.78	200	87.00	100	85.07
$DWTLBP^{ri}$	4	100	92.00	250	92.00	250	89.50	100	88.53
	5	200	92.33	250	92.22	200	90.50	100	89.47
	6	100	92.67	300	92.22	200	91.00	100	89.47
	7	250	92.33	200	92.22	150	90.00	100	89.07
	1	30	76.00	35	71.78	35	70.33	30	66.67
	2	50	88.33	50	84.89	50	83.33	60	78.13
	3	50	89.67	100	88.00	110	85.83	50	84.00
$DWTLBP^{riu2}$	4	100	90.00	100	90.00	100	87.67	100	86.67
	5	150	89.67	100	89.11	100	88.17	100	86.80
	6	150	90.33	150	89.78	150	87.86	150	87.20
	7	150	89.67	150	90.00	150	88.33	100	87.33
	1	50	75.00	50	74.00	50	71.17	50	68.53
	2	100	89.00	100	86.67	100	85.33	100	82.27
	3	100	92.00	150	90.44	100	89.33	100	87.33
DWTLBP-HF	4	150	93.33	250	92.44	150	91.17	150	89.60
	5	100	94.00	250	93.33	150	92.33	100	90.67
	6	150	93.00	150	93.78	100	92.50	150	91.73
	7	100	93.00	150	94.22	200	92.83	200	91.73
	1	100	89.33	250	85.33	250	80.50	300	77.20
	2	150	90.67	150	89.33	100	88.17	150	85.73
	3	300	95.00	300	94.00	200	91.67	200	90.53
$DWTCLBP^{u2}$	4	200	95.33	150	94.67	250	93.67	350	91.87
	5	150	95.67	150	95.33	250	93.67	250	92.40
	6	200	95.67	200	95.33	250	93.50	400	92.27
	7	**200**	**96.00**	**250**	**95.56**	**300**	**93.83**	**300**	**92.80**

Table 5.11 Classification accuracy achieved by mRMR feature selection based reduced feature vector data for different proportions of training and testing data of RDD using RF classifier.

Technique	IDL	NoF	80/20	NoF	70/30	NoF	60/40	NoF	50/50
	1	100	78.67	150	73.56	250	71.33	100	70.80
	2	450	85.67	400	83.78	250	82.83	200	80.13
	3	200	88.67	100	88.89	100	86.50	400	84.67
DWTLBP	4	250	89.00	150	89.11	250	87.83	300	86.00
	5	550	90.00	150	89.11	200	88.67	350	86.67
	6	150	90.00	350	89.78	150	88.38	300	86.13
	7	350	89.67	300	89.11	250	88.16	250	86.53
	1	100	74.00	50	68.00	100	66.83	150	64.93
	2	250	83.67	200	80.89	200	78.50	200	76.53
	3	150	88.67	100	85.56	350	84.67	150	81.60
$DWTLBP^{u2}$	4	150	89.33	50	87.56	100	86.33	150	84.00
	5	200	89.67	50	87.78	350	86.83	250	85.07
	6	200	90.33	150	88.22	350	87.17	50	85.47
	7	100	89.67	100	88.00	150	88.00	150	85.20
	1	100	68.00	100	63.78	100	62.33	100	59.73
	2	100	83.67	150	78.89	100	78.67	200	74.53
	3	50	86.33	300	82.89	150	82.33	300	79.33
$DWTLBP^{ri}$	4	50	88.67	100	86.22	50	85.11	100	82.13
	5	250	88.00	200	86.67	100	86.17	50	84.13
	6	200	89.67	300	87.33	100	86.00	150	83.33
	7	50	89.00	100	87.11	150	85.83	100	84.00
	1	30	57.67	20	54.89	20	53.83	20	51.73
	2	50	81.67	75	76.00	50	73.17	50	68.17
	3	115	82.33	50	80.22	100	79.00	100	76.40
$DWTLBP^{riu2}$	4	50	84.33	100	83.56	50	83.30	50	79.56
	5	175	86.33	100	84.22	100	83.33	50	81.73
	6	50	86.33	100	85.11	100	84.50	50	82.40
	7	150	87.67	50	85.11	150	84.00	150	81.87
	1	50	74.67	50	72.00	50	67.83	50	67.07
	2	150	83.67	250	79.78	100	79.00	50	77.33
	3	250	88.67	200	86.00	100	85.17	50	82.13
DWTLBP-HF	4	200	90.00	100	89.11	100	87.17	100	85.07
	5	50	90.00	100	89.33	100	88.33	100	86.40
	6	50	91.00	50	89.56	150	89.17	150	86.27
	7	50	91.00	50	89.56	100	87.83	100	86.40
	1	100	80.67	100	77.56	150	74.33	150	71.73
	2	150	86.33	100	83.33	100	83.67	100	81.20
	3	150	92.00	300	88.67	50	88.17	300	85.60
$DWTCLBP^{u2}$	**4**	**200**	**92.67**	150	90.44	150	89.17	300	87.60
	5	250	91.33	350	89.56	250	89.33	350	87.73
	6	200	91.67	150	90.89	**100**	**90.33**	**450**	**88.27**
	7	200	92.00	**200**	**91.56**	150	89.83	100	88.13

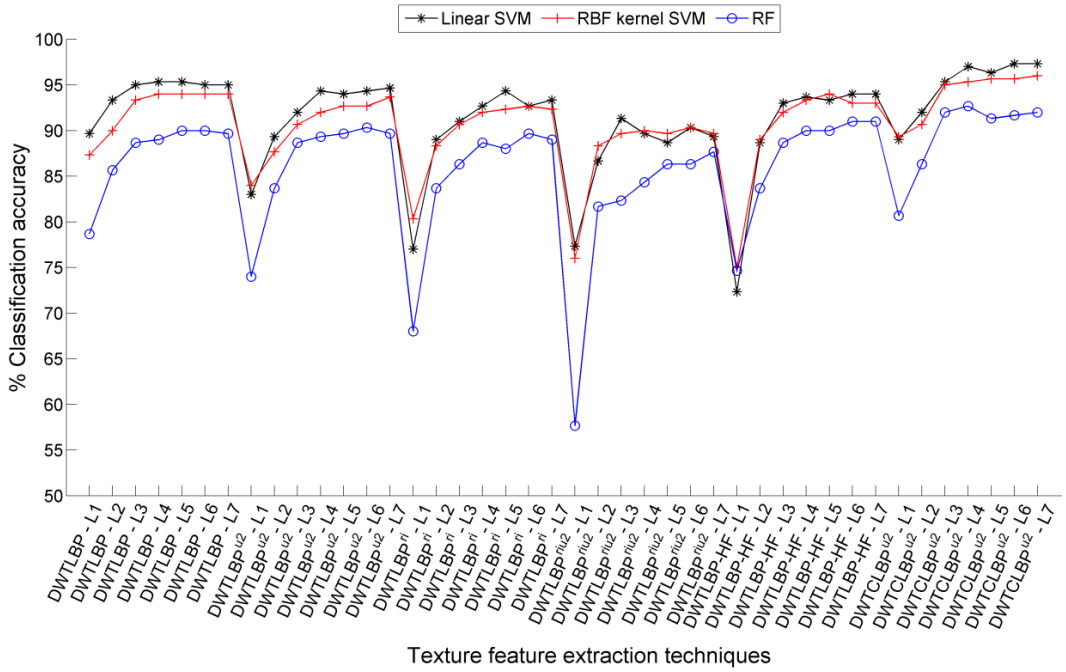

Fig. 5.18 Classification accuracy achieved for 80/20 proportion of training and testing data of RDD.

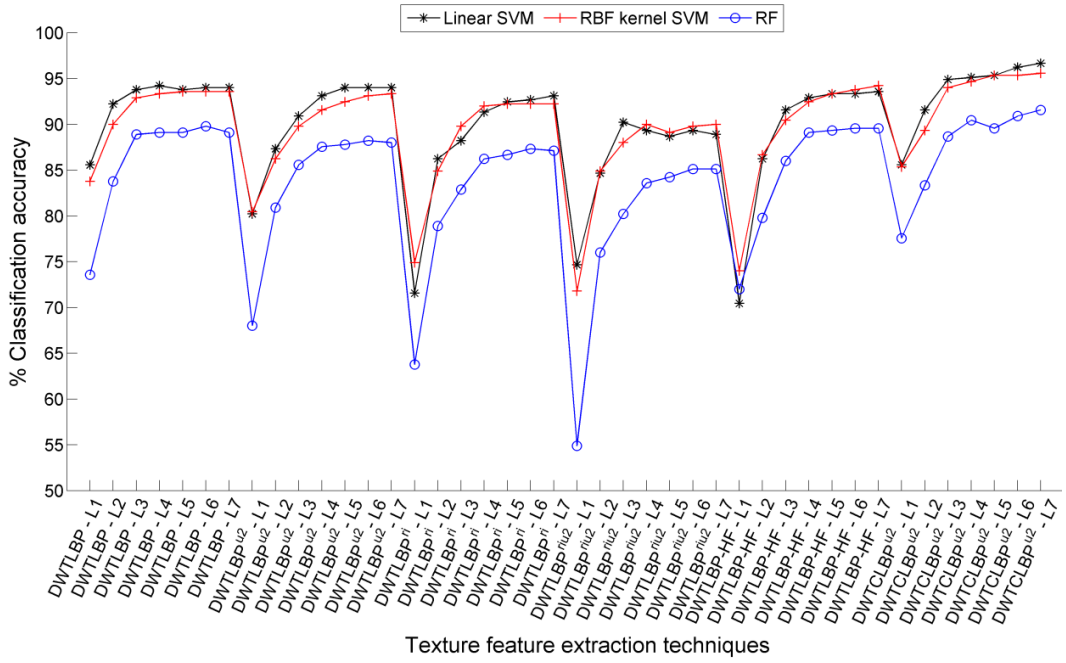

Fig. 5.19 Classification accuracy achieved for 70/30 proportion of training and testing data of RDD.

The classification accuracies obtained by three different classifiers are compared for each of the four (80/20, 70/30, 60/40 and 50/50) training and testing ratios, and are illustrated in Fig. 5.18, Fig. 5.19, Fig. 5.20 and Fig. 5.21, respectively. The analysis of these graphs advocates that among the MRLBP variants based texture feature extraction techniques, the DWTCLBP^{u2} has obtained the best classification accuracy with linear SVM classifier; whereas comparatively lower classification accuracy has been reported by RF classifier.

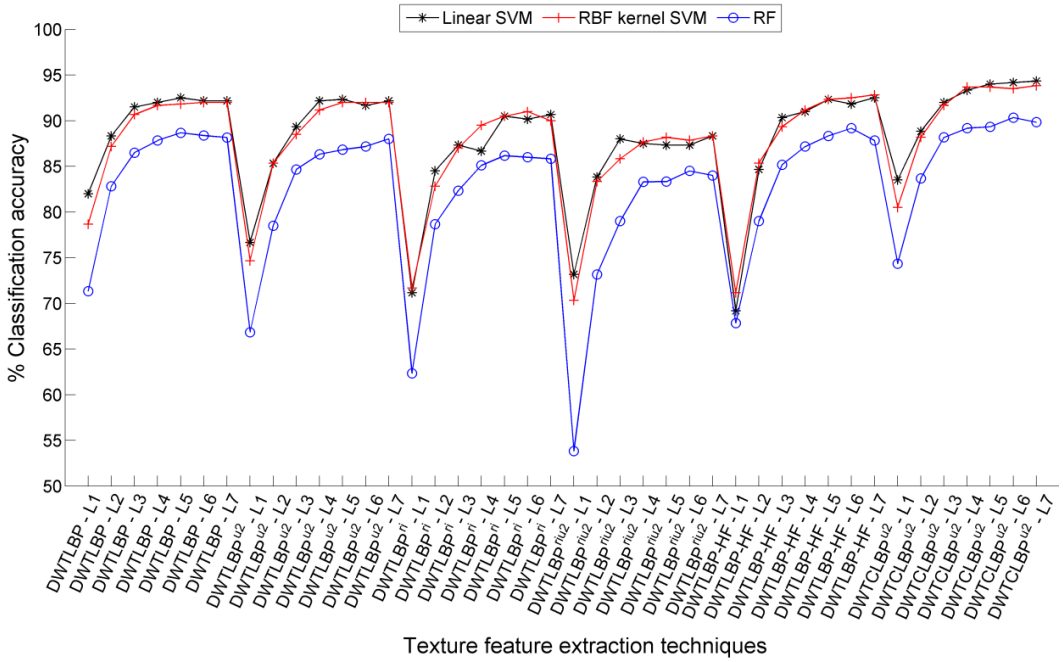

Fig. 5.20 Classification accuracy achieved for 60/40 proportion of training and testing data of RDD.

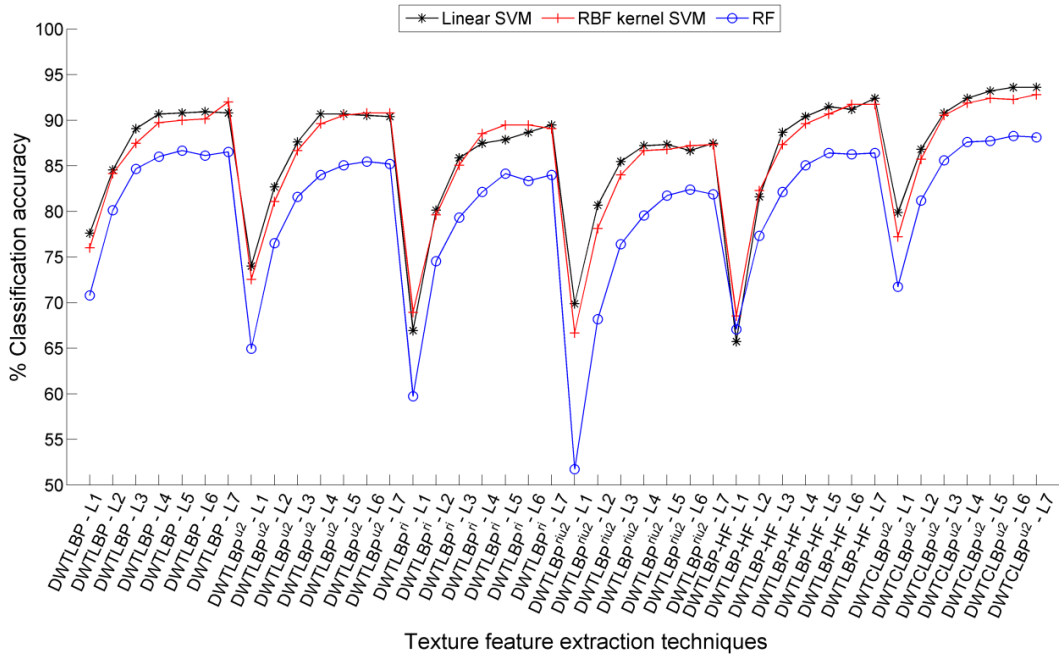

Fig. 5.21 Classification accuracy achieved for 50/50 proportion of training and testing data of RDD.

Thus, employing feature dimensionality reduction/feature selection technique has not only reduced the computational time but also shown considerable improvement in the classification accuracy for hardwood species classification. It is also observed that the performance of variants of LBP texture features have been improved by involving DWT for analysing images at multiresolution followed by extraction of texture features from these transformed images.

The above analysis suggests that MRLBP variants based texture feature extraction techniques do acquire significant texture features of the images and have performed well for both 10-fold cross validation and RDD. An important observation which is worth to be noted is that incorporating DWT with LBP variants for extracting texture features have improved the significant texture features of individual LBP variants which in turn have produced better classification accuracy for hardwood species.

It is worth pointing out that amongst the variants of MRLBP techniques, the DWTCLBP^{u2} has given the best classification accuracy for hardwood species classification and validate the superiority of CLBP^{u2} compared to other LBP variants as discussed in Chapter 2. The gray scale image of *Aurantium* species has been processed with LBP variants and is depicted in Fig. 5.22. The comparison of the processed images reveals that CLBP^{u2} (CLBP^{u2}_S and CLBP^{u2}_M) image has more information compared to other LBP variants as it combines the *CLBP_S* and *CLBP_M* information together which is evident from Fig. 5.22(g) and Fig. 5.22(h).

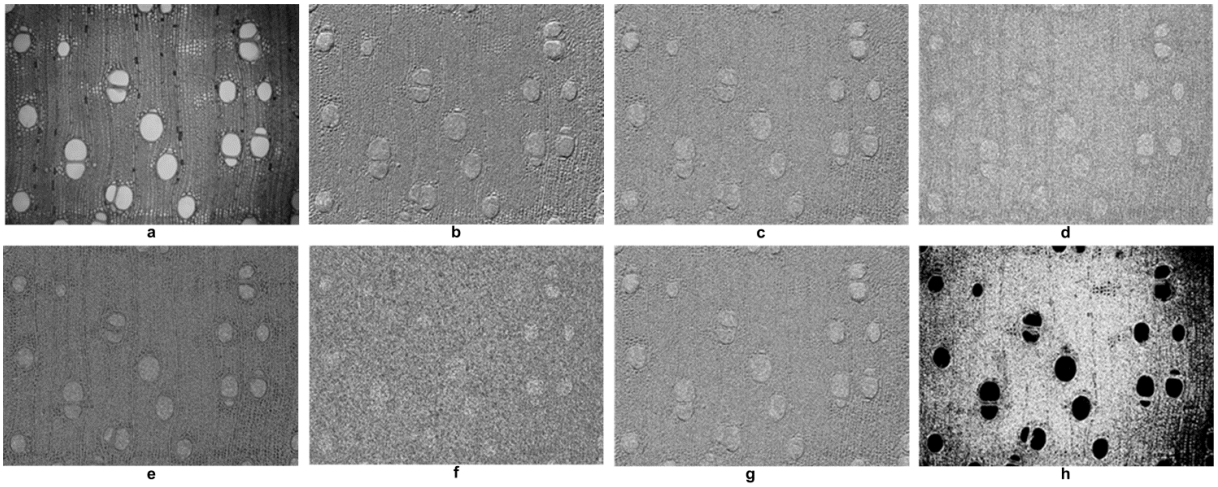

Fig. 5.22 The *Aurantium* species image, (a) Grayscale image, (b) LBP image, (c) LBP^{u2} image, (d) LBP-HF image, (e) LBP^{ri} image, (f) LBP^{riu2} image, (g) CLBP^{u2}_S image, and (h) CLBP^{u2}_M image

Further, the performance of other MRLBP techniques are also comparable with DWTCLBP^{u2} technique. The performance of individual LBP variants have been significantly improved by MRLBP techniques for hardwood species classification. The FFVD obtained by most of the variants of MRLBP techniques beyond 3rd to 5th level of image decomposition could not improve the classification accuracy significantly rather produced the same or the lower classification accuracy. The obvious reason is that the subimages obtained beyond the 3rd level of image decomposition do not have qualitative visible information (though statistically significant features do exist). Thus, additional higher level of image decompositions have not been investigated.

The possible reasons for MRLBP techniques exhibiting comparatively better performance are as follows: As it is known, that the images of hardwood species have numerous objects that

too of different sizes and shapes. Thus, to recognize the information contents of such images effectively, it must be analyzed at various resolutions. The large size objects are better to be examined at coarse view (lower) resolutions while smaller objects are the candidates to be examined at higher resolutions. Therefore, hardwood species image is decomposed by DWT to represent it into a set of frequency channels that carry the information of the grayscale image at various scales and orientations. The results of the DWT transformation contain more valuable information, and the DWT coefficients of each level are different for the same characterization of the signal. Further, to extract features from several scale images, LBP (most prominent and established texture descriptors) variants are preferred due to the simple computational requirement. Though, distinctive features are obtained from low resolution subimages but alone they are not capable enough to discriminate the hardwood species. Thus the features (obtained by LBP variants) of several resolution images are combined to get more significant feature vector data to discriminate among the hardwood species database.

5.4 SUMMARY

In this chapter, the MRLBP variants texture feature extraction techniques have been proposed to enhance the classification accuracy of microscopic images of hardwood species. In the proposed techniques, the DWT has been employed to decompose the image up to 7 different levels, followed by texture feature extraction with LBP variants. The resultant DWT subimages coefficients obtained using proposed methodology are distinct at each level and contain valuable information. Extracting texture features by variants of LBP from several level (L1 - L7) resolutions subimages have increased the number of significant features. Combining the texture features of several levels (L1 - L7) generate significant feature vector useful in discrimination among the hardwood species. Further, four classifiers namely, linear SVM, RBF kernel SVM, LDA and RF have been used for assessing the performance of the proposed texture features obtained at 7 different levels of image decomposition by DWT.

Critical analysis of the results obtained with 10-fold cross validation approach revealed that among all the proposed techniques, DWTCLBP^{u2} generates the most discriminative texture features. The best classification accuracy of 97.40±1.06% is obtained for DWTCLBP^{u2} texture features at the 3rd level of image decomposition (1416 features) using linear SVM classifier. Further, reduction in feature dimensions is obtained using PCA and it is observed that the DWTCLBP^{u2} texture features have achieved superlative classification accuracy of 97.87±0.82% at the 3rd level of image decomposition (325 features) with LDA classifier. Furthermore, incorporating the mRMR feature selection based subset of full feature vector data, the DWTCLBP^{u2} texture features have again obtained the best classification accuracy of 98.40±1.00% at the 4th level of image decomposition (550 features) with RBF kernel SVM classifier. The accuracy thus, achieved by MRLBP based texture features are better than the

state-of-the-art texture features for hardwood species. It is important to note that the higher level of image decomposition by DWT produce low resolution images that do not carry qualitative visual information. Therefore, most of the MRLBP techniques have shown decrement in classification accuracy beyond the 3rd level of image decomposition (using full feature vector data).

In addition, the classification accuracy obtained using randomly divided database into fixed training and testing ratio of hardwood species by DWTCLBP^{u2} texture features have also established the superiority of MRLBP techniques. Amongst the proposed texture feature extraction techniques, the FFVD of DWTCLBP^{u2} technique achieved the best classification accuracy of 94.33%, 92.67%, 92.17% and 90.93% for 80/20, 70/30, 60/40 and 50/50 training and testing ratios of RDD, respectively, using linear SVM classifier. The PCA dimensionality reduced feature vector data of DWTCLBP^{u2} technique has obtained the best classification accuracy results of 95.67% (350 features), 94.22% (200 features), 92.67% (250 features) and 92% (100 features) for 80/20, 70/30, 60/40 and 50/50 training and testing ratios of RDD, respectively, using LDA classifier. The subset of feature vector data of DWTCLBP^{u2} technique selected by mRMR feature selection technique yields the best classification accuracy of 97.33% (350 features), 96.67% (350 features), 94.33% (400 features) and 93.60% (350 features) for 80/20, 70/30, 60/40 and 50/50 training and testing ratios of RDD, respectively, using linear SVM classifier. Hence, it can be concluded that the texture features extracted by the MRLBP variants based texture feature extraction techniques for hardwood species are of excellent quality, as is evident from the classification accuracy obtained by all the classifiers.

CHAPTER 6. DWT BASED HYBRID TEXTURE FEATURE EXTRACTION TECHNIQUES

This chapter explores the effectiveness of discrete wavelet transform (DWT) based hybrid texture feature extraction techniques for classification of hardwood species. Here, the texture features of grayscale and RGB images are obtained and investigated for the classification of hardwood species. The chapter starts with concise introduction of the DWT technique, proposed DWT based hybrid texture features methodology and subsequently evaluation of effectiveness of these techniques for classification of hardwood species using different classifiers.

6.1 INTRODUCTION

The DWT has been used here due to its multiresolution capability for analyzing images at different frequencies for several levels of resolutions [121,133] and is detailed in Section 5.1. Further, the Daubechies wavelet family designed by Ingrid Daubechies has been chosen as a decomposition filter in 2D-DWT [194]. The db3 wavelet of Daubechies family has been widely used in image analysis applications like face recognition [214]. The reason for selecting db3 as decomposition filter are its properties such as compact support, orthogonal, symmetrical behaviour and use of overlapping windows to show changes between all the pixel intensities [89]. Further, the FOS is one of the simplest and computationally efficient technique for describing texture by using the intensity histogram of an image [103]. In FOS, the features that are taken into consideration are mean, SD, kurtosis and skewness. Thus, the effort has been made to combine the FOS and LBP variants features obtained from the DWT images. In the light of the above reasoning, the DWT based hybrid texture feature extraction technique capable of acquiring significant features of hardwood species have been proposed here.

6.2 PROPOSED METHODOLOGY

6.2.1 Procedural Steps

The hardwood species classification using DWT based hybrid texture feature extraction technique is illustrated in Fig. 6.1. The classification procedure is implemented in four major steps, namely, pre-processing, texture feature extraction, feature dimensionality reduction/ selection and classification. The individual blocks are concisely described as follows:

1. The pre-processing step is employed to acquire grayscale images from color (RGB) images using Eq. (2.41). This transformation facilitates significant reduction in computational time during feature extraction process.
2. Initially, the grayscale images are decomposed up to the seven (1 to 7) levels/scales by DWT using Daubechies (db3) wavelet as decomposition filter. At the 1^{st} level of image decomposition by DWT, the grayscale image is subdivided into four identical, quarter-size

subimages, namely, approximation (LL1), horizontal (LH1), vertical (HL1) and diagonal (HH1) components. Thereafter, the LL1 component is decomposed into four equal quarter-size subimages (LL2, LH2, HL2 and HH2) at the 2nd level of image decomposition. The process of partitioning the approximation component is repeated till the required level of image decomposition has been reached. As an illustration, the color image of *Pachycarpa* specie is shown in Fig. 6.2(a), whereas DWT based 5th level image decomposition of the grayscale image of *Pachycarpa* specie is shown in Fig. 6.2(b). It is evident that each scale subimages have distinctive information.

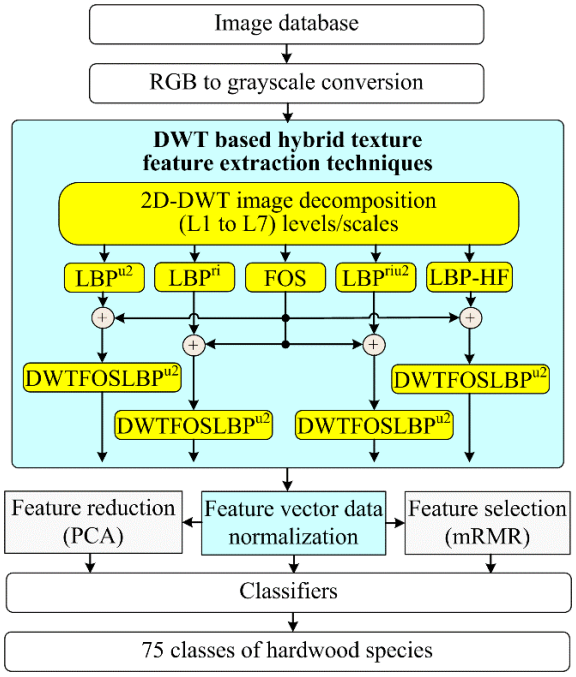

Fig. 6.1 Block diagram of hardwood species classification using DWT based hybrid texture feature extraction techniques.

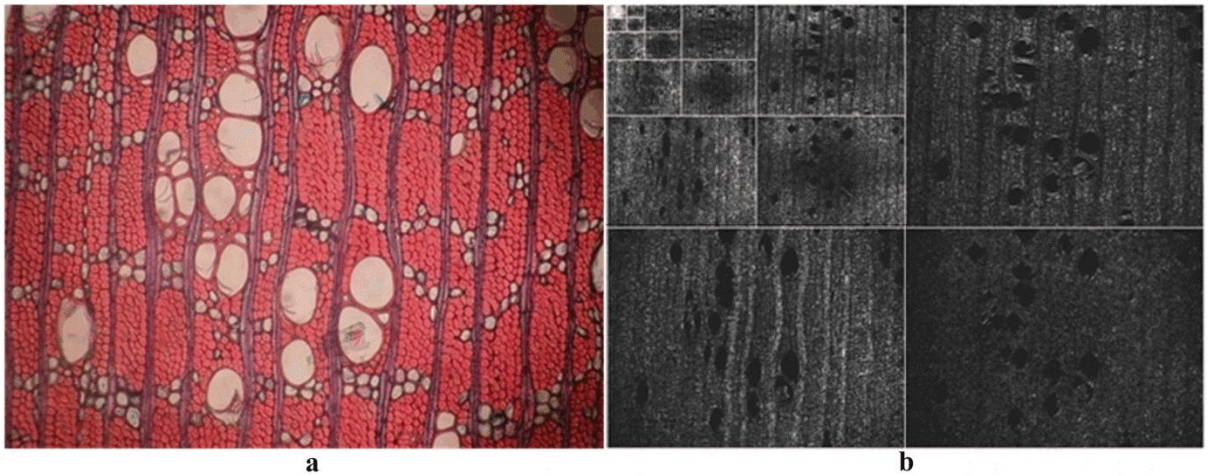

Fig. 6.2 (a) Color image of *Pachycarpa* specie (b) the *Pachycarpa* specie grayscale image obtained at the 5th level of image decomposition using DWT.

Subsequently, five texture descriptors are employed to extract distinct features from each of the subimages at different (1 to 7) levels of image decomposition. The texture

feature descriptors used in this work are, FOS and four variants of LBP (LBP^{u2}, LBP^{ri}, LBP^{riu2} and LBP-HF). The FOS features are chosen as they reveal the global features of image. The LBP variants are selected to depict the local texture descriptors of the image. Further, at each level of image decomposition the FOS features are concatenated with LBP variants features to construct feature vector data. The expression for obtaining DWTFOSLBP feature vector data for each image at the L^{th} level of image decomposition is given by Eq. (6.1):

$$\text{DWTFOSLBP}^{L}=\sum_{l=1}^{L}\begin{bmatrix}\left(LBP_{P,R}\left(W_{\varphi}^{\ l}\right)+LBP_{P,R}\left(W_{\psi}^{H^{l}}\right)+LBP_{P,R}\left(W_{\psi}^{V^{l}}\right)+LBP_{P,R}\left(W_{\psi}^{D^{l}}\right)\right)\\+\left(m\left(W_{\varphi}^{\ l}\right)+m\left(W_{\psi}^{H^{l}}\right)+m\left(W_{\psi}^{V^{l}}\right)+m\left(W_{\psi}^{D^{l}}\right)\right)\\+\left(\sigma\left(W_{\varphi}^{\ l}\right)+\sigma\left(W_{\psi}^{H^{l}}\right)+\sigma\left(W_{\psi}^{V^{l}}\right)+\sigma\left(W_{\psi}^{D^{l}}\right)\right)\\+\left(\mu_3\left(W_{\varphi}^{\ l}\right)+\mu_3\left(W_{\psi}^{H^{l}}\right)+\mu_3\left(W_{\psi}^{V^{l}}\right)+\mu_3\left(W_{\psi}^{D^{l}}\right)\right)\\+\left(\mu_4\left(W_{\varphi}^{\ l}\right)+\mu_4\left(W_{\psi}^{H^{l}}\right)+\mu_4\left(W_{\psi}^{V^{l}}\right)+\mu_4\left(W_{\psi}^{D^{l}}\right)\right)\end{bmatrix} \quad (6.1)$$

where, L stands for number of image decomposition levels and $LBP_{P,R}$ represents one of the LBP variants (i.e., LBP^{u2}, LBP^{ri}, LBP^{riu2} and LBP-HF) features. The, m, σ, μ_3 and μ_4 represents mean, SD, kurtosis and skewness features of FOS, respectively. Thus, on the basis of integration of DWT with FOS and LBP variants, following four hybrid texture feature extraction techniques have been proposed:

$DWTFOSLBP^{u2}$	Discrete wavelet transform based first-order statistics and uniform local binary pattern
$DWTFOSLBP^{ri}$	Discrete wavelet transform based first-order statistics and rotation invariant local binary pattern
$DWTFOSLBP^{riu2}$	Discrete wavelet transform based first-order statistics and rotation invariant uniform local binary pattern
DWTFOSLBP-HF	Discrete wavelet transform based first-order statistics and local binary pattern histogram Fourier features

3. The feature vector dataset produced by these techniques have different range of values, which is normalized in the range 0 to 1 using Eq. (2.42), thus rendering it in the form useful as an input to the classifier.
4. The PCA and mRMR techniques are employed in the third stage to reduce the dimensions of feature vector data.
5. The fourth stage employs, LDA, RF, linear SVM and RBF kernel SVM classifiers for the classification of hardwood species into 75 categories. The effectiveness of the DWT based hybrid texture feature extraction techniques has been observed on the basis of the

classification accuracy obtained through the classifiers. Consequently, the best combination of DWT based hybrid texture features and the classifier is identified on the basis of the best classification accuracy.

6.2.2 Approaches used for Performance Evaluation of Feature Extraction Techniques

The performance of the DWT based hybrid texture feature extraction techniques for classification of hardwood species have been investigated employing two strategies: (1) 10-fold cross validation and (2) randomly dividing the database (Section 2.5.2).

6.3 EXPERIMENTAL RESULTS AND DISCUSSION

The experimental work presented in this section investigates the efficiency of the DWT based hybrid texture feature extraction techniques for the classification of microscopic images of hardwood species database into 75 classes with the help of four different classifiers.

6.3.1 Parameter Selection

The selection of parameters for efficient implementation of various feature extraction techniques and classifiers have been discussed in detail in Section 2.6.1 and the same are used here also. The texture features of grayscale and RGB images are extracted with the help of DWT based hybrid texture feature extraction techniques.

6.3.2 Experimental Results

The classification accuracy obtained by the DWT based hybrid texture feature extraction techniques (for both RGB and grayscale image) for microscopic images of hardwood species have been computed using four classifiers. Similar to presentation of results in previous chapters, here also results have been presented for different categories, and different sets of feature vector data (Section 2.6.2).

6.3.3 Performance Evaluation of DWT based Hybrid Texture Feature Extraction Techniques for Grayscale Images using 10-fold Cross Validation Approach

6.3.3.1 Full feature vector data (FFVD)

The percentage classification accuracy attained by the DWT based hybrid texture feature extraction techniques for grayscale image of hardwood species database is presented in Table 6.1. The classification accuracy obtained with the proposed texture features using three different classifiers is discussed below:

Linear SVM classifier: The feature vector data of DWTFOSLBP^{u2} texture feature extraction technique has achieved the best classification accuracy of 97.67±0.79% with feature vector dimension of 1008 (obtained at the 4th level of image decomposition). Further, the same classification accuracy (97.67±0.79%) has been achieved by FFVD produced by

DWTFOSLBP^{riu2} texture feature extraction technique, but using only 280-dimensional feature vector data (obtained at the 5th level of image decomposition). The least classification accuracy of 96.60±1.46% (1008 features) has been achieved by using FFVD of DWTFOSLBP-HF (obtained at the 5th level of image decomposition), among the proposed feature extraction techniques.

RBF kernel SVM classifier: By means of this classifier, the best classification accuracy of 97.67±1.14% has been attained using FFVD (1260 features) produced by DWTFOSLBP^{u2} texture feature extraction technique, which is the best among the proposed feature extraction techniques. The FFVD of DWTFOSLBP^{riu2} texture feature extraction technique has achieved the second best classification accuracy of 97.53±0.83% using 280-dimensional feature vector data. On the other hand, the least classification accuracy of 96.47±1.69% (840 features) has been achieved by FFVD of DWTFOSLBP-HF texture feature extraction technique. All these classification accuracies are achieved for texture feature vector data produced at the 5th level of image decomposition.

Table 6.1 Classification accuracy achieved using full feature vector data.

Technique	IDL	Feature extraction time in seconds	% CA±SD achieved by classifiers			
			NoF	Linear SVM	RBF kernel SVM	RF
DWTFOSLBP^{u2}	1	0.3468	252	90.67±1.81	90.33±2.07	82.60±3.05
	2	0.4139	504	95.73±1.38	94.33±1.55	88.93±2.54
	3	0.4428	756	97.13±1.51	96.33±1.64	93.20±1.25
	4	**0.4602**	**1008**	**97.67±0.79**	97.33±1.18	94.13±1.17
	5	0.4710	1260	97.33±1.09	**97.67±1.14**	94.47±1.09
	6	0.4790	1512	97.07±1.00	96.93±1.30	**95.00±1.23**
	7	0.4969	1764	96.73±1.24	96.67±1.44	94.13±1.08
DWTFOSLBP^{ri}	1	0.3604	160	84.87±2.65	87.07±2.40	81.53±2.20
	2	0.4438	320	92.73±2.05	92.87±2.53	88.13±1.85
	3	0.4858	480	95.73±1.23	95.73±1.78	92.27±1.18
	4	0.5065	640	96.73±1.24	96.53±1.36	93.73±1.38
	5	0.5114	800	96.47±1.00	96.33±1.48	94.13±1.47
	6	0.5209	960	96.07±1.49	96.13±1.96	94.00±1.41
	7	0.5407	1120	95.40±1.46	95.53±2.03	**94.33±1.34**
DWTFOSLBP^{riu2}	1	0.3469	56	86.00±3.10	87.20±1.88	79.73±3.59
	2	0.4165	112	92.87±1.94	92.60±1.52	86.07±1.97
	3	0.4453	168	96.60±0.66	96.07±1.02	91.00±1.81
	4	0.4540	224	97.53±0.71	97.13±1.69	93.73±1.05
	5	**0.4609**	**280**	**97.67±0.79**	**97.53±0.83**	94.67±1.47
	6	0.4706	336	97.40±1.11	97.13±1.37	94.80±1.43
	7	0.4780	392	96.07±1.59	96.73±1.46	94.67±1.47
DWTFOSLBP-HF	1	0.3652	168	84.53±2.41	85.47±3.94	82.87±3.14
	2	0.4447	336	91.80±1.48	92.33±1.64	89.20±1.60
	3	0.4851	504	95.87±1.36	95.53±1.35	93.33±1.30
	4	0.4972	672	96.27±1.10	96.20±1.04	94.07±1.55
	5	0.5131	840	96.47±1.60	**96.47±1.69**	95.13±1.26
	6	0.5417	**1008**	**96.60±1.46**	96.27±1.51	**95.27±1.87**
	7	0.5483	1176	95.40±1.73	95.87±1.40	95.07±1.55

RF classifier: This classifier has given the best classification accuracy of 95.27±1.87% for

FFVD (1008 features) produced by DWTFOSLBP-HF texture feature extraction technique. Further, the FFVD produced by of DWTFOSLBP^{u2} technique has obtained the 2nd best classification accuracy of 95.00±1.23% for 1512-dimensional feature vector data**.** In addition, among the proposed feature extraction techniques, the least classification accuracy of 94.33±1.34% (1120 features) has been attained by using FFVD of DWTFOSLBP^{ri} feature extraction technique. These classification accuracies are obtained for FFVD produced at the 6th level (DWTFOSLBP-HF and DWTFOSLBP^{u2} techniques) and 7th level (DWTFOSLBP^{ri} techniques) of image decomposition.

Here, it is observed that the best classification accuracy has been achieved by most of the DWT based hybrid texture features obtained between the 4th to 6th levels of image decomposition with all the three classifiers. In addition, the linear and RBF kernel SVM classifiers, both have presented excellent classification accuracy; whereas, RF classifier yields comparatively lower classification accuracy. The classification accuracy obtained by three classifiers have been compared and the same is illustrated in Fig. 6.3. The graphical illustration also reveals that DWTFOSLBP^{u2} texture feature extraction technique has given the best classification accuracy.

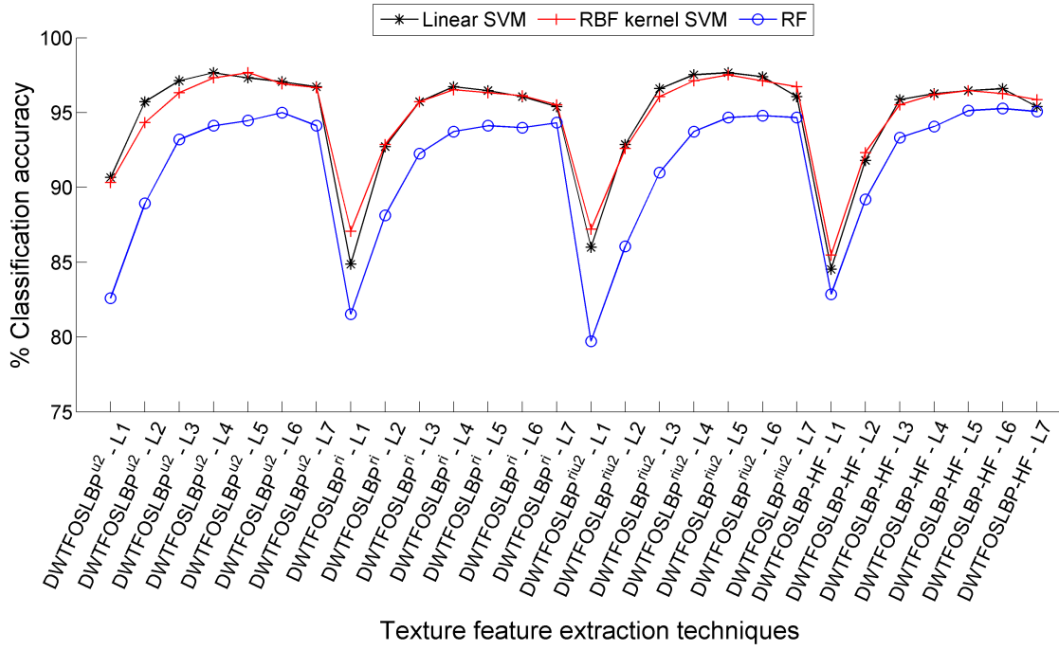

Fig. 6.3 Classification accuracy achieved using FFVD.

Further, the time required by the DWT based hybrid texture feature extraction techniques for FFVD generation for single image is also listed in Table 6.1. The DWTFOSLBP^{u2} feature extraction technique has achieved best classification accuracy of 97.67±0.79% at the 4th level of image decomposition, which requires 0.4602 second for extracting texture features of an individual image as shown in Fig. 6.4. This feature extraction time is relatively lesser than the BWTCLBP^{ri} feature extraction technique, which requires 0.6929 second for extracting the

texture features of given individual images. The error bar plot for FFVD is shown in Fig. 6.5. The assessment of Fig. 6.5 reveals that the FFVD of DWTFOSLBP^{u2} feature extraction technique at the 4th level of image decomposition yields the best classification accuracy of 97.67±0.79% with lower SD value. The DWTFOSLBP^{u2} feature extraction technique has also achieved the same classification accuracy (97.67±1.14%) but with slightly higher SD value with RBF kernel SVM classifier.

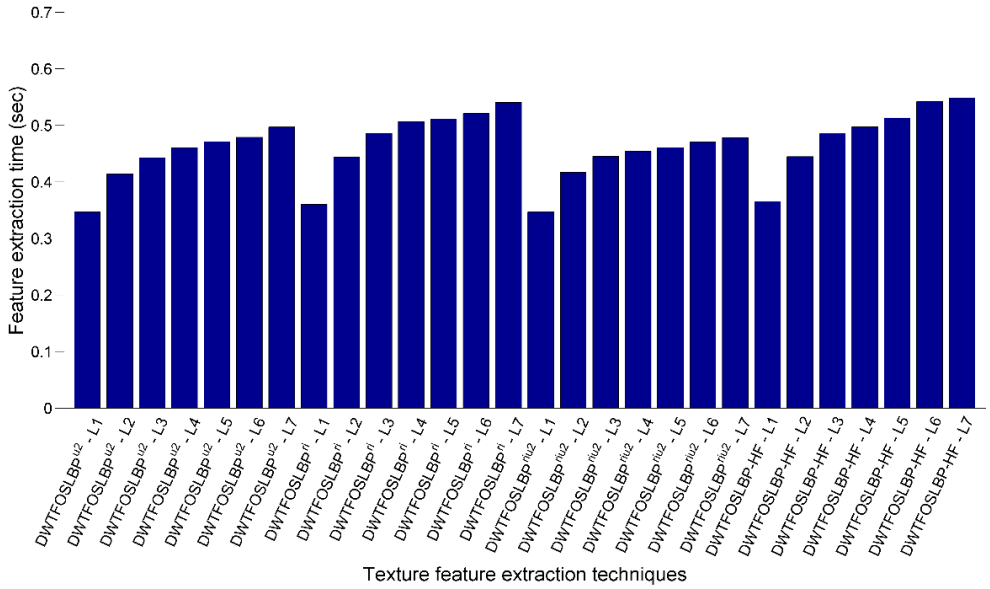

Fig. 6.4 Feature extraction time for single grayscale image.

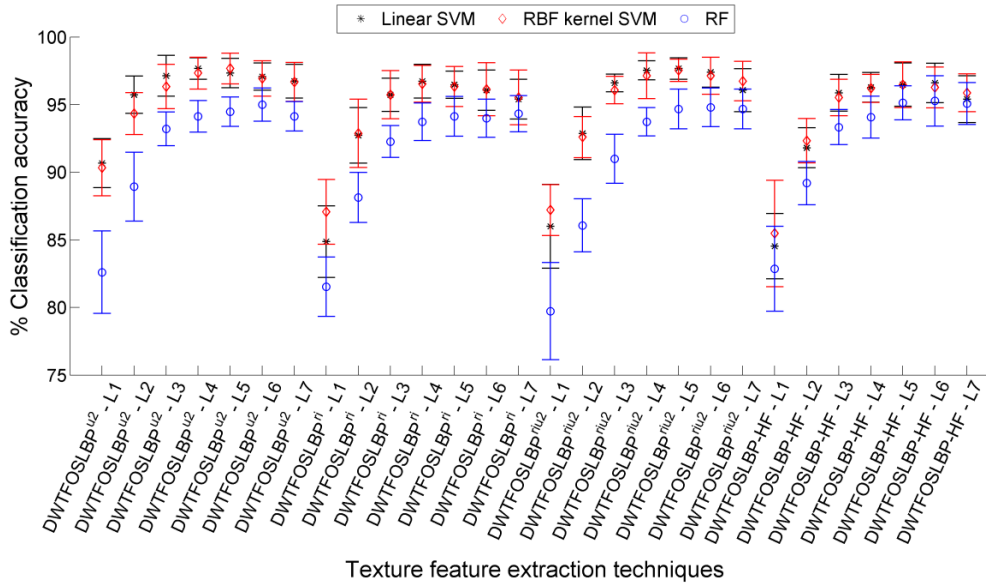

Fig. 6.5 Error bar plot with SD using FFVD.

6.3.3.2 The PCA dimensionality reduced feature vector data

The performance evaluation of texture feature extraction techniques with PCA reduced feature vector data with different classifiers are listed in Table 6.2 and has been concisely discussed henceforth:

Linear SVM classifier: Here, the PCA reduced feature vector data of DWTFOSLBP^{riu2} feature extraction technique yields the best classification accuracy of 97.73±0.84%, which is slightly better than the FFVD (97.67±0.79%) of DWTFOSLBP^{riu2} technique. The classification accuracy has been achieved using only 200-dimensional feature vector data generated at the 5th level of image decomposition compared to 200-dimensional FFVD produced at the 5th level of image decomposition. Further, the PCA reduced feature vector data of DWTFOSLBP^{u2} feature extraction technique has achieved the same classification accuracy (97.73±0.95%, 300 features) but with slightly higher SD value. This classification accuracy is again slightly better than the accuracy achieved by the FFVD of DWTFOSLBP^{u2} (97.67±0.79%, 1008 features).

Table 6.2 Classification accuracy achieved using PCA based reduced feature vector data.

Technique	IDL	% CA±SD achieved by classifiers							
		NoF	Linear SVM	NoF	RBF kernel SVM	NoF	RF	NoF	LDA
	1	200	90.33±2.52	225	90.87±2.18	50	86.67±2.39	225	91.60±1.55
	2	400	95.13±1.83	150	94.87±1.30	50	90.53±2.13	300	95.60±1.73
	3	300	97.07±1.14	100	96.53±1.50	50	93.47±2.08	300	96.93±1.10
DWTFOSLBP^{u2}	4	400	97.60±0.72	250	97.60±1.41	50	94.27±1.18	250	97.07±1.14
	5	**300**	**97.73±0.95**	**100**	**97.93±1.39**	**50**	**95.07±1.55**	350	97.27±0.80
	6	550	97.00±1.01	100	97.60±1.23	50	95.00±1.52	300	96.67±0.83
	7	600	96.87±1.18	50	97.40±1.42	50	94.00±0.94	350	96.60±1.35
	1	150	84.67±2.11	150	87.00±2.46	50	79.07±2.52	150	90.27±1.86
	2	300	92.33±1.67	300	92.93±2.44	50	87.07±1.76	312	95.80±1.44
	3	250	95.53±1.30	350	95.87±1.77	50	92.00±1.33	450	97.13±1.30
DWTFOSLBP^{ri}	4	350	96.27±1.14	400	96.60±1.06	50	92.93±1.89	600	97.00±1.05
	5	400	96.47±1.26	50	96.87±1.66	50	92.93±1.78	600	96.40±0.78
	6	550	96.07±1.46	50	97.27±1.90	50	92.93±1.67	500	95.40±1.49
	7	400	94.67±1.09	200	96.13±1.57	50	91.67±1.23	100	94.80±1.96
	1	50	84.80±2.55	40	87.27±2.34	50	84.27±2.31	52	87.73±1.22
	2	100	92.60±2.02	100	92.80±1.69	100	90.33±2.42	104	94.80±1.60
	3	150	96.53±1.12	100	96.07±0.97	100	92.73±2.05	150	97.33±1.72
DWTFOSLBP^{riu2}	4	150	97.67±0.90	200	97.27±1.59	100	93.40±1.71	200	98.00±1.09
	5	**200**	**97.73±0.84**	**200**	**97.67±0.90**	50	92.27±1.45	**250**	**98.27±1.10**
	6	200	97.27±1.15	200	97.13±1.51	50	90.87±2.33	300	98.20±1.14
	7	350	95.93±1.46	200	96.73±1.46	50	89.33±1.30	350	98.27±1.14
	1	150	83.93±2.70	150	85.47±4.39	125	76.07±4.01	164	91.67±1.01
	2	250	91.73±1.14	300	92.40±1.70	150	83.20±2.10	326	96.40±1.26
	3	400	96.00±1.78	350	95.60±1.41	50	89.47±1.74	**492**	**97.87±1.43**
DWTFOSLBP-HF	4	450	96.33±0.96	350	96.27±1.10	50	90.87±2.22	550	97.47±1.25
	5	600	96.33±1.31	450	96.60±1.56	50	92.27±1.38	500	96.53±1.61
	6	600	96.47±1.30	300	96.40±1.58	50	91.67±1.81	600	96.40±1.92
	7	500	95.40±1.68	350	95.87±1.60	50	91.27±2.25	600	95.73±1.55

RBF kernel SVM classifier: Amongst the proposed feature extraction techniques, the PCA reduced feature vector data of DWTFOSLBP^{u2} technique, has attained slightly better classification accuracy of 97.93±1.39% (100 features) compared to 97.67±1.14% (1260 features) presented by FFVD of DWTFOSLBP^{u2} technique. In addition, the aforesaid feature vector data are obtained at the 5th level of image decomposition. Further, the PCA reduced feature vector data of DWTFOSLBP^{riu2} techniques (at the 5th level of image decomposition) has achieved the 2nd best classification accuracy (97.67±0.90%), which is slightly better than 97.53±0.83% (280 features) presented by FFVD of DWTFOSLBP^{riu2} technique.

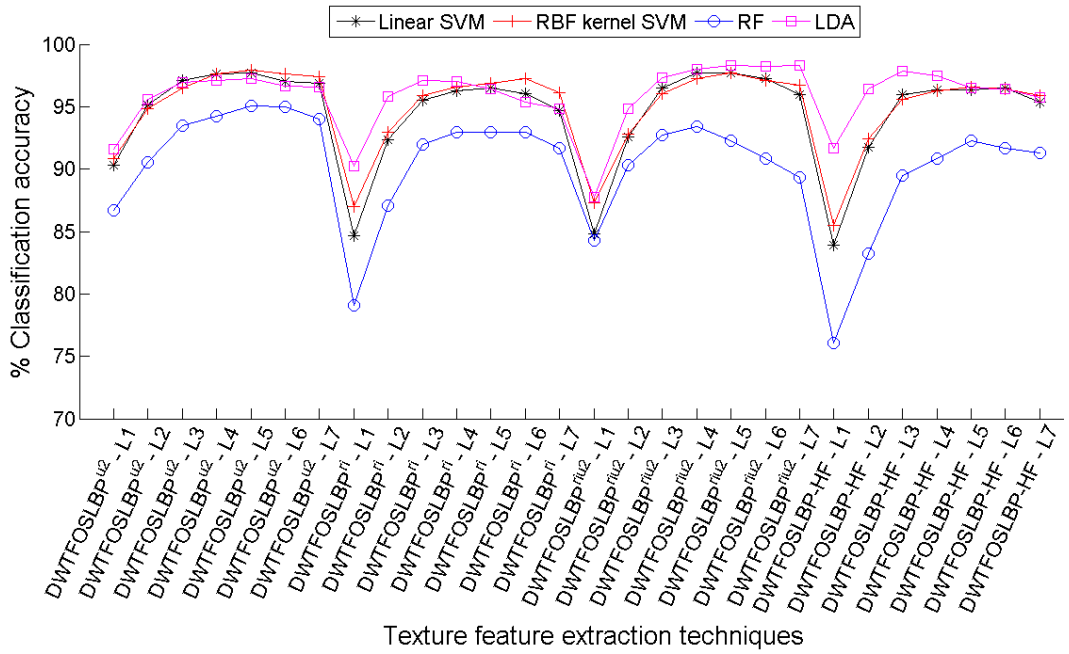

Fig. 6.6 Classification accuracy achieved using PCA reduced feature vector data.

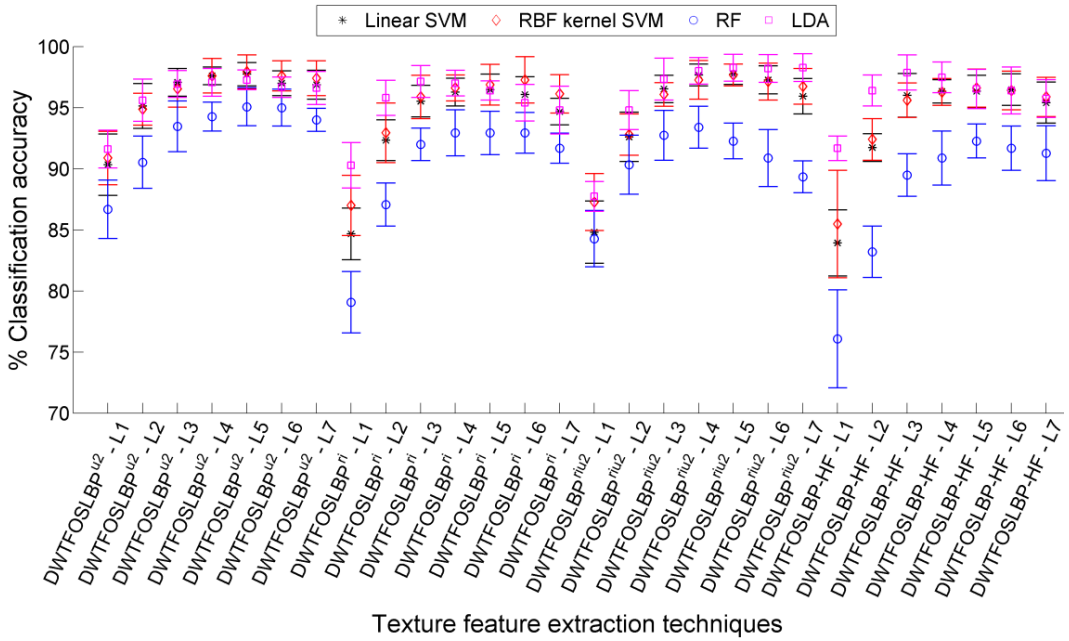

Fig. 6.7 Error bar plot with SD using PCA reduced feature vector data.

RF classifier: The PCA reduced feature vector data of DWTFOSLBP^{u2} texture feature extraction technique has achieved the best classification accuracy of 95.07±1.55% using 300-dimensional feature vector data only, which is slightly better than the classification accuracy (95.00±1.23%) yielded by the FFVD of DWTFOSLBP^{u2} technique(1512 features).

LDA classifier: This classifier has given the best classification accuracy of 98.27±1.10% for PCA reduced feature vector data of DWTFOSLBP^{riu2} texture feature extraction technique with 250-dimemnsional feature vector data. The aforementioned classification accuracy has been achieved for the feature vector data produced at the 5th level of image decomposition. Further, the PCA reduced feature vector data of DWTFOSLBP-HF texture feature extraction technique

has obtained the 2nd best classification accuracy of 97.87±1.43% (492 features, produced at the 3rd level of image decomposition).

The classification accuracy achieved with PCA reduced dimensional feature vector data are at par/superior than the FFVD, but has been obtained using lower-dimensional features. Among the four classifiers, the LDA classifier has obtained maximum classification accuracy (98.27±1.10%) for the feature vector data produced at the 5th level of image decomposition by $DWTFOSLBP^{riu2}$ texture feature extraction technique. The graph depicting the comparison of the classification accuracy obtained by four different classifiers is shown in Fig. 6.6. In addition, the error bar plot representation of the same is given in Fig. 6.7. The graphical illustration also supports the claim that $DWTFOSLBP^{riu2}$ texture features classified with LDA classifier achieves the best/superlative classification accuracy amongst the proposed techniques with different classifiers.

6.3.3.3 The mRMR feature selection based reduced feature vector data

The subset of feature vector data obtained by mRMR feature selection method has been investigated here to see their effect on the classification accuracy produced for hardwood species classification. The classification accuracy results achieved by three different classifiers are listed in Table 6.3. These results are plotted in Fig. 6.8 and the error bar plot for the same has been illustrated in Fig. 6.9. The performance of texture feature extraction techniques with different classifiers are as follows:

Linear SVM classifier: Amongst the proposed feature extraction techniques, the highest classification accuracy of 99.00±0.79% has been achieved by the mRMR processed subset (275 features) of FFVD produced by DWTFOSLBP-HF technique at the 5th level of image decomposition. This classification accuracy is comparatively better than 96.60±1.46% accuracy obtained by FFVD of DWTFOSLBP-HF technique (1008 features) at the 6th level of image decomposition. The 2nd best classification accuracy of 98.60±0.66% has been obtained by the mRMR processed subset (300 features) of FFVD of $DWTFOSLBP^{u2}$ technique (obtained at the 7th level of image decomposition).

RBF kernel SVM classifier: The mRMR selected feature subset (275 features) of DWTFOSLBP-HF texture feature extraction technique (FFVD produced at the 7th level of image decomposition) has achieved the best classification accuracy of 98.80±0.69%, which is relatively better than 96.47±1.69% classification accuracy obtained by full feature vector data of DWTFOSLBP-HF technique (840 features) at the 5th level of image decomposition. The $DWTFOSLBP^{u2}$ texture feature extraction techniques feature vector data processed with mRMR feature selection method has also produced 2nd best classification accuracy of 98.33±0.79% (300 features), better than 97.67±1.14% classification accuracy obtained with their full feature vector data (1260 features).

Table 6.3 Classification accuracy achieved using mRMR feature selection based reduced feature vector data.

Technique	IDL	% CA±SD achieved by classifiers					
		NoF	Linear SVM	NoF	RBF kernel SVM	NoF	RF
DWTFOSLBP^{u2}	1	150	91.33±2.08	150	91.87±2.01	100	84.60±2.85
	2	200	96.20±1.26	200	95.80±1.29	300	90.60±2.38
	3	300	97.73±0.72	300	97.53±1.51	300	93.67±1.45
	4	300	98.13±0.88	300	98.33±0.79	175	95.00±1.76
	5	275	98.40±0.84	300	98.27±0.47	150	95.47±1.21
	6	300	98.33±0.79	250	98.33±0.96	**175**	**95.93±0.91**
	7	**300**	**98.60±0.66**	**250**	**98.33±0.79**	175	95.80±1.04
DWTFOSLBP^{ri}	1	155	85.00±1.92	155	87.13±2.37	75	83.27±3.05
	2	275	92.80±1.45	75	93.80±1.96	200	89.53±2.01
	3	150	96.87±1.37	225	97.00±0.72	175	93.53±1.63
	4	100	97.47±0.88	175	97.93±0.86	150	94.87±1.48
	5	200	98.20±1.09	175	98.13±0.76	125	95.93±1.57
	6	300	98.27±0.90	200	98.20±0.63	150	95.80±1.99
	7	150	98.33±0.79	200	98.27±0.78	150	95.93±1.52
DWTFOSLBP^{riu2}	1	50	86.00±3.68	55	86.93±2.29	40	79.20±3.15
	2	110	93.13±1.63	75	93.13±1.75	100	86.93±1.89
	3	160	96.73±0.86	100	96.67±0.89	165	91.40±1.31
	4	200	97.80±0.71	175	97.73±1.10	75	93.80±1.69
	5	150	98.13±0.76	150	97.80±0.55	175	94.73±1.11
	6	175	98.13±0.82	175	98.00±0.83	300	94.93±1.51
	7	175	98.13±0.53	175	98.13±0.69	175	94.87±1.63
DWTFOSLBP-HF	1	50	86.53±2.56	100	86.07±3.83	50	84.93±1.67
	2	100	94.06±1.61	150	94.53±1.60	125	90.33±1.73
	3	175	97.67±1.38	150	97.53±0.63	175	94.20±1.81
	4	275	98.53±0.47	250	98.47±0.89	175	95.00±1.01
	5	**275**	**99.00±0.79**	225	98.60±0.49	175	95.93±1.52
	6	275	98.80±0.53	275	98.73±0.58	**175**	**96.20±1.51**
	7	200	98.73±0.38	**275**	**98.80±0.69**	175	95.93±1.55

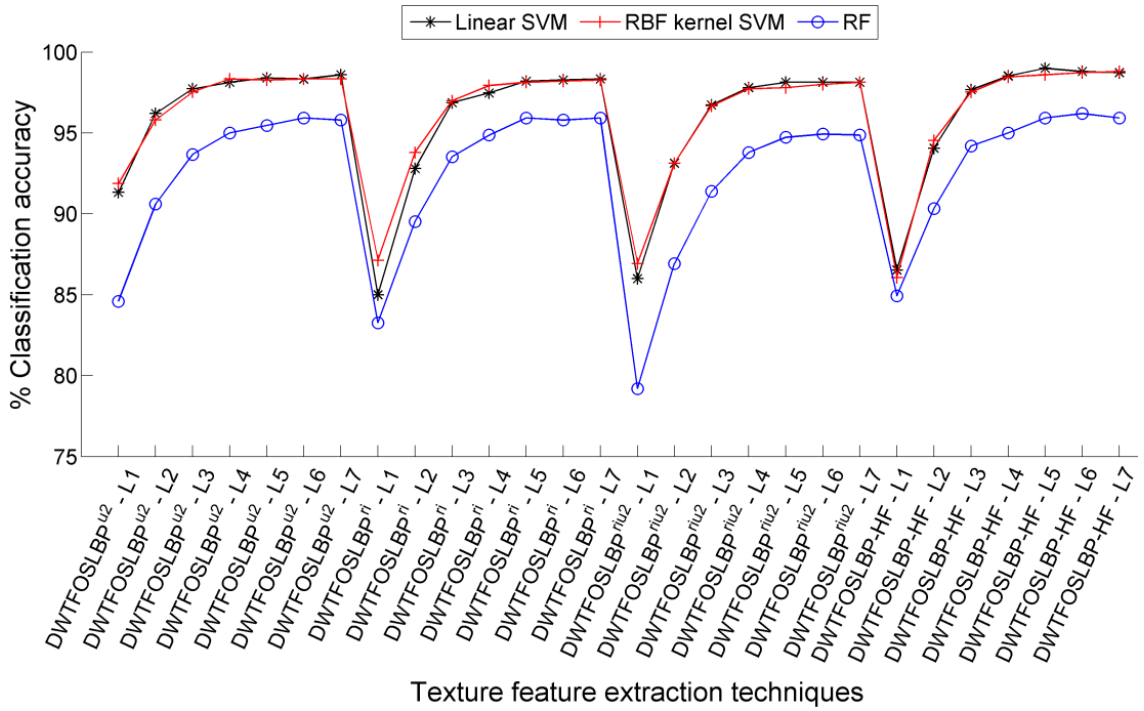

Fig. 6.8 Classification accuracy achieved using mRMR feature selection based reduced feature vector data.

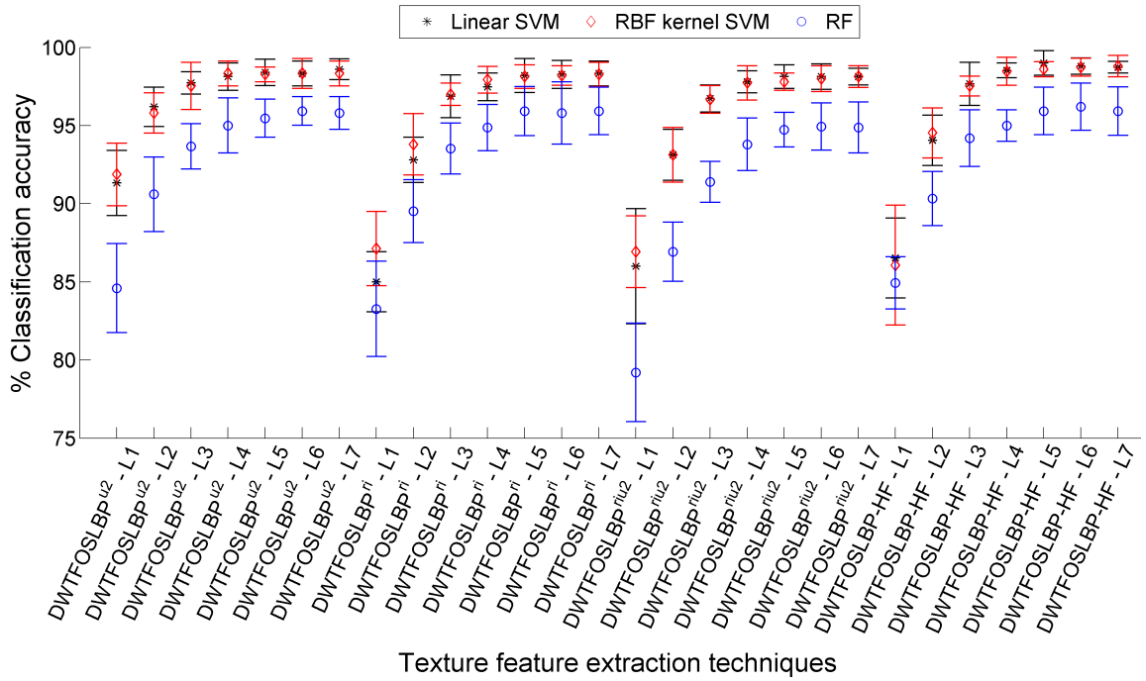

Fig. 6.9 Error bar plot with SD using mRMR feature selection based reduced feature vector data.

RF classifier: The RF classifier has achieved the best classification accuracy of 96.20±1.51% for mRMR selected feature subset (175 features) of DWTFOSLBP-HF texture feature extraction technique (at the 6th level of image decomposition). This accuracy is reasonably better than the highest classification accuracy (95.27±1.87%) obtained by the DWTFOSLBP-HF texture feature extraction technique for full feature vector dataset (1008 features) at the 6th level of image decomposition.

The analysis of Table 6.3 suggests that among the proposed texture feature extraction techniques, the mRMR selected feature subset of DWTFOSLBP-HF technique has achieved the best classification accuracy of 99.00±0.79% with linear SVM classifier**.**

Further, it is observed from Table 6.1 that as the level of image decomposition increases, the length of the feature vector data also increases. The classification accuracy results for FFVD of DWT based hybrid texture feature extraction techniques with different classifiers have gone up in the range of 4th to 6th level of image decomposition and after that either it remains same or decreases a little bit. It is noticeable that the increase in the classification accuracy has been attained at the cost of additional computation time. Therefore, the DWT based hybrid texture descriptors beyond 7th level of image decomposition has not been investigated.

It is worth noting that employing PCA (dimensionality reduction) and mRMR (feature selection) technique has not only reduced the computational time during classification, but at the same time has shown considerable improvement in the classification accuracy of hardwood species. It is also observed from Table 6.1, Table 6.2 and Table 6.3, that the DWT based hybrid texture feature extraction techniques for grayscale images have achieved better classification

accuracy compared to the state-of-the-art LBP variants feature extraction techniques as given in Chapter 2.

6.3.4 Performance Evaluation of DWT based Hybrid Texture Feature Extraction Techniques for Grayscale Images using Randomly Divided Database (RDD)

6.3.4.1 Full feature vector data (FFVD)

The classification accuracy achieved by DWT based hybrid texture feature extraction techniques for different ratios of training and testing data is listed in Table 6.4.

Table 6.4 Classification accuracy achieved by full feature vector data for different proportions of training and testing data of RDD using three classifiers.

Technique	IDL	% CA achieved by classifiers for different proportions of training and testing											
		Linear SVM				RBF kernel SVM				RF			
		80/20	70/30	60/40	50/50	80/20	70/30	60/40	50/50	80/20	70/30	60/40	50/50
$DWTFOSLBP^{u2}$	1	86.00	83.33	80.00	78.67	84.33	80.67	75.83	73.60	75.33	71.56	69.50	68.13
	2	90.00	88.67	86.50	83.33	88.33	85.56	83.83	81.60	86.00	80.89	80.17	77.73
	3	92.67	92.00	90.00	88.67	90.00	88.67	87.50	85.20	90.33	85.78	86.50	83.60
	4	93.00	93.33	92.00	90.40	92.00	91.33	89.17	88.27	89.33	87.33	88.50	85.73
	5	93.33	93.33	92.33	90.80	91.33	91.33	90.67	88.93	91.00	88.22	90.53	87.47
	6	93.33	92.44	90.67	90.27	92.33	90.89	90.33	88.53	91.67	88.44	89.83	87.33
	7	93.00	90.67	90.67	89.87	91.00	90.44	89.83	88.67	90.33	89.11	89.50	87.20
$DWTFOSLBP^{ri}$	1	82.00	74.00	72.67	71.20	82.67	77.33	75.17	72.67	77.00	70.44	68.50	65.87
	2	87.67	87.33	84.33	81.60	86.67	85.11	83.00	80.93	86.00	83.56	80.67	77.20
	3	93.33	92.22	90.17	86.93	89.67	87.78	87.33	84.67	90.00	88.00	87.00	82.53
	4	95.00	92.89	91.50	87.73	93.33	91.56	89.50	86.93	92.00	89.11	88.17	84.67
	5	94.67	93.11	91.67	88.53	93.00	91.78	89.50	87.73	91.00	90.89	89.50	86.00
	6	95.33	93.56	91.33	88.40	93.33	92.00	89.67	87.87	91.67	89.56	88.33	88.00
	7	93.67	92.44	89.50	87.47	92.33	90.67	88.50	87.07	92.00	90.44	89.50	87.60
$DWTFOSLBP^{riu2}$	1	82.67	77.33	72.67	72.93	80.33	76.89	74.17	73.60	76.33	68.44	64.17	65.60
	2	89.00	89.11	86.33	83.47	89.33	86.22	84.17	82.00	84.00	82.44	79.50	77.73
	3	92.67	92.44	90.50	87.87	90.67	89.56	86.50	86.00	87.00	85.78	84.83	81.73
	4	**95.33**	**94.22**	91.50	90.67	93.67	92.89	90.33	89.33	90.00	88.67	88.50	85.60
	5	94.33	94.00	**92.83**	**91.73**	93.33	92.89	90.50	**90.27**	90.67	90.00	89.50	87.07
	6	94.33	94.22	91.50	90.53	**94.33**	**94.00**	**91.00**	90.00	91.67	89.78	88.67	87.73
	7	94.00	92.00	89.33	88.67	93.67	93.78	91.00	88.80	91.33	90.00	89.17	88.00
DWTFOSLBP-HF	1	79.33	75.33	71.00	69.33	75.33	73.11	69.83	67.33	80.67	73.78	70.17	68.13
	2	86.67	85.33	82.33	79.47	87.67	86.22	83.67	81.20	86.00	83.33	81.50	79.87
	3	91.33	90.22	88.50	85.73	91.00	90.22	87.00	85.73	89.33	86.44	86.17	83.47
	4	93.67	93.33	90.50	88.80	93.33	91.56	89.67	87.60	89.67	89.56	89.00	86.93
	5	93.67	93.33	91.50	90.27	91.67	91.56	90.67	89.60	91.67	90.44	**90.50**	87.47
	6	93.33	92.44	90.83	89.60	92.33	92.00	90.17	89.07	92.33	91.56	89.83	**89.33**
	7	92.67	91.56	89.17	88.93	92.00	90.89	89.50	88.53	**92.67**	**91.56**	89.67	88.40

Linear SVM classifier: Amongst the proposed texture feature extraction techniques, $DWTFOSLBP^{riu2}$ has produced significant feature vector data that yields best classification accuracy of 95.33%, 94.22%, 92.83% and 91.73% for 80/20, 70/30, 60/40 and 50/50 training and testing ratios of RDD, respectively. These classification accuracies have been achieved for FFVD of the $DWTFOSLBP^{riu2}$ feature extraction technique at the 4^{th} level (80/20 and 70/30) and 5^{th} level (60/40 and 50/50) of image decomposition as listed in Table 6.4.

RBF kernel SVM classifier: Using RBF kernel SVM classifier, the best classification accuracy of 94.33%, 94%, 91% and 90.27% has been achieved for 80/20, 70/30, 60/40 and 50/50 training

and testing ratios of RDD, respectively. The classification accuracies have been achieved for FFVD of DWTFOSLBP^{riu2} technique obtained at the 6th level (80/20, 70/30 and 60/40) and 5th level (50/50) of image decomposition as listed in Table 6.4.

RF classifier: As listed in Table 6.4 the FFVD produced by DWTFOSLBP-HF feature extraction technique has given the best classification accuracy for different proportions of training and testing data of RDD, amongst the proposed techniques using RF classifier. The DWTFOSLBP-HF features have achieved classification accuracy of 92.67%, 91.56%, 90.50% and 89.33% for 80/20, 70/30, 60/40 and 50/50 training and testing ratios of RDD, respectively, at the 5th (60/40), 6th (50/50) and 7th (80/20 and 70/30) levels of image decomposition.

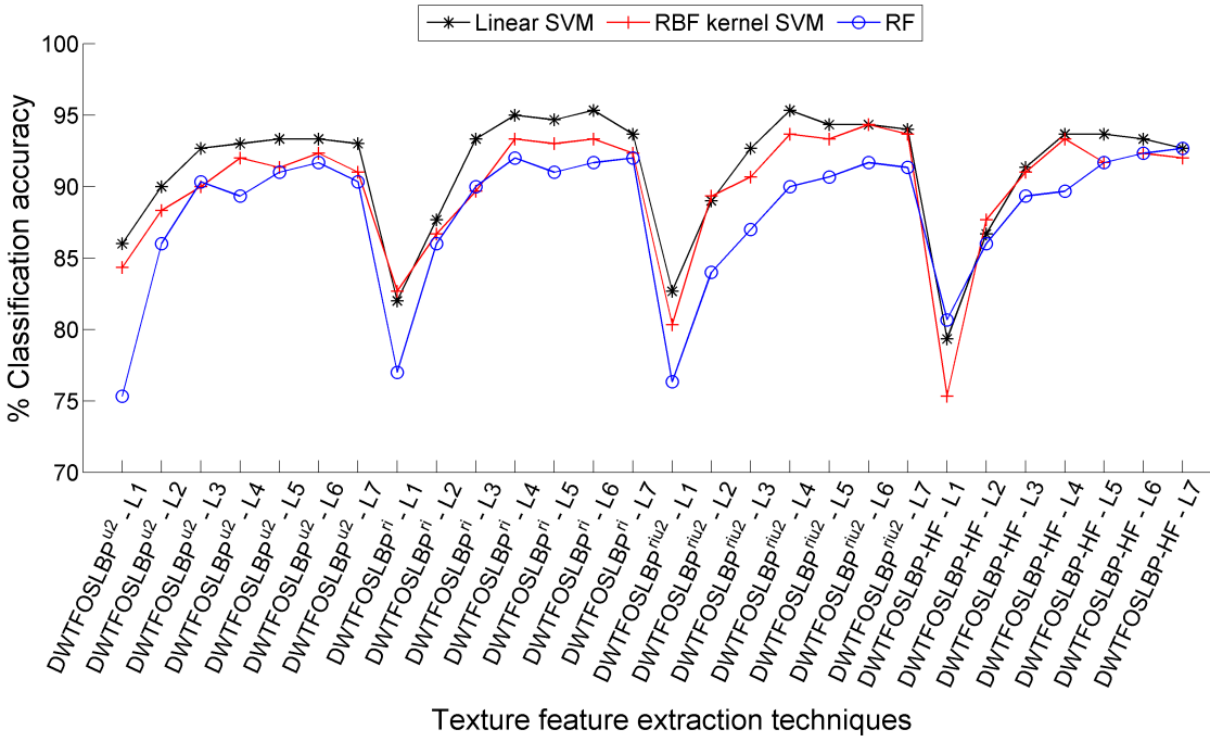

Fig. 6.10 Classification accuracy achieved for 80/20 proportion of training and testing data of RDD.

The classification accuracies obtained by the three different classifiers are compared for each of the four (80/20, 70/30, 60/40 and 50/50) training and testing ratios, and are graphically illustrated in Fig. 6.10, Fig. 6.11, Fig. 6.12 and Fig. 6.13, respectively. It is apparent from these figures that texture feature vector data produced by most of the DWT based hybrid texture feature extraction techniques yields best classification accuracy with linear SVM classifier. Whereas, the least classification accuracy has been achieved with RF classifier. Further, the classification accuracy obtained by other DWT based hybrid texture feature extraction techniques have also achieved comparably better classification accuracy compared to the classification accuracy achieved by LBP variants (state-of-the-art) texture feature extraction techniques.

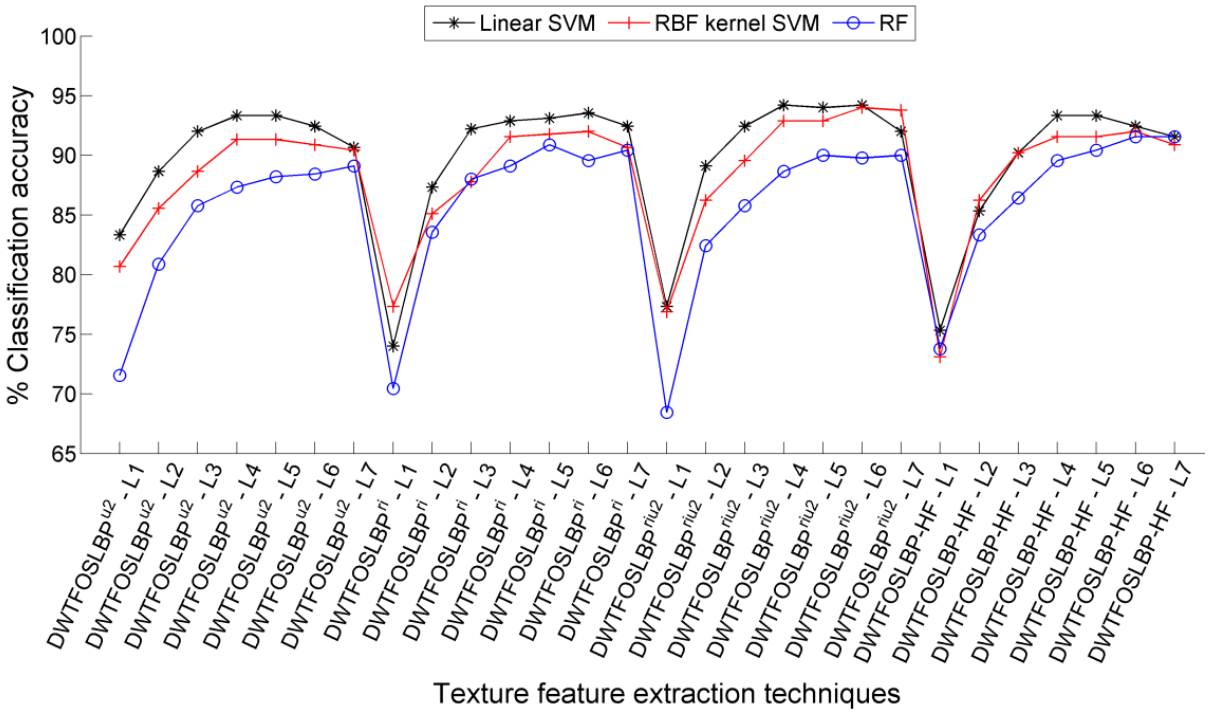

Fig. 6.11 Classification accuracy achieved for 70/30 proportion of training and testing data of RDD.

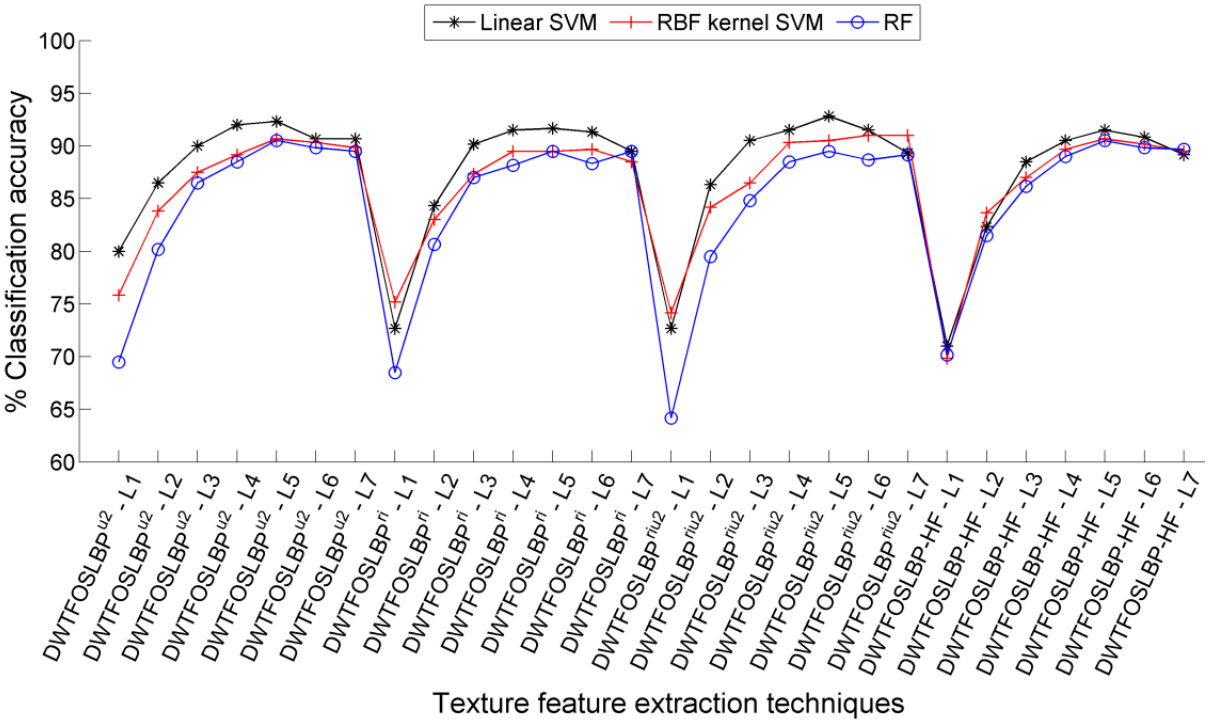

Fig. 6.12 Classification accuracy achieved for 60/40 proportion of training and testing data of RDD.

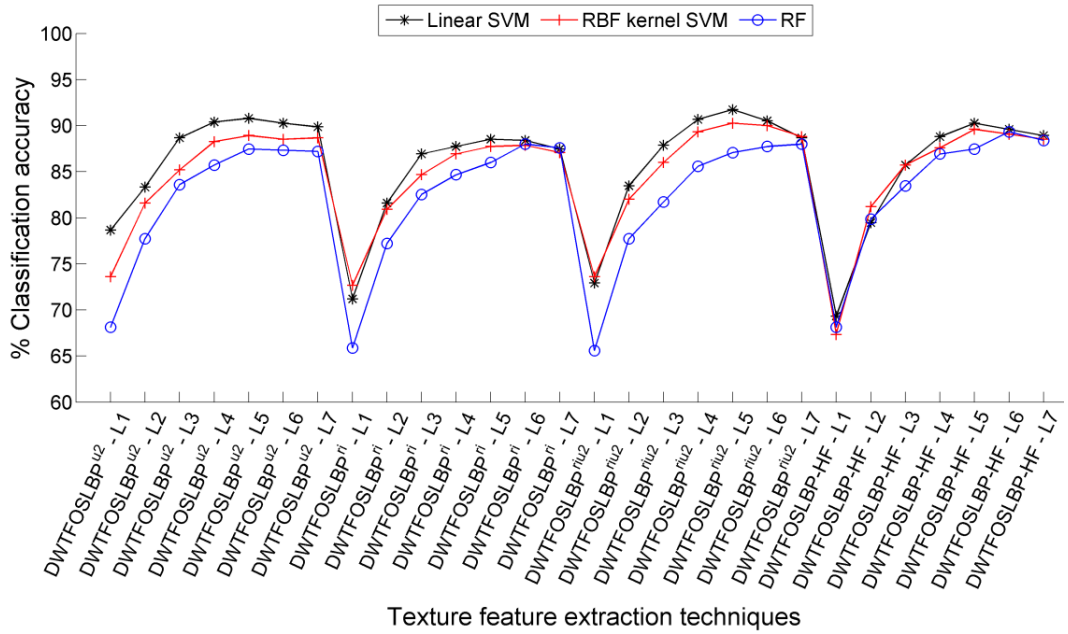

Fig. 6.13 Classification accuracy achieved for 50/50 proportion of training and testing data of RDD.

6.3.4.2 The PCA dimensionality reduced feature vector data

The classification accuracy results obtained by the PCA reduced feature vector data using four different classifiers are concisely discussed below:

Linear SVM classifier: The PCA dimensionality reduced feature vector data of the DWTFOSLBP^{riu2} technique has yielded the best classification accuracy of 95% (200 features), 94.22% (200 features), 92.83% (200 features) and 90.67% (200 features) for 80/20, 70/30, 60/40 and 50/50 training and testing ratios of RDD, respectively. The aforesaid classification accuracies are obtained for feature vector data produced at the 5th level of image decomposition. This classification accuracy is comparable to the accuracy achieved with FFVD of DWTFOSLBP^{riu2} technique with high-dimensional feature vector data (Table 6.5).

RBF kernel SVM classifier: A classification accuracy of 94.67% (250 features), 94.22% (250 features), 91.17% (250 features) and 90.27% (150 features) has been obtained for 80/20, 70/30, 60/40 and 50/50 training and testing ratios of RDD, respectively. These results have been achieved by PCA dimensionality reduced feature vector data of the DWTFOSLBP^{riu2} technique at the 5th level (50/50) and 6th level (80/20, 70/30 & 60/40) of image decomposition. The classification accuracies are slightly better than the accuracy presented by the FFVD of the DWTFOSLBP^{riu2} technique (Table 6.6).

RF classifier: In this case, the classification accuracy of 93% (50 features), 89.11% (100 features), 88.50% (100 features) and 86.93% (50 features) for 80/20, 70/30, 60/40 and 50/50 training and testing ratios of RDD, respectively, has been obtained by DWTFOSLBP^{ri} technique with PCA dimensionality reduced feature vector data. The said classification accuracy results

are obtained by the feature vector data produced at the 4th level (70/30) and 5th level (80/20, 60/40 & 50/50) of image decomposition (Table 6.7).

Table 6.5 Classification accuracy achieved by PCA reduced feature vector data for different proportions of training and testing data of RDD using linear SVM classifier.

Technique	IDL	NoF	80/20	NoF	70/30	NoF	60/40	NoF	50/50
	1	100	85.67	100	82.89	150	79.67	225	78.53
	2	250	90.33	200	87.78	250	86.67	350	84.00
	3	350	92.33	200	91.78	300	90.17	300	88.93
$DWTFOSLBP^{u2}$	4	50	93.67	250	92.67	250	92.17	300	90.27
	5	350	94.00	350	93.33	350	92.33	350	90.67
	6	100	92.33	100	92.22	100	90.83	500	89.87
	7	50	93.00	100	92.22	200	91.17	100	90.27
	1	150	80.33	150	75.11	150	72.50	150	72.40
	2	250	88.00	300	88.00	300	85.50	300	81.33
	3	350	93.33	350	91.78	300	90.17	300	87.07
$DWTFOSLBP^{ri}$	4	450	94.33	450	92.67	550	91.83	450	88.67
	5	400	94.67	400	92.67	550	91.50	350	88.53
	6	450	94.00	400	93.11	400	90.33	550	88.53
	7	200	93.67	150	92.22	200	89.33	400	88.40
	1	50	82.00	50	76.22	50	73.67	40	72.80
	2	50	88.67	100	89.33	75	85.83	100	83.33
	3	100	93.00	100	92.22	150	90.67	100	88.40
$DWTFOSLBP^{riu2}$	4	200	94.67	200	93.33	150	91.50	200	90.53
	5	**200**	**95.00**	**200**	**94.22**	**200**	**92.83**	**200**	**90.67**
	6	200	94.67	300	93.33	250	90.50	300	90.40
	7	150	94.00	250	91.33	350	90.17	300	88.53
	1	150	78.67	150	74.22	125	71.00	125	69.07
	2	200	84.33	200	84.44	300	81.17	250	78.93
	3	350	91.00	450	89.78	300	89.17	350	85.47
DWTFOSLBP-HF	4	350	93.33	400	93.11	400	90.50	500	88.67
	5	350	93.67	350	93.11	400	91.00	450	90.53
	6	200	93.33	250	92.67	550	90.50	450	88.93
	7	550	93.00	500	91.33	550	89.33	350	88.67

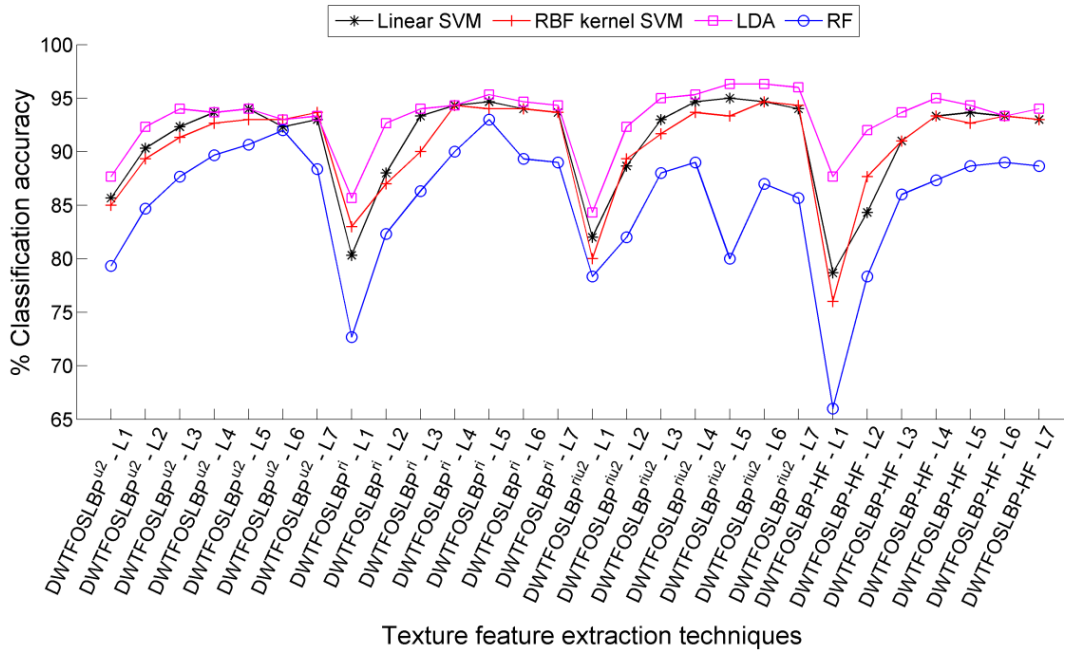

Fig. 6.14 Classification accuracy achieved for 80/20 proportion of training and testing data of RDD.

Table 6.6 Classification accuracy achieved by PCA reduced feature vector data for different proportions of training and testing data of RDD using RBF kernel SVM classifier.

Technique	IDL	NoF	80/20	NoF	70/30	NoF	60/40	NoF	50/50
	1	50	85.00	100	81.56	200	76.50	150	73.87
	2	150	89.33	150	87.33	200	84.50	250	82.00
	3	100	91.33	150	89.78	150	88.17	200	85.60
$DWTFOSLBP^{u2}$	4	100	92.67	50	92.44	50	90.17	250	89.20
	5	200	93.00	50	92.89	50	91.17	200	89.87
	6	350	93.00	50	92.89	150	91.67	100	89.87
	7	50	93.67	100	93.11	100	92.50	50	90.27
	1	125	83.00	125	76.89	125	75.33	100	72.53
	2	200	87.00	250	85.11	100	83.33	150	81.33
	3	50	90.00	50	89.11	50	87.67	50	85.33
$DWTFOSLBP^{ri}$	4	100	94.33	100	92.00	50	90.17	100	88.67
	5	100	94.00	150	93.11	300	90.50	150	89.73
	6	200	94.00	50	93.11	150	90.33	200	88.80
	7	300	93.67	50	92.22	100	89.33	50	87.60
	1	30	80.00	40	76.67	50	74.33	40	74.00
	2	75	89.33	100	86.44	100	84.17	75	82.00
	3	150	91.67	150	90.00	150	87.00	100	86.00
$DWTFOSLBP^{riu2}$	4	150	93.67	100	93.11	200	90.67	100	89.60
	5	100	93.33	100	92.89	150	90.67	**150**	**90.27**
	6	**250**	**94.67**	**250**	**94.22**	**250**	**91.17**	250	89.87
	7	100	94.33	250	93.56	250	91.00	300	88.93
	1	125	76.00	125	72.89	125	69.67	125	67.33
	2	200	87.67	250	86.44	250	83.50	300	80.93
	3	50	91.00	100	90.67	100	87.33	100	85.87
DWTFOSLBP-HF	4	300	93.33	150	91.78	100	90.17	300	87.87
	5	150	92.67	150	92.44	150	91.00	100	89.33
	6	150	93.33	100	93.11	100	90.83	100	89.20
	7	300	93.00	100	92.22	200	90.17	150	88.93

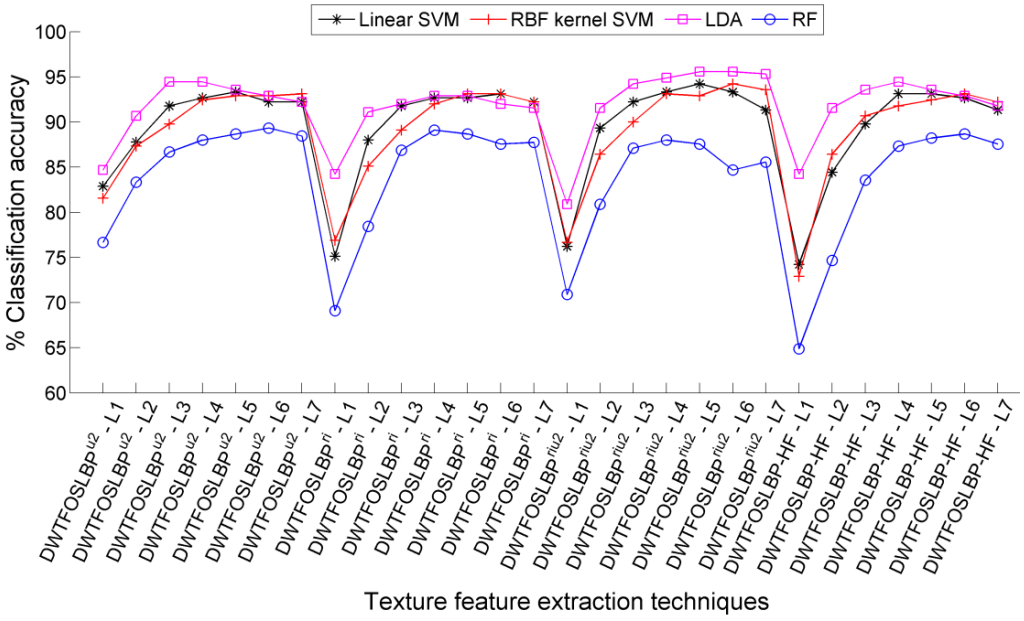

Fig. 6.15 Classification accuracy achieved for 70/30 proportion of training and testing data of RDD.

LDA classifier: Amongst the proposed feature extraction techniques, the PCA dimensionality reduced feature vector data of the $DWTFOSLBP^{riu2}$ technique has achieved the best classification accuracy of 96.33% (150 features), 95.56% (260 features), 94.17% (200 features)

and 93.73% (200 features) for 80/20, 70/30, 60/40 and 50/50 training and testing ratios of RDD, respectively. These classification accuracies are obtained for the feature vector data produced at the 4th level (60/40) and 5th level (80/20, 70/30 & 50/50) of image decomposition (Table 6.8).

Table 6.7 Classification accuracy achieved by PCA reduced feature vector data for different proportions of training and testing data of RDD using RF classifier.

Technique	IDL	NoF	80/20	NoF	70/30	NoF	60/40	NoF	50/50
	1	100	79.33	50	76.67	50	71.83	50	69.87
	2	50	84.67	200	83.33	50	82.83	50	79.20
	3	100	87.67	50	86.67	150	85.67	50	82.93
$DWTFOSLBP^{u2}$	4	100	89.67	150	88.00	100	86.67	50	84.93
	5	50	90.67	50	88.67	50	88.67	50	88.67
	6	100	92.00	100	89.33	50	88.83	50	88.40
	7	50	88.38	100	88.44	50	87.50	50	87.07
	1	125	72.67	50	69.11	50	65.83	50	65.07
	2	50	82.33	50	78.44	50	78.33	50	74.27
	3	50	86.33	50	86.89	50	84.33	50	83.73
$DWTFOSLBP^{ri}$	4	100	90.00	**100**	**89.11**	100	87.33	50	83.87
	5	**50**	**93.00**	50	88.67	**100**	**88.50**	**50**	**86.93**
	6	50	89.33	50	87.56	50	87.33	50	84.80
	7	100	89.00	50	87.73	100	87.50	100	84.53
	1	40	78.33	40	70.89	40	71.33	50	70.53
	2	75	82.00	100	80.89	100	80.67	75	78.13
	3	150	88.00	150	87.11	50	85.83	50	84.67
$DWTFOSLBP^{riu2}$	4	50	89.00	50	88.00	150	87.50	100	87.33
	5	100	80.00	50	87.56	150	87.00	100	85.60
	6	250	87.00	50	84.67	100	84.17	50	83.07
	7	100	85.67	50	85.56	50	83.17	200	80.40
	1	125	66.00	150	64.89	125	62.67	150	59.33
	2	50	78.33	300	74.67	100	71.50	50	68.67
	3	50	86.00	100	83.56	50	83.00	100	80.27
DWTFOSLBP-HF	4	100	87.33	100	87.33	50	85.50	100	83.07
	5	100	88.67	150	88.22	50	86.50	50	84.53
	6	50	89.00	100	88.67	50	87.50	50	85.60
	7	50	88.67	50	87.56	50	85.50	50	83.33

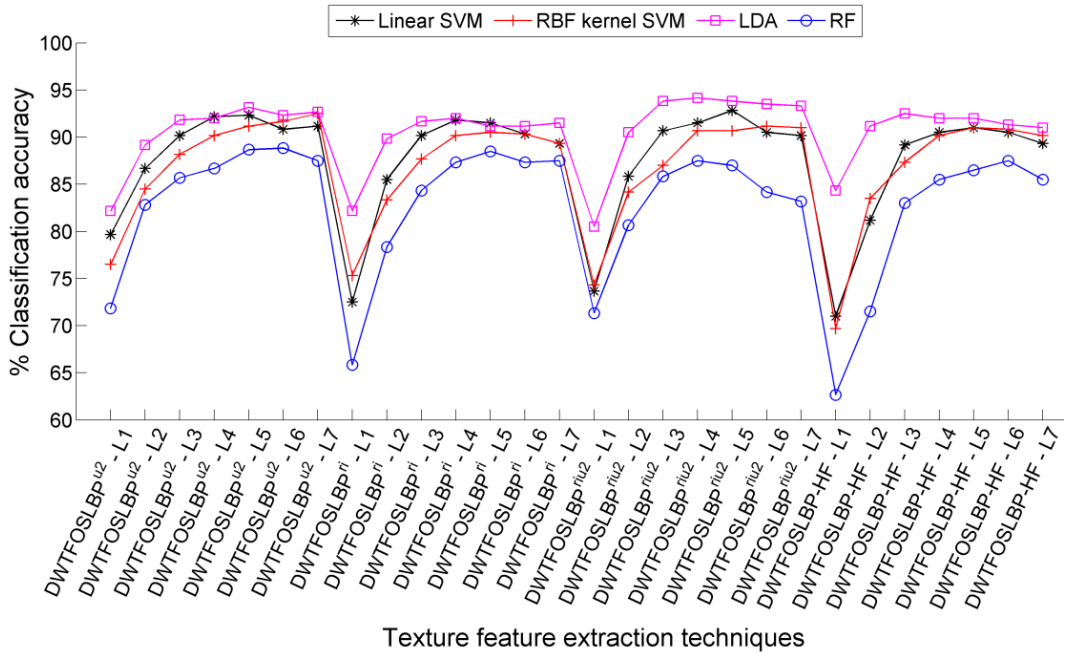

Fig. 6.16 Classification accuracy achieved for 60/40 proportion of training and testing data of RDD.

Table 6.8 Classification accuracy achieved by PCA reduced feature vector data for different proportions of training and testing data of RDD using LDA classifier.

Technique	IDL	NoF	80/20	NoF	70/30	NoF	60/40	NoF	50/50
	1	225	87.67	125	84.67	100	82.17	100	80.53
	2	300	92.33	250	90.67	200	89.17	50	86.40
	3	300	94.00	300	94.44	100	91.83	150	90.53
$DWTFOSLBP^{u2}$	4	200	93.67	400	94.44	100	92.00	50	91.60
	5	50	94.00	100	93.56	100	93.17	100	92.13
	6	100	93.00	100	92.89	100	92.33	100	91.33
	7	150	93.33	100	92.22	100	92.67	50	91.73
	1	150	85.67	150	84.22	150	82.17	150	81.07
	2	300	92.67	300	91.11	300	89.83	300	86.27
	3	50	94.00	50	92.00	50	91.67	50	88.80
$DWTFOSLBP^{ri}$	4	250	94.33	100	92.89	50	92.00	50	91.07
	5	50	95.33	50	92.89	50	91.17	50	90.80
	6	400	94.67	50	92.00	50	91.17	50	90.27
	7	300	94.33	50	91.56	50	91.50	100	90.80
	1	50	84.33	52	80.89	52	80.50	50	80.00
	2	100	92.33	104	91.56	104	90.50	104	89.33
	3	150	95.00	156	94.22	150	93.83	156	92.27
$DWTFOSLBP^{riu2}$	4	100	95.33	200	94.89	**200**	**94.17**	200	93.33
	5	**150**	**96.33**	**260**	**95.56**	260	93.83	**200**	**93.73**
	6	200	96.33	312	95.56	250	93.50	312	92.80
	7	364	96.00	350	95.33	364	93.33	350	91.87
	1	150	87.67	150	84.22	150	84.33	164	82.00
	2	300	92.00	250	91.56	300	91.17	250	87.20
	3	492	93.67	450	93.56	250	92.50	350	89.87
DWTFOSLBP-HF	4	350	95.00	400	94.44	350	92.00	250	88.67
	5	350	94.33	450	93.56	150	92.00	150	89.60
	6	600	93.33	100	92.89	100	91.33	50	89.73
	7	100	94.00	150	91.78	100	91.00	100	89.87

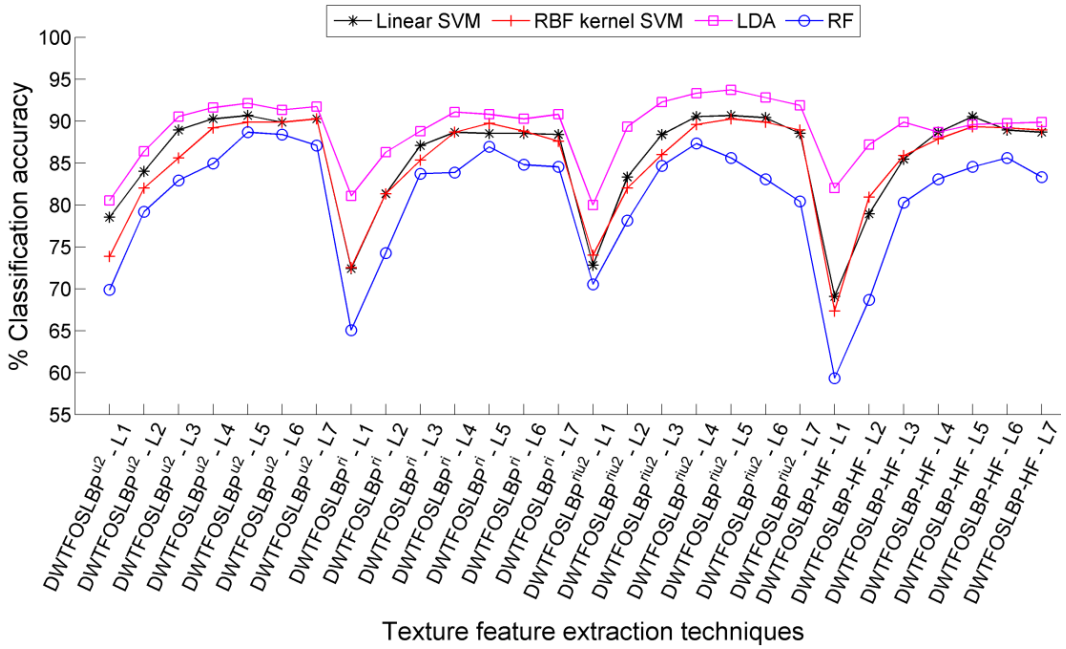

Fig. 6.17 Classification accuracy achieved for 50/50 proportion of training and testing data of RDD.

The graphical illustration of PCA reduced feature vector data of DWT based hybrid texture feature extraction techniques for grayscale images are shown in Fig. 6.14, Fig. 6.15, Fig. 6.16

and Fig. 6.17 for 80/20, 70/30, 60/40 and 50/50 training and testing ratios of RDD, respectively. It is clearly visible that the PCA reduced feature vector data has obtained the best classification accuracy with LDA classifier, whereas RF classifier has achieved lowest classification accuracy among the four classifiers. Thus, incorporating PCA for feature dimensionality reduction has improved the performance of DWT based hybrid texture feature extraction techniques for hardwood species classification with low-dimensional feature vector data.

6.3.4.3 The mRMR feature selection based reduced feature vector data

The classification accuracy achieved by the mRMR feature selection based reduced feature vector data of DWT based hybrid texture feature extraction techniques with three different classifiers have been presented in Table 6.9, Table 6.10 and Table 6.11, respectively. The classification accuracy obtained by each of the classifiers for proposed texture feature extraction techniques are discussed below:

Table 6.9 Classification accuracy achieved by mRMR feature selection based reduced feature vector data for different proportions of training and testing data of RDD using linear SVM classifier.

Technique	IDL	NoF	80/20	NoF	70/30	NoF	60/40	NoF	50/50
	1	100	87.00	150	83.56	150	80.67	150	79.87
	2	200	91.67	200	89.78	200	87.83	300	85.07
	3	200	93.67	400	92.44	400	90.50	400	89.47
$DWTFOSLBP^{u2}$	4	500	95.00	350	94.67	350	93.17	400	92.67
	5	350	95.00	250	94.89	500	93.00	350	92.67
	6	450	95.67	350	94.89	500	93.17	400	93.07
	7	450	96.00	600	94.89	350	93.00	400	93.33
	1	125	81.67	125	74.89	100	73.00	150	71.47
	2	100	90.00	100	87.11	150	85.33	150	83.20
	3	100	94.33	150	92.89	150	90.17	150	89.47
$DWTFOSLBP^{ri}$	4	100	95.67	200	95.11	250	92.83	400	91.20
	5	300	95.00	100	94.89	250	93.67	300	91.87
	6	150	95.67	200	95.56	200	93.83	100	92.40
	7	150	95.33	150	95.11	300	93.67	350	92.27
	1	45	82.67	45	78.00	50	74.17	50	73.20
	2	100	89.00	100	88.89	100	86.00	50	83.73
	3	100	92.67	150	92.67	150	90.67	100	88.40
$DWTFOSLBP^{riu2}$	4	200	95.67	200	94.22	150	92.33	150	91.33
	5	150	96.00	150	95.56	150	93.17	250	91.87
	6	150	95.33	250	95.11	150	92.50	100	91.20
	7	150	95.67	150	95.33	200	93.33	200	91.60
	1	50	84.00	50	80.44	50	76.50	50	76.13
	2	150	90.67	150	88.89	150	86.67	150	83.60
	3	50	93.33	100	92.22	200	91.67	200	90.67
DWTFOSLBP-HF	4	250	95.67	300	95.33	100	93.33	200	92.80
	5	500	95.67	200	95.33	350	93.50	150	93.47
	6	200	96.00	350	95.33	150	93.33	400	92.80
	7	**200**	**96.33**	**200**	**95.56**	**200**	**94.00**	**150**	**93.47**

Linear SVM classifier: The subset of feature vector data of DWTFOSLBP-HF texture feature extraction technique, processed by mRMR feature selection technique, yields the best classification accuracy of 96.33% (200 features), 95.56% (200 features), 94% (200 features) and 93.47% (150 features) for 80/20, 70/30, 60/40 and 50/50 training and testing ratios of RDD,

respectively. The aforesaid classification accuracies have been achieved by the feature vector data of DWTFOSLBP-HF technique obtained at the 7th level of image decomposition (Table 6.9).

RBF kernel SVM classifier: Here also the subset of feature vector data of DWTFOSLBP-HF texture feature extraction technique processed through mRMR feature selection technique has achieved the best classification accuracy of 96.33% (200 features), 95.11% (300 features), 93.50% (250 features) and 93.07% (250 features) for 80/20, 70/30, 60/40 and 50/50 training and testing ratios of RDD, respectively (Table 6.10). The accuracy is reported for feature vector data obtained at the 6th level (80/20 & 70/30) and 7th level (60/40 & 50/50) of image decomposition. Further, relatively comparable classification accuracy 96.67% (300 features), 95.56% (450 features), 93.17% (400 features) and 91.87% (350 features) for 80/20, 70/30, 60/40 and 50/50 training and testing ratios of RDD, respectively, has been achieved for mRMR processed feature vector data of DWTFOSLBP^{ri} technique. The accuracy is reported for feature vector data obtained at the 5th level (60/40), 6th level (70/30) and 7th level (80/20 & 50/50) of image decomposition.

Table 6.10 Classification accuracy achieved by mRMR feature selection based reduced feature vector data for different proportions of training and testing data of RDD using RBF kernel SVM classifier.

Technique	IDL	NoF	80/20	NoF	70/30	NoF	60/40	NoF	50/50
	1	150	86.00	100	81.11	200	78.00	100	75.33
	2	100	90.33	200	88.44	150	85.67	200	83.60
	3	300	92.67	300	91.78	300	89.33	300	88.27
DWTFOSLBP^{u2}	4	200	95.00	200	93.78	150	92.17	200	92.13
	5	250	95.33	200	94.22	300	93.17	300	92.40
	6	300	95.33	200	94.67	250	93.00	150	92.53
	7	150	95.67	200	95.11	250	93.17	250	92.53
	1	125	82.00	125	76.44	150	75.33	150	72.93
	2	20	90.00	50	88.67	50	86.50	50	84.40
	3	100	94.67	150	93.11	150	90.83	150	89.07
DWTFOSLBP^{ri}	4	150	96.33	150	94.67	150	92.00	200	91.47
	5	100	96.00	250	95.11	**400**	**93.17**	250	91.47
	6	200	96.33	**450**	**95.56**	200	92.83	250	91.73
	7	**300**	**96.67**	300	95.33	350	92.83	**350**	**91.87**
	1	40	80.67	40	79.11	50	75.67	50	74.00
	2	50	88.67	50	86.67	100	84.67	75	83.73
	3	50	91.67	100	91.78	100	88.00	100	87.47
DWTFOSLBP^{riu2}	4	100	94.67	100	93.78	100	91.67	150	91.60
	5	150	95.67	150	94.67	150	92.17	100	91.07
	6	200	95.33	325	94.67	150	92.50	100	91.20
	7	200	96.00	200	94.89	150	92.50	200	91.20
	1	50	84.33	50	79.11	50	76.50	50	76.27
	2	50	90.67	50	88.22	50	86.50	50	84.67
	3	100	93.00	250	92.67	150	90.83	150	90.13
DWTFOSLBP-HF	4	200	95.00	200	94.67	200	92.33	200	93.20
	5	100	95.67	300	94.22	350	93.00	100	92.80
	6	**200**	**96.33**	**300**	**95.11**	150	93.33	250	92.80
	7	200	95.67	250	94.89	**250**	**93.50**	**250**	**93.07**

RF classifier: The mRMR feature selection based feature vector data of DWTFOSLBP^{ri} technique yields the best classification accuracy result of 93.67% (450 features), 92.22% (150 features), 91.50% (150 features) and 90% (150 features) for 80/20, 70/30, 60/40 and 50/50

training and testing ratios of RDD, respectively (Table 6.11). The aforesaid classification accuracies have been achieved for the feature vector data of DWTFOSLBP^{ri} technique produced at the 6th level (70/30) and 7th level (80/20, 60/40 & 50/50) of image decomposition.

Table 6.11 Classification accuracy achieved by mRMR feature selection based reduced feature vector data for different proportions of training and testing data of RDD using RF classifier.

Technique	IDL	NoF	80/20	NoF	70/30	NoF	60/40	NoF	50/50
DWTFOSLBP^{u2}	1	125	81.67	50	75.33	50	72.00	100	70.00
	2	250	87.00	100	85.11	100	83.50	150	80.67
	3	50	90.33	400	87.78	350	87.50	450	85.60
	4	200	91.00	250	89.33	250	89.33	500	87.87
	5	200	93.00	550	91.56	450	90.67	150	89.47
	6	250	93.67	250	91.56	500	90.33	550	88.93
	7	250	92.67	550	90.89	350	90.33	300	89.20
DWTFOSLBP^{ri}	1	50	80.33	50	73.33	50	70.67	50	70.40
	2	100	88.33	100	86.00	200	83.17	100	80.13
	3	200	91.33	200	90.22	250	89.00	100	86.13
	4	300	92.00	300	91.33	300	90.50	150	88.53
	5	250	92.33	150	92.00	300	91.33	150	59.33
	6	150	93.33	**150**	**92.22**	150	91.17	200	89.60
	7	**450**	**93.67**	150	92.00	**150**	**91.50**	**150**	**90.00**
DWTFOSLBP^{riu2}	1	30	77.00	30	70.22	40	66.50	30	65.33
	2	75	86.67	75	83.56	50	81.00	50	78.27
	3	160	89.33	150	86.67	100	85.67	100	83.47
	4	100	91.00	215	90.00	200	88.67	150	86.53
	5	150	92.00	200	90.67	200	89.67	150	88.40
	6	200	92.00	250	90.89	250	89.83	100	88.27
	7	200	92.33	350	91.11	200	89.50	250	88.80
DWTFOSLBP-HF	1	100	80.67	50	76.44	50	73.00	50	70.67
	2	150	87.33	150	85.11	100	83.17	100	82.27
	3	150	90.33	150	88.89	350	88.00	250	85.73
	4	450	91.67	250	90.67	300	90.50	350	83.40
	5	100	92.33	250	92.22	300	91.17	350	89.87
	6	150	92.33	250	90.89	150	90.50	250	89.07
	7	400	93.00	350	91.56	400	91.67	350	89.87

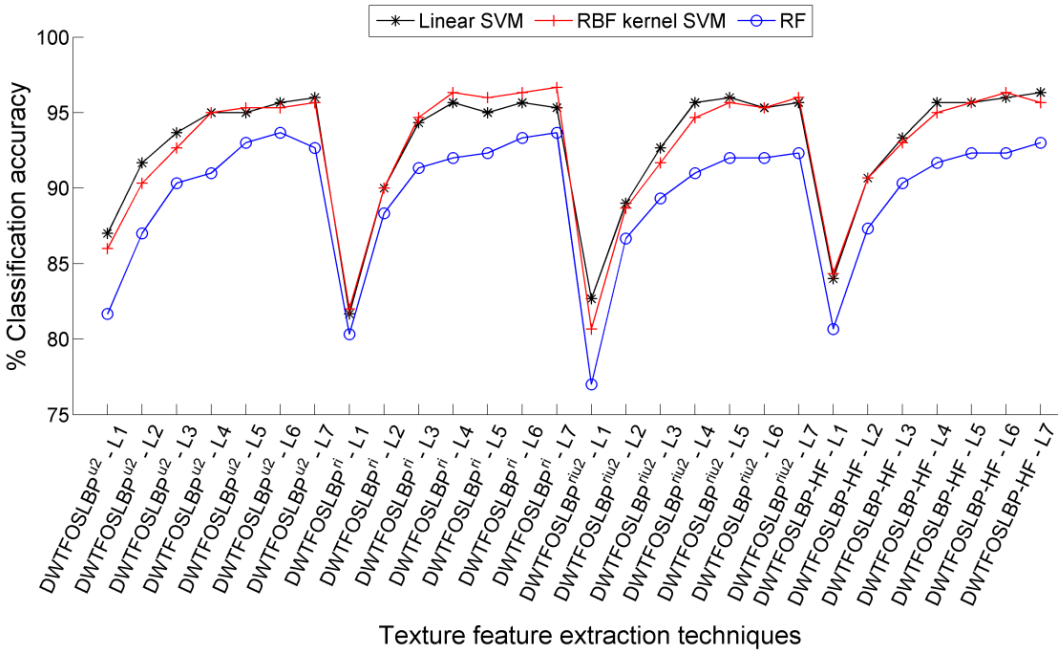

Fig. 6.18 Classification accuracy achieved for 80/20 proportion of training and testing data of RDD.

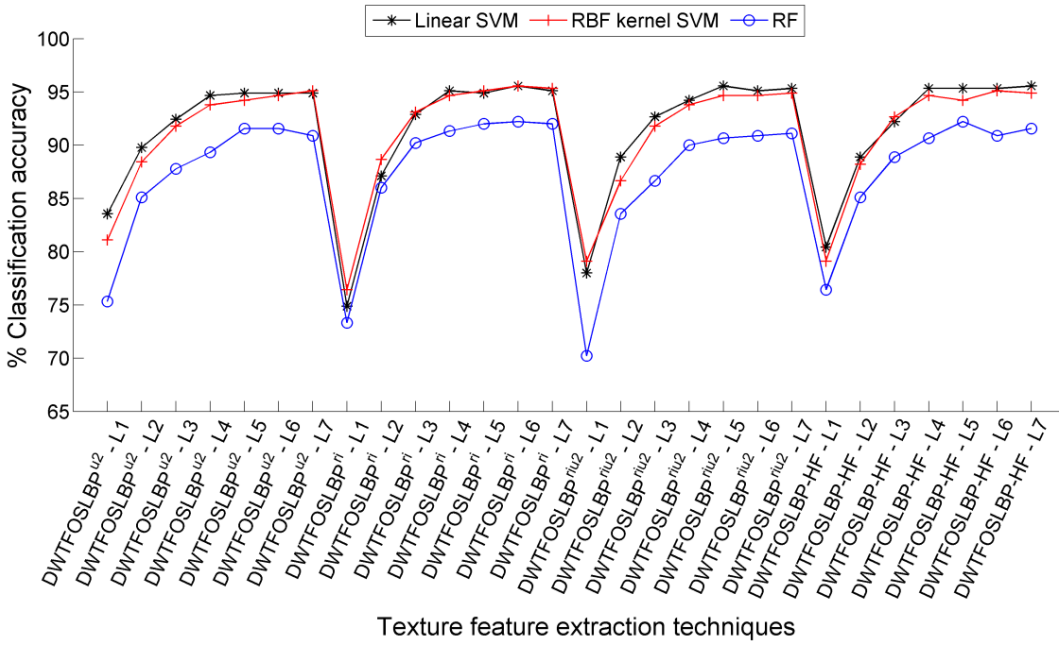

Fig. 6.19 Classification accuracy achieved for 70/30 proportion of training and testing data of RDD.

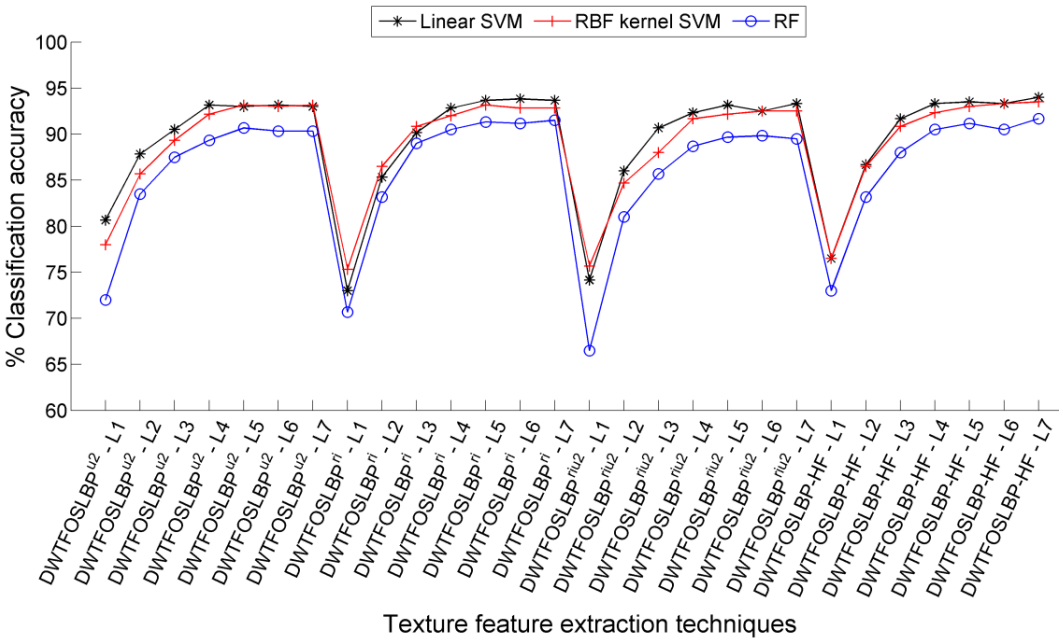

Fig. 6.20 Classification accuracy achieved for 60/40 proportion of training and testing data of RDD.

Interestingly, all the three classifiers have achieved the best classification accuracies for feature vector data produced by the DWT based hybrid texture feature extraction techniques from 5th to 7th level of image decomposition. Also, employing mRMR feature selection technique for reducing the number of features has given much better classification accuracy compared to their FFVD, that too with lower-dimensional features. Further, other DWT based hybrid texture feature extraction techniques have also attained improved classification accuracy in comparison with the LBP variants (state-of-the-art) texture feature extraction techniques.

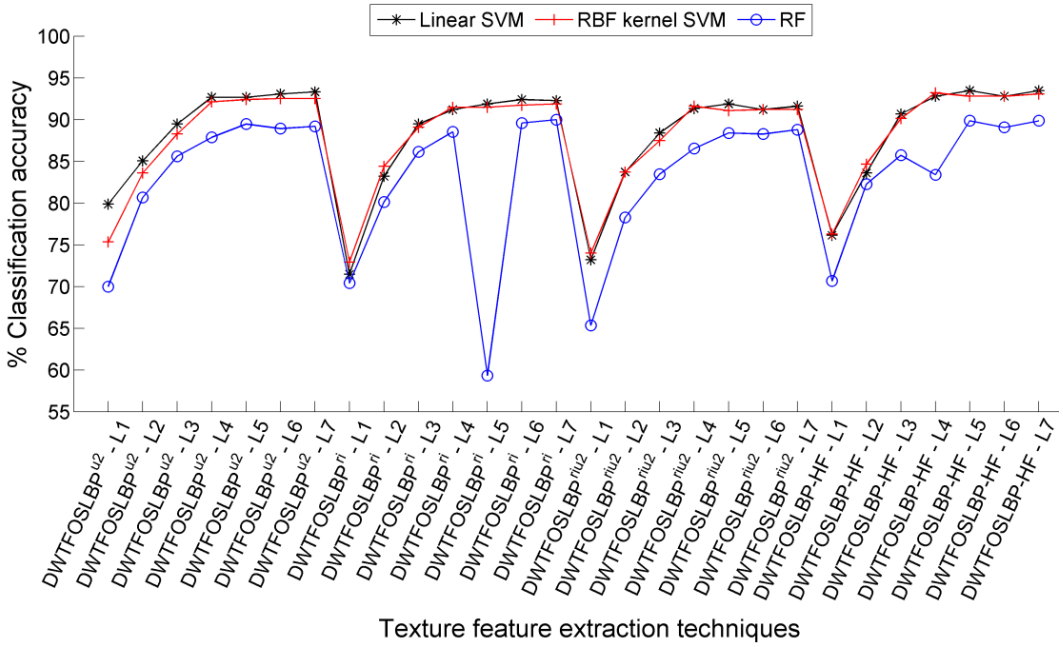

Fig. 6.21 Classification accuracy achieved for 50/50 proportion of training and testing data of RDD.

6.3.5 Performance Evaluation of DWT based Hybrid Texture Feature Extraction Techniques for RGB Images using 10-fold Cross Validation Approach

6.3.5.1 Full feature vector data (FFVD)

The percentage classification accuracy attained by the DWT based hybrid texture feature extraction techniques for RGB image [174, 175] of hardwood species database is presented in Table 6.12. The classification accuracy obtained by the proposed texture features using three different classifiers are discussed below:

Linear SVM classifier: The FFVD produced by DWTFOSLBP^{u2} texture feature extraction technique has achieved the best classification accuracy of 98.40±0.64% using 1008 features obtained at the 4th level of image decomposition. Further, a classification accuracy of 98.27±0.78% has been achieved by FFVD of DWTFOSLBP^{riu2} texture feature extraction technique using only 280 features (obtained at the 5th level of image decomposition). The least classification accuracy of 97.67±1.00% (672 features) has been achieved by using FFVD (obtained at the 4th level of image decomposition) produced by DWTFOSLBP-HF technique, among the proposed feature extraction techniques.

RBF kernel SVM classifier: By means of this classifier, the best classification accuracy of 98.13±0.75% has been attained using FFVD (336 features) produced by DWTFOSLBP^{riu2} texture feature extraction technique (at the 6th level of image decomposition), which is the best among the proposed feature extraction techniques. The FFVD of DWTFOSLBP^{u2} texture feature extraction technique has achieved the 2nd best classification accuracy of 98.13±0.88% using 1008-dimensional feature vector data produced at the 4th level of image decomposition. On the other hand, the least classification accuracy of 97.33±0.83% (640 features) has been achieved

by FFVD of DWTFOSLBP^{ri} texture feature extraction technique (at the 4th level of image decomposition).

Table 6.12 Classification accuracy achieved using full feature vector data.

Technique	IDL	Feature extraction time in seconds	% CA±SD achieved by classifiers			
			NoF	Linear SVM	RBF kernel SVM	RF
	1	1.0725	252	92.67±1.81	91.60±1.76	85.07±2.69
	2	1.3157	504	96.47±1.86	95.20±1.69	92.40±2.23
	3	1.3437	756	97.73±1.05	97.00±1.64	95.13±1.26
DWTFOSLBP^{u2}	**4**	1.3889	**1008**	**98.40±0.64**	**98.13±0.88**	96.00±1.13
	5	1.4077	1260	97.73±1.14	97.67±1.41	96.33±1.23
	6	1.4237	1512	97.73±1.14	97.40±1.27	96.53±1.03
	7	1.4352	1764	97.87±1.29	97.73±1.00	96.27±1.26
	1	1.0935	160	88.93±1.81	90.53±2.08	84.73±2.71
	2	1.3493	320	95.20±1.40	94.60±1.82	91.27±2.11
	3	1.3919	480	97.60±1.23	96.73±1.19	95.13±1.18
DWTFOSLBP^{ri}	**4**	1.4363	640	97.73±0.90	**97.33±0.83**	95.33±0.89
	5	1.4581	800	97.80±0.77	97.27±0.91	96.00±0.89
	6	1.4690	960	97.93±0.97	97.20±0.98	**96.73±1.23**
	7	1.4927	1120	97.67±0.85	96.80±1.43	96.13±0.98
	1	1.0645	56	87.07±2.74	88.67±2.92	83.00±2.63
	2	1.2908	112	94.33±1.61	94.20±1.54	89.73±1.84
	3	1.3469	168	97.40±1.42	96.27±1.55	93.73±1.10
DWTFOSLBP^{riu2}	4	1.3710	224	98.07±1.42	97.60±1.10	95.87±0.98
	5	1.3885	**280**	**98.27±0.78**	97.87±0.98	96.00±1.30
	6	1.3937	336	97.87±1.12	**98.13±0.75**	**96.13±0.93**
	7	1.4012	392	97.33±0.90	97.47±1.60	95.80±1.48
	1	1.0797	168	87.07±3.00	88.07±2.32	86.13±2.01
	2	1.3200	336	93.93±2.10	94.20±1.55	91.53±1.63
	3	1.4195	504	96.20±0.90	96.73±1.35	95.13±1.21
DWTFOSLBP-HF	**4**	1.4415	**672**	**97.67±1.00**	97.60±1.05	96.13±1.21
	5	1.4615	840	97.47±0.82	97.73±1.48	96.53±0.69
	6	1.4804	1008	97.60±1.05	97.60±1.18	96.33±1.05
	7	1.4890	1176	97.27±1.11	97.47±1.21	**96.60±1.19**

RF classifier: This classifier has given the best classification accuracy of 96.73±1.23% for FFVD (960 features) produced by DWTFOSLBP^{ri} texture feature extraction technique (at the 6th level of image decomposition). Further, the FFVD of DWTFOSLBP-HF technique (at the 7th level of image decomposition) has achieved the 2nd best classification accuracy of 96.60±1.19% for 1176-dimensional feature vector data**.** In addition, among the proposed feature extraction techniques, the least classification accuracy of 96.13±0.93% (336 features) has been attained by using FFVD produced by DWTFOSLBP^{riu2} feature extraction technique (at the 6th level of image decomposition).

Here, it has been observed that the better classification accuracy has been achieved by most of the DWT based hybrid texture features obtained between the 4th to 7th levels of image decomposition with all the three classifiers. In addition, the linear and RBF kernel SVM classifiers, both have presented the best classification accuracy; whereas, RF classifier yields comparatively lower classification accuracy. The classification accuracy obtained by the three classifiers have been compared and the same is illustrated in Fig. 6.22. The graphical illustration also reveals that DWTFOSLBP^{u2} texture feature extraction technique has given the best

classification accuracy with linear SVM classifier.

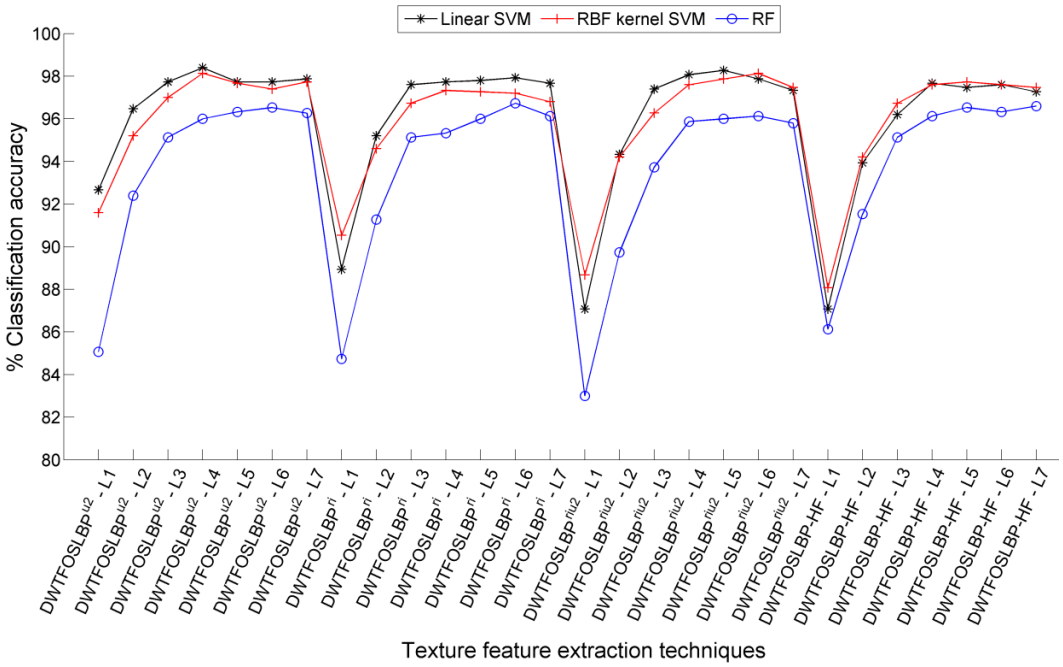

Fig. 6.22 Classification accuracy achieved using FFVD

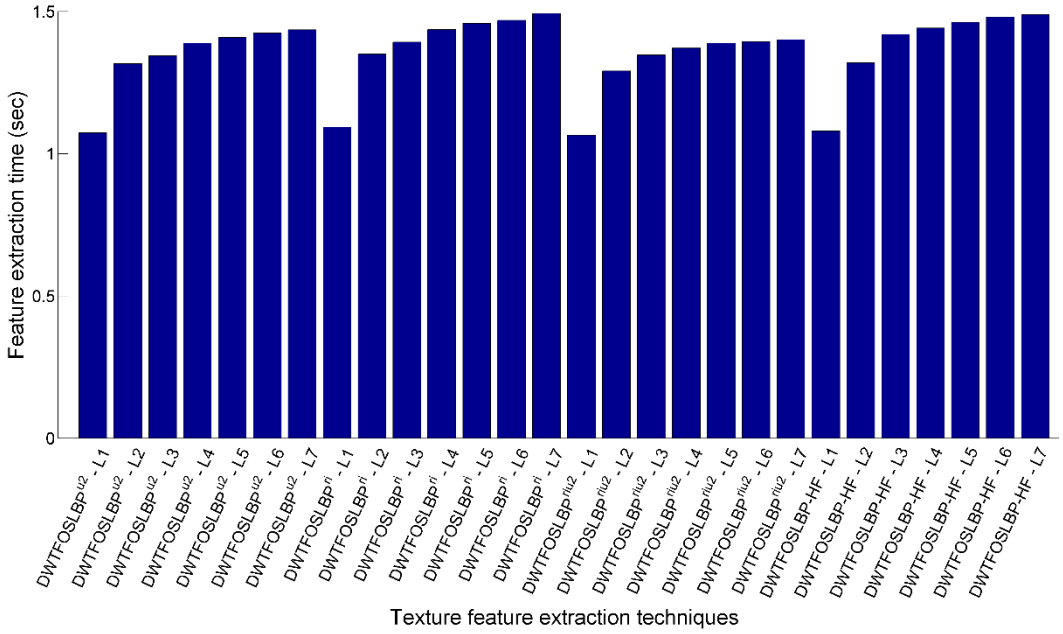

Fig. 6.23 Feature extraction time for single RGB image.

Further, the time required by the DWT based hybrid texture feature extraction techniques for feature vector data generation for single RGB image is also listed in Table 6.12. The DWTFOSLBP^{u2} feature extraction technique has achieved best classification accuracy of 98.40±0.64% at the 4th level of image decomposition, which requires 1.3889 seconds for extracting the texture features of given individual image as shown in Fig. 6.24. This feature extraction time is almost thrice than the DWTFOSLBP^{u2} feature extraction technique (grayscale image) which requires 0.4602 second for extracting the texture features of given individual

grayscale image. The error bar plot with SD for FFVD is shown in Fig. 6.24. The assessment of Fig. 6.24 reveals that the feature vector data achieved by DWTFOSLBP^{u2} feature extraction technique at the 4th level of image decomposition yields the best classification accuracy of 98.40±0.64% with lesser value of standard deviation. Also, the DWTFOSLBP^{riu2} feature extraction technique has achieved comparable classification accuracy (98.13±0.75%) with RBF kernel SVM classifier.

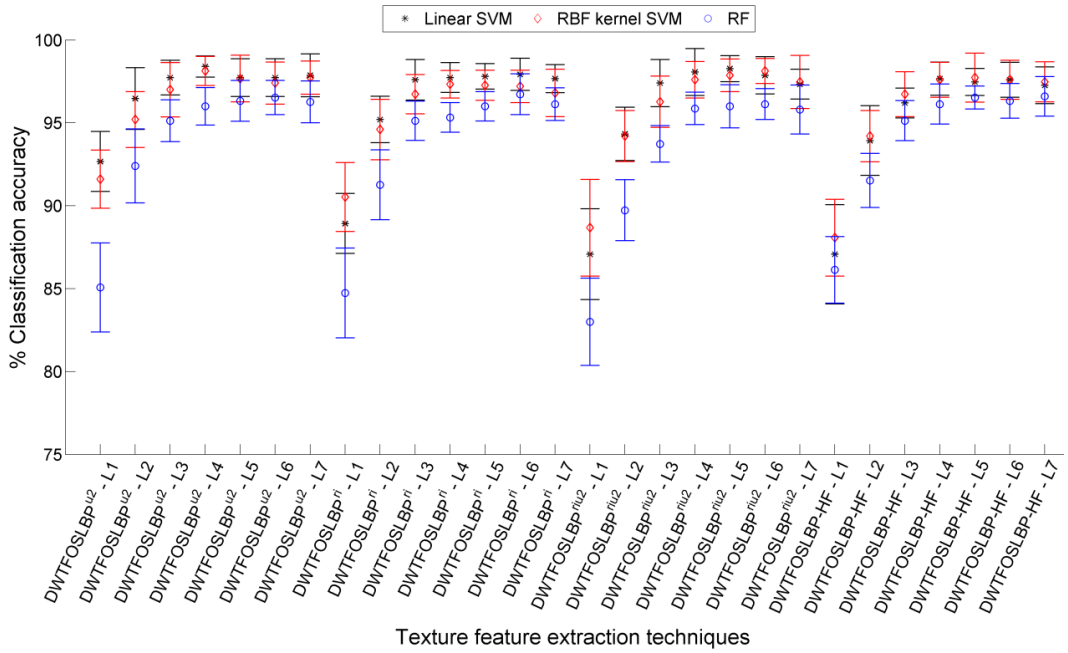

Fig. 6.24 Error bar plot with SD using FFVD.

6.3.5.2 The PCA dimensionality reduced feature vector data

The performance evaluation of texture feature extraction techniques of RGB images with PCA reduced feature vector data with different classifiers are listed in Table 6.13 and has been concisely described henceforth:

Linear SVM classifier: The PCA reduced feature vector data of DWTFOSLBP^{u2} feature extraction technique yields the best classification accuracy of 98.53±0.69%, which is slightly better than the FFVD (98.40±0.64%) of DWTFOSLBP^{u2} technique. The classification accuracy has been achieved using only 450 features produced at the 4th level of image decomposition, compared to FFVD (1008 features). Further, the PCA reduced feature vector data of DWTFOSLBP^{riu2} feature extraction technique has achieved marginally lower classification accuracy (97.93±1.49%**)** with 100 features only. This classification accuracy is slightly lower than the accuracy achieved by the FFVD of DWTFOSLBP^{riu2} (98.27±0.78%) with 280-dimesional features.

RBF kernel SVM classifier: Amongst the proposed feature extraction techniques, the PCA reduced feature vector data of DWTFOSLBP^{u2}, has attained slightly better classification accuracy of 98.27±0.90% (350 features) compared to 98.13±0.88% (1008 features) presented

by FFVD of DWTFOSLBP^{u2} technique. In addition, the aforesaid feature vector data are obtained at the 4th level of image decomposition. Further, the PCA reduced feature vector data of DWTFOSLBP^{ri} techniques (at the 6th level of image decomposition) has achieved the 2nd best classification accuracy (98.13±0.61%, 50 features), slightly better than (97.93±0.97%, 960 features) presented by FFVD of DWTFOSLBP^{ri} technique.

Table 6.13 Classification accuracy achieved using PCA based reduced feature vector data.

Technique	IDL	% CA±SD achieved by classifiers							
		NoF	Linear SVM	NoF	RBF kernel SVM	NoF	RF	NoF	LDA
	1	200	92.73±0.97	125	91.27±1.68	50	89.70±2.09	225	93.47±1.25
	2	200	96.13±1.57	150	95.20±1.57	50	93.00±1.73	350	96.93±0.95
	3	350	97.87±0.93	250	97.20±1.40	50	95.07±1.23	400	98.33±0.90
DWTFOSLBP^{u2}	**4**	**450**	**98.53±0.69**	**350**	**98.27±0.90**	50	96.33±1.55	200	98.20±1.22
	5	250	98.07±1.02	200	98.20±1.18	150	96.20±1.04	400	98.13±0.69
	6	250	98.07±1.09	50	98.13±1.08	100	95.33±1.09	300	98.07±1.24
	7	300	97.80±1.26	100	98.00±1.37	50	95.13±1.22	350	97.93±0.97
	1	150	88.60±2.10	100	90.60±2.12	100	84.20±1.86	150	92.00±2.04
	2	300	95.13±1.30	200	94.60±1.95	100	91.13±1.22	300	97.00±0.96
	3	300	97.33±1.22	150	96.87±1.48	50	93.87±1.63	450	98.13±1.43
DWTFOSLBP^{ri}	4	250	97.60±0.64	100	97.53±1.04	100	95.07±0.78	600	98.40±0.89
	5	250	97.40±0.73	100	97.87±0.82	100	94.87±1.26	500	97.80±0.83
	6	350	97.33±1.30	**50**	**98.13±0.61**	50	95.20±1.21	600	97.47±1.60
	7	500	97.13±1.09	100	97.67±0.72	50	94.27±1.10	200	97.33±1.09
	1	50	86.87±1.91	50	89.07±2.83	50	87.47±2.57	50	90.27±1.61
	2	100	94.00±1.04	75	94.33±1.31	75	91.87±2.06	100	96.00±0.63
	3	150	97.07±1.41	160	96.40±1.55	100	95.07±1.61	150	98.13±1.17
DWTFOSLBP^{riu2}	**4**	**100**	**97.93±1.49**	150	97.67±1.14	**100**	**96.40±1.55**	175	98.33±1.05
	5	250	97.87±1.03	150	98.00±1.04	100	94.53±1.53	200	98.60±0.86
	6	325	97.67±1.34	200	98.13±0.76	100	94.40±1.58	**300**	**98.73±0.86**
	7	300	96.80±1.17	250	97.47±1.60	100	92.67±1.41	350	98.40±0.95
	1	150	87.80±2.01	150	88.07±2.32	150	81.47±2.89	150	92.47±1.86
	2	300	93.73±1.67	300	94.20±1.54	50	88.07±2.05	300	97.13±0.89
	3	400	96.20±1.41	400	96.80±1.36	50	91.27±2.02	450	98.20±0.95
DWTFOSLBP-HF	4	450	97.47±0.98	400	97.60±1.05	50	92.80±0.88	**600**	**98.47±0.77**
	5	550	97.53±0.63	300	97.80±1.60	50	93.73±1.38	500	97.87±0.98
	6	550	97.53±0.95	50	98.00±1.13	50	93.87±1.17	550	97.67±0.85
	7	550	97.47±1.33	100	97.87±1.50	50	93.07±1.14	200	97.00±1.45

RF classifier: The PCA reduced feature vector data of DWTFOSLBP^{riu2} texture feature extraction technique has achieved the best classification accuracy of 96.40±1.55% using 100-dimensional feature vector data only (at the 4th level of image decomposition), which is slightly better than the classification accuracy (96.13±0.93%) yielded by the FFVD of DWTFOSLBP ^{riu2} technique with 336-dimensional features (at the 6th level of image decomposition).

LDA classifier: This classifier has given the best classification accuracy of 98.73±0.86% for PCA reduced feature vector data of DWTFOSLBP^{riu2} texture feature extraction technique with 300-dimemnsional feature vector data. The afore-said classification accuracy has been achieved for the feature vector data produced at the 6th level of image decomposition. Further, the PCA reduced feature vector data of DWTFOSLBP-HF texture feature extraction technique has obtained the 2nd best classification accuracy of 98.47±0.77% (600 features) for feature vector data produced at the 4th level of image decomposition.

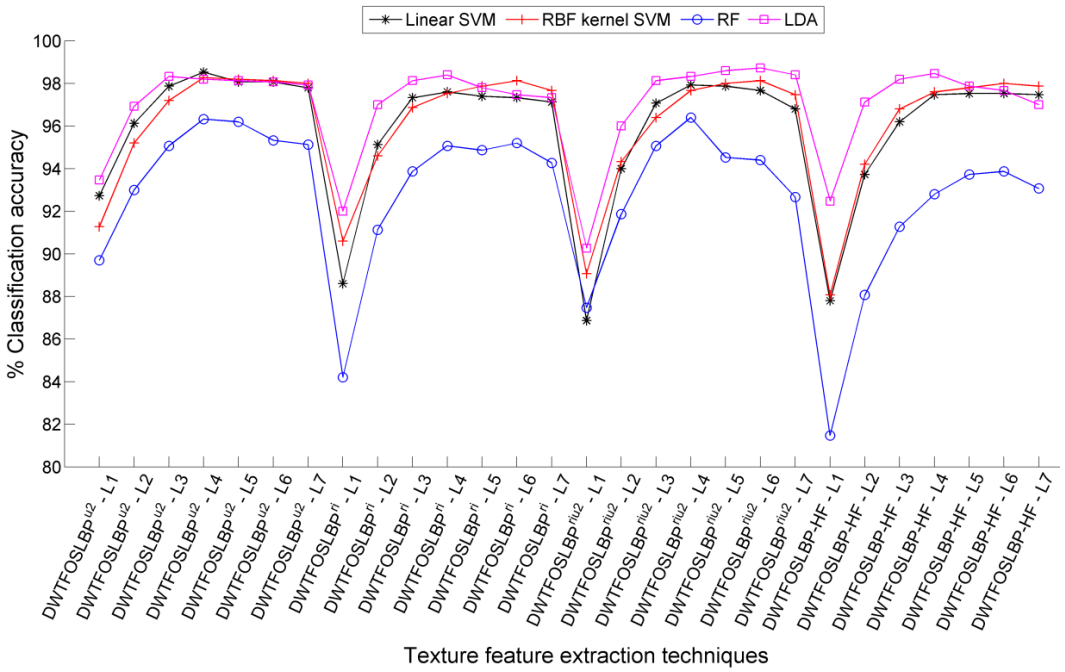

Fig. 6.25 Classification accuracy achieved using PCA reduced feature vector data.

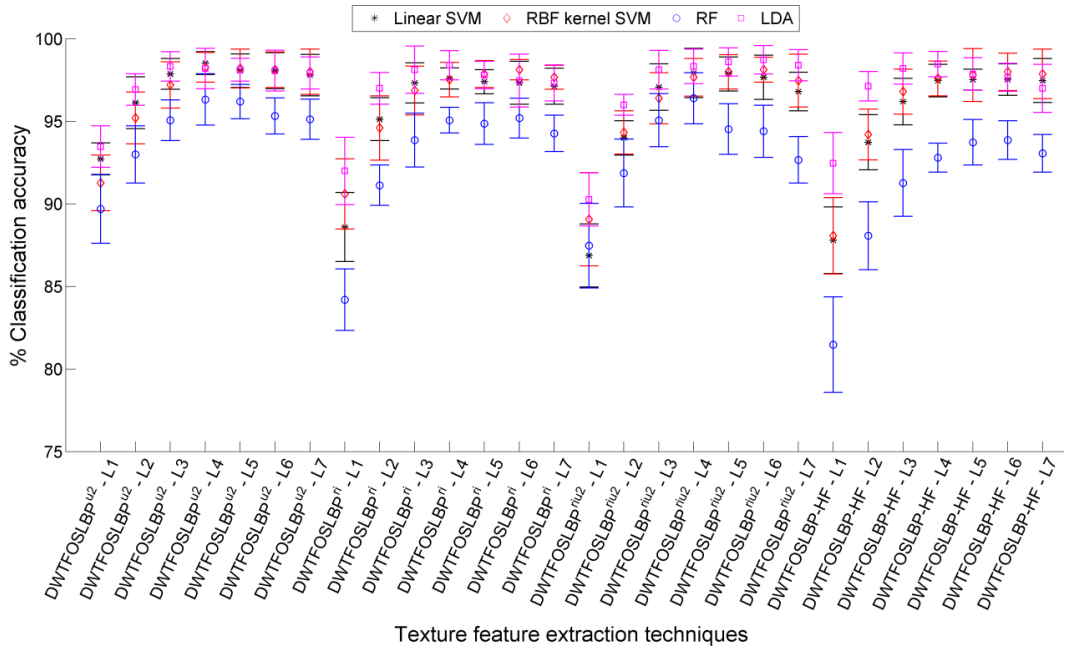

Fig. 6.26 Error bar plot with SD using PCA reduced feature vector data.

The classification accuracy achieved with PCA reduced dimensional feature vector data are at par/superior than their FFVD, but has been obtained using lower-dimensional features. Among the four classifiers, the LDA classifier has obtained maximum classification accuracy (98.73±0.86%) for the feature vector data produced at the 6th level of image decomposition by DWTFOSLBP^{riu2} texture feature extraction technique. The graph depicting the comparison of the classification accuracy obtained by four different classifiers is shown in Fig. 6.25. In addition, the error bar plot of the same is shown in Fig. 6.26. The graphical illustration also supports the claim that DWTFOSLBP^{riu2} texture features classified with LDA classifier has achieved the

best/superlative classification accuracy amongst the proposed techniques with different classifiers.

6.3.5.3 The mRMR feature selection based reduced feature vector data

The subset of feature vector data obtained by mRMR feature selection method has been investigated here to see their effect on the classification accuracy produced for hardwood species classification. The classification accuracy achieved by three different classifiers are listed in Table 6.14. The classification accuracy results are plotted in Fig. 6.27, and error bar plot for the same has been illustrated in Fig. 6.28. The performance of texture feature extraction techniques with different classifiers are as follows:

Table 6.14 Classification accuracy achieved using mRMR feature selection based reduced feature vector data.

Technique	IDL	% CA±SD achieved by classifiers					
		NoF	Linear SVM	NoF	RBF kernel SVM	NoF	RF
$DWTFOSLBP^{u2}$	1	175	93.13±1.81	100	92.80±1.69	50	87.87±2.21
	2	300	96.93±1.64	225	96.73±1.31	125	93.00±1.67
	3	225	97.73±0.78	225	97.87±0.88	150	95.80±1.34
	4	225	98.53±0.82	225	98.67±0.70	125	96.47±1.14
	5	200	98.60±1.06	275	98.87±0.55	200	97.27±1.18
	6	225	98.80±0.82	250	98.93±0.56	175	96.93±1.18
	7	225	98.80±0.82	250	98.93±0.47	175	97.07±1.23
$DWTFOSLBP^{ri}$	1	150	89.53±1.48	150	90.73±1.42	50	86.33±2.02
	2	250	95.27±1.29	125	96.07±1.42	200	92.27±1.61
	3	225	97.87±0.88	200	98.00±1.30	175	95.80±1.63
	4	175	98.47±0.77	225	98.67±0.44	175	96.73±1.06
	5	175	98.53±0.76	175	98.87±0.45	300	96.93±1.05
	6	300	98.80±0.76	225	99.13±0.45	150	97.13±1.44
	7	200	98.87±0.63	250	98.93±0.34	225	96.93±0.84
$DWTFOSLBP^{riu2}$	1	55	87.07±1.51	50	89.27±2.91	55	82.73±2.25
	2	100	94.53±1.50	75	94.73±1.39	100	90.20±1.96
	3	150	97.87±0.93	125	97.06±1.26	165	94.47±1.81
	4	200	98.20±1.26	150	98.13±1.47	150	95.80±1.21
	5	150	98.40±0.84	175	98.40±0.78	200	96.27±1.05
	6	125	98.67±0.88	150	98.60±0.66	150	96.33±1.34
	7	125	98.87±0.77	125	98.60±0.73	75	96.40±1.45
DWTFOSLBP-HF	1	150	87.33±2.72	125	88.47±2.01	100	87.13±2.55
	2	150	94.33±1.76	150	94.87±1.26	200	92.87±1.18
	3	200	98.20±1.00	175	97.87±1.25	150	95.33±1.66
	4	300	98.93±0.47	300	98.47±0.77	300	96.80±1.12
	5	300	99.07±0.47	250	98.87±0.55	300	97.07±1.26
	6	300	99.20±0.42	275	98.93±0.47	175	97.13±1.14
	7	300	99.13±0.55	250	99.07±0.47	300	97.33±0.94

Linear SVM classifier: Amongst the proposed feature extraction techniques, the highest classification accuracy of 99.20±0.42% has been achieved by the mRMR processed subset (300 features) of FFVD of DWTFOSLBP-HF technique at the 6^{th} level of image decomposition. This classification accuracy is comparably better than 97.67±1.00% accuracy obtained by the FFVD of DWTFOSLBP-HF technique (672 features, at the 4^{th} level of image decomposition). The 2^{nd} best classification accuracy of 98.87±0.63% has been obtained by the mRMR processed

subset (200 features) of FFVD of DWTFOSLBP^{ri} technique (at the 7th level of image decomposition).

RBF kernel SVM classifier: The mRMR selected feature subset (225 features) of FFVD of DWTFOSLBP^{ri} texture feature extraction technique (produced at the 6th level of image decomposition) has achieved the best classification accuracy of 99.13±0.45%. This classification accuracy is relatively better than 97.33±0.83% accuracy obtained by the FFVD of DWTFOSLBP^{ri} technique (640 features, at the 4th level of image decomposition). Further, the DWTFOSLBP-HF texture feature extraction techniques feature vector data processed with mRMR feature selection method has also obtained 2nd best classification accuracy of 99.07±0.47% (250 features), better than 97.73±1.48% classification accuracy achieved with their FFVD (840 features).

RF classifier: The RF classifier has achieved the best classification accuracy of 97.33±0.94% for mRMR selected feature subset (300 features) of DWTFOSLBP-HF texture feature extraction technique (at the 7th level of image decomposition). This accuracy is reasonably better than the highest classification accuracy (96.60±1.19%) achieved by the DWTFOSLBP-HF texture feature extraction technique for their FFVD (1176 features, at the 7th level of image decomposition).

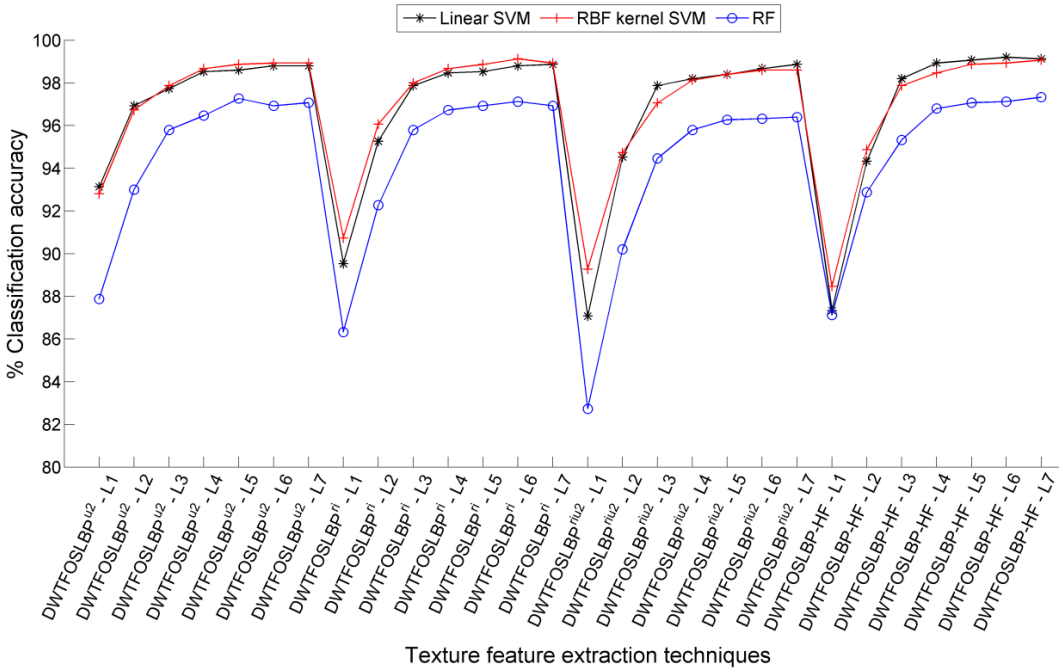

Fig. 6.27 Classification accuracy achieved using mRMR feature selection based reduced feature vector data.

The analysis of Table 6.14 suggests that among the proposed texture feature extraction techniques, the mRMR selected feature subset of DWTFOSLBP-HF technique has achieved the best classification accuracy of 99.20±0.42% with linear SVM classifier. Further, it is observed from Table 6.12 that as the level of image decomposition increases, the length of the feature vector data also increases. The classification accuracy results for FFVD of DWT based hybrid

texture feature extraction techniques with different classifiers have gone up in the range of 4th to 5th level of image decomposition for linear and RBF kernel SVM classifier, and after that either it remains same or decreases little bit. In case of RF classifier the rise in the classification accuracy has been witnessed in the range of 5th to 7th level of image decomposition and after that either it remains same or decreases little bit. It is noticeable that the increase in the classification accuracy has been attained at the cost of additional computation time. Therefore, the DWT based hybrid texture descriptors beyond 7th level of image decomposition have not been investigated.

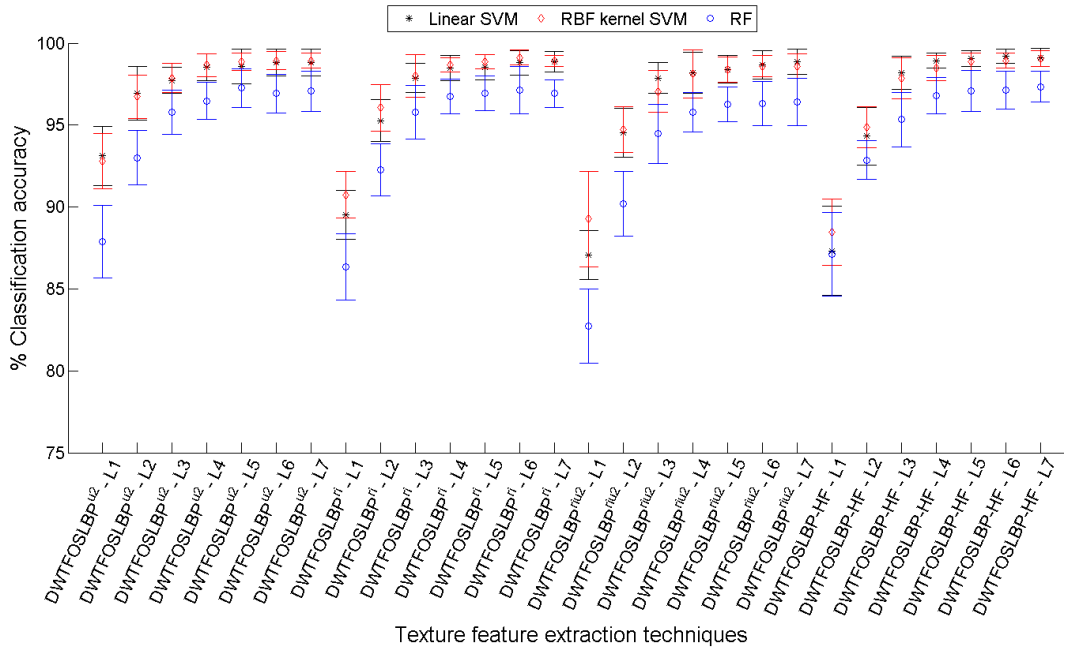

Fig. 6.28 Error bar plot with SD using mRMR feature selection based reduced feature vector data.

It is worth noting that employing PCA and mRMR technique, has not only reduced the computational time of classifiers but at the same time has shown considerable improvement in the classification accuracy of hardwood species. It is also observed from Table 6.12, Table 6.13 and Table 6.14, that DWT based hybrid texture feature extraction techniques for RGB images have achieved better classification accuracy compared to the LBP variants and DWT based hybrid texture feature extraction techniques for grayscale images.

6.3.6 Performance Evaluation of DWT based Hybrid Texture Feature Extraction Techniques for RGB Images using Randomly Divided Database (RDD)

6.3.6.1 Full feature vector data (FFVD)

The classification accuracy achieved by DWT based hybrid texture feature extraction techniques for different ratios of training and testing data is listed in Table 6.15.

Linear SVM classifier: Amongst the proposed texture feature extraction techniques, DWTFOSLBP^{riu2} has produced significant feature vector data that yields best classification

accuracy of 96.67%, 96.44%, 93.83% and 92.27% for 80/20, 70/30, 60/40 and 50/50 training and testing ratios of RDD, respectively. These classification accuracies have been achieved for feature vector data produced by the DWTFOSLBP^{riu2} feature extraction technique at the 5th (70/30, 60/40 & 50/50) and 6th (80/20) levels of image decomposition (Table 6.15).

RBF kernel SVM classifier: Using RBF kernel SVM classifier the best classification accuracy of 96.33%, 95.56%, 93.50% and 92.27% has been achieved for 80/20, 70/30, 60/40 and 50/50 training and testing ratios of RDD, respectively. The classification accuracies have been achieved for feature vector data of DWTFOSLBP^{riu2} technique obtained at the 6th level of image decomposition (Table 6.15).

Table 6.15 Classification accuracy achieved by full feature vector data for different proportions of training and testing data of RDD using three classifiers.

Technique	IDL	% CA achieved by classifiers for different proportions of training and testing data											
		Linear SVM				RBF kernel SVM				RF			
		80/20	70/30	60/40	50/50	80/20	70/30	60/40	50/50	80/20	70/30	60/40	50/50
DWTFOSLBP^{u2}	1	86.00	84.44	83.67	81.60	84.33	81.56	77.17	75.33	77.33	74.44	71.50	71.87
	2	91.67	90.22	87.00	85.33	88.67	86.44	85.17	82.27	86.00	85.56	83.17	81.33
	3	93.33	92.67	91.00	89.07	92.67	91.78	88.83	86.80	91.00	90.44	88.17	86.67
	4	94.33	94.89	93.50	91.47	94.00	93.56	91.00	89.60	91.67	92.44	91.50	90.13
	5	94.67	94.89	93.50	92.40	94.33	94.00	91.50	90.53	93.00	93.11	92.00	90.67
	6	95.00	94.00	93.50	92.27	94.00	93.56	91.83	90.13	93.00	93.56	92.50	90.93
	7	94.33	93.11	94.00	92.00	94.00	93.11	91.67	89.60	93.00	93.11	92.17	90.13
DWTFOSLBP^{ri}	1	87.67	81.33	78.33	76.67	81.33	79.78	78.33	74.80	79.00	74.89	71.33	69.20
	2	90.00	89.56	87.67	84.53	88.67	86.89	85.50	82.13	89.00	86.00	82.33	78.67
	3	94.67	94.00	92.50	89.60	93.00	92.22	90.50	87.47	92.67	92.00	89.33	86.13
	4	95.67	95.11	93.17	92.00	95.00	92.44	91.67	89.87	94.33	92.89	91.00	88.53
	5	95.33	95.11	93.83	92.53	96.00	93.56	92.00	90.67	93.33	92.67	91.67	89.47
	6	95.67	94.00	94.17	92.00	95.67	93.33	92.00	91.20	94.00	93.33	91.50	90.27
	7	96.33	94.22	93.17	91.33	95.67	92.44	92.00	89.47	94.00	92.67	91.67	89.60
DWTFOSLBP^{riu2}	1	83.00	78.00	76.33	75.60	81.00	77.78	74.67	73.60	76.67	73.78	69.33	66.13
	2	91.33	90.67	88.17	86.27	89.67	86.67	85.67	83.20	87.67	85.33	81.83	78.67
	3	94.67	94.00	91.17	89.60	93.33	91.33	89.67	87.47	92.00	89.56	88.67	85.60
	4	96.00	95.78	92.83	92.13	95.00	94.89	92.17	91.07	93.67	91.78	91.00	89.33
	5	96.33	**96.44**	**93.83**	**92.27**	95.67	95.33	92.83	91.33	94.33	92.44	92.17	89.33
	6	**96.67**	95.78	93.33	92.27	**96.33**	**95.56**	**93.50**	**92.27**	94.33	93.33	91.50	90.40
	7	95.67	95.56	92.50	90.67	94.67	94.67	92.33	91.60	94.00	91.78	91.50	89.07
DWTFOSLBP-HF	1	83.00	78.22	74.83	72.27	81.67	76.00	74.67	71.73	81.33	76.89	73.00	71.07
	2	89.67	85.33	85.00	83.47	89.33	87.78	86.33	82.93	88.33	87.11	85.00	82.67
	3	92.67	90.67	89.33	88.27	92.67	91.33	90.17	87.73	91.00	91.33	88.83	86.27
	4	93.67	92.44	91.83	90.93	94.33	93.33	91.83	89.87	92.67	93.11	91.50	89.20
	5	93.67	92.89	92.67	91.07	94.67	93.56	92.83	92.83	94.00	93.11	92.00	**91.20**
	6	94.00	92.44	92.67	90.93	95.00	94.00	92.83	91.07	93.33	93.33	91.83	90.13
	7	94.67	92.67	92.17	90.13	95.33	93.78	92.33	90.53	**95.00**	**93.33**	**92.33**	90.67

RF classifier: As listed in Table 6.15, the feature vector data produced by DWTFOSLBP-HF feature extraction technique has given the best classification accuracy for different proportions of training and testing data of RDD, amongst the proposed techniques using RF classifier. The DWTFOSLBP-HF features have achieved classification accuracy of 95% (at 7th IDL), 93.33%

(at 7th IDL), 92.33% (at 7th IDL) and 91.27% (at 5th IDL) for 80/20, 70/30, 60/40 and 50/50 training and testing ratios, respectively.

The classification accuracies obtained by the three different classifiers are compared for each of the four (80/20, 70/30, 60/40 and 50/50) training and testing ratios, and are graphically illustrated in Fig. 6.29, Fig. 6.30, Fig. 6.31 and Fig. 6.32, respectively. It is apparent from these figures that texture feature vector data produced by most of the DWT based hybrid texture feature extraction techniques for RGB images yields the best classification accuracy with linear SVM classifier,whereas, the least classification accuracy has been achieved with RF classifier.

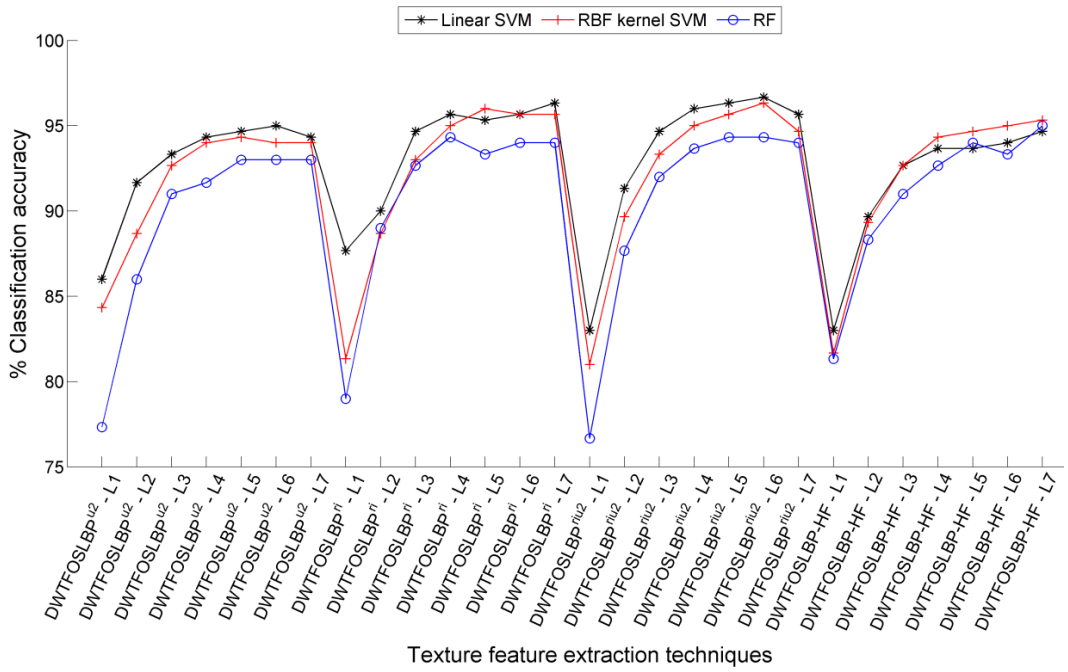

Fig. 6.29 Classification accuracy achieved for 80/20 proportion of training and testing data of RDD.

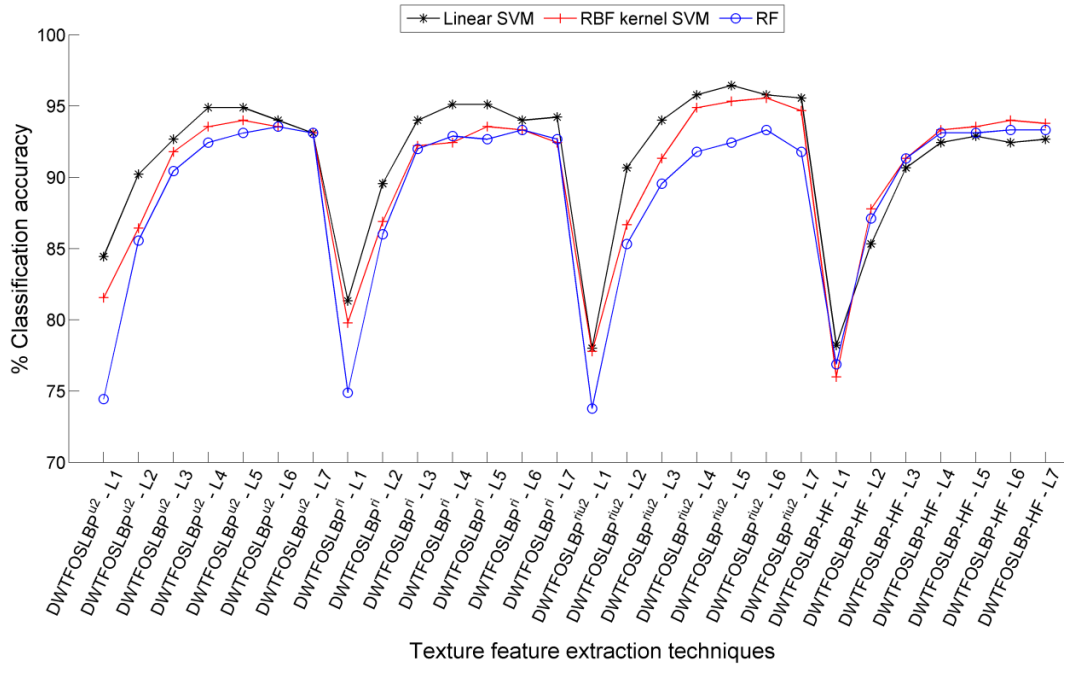

Fig. 6.30 Classification accuracy achieved for 70/30 proportion of training and testing data of RDD.

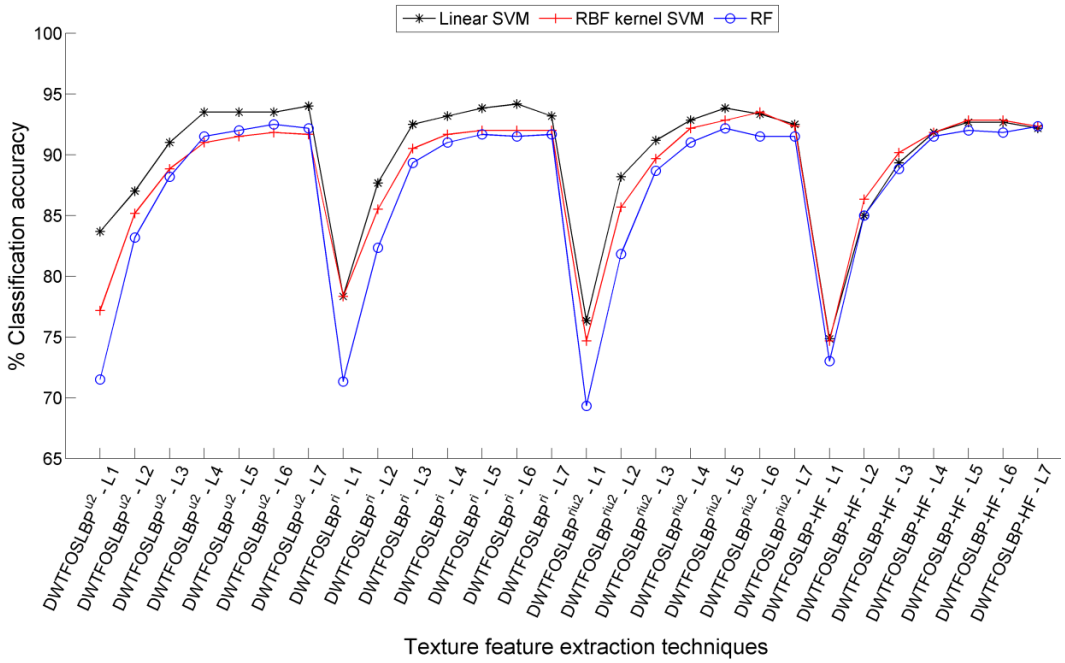

Fig. 6.31 Classification accuracy achieved for 60/40 proportion of training and testing data of RDD.

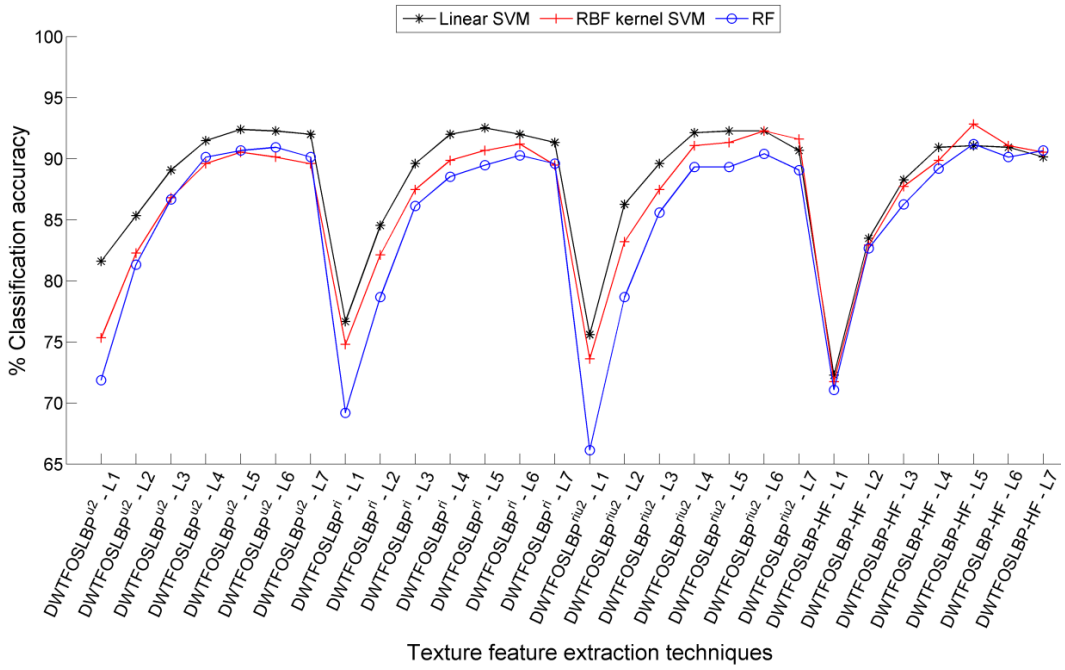

Fig. 6.32 Classification accuracy achieved for 50/50 proportion of training and testing data of RDD.

Further, the classification accuracy obtained by other DWT based hybrid texture feature extraction techniques for RGB images have achieved relatively better classification accuracy compared to the classification accuracy achieved by the DWT based hybrid texture feature extraction techniques for grayscale images.

6.3.6.2 The PCA dimensionality reduced feature vector data

The classification accuracy results obtained by the PCA reduced feature vector data using four different classifiers are concisely discussed below:

Linear SVM classifier: The PCA dimensionality reduced feature vector data of the DWTFOSLBP^{riu2} technique yields the best classification accuracy of 96.33% (150 features), 96.22% (150 features), 93.67% (200 features) and 92.27% (150 features) for 80/20, 70/30, 60/40 and 50/50 training and testing ratios of RDD, respectively. The aforesaid classification accuracy is obtained for feature vector data produced at the 5th level of image decomposition (Table 6.16). This classification accuracy is comparable to the accuracy achieved with FFVD of DWTFOSLBP^{riu2} technique with high-dimensional features.

Table 6.16 Classification accuracy achieved by PCA reduced feature vector data for different proportions of training and testing data of RDD using linear SVM classifier.

Technique	IDL	NoF	80/20	NoF	70/30	NoF	60/40	NoF	50/50
DWTFOSLBP^{u2}	1	100	86.00	225	85.11	225	83.00	200	80.53
	2	200	91.00	200	90.44	250	87.50	400	85.60
	3	100	93.00	150	92.44	100	91.33	200	89.20
	4	200	95.00	150	94.44	400	93.33	450	91.33
	5	100	95.00	250	95.11	250	93.83	350	92.00
	6	150	95.33	300	93.56	500	93.33	300	92.80
	7	350	95.33	300	92.27	250	92.50	600	92.00
DWTFOSLBP^{ri}	1	100	86.00	125	78.89	100	78.00	150	76.27
	2	250	89.00	200	88.89	200	87.50	200	84.40
	3	250	94.67	250	93.78	350	92.67	200	89.87
	4	300	94.33	250	94.44	300	93.33	300	91.87
	5	100	94.67	100	94.44	400	93.50	550	92.40
	6	150	95.33	150	94.00	550	93.83	350	92.40
	7	550	96.00	600	94.89	600	93.33	250	90.80
DWTFOSLBP^{riu2}	1	40	82.00	40	77.56	40	77.17	50	74.93
	2	50	91.00	100	89.56	100	88.17	75	85.33
	3	100	92.67	100	92.44	100	90.83	150	89.33
	4	200	96.33	100	95.33	200	92.83	100	91.33
	5	**150**	**96.33**	**150**	**96.22**	**200**	**93.67**	**150**	**92.27**
	6	250	95.67	250	95.56	300	93.17	300	92.00
	7	200	95.00	200	94.89	250	93.17	350	90.67
DWT FOSLBP-HF	1	150	84.67	125	77.11	150	74.50	125	71.73
	2	250	89.33	250	85.78	300	85.33	250	82.93
	3	350	92.00	350	89.78	300	90.50	350	88.53
	4	300	93.67	500	92.44	450	91.67	500	90.40
	5	350	94.00	500	93.11	450	92.33	500	91.20
	6	250	94.00	500	92.67	450	92.33	600	91.20
	7	450	94.67	600	93.11	550	92.50	600	90.80

RBF kernel SVM classifier: A classification accuracy of 96.67% (50 features), 95.33% (50 features), 93% (250 features) and 92% (100 features) has been obtained for 80/20, 70/30, 60/40 and 50/50 training and testing ratios of RDD, respectively. These results have been achieved by PCA dimensionality reduced feature vector data of the DWTFOSLBP^{ri} technique at the 6th (50/50) and 7th (80/20, 70/30 & 60/40) levels of image decomposition (Table 6.17). The classification accuracies are slightly better than the accuracy presented by the FFVD of DWTFOSLBP^{ri} technique.

Table 6.17 Classification accuracy achieved by PCA reduced feature vector data for different proportions of training and testing data of RDD using RBF kernel SVM classifier.

Technique	IDL	NoF	80/20	NoF	70/30	NoF	60/40	NoF	50/50
	1	200	84.67	50	82.22	100	77.83	250	75.33
	2	50	89.00	50	88.00	100	85.67	250	83.07
	3	250	92.67	450	92.00	200	89.50	450	89.33
$DWTFOSLBP^{u2}$	4	400	94.67	150	94.22	100	92.17	200	90.67
	5	250	94.67	350	94.44	50	92.67	150	91.20
	6	350	95.00	100	94.44	100	93.33	250	91.20
	7	50	95.00	100	94.89	100	93.17	100	91.60
	1	100	82.33	150	80.22	100	79.00	50	75.20
	2	50	89.33	100	87.56	150	85.50	200	82.13
	3	200	92.67	250	92.22	200	90.67	450	87.60
$DWTFOSLBP^{ri}$	4	250	95.00	100	93.33	100	92.17	500	89.87
	5	500	96.00	150	94.89	200	92.67	200	91.07
	6	50	96.67	50	95.11	100	92.67	**100**	**92.00**
	7	**50**	**96.67**	**50**	**95.33**	**250**	**93.00**	50	91.20
	1	30	80.67	40	77.11	40	75.33	50	73.60
	2	50	90.67	50	87.11	50	85.50	100	83.07
	3	100	93.67	100	91.33	100	89.83	150	87.47
$DWTFOSLBP^{riu2}$	4	100	96.00	100	94.89	150	92.17	100	91.07
	5	100	95.67	150	95.33	150	93.17	250	91.60
	6	250	95.67	200	95.56	200	93.00	250	92.13
	7	200	94.33	150	94.44	250	92.17	300	91.47
	1	100	82.00	150	75.78	150	74.33	150	71.87
	2	300	89.33	150	88.22	300	83.33	250	83.20
	3	200	92.67	150	91.56	150	90.17	250	87.87
DWT FOSLBP-HF	4	300	94.67	300	93.33	450	92.17	350	90.00
	5	50	95.33	50	94.89	50	93.00	50	91.07
	6	50	95.33	50	94.89	450	92.83	400	91.60
	7	250	96.00	50	94.89	50	92.83	50	92.00

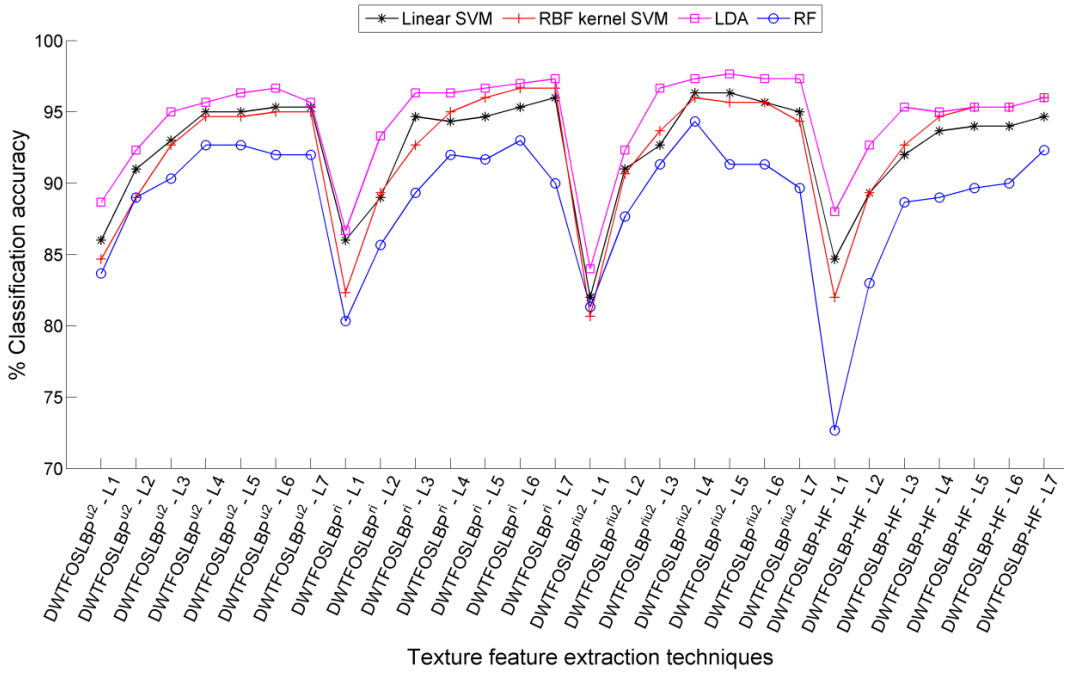

Fig. 6.33 Classification accuracy achieved for 80/20 proportion of training and testing data of RDD.

RF classifier: In this case, the classification accuracy results of 94.33% (100 features), 91.56% (50 features), 90.67% (50 features) and 89.07% (150 features) for 80/20, 70/30, 60/40 and 50/50 training and testing ratios of RDD, respectively, has been obtained by $DWTFOSLBP^{riu2}$

technique with PCA dimensionality reduced feature vector data. The said classification accuracy results are obtained by the feature vector data produced at the 4th level (80/20, 70/30 & 50/50) and 6th level (60/40) of image decomposition, respectively (Table 6.18).

Table 6.18 Classification accuracy achieved by PCA reduced feature vector data for different proportions of training and testing data of RDD using RF classifier.

Technique	IDL	NoF	80/20	NoF	70/30	NoF	60/40	NoF	50/50
	1	100	83.67	100	76.67	50	76.00	100	72.93
	2	50	89.00	50	86.44	50	84.17	100	80.93
	3	100	90.33	100	88.89	150	87.83	150	85.60
$DWTFOSLBP^{u2}$	4	50	92.67	100	91.33	100	89.83	150	88.80
	5	50	92.67	50	91.00	100	90.33	50	89.33
	6	200	92.00	50	90.78	50	89.33	100	89.60
	7	50	92.00	50	90.89	50	88.83	50	87.87
	1	150	80.33	50	74.22	100	73.33	50	70.13
	2	250	85.67	100	84.44	100	82.50	50	79.87
	3	50	89.33	50	87.56	100	86.67	100	85.20
$DWTFOSLBP^{ri}$	4	100	92.00	50	90.44	100	90.00	50	87.20
	5	150	91.67	50	90.67	50	90.17	100	88.13
	6	50	93.00	50	91.33	100	91.17	50	88.93
	7	50	90.00	150	89.78	50	88.33	50	88.13
	1	40	81.33	50	77.33	50	76.83	50	76.53
	2	50	87.67	50	83.33	75	82.67	100	81.73
	3	100	91.33	100	87.56	50	87.33	160	85.33
$DWTFOSLBP^{riu2}$	**4**	**100**	**94.33**	**50**	**91.56**	100	89.33	**150**	**89.07**
	5	50	91.33	50	90.89	50	90.33	50	88.00
	6	50	91.33	50	90.89	**50**	**90.67**	100	87.60
	7	100	89.67	100	88.89	50	87.50	50	85.07
	1	150	72.67	150	71.56	125	67.67	125	63.07
	2	200	83.00	50	78.67	150	77.33	50	73.33
	3	50	88.67	50	87.11	100	85.17	50	82.00
DWT FOSLBP-HF	4	100	89.00	100	86.89	100	85.67	100	83.60
	5	50	89.67	50	87.78	100	87.17	50	85.87
	6	50	90.00	50	89.56	50	87.83	100	86.40
	7	50	92.33	50	89.33	50	88.33	50	85.33

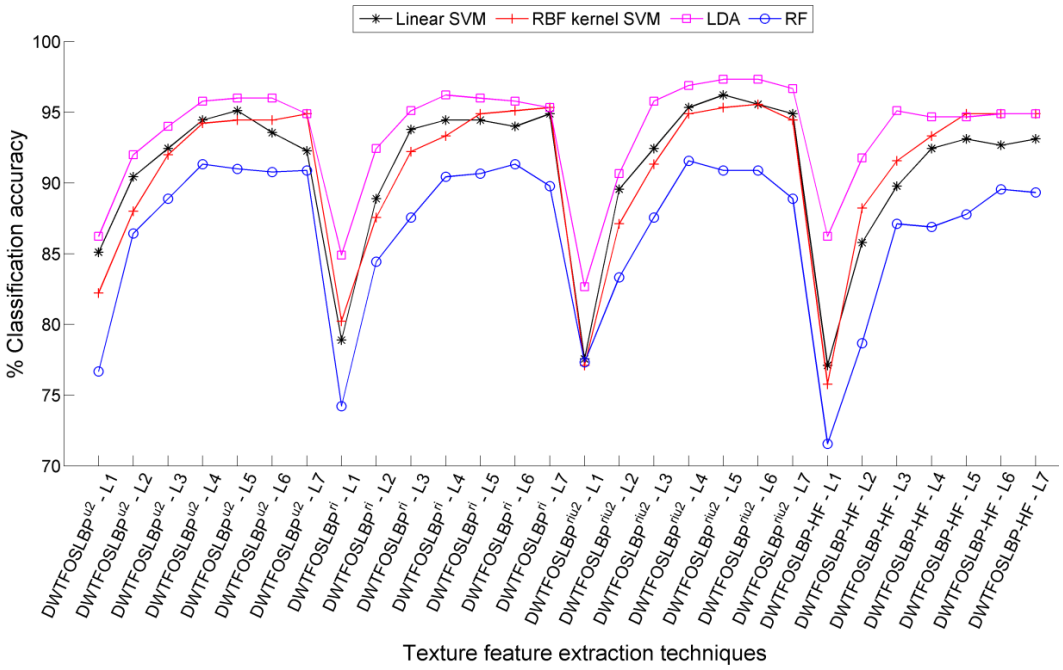

Fig. 6.34 Classification accuracy achieved for 70/30 proportion of training and testing data of RDD.

Table 6.19 Classification accuracy achieved by PCA reduced feature vector data for different proportions of training and testing data of RDD using LDA classifier.

Technique	IDL	NoF	80/20	NoF	70/30	NoF	60/40	NoF	50/50
	1	225	88.67	50	86.22	50	85.83	50	84.00
	2	200	92.33	300	92.00	100	90.83	100	89.07
	3	100	95.00	300	94.00	100	93.33	100	93.07
DWTFOSLBP^{u2}	4	100	95.67	300	95.78	100	95.00	100	94.00
	5	300	96.33	200	96.00	50	94.67	200	94.00
	6	300	96.67	200	96.00	150	94.67	200	94.40
	7	100	95.67	100	94.89	150	94.17	100	92.67
	1	125	86.67	150	84.89	150	84.00	125	82.13
	2	300	93.33	300	92.44	250	91.50	300	89.07
	3	450	96.33	350	95.11	250	93.33	200	92.00
DWTFOSLBP^{ri}	4	100	96.33	300	96.22	100	94.33	100	93.60
	5	100	96.67	200	96.00	250	95.17	100	94.13
	6	100	97.00	100	95.78	100	94.67	100	93.73
	7	200	97.33	200	95.33	50	94.50	50	92.53
	1	50	84.00	50	82.67	50	83.83	50	81.87
	2	100	92.33	100	90.67	75	90.17	75	89.87
	3	125	96.67	150	95.78	150	94.50	150	92.80
DWTFOSLBP^{riu2}	4	200	97.33	200	96.89	200	95.33	175	94.00
	5	**200**	**97.67**	**150**	**97.33**	**150**	**95.50**	**200**	**94.40**
	6	312	97.33	300	97.33	300	95.33	300	94.27
	7	350	97.33	350	96.67	350	95.00	350	93.60
	1	150	88.00	150	86.22	125	85.83	150	85.20
	2	250	92.67	300	91.77	300	91.67	300	88.93
	3	400	95.33	400	95.11	350	93.83	250	92.67
DWT FOSLBP-HF	4	350	95.00	450	94.67	400	93.83	350	92.40
	5	450	95.33	200	94.67	200	93.33	200	92.13
	6	50	95.33	100	94.89	50	93.83	50	92.00
	7	50	96.00	100	94.89	50	94.33	100	92.00

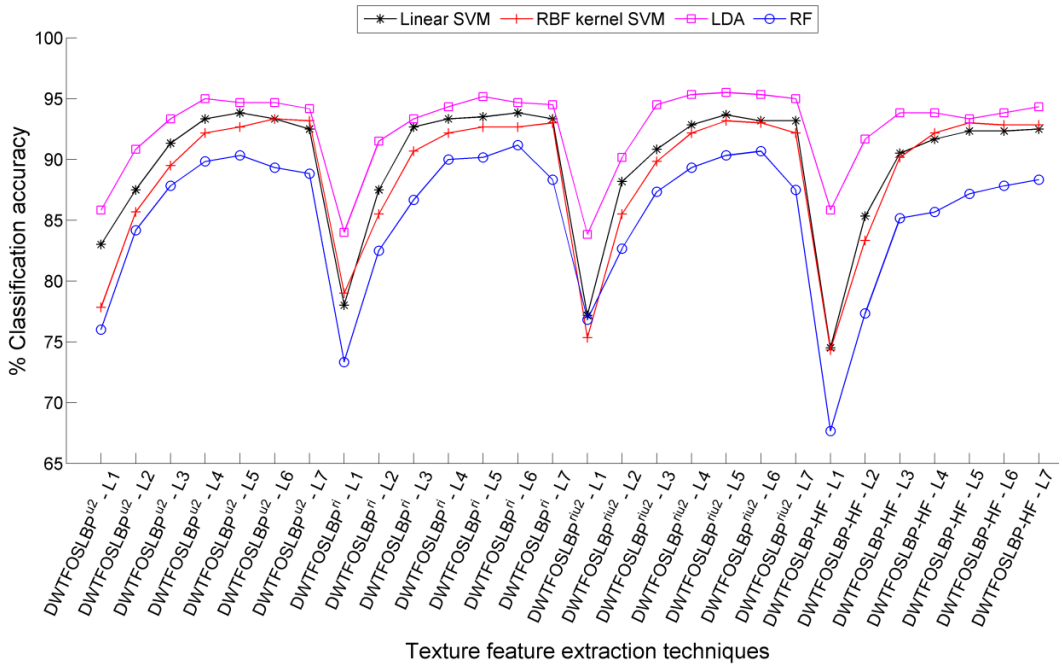

Fig. 6.35 Classification accuracy achieved for 60/40 proportion of training and testing data of RDD.

LDA classifier: Amongst the proposed feature extraction techniques, the PCA dimensionality reduced feature vector data of the DWTFOSLBP^{riu2} technique has achieved classification

accuracy of 97.67% (200 features), 97.33% (150 features), 95.50% (150 features) and 94.40% (200 features) for 80/20, 70/30, 60/40 and 50/50 training and testing ratios of RDD, respectively. These classification accuracies are obtained for PCA reduced feature vector data produced at the 5th level of image decomposition (Table 6.19).

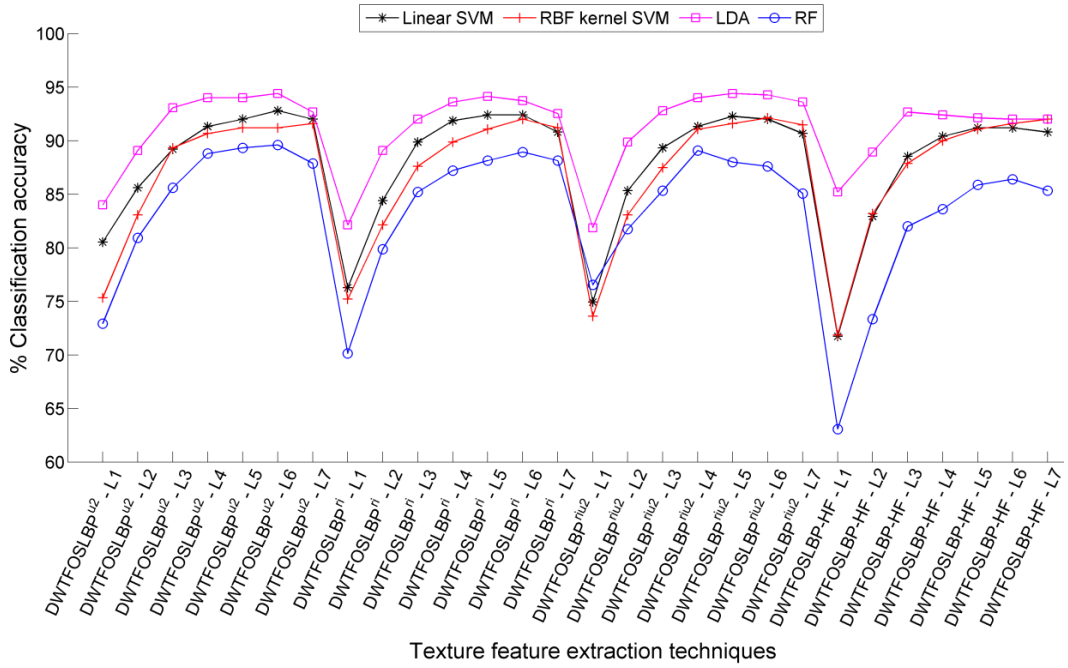

Fig. 6.36 Classification accuracy achieved for 50/50 proportion of training and testing data of RDD.

The graphical illustration of PCA reduced feature vector data of DWT based hybrid texture feature extraction techniques for RGB images are shown in Fig. 6.33, Fig. 6.34, Fig. 6.35 and Fig. 6.36 for 80/20, 70/30, 60/40 and 50/50 training and testing ratios of RDD, respectively. It is clearly visible that the PCA reduced feature vector data has given the best classification accuracy with LDA classifier, whereas RF classifier has achieved lowest classification accuracy among the four classifiers. Thus, incorporating PCA for feature dimensionality reduction has improved the performance of DWT based hybrid texture feature extraction techniques (RGB images) for hardwood species classification with low-dimensional feature vector data.

6.3.6.3 The mRMR feature selection based reduced feature vector data

The classification accuracy results achieved by the mRMR feature selection reduced feature vector data of DWT based hybrid texture feature extraction techniques with three different classifiers have been presented in Table 6.20, Table 6.21 and Table 6.22, respectively. The classification accuracy obtained by each of the classifiers for proposed texture feature extraction techniques are discussed below:

Linear SVM classifier: The subset of feature vector data of DWTFOSLBP^{ri} texture feature extraction technique, chosen with mRMR feature selection method, yields the best classification accuracy of 97.33% (600 features), 97.33% (500 features), 94.67% (350 features) and 94%

(550 features) for 80/20, 70/30, 60/40 and 50/50 training and testing ratios of RDD, respectively (Table 6.20). The aforesaid classification accuracies have been achieved by the feature vector data of DWTFOSLBP^{ri} technique at the 6th (50/50) and 7th (80/20, 70/30 & 60/40) levels of image decomposition.

Table 6.20 Classification accuracy achieved by mRMR feature selection based reduced feature vector data for different proportions of training and testing data of RDD using linear SVM classifier.

Technique	IDL	NoF	80/20	NoF	70/30	NoF	60/40	NoF	50/50
	1	100	86.00	200	85.56	200	84.00	225	81.33
	2	350	92.33	200	90.22	350	88.00	250	86.13
	3	200	94.33	400	93.33	400	91.00	350	91.07
DWTFOSLBP^{u2}	4	250	96.00	250	95.56	350	93.33	550	93.33
	5	450	97.00	250	96.00	250	93.50	350	93.47
	6	400	96.33	250	95.78	250	93.93	400	93.60
	7	450	97.00	350	96.22	300	93.67	300	93.33
	1	150	88.67	150	80.89	150	78.83	150	76.67
	2	250	91.00	300	89.56	250	87.50	150	86.27
	3	300	95.33	100	94.89	300	92.83	200	90.27
DWTFOSLBP^{ri}	4	600	96.00	100	96.00	450	93.83	400	92.40
	5	400	96.33	500	96.22	550	94.67	400	93.47
	6	500	97.33	150	97.11	500	94.67	**550**	**94.00**
	7	**600**	**97.33**	**500**	**97.33**	**350**	**94.67**	600	93.87
	1	50	83.67	40	79.33	40	78.17	40	77.20
	2	75	90.67	100	89.78	100	88.17	75	86.00
	3	100	94.33	100	93.56	150	91.67	150	90.27
DWTFOSLBP^{riu2}	4	200	96.00	200	95.56	200	93.50	100	92.80
	5	250	96.33	150	96.00	200	93.83	250	92.27
	6	200	96.67	200	96.67	250	93.67	150	92.40
	7	150	96.67	200	96.67	300	94.00	150	92.93
	1	150	82.33	50	80.67	50	75.33	50	74.67
	2	150	91.00	100	89.33	100	88.33	50	85.60
	3	100	94.67	100	93.56	200	91.00	150	89.47
DWT FOSLBP-HF	4	200	97.00	150	95.56	200	93.33	200	92.33
	5	200	96.00	200	96.67	250	94.33	250	93.73
	6	550	96.33	400	96.00	200	94.50	200	93.33
	7	600	97.00	400	96.67	250	94.67	400	93.87

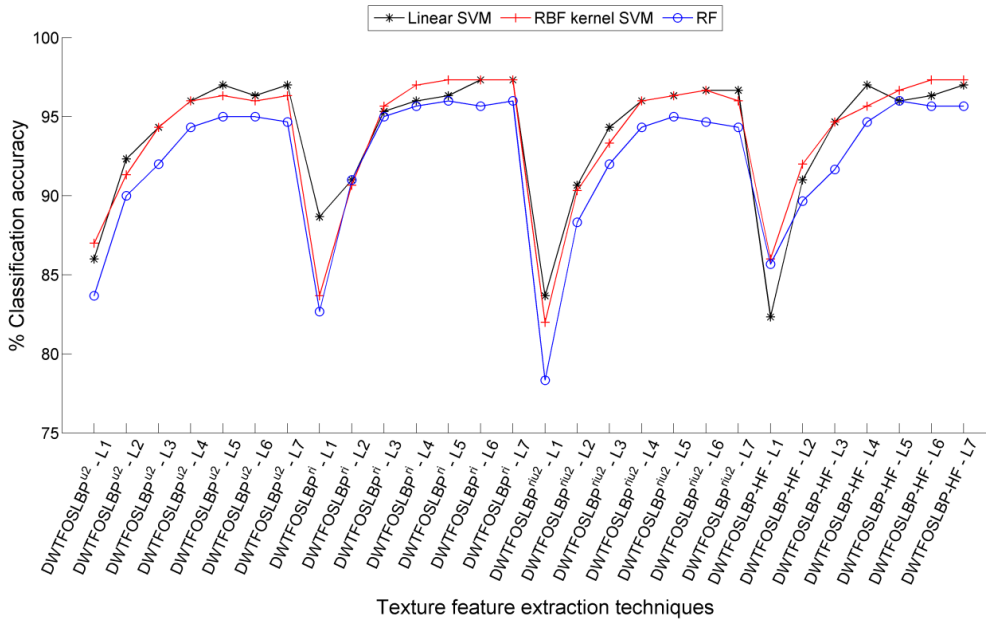

Fig. 6.37 Classification accuracy achieved for 80/20 proportion of training and testing data of RDD.

Table 6.21 Classification accuracy achieved by mRMR feature selection based reduced feature vector data for different proportions of training and testing data of RDD using RBF kernel SVM classifier.

Technique	IDL	NoF	80/20	NoF	70/30	NoF	60/40	NoF	50/50
	1	50	87.00	50	82.89	200	79.17	150	76.67
	2	150	91.33	100	91.78	150	87.83	150	86.40
	3	250	94.33	250	94.22	100	91.33	100	90.13
$DWTFOSLBP^{u2}$	4	150	96.00	150	95.78	200	93.33	200	92.93
	5	300	96.33	300	95.78	550	94.00	150	93.60
	6	400	96.00	300	96.00	250	94.17	300	93.20
	7	400	96.33	400	96.22	350	94.33	300	93.20
	1	50	83.67	50	81.11	50	78.67	50	75.20
	2	50	90.67	50	90.00	100	87.50	50	86.27
	3	100	95.67	50	94.67	200	92.50	150	90.83
$DWTFOSLBP^{ri}$	4	100	97.00	100	96.67	100	94.17	50	93.07
	5	450	97.33	450	96.89	350	94.17	300	93.47
	6	450	97.33	500	97.11	350	94.67	350	94.00
	7	**500**	**97.33**	**500**	**97.11**	**400**	**94.67**	**400**	**94.13**
	1	30	82.00	30	78.22	30	76.83	50	74.53
	2	50	90.33	50	89.33	50	87.33	50	85.20
	3	50	93.33	50	93.33	50	91.00	100	89.33
$DWTFOSLBP^{riu2}$	4	150	96.00	100	95.33	150	93.67	50	92.40
	5	200	96.33	200	96.00	200	94.17	200	93.33
	6	200	96.67	150	96.22	250	94.17	150	93.33
	7	200	96.00	150	96.22	250	93.67	200	93.20
	1	50	86.00	50	81.56	50	77.17	50	74.67
	2	50	92.00	50	91.78	100	89.50	50	85.87
	3	150	94.67	150	94.44	200	92.17	200	90.53
DWT FOSLBP-HF	4	150	95.67	150	95.33	100	94.17	100	93.60
	5	250	96.67	200	96.44	200	94.67	150	94.00
	6	250	97.33	150	97.11	350	94.67	200	94.40
	7	**500**	**97.33**	**200**	**97.11**	**350**	**95.00**	**200**	**94.93**

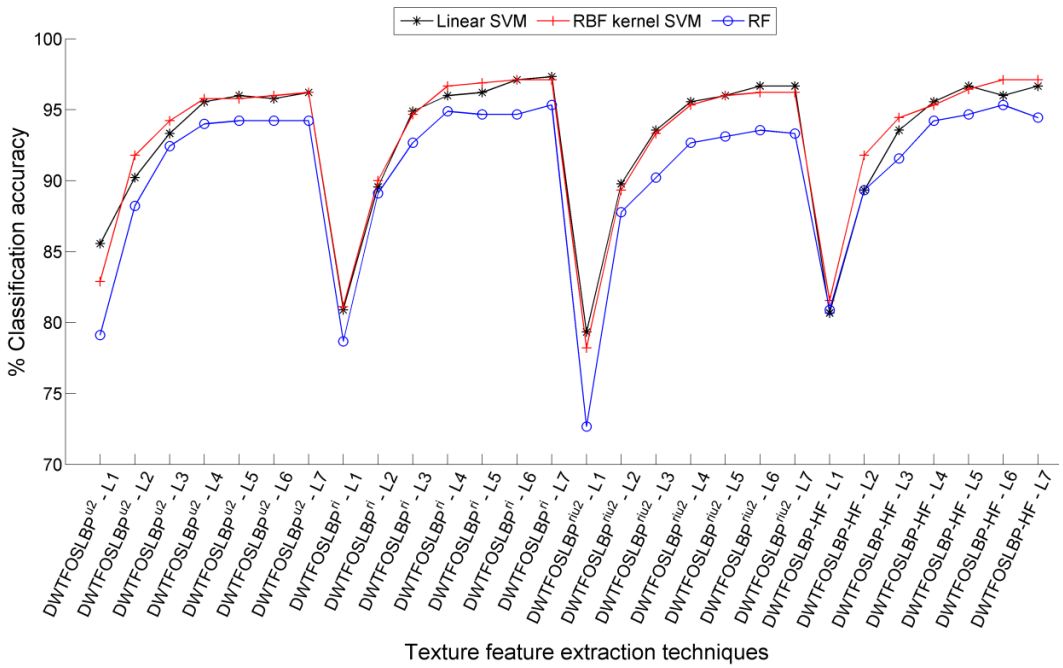

Fig. 6.38 Classification accuracy achieved for 70/30 proportion of training and testing data of RDD.

RBF kernel SVM classifier: The subset of feature vector data of DWTFOSLBP-HF texture feature extraction technique processed through mRMR feature selection method has achieved

the best classification accuracy of 97.33% (500 features), 97.11% (200 features), 95% (350 features) and 94.93% (200 features) for 80/20, 70/30, 60/40 and 50/50 training and testing ratios of RDD, respectively. The accuracy is achieved for feature vector data obtained at the 7th level of image decomposition. Further, comparable classification accuracy of 97.33% (500 features), 97.11% (500 features), 94.67% (400 features) and 94.13% (400 features) for 80/20, 70/30, 60/40 and 50/50 training and testing ratios of RDD, respectively, has been achieved for mRMR processed feature vector data of DWTFOSLBP^{ri} technique at the 7th level of image decomposition (Table 6.21).

Table 6.22 Classification accuracy achieved by mRMR feature selection based reduced feature vector data for different proportions of training and testing data of RDD using RF classifier.

Technique	IDL	NoF	80/20	NoF	70/30	NoF	60/40	NoF	50/50
	1	50	83.67	50	79.11	50	76.83	50	74.27
	2	350	90.00	100	88.22	150	86.50	150	84.93
	3	200	92.00	300	92.44	300	90.83	350	88.80
DWTFOSLBP^{u2}	4	400	94.33	400	94.00	350	93.00	200	91.20
	5	300	95.00	350	94.22	250	93.17	200	91.60
	6	350	95.00	450	94.22	400	93.00	400	91.60
	7	100	94.67	400	94.22	350	93.17	350	91.60
	1	50	82.67	50	78.67	50	76.17	50	73.87
	2	100	91.00	150	89.11	100	85.83	50	83.07
	3	150	95.00	150	92.67	100	90.83	200	88.80
DWTFOSLBP^{ri}	4	150	95.67	300	94.89	200	92.67	250	91.20
	5	400	96.00	200	94.67	250	93.67	50	91.33
	6	150	95.67	150	94.67	**350**	**94.00**	300	91.20
	7	**250**	**96.00**	**400**	**95.33**	400	93.33	**250**	**91.47**
	1	30	78.33	30	72.67	50	70.33	30	68.33
	2	50	88.33	50	87.78	75	84.50	50	80.67
	3	100	92.00	50	90.22	100	88.33	100	87.60
DWTFOSLBP^{riu2}	4	150	94.33	100	92.67	150	92.83	150	90.27
	5	150	95.00	100	93.11	150	92.50	150	90.27
	6	150	94.67	200	93.56	150	92.67	100	90.13
	7	250	94.33	200	93.33	200	92.67	250	90.00
	1	100	85.67	50	80.89	50	78.17	50	76.80
	2	200	89.67	150	89.33	150	86.33	250	84.00
	3	100	91.67	200	91.56	200	89.67	200	88.53
DWT FOSLBP-HF	4	250	94.67	250	94.22	250	93.33	150	90.67
	5	300	96.00	400	94.67	150	93.00	300	91.60
	6	150	95.67	150	95.33	400	93.33	300	91.60
	7	550	95.67	400	94.44	250	93.67	400	91.47

RF classifier: The mRMR feature selection based feature vector data of DWTFOSLBP^{ri} technique yields the best classification accuracy of 96% (250 features), 95.33% (400 features), 94% (350 features) and 91.47% (250 features) for 80/20, 70/30, 60/40 and 50/50 training and testing ratios of RDD, respectively (Table 6.22). The aforesaid classification accuracies have been achieved for the feature vector data of DWTFOSLBP^{ri} technique at the 6th (60/40) and 7th (80/20, 70/30 & 50/50) levels of image decomposition.

The graphical illustration of mRMR feature selection reduced feature vector data of DWT based hybrid texture feature extraction techniques for RGB images are shown in Fig. 6.37, Fig. 6.38, Fig. 6.39 and Fig. 6.40 for 80/20, 70/30, 60/40 and 50/50 training and testing ratios of

RDD, respectively. It is clearly visible that the mRMR feature selection reduced feature vector data has given the best classification accuracy with both linear SVM and RBF kernel SVM classifier, whereas RF classifier has achieved lowest classification accuracy among the three classifiers. Thus, incorporating mRMR method for feature selection has improved the performance of DWT based hybrid texture feature extraction techniques (RGB images) for hardwood species classification with low-dimensional feature vector data.

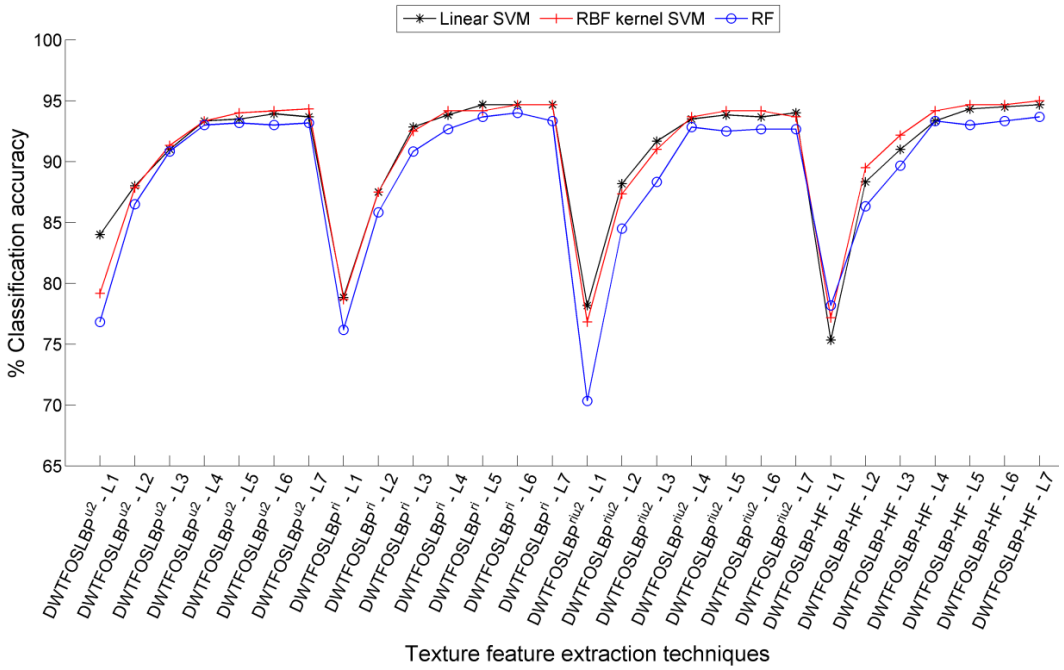

Fig. 6.39 Classification accuracy achieved for 60/40 proportion of training and testing data of RDD.

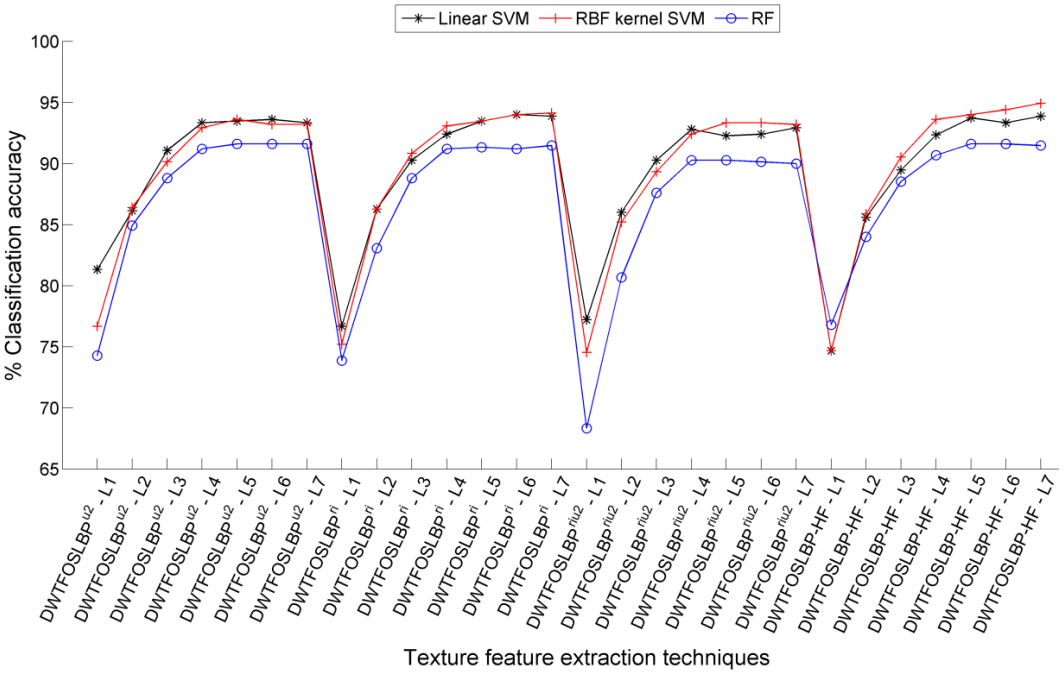

Fig. 6.40 Classification accuracy achieved for 50/50 proportion of training and testing data of RDD.

Further, other DWT based hybrid texture feature extraction techniques (RGB images) have improved the classification accuracy in comparison to the DWT based hybrid texture feature extraction techniques (grayscale images) and LBP variants texture feature extraction techniques. Also, employing mRMR feature selection technique for reducing the number of features has given much better classification accuracy results compared to the FFVD, that too with lower-dimensional feature vector data. The above analysis suggests that DWT based hybrid texture feature extraction techniques acquire significant features of the images and are well suited for the classification of hardwood species using both the 10-fold cross validation and RDD approaches.

The FOS and variants of LBP techniques are simple yet computationally efficient feature extraction techniques. For a given image, the LBP variants produce local texture descriptors while the FOS is a global texture descriptor. Thus, an effort has been made here to combine these descriptors to get the significant features of images at multiresolution without involving large increase in the number of features. This is the reason why combination of FOS and variants of LBP at multiresolution have been chosen here.

Furthermore, the FFVD produced by most of the variants of DWTFOSLBP techniques (for grayscale and RGB images) could not improve the classification accuracy significantly beyond the 4^{th} to 6^{th} levels of image decomposition, rather same or the lower classification accuracy have been reported as shown in Table 6.1 and Table 6.12. This happens because the subimages produced by DWT decomposition beyond the 4^{th}/6^{th} level of image decomposition do not encompass qualitative visible information (though statistically significant features do exist). In addition, inclusion of further levels of image decomposition gives rise to computation time without considerable improvement in the classification accuracy. Therefore, in this work up to 7 levels of image decomposition by DWT has been performed. An important observation which is worthy to be noted here is that incorporating DWT with FOS and LBP variants has extracted distinct texture features of hardwood species image. Further, combining FOS and LBP features together at different levels of image decomposition improves discrimination capability of a classifier for hardwood species.

6.4 SUMMARY

The proposed work demonstrated the effectiveness of four variants of LBP texture features for the classification of hardwood species into 75 different categories by using DWT based hybrid texture feature extraction techniques. These techniques integrate the multiresolution capability of DWT with FOS and variants of LBP. Initially, the images have been decomposed using DWT and then texture features are extracted from these images by FOS and LBP variants. The effectiveness of the proposed techniques has been investigated on an open access database of hardwood species consisting of 1500 microscopic images samples of 75 hardwood species

using 10-fold cross validation and RDD approach. The performance of the texture features obtained by the proposed techniques at 7 different levels of images decomposition is evaluated in terms of classification accuracy by using linear SVM, RBF kernel SVM, LDA and RF classifiers.

The comprehensive analysis of the results produced by 10-fold cross validation approach shows that amongst the proposed texture feature extraction techniques the $DWTFOSLBP^{u2}$ has obtained best classification accuracy of 97.67±0.79% and 98.40±0.64% for grayscale and RGB images, respectively. These accuracies are achieved for FFVD of $DWTFOSLBP^{u2}$ using linear SVM classifier.

Further, the PCA dimensionality reduced feature vector data of the $DWTFOSLBP^{u2}$ texture feature extraction technique has achieved the best classification accuracy of 97.93±1.39% (100 features) using RBF kernel SVM classifier (at the 5^{th} level of image decomposition) for grayscale images; while a classification accuracy of 98.53±0.69% (450 features) has been achieved for the $DWTFOSLBP^{u2}$ texture feature extraction technique (at the 4^{th} level of image decomposition) for RGB images using linear SVM classifier.

Furthermore, the reduction in feature vector data is achieved by mRMR feature selection method and it is seen that DWTFOSLBP-HF texture features using linear SVM classifier produces the best classification accuracy of 99.00±0.79% (275 features) and 99.20±0.42% (300 features) at the 5^{th} and 6^{th} level of image decomposition for grayscale and RGB images, respectively. Also, texture features obtained by proposed techniques classified by RBF kernel SVM classifier has also delivered comparable classification accuracy for both RGB and grayscale images.

In case of randomly dividing the database into fixed proportions (80/20, 70/30, 60/40 and 50/50) of training and testing ratios, the usage of DWT based hybrid texture features have achieved superior results. Amongst the proposed texture feature extraction techniques the $DWTFOSLBP^{riu2}$ has obtained the best classification accuracy of 95.33, 94.22, 92.83, 91.73 and 96.67, 96.44, 93.83, 92.27 for grayscale and RGB images, respectively. These accuracies are achieved for FFVD of $DWTFOSLBP^{riu2}$ technique at the 4^{th} and 6^{th} levels of image decomposition for grayscale and RGB images, respectively, using linear SVM classifier.

Further, the PCA dimensionality reduced feature vector data of the $DWTFOSLBP^{riu2}$ texture feature extraction technique using LDA classifier has achieved the best classification accuracy of 96.33% (150 features), 95.56% (260 features), 94.17% (200 features), 93.73% (200 features) and 97.67% (200 features), 97.33% (150 features), 95.50% (150 features) 94.40% (200 features) for grayscale and RGB images, respectively.

Furthermore, the reduction in feature vector data is achieved by mRMR feature selection method and it is seen that DWTFOSLBP-HF texture features achieved the best classification accuracy of 96.33% (200 features), 95.56% (200 features), 94% (200 features), and 93.47%

(150 features) with linear SVM classifier for grayscale images. Further, DWTFOSLBP-HF texture features achieved the best classification accuracy of 97.33% (500 features), 97.11% (200 features), 95.00% (350 features) 94.93% (200 features) for RGB images using RBF kernel SVM classifier.

The classification accuracy achieved by the features produced by the proposed techniques is based on the use of Daubechies wavelet (db3) for image decomposition. It worth pointing out that, the texture features acquired by DWT based hybrid texture feature extraction techniques for hardwood species are of excellent quality and no significant information loss is reported when features of grayscale image is employed for the classification. Further the slight improvement in the classification accuracy for the RGB images (99.20±0.42%) compared to grayscale images (99.00±0.79%) for mRMR based reduced feature dataset of DWTFOSLBP-HF technique is achieved at the cost of almost thrice the computational time taken by RGB images to extract features from these images.

CHAPTER 7. SEGMENTATION AND DETERMINATION OF VESSEL ELEMENTS

This chapter observes the digital image processing methods used to extract the vessel elements of hardwood species images and measure the hydraulic conductivity of each of the vessels and thereby specifying the hydraulic conductivity of the hardwood trees. It starts with concise introduction of techniques used for accomplishing the task, the methodology of vessel elements determination and finding their hydraulic conductivity.

7.1 INTRODUCTION

There are lot of variations in the density [123] and strength of wood of different species. These variations are characterized by the size and density of vessel elements present in the secondary xylem. The heartwood of balsa (*Ochroma pyramidale*) possess large vessel elements, and is correspondingly light in density, while the heartwood of the Brazilian ironwood (*Caesalpinia ferrea*) has small vessel elements and are found to be very dense [256].

The examination of vessel elements (especially secondary xylem vessel elements) provides significant information that may be quite useful to the wood anatomist. Some of the useful features are the wall size (thick or thin), diameter (narrow or wide), length of vessel elements and number of vessel elements per mm^2. The part of the deviation in the vessel characters may be the outcome of functional adaptations to different climatic zones and environments, particularly with reference to conductive efficiency and safety [110]. The plants having thick-walled vessel elements are likely to be found in dry areas [13, 29] and these thick-walled vessel elements might contribute to the strength of the wood.

The large diameter vessel elements offer minimal friction and add in to greater conductive efficiency [11, 245]. However, the narrow vessel elements may not be considered as a form of conductive inefficiency. Further, the plants have various lengths of vessels. The long vessels characterize the wide earlywood vessels; vessels in latewood are shorter. The longer vessels endorse better conductive efficiency, whereas, shorter vessels advocate greater safety.

The above discussion suggests that the study of wood anatomical structures may be helpful in describing the contribution of each of the elements of hardwood species. In this study, the work is confined to the extraction of vessel elements of hardwood species. The vessel elements have key contribution in the transportation of water from the roots to leaves of tree. Once, the vessel elements are delineated from other elements (rays, parenchyma and fibers) of hardwood species, the next task is to measure area and diameter of these elements. In addition, the hydraulic conductivity and lumen resistivity of each of the vessel elements are calculated.

In the year 2013, Scholz *et al*., [182] have carried out an investigation on various techniques useful for the quantification of wood conduits. The study reports several image

analysis tools [50] for the quantification of wood; which are useful in better understanding of wood anatomy. The traditional techniques of vessel elements measurement (diameter, number of vessels per mm^2) make use of light microscopy images. Since the definitions and methodology used to acquire the anatomical features amongst the anatomist vary considerably, the difficulty arises in achieving reliable and unbiased data. Several techniques of quantification of xylem conduits (vessels, tracheid) are available. These techniques have certain advantages and disadvantages associated with them [185].

In the year 2009, Yu *et al*., [229] have suggested use of computers to measure the cellular tissue proportions of broad leaved (vessel, fiber and xylem ray) and coniferous (resin canal tracheid and ray) trees. The results attained with the machine vison based systems are found to be accurate, efficient and time saving compared to conventional methods (weighing and grid counting). Further, the pore (vessel elements present in cross-sectional view) features of hardwood species have been extracted using mathematical morphology by QI *et al*. [178]. An adaptive method (genetic algorithm) was employed by Wang *et al*. [209] to obtain optimal threshold of closed region area for pore segmentation.

Pan and Kudo [159] have used the radius of structuring element decided by the mathematical morphology with a variable structuring element, which has resulted into decent quality segmentation for 25 out of 30 wood samples, whereas 5 samples were found to have conflicting radii. The only shortcoming noticeable was, the time required to execute the segmentation task was considerably on the higher side. Though there are several machine vision based techniques proposed for wood quantification [128,182], but each of them have related drawbacks.

Some other approaches of vessel elements extraction from the microscopic images have also been suggested by the researchers. The ROXAS is one such software available for segmentation and extraction of elements of hardwood species [206, 207, 215]. But, the ROXAS software only works with Image Pro Plus software. Thus, in this work an effort has been made to propose a platform independent tool based on simple digital image processing technique to quantify wood vessel elements and measure the hydraulic conductivity and lumen resistivity of the vessel elements.

7.2 IMAGE DATABASE

Wood samples were obtained from the Xylarium (DDw) of the Wood Anatomy Discipline of the Forest Research Institute, Dehradun. Small blocks of the authentic wood samples were boiled for softening and then cooled. Small wood blocks were taken out and cross, radial and tangential sections were prepared (sections were cut on a Reichert sliding microtome). These sections were stained in haematoxylin and then counter stained in safranin. Standard laboratory procedure was followed for mounting the sections after dehydrating them through the alcohol

series. Photomicrographs of cross, radial and tangential sections and other diagnostic features were prepared. The images are acquired at 5x zoom by Carl Zeiss Axio Scope.A1 polarized light microscope. These images have a resolution of 1044×1388, and each pixel value corresponds to 1.2824 µm

7.3 METHODOLOGY

The procedure adapted to accomplish the task of vessel elements delineation out of the four key elements of hardwood species are illustrated in Fig. 7.1. A brief description of these procedures are presented below:

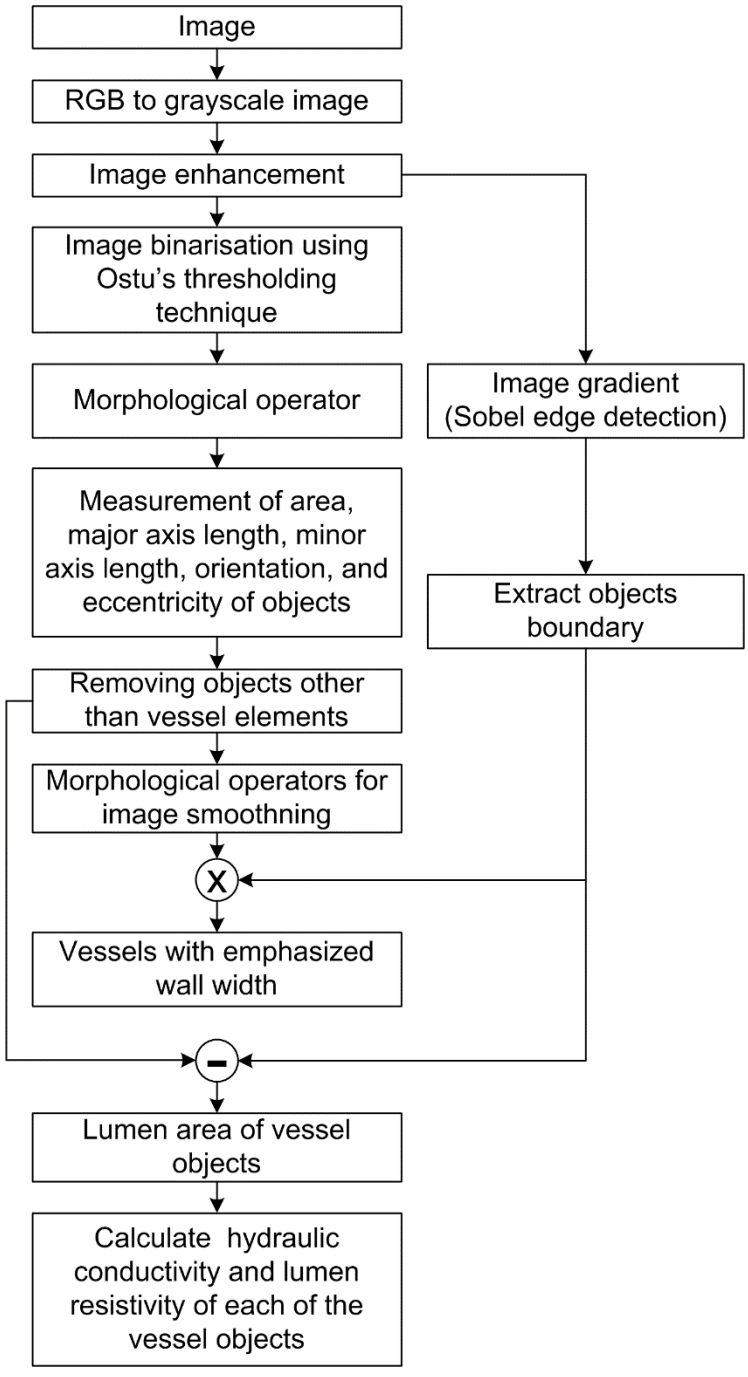

Fig. 7.1 Flow chart to compute the hydraulic conductivity of the vessel elements

7.3.1 RGB to Grayscale Conversion

The RGB images acquired by light microscopes' were converted to grayscale image with the help of Eq. (2.41) in order to reduce the computational burden of the system.

7.3.2 Image Enhancement

The grayscale images are required to be processed in order to enhance the image quality. Thus, gray level enhancement techniques such as contrast stretching, histogram equalization and contrast-limited adaptive histogram equalization are investigated here. All the three techniques have given more or less comparable results. Therefore, in this work to enhance the quality of grayscale image the contrast of the image is increased by mapping the values of the input grayscale images to new values in such a way that 1% of the data is saturated at lower and higher intensity levels of the input data.

7.3.3 Image Gradient

The visually enhanced grayscale images are processed by edge detection algorithms. Amongst the available basic edge detection algorithms, Sobel operator is a widely used algorithm (gives isotropic results for horizontal and vertical edges), which produces an image having emphasized edges and transitions [190]. The reason for selection of Sobel mask is its immunity to noise (an important concern to be dealt with derivatives) during the process of detection of edges. This operator uses two 3×3 kernels namely g_x and g_y, which are convolved with the grayscale images to compute the derivatives in vertical and horizontal directions, respectively.

7.3.4 Image Segmentation and Morphological Operations

The most important task of this method is to precisely segment the grayscale images in order to obtain the binary image. Though several techniques are available for image segmentation such as edge based, region based and now a days active contour based techniques are preferred. But the region based and contour based image segmentation methods have prior requirement of providing seed points and region of interest (ROI), respectively, for optimal image segmentation. The key problem that arises in the segmentation of microscopic images of hardwood specie is large number of object having different shapes and sizes. Therefore, the selection of seed points and ROI for region based and active contour based images segmentation techniques is a difficult issue to deal with. Therefore, out of the several widely used thresholding based image segmentation techniques, Otsu's [131, 155] thresholding technique has been chosen. The Otsu's thresholding algorithms has been widely used for grayscale image segmentation because of optimal thresholding and minimal computational time requirement [64]. The optimum threshold value produced by the thresholding technique is then used to binarize the images by setting value 1 (white) to pixels having intensity value greater

than optimum threshold values and all other pixel intensity values are set to 0 (black). Further, the morphological operator hole filling is employed to fill the smaller regions that give impression of background region, but in fact it is part of the object of interest.

7.3.5 Measurement of Objects

The next important task has been to compute the area, major axis length, minor axis length, orientation and eccentricity of each of the objects detected in the binary images. This has been accomplished with the help of Matlab command "*regionprops*", which returns measurements for the set of properties specified by properties for each of the connected components (object) in the binary image. The binary image of the hardwood species contains four key elements, namely, vessels, rays, parenchymas and fibers. It is observed that the vessel elements of the microscopic image have large variation in their size and shape (most of the time they have elliptical shape). Thus, there are chances of false recognition of vessel elements as the parenchyma elements are of similar shape but they differ in size (tiny elements) only. Thus, to differentiate the vessel elements from parenchymas, the size of the objects has been considered. Further, to differentiate vessel elements from ray and fiber elements, the orientation, eccentricity, major axis length and minor axis length of the objects has been taken into consideration.

The traditional approach of computing the tangential diameter of the vessel element is to measure it along its widest tangential axis for a minimum number of randomly selected specified vessels and calculate the minimum, maximum and average values of it. Though, the approach is simple, it has a drawback that the shape and hydraulic conductance of the conduits (vessels) are not considered [28]. Also, the conduits are frequently elliptical and rarely found to have circular shape in the cross-sectional area, therefore, it is preferable to calculate the arithmetic diameter rather than the tangential diameter. The alternate solution is to calculate the equivalent circle diameter as suggested by [47, 112, 192, 193] and expressed as:

$$D = \sqrt{4A/\pi} \tag{7.1}$$

where, A represents the conduit surface area and D is the equivalent circle diameter.

7.3.6 Vessel Elements and their Hydraulic Conductivity

The size and shape of vessel elements vary among different species. Thus, here the vessel elements are separated from other three key elements based on defining the minimum diameter of the vessel as threshold parameter. These steps will retain only vessel elements in the image. Further, morphological operator namely erosion may be used to separate connectivity between the vessel and misleading objects connected to it. Further, these objects (vessel elements) have area which contains both wall width and lumen area. Therefore, to delineate the wall width and lumen area of the vessel elements, the image having vessel elements only are multiplied with

complement of the image gradient obtained by application of Sobel masks' to the enhanced gray scale image. The resulting images emphasizes the wall width of the vessel elements. From the Sobel gradient images, the wall width of the vessel element is obtained by boundary extraction method. Then, from this image the separated vessel elements' image have been subtracted to obtain the information about the lumen area of the vessel elements. Once the image containing vessel lumen area is produced, the diameter of each of the elements are calculated. Finally, the hydraulic conductivity (K_h) [112] of the vessel elements are computed using Eq. (7.2) which is based on Hagen-Poiseuille law [204]:

$$K_h = \pi D^4 / 128\eta \tag{7.2}$$

where, D represents the equivalent circle diameter of the vessels as given by Eq. (7.1), and η (1.002×10^{-9} MPa at 20° C) signifies the viscosity index of water. The unit of K_h is $\mathrm{m}^4/\mathrm{MPa}^{-1}\times\mathrm{s}^{-1}$. Also, the lumen resistivity (R_L) is measured by Eq. (7.3), or lumen resistivity is reciprocal of hydraulic conductivity as given by Eq. (7.4),

$$R_L = 128\eta / \pi D^4 \tag{7.3}$$

$$R_L = 1 / K_h \tag{7.4}$$

The unit of R_L is $\mathrm{m}^{-4}\,\mathrm{MPa\,s}$.

7.4 EXPERIMENTAL RESULTS AND DISCUSSION

In this experimentation work, light microscopic images of 14 species have been used to examine the performance of proposed segmentation, vessel elements extraction and measurement of their hydraulic conductivity. The hardwood species used in the present work are listed in Table 7.1. Here, Sr. No. 10 and 11 presents two different images of *Elaeagnus latifolia* specie, whereas, Sr. No. 15 and 16 presents different images of *Carissa opaca* species whose accession numbers are also listed in Table 7.1.

The *Tectona grandis* specie image examined with the proposed technique has produced promising results which are illustrated in Fig. 7.2 and Fig. 7.3. The Fig. 7.2 (a) to (f) presents RGB image, grayscale image, grayscale image enhanced with contrast adjustment, Sobel mask based gradient image, complement of gradient image and the binary image obtained using Otsu's thresholding algorithm. It has been observed that incorporating the image enhancement technique results in better image quality, which further improves the binary image conversion process. The Sobel mask based image gradient of the enhanced grayscale image is shown in Fig. 7.2 (d).To obtain the wall width region of the vessel elements complement of the gradient image has been implemented which is illustrated in Fig. 7.2 (e). Subsequently, the vessel elements are extracted by setting the following parameters, the structuring element of disk shape (d=1) has been used in the erosion process in order to separate two distinct objects

touching each other, equivalent diameter of the vessel (D=30), orientation (between 65° to 98°) and the ratio of major axis length to minor axis length. The need for ratio parameter arises because the vessel elements are not necessarily bound to have circular shapes; most of the time they have elliptical or tubular shape.

Table 7.1 List of the 14 hardwood species

Sr. No.	Family	Species	Accession number
1	Lamiaceae	*Tectona grandis*	DDw3714
2	Bignoniaceae	*Spathodea campanulata*	DDw3975
3	Rosaceae	*Rubus ellipticus*	DDw2367
4	Rosaceae	*Rosa lechenauitiana*	DDw3801
5	Punicaceae	*Punica granatum*	DDw4706
6	Asclepidaceae	*Ardisia humilis*	DDw3463
7	Myrsinaceae	*Embelia floribunda*	DDw3294
8	Menispermiaceae	*Stephania rotunda*	DDw5367
9	Loganiaceae	*Buddleja paniculata*	DDw2882
10	Elaeagnaceae	*Elaeagnus latifolia*	DDw4454
11	Elaeagnaceae	*Elaeagnus latifolia*	DDw3804
12	Gesneraceae	*Haematoxylon campechianum*	DDw4559
13	Berberidaceae	*Berberis lyceum*	DDw3054
14	Asteraceae	*Senecio corymbosus*	DDw3787
15	Apocynaceae	*Carissa opaca*	DDw3511
16	Apocynaceae	*Carissa opaca*	DDw3518

Further, ray elements sometimes may have shape that matches with vessel elements, but since the rays mostly have vertical orientation (between 60° to 110°). Therefore, the orientation parameter has also been taken in to consideration to differentiate between vessel and ray elements. Using the above discussed parameters, it became possible to extract the vessels elements of the light microscopic image as shown in Fig. 7.3 (a). The multiplication of complement gradient image with extracted vessel elements are shown in Fig. 7.3(c), which emphasizes the information about the wall width of the vessel elements. Further, the vessel wall width area has been shown in Fig. 7.3 (d). Though, some openings are visible but it gives the overall idea about the width and shape of the wall. The lumen area of the vessel element is also illustrated in Fig. 7.3 (e). The visual comparison of Fig. 7.3 (b) and Fig. 7.3 (e) depicts that there is considerable difference between these two images.

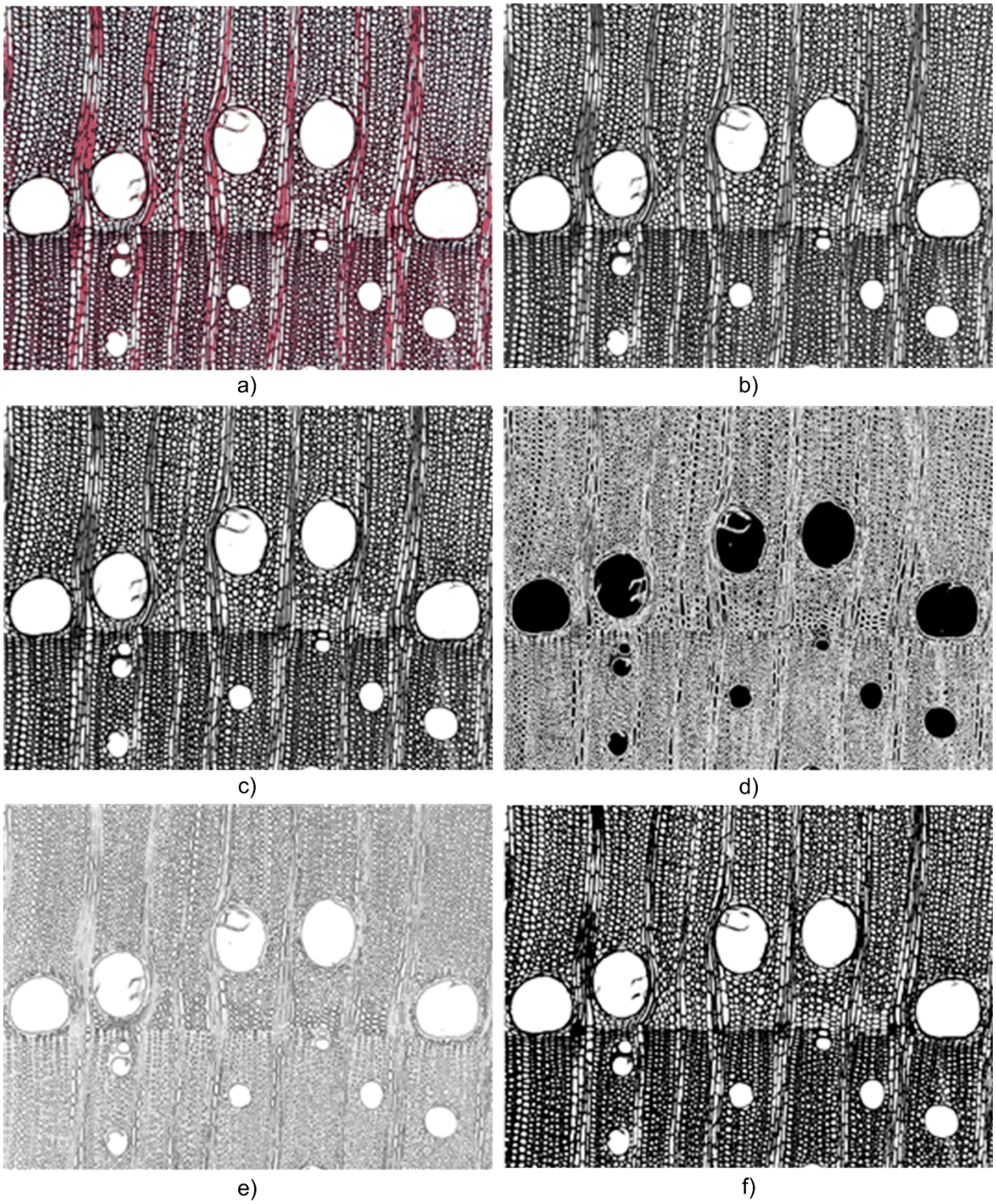

Fig. 7.2 (a) RGB image, b) grayscale image, (c),image enhancement using contrast adjustment, (d), gradient image obtained by application of Sobel mask to the enhanced grayscale image (e) complement of gradient image, and (f) binary image, for *Tectona grandis* specie image.

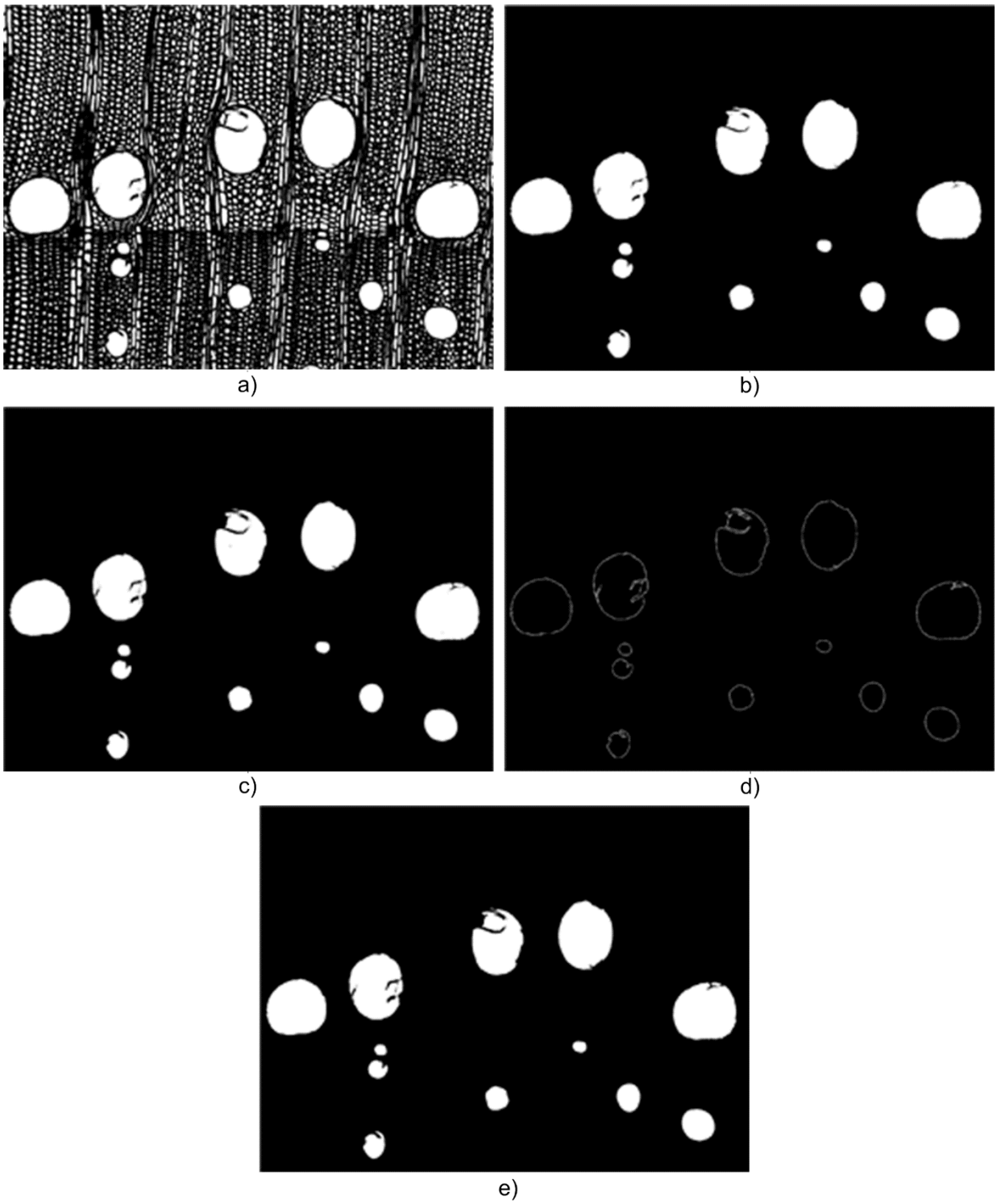

Fig. 7.3 (a) binary image with hole filling, (b) extracted vessel elements, (c) image produced by multiplication of complement gradient image and extracted vessel elements objects, (d) wall width of vessel elements, and (e) vessel lumen area, for *Tectona grandis* specie image.

Finally, the hydraulic conductivity (K_h) and lumen resistivity (R_L) of each of the vessel elements are calculated by considering the lumen area of the vessel elements. For *Tectona grandis* specie image the average value of K_h and R_L are found to be 8.87669E+15 and 4.45321E-15, respectively.

Table 7.2 Parameters chosen for vessel elements extraction and the average hydraulic conductivity and lumen resistivity of the given specie image.

Sr. No.	Species	Vessel segmentation parameters	Hydraulic conductivity (K_h) $m^4/MPa^{-1}\times s^{-1}$	Lumen Resistivity (R_L) $m^{-4}MPas$ (E= 10)
1	*Tectona grandis*	d=1, D=30	8.87669E+15	4.45321E-15
2	*Spathodea campanulata*	d=3, D=25	1.08031E+15	2.98923E-15
3	*Rubus ellipticus*	d=1, D=15	1.29643E+14	5.12067E-14
4	*Rosa lechenauitiana*	d=4, D=20	1.0365E+15	1.67685E-14
5	*Punica granatum*	d=4, D=8	6.6544E+13	9.50128E-14
6	*Ardisia humilis*	d=4, D=25	1.17369E+14	1.46358E-14
7	*Embelia floribunda*	d=4, D=20	3.79676E+15	5.96173E-15
8	*Stephania rotunda*	d=4, D=35	9.43799E+15	1.06875E-15
9	*Buddleja paniculata*	d=1, D=5	1.21167E+12	4.67416E-12
10	*Elaeagnus latifolia*	d=2, D=15	9.7993E+13	3.20037E-14
11	*Elaeagnus latifolia*	d=2, D=10	1.01237E+14	4.46697E-14
12	*Haematoxylon*	d=3, D=15	3.34495E+13	5.8297E-14
13	*Berberis lyceum*	d=3, D=8	4.9398E+12	4.44056E-13
14	*Senecio corymbosus*	d=4, D=8	2.89239E+13	1.00074E-13
15	*Carissa opaca*	d=2, D=4	1.22475E+12	1.75879E-12
16	*Carissa opaca*	d=1, D=4	1.35794E+12	3.4172E-12

The *Spathodea campanulata* specie image has also been processed by using the proposed methodology and the obtained results are being illustrated in Fig. 7.4 (a) to (f) and Fig. 7.5 (a) to (e). Using the selected set of parameters listed in Table 7.2, the vessel elements have been easily separable with the proposed approach. Further, the hydraulic conductivity and the lumen resistivity of the vessel elements have been computed and the average values of these parameters are listed in Table 7.2.

The average value of hydraulic conductivity and lumen resistivity for rest of the specie images listed in Table 7.2 are also presented here to show that the proposed methodology has also performed well for variety of images. The results obtained for each of the specie images are illustrated in Fig. 7.6 (a) to (e), Fig. 7.7 (a) to (e), and Fig. 7.8 (a) to (d). In these figures, column 1, 2, and 3 depicts RGB image, enhanced grayscale image and extracted vessel elements, respectively.

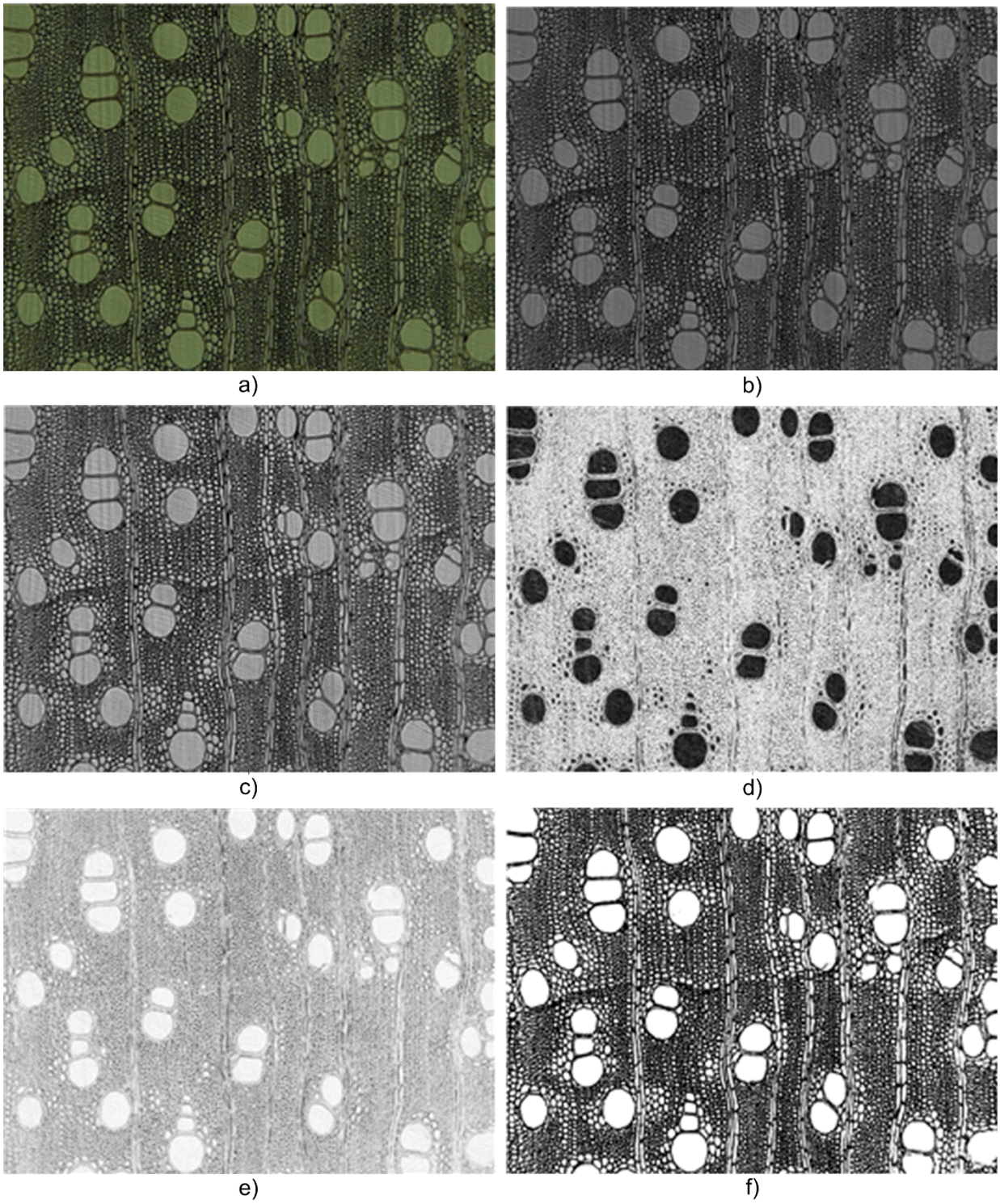

Fig. 7.4 (a) RGB image, b) grayscale image, (c),image enhancement using contrast adjustment, (d), gradient image obtained by application of Sobel mask to the enhanced grayscale image (e) complement of gradient image, and (f) binary image, for *Spathodea campanulata* specie image

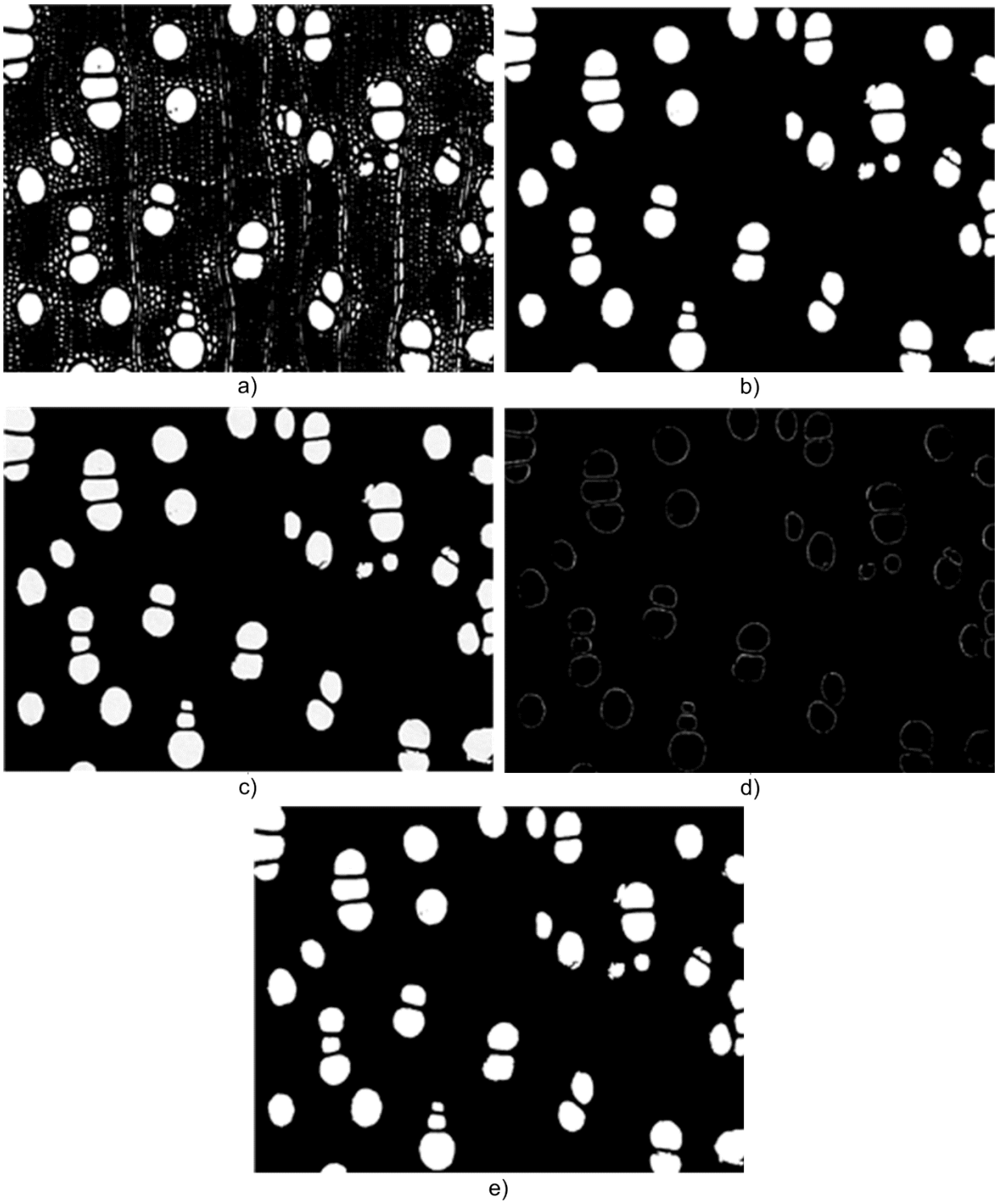

Fig. 7.5 (a) binary image with hole filling, (b) extracted vessel elements, (c) image produced by multiplication of complement gradient image and extracted vessel elements objects, (d) wall width of vessel elements, and (e) vessel lumen area, for *Spathodea campanulata* specie image.

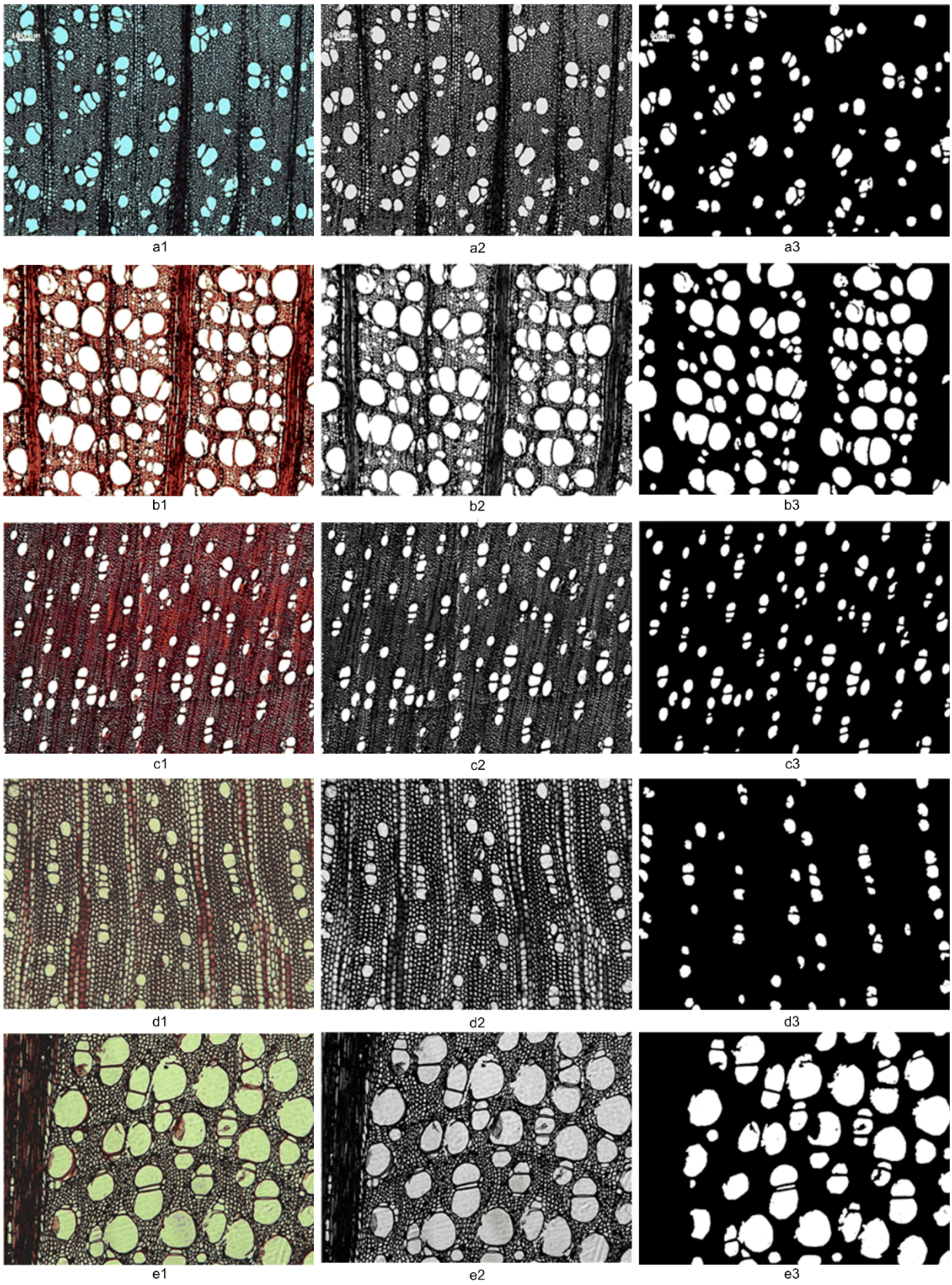

Fig. 7.6 Column 1, 2, and 3 depicts RGB image, enhanced grayscale image and extracted vessel elements, respectively for microscopic images of a) *Rubus ellipticus* (DDw2367), b) *Rosa lechenauitiana* (DDw3801), c) *Punica granatum* (DDw4706), d) *Ardisia humilis* (DDw3463), and e) *Embelia floribunda* (DDw 3294) species.

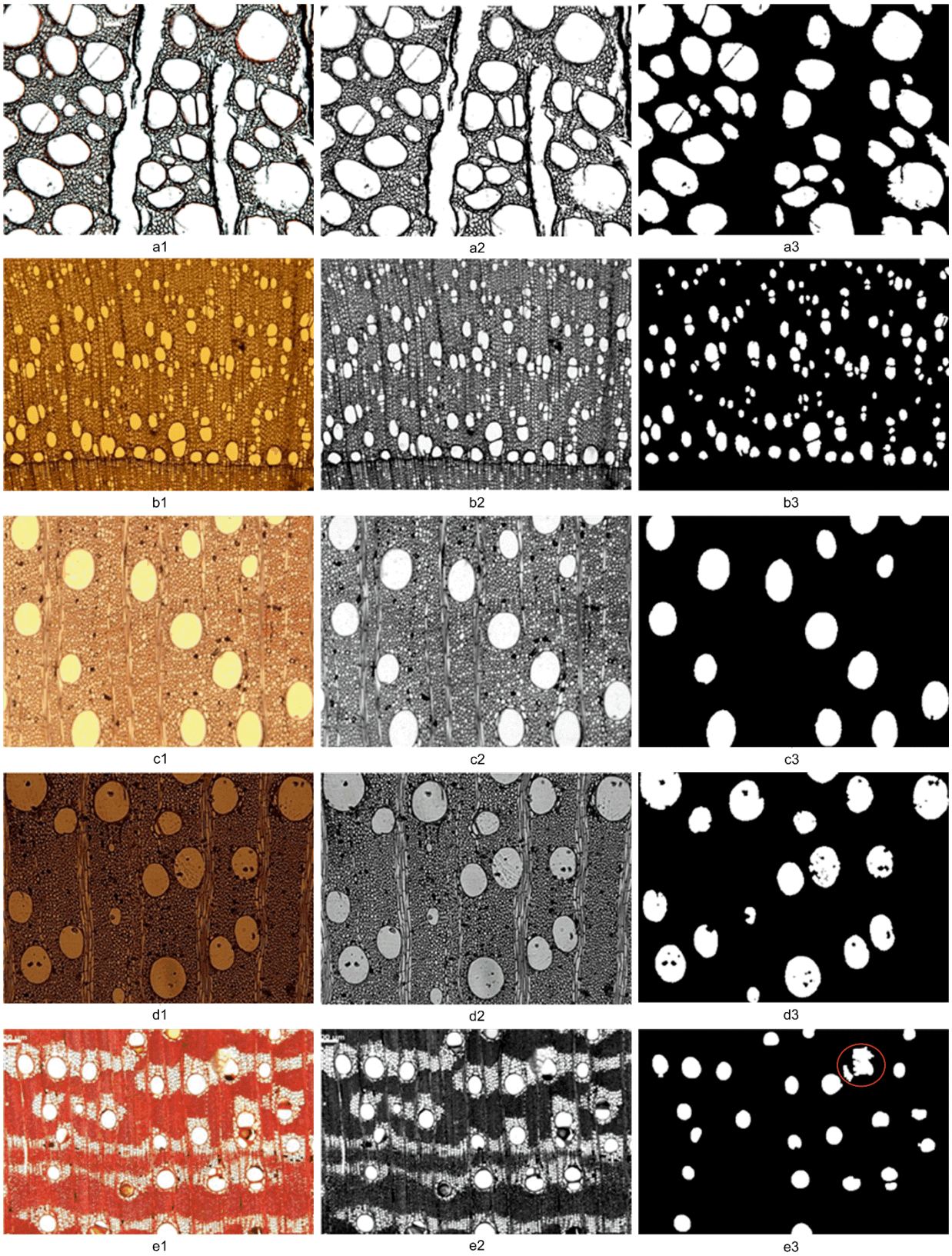

Fig. 7.7 Column 1, 2, and 3 depicts RGB image, enhanced grayscale image and extracted vessel elements, respectively for microscopic images of a) *Stephania rotunda* (DDw5367), b) *Buddleja paniculata* (DDw2882), c) *Elaeagnus latifolia* (DDw4454), d) *Elaeagnus latifolia* (DDw3804), and e) *Haematoxylon campechianum* (DDw4559) species.

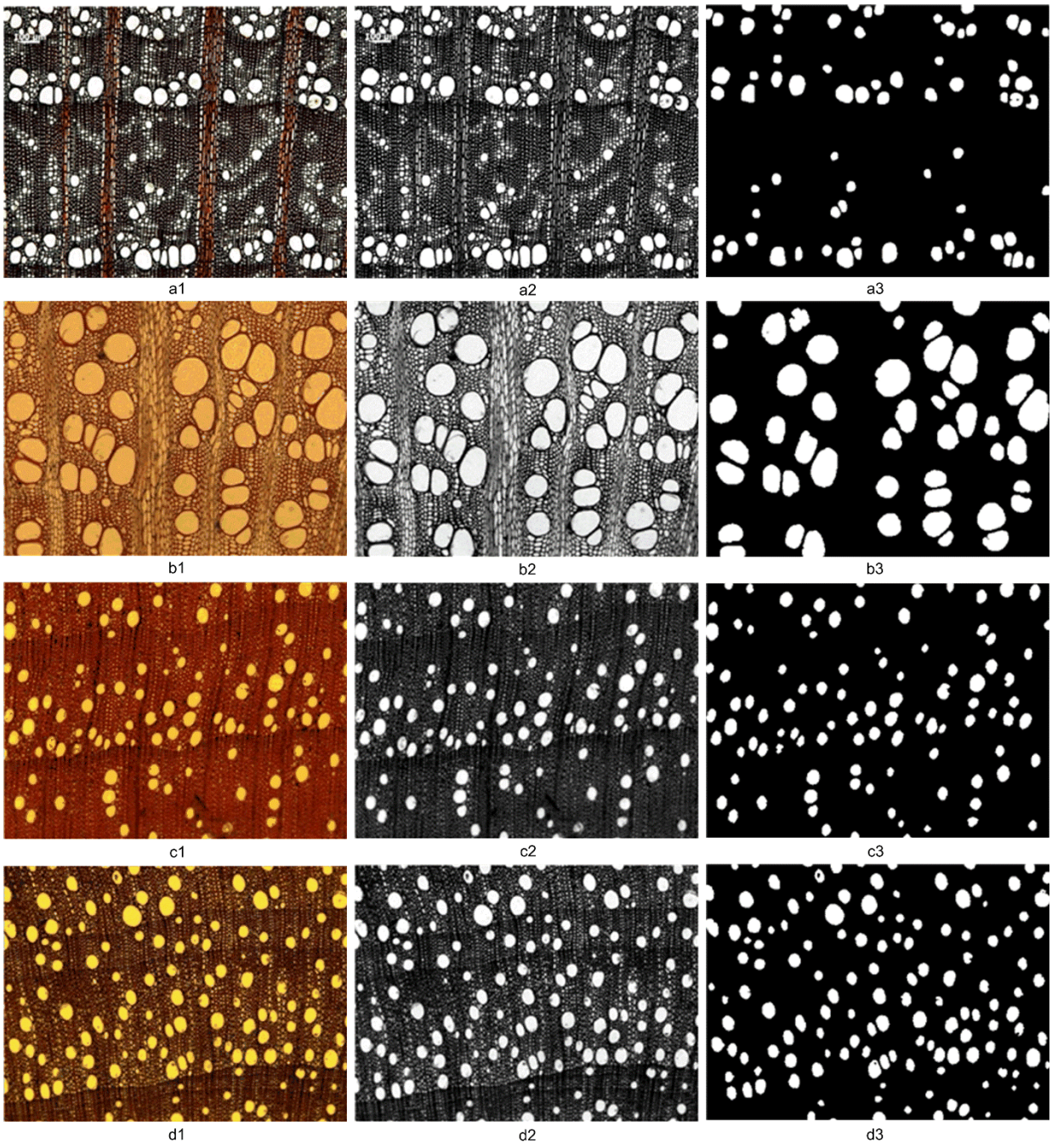

Fig. 7.8 Column 1, 2, and 3 depicts RGB image, enhanced grayscale image and extracted vessel elements, respectively for microscopic images of a) *Berberis lyceum* (DDw3054), b) *Senecio corymbosus* (DDw3787), c) *Carissa opaca* (DDw3511), and d) *Carissa opaca* (DDw3518) species.

The analysis of the segmentation results suggests that the proposed approach has been able to extract the vessel elements clearly for most of the images. But in Fig. 7.7 (e) it is found that in 3rd column, one of the object extracted as vessel element is in fact combination of vessel and parenchyma elements which has been highlighted with red circle. This has happened because the RGB image of the same specie has blurred parenchyma section surrounding that particular vessel element.

7.5 SUMMARY

This chapter presents an approach to segment the light microscopic images of hardwood species and then extract only the vessel elements of these images. In this work an effort has been made to propose a platform independent tool based on simple digital image processing technique to quantify wood conduits (especially vessel elements at present). A prototype model has been developed and has been tested on several microscopic images prepared at the Xylarium (DDw) of the Wood Anatomy Discipline of the Forest Research Institute, Dehradun. The analysis of the experimental work suggest that for most of the images, with the help of appropriate parameter selection, the vessel elements were being extracted. In one of the case the identified vessel element area was in fact the area of vessel element plus the surrounding parenchyma elements area. The close observation of the aforesaid object in original RGB image suggests that the parenchyma elements surrounding the vessel elements have higher intensity level compared to other parenchyma elements. Further, since the binarization process is accomplished by intensity based thresholding approach, which allows parenchyma elements to be treated as vessel elements. Further, along with the extraction of vessel elements the proposed model is capable of computing the hydraulic conductivity and lumen resistivity of the vessel elements.

CHAPTER 8. CONCLUSIONS AND SCOPE FOR FUTURE WORK

8.1 CONCLUSIONS

In this research work, the emphasis has been given to the design and development of some suitable texture feature extraction techniques for the classification of microscopic images of hardwood species into 75 categories. The effectiveness of the proposed techniques have been investigated on an open access database of hardwood species consisting of 1500 microscopic images samples of 75 hardwood species.

To accomplish the classification task efficiently, a comparative study of several state-of-the-art texture feature extraction techniques have been carried out to select the simple yet computationally efficient texture feature extraction techniques. Further, the performance of these techniques have been improved by extracting the texture features from multiresolution images and concatenating them to form a feature vector data. The feature vector data produced by these techniques have been normalized in the range 0 to 1, to give equal weightage to all the features, before applying it as input to the classifiers.

The multiresolution feature extraction techniques have produced large number of complex features that may limit the classification accuracy. Therefore, PCA (as dimensionality reduction) and mRMR (feature selection) techniques have been employed to reduce the feature vector data dimension. Further, to enhance the classification accuracy, four widely used classification algorithms namely, linear SVM, RBF kernel SVM, LDA and RF classifiers have been employed. To evaluate the performance of the state-of-the-art and proposed multiresolution feature extraction techniques, two approaches, namely 10-fold cross validation and randomly divided database have been adopted. Also, in both the approaches three cases are discussed (viz., FFVD, PCA reduced and mRMR feature selection based feature vector data). The best combination of the multiresolution feature extraction technique and classification algorithm has been selected based upon the maximum classification accuracy presented by them.

In addition, a prototype for determination of vessel elements and computation of their hydraulic conductivity for hardwood species have been carried out; which in turn would assist the wood anatomist to characterize the wood species.

Based upon the experimental outcomes, distinct conclusions have been drawn at different phases of the present work, which are summarized in the following subsections:

8.1.1 Performance of State-of-the-art Texture Feature Extraction Techniques

The experimental results accomplished for 10-fold cross validation approach suggest that the FFVD and mRMR feature selection based feature vector data of BGP texture feature extraction technique has achieved best classification accuracy of 95.93±1.52% and 95.60±1.78% with linear SVM classifier. Moreover, the best classification accuracy of 96.33±1.14% has been

obtained on the PCA reduced feature vector data using CoALBP24 texture feature extraction technique with the help of LDA classifier, amongst several techniques examined here. The CoALBP12, CoALBP24, CoALBP48, Gabor filter, LBP and LTCoP feature extraction techniques have also produced results better than the rest of the other state-of-the-art texture feature extraction techniques.

In case of RDD, the BGP texture feature extraction technique has achieved classification accuracy better than rest of the feature extraction techniques in all the three cases. However, the FFVD of BGP texture feature extraction technique has attained the best classification accuracies of 94.33%, 88%, 85.33% and 82.40% for 80/20, 70/30, 60/40 and 50/50 training and testing ratios of RDD, respectively, using linear SVM classifier.

It is to be emphasized that Gabor filter, LTCoP and BGP techniques took around 9.3753, 4.5533 and 2.6857 seconds, respectively, to extract the texture features of individual image. In addition, feature vector data of FOS technique has obtained lowest classification accuracy amongst the techniques tested here. The linear SVM, RBF kernel SVM and LDA classifier give better performance, whereas RF classifier gives poor performance, comparatively.

8.1.2 Performance of BWT based Texture Feature Extraction Techniques

In this case, the mRMR feature selection based feature subset (200 features) of $BWTCLBP^{ri}$ feature extraction technique (among all the variants of BWT based feature extraction techniques) has obtained maximum classification accuracy (96.87±1.18%) using RBF kernel SVM classifier for 10-fold cross validation approach. Further, the FFVD produced by $BWTCLBP^{ri}$ feature extraction technique at the 3rd level of image decomposition yields 95.47±1.75% classification accuracy using linear SVM classifier. However, the LDA classifier has produced a classification accuracy of 95.73±0.84% for PCA reduced feature vector data of $BWTCLBP^{riu2}$ texture feature extraction technique (288 features). Thus, classification accuracy achieved by $BWTCLBP^{ri}$ texture feature extraction technique is relatively better than the classification accuracy achieved by CoALBP24 texture feature extraction technique.

Further, in RDD approach, amongst the three cases, the subset of feature vector data of $BWTCLBP^{ri}$ technique selected by mRMR feature selection technique yields the best classification accuracies of 95.67% (250 features), 93.78% (150 features), 91.50% (250 features) and 90.53% (250 features) for 80/20, 70/30, 60/40 and 50/50 training and testing ratios of RDD, respectively, with linear SVM classifier. The aforementioned classification accuracies are much better than the classification accuracy produced by BGP (state-of-the-art) feature extraction technique.

Further, it is worthwhile to point out that only MSB bit-plane of the gray scale image used by BWT based LBP variants texture feature extraction technique has achieved slightly better classification accuracy compared to 8-bit plane (grayscale) image used by CoALBP24 texture

feature extraction technique. Thus, the performance of LBP variants texture feature extraction techniques have been significantly improved by incorporating grayscale image transformation with gray-level slicing and BWT, followed by extraction of texture features from these transformed images. The MSB bit of grayscale image has significant information which can be used to deliver comparatively good classification accuracy using BWT transform.

8.1.3 Performance of GP based Texture Feature Extraction Techniques

For 10-fold cross validation approach, amongst the GP based texture feature extraction techniques, the PCA reduced feature vector data of GPLPQ technique (500 features) yields the best classification accuracy of 98.73±1.15% with LDA classifier. However, the FFVD (1024 features), and mRMR selected feature subset (550 features) of GPLPQ techniques have achieved the best classification accuracy of 98.20±1.04%, and 98.13±0.93%, respectively, by linear SVM classifier**.**

In case of RDD, amongst the proposed texture feature extraction techniques, the PCA dimensionality reduced feature vector data of $GPLCP^{riu2}$ technique has obtained the best classification accuracies of 96.33% (250 features), 96.22% (250 features), 94.67% (300 features) and 93.73% (250 features) for 80/20, 70/30, 60/40 and 50/50 training and testing ratios of RDD, respectively, using LDA classifier. Moreover, subset of feature vector data of GPLPQ technique selected by mRMR feature selection method yields relatively lower classification accuracy (95.67% (450 features), 92.89% (550 features), 90.67% (550 features) and 89.20% (400 features) for 80/20, 70/30, 60/40 and 50/50 training and testing ratios of RDD, respectively), using linear SVM classifier.

The analysis of the GP based texture feature extraction techniques suggests that the performance of variants of LBP, LCP and LPQ techniques have been significantly improved by incorporating Gaussian image pyramid based image decomposition, followed by extraction of texture features from these transformed images.

8.1.4 Performance of DWT based Texture Feature Extraction Techniques

Critical analysis of the results obtained with 10-fold cross validation approach revealed that among all the proposed techniques, $DWTCLBP^{u2}$ generates most discriminative texture features. The best classification accuracy of 97.40±1.06% has been obtained for $DWTCLBP^{u2}$ texture features at the 3rd level of image decomposition (1416 features) using linear SVM classifier.

Further, reduced by PCA approach, the $DWTCLBP^{u2}$ texture features have achieved superlative classification accuracy of 97.87±0.82% (325 features) with LDA classifier. Furthermore, incorporating the mRMR feature selection based texture features of $DWTCLBP^{u2}$

technique have again obtained the best classification accuracy having value of 98.40±1.00% (550 features) with RBF kernel SVM classifier.

It is important to note that the higher level of image decomposition by DWT produce low resolution images that do not carry qualitative visual information. Therefore, most of these techniques have shown decrement in classification accuracy beyond the 3rd level of image decomposition using full feature vector data.

Similarly for RDD aaproach, amongst the proposed texture feature extraction techniques, the subset of feature vector data of DWTCLBP^{u2} selected by mRMR feature selection technique yields the best classification accuracies of 97.33% (350 features), 96.67% (350 features), 94.33% (400 features) and 93.60% (350 features) for 80/20, 70/30, 60/40 and 50/50 training and testing ratios of RDD, respectively, using linear SVM classifier. Further, the PCA dimensionality reduced feature vector data of DWTCLBP^{u2} technique has obtained the classification accuracies of 95.67% (350 features), 94.22% (200 features), 92.67% (250 features) and 92% (100 features) for 80/20, 70/30, 60/40 and 50/50 training and testing ratios of RDD, respectively, using LDA classifier. Furthermore, the FFVD of DWTCLBP^{u2} technique achieved a classification accuracy of 94.33%, 92.67%, 92.17% and 90.93% for 80/20, 70/30, 60/40 and 50/50 training and testing ratios of RDD, respectively, using linear SVM classifier.

Hence, it can be concluded that the texture features extracted by the DWT based texture feature extraction techniques for hardwood species are also of excellent quality, as it is evident from the classification accuracy obtained by all the classifiers.

8.1.5 Performance of DWT based Hybrid Texture Feature Extraction Techniques

The DWT based hybrid texture feature extraction techniques integrate the multiresolution capability of DWT with FOS and variants of LBP. The comprehensive analysis of the results produced by 10-fold cross validation approach shows that amongst the proposed texture feature extraction techniques the FFVD of DWTFOSLBP^{u2} has obtained classification accuracy of 97.67±0.79% and 98.40±0.64% for grayscale and RGB images, respectively, using linear SVM classifier. Further, the PCA reduced feature vector data of the DWTFOSLBP^{u2} texture feature extraction technique has achieved 97.93±1.39% (100 features) classification accuracy using RBF kernel SVM classifier for grayscale images. While a classification accuracy of 98.53±0.69% (450 features) has been achieved for the DWTFOSLBP^{u2} texture feature extraction technique for RGB images using linear SVM classifier. Furthermore, the mRMR feature selection based subset of DWTFOSLBP-HF texture features produces the best classification accuracy of 99.00±0.79% (275 features) and 99.20±0.42% (300 features) for grayscale and RGB images, respectively, using linear SVM classifier.

In case of RDD, the FFVD of DWTFOSLBP^{riu2} technique has obtained the classification accuracies of 95.33%, 94.22%, 92.83%, 91.73% and 96.67%, 95.78%, 93.33%, 92.20%,

respectively for grayscale and RGB images (for 80/20, 70/30, 60/40 and 50/50 training and testing ratios). These accuracies are achieved at the 4^{th} and 6^{th} IDL for grayscale and RGB images, respectively, using linear SVM classifier. Further, the PCA reduced feature vector data of the $DWTFOSLBP^{riu2}$ texture feature extraction technique using LDA classifier has achieved classification accuracies of 96.33% (150 features), 95.56% (260 features), 93.83% (260 features), 93.73% (200 features), and 97.67% (200 features), 97.33% (150 features), 95.50% (150 features) 94.40% (200 features) for grayscale and RGB images, respectively. These accuracies are achieved for the feature vector data produced at the 5^{th} IDL for grayscale and RGB images. Likewise, mRMR feature selection based subset of DWTFOSLBP-HF texture features achieved classification accuracies of 96.33% (200 features), 95.56% (200 features), 94% (200 features), and 93.47% (150 features) with linear SVM classifier for grayscale images. Moreover, mRMR feature selection based subset of DWTFOSLBP-HF texture features achieved best classification accuracies of 97.33% (500 features), 97.11% (200 features), 95% (350 features) 94.93% (200 features) for RGB images using RBF kernel SVM classifier.

It is worth pointing out here that, in the case of texture features acquired by DWT based hybrid texture feature extraction techniques for hardwood species no significant information loss is observed when features of grayscale image is employed for the classification in place of RGB image. As it is seen that only a slight improvement (99.20±0.42% as compared to 99.00±0.79% for grayscale image) in the classification accuracy is achieved for the RGB images, at the cost of almost thrice the computational time taken by feature extraction techniques to extract texture features from grayscale image.

8.1.6 Segmentation and Determination of Vessel Elements

In this section of work, an approach to segment the light microscopic images of hardwood species followed by vessel elements extraction has been proposed. A prototype model has been developed and has been tested on several microscopic images prepared at the Xylarium (DDw) of the Wood Anatomy Discipline of the Forest Research Institute, Dehradun. The analysis of the experimental work suggests that for most of the images, with the help of appropriate parameter selection, the vessel elements were being extracted. Moreover, in one of the case the identified vessel element area was in fact the area of vessel element plus the surrounding parenchyma elements area. The close observation of the aforesaid object in original RGB image suggests that the parenchyma elements surrounding the vessel elements have higher intensity level compared to other parenchyma elements. Besides, the extraction of vessel elements the proposed model is also capable of computing the hydraulic conductivity and lumen resistivity of the vessel elements.

Finally, it is stated that the multiresolution feature extraction techniques proposed for the classification of microscopic images of hardwood species have extracted significant features of

the images. Further, employing the PCA and mRMR as feature dimensionality reduction and feature selection techniques have given value addition to the proposed approaches. Amongst all the proposed techniques the DWTFOSLBP-HF texture feature extraction technique has given the best classification accuracy. Another important finding of this work has been that texture features extracted from grayscale images do not suffer from information loss compared to texture features extracted from RGB images.

8.2 SCOPE FOR THE FUTURE WORK

Even though comprehensive experimental work has been done here, to improve the classification accuracy of hardwood species, following are some of the suggestions for implementation in future research work in this field:

- The proposed approach has used selected mother wavelets to decompose the images by DWT. Several other mother wavelets may be investigated to see their effect on the feature extraction and classification of hardwood species.
- In this study, the PCA (dimensionality reduction) and mRMR (features selection) techniques have been used to reduce the dimension of feature vector data. Some other techniques such as Kernel PCA (dimensionality reduction), genetic algorithm, and correlation based feature selection may be investigated to reduce the feature vector data.
- Further, to get the multiresolution images, the BWT, GP and DWT have been employed. Several other multiresolution techniques, namely, fractional wavelet transform (FRWT) and dual tree complex wavelet transform (DTCWT) may be investigated to produce significant texture features
- In this work, a prototype model has been proposed for the segmentation and determination of conduits of wood (especially vessel elements). This can further be extended to delineate the other key elements of hardwood species viz., parenchymas, rays and fibres.
- A single enhancement technique may not be helpful in improving the quality of all the hardwood species images. Thus, other enhancements techniques may further be employed to improve the visual quality of the image.
- Further, In order to extract the vessel elements, Otsu's thresholding algorithm has been used in this work. Since the threshloding algorithm plays vital role in the segmentation of grayscale image to obtain binary image, the nature inspired algorithms namely artificial bee colony (ABC) and cuckoo search (CS) optimization algorithms may be investigated for determination of optimal thresholding value.
- After compiling the ideas proposed in the present work, an expert system can also be designed and developed to assist the wood anatomist in characterising the key elements of hardwood species.

PUBLICATIONS FROM THE WORK

Journals

1. Yadav, A. R., Anand, R. S., Dewal, M. L., and Gupta, S., “Multiresolution local binary pattern variants based texture feature extraction techniques for efficient classification of microscopic images of hardwood species,” *Applied Soft Computing,* vol. 32, pp. 101-112, 2015.
2. Yadav, A. R., Anand, R. S., Dewal, M. L., and Gupta, S., “Hardwood species classification with DWT based hybrid texture feature extraction techniques,” in Sadhana-Academy Proceedings in Engineering Science, Springer (Accepted for publication on 2nd August 2015)
3. Yadav, A. R., Anand, R. S., Dewal, M. L., and Gupta, S., “Gaussian image pyramid based texture features for classification of microscopic images of hardwood species,” Optik International Journal for Light and Electron Optic , Elsevier (Under review)

Conference

4. Yadav, A. R., Dewal, M. L., Anand, R. S., and Gupta, S., "Classification of hardwood species using ANN classifier," in *IEEE Fourth National Conference on Computer Vision, Pattern Recognition, Image Processing and Graphics (NCVPRIPG), 2013*, pp. 1-5.
5. Yadav, A. R., Anand, R. S., Dewal, M. L., and Gupta, S., "Analysis and classification of hardwood species based on Coiflet DWT feature extraction and WEKA workbench," in *IEEE International Conference on Signal Processing and Integrated Networks (SPIN), 2014*, pp. 9-13.
6. Yadav, A. R., Anand, R. S., Dewal, M. L., and Gupta, S., "Performance analysis of discrete wavelet transform based first-order statistical texture features for hardwood species classification," *in 3rd International Conference on Recent Trends in Computing (ICRTC), 2015,*pp .1-8, Elsevier. (Accepted for Publication in Proceedia computer science, Elsevier).

REFERENCES

[1] Adelson, E. H., Anderson, C. H., Bergen, J. R., Burt, P. J., and Ogden, J. M., “Pyramid methods in image processing,” *RCA engineer,* vol. 29, no. 6, pp. 33-41, 1984.

[2] Ahmad, A., and Yusof, R., “The implementation of ant clustering algorithm (ACA) in clustering and classifying the tropical wood species,” in International Conference on Signal-Image Technology & Internet-Based Systems (SITIS), 2013, pp. 720-725.

[3] Ahmad, A., and Yusof, R., “Clustering the tropical wood species using kohonen self-organizing map (KSOM),” in Proceedings of the 2nd International Conference on Advances in Computer Science and Engineering, 2013, pp. 16-19.

[4] Ahonen, T., Matas, J., He, C., and Pietikäinen, M., "Rotation invariant image description with local binary pattern histogram fourier features," *Image Analysis*, pp. 61-70: Springer, 2009.

[5] Ai, F.-f., Bin, J., Zhang, Z.-m., Huang, J.-h., Wang, J.-b., Liang, Y.-z., Yu, L., and Yang, Z.-y., “Application of random forests to select premium quality vegetable oils by their fatty acid composition,” *Food chemistry,* vol. 143, pp. 472-478, 2014.

[6] Albregtsen, F., “Statistical texture measures computed from gray level run length matrices,” *IMAGE,* vol. 1, no. 2, pp. 3-4, 1995.

[7] Alexandre, L. A., “Gender recognition: A multiscale decision fusion approach,” *Pattern Recognition Letters,* vol. 31, no. 11, pp. 1422-1427, 2010.

[8] Anand, C. S., and Sahambi, J. S., “Wavelet domain non-linear filtering for MRI denoising,” *Magnetic Resonance Imaging,* vol. 28, no. 6, pp. 842-861, 2010.

[9] Apatean, A., Rogozan, A., Emerich, S., and Bensrhair, A., “Wavelets as features for objects recognition,” *Acta Tehnica Napocensis,* vol. 49, no. 2, 2008.

[10] Avci, E., “Comparison of wavelet families for texture classification by using wavelet packet entropy adaptive network based fuzzy inference system,” *Applied Soft Computing,* vol. 8, no. 1, pp. 225-231, 2008.

[11] Baas, P., “Some functional and adaptive aspects of vessel member morphology,” Leiden Botanical Series, vol. 3, pp. 157-181, 1976.

[12] Baas, P., Wheeler, E., and Gasson, P., “IAWA list of microscopy features for hardwood identification,” *IAWA Committee*, 1989.

[13] Baas, P., Werker, E., and Fahn, A., “Some ecological trends in vessel characters,” Iawa Bull, vol. 4, pp. 141-59, 1983.

[14] Balan Menon, P., “Structure and identification of Malayan woods,” *Malay. Forest Rec*, no. 25, pp. 1-121, 1967.

[15] Belhumeur, P. N., Hespanha, J. P., and Kriegman, D., “Eigenfaces vs. fisherfaces: Recognition using class specific linear projection,” *IEEE Transactions on Pattern Analysis and Machine Intelligence* vol. 19, no. 7, pp. 711-720, 1997.

[16] Ben-Hur, A., Ong, C. S., Sonnenburg, S., Schölkopf, B., and Rätsch, G., “Support vector machines and kernels for computational biology,” *PLoS computational biology,* vol. 4, no. 10, pp. e1000173, 2008.

[17] Bhuyan, M., Ghosh, D., and Bora, P., “Feature extraction from 2D gesture trajectory in dynamic hand gesture recognition,” in IEEE Conference on Cybernetics and Intelligent Systems, 2006 pp. 1-6.

[18] Biswas, K. K., and Basu, S. K., “Gesture recognition using Microsoft Kinect®,” in 5th International Conference on Automation, Robotics and Applications (ICARA) 2011, pp. 100-103.

[19] Bond, B., *Wood Identification for hardwood and softwood species native to Tennessee*: Agricultural Extension Service, University of Tennessee, 2002.

[20] Brazier, J., and Franklin, G., “Identification of hardwoods: a microscopic key,” *For. Prod. Res. Bull,* vol. 46, 1961.

[21] Breiman, L., “Random forests,” *Machine learning,* vol. 45, no. 1, pp. 5-32, 2001.

[22] Bremananth, R., Nithya, B., and Saipriya, R., “Wood species recognition using GLCM and correlation,” in International Conference on Advances in Recent Technologies in Communication and Computing (ARTCom'09), 2009, pp. 615-619.

[23] Bruce, L. M., Koger, C. H., and Li, J., “Dimensionality reduction of hyperspectral data using discrete wavelet transform feature extraction,” *IEEE Transactions on Geoscience and Remote Sensing,* vol. 40, no. 10, pp. 2331-2338, 2002.

[24] Burt, P. J., “Fast algorithms for estimating local image properties,” *Computer Vision, Graphics, and Image Processing,* vol. 21, no. 3, pp. 368-382, 1983.

[25] Burt, P. J., and Adelson, E. H., “The Laplacian pyramid as a compact image code,” *IEEE Transactions on Communications,* vol. 31, no. 4, pp. 532-540, 1983.

[26] Camastra, F., “Data dimensionality estimation methods: a survey,” *Pattern recognition,* vol. 36, no. 12, pp. 2945-2954, 2003.

[27] Canuto, A. M., Vale, K. M., Feitos, A., and Signoretti, A., “ReinSel: A class-based mechanism for feature selection in ensemble of classifiers,” *Applied Soft Computing,* vol. 12, no. 8, pp. 2517-2529, 2012.

[28] Carlquist, S., *Comparative wood anatomy: systematic, ecological, and evolutionary aspects of dicotyledon wood*: Springer Science & Business Media, 2013.

[29] Carlquist, S., “Further concepts in ecological wood anatomy, with comments on recent work in wood anatomy and evolution,” Aliso, vol. 9, no. 4, pp. 499-553, 1980.

[30] Carolina, S., Pierre, D., Christine, H., Jean-François, M., Pierre, G., and Pierre, B., "Pl@ntwood: a computer-assisted identification tool for 110 species of Amazon trees based on wood anatomical features," *IAWA Journal,* vol. 32, no. 2, pp. 221-232, 2011.

[31] Cavalin, P. R., Kapp, M. N., Martins, J., and Oliveira, L. E., "A multiple feature vector framework for forest species recognition," in Proceedings of the 28th Annual ACM Symposium on Applied Computing, 2013, pp. 16-20.

[32] Chandrashekar, G., and Sahin, F., "A survey on feature selection methods," *Computers & Electrical Engineering,* vol. 40, no. 1, pp. 16-28, 2014.

[33] Chang, C.-C., and Lin, C.-J., "LIBSVM: a library for support vector machines," *ACM Transactions on Intelligent Systems and Technology (TIST),* vol. 2, no. 3, pp. 27, 2011.

[34] Chowdhury, S., Sing, J. K., Basu, D. K., and Nasipuri, M., "Face recognition by generalized two-dimensional FLD method and multi-class support vector machines," *Applied Soft Computing,* vol. 11, no. 7, pp. 4282-4292, 2011.

[35] Chu, A., Sehgal, C. M., and Greenleaf, J. F., "Use of gray value distribution of run lengths for texture analysis," *Pattern Recognition Letters,* vol. 11, no. 6, pp. 415-419, 1990.

[36] Chu, W.-S., Huang, C.-R., and Chen, C.-S., "Gender classification from unaligned facial images using support subspaces," *Information Sciences,* vol. 221, pp. 98-109, 2013.

[37] Clarke, S., "A multiple-entry perforated-card key with special reference to the identification of hardwoods," *New phytologist,* vol. 37, no. 4, pp. 369-374, 1938.

[38] Clemmensen, L., Hastie, T., Witten, D., and Ersbøll, B., "Sparse discriminant analysis," *Technometrics,* vol. 53, no. 4, pp. 406-413, 2011.

[39] Conners, R. W., Cho, T.-H., Ng, C. T., Drayer, T. H., Araman, P. A., and Brisbin, R. L., "A machine vision system for automatically grading hardwood lumber," *Industrial Metrology,* vol. 2, no. 3, pp. 317-342, 1992.

[40] Conners, R. W., Kline, D. E., Araman, P. A., and Drayer, T. H., "Machine vision technology for the forest products industry," *Computer*, no. 7, pp. 43-48, 1997.

[41] Cortes, C., and Vapnik, V., "Support-vector networks," *Machine learning,* vol. 20, no. 3, pp. 273-297, 1995.

[42] Coussement, K., and Van den Poel, D., "Churn prediction in subscription services: An application of support vector machines while comparing two parameter-selection techniques," *Expert systems with applications,* vol. 34, no. 1, pp. 313-327, 2008.

[43] Crammer, K., and Singer, Y., "On the learnability and design of output codes for multiclass problems," *Machine Learning,* vol. 47, no. 2-3, pp. 201-233, 2002.

[44] Cui, K.-p., Zhai, X.-r., and Wang, H.-j., "A survey on wood recognition using machine vision," *Advances in Forestry Letters (AFL),* vol. 2, no. 4, pp. 61-66, 2013.

[45] Datta, A., Dutta, S., Pal, S. K., Sen, R., and Mukhopadhyay, S., “Texture analysis of turned surface images using grey level co-occurrence technique,” in Advanced Materials Research, 2012, pp. 38-43.

[46] Daugman, J. G., “Uncertainty relation for resolution in space, spatial frequency, and orientation optimized by two-dimensional visual cortical filters,” *JOSA A,* vol. 2, no. 7, pp. 1160-1169, 1985.

[47] Davis, S. D., Sperry, J. S., and Hacke, U. G., “The relationship between xylem conduit diameter and cavitation caused by freezing,” American journal of botany, vol. 86, no. 10, pp. 1367-1372, 1999.

[48] Deka, B., and Bora, P. K., “Wavelet-based despeckling of medical ultrasound images,” *IETE Journal of Research,* vol. 59, no. 2, pp. 97-108, 2013.

[49] DiFranco, M. D., O’Hurley, G., Kay, E. W., Watson, R. W. G., and Cunningham, P., “Ensemble based system for whole-slide prostate cancer probability mapping using color texture features,” *Computerized medical imaging and graphics,* vol. 35, no. 7, pp. 629-645, 2011.

[50] Dutta, S., Pal, S., Mukhopadhyay, S., and Sen, R., “Application of digital image processing in tool condition monitoring: A review,” *CIRP Journal of Manufacturing Science and Technology,* vol. 6, no. 3, pp. 212-232, 2013.

[51] Fahn, A., Werker, E., and Baas, P., *Wood anatomy and identification of trees and shrubs from Israel and adjacent regions*: Israel Academy of Sciences and Humanities, 1986.

[52] Fan, R.-E., Chang, K.-W., Hsieh, C.-J., Wang, X.-R., and Lin, C.-J., “LIBLINEAR: A library for large linear classification,” *The Journal of Machine Learning Research,* vol. 9, pp. 1871-1874, 2008.

[53] Fisher, R. A., “The use of multiple measurements in taxonomic problems,” *Annals of eugenics,* vol. 7, no. 2, pp. 179-188, 1936.

[54] Fortuner, R., “The NEMISYS solution to problems in nematode identification. Chapter 9,” *Advances in computer methods for systematic biology. John Hopkins Univ. Press: Baltimore, USA*, pp. 137-164, 1993.

[55] Galloway, M. M., “Texture analysis using gray level run lengths,” *Computer graphics and image processing,* vol. 4, no. 2, pp. 172-179, 1975.

[56] Gasim, Harjoko, A., Seminar, K. B., and Hartati, S., “Merging feature method on RGB image and edge detection image for wood identification,” *International Journal of Computer Science and Information Technologies (IJCSIT),* vol. 4, no. 1, pp. 188-193, 2013.

[57] Gasim, Harjoko, A., Seminar, K. B., and Hartati, S., “Image blocks model for improving accuracy in identification systems of wood type,” *(IJACSA) International Journal of Advanced Computer Science and Applications,* vol. 4, no. 6, pp. 48-53, 2013.

[58] Geisser, S., *Predictive inference*: CRC Press, 1993.

[59] Ghorai, S., Mukherjee, A., and Dutta, P. K., "Discriminant analysis for fast multiclass data classification through regularized kernel function approximation," *IEEE Transactions on Neural Networks,* vol. 21, no. 6, pp. 1020-1029, 2010.

[60] Gonzalez, R. C., and Woods, R. E., *Digital image processing*, 3 ed.: Pearson Education, 2011.

[61] Gragnaniello, D., Poggi, G., Sansone, C., and Verdoliva, L., "Fingerprint liveness detection based on Weber local image descriptor," in IEEE Workshop on Biometric Measurements and Systems for Security and Medical Applications (BIOMS) 2013, pp. 46-50.

[62] Grigorescu, S. E., Petkov, N., and Kruizinga, P., "Comparison of texture features based on Gabor filters," *IEEE Transactions on Image Processing,* vol. 11, no. 10, pp. 1160-1167, 2002.

[63] Guang-Sheng, C., and Peng, Z., "Wood cell recognition using geodesic active contour and principal component analysis," *Optik-International Journal for Light and Electron Optics,* vol. 124, no. 10, pp. 949-952, 2013.

[64] Guijarro, M., Pajares, G., Riomoros, I., Herrera, P., Burgos-Artizzu, X., and Ribeiro, A., "Automatic segmentation of relevant textures in agricultural images," Computers and Electronics in Agriculture, vol. 75, no. 1, pp. 75-83, 2011.

[65] Guo, Y., Zhao, G., and Pietikäinen, M., "Texture classification using a linear configuration model based descriptor," in BMVC, 2011, pp. 1-10.

[66] Guo, Y., Zhao, G., and Pietikäinen, M., "Discriminative features for texture description," *Pattern Recognition,* vol. 45, no. 10, pp. 3834-3843, 2012.

[67] Guo, Z., and Zhang, D., "A completed modeling of local binary pattern operator for texture classification," *IEEE Transactions on Image Processing* vol. 19, no. 6, pp. 1657-1663, 2010.

[68] Guo, Z., Zhang, D., and Zhang, S., "Rotation invariant texture classification using adaptive LBP with directional statistical features," in 17th IEEE International Conference on Image Processing (ICIP), 2010, pp. 285-288.

[69] Gupta, R. D., Dash, J. K., and Mukhopadhyay, S., "Rotation invariant textural feature extraction for image retrieval using eigen value analysis of intensity gradients and multi-resolution analysis," Pattern Recognition, vol. 46, no. 12, pp. 3256-3267, 2013.

[70] Gupta, S., Kulshreshta, S., and Chauhan, L., "An expert system for wood anatomy research, image display and wood identification," *Indian forester,* vol. 128, no. 8, pp. 917-925, 2002.

[71] Gurau, L., Timar, M., Porojan, M., and Ioras, F., "Image processing method as a supporting tool for wood species identification," *Wood and fiber Science,* vol. 45, no. 3, pp. 1-11, 2013.

[72] Hafemann, L. G., Oliveira, L. S., and Cavalin, P., “Forest species recognition using deep convolutional neural networks,” in 22nd International Conference on Pattern Recognition (ICPR) 2014, pp. 1103-1107.

[73] Haghighat, M., Zonouz, S., and Abdel-Mottaleb, M., “Identification using encrypted biometrics,” in Computer Analysis of Images and Patterns, 2013, pp. 440-448.

[74] Haralick, R. M., Shanmugam, K., and Dinstein, I. H., “Textural features for image classification,” *IEEE Transactions on Systems, Man and Cybernetics*, no. 6, pp. 610-621, 1973.

[75] Harjoko, A., and Gasim, “Comparison of some features extraction method in wood identification,” in IEEE International Conference on Distributed Framework and Applications (DFmA) 2010, pp. 1-6.

[76] Harjoko, A., Gasim, S, S. R., and Damayanti, R., “Identification method for 15 names of commercial wood with image of texture pores as an input,” in International Conference on informatics for Development (ICID), Yogyakarta, Indonesia, 2011, pp. C2-129 - C2-133.

[77] Harjoko, A., Seminar, K. B., and Hartati, S., “Image blocks model for improving accuracy in identification systems of wood type,” *Image,* vol. 4, no. 6, 2013.

[78] Hasan, A. F., Ahmad, M. F., Ayob, M. N., Rais, S. A. A., Saad, N. H., Faiz, A., Abidin, Z., Abussal, A., Nordin, N. A., and Mohamad, S. H., “Application of binary particle swarm optimization in automatic classification of wood species using gray level co-occurence matrix and K-nearest neighbor,” *Int. J. Sci. Eng. Res,* vol. 4, pp. 50-55, 2013.

[79] Hayek, E. W., Krenmayr, P., Lohninger, H., Jordis, U., Moche, W., and Sauter, F., “Identification of archaeological and recent wood tar pitches using gas chromatography/mass spectrometry and pattern recognition,” *Analytical Chemistry,* vol. 62, no. 18, pp. 2038-2043, 1990.

[80] Heikkilä, M., Pietikäinen, M., and Schmid, C., “Description of interest regions with local binary patterns,” *Pattern recognition,* vol. 42, no. 3, pp. 425-436, 2009.

[81] Hellwich, O., Laptev, I., and Mayer, H., “Extraction of linear objects from interferometric SAR data,” International Journal of Remote Sensing, vol. 23, no. 3, pp. 461-475, 2002.

[82] Hermanson, J. C., and Wiedenhoeft, A. C., “A brief review of machine vision in the context of automated wood identification systems,” *IAWA Journal,* vol. 32, no. 2, pp. 233-250, 2011.

[83] Hingley, B. D., *Furniture repair & restoration*: Creative Homeowner, 2010.

[84] Hoadley, R. B., *Understanding wood: a craftsman's guide to wood technology*: Taunton press, 2000.

[85] Huang, S., Cai, C., Zhao, F., He, D., and Zhang, Y., “An efficient wood image retrieval using SURF descriptor,” in International Conference on Test and Measurement, ICTM'09, 2009, pp. 55-58.

[86] Ilic, J., “Computer aided wood identification using CSIROID,” *IAWA Journal,* vol. 14, no. 4, pp. 333-340, 1993.

[87] Jabid, T., Kabir, M. H., and Chae, O., “Local directional pattern (LDP) for face recognition,” in IEEE International Conference on Consumer Electronics, 2010, pp. 329-330.

[88] Jack, L., and Nandi, A., “Support vector machines for detection and characterization of rolling element bearing faults,” *Proceedings of the Institution of Mechanical Engineers, Part C: Journal of Mechanical Engineering Science,* vol. 215, no. 9, pp. 1065-1074, 2001.

[89] Jadhav, D. V., and Holambe, R. S., “Feature extraction using Radon and wavelet transforms with application to face recognition,” *Neurocomputing*, vol. 72, no. 7, pp. 1951-1959, 2009.

[90] Jaeger, M., Reigber, A., and Hellwich, O., “A non-parametric texture descriptor for polarimetric sar data with applications to supervised classification,” in Proceedings of 10th European Conference on Synthetic Aperture Radar,EUSAR 2014, pp. 1-4.

[91] Jain, V., and Sahambi, J., "Neural network and wavelets in arrhythmia classification," *Applied Computing*, pp. 92-99: Springer, 2004.

[92] Kanan, C., and Cottrell, G. W., “Color-to-grayscale: does the method matter in image recognition?,” PloS one, vol. 7, no. 1, pp. e29740, 2012.

[93] Kanumuri, T., Dewal, M., and Anand, R., “Progressive medical image coding using binary wavelet transforms,” *Signal, Image and Video Processing,* vol. 8, no. 5, pp. 883-899, 2014.

[94] Kapp, M. N., Bloot, R., Cavalin, P. R., and Oliveira, L. E., “Automatic forest species recognition based on multiple feature sets,” in International Joint Conference on Neural Networks (IJCNN), 2014, pp. 1296-1303.

[95] Kennel, P., Subsol, G., Guéroult, M., and Borianne, P., “Automatic identification of cell files in light microscopic images of conifer wood,” in 2nd International Conference on Image Processing Theory Tools and Applications (IPTA), 2010, pp. 98-103.

[96] Khadtare, M. S., and Sahambi, J., "ECG arrhythmia analysis by multicategory support vector machine," *Applied Computing*, pp. 100-107: Springer, 2004.

[97] Khairuddin, A. S. M., Khalid, M., and Yusof, R., "Using two stage classification for improved tropical wood species recognition system," *Intelligent Interactive Multimedia Systems and Services*, pp. 305-314: Springer, 2011.

[98] Khalid, M., Lee, E. L. Y., Yusof, R., and Nadaraj, M., “Design of an intelligent wood species recognition system,” *International Journal of Simulation System, Science and Technology,* vol. 9, no. 3, pp. 9-19, 2008.

[99] Khalid, M., Yusof, R., and Khairuddin, A. S. M., “Tropical wood species recognition system based on multi-feature extractors and classifiers,” in 2nd International Conference on Instrumentation Control and Automation (ICA), 2011, pp. 6-11.

[100] Khalid, M., Yusof, R., and Khairuddin, A. S. M., “Improved tropical wood species recognition system based on multi-feature extractor and classifier,” *World Academy of Science Engineering and Technology,* vol. 59, pp. 1189-1195, 2011.

[101] Klaghstan, M., Haensch, R., Coquil, D., and Hellwich, O., “Impact of hierarchical structures in image categorization systems,” in 3rd International Conference on Image Processing Theory, Tools and Applications (IPTA) 2012, pp. 367-370.

[102] Kobayashi, T., and Otsu, N., "Image feature extraction using gradient local auto-correlations," *Computer Vision–ECCV 2008*, pp. 346-358: Springer, 2008.

[103] Koenderink, J. J., “The structure of images,” *Biological cybernetics,* vol. 50, no. 5, pp. 363-370, 1984.

[104] Kruizinga, P., and Petkov, N., “Nonlinear operator for oriented texture,” *IEEE Transactions on Image Processing,* vol. 8, no. 10, pp. 1395-1407, 1999.

[105] Kruizinga, P., Petkov, N., and Grigorescu, S. E., “Comparison of texture features based on Gabor filters,” in International Conference on Image Analysis and Processing, 1999, pp. 142-147.

[106] Kusuma, E. D., Yusof, R., and Othman, M. F., “Fixed-point implementation of classifier for Tropical wood recognition system,” in International Conference on Communications, Signal Processing and Computers (CSCP’14), Interlaken, Switzerland, 2014, pp. 161-166.

[107] Kusuma, E. D., Yusof, R., and Othman, M. F., “Floating-point to fixed-point conversion of Tropical wood recognition system classifier,” *International journal of circuits, systems and signal processing,* vol. 8, pp. 376-387, 2014.

[108] Larkin, L., and Burt, P., “Multi-resolution texture energy measures,” in Proceedings IEEE Computer Society Conference on Computer Vision and Pattern Recognition. Washington, DC, 1983, pp. 519-520.

[109] Lei, Z., and Yan, M., “Timber species recognition approach based on mathematic simulation theory,” in International Conference of Information Science and Management Engineering (ISME), 2010, pp. 197-202.

[110] Lens, F., Luteyn, J. L., Smets, E., and Jansen, S., “Ecological trends in the wood anatomy of Vaccinioideae (Ericaceae sl),” Flora-Morphology, Distribution, Functional Ecology of Plants, vol. 199, no. 4, pp. 309-319, 2004.

[111] Lew, E. Y. L., “Design of an intelligent wood recognition system for the classification of Tropical wood species,” Universiti Teknologi Malaysia, Faculty of Electrical Engineering, 2005.

[112] Lewis, A. M., “Measuring the hydraulic diameter of a pore or conduit,” American Journal of Botany, pp. 1158-1161, 1992.

[113] Li, T., Zhu, S., and Ogihara, M., “Using discriminant analysis for multi-class classification: an experimental investigation,” *Knowledge and information systems,* vol. 10, no. 4, pp. 453-472, 2006.

[114] Li, W., You, J., and Zhang, D., “Texture-based palmprint retrieval using a layered search scheme for personal identification,” *IEEE Transactions on Multimedia,* vol. 7, no. 5, pp. 891-898, 2005.

[115] Liu, M., Wang, M., Wang, J., and Li, D., “Comparison of random forest, support vector machine and back propagation neural network for electronic tongue data classification: Application to the recognition of orange beverage and Chinese vinegar,” *Sensors and Actuators B: Chemical,* vol. 177, pp. 970-980, 2013.

[116] Livens, S., Scheunders, P., Van de Wouwer, G., and Van Dyck, D., “Wavelets for texture analysis, an overview,” in 6th International Conference on Image Processing and Its Applications, 1997, pp. 581-585.

[117] Lyle, J. R., Miller, P. E., Pundlik, S. J., and Woodard, D. L., “Soft biometric classification using local appearance periocular region features,” *Pattern Recognition,* vol. 45, no. 11, pp. 3877-3885, 2012.

[118] Ma, L.-j., and Wang, H.-j., “A new method for wood recognition based on blocked HLAC,” in 8th International Conference on Natural Computation (ICNC), 2012, pp. 40-43.

[119] Mäenpää, T., *The local binary pattern approach to texture analysis: extenxions and applications*: Oulun yliopisto, 2003.

[120] Malhotra, R., “Comparative analysis of statistical and machine learning methods for predicting faulty modules,” *Applied Soft Computing,* vol. 21, pp. 286-297, 2014.

[121] Mallat, S. G., “A theory for multiresolution signal decomposition: the wavelet representation,” *IEEE Transactions on Pattern Analysis and Machine Intelligence,* vol. 11, no. 7, pp. 674-693, 1989.

[122] Mallik, A., Tarrío-Saavedra, J., Francisco-Fernández, M., and Naya, S., “Classification of wood micrographs by image segmentation,” *Chemometrics and intelligent laboratory systems,* vol. 107, no. 2, pp. 351-362, 2011.

[123] Martínez-Cabrera, H. I., Jones, C. S., Espino, S., and Schenk, H. J., “Wood anatomy and wood density in shrubs: responses to varying aridity along transcontinental transects,” *American Journal of Botany,* vol. 96, no. 8, pp. 1388-1398, 2009.

[124] Martins, J., Oliveira, L., Britto Jr, A., and Sabourin, R., “Forest species recognition based on dynamic classifier selection and dissimilarity feature vector representation,” *Machine Vision and Applications,* vol. 26, no. 2-3, pp. 279-293, 2015.

[125] Martins, J., Oliveira, L., Nisgoski, S., and Sabourin, R., “A database for automatic classification of forest species,” *Machine Vision and Applications,* vol. 24, pp. 567-578, 2013.

[126] Martins, J., Oliveira, L., and Sabourin, R., “Combining textural descriptors for forest species recognition,” in 38th Annual Conference on IEEE Industrial Electronics Society (IECON), 2012, pp. 1483-1488.

[127] McNeill, J., “A botanist's view of automatic identification,” *Biological identification with computers*, pp. 283-289, 1975.

[128] Mencuccini, M., Martinez-Vilalta, J., Piñol, J., Loepfe, L., Burnat, M., Alvarez, X., Camacho, J., and Gil, D., “A quantitative and statistically robust method for the determination of xylem conduit spatial distribution,” *American journal of botany,* vol. 97, no. 8, pp. 1247-1259, 2010.

[129] Metcalfe, C., and Chalk, L., *Anatomy of the dicotyledons. Wood structure and conclusion of the general introduction. Vol. II*: Clarendon Press, Oxford, 1983.

[130] Metcalfe, C. R., and Chalk, L., “Anatomy of the dicotyledons, Vols. 1 & 2, 1950.

[131] Min, T.-H., and Park, R.-H., “Eyelid and eyelash detection method in the normalized iris image using the parabolic Hough model and Otsu’s thresholding method,” Pattern recognition letters, vol. 30, no. 12, pp. 1138-1143, 2009.

[132] Modasia, B., and De Silva, M., “An intelligent system to classify varieties of wood,” in Proceedings of 2nd Annual Session Sri Lanka Association for Artificial Intelligence (SLAAI), Colombo, 2005, pp. 61-69.

[133] Mohamed, A. A., and Yampolskiy, R. V., “Wavelet-based multiscale adaptive LBP with directional statistical features for recognizing artificial faces,” *ISRN Machine Vision,* vol. 2012, 2012.

[134] Mu, H., Li, L., Yu, L., Zhang, M., and Qi, D., “Detection and classification of wood defects by ANN,” in Proceedings of the IEEE International Conference on Mechatronics and Automation, 2006, pp. 2235-2240.

[135] Mu, T., Nandi, A. K., and Rangayyan, R. M., “Classification of breast masses via nonlinear transformation of features based on a kernel matrix,” *Medical & biological engineering & computing,* vol. 45, no. 8, pp. 769-780, 2007.

[136] Mu, T., Nandi, A. K., and Rangayyan, R. M., “Classification of breast masses using selected shape, edge-sharpness, and texture features with linear and kernel-based classifiers,” *Journal of digital imaging,* vol. 21, no. 2, pp. 153-169, 2008.

[137] Mukhopadhyay, S., Dash, J. K., and Gupta, R. D., “Content-based texture image retrieval using fuzzy class membership,” *Pattern Recognition Letters,* vol. 34, no. 6, pp. 646-654, 2013.

[138] Murala, S., Maheshwari, R., and Balasubramanian, R., “Directional binary wavelet patterns for biomedical image indexing and retrieval,” *Journal of medical systems,* vol. 36, no. 5, pp. 2865-2879, 2012.

[139] Murala, S., and Wu, Q. J., “Local ternary co-occurrence patterns: A new feature descriptor for MRI and CT image retrieval,” *Neurocomputing,* vol. 119, pp. 399-412, 2013.

[140] Nandi, R., Nandi, A. K., Rangayyan, R. M., and Scutt, D., “Classification of breast masses in mammograms using genetic programming and feature selection,” *Medical and biological engineering and computing,* vol. 44, no. 8, pp. 683-694, 2006.

[141] Nanni, L., Brahnam, S., and Lumini, A., “Combining different local binary pattern variants to boost performance,” *Expert Systems with Applications,* vol. 38, no. 5, pp. 6209-6216, 2011.

[142] Nanni, L., Lumini, A., and Brahnam, S., “Local binary patterns variants as texture descriptors for medical image analysis,” *Artificial intelligence in medicine,* vol. 49, no. 2, pp. 117-125, 2010.

[143] Nanni, L., Lumini, A., and Brahnam, S., “Survey on LBP based texture descriptors for image classification,” *Expert Systems with Applications,* vol. 39, no. 3, pp. 3634-3641, 2012.

[144] Nanni, L., Paci, M., Brahnam, S., Ghidoni, S., and Menegatti, E., “Local phase quantization texture descriptor for protein classification,” in 14th International Conference on Bioinformatics and Computational Biology (BIOCOMP’13), Las Vegas, 2013, pp. 56-61.

[145] Nasirzadeh, M., Khazael, A. A., and bin Khalid, M., “Woods recognition system based on local binary pattern,” in 2nd International Conference on Computational Intelligence, Communication Systems and Networks (CICSyN), 2010, pp. 308-313.

[146] Nikam, S. B., and Agarwal, S., “Wavelet energy signature and GLCM features-based fingerprint anti-spoofing,” in International Conference on Wavelet Analysis and Pattern Recognition (ICWAPR'08), 2008, pp. 717-723.

[147] Nirmala, S., Dandapat, S., and Bora, P., “Wavelet weighted blood vessel distortion measure for retinal images,” *Biomedical Signal Processing and Control,* vol. 5, no. 4, pp. 282-291, 2010.

[148] Nirmala, S., Dandapat, S., and Bora, P., “Wavelet weighted distortion measure for retinal images,” *Signal, Image and Video Processing,* vol. 7, no. 5, pp. 1005-1014, 2013.

[149] Nosaka, R., Ohkawa, Y., and Fukui, K., "Feature extraction based on co-occurrence of adjacent local binary patterns," *Advances in Image and Video Technology*, pp. 82-91: Springer, 2012.

[150] Ojala, T., Pietikainen, M., and Harwood, D., “Performance evaluation of texture measures with classification based on Kullback discrimination of distributions,” in Proceedings of the 12th IAPR International Conference on Pattern Recognition, Vol. 1-Conference A: Computer Vision & Image Processing, 1994, pp. 582-585.

[151] Ojala, T., Pietikäinen, M., and Harwood, D., “A comparative study of texture measures with classification based on featured distributions,” *Pattern recognition,* vol. 29, no. 1, pp. 51-59, 1996.

[152] Ojala, T., Pietikainen, M., and Maenpaa, T., “Multiresolution gray-scale and rotation invariant texture classification with local binary patterns,” *IEEE Transactions on Pattern Analysis and Machine Intelligence,* vol. 24, no. 7, pp. 971-987, 2002.

[153] Ojansivu, V., and Heikkilä, J., "Blur insensitive texture classification using local phase quantization," *Image and signal processing*, pp. 236-243: Springer, 2008.

[154] Ojansivu, V., Rahtu, E., and Heikkila, J., “Rotation invariant local phase quantization for blur insensitive texture analysis,” in 19th International Conference on Pattern Recognition (ICPR) 2008, pp. 1-4.

[155] Otsu, N., “A threshold selection method from gray-level histograms,” Automatica, vol. 11, no. 285-296, pp. 23-27, 1975.

[156] Pan, H., Jin, L.-Z., Yuan, X.-H., Xia, S.-Y., and Xia, L.-Z., “Context-based embedded image compression using binary wavelet transform,” *Image and Vision Computing,* vol. 28, no. 6, pp. 991-1002, 2010.

[157] Pan, H., Siu, W.-C., and Law, N.-F., “Lossless image compression using binary wavelet transform,” *IET Image Processing,* vol. 1, no. 4, pp. 353-362, 2007.

[158] Pan, S., and Kudo, M., "Recognition of porosity in wood microscopic anatomical images," *Advances in Data Mining. Applications and Theoretical Aspects*, pp. 147-160: Springer, 2011.

[159] Pan, S., and Kudo, M., “Segmentation of pores in wood microscopic images based on mathematical morphology with a variable structuring element,” *Computers and Electronics in Agriculture,* vol. 75, no. 2, pp. 250-260, 2011.

[160] Pan, S., and Kudo, M., “Recognition of wood porosity based on direction insensitive feature sets,” *Transactions on Machine Learning and Data Mining,* vol. 5, no. 1, pp. 45-62, 2012.

[161] Pankhurst, R., “Principles and problems of identification,” *Advances in computer methods for systematic biology. John Hopkins Univ. Press: Baltimore, USA*, pp. 125-136, 1993.

[162] Pankhurst, R. J., *Biological identification. The principles and practice of identification methods in biology*: Edward Arnold (Publishers) Ltd., 1978.

[163] Pankhurst, R. J., *Practical taxonomic computing*: Cambridge University Press, 1991.

[164] Patil, H. A., Dutta, P. K., and Basu, T., “Comparison of performance of different speech features for identification of professional mimics in Hindi and Urdu languages,” in National Symposium on Acoustics, 2004, pp. 25-27.

[165] Paul, R. R., Mukherjee, A., Dutta, P. K., Banerjee, S., Pal, M., Chatterjee, J., Chaudhuri, K., and Mukkerjee, K., “A novel wavelet neural network based pathological stage detection

technique for an oral precancerous condition," *Journal of clinical pathology,* vol. 58, no. 9, pp. 932-938, 2005.

[166] Paula Filho, P. L., Oliveira, L. S., and Britto Jr, A. S., "A database for forest species recognition," in Proceedings of the XXII Brazilian Symposium on Computer Graphics and Image Processing, 2009.

[167] Paula Filho, P. L., Oliveira, L. S., Nisgoski, S., and Britto Jr, A. S., "Forest species recognition using macroscopic images," *Machine Vision and Applications,* vol. 25, no. 4, pp. 1019-1031, 2014.

[168] Peng, H., Long, F., and Ding, C., "Feature selection based on mutual information criteria of max-dependency, max-relevance, and min-redundancy," *IEEE Transactions on Pattern Analysis and Machine Intelligence* vol. 27, no. 8, pp. 1226-1238, 2005.

[169] Pietikäinen, M., Hadid, A., Zhao, G., and Ahonen, T., "Computer vision using local binary patterns," *Computational Imaging and Vision*, 2011.

[170] Pietikäinen, M., Ojala, T., and Xu, Z., "Rotation-invariant texture classification using feature distributions," *Pattern Recognition,* vol. 33, no. 1, pp. 43-52, 2000.

[171] Piuri, V., and Scotti, F., "Design of an automatic wood types classification system by using fluorescence spectra," *IEEE Transactions on Systems, Man, and Cybernetics, Part C: Applications and Reviews,* vol. 40, no. 3, pp. 358-366, 2010.

[172] Platt, J. C., Cristianini, N., and Shawe-Taylor, J., "Large margin DAGs for multiclass classification," in Proceedings of Neural Information Processing Systems (NIPS), 1999, pp. 547-553.

[173] Prasad, A. M., Iverson, L. R., and Liaw, A., "Newer classification and regression tree techniques: bagging and random forests for ecological prediction," *Ecosystems,* vol. 9, no. 2, pp. 181-199, 2006.

[174] Prasad, B., Biswas, K. K., and Gupta, S., "Region-based image retrieval using integrated color, shape, and location index," *computer vision and image understanding,* vol. 94, no. 1, pp. 193-233, 2004.

[175] Prasad, B., Gupta, S., and Biswas, K. K., "Color and shape index for region-based image retrieval," *Visual Form 2001*, pp. 716-725: Springer, 2001.

[176] Prasad, G. K., and Sahambi, J., "Classification of ECG arrhythmias using multi-resolution analysis and neural networks," in Conference on Convergent Technologies for the Asia-Pacific Region TENCON 2003, 2003, pp. 227-231.

[177] Pujara, C., Bhardwaj, A., Gadre, V. M., and Khire, S., "Secure watermarking in fractional wavelet domains," *IETE Journal of Research,* vol. 53, no. 6, pp. 573-580, 2007.

[178] Qi, H.-n., Chen, F.-n., and Wang, H.-j., "Analysis of quantitative pore features based on mathematical morphology," *Forestry Studies in China,* vol. 10, no. 3, pp. 193-198, 2008.

[179] Rangayyan, R. M., and Ayres, F. J., “Gabor filters and phase portraits for the detection of architectural distortion in mammograms,” *Medical and biological engineering and computing,* vol. 44, no. 10, pp. 883-894, 2006.

[180] Saeys, Y., Inza, I., and Larrañaga, P., “A review of feature selection techniques in bioinformatics,” *bioinformatics,* vol. 23, no. 19, pp. 2507-2517, 2007.

[181] Sarfraz, M. S., and Hellwich, O., “Probabilistic learning for fully automatic face recognition across pose,” Image and Vision Computing, vol. 28, no. 5, pp. 744-753, 2010.

[182] Scholz, A., Klepsch, M., Karimi, Z., and Jansen, S., “How to quantify conduits in wood?,” *Frontiers in plant science,* vol. 4, no. 56, pp. 1-11, 2013.

[183] Sengar, R. S., Upadhyay, A. K., Singh, M., and Gadre, V. M., “Segmentation of two dimensional electrophoresis gel image using the wavelet transform and the watershed transform,” in National Conference on Communications (NCC), 2012, pp. 1-5.

[184] Sengur, A., Turkoglu, I., and Ince, M. C., “Wavelet packet neural networks for texture classification,” *Expert systems with applications,* vol. 32, no. 2, pp. 527-533, 2007.

[185] Shan, C., Gong, S., and McOwan, P. W., “Facial expression recognition based on local binary patterns: A comprehensive study,” *Image and Vision Computing,* vol. 27, no. 6, pp. 803-816, 2009.

[186] Sharma, H., Zerbe, N., Heim, D., Wienert, S., Behrens, H.-M., Hellwich, O., and Hufnagl, P., “A multi-resolution approach for combining visual information using nuclei segmentation and classification in histopathological images,” in Proceedings of the International Conference on Computer Vision Theory and Applications (VISAPP 2015), Berlin Germany, 2015, pp. 37-46.

[187] Sharma, L., Tripathy, R., and Dandapat, S., “Multiscale energy and eigenspace approach to Detection and Localization of Myocardial Infarction,” *IEEE Transactions on Biomedical Engineering*, vol. 62, no. 7, pp. 1827-1837, 2015.

[188] Sharma, M., Gadre, V. M., and Porwal, S., “An eigenfilter-based approach to the design of time-frequency localization optimized two-channel linear phase biorthogonal filter banks,” *Circuits, Systems, and Signal Processing,* vol. 34, no. 3, pp. 931-959, 2015.

[189] Sharma, M., Kolte, R., Patwardhan, P., and Gadre, V., “Time-frequency localization optimized biorthogonal wavelets,” in International Conference on Signal Processing and Communications (SPCOM), 2010, pp. 1-5.

[190] Sobel, I., “Camera models and machine perception,” DTIC Document, Stanford University, Palo Alto, Calif, 1970.

[191] Soh, L.-K., and Tsatsoulis, C., “Texture analysis of SAR sea ice imagery using gray level co-occurrence matrices,” *IEEE Transactions on Geoscience and Remote Sensing,* vol. 37, no. 2, pp. 780-795, 1999.

[192] Sperry, J. S., and Sullivan, J. E., “Xylem embolism in response to freeze-thaw cycles and water stress in ring-porous, diffuse-porous, and conifer species,” Plant Physiology, vol. 100, no. 2, pp. 605-613, 1992.

[193] Sperry, J. S., Nichols, K. L., Sullivan, J. E., and Eastlack, S. E., “Xylem embolism in ring-porous, diffuse-porous, and coniferous trees of northern Utah and interior Alaska,” Ecology, pp. 1736-1752, 1994.

[194] Sripath, D., “Efficient implementations of discrete wavelet transforms using FPGAs,” Open Access, Department of Electrical and Computer Engineering, The Florida State University, 2003.

[195] Steppe, K., Cnudde, V., Girard, C., Lemeur, R., Cnudde, J.-P., and Jacobs, P., “Use of X-ray computed microtomography for non-invasive determination of wood anatomical characteristics,” *Journal of structural biology,* vol. 148, no. 1, pp. 11-21, 2004.

[196] Sun, L. J., Ji, Z. W., and Wang, H. J., “A new wood recognition method based on texture analysis,” in Applied Mechanics and Materials, 2011, pp. 613-617.

[197] Taman, I., Rosid, M., Atika, N., Karis, M. S., Hasim, S. H., Zainal Abidin, A. F., Nordin, N. A., Omar, N., Jaafar, H. I., and Ab Ghani, Z., “Classification system for wood recognition using k-nearest neighbor with optimized features from binary gravitational algorithm,” in International Conference on Recent treads in Engineering & Technology (ICRET), Batam (Indonesia), 2014, pp. 1-6.

[198] Tan, X., and Triggs, B., “Enhanced local texture feature sets for face recognition under difficult lighting conditions,” *IEEE Transactions on Image Processing* vol. 19, no. 6, pp. 1635-1650, 2010.

[199] Tian, Q., Yu, J., and Huang, T. S., "Boosting multiple classifiers constructed by hybrid discriminant analysis," *Multiple Classifier Systems*, pp. 42-52: Springer, 2005.

[200] Tou, J. Y., Lau, P. Y., and Tay, Y. H., “Computer vision-based wood recognition system,” in Proceedings of International Workshop on Advanced Image Technology (IWAIT), 2007.

[201] Tou, J. Y., Tay, Y. H., and Lau, P. Y., “Rotational invariant wood species recognition through wood species verification,” in 1st Asian Conference on Intelligent Information and Database Systems (ACIIDS), 2009, pp. 115-120.

[202] Tou, J. Y., Tay, Y. H., and Lau, P. Y., “A comparative study for texture classification techniques on wood species recognition problem,” in 5th International Conference on Natural Computation (ICNC) 2009, pp. 8-12.

[203] Travis, A., Hirst, D., and Chesson, A., “Automatic classification of plant cells according to tissue type using anatomical features obtained by the distance transform,” *Annals of Botany,* vol. 78, no. 3, pp. 325-331, 1996.

[204] Tyree, M. T., and Zimmermann, M. H., Xylem Structure and the Ascent of Sap, Springer Series in Wood Science 2nd ed.: Springer-Verlag Berlin Heidelberg, 2002.

[205] Van Vliet, G., “Wood anatomy of the Combretaceae,” *Blumea,* vol. 25, pp. 141-223, 1979.

[206] Von Arx, G., Kueffer, C., and Fonti, P., “Quantifying plasticity in vessel grouping–added value from the image analysis tool RoXAS,” IAWA Journal, vol. 34, no. 4, pp. 433-445, 2013.

[207] Von Arx, G., and Carrer, M., “ROXAS–A new tool to build centuries-long tracheid-lumen chronologies in conifers,” Dendrochronologia, vol. 32, no. 3, pp. 290-293, 2014.

[208] Wang, B.-h., Wang, H.-j., and Qi, H.-n., “Wood recognition based on grey-level co-occurrence matrix,” in IEEE International Conference on Computer Application and System Modeling (ICCASM), 2010, pp. V1-269 - V1-272.

[209] Wang, H., Qi, H., Li, W., Zhang, G., and Wang, P., “A GA-based automatic pore segmentation algorithm,” in Proceedings of the first ACM/SIGEVO Summit on Genetic and Evolutionary Computation, 2009, pp. 985-988.

[210] Wang, H., Zhang, G., Qi, H., and Ma, L., “Multi-objective optimization on pore segmentation,” in 5th International Conference on Natural Computation (ICNC), 2009, pp. 613-617.

[211] Wang, H.-j., Qi, H.-n., and Wang, X.-F., "A new wood recognition method based on Gabor entropy," *Advanced Intelligent Computing Theories and Applications. With Aspects of Artificial Intelligence*, pp. 435-440: Springer, 2012.

[212] Wang, H.-j., Qi, H.-n., and Wang, X.-F., “A new Gabor based approach for wood recognition,” *Neurocomputing,* vol. 116, pp. 192-200, 2013.

[213] Wang, H.-j., Zhang, G.-q., and Qi, H.-n., “Wood recognition using image texture features,” *PloS one,* vol. 8, no. 10, pp. e76101, 2013.

[214] Wang, J. Z., Wiederhold, G., Firschein, O., and Wei, S. X., “Content-based image indexing and searching using Daubechies' wavelets,” *International Journal on Digital Libraries,* vol. 1, no. 4, pp. 311-328, 1998.

[215] Wegner, L., von Arx, G., Sass-Klaassen, U., and Eilmann, B., “ROXAS–an efficient and accurate tool to detect vessels in diffuse-porous species,” Iawa Journal, vol. 34, no. 4, pp. 425-432, 2013.

[216] Wheeler, E. A., “Inside Wood–A Web resource for hardwood anatomy,” *IAWA Journal,* vol. 32, no. 2, pp. 199-211, 2011.

[217] Wheeler, E. A., and Baas, P., “Wood identification: a review,” *IAWA Journal (Netherlands),* vol. 19, no. 3, pp. 241-264, 1998.

[218] Wheeler, E. A., Pearson, R., LaPasha, C., Zack, T., and Hatley, W., “Computer-aided wood identification. Reference manual,” *Bull. N. Carolina Agric. Res. Serv*, no. 474, pp. 160, 1986.

[219] Xu, H., Caramanis, C., and Mannor, S., “Robustness and regularization of support vector machines,” *The Journal of Machine Learning Research,* vol. 10, pp. 1485-1510, 2009.

[220] Yaghouby, F., and Ayatollahi, A., “An arrhythmia classification method based on selected features of heart rate variability signal and support vector machine-based classifier,” in World Congress on Medical Physics and Biomedical Engineering, September 7-12, 2009, Munich, Germany, 2010, pp. 1928-1931.

[221] Yaghouby, F., Ayatollahi, A., Bahramali, R., and Yaghouby, M., “Robust genetic programming-based detection of atrial fibrillation using RR intervals,” *Expert Systems,* vol. 29, no. 2, pp. 183-199, 2012.

[222] Yaghouby, F., Ayatollahi, A., Bahramali, R., Yaghouby, M., and Alavi, A. H., “Towards automatic detection of atrial fibrillation: A hybrid computational approach,” *Computers in biology and medicine,* vol. 40, no. 11, pp. 919-930, 2010.

[223] Yaghouby, F., Ayatollahi, A., and Soleimani, R., “Classification of cardiac abnormalities using reduced features of heart rate variability signal,” *World Applied Sciences Journal,* vol. 6, no. 11, pp. 1547-1554, 2009.

[224] Yang, J., and Yang, J.-y., “Why can LDA be performed in PCA transformed space?,” *Pattern recognition,* vol. 36, no. 2, pp. 563-566, 2003.

[225] Ylioinas, J., Hadid, A., Guo, Y., and Pietikäinen, M., "Efficient image appearance description using dense sampling based local binary patterns," *Computer Vision–ACCV 2012*, pp. 375-388: Springer, 2013.

[226] You, J., and Bhattacharya, P., “A wavelet-based coarse-to-fine image matching scheme in a parallel virtual machine environment,” *IEEE Transactions on Image Processing,* vol. 9, no. 9, pp. 1547-1559, 2000.

[227] You, J., Li, W., and Zhang, D., “Hierarchical palmprint identification via multiple feature extraction,” *Pattern recognition,* vol. 35, no. 4, pp. 847-859, 2002.

[228] You, M., and Cai, C., “Wood classification based on PCA, 2DPCA,$(2D)^2$PCA and LDA,” in 2nd International Symposium on Knowledge Acquisition and Modeling,KAM'09, 2009, pp. 371-374.

[229] Yu, H., Liu, Y., Han, G., and Cui, Y., “Comparison of image analysis and conventional methods for cellular tissue proportion measurement of wood,” in International Conference on Information and Automation (ICIA'09), 2009, pp. 133-137.

[230] Yuan, G.-X., Ho, C.-H., and Lin, C.-J., “Recent advances of large-scale linear classification,” *Proceedings of the IEEE,* vol. 100, no. 9, pp. 2584-2603, 2012.

[231] Yusof, R., Khalid, M., and Khairuddin, A. S. M., “Fuzzy data management on pores arrangement for tropical wood species recognition system,” in Science and Information Conference (SAI), 2013, pp. 529-535.

[232] Yusof, R., Khalid, M., and Khairuddin, A. S. M., “Fuzzy logic-based pre-classifier for tropical wood species recognition system,” *Machine vision and applications,* vol. 24, no. 8, pp. 1589-1604, 2013.

[233] Yusof, R., Khalid, M., and M Khairuddin, A. S., “Application of kernel-genetic algorithm as nonlinear feature selection in tropical wood species recognition system,” *Computers and Electronics in Agriculture,* vol. 93, pp. 68-77, 2013.

[234] Yusof, R., Rosli, N. R., and Khalid, M., “Using Gabor filters as image multiplier for tropical wood species recognition system,” in 12th International Conference on Computer Modelling and Simulation (UKSim), 2010, pp. 289-294.

[235] Zhang, D., Kong, W.-K., You, J., and Wong, M., “Online palmprint identification,” *IEEE Transactions on Pattern Analysis and Machine Intelligence,* vol. 25, no. 9, pp. 1041-1050, 2003.

[236] Zhang, L., Zhou, Z., and Li, H., “Binary Gabor pattern: An efficient and robust descriptor for texture classification,” in 19th IEEE International Conference on Image Processing (ICIP), 2012, pp. 81-84.

[237] Zhang, Z., Ye, N., Wu, D., and Wang, Y., “Automatic wood defects recognition comparative research,” in International Workshop on Geoscience and Remote Sensing, Education Technology and Training (ETT and GRS) 2008, pp. 649-653.

[238] Zhao, G., Ahonen, T., Matas, J., and Pietikainen, M., “Rotation-invariant image and video description with local binary pattern features,” *IEEE Transactions on Image Processing,* vol. 21, no. 4, pp. 1465-1477, 2012.

[239] Zhao, M., Chai, Q., and Zhang, S., "A method of image feature extraction using wavelet transforms," *Emerging Intelligent Computing Technology and Applications*, pp. 187-192: Springer, 2009.

[240] Zhao, P., “Robust wood species recognition using variable color information,” *Optik-International Journal for Light and Electron Optics,* vol. 124, no. 17, pp. 2833-2836, 2013.

[241] Zhao, P., Dou, G., and Chen, G.-S., “Wood species identification using feature-level fusion scheme,” *Optik-International Journal for Light and Electron Optics,* vol. 125, no. 3, pp. 1144-1148, 2014.

[242] Zhao, P., Dou, G., and Chen, G.-S., “Wood species identification using improved active shape model,” *Optik-International Journal for Light and Electron Optics,* vol. 125, no. 18, pp. 5212-5217, 2014.

[243] Zheng, Y., Shen, C., Hartley, R., and Huang, X., “Effective pedestrian detection using center-symmetric local binary/trinary patterns,” *arXiv preprint arXiv:1009.0892*, 2010.

[244] Zhong, F., and Zhang, J., “Face recognition with enhanced local directional patterns,” *Neurocomputing,* vol. 119, pp. 375-384, 2013.

[245] Zimmermann, M., "Structural requirements for optimal water conduction in tree stems," Cambridge University Press, 1978, pp. 517-532.

[246] Arrangement of cells and tissues in the stem," July 4, 2015; http://www.trada.co.uk/images/onlinebooks/FA4C5C32-D645-4155-AF8B-20DE2FEE2A66/ ar01s02.html.

[247] Database of Japanese woods, Wood identification database team, FFPRI, 2002," http://f030091.ffpri.affrc.go.jp/index-E1.html.

[248] Enger, N., "Wood botany," July 4, 2015; http://workshopcompanion.com/KnowHow/Wood/Hardwoods_&_Softwoods/1_Wood_Botany/1_Wood_Botany.htm.

[249] Jaiantilal, A., "Random forest (regression, classification and clustering) implementation for MATLAB (and standalone)," https://code.google.com/p/randomforest-matlab/downloads/detail?name=Windows-Precompiled-RF_MexStandalone-v0.02-.zip.

[250] Jensen, E., Zahler, D., Patterson, B., and Littlefield, B., "Dichotomous key," July 1, 2015; http://oregonstate.edu/trees/dichotomous_key/index.html.

[251] Karch, E., "Simple hardwood identification for turners," July 7, 2015; http://www.karch.com/K/idwood.htm.

[252] Laboratories 11 and 12 the movement of sap in trees, "cellular structure of maple (Acer)", July 4, 2015; http://www.uvm.edu/~biology/Classes/past-classes/002B/laboratories11_12.htm.

[253] Massengle, C., "Dichotomous keying," July 1, 2015; http://www.biologyjunction.com/dichotomous_keying.htm.

[254] Nunlist, T., "Understanding wood: Four structure types," July 4, 2015; http://www.popularwoodworking.com/techniques/understanding-wood-four-structure-types.

[255] Wheeler, E., "InsideWood 2004-onwards," July 2, 2015; http://insidewood.lib.ncsu.edu/search.

[256] Wood , April 10, 2015; http://science.jrank.org/pages/7409/Wood.html